**This is a digital document from the collections of the *Wyoming Water Resources Data System* (WRDS) Library.**

For additional information about this document and the document conversion process, please contact WRDS at wrds@uwyo.edu and include the phrase **"Digital Documents"** in your subject heading.

To view other documents please visit the WRDS Library online at:
http://library.wrds.uwyo.edu

**Mailing Address**:
Water Resources Data System
University of Wyoming, Dept 3943
1000 E University Avenue
Laramie, WY 82071

**Physical Address:**
Wyoming Hall, Room 249
University of Wyoming
Laramie, WY 82071

**Phone:** (307) 766-6651
**Fax:** (307) 766-3785

***Funding for WRDS and the creation of this electronic document was provided by the Wyoming Water Development Commission (http://wwdc.state.wy.us)***



# Weather Modification–
# Bighorn Mountains Siting and Design Study

## Final Report

**prepared for**

**Wyoming Water Development Commission**
**State of Wyoming**

by

National Center for Atmospheric Research
Research Applications Laboratory
3090 Center Green Drive
Boulder, CO 80301

NCAR

Investigators:
Sarah Tessendorf[1], Roy Rasmussen[1], Lulin Xue[1], Courtney Weeks[1], Kyoko Ikeda[1], Jamie Wolff[1], Michelle Harrold[1], Scott Landolt[1], Duncan Axisa[1], Bruce Boe[2], Patrick Golden[3]

[1]Research Applications Laboratory, National Center for Atmospheric Research (NCAR)
[2]Weather Modification International (WMI)
[3]Heritage Environmental Consultants (HEC)

2 March 2017

**Weather Modification—Bighorn Mountains Siting and Design Study**

## Table of Contents


Executive Summary ..... i
1. Introduction ..... 1
  1.1 Task Overview ..... 1
  1.2 Personnel and Organizations ..... 2
2. Task 1: Scoping Meeting/Project Meetings ..... 4
  2.1 Scoping Meetings in Sheridan and Worland, WY ..... 4
  2.2 27 January 2016, Cheyenne, WY ..... 4
3. Task 2: Review and Summarization of Previous Data ..... 6
  3.1 Background ..... 6
    3.1.1 Conceptual Model ..... 7
  3.2 History of Wintertime Orographic Cloud Seeding ..... 10
    3.2.1 Randomized Studies - Historical ..... 10
    3.2.2 Randomized Studies - Recent ..... 11
    3.2.3 Physical Experiments ..... 13
    3.2.4 Numerical Modeling ..... 14
  3.3 Meteorological Observations Relevant to the Bighorn Mountains ..... 14
  3.4 History of Cloud Seeding In and Near the Bighorn Mountains ..... 15
4. Task 3: Climatology of the Project Area ..... 18
  4.1 Data and Methodology ..... 19
    4.1.1 Observations ..... 19
    4.1.2 Model ..... 20
  4.2 Characteristics of Wintertime Clouds and Precipitation ..... 25
    4.2.1 SNOTEL Precipitation Observations ..... 25
    4.2.2 Comparison of model vs SNOTEL ..... 30
    4.2.3 Riverton Sounding Analysis ..... 36
    4.2.4 Model-based Analysis Results ..... 37
  4.3 Climatology of Cloud-Seeding Opportunities ..... 58
    4.3.1 Model-based Analysis Results ..... 58
  4.4 Seedable Precipitation Calculations ..... 77
  4.5 Summary ..... 78
5. Task 4: Development of Preliminary Project Design ..... 80
  5.1 Project Scope and Targeting ..... 80
  5.2 Delivery Methods and Seeding Agent Selection ..... 81
  5.3 Selection of Test Cases ..... 82
  5.4 Initial Exploratory Ground-based Tests ..... 83
  5.5 Airborne Tests ..... 84
  5.6 Additional Tests ..... 86
  5.7 Final Ground-based Generator Locations ..... 87
  5.8 Summary Remarks ..... 88
6. Task 5: Model Evaluation of Preliminary Project Design ..... 90
  6.1 Model setup ..... 90
    6.1.1 Cloud-Seeding Parameterization in WRF ..... 91

6.2 Case Selection and Overviews ..... 93
6.2.1 Case Selection using WRF-CONUS Model ..... 93
6.2.2 Case Selection Using Observations from 2015–2016 ..... 94
6.3 Case Study Simulation Results ..... 95
6.3.1 13 November 2007 case ..... 96
6.3.2 20 November 2007 case ..... 121
6.3.3 17 January 2016 case ..... 143
6.4 Summary of Model Evaluation ..... 160
7. Task 6: Field Surveys: Proposed Ground Generator Locations ..... 162
7.1 Selection of Ground-based Generator Locations ..... 162
7.1.1 Remote Generator Locations – Pre-Field Survey ..... 163
7.1.2 Generator Locations - Post-Field Survey ..... 165
8. Task 7: Access/Easements & Environmental Permitting/Reporting ..... 171
8.1 Private Lands ..... 171
8.2 Public Lands ..... 172
8.3 Ownership Summary – Final Configuration of Generator Locations ..... 172
8.4 Weather Modification Program Permitting ..... 172
8.4.1 State of Wyoming Permit Requirements ..... 172
8.4.2 Wyoming Game and Fish Department ..... 173
8.4.3 National Oceanic and Atmospheric Administration Reporting ..... 173
9. Task 8: Establishment of Operational Criteria ..... 174
9.1 Information Sources ..... 174
9.1.1 Soundings ..... 174
9.1.2 Radiometer ..... 174
9.1.3 Additional Information ..... 174
9.2 Ground-based Seeding with Ice Nuclei ..... 175
9.3 Airborne Seeding with Ice Nuclei ..... 176
9.4 Seeding Season ..... 177
9.5 Suspension Criteria ..... 178
10. Task 9: Environmental and Legal Considerations ..... 180
10.1 Downwind (Extra-area) Effects ..... 180
10.2 Environmental Impacts of Seeding Agents ..... 183
10.3 General Statements on Potential Environmental Impacts of Cloud Seeding ..... 185
10.4 Legal Implications ..... 187
11. Task 10: Evaluation Methodology ..... 188
11.1 Statistical Evaluation ..... 188
11.1.1 Target/Control Method ..... 188
11.1.2 Evaluation by Historical Regression ..... 189
11.1.3 Evaluation by Ratio Statistics ..... 190
11.2 Numerical Model Evaluation ..... 191
11.3 Physical Evaluation ..... 192
11.4 Evaluation Methodology Summary ..... 194
12. Task 11: Hydrologic Assessment ..... 195
12.1 WRF model simulation of runoff ..... 195
12.2 Observational Streamflow Data and Snowpack ..... 200
12.3 Other parameters for Estimating Seeding Effects ..... 206

12.3.1 Seasonal Percentage of Seedable Snowpack ..... 206
12.3.2 Areal Coverage ..... 207
12.4 Estimates of Streamflow Changes due to Seeding ..... 207
13. Task 12: Cost Estimates ..... 211
13.1 Project Scope ..... 211
13.2 Deployment of Ground-based Ice Nucleus Generators ..... 211
13.3 Length of Program Season ..... 212
13.4 Airborne Seeding ..... 212
13.5 Possible Cost Savings ..... 213
13.5.1 Sharing Operational Resources ..... 213
13.5.2 The Number of Operational Seasons ..... 214
13.5.3 Project Implementation Mode ..... 214
13.6 Water Quantity, Use, and Value ..... 217
13.6.1 Wind/Bighorn Basin ..... 217
13.6.2 Powder/Tongue River Basin ..... 219
13.6.3 The Value of Water near the Bighorn Mountains ..... 221
14. Task 13: Preliminary Cost/Benefit Analyses ..... 222
14.1 Value of Augmented April-July Streamflow ..... 222
14.2 Cost per Acre-Foot Estimates ..... 223
14.3 Cost/Benefit Summary Remarks ..... 225
14.3.1 Uncertainties in the Analysis ..... 226
15. Task 14: Reports and Executive Summaries ..... 228
16. Task 15: Report Presentations ..... 229
17. Task 16: Climatological Monitoring of the Study Area ..... 231
17.1 Available Datasets on the Internet ..... 231
17.2 Additional Instrument Deployments ..... 231
17.2.1 Radiometer ..... 231
17.2.2 Snow Gauges ..... 238
18. Summary and Recommendations ..... 246
18.1 Summary ..... 246
18.2 Conclusions and Recommendations ..... 251
18.2.1 Recommendations ..... 251
19. References ..... 253
20. List of Acronyms ..... 261
21. Appendix A ..... 263
22. Appendix B ..... 282

## LIST OF FIGURES

Figure 3.1. Wyoming county borders. ..... 16
Figure 4.1. SNOTEL site locations (magenta dots) in the Bighorn mountain range. Near-by towns are indicated by filled squares. ..... 20
Figure 4.2. WRF-CONUS model domain and elevation. Red box indicates the region of the Bighorn Mountains where the analysis focuses. For a close-up image of the study region see Figure 4.1. ..... 21
Figure 4.3. Map of the model terrain height highlighting the grid points used in the seeding potential analysis along with other key sites where model output was analyzed. The west area is shown in blue, the east area in red, and the south area in black. Precipitation sites are marked by yellow circles. Sites used for analysis of 700-hPa conditions are marked by white circles. ..... 23
Figure 4.4. (a) – (h) Monthly observed precipitation averaged from 14 SNOTEL sites in the study area in each water year. (i) The 8-year climatology of monthly SNOTEL-observed precipitation. Magenta vertical bars indicate +/– one standard deviation from the areal average, indicating spatial variability. ..... 27
Figure 4.5. The November – April precipitation at SNOTEL sites in each water year. Contours indicate elevation. The color scale is intended to match the range of model precipitation shown in Figure 4.9. ..... 28
Figure 4.6. Temporal correlation coefficients of daily precipitation over eight years at each pair of SNOTEL sites based on the November – April measurements from eight water years. Site names in black, red, and blue indicate sites in the western, southern, and eastern regions of the Bighorn Mountains. ..... 29
Figure 4.7. Same as Figure 4.6 but for each water year. ..... 30
Figure 4.8. Map of the 8-year average accumulated wintertime precipitation (mm) between November–April from SNOTEL (left) and the WRF-CONUS model (right). ..... 31
Figure 4.9. The November – April precipitation in each water year from the WRF-CONUS model simulation. Magenta circles mark the SNOTEL site locations. ..... 32
Figure 4.10. Maps of 8-year average monthly precipitation accumulation (mm) from the WRF-CONUS model for the months of October to May. ..... 32
Figure 4.11. 8-year average of annual precipitation accumulation at each SNOTEL site (SNOTEL in black, model in red). Vertical bars are one standard deviation about the 8-year mean. The difference (in mm) between the model and SNOTEL precipitation observations for November–April (winter) and the full year is indicated in the upper left corners. Values in parentheses indicate percent bias in the seasonal and annual biases with respect to the observations. Refer to the inlay map for the SNOTEL site locations. ..... 34
Figure 4.12. Time history of observed and simulated precipitation accumulation averaged over SNOTEL sites in each water year. The difference (in mm) between the model and SNOTEL precipitation observations for November–April (winter) and the full year is indicated in the upper left corners. Values in parentheses are the percent bias from the observations. The biases are taken as model minus observation. Vertical bars present +/– one standard deviation from the areal mean, indicating spatial variability. ..... 35

Figure 4.13. The 8-year climatology of precipitation accumulation averaged over the SNOTEL sites in the study region. Vertical bars are one standard deviation from the 8-year mean, representing the year-to-year variability. The model bias in November – April (grey shaded) and annual precipitation (in mm) is indicated in the upper right corner. Values in parentheses are the percent bias from the observations. The biases are taken as model minus observation. ..... 36
Figure 4.14. Wind rose showing the frequency of (a) observed and (b) modeled 700-hPa wind direction over Riverton, Wyoming when precipitation occurred over the Bighorn Mountains, using daily observed data from the Grave Springs SNOTEL site in (a) and three-hourly modeled precipitation at Grave Springs in (b), over the 8-year period from November–April. The magnitude of daily observed or 3-hourly modeled precipitation for each wind direction is indicated by the color within each wind direction bin. ..... 37
Figure 4.15. Histogram counts (left ordinate) of the (a) observed and (b) modeled 700-hPa temperature at Riverton, Wyoming. In (a), it is shown for all soundings (red) from November–April during the 8-year period of study (water years 2001–2008) and for all soundings that had precipitation observed at the Grave Springs SNOTEL site (blue); in (b) counts of modeled 700-hPa temperature at Riverton, Wyoming for all three-hour model periods (red) and three-hour model periods with modeled precipitation at the Grave Springs SNOTEL site (blue). Cumulative distributions for all (red) and with precipitation (blue dotted) are also overlaid using the right ordinate (%). ..... 37
Figure 4.16. Wind rose showing the frequency of modeled 700-hPa wind direction over Sheridan, Wyoming when precipitation occurred over the Bighorn Mountains (using the Sucker Creek SNOTEL site) over the 8-year period from November–April. The magnitude of precipitation per 3-hourly model output time for each wind direction is indicated by the color within each wind direction bin. ..... 38
Figure 4.17. As in Figure 4.16, except for modeled 700-hPa winds over Kaycee when precipitation occurred at the Bear Trap Meadow SNOTEL site. ..... 39
Figure 4.18. As in Figure 4.16, except for modeled 700-hPa winds over Worland when precipitation occurred at the Shell Creek SNOTEL site. ..... 39
Figure 4.19. As in Figure 4.16, except for modeled 700-hPa winds over Twenty Mile Creek when precipitation occurred at the Bone Springs SNOTEL site. ..... 40
Figure 4.20. Month-by-month model wind roses of 700-hPa wind direction over Sheridan during model hours with seedable conditions and precipitation at the Sucker Creek SNOTEL site from November–April. ..... 41
Figure 4.21. As in Figure 4.20, but for model winds over Kaycee and precipitation at the Bear Trap Meadow SNOTEL site. ..... 42
Figure 4.22. As in Figure 4.20, but for model winds over Worland and precipitation at the Shell Creek SNOTEL site. ..... 43
Figure 4.23. As in Figure 4.20, but for model winds over Twenty Mile Creek and precipitation at the Bone Springs SNOTEL site. ..... 44
Figure 4.24. Histogram counts (left ordinate) of the modeled 700-hPa temperature at Sheridan, Wyoming for all 3-hourly output from November–April from the 8-year (water years 2001–2008) model runs (red) and for all 3-hourly output that had precipitation at the Sucker Creek SNOTEL site (blue). Cumulative distributions for all

(red) and with precipitation (blue dotted) are also overlaid using the right ordinate (%)..... 45
Figure 4.25. As in Figure 4.24, but using modeled 700-hPa temperature at the Kaycee, Wyoming site and precipitation from the Bear Trap Meadow SNOTEL site. ..... 46
Figure 4.26. As in Figure 4.24, but using modeled 700-hPa temperature at the Worland site and precipitation from the Shell Creek SNOTEL site..... 46
Figure 4.27. As in Figure 4.24, but using modeled 700-hPa temperature at the Twenty Mile Creek site and precipitation from the Bone Springs SNOTEL site..... 47
Figure 4.28. Histogram counts (left ordinate) of the west region average 0–1 km AGL temperature (left) and 0–1 km AGL LWC (right) for ground seeding (GS) for all three-hourly output from Nov–Apr from the 8-year (Water Years 2001–2008) model runs (red) and for all three-hourly model output that had precipitation at the Shell Creek precipitation site (blue). Cumulative distributions for all (red) and output hours with precipitation (blue dotted) are also overlaid using the right ordinate (%). The bar to the left of the zero includes all values equal to zero..... 48
Figure 4.29. As in Figure 4.28, but areal-averaged values from the eastern region and precipitation from the Sucker Creek site..... 48
Figure 4.30. As in Figure 4.28, but areal-averaged values from the southern region and precipitation from the Grave Springs site..... 49
Figure 4.31. As in Figure 4.28, except for average model LWP in the western (top left), eastern (top right), and southern (bottom) regions. The model precipitation was from the Shell Creek (west), Sucker Creek (east), and Grave Springs (south) sites..... 50
Figure 4.32. As in Figure 4.28, except for average Froude number..... 51
Figure 4.33 As in Figure 4.28, except for average cloud base height in the western (left), eastern (right), and southern (bottom) regions. The model precipitation was from the Shell Creek (west), Sucker Creek (east), and Grave Springs (south) sites..... 52
Figure 4.34. As in Figure 4.28, except for average cloud depth in the western (left), eastern (right), and southern (bottom) regions. The model precipitation was from the Shell Creek (west), Sucker Creek (east), and Grave Springs (south) sites..... 53
Figure 4.35. As in Figure 4.28, except for average cloud top temperature in the western (left), eastern (right), and southern (bottom) regions. The model precipitation was from the Shell Creek (west), Sucker Creek (east), and Grave Springs (south) sites..... 54
Figure 4.36. As in Figure 4.28, except for in the 3.5–4.5 km MSL layer (for airborne seeding; AS). ..... 56
Figure 4.37. As in Figure 4.29, except for in the 3.5–4.5 km MSL layer. ..... 57
Figure 4.38. As in Figure 4.30, except for in the 3.5–4.5 km MSL layer. ..... 57
Figure 4.39. Histogram counts (left ordinate) of the western region average 0–1 km AGL temperature when LWC was present (> 0) in the layer (left) and 3.5–4.5 km MSL temperature when LWC was present in the layer (right) for all hourly output between November and April from the 8-year (Water Years 2001–2008) model runs (red) and for all hourly output that had precipitation at the Shell Creek SNOTEL site (blue). Cumulative distributions are included as in Figure 4.28..... 58
Figure 4.40. Frequency (fraction of time) that seeding criteria are met within the 0–1 km AGL layer for all seasons (2000–2008): a) LWP, b) LWC, c) Temperature, d) LWC and Temperature concurrently. Note: the colorbar has a maximum value of 40% (same

across all figures) and values greater than 40% are not shown. Thin black contours indicate the topography. 60
Figure 4.41. As in Figure 4.40, but for the 3.5–4.5 km MSL airborne seeding layer. 62
Figure 4.42. Bar chart showing the average fraction of hours per month that met the temperature and LWC criteria averaged over the western area for ground-based seeding (0–1 km AGL; blue) and the same for hours that also had precipitation in the model near the Shell Creek SNOTEL site (green). 63
Figure 4.43. Bar chart showing the number of hours in a given month that met the temperature and LWC criteria averaged over the western area for ground-based seeding (0–1 km AGL). Each color represents one of the 8 years simulated by the model. 64
Figure 4.44. Bar chart showing the average fraction of hours in a winter season (Nov–Apr) that met the temperature and LWC criteria averaged over the western area for ground-based seeding (0–1 km AGL; blue) and the same for hours that also had precipitation in the model near the Shell Creek SNOTEL site (green). 64
Figure 4.45. As in Figure 4.44, except also including 700-hPa wind direction as an additional criterion for ground seeding potential. 65
Figure 4.46. As in Figure 4.44, except also including 700-hPa wind direction and Froude number > 0.5 as additional criteria for ground seeding potential. 65
Figure 4.47. As in Figure 4.42, but over the eastern area and using precipitation near the Sucker Creek SNOTEL site. 66
Figure 4.48. As in Figure 4.42, but over the southern area and using precipitation near the Grave Springs SNOTEL site. 66
Figure 4.49. Bar chart showing the average fraction of 3-hour periods in a month that met the temperature and LWC criteria averaged over the western area for airborne seeding (3.5–4.5 km MSL; blue) and the same for hours that also had any precipitation (cyan) and snow (green) in the model near the Shell Creek SNOTEL site. 67
Figure 4.50. Fraction of 3-hourly periods in the November–April period for each water year meeting the temperature and LWC criteria in the 3.5–4.5 km MSL layer over the western area (blue), and the same using the Shell Creek SNOTEL site for precipitation (cyan) and snow (green). 68
Figure 4.51. As in Figure 4.43, except for airborne seeding (3.5–4.5 km MSL). 68
Figure 4.52. As in Figure 4.50, except for number of 3-hourly periods rather than fraction. 69
Figure 4.53. As in Figure 4.50, except for number of 3-hourly periods in the extended October–June period. 69
Figure 4.54. As in Figure 4.49, except for the 4.5–5.5 km MSL layer. 70
Figure 4.55. As in Figure 4.49, except for the eastern region and the Sucker Creek SNOTEL site. 70
Figure 4.56. As in Figure 4.49, except for the eastern region and Sucker Creek SNOTEL site, in the 4.5–5.5 km MSL layer. 71
Figure 4.57. As in Figure 4.49, except for the southern region and the Grave Springs SNOTEL site. 71
Figure 4.58. As in Figure 4.49, except for the southern region and Grave Springs SNOTEL site, in the 4.5–5.5 km MSL layer. 72

Figure 4.59. Fraction of seedable three-hour periods meeting temperature and LWC criteria in the 3.5–4.5 km MSL airborne seeding layer for the western (blue) and eastern (green) areas, and the union of the two (yellow). ..... 72
Figure 4.60. As in Figure 4.59, except including the southern area as well (olive). ..... 73
Figure 4.61. Ground (0–1 km AGL; blue) versus airborne (3.5–4.5 km MSL; green) seeding opportunities by month in the western region (fraction of hours in the month that meet the designated criteria, listed atop the figure, on average over the 8-year period). The frequency of occurrence of cases from the union of both ground and airborne seeding potential is shown in the yellow bar for each time period. ..... 74
Figure 4.62. Ground (0–1 km AGL; blue) versus airborne (3.5–4.5 km MSL; green) seeding opportunities by November–April season in the western region (fraction of hours in the season that meet the designated criteria, listed atop the figure), and the 8-year average. The frequency of occurrence of cases from the union of both ground and airborne seeding potential is shown in the yellow bar for each time period. ..... 74
Figure 4.63. Lower airborne (3.5–4.5 km MSL; blue) versus higher airborne (4.5–5.5 km MSL; green) seeding opportunities by month in the western region (fraction of hours in the month that meet the designated criteria, listed atop the figure, on average over the 8-year period). The frequency of occurrence of cases from the union of both ground and airborne seeding potential is shown in the yellow bar for each time period. ..... 75
Figure 4.64. Ground (0–1 km AGL; dark blue), lower airborne (3.5–4.5 km MSL; light blue), and upper airborne (4.5–5.5 km MSL; green) seeding opportunities in the western region by November–April season (total number of 3-hourly periods in the month that meet the designated criteria, listed atop the figure) and the 8-year average. The frequency of occurrence of cases from the union of both ground and airborne seeding potential is shown in the yellow bar for each time period. ..... 75
Figure 4.65. As in Figure 4.64 but for the October–June period. ..... 76
Figure 4.66. As in Figure 4.63 but for the eastern region. ..... 76
Figure 4.67. As in Figure 4.63 but for the southern region. ..... 77
Figure 5.1. Example of a remotely-controlled AgI generator. ..... 81
Figure 5.2. Example seeding aircraft ..... 82
Figure 5.3. Topography map of the Bighorn Mountains (m) illustrating the locations of all ground-based generator design groups. ..... 84
Figure 5.4. Map of the proposed ground generator groups and potential airborne seeding flight tracks tested with the model. ..... 86
Figure 5.5. Map of the Bighorn Mountains with the locations of potential ground-based generators. The thick gray line illustrates the divide between the Bighorn and Powder/Tongue River basins. ..... 88
Figure 6.1. Model domain for all cloud seeding project design evaluation simulations. ..... 90
Figure 6.2. Interactions between AgI and hydrometeors simulated in the cloud-seeding parameterization (updated from Xue et al. 2013a to include coagulation, impact scavenging, and dry deposition for AgI). ..... 93
Figure 6.3. The Bighorn sub-domain extracted from the WRF-CONUS model runs. The three black boxes indicate the three sub-regions used by WASCA to assess conditions suitable for seeding. The black line at 45°N is the Wyoming-Montana state border. ..... 94

Figure 6.4. Three sub-regions (areas with terrain greater than 2100 m within each red box) for WASCA. ..... 96
Figure 6.5. Microphysical seeding criteria plots for ground seeding, airborne seeding (3750 m MSL) and higher level airborne seeding (4250 m MSL) for the BHN, BHC and BHS regions for the 13 November 2007 case. Each horizontal panel (and color) represents a different criterion assessed and the horizontal dashed line indicates the threshold that must be reached for the algorithm to consider that criterion met. Not all microphysical criteria assessed are required to be met for a case to be called, and even if all microphysical criteria are met there are additional criteria (especially for ground seeding, such as atmospheric stability and wind direction) that need to be met as well (not shown). Gray shading indicates time periods when seeding cases were identified. For airborne seeding, a 2-hr window is shaded in dark gray, representing the "best" period for seeding (given shorter time on station using a single aircraft). ..... 99
Figure 6.6. Liquid water path below 1 km AGL (kg $m^{-2}$) from 18 UTC 13 November to 08 UTC 14 November every 2 hours. The scale ranges from 0 to 0.5 kg $m^{-2}$. The horizontal solid black line is the Montana-Wyoming state border, and the curved dark black line indicates temperature isotherm of –6 $^{o}$C at 700 hPa. The vertical short black line is the southern flight track. ..... 100
Figure 6.7. The 700-hPa temperature (°C) and wind field for the same period as Figure 6.6. Temperature ranges from -14 to 14 °C. The red line indicates the temperature contour at -6°C. ..... 101
Figure 6.8. Accumulated precipitation (mm) of the 13 November 2007 control simulation. ..... 102
Figure 6.9. Maps of observed precipitation accumulation (mm) over the simulation period for the 13 November 2007 case from SNOTEL sites, with minimum accumulation in (a) and maximum accumulation in (b), compared to model-simulated precipitation accumulation at the SNOTEL sites (c) and the complete simulation of precipitation across the domain (d). ..... 102
Figure 6.10. Scatterplot comparing observed precipitation accumulation at SNOTEL sites versus the modeled precipitation accumulation at the same sites for 13 November 2007. Dots represent the average of the maximum and minimum possible precipitation accumulation at each SNOTEL site during the simulation period. Vertical bars represent the range of possible observation (i.e., minimum to maximum observation amount). Each point (color coded) represents single SNOTEL site. ..... 103
Figure 6.11. The absolute simulated seeding effect (mm) on the left and relative simulated seeding effect (%) on the right for the group D simulation on the top and the group E simulation at the bottom. ..... 104
Figure 6.12. Plan view maps of average simulated AgI concentration below 1 km AGL on the left and vertical cross sections of simulated AgI concentration (color shaded), liquid water mixing ratio (black contours in g/kg), temperature (red contours), ice supersaturation at 1.04 and wind vectors on the right. The cross section locations are indicated by red dashed lines on the plan view maps. The time was 05 UTC 14 November 2007 for ground D simulation (top) and 09 UTC 14 November 2007 for group E (bottom). ..... 105

Figure 6.13. Three flight tracks, the corresponding altitude or seeding rates for the airborne seeding experiments in the 13 November 2007 case. The seeding times for each are also annotated atop each map. 106
Figure 6.14. The simulated seeding effect (mm) at the end of the simulation, average LWP difference (mm), and the relative LWP difference (%) for the AS_N case on 13 November 2007. The straight black horizontal line is the Wyoming-Montana state border. The thin black curves are the underlying terrain contours. The thick black curves in the left panel are the basin divides. The AS_N flight track is overlaid in the center panel. 107
Figure 6.15. The average simulated AgI number concentration between 1 and 3 km MSL at 1113 2300 UTC and 1114 0100 UTC. The red dashed lines indicate the cross section location as show in Figure 6.17. The AS_N flight track is overlaid as a thick black line. 108
Figure 6.16. The LWP between 1 and 3 km MSL at 1113 2300 UTC and 1114 0100 UTC. The black contour represents the isotherm of -6 °C at 700 hPa. The AS_N flight track is overlaid as a thick black line. 109
Figure 6.17. South-north cross sections at 1113 2300 UTC and 1114 0100 UTC for the AS_N case. The left panels show the simulated AgI number concentration in logarithmic scale (color shaded), the cloud water mixing ratio in black starting at 0.01 g $kg^{-1}$ with an interval of 0.2 g $kg^{-1}$, the ice saturation ratio of 1.04 in purple, isotherm in every 10 °C and wind vectors. The right panels show the cloud water mixing ratio difference in black (g $kg^{-1}$) and ice-phase mixing ratio difference in color (g $kg^{-1}$). 110
Figure 6.18. The simulated seeding effect (mm) at the end of the simulation, average LWP difference (mm), and the relative LWP difference (%) for AS_C case. The straight black horizontal line is the Wyoming-Montana state border. The thin black curves are the underlying terrain contours. The thick black curves in the left panel are the basin divides. The AS_C flight track is overlaid in the center panel. 111
Figure 6.19. The average simulated AgI number concentration between 1 and 3 km MSL at 1113 2300 UTC and 1114 0100 UTC for AS_C case. The red dashed lines indicate the cross section location. The AS_C flight track is overlaid as a thick black line. 111
Figure 6.20. The LWP between 1 and 3 km MSL at 1113 23 UTC and 1114 01 UTC for AS_C case. The black contour represents the isotherm of -6 °C at 700 hPa. The AS_C flight track is overlaid as a thick black line. 112
Figure 6.21. West-east cross sections at 1114 0330 UTC and 1114 0530 UTC for the AS_C case. The left panels show the simulated AgI number concentration in logarithmic scale (color shaded), the cloud water mixing ratio in black starting at 0.01 g $kg^{-1}$ with an interval of 0.2 g $kg^{-1}$, the ice saturation ratio of 1.04 in purple, isotherm in every 10 °C and wind vectors. The right panels show the cloud water mixing ratio difference in black (g $kg^{-1}$) and ice-phase mixing ratio difference in color (g $kg^{-1}$). 113
Figure 6.22. The simulated seeding effect (mm) at the end of the simulation, average LWP difference (mm), and the relative LWP difference (%) for ASH_C case. The straight black horizontal line is the Wyoming-Montana state border. The thin black curves are the underlying terrain contours. The thick black curves in the left panel are the basin divides. The AS_C flight track is overlaid as a thick black line (left and center). 113

Figure 6.23. The average simulated AgI number concentration between 1 and 3 km MSL at 1113 2300 UTC and 1114 0100 UTC for ASH_C case. The red dashed lines indicate the cross section location. 114
Figure 6.24. Same as Figure 6.16, but for ASH_C case. 114
Figure 6.25. West-east cross sections at 1114 0230 UTC and 1114 0430 UTC for the ASH_C case. The left panels show the simulated AgI number concentration in logarithmic scale (color shaded), the cloud water mixing ratio in black starting at 0.01 g $kg^{-1}$ with an interval of 0.2 g $kg^{-1}$, the ice saturation ratio of 1.04 in purple, isotherm in every 10 °C and wind vectors. The right panels show the cloud water mixing ratio difference in black (g $kg^{-1}$) and ice-phase mixing ratio difference in color (g $kg^{-1}$). 115
Figure 6.26. The simulated seeding effect of ASH_CS (left) and ASH_CSQ (right) cases (mm). The location of the cross section shown in Figure 6.28 is indicated by the red dashed lines. 116
Figure 6.27. The average simulated AgI number concentration between 1 and 3 km MSL at 1113 2300 UTC and 1114 0100 UTC for ASH_CS (top) and ASH_CSQ (bottom) cases. The red dashed lines indicate the cross section. 117
Figure 6.28. West-east cross section at 0230 and 0430 UTC for ASH_CS (left) and ASH_CSQ (right). 118
Figure 6.29. Watersheds in the simulation domain (Bighorn =BH, Powder/Tongue =PT). The orange area is the Bighorn basin above 8000 ft (BH mtns) and the red area is the Powder/Tongue basin above 8000 ft (PT mtns). 119
Figure 6.30. Microphysical seeding criteria plots for ground seeding, airborne seeding (3750 m MSL) and higher level airborne seeding (4250 m MSL) for the BHN, BHC and BHS regions for the 20 November 2007 case. Each horizontal panel (and color) represents a different criterion assessed and the horizontal dashed line indicates the threshold that must be reached for the algorithm to consider that criterion met. Not all microphysical criteria assessed are required to be met for a case to be called, and even if all microphysical criteria are met there are additional criteria (especially for ground seeding, such as atmospheric stability and wind direction) that need to be met as well (not shown). Gray shading indicates time periods when seeding cases were identified. For airborne seeding, a 2-hr window is shaded in dark gray, representing the "best" period for seeding (given shorter time on station using a single aircraft). 124
Figure 6.31. Model simulation accumulated precipitation (mm), as Figure 6.8, but for the 20 November 2007 case. 126
Figure 6.32. Plan views of LWP below 1 km AGL (mm) from 1300 UTC 20 November to 0400 UTC 21 November every 3 hours. Black contour indicates the -6 °C isotherm at 700 hPa. 127
Figure 6.33. Maps of observed precipitation accumulation (mm) over the simulation period for the 20 November 2007 case from SNOTEL sites, with minimum accumulation in (a) and maximum accumulation in (b), compared to model-simulated precipitation accumulation at the SNOTEL sites (c) and the complete simulation of precipitation across the domain (d). 128
Figure 6.34. Scatterplot comparing observed precipitation accumulation at SNOTEL sites versus the modeled precipitation accumulation at the same sites for 20 November 2007. Dots represent the average of the maximum and minimum possible precipitation accumulation at each SNOTEL site during the simulation period. Vertical

bars represent the range of possible observation (i.e., minimum to maximum observation amount). Each point (color coded) represents single SNOTEL site..... 128
Figure 6.35. 700-hPa temperature (color shaded) and wind barbs at the same times as Figure 6.32. Red line indicates the -6 °C isotherm. ..... 129
Figure 6.36. Average simulated AgI concentration below 1 km AGL at the end of the seeding period of each ground seeding case. Red dashed lines indicate the cross section locations. ..... 130
Figure 6.37. West-east (top) and south-north (bottom) cross sections at 0300 UTC for the GS_D (left) and GS_D+F (right) experiments. ..... 131
Figure 6.38. The simulated seeding effect (mm) for all ground seeding experiments on 20 November 2007. ..... 132
Figure 6.39. The aircraft track location for the AS_UC (left) and AS4km_S (right) experiments. ..... 133
Figure 6.40. The simulated seeding effect (mm) at the end of the simulation, average LWP difference (mm), and the relative LWP difference (%) for the AS_UC experiment in the 20 November 2007 case. The straight black horizontal line is the Wyoming-Montana state border. The thin black curves are the underlying terrain contours. The thick black curves in the left panel are the basin divides. The AS_C flight track is overlaid in the left and center panels. ..... 134
Figure 6.41. Average simulated AgI concentration between 1 and 3 km MSL at 1121 00 and 02 UTC for the AS_UC experiment. The AS_C flight track is overlaid as thick black line. ..... 135
Figure 6.42. The LWP between 1 and 3 km MSL at1121 00 and 02 UTC for the AS_UC experiment. ..... 136
Figure 6.43. West-east cross sections at 1121 0000 UTC and 1121 0200 UTC for the AS_UC case. The left panels show the simulated AgI number concentration in logarithmic scale (color shaded), the cloud water mixing ratio in black starting at 0.01 g $kg^{-1}$ with an interval of 0.2 g $kg^{-1}$, the ice saturation ratio of 1.04 in purple, isotherm in every 10 °C and wind vectors. The right panels show the cloud water mixing ratio difference in black (g $kg^{-1}$) and ice-phase mixing ratio difference in color (g $kg^{-1}$). ..... 137
Figure 6.44. The simulated seeding effect (mm) at the end of the simulation, average LWP difference (mm), and the relative LWP difference (%) for the AS4km_S experiment. The straight black horizontal line is the Wyoming-Montana state border. The thin black curves are the underlying terrain contours. The thick black curves in the left panel are the basin divides. The AS_S flight track is overlaid in the left and center panels. ..... 138
Figure 6.45. Average simulated AgI concentration between 1 and 3 km MSL at 1121 00 and 02 UTC for the AS4km_S experiment. ..... 139
Figure 6.46. The LWP between 1 and 3 km MSL at1121 00 and 02 UTC for the AS4km_S experiment. ..... 140
Figure 6.47. West-east cross sections at 1121 0430 UTC and 1121 0630 UTC for the AS4km_S case. The left panels show the simulated AgI number concentration in logarithmic scale (color shaded), the cloud water mixing ratio in black starting at 0.01 g $kg^{-1}$ with an interval of 0.2 g $kg^{-1}$, the ice saturation ratio of 1.04 in purple, isotherm in every 10 °C and wind vectors. The right panels show the cloud water mixing ratio difference in black (g $kg^{-1}$) and ice-phase mixing ratio difference in color (g $kg^{-1}$). .. 141

Figure 6.48. Microphysical seeding criteria plots for ground seeding, airborne seeding (3750 m MSL) and higher level airborne seeding (4250 m MSL) for the BHN, BHC and BHS regions for the 17 January 2016 case. Each horizontal panel (and color) represents a different criterion assessed and the horizontal dashed line indicates the threshold that must be reached for the algorithm to consider that criterion met. Not all microphysical criteria assessed are required to be met for a case to be called, and even if all microphysical criteria are met there are additional criteria (especially for ground seeding, such as atmospheric stability and wind direction) that need to be met as well (not shown). Gray shading indicates time periods when seeding cases were identified. For airborne seeding, a 2-hr window is shaded in dark gray, representing the "best" period for seeding (given shorter time on station using a single aircraft). ..... 146
Figure 6.49. Time series plot comparing the observed LWP from the Lovell radiometer (blue) against the modeled LWP at the same site (red). ..... 147
Figure 6.50. Accumulated precipitation (mm) of the 17 January 2016 control simulation. ..... 149
Figure 6.51. Maps of observed precipitation accumulation (mm) over the simulation period for the 17 January 2016 case from SNOTEL sites, with minimum accumulation in (a) and maximum accumulation in (b), compared to model-simulated precipitation accumulation at the SNOTEL sites (c) and the complete simulation of precipitation across the domain (d). ..... 150
Figure 6.52. Scatterplot comparing observed precipitation accumulation at SNOTEL sites versus the modeled precipitation accumulation at the same sites for 17 January 2016. Dots represent the average of the maximum and minimum possible precipitation accumulation at each SNOTEL site during the simulation period. Vertical bars represent the range of possible observation (i.e., minimum to maximum observation amount). Each point (color coded) represents single SNOTEL site. ..... 150
Figure 6.53. Plan views of LWP below 1 km AGL (mm) from 2000 UTC 17 January 2016 to 0600 UTC 18 January 2016 every 2 hours. Black contour indicates the -6 °C isotherm at 700 hPa. ..... 151
Figure 6.54. 700-hPa temperature (color shaded) and wind barbs at the same times as Figure 6.53 for the 17 January 2016 case. Red line indicates the -6 °C isotherm. ..... 152
Figure 6.55. Average simulated AgI concentration below 1 km AGL at the end of the seeding period of each ground seeding case on 17 January 2016. Red dashed lines indicate the cross section locations. ..... 153
Figure 6.56. West-east (top) and south-north (bottom) cross sections at 0600 UTC for the GS_D (left) and GS_F (right) experiments.for the 17 January 2016 case. ..... 154
Figure 6.57. The simulated seeding effect (mm) for all ground seeding experiments for the 17 January 2016 case. ..... 155
Figure 6.58. The simulated seeding effect (mm) at the end of the simulation, average LWP difference (mm), and the relative LWP difference (%) for the AS experiment in the 17 January 2016 case. The straight black horizontal line is the Wyoming-Montana state border. The thin black curves are the underlying terrain contours. The thick black curves in the left panel are the basin divides. The AS_C and AS_S flight tracks are overlaid in the center panel. ..... 156
Figure 6.59. Average AgI concentration between 1 and 3 km MSL at 17 January 1130 and 0118 0030 UTC for the AS experiment. ..... 157

Figure 6.60. The LWP between 1 and 3 km MSL at 17 January 1130 and 18 January 0030 UTC for the AS experiment. ..... 158
Figure 6.61. West-east cross sections at 0117 1130 UTC and 0118 0030 UTC for the AS case. The left panels show the simulated AgI number concentration in logarithmic scale (color shaded), the cloud water mixing ratio in black starting at 0.01 g $kg^{-1}$ with an interval of 0.2 g $kg^{-1}$, the ice saturation ratio of 1.04 in purple, isotherm in every 10 °C and wind vectors. The right panels show the cloud water mixing ratio difference in black (g $kg^{-1}$) and ice-phase mixing ratio difference in color (g $kg^{-1}$). ..... 159
Figure 7.1. Satellite-generated image of the project area with potential generator locations. These locations were selected prior to the field surveys. ..... 163
Figure 7.2. Satellite-generated image of the project area with potential generator locations and alternate sites based on field surveys. ..... 169
Figure 7.3. Land ownership map indicating proposed generator sites. ..... 170
Figure 9.1. Yield as a function of supercooling for a condensation-freezing nucleus produced by the seeding solution used in the WWMPP (blues), and another condensation-freezing nucleus produced by pyrotechnics manufactured by Ice Crystal Engineering (red, yellow). (Data from DeMott 1997, 1999.) ..... 176
Figure 12.1. WRF simulation of (a) precipitation, (b) total runoff (surface and sub-surface runoff), and (c) evapotranspiration averaged over 2000–2008. Top panels show annual precipitation, runoff, and evapotranspiration. Middle and bottom panels are for November – April, and May – October, respectively. Black solid lines indicate hydrological basins. West of the divide is the Bighorn basin and east of the divide is the Powder/Tongue River basin. ..... 196
Figure 12.2. Ratio of annual total runoff to annual precipitation from the 8-year averaged model data. ..... 197
Figure 12.3. 2000–2008 average snowfall in (a) November – April and (b) May – October. ..... 198
Figure 12.4. Monthly precipitation, snow, SWE, and runoff (total, surface, and sub-surface) averaged over the (a) Bighorn and Powder/Tongue River basins, (b) Bighorn basin, and (c) Powder/Tongue River basin. The annual cycle is based on the 2000 – 2008 WRF simulation. ..... 199
Figure 12.5. USGS streamflow gauge sites. For this study, streamflow measurements from Tongue River gauge near Dayton and Shell Creek gauge above Shell Creek Reservoir were used. Correspondence of streamflow to snowpack were examined with SWE data from near-by SNOTEL sites (stars). ..... 201
Figure 12.6. (a) Annual cycle of daily mean discharge ($ft^3$ $s^{-1}$) measured at the Shell Creek gauge above Shell Creek Reservoir over three different climatological periods: 1971–2015, 1980–2015, and 1995–2015. Lines are the median values of the data. Shaded region indicate $25^{th}$ to $75^{th}$ percentile of the data for each climatological period. (b) Annual cycle of SWE at Shell Creek SNOTEL site for the 1980–2015 period. Median (line) and the 25–$75^{th}$ percentile range (shaded) of the data are shown. ..... 202
Figure 12.7. Scatter plot of total streamflow (AF) from April through July compared to SWE (mm) on 1 May for Shell at Shell Creek SNOTEL site. Red line shows the least-squared fit. $r^2$ is the coefficient of determination and r is the linear correlation coefficient..... 203

Figure 12.8. Same as Figure 12.6 but for (a) the streamflow measurements at Tongue River near Dayton and SNOTEL SWE measurements at (b) Tie Creek and (c) Burgess Junction. ..... 205
Figure 12.9. Same as Figure 12.7 but for the (a) Tongue River streamflow gauge and Burgess Junction SNOTEL SWE, and (b) Tongue River streamflow gauge and Tie Creek SNOTEL SWE..... 205
Figure 12.10. Estimates of streamflow increases in acre-feet (left ordinate) and percent increase relative to annual streamflow (right ordinate) into the (a) Bighorn River Basin and (b) Powder/Tongue River Basin using the levels of seasonal seeding effects for seedable storms from the draft WWMPP report. The streamflow calculations include adjustments to relate the seeding effects to total target area precipitation, which requires an estimate of target area seeding coverage. The streamflow estimates for the various levels of area coverage (30–80%) are denoted by the different linestyles. Different line colors represent the estimates based on a ground-based (green) or airborne-based (blue) seeding program. The 50% area coverage (solid lines) are used for streamflow estimates assumed in the benefit/cost calculations.. 209
Figure 13.1. Map of the river basins, and their respective sub-basins, surrounding the Bighorn Mountains. The Powder/Tongue Basin is in shades of pink, while the Wind/Bighorn Basin is in shades of blue. The darker blue shaded sub-basin is the Bighorn Lake drainage (that includes Shell Creek), while the darker pink shaded sub-basin is the Tongue River drainage. Streamflow gauges in each of these sub-basins were utilized in the hydrological assessment. ..... 219
Figure 14.1. Cost of water for usage categories and for two estimates of annual seeding program costs (using 50% impact area) for the three levels of estimated streamflow increases resulting from WWMPP annual seeding effects for seedable storms (5, 10. 15%; Section 12). Gray shading indicates estimated water costs ($30–$50/AF). The solid green and red lines indicate the cost for the 15 remote generator ground-seeding option versus the single aircraft airborne seeding option, respectively, expressed as program costs per acre-feet of streamflow increase (essentially a 1:1 ratio). The dashed green and red lines show the corresponding 5:1 ratios of water costs to program costs..... 224
Figure 17.1. Google Earth map of the Lovell radiometer. ..... 232
Figure 17.2. Google Earth map of the pointing angle from the Lovell radiometer over Sheep Mountain..... 233
Figure 17.3. Photos of the radiometer installation. ..... 234
Figure 17.4. Histogram of LW period duration (hours)..... 236
Figure 17.5. Liquid water path (blue) and identified LW periods (gray) from the Lovell radiometer for the month of November, 2015. ..... 236
Figure 17.6. As in Figure 17.5, but for December 2015. ..... 237
Figure 17.7. As in Figure 17.5, but for January 2016. ..... 237
Figure 17.8. As in Figure 17.5, but for February 2016. ..... 237
Figure 17.9. As in Figure 17.5, but for March 2016. ..... 238
Figure 17.10. As in Figure 17.5, but for April 2016. ..... 238
Figure 17.11. Photo of the Bald Mountain SNOTEL gauge. ..... 239
Figure 17.12. Southern permitted potential site locations..... 240
Figure 17.13. Northern potential site locations. ..... 241

Figure 17.14. North-facing view (left) and South-facing view (right) of the Rd 14 gauge installation. 242
Figure 17.15. East-facing view of the Rd 14 gauge installation. 243
Figure 17.16. West-facing view of the Rd 14 gauge installation. 243
Figure 17.17. Time series plot of accumulated precipitation (mm) measured by the Rd 14 Geonor (three wires each labeled VM1, VM2, VM3) and ETI gauge compared to the Bald Mountain SNOTEL for the period 1 January–1 May 2016. 244
Figure 17.18. Same as Figure 17.17, except this figure starts on 16 January 2016 in order to show that after the 15 January event, the Bald Mountain SNOTEL site compares fairly well with the Rd 14 gauges. 245

## LIST OF TABLES

Table 1.1. List of key personnel from each institution that was involved in conducting this study. 3
Table 2.1. List of attendees (other than presenters) at the scoping meeting in Sheridan. 4
Table 2.2. List of attendees (other than presenters) at the scoping meeting in Worland. 4
Table 2.3. List of attendees at the January 2016 TAT meeting in Cheyenne. 5
Table 3.1. Advantages and disadvantages of various seeding types and modes. 9
Table 4.1. WRF model physics options 22
Table 4.2. Average annual precipitation from SNOTEL sites and the fraction of the annual precipitation that fell between 1 November and 30 April in each water year 27
Table 4.3. Seasonal (November–April) model precipitation totals from Shell Creek and the amount of precipitation that fell when the western area average 700-hPa temperature was < −6°C 55
Table 4.4. As in Table 4.3, but precipitation totals from Sucker Creek and 700-hPa temperatures averaged over the eastern area. 55
Table 4.5. As in Table 4.3, but precipitation totals from Grave Springs and 700-hPa temperatures averaged over the southern area 55
Table 4.6. Seasonal (November–April) 8-year average simulated total precipitation (mm) compared to the seasonal precipitation that fell during ground-seedable ("GS", 0–1 km AGL) time periods versus lower airborne-seedable ("AS", 3.5–4.5 km MSL) and upper airborne seedable ("ASH", 4.5–5.5 km MSL) times. The percent of the total seasonal precipitation that was seedable is provided in parentheses next to the absolute seedable precipitation. For the ground-seeding layer, the criteria builds starting with the basic temperature criteria, the the primary criteria (temperature and LWC), then the wind direction (WDIR) is included (T+LWC+WDIR) and finally the scenario with all additional criteria is included (T+LWC+ WDIR+Fr, "GS_all"). 78
Table 4.7. Extended-seasonal (October–June) 8-year average simulated total precipitation (mm) compared to the extended-seasonal precipitation that fell during ground-seedable ("GS", 0–1 km AGL) time periods versus lower airborne-seedable ("AS", 3.5–4.5 km MSL) and upper airborne seedable ("ASH", 4.5–5.5 km MSL) times. The percent of the total precipitation that was seedable is provided in parentheses next to the absolute seedable precipitation. For the ground-seeding layer, the criteria builds starting with the basic temperature criteria, the the primary criteria (temperature and LWC), then the wind direction (WDIR) is included (T+LWC+WDIR) and finally the scenario with all additional criteria is included (T+LWC+ WDIR+Fr, "GS_all"). 78
Table 6.1. Model configuration for cloud seeding project design evaluation simulations. 91
Table 6.2. Summary of wind regime and precipitation for the selected cases. 95
Table 6.3. WASCA output for the 13 November 2007 experiment. 97
Table 6.4. Seeding times of the ground seeding simulations for the 13 November 2007 case. 103
Table 6.5. Seeding times for the airborne seeding simulations of the 13 November 2007 case 106
Table 6.6. Control precipitation and simulated seeding effects for each seeding simulation (acre-feet on top and % effect on bottom for each experiment row) over the full model

domain and in the two primary watersheds (entirely, BH and PT, and just above 8,000 ft in those watersheds, BH mtns and PT mtns) for each of the seeding experiments. The experiment with the best simulated seeding effects is shaded. Relative simulated seeding effects within the target regions (BH mtns and PT mtns) > 1% are listed in bold. Results shown for the 13 November 2007 case. ..... 120
Table 6.7. Simulated seeding areas of impact for the 13 November 2007 case. The simulated positive seeding areal impacts are listed as area in km$^2$ (rows labeled A_SE) and the portion of the seeding impacted area relative to the total area in percentage (rows labeled P_SE). The CTRL precipitation impacted area is calculated based on grid points with accumulated precipitation greater than 0.01 mm (in km$^2$, "A", and in percent of total area, "P"). The total area (A_total) within each domain is listed in the first row (km$^2$). For experiments and target areas (either BH mtns or PT mtns) with simulated seeding impacts > 1% (shown in Table 6.6), the P_SE values have been listed in bold. ..... 121
Table 6.8. WASCA output for the 20 November 2007 case. ..... 122
Table 6.9. Seeding times of the ground seeding simulations for the 20 November 2007 case. ..... 125
Table 6.10. Seeding times of the airborne seeding simulations.for the 20 November 2007 case. ..... 132
Table 6.11. Control precipitation and simulated seeding effects for each seeding simulation (acre-feet on top and % effect on bottom for each experiment row) over the full model domain and in the two primary watersheds (entirely, BH and PT, and just above 8,000 ft in those watersheds, BH mtns and PT mtns) for each of the seeding experiments. The experiment with the best simulated seeding effects is shaded. Relative simulated seeding effects within the target regions (BH mtns and PT mtns) > 1% are listed in bold. Results shown for the 20 November 2007 case. ..... 142
Table 6.12. Simulated seeding areas of impact for the 20 November 2007 case. The simulated positive seeding areal impacts are listed as area in km$^2$ (rows labeled A_SE) and the portion of the seeding impacted area relative to the total area in percentage (rows labeled P_SE). The CTRL precipitation impacted area is calculated based on grid points with accumulated precipitation greater than 0.01 mm (in km$^2$, "A", and in percent of total area, "P"). The total area (A_total) within each domain is listed in the first row (km$^2$). For experiments and target areas (either BH mtns or PT mtns) with simulated seeding impacts > 1% (shown in Table 6.11), the P_SE values have been listed in bold. ..... 143
Table 6.13. WASCA output for the 17 January 2016 case. ..... 144
Table 6.14. Seeding times of the ground and airborne seeding simulations.for the 17 January 2016 case. ..... 147
Table 6.15. Control precipitation and simulated seeding effects for each seeding simulation (acre-feet on top and % effect on bottom for each experiment row) over the full model domain and in the two primary watersheds (entirely, BH and PT, and just above 8,000 ft in those watersheds, BH mtns and PT mtns) for each of the seeding experiments. The experiment with the best simulated seeding effects is shaded. Relative simulated seeding effects within the target regions (BH mtns and PT mtns) > 1% are listed in bold. Results shown for the 17 January 2016 case. ..... 159

Table 6.16. Simulated seeding areas of impact for the 17 January 2016 case. The simulated positive seeding areal impacts are listed as area in km$^2$ (rows labeled A_SE) and the portion of the seeding impacted area relative to the total area in percentage (rows labeled P_SE). The CTRL precipitation impacted area is calculated based on grid points with accumulated precipitation greater than 0.01 mm (in km$^2$, "A", and in percent of total area, "P"). The total area (A_total) within each domain is listed in the first row (km$^2$). For experiments and target areas (either BH mtns or PT mtns) with simulated seeding impacts > 1% (shown in Table 6.15), the P_SE values have been listed in bold. ..... 160
Table 7.1. Proposed Generator Locations Post-Field Survey ..... 166
Table 12.1: 8-year average annual precipitation, runoff, runoff ratio, snowfall and rainfall averaged over the study area (Figure 12.1), Bighorn basin, and Powder/Tongue River basin. Values in parentheses for the snowfall and rainfall indicate the ratio of snowfall and rainfall to total precipitation. Note that the basin-averaged values are only for the area that appears in Figure 12.1, not including the entire basin. ..... 199
Table 12.2. 8-yr (2000–2008) average annual and April–July total runoff per river basin in acre feet for areas > 8000 ft in elevation calculated from the WRF-CONUS model simulations. ..... 199
Table 12.3. List of site name, measurements, and site elevation used. ..... 201
Table 12.4. Summary of relation between the April – July streamflow and the 1 May Snowpack from each pairs of streamflow gauge and SNOTEL site. Total annual runoff, average seasonal runoff and mean 1 May Snowpack are data values averaged over the regression period. Dry and wet season streamflow are determined from the best-fit equation shown in Figure 12.9. Ratio of % change in streamflow to % change in snowpack (in bold) are based on the "Dry" and "Wet" season streamflow estimates. ..... 206
Table 12.5. Streamflow increase estimates using various seeding impact parameters for a ground-based seeding program (5, 10, 15% seeding effect and 30–80% seeding impact area). *Estimated April–July streamflow increase per basin is provided for the 50% impact area scenario. ..... 210
Table 12.6. Same as Table 12.5, except for an airborne seeding program. ..... 210
Table 12.7. Same as Table 12.5, except for a combined ground and airborne seeding program. ..... 210
Table 13.1. Estimated Operational Costs of Possible Five-Month Programs for the Bighorn Mountains. ..... 213
Table 13.2. Contracted vs. Self-Run Projects, or Project Components. ..... 215
Table 13.3. Summary of Current (2010) Water Use by Category[4] ..... 217
Table 13.4. Summary of Natural Annual Streamflows by Sub-basin, Wind/Bighorn. ..... 218
Table 13.5. Summary of Current (2002) Water Use By Category[1] ..... 220
Table 13.6. Summary of Natural Annual Streamflows by Sub-basin, Powder/Tongue. ..... 220
Table 14.1. Cost of a Ground-based Program to Generate Different Benefit/Cost Ratios, assuming a water cost of $50 and impact area of 50%. ..... 223
Table 14.2. Cost of an Airborne Program to Generate Different Benefit/Cost Ratios (assuming $50 water cost and 50% impact area). ..... 223

Table 14.3. Cost of an Airborne Program to Generate Different Benefit/Cost Ratios (assuming $50 water cost and 80% impact area). ..... 223
Table 14.4. Annual Costs Breakdown of Seeding Options for the Proposed Bighorn Mountains Winter Cloud-Seeding Program and Estimated Cost/AF of augmented streamflow (using 50% impact area assumption for ground, and both the 50 and 80% assumption for airborne). ..... 224
Table 16.1. List of attendees (other than presenters) at the results meeting in Sheridan. 229
Table 16.2. List of attendees (other than presenters) at the results meeting in Worland. 230
Table 17.1. Location information about the radiometer site. ..... 232
Table 17.2. Monthly break down of number and duration of LW periods. ..... 235
Table 17.3. Loaction information for the deployed snow gauge sites. ..... 239

## Executive Summary

A conceptual siting and design study was completed to assess the feasibility of conducting an operational weather modification program targeting the Bighorn Mountains in north central Wyoming.

A review of previous reports indicated that there were previous cloud-seeding activities in the Bighorn Mountains, spanning the period of 1951–1954. Since that time, no additional permits for cloud-seeding operations in the Bighorns were issued. These previous programs utilized ground-based silver iodide (AgI) generators, and most operations targeted clouds in the summer months.

In more recent years, numerous research investigations have improved the understanding of how to use AgI seeding to enhance snowfall in winter orographic clouds. These include the Wyoming Range Phase I and Phase II Feasibility Studies and the Wyoming Weather Modification Pilot Program (WWMPP). These results were reviewed prior to preparation of this report to ensure it remains consistent with the most recent recommendations for cloud-seeding program design. Noteworthy results from the draft WWMPP report are that while the randomized seeding experiment was statistically inconclusive, an accumulation of evidence analysis approach suggested seasonal precipitation increases of 5–15% in seedable storms. It also demonstrated the capability of numerical models to realistically simulate snowfall distributions. Furthermore, a new modeling capability that simulates seeding effects via a cloud-seeding parameterization was developed and applied to estimate seeding effects, but complete evaluation of this new tool has so far been limited by a lack of necessary observations. The results from this program were utilized by the present study.

In the review of previous reports, the various options for cloud seeding were summarized. It was determined that liquid propane seeding would likely not be an efficient option, given it has very spatially-limited impacts due to the need to release it directly in the presence of supercooled liquid water (SLW). In addition, manual AgI generators were determined to be challenging to implement in the region given the limited number of sites where on-site operators reside. For manual generators to be activated and deactivated during the winter months, siting would need to be at lower elevations in the Bighorn River Basin, and the AgI plume would frequently be trapped and unable to disperse over the mountains at these lower elevations.

### Climatology of the Project Area

A climatological study of the project area was conducted to determine the characteristics of wintertime precipitation in the Bighorn Mountains and to estimate how frequently meteorological conditions are appropriate for AgI seeding. The climatology analysis

indicated that the typical wind regimes in the Bighorn Mountains are westerly to northwesterly, with few easterly (upslope) events on the eastern slopes. The spatial mapping analysis revealed that liquid water content (LWC) most frequently develops on the western and northeastern slopes of the Bighorn Mountains, while the most frequent seeding opportunities occur on the western slopes.

Based on 0–1 km above ground level (AGL) average temperature and LWC criteria, ground seeding had equal or more frequent opportunities than airborne seeding during the November–April wintertime period. When considering additional criteria for ground-based seeding to be able to reach the clouds, ground-seeding opportunities dropped to nearly zero in the eastern and southern regions, and were substantially reduced in the western region. This was due to the frequent occurrence of stable conditions causing the flow of AgI to pass around the Bighorn Mountains rather than go over. The stability limitation issue for ground-based seeding results in airborne seeding potential in the western region to be greater than ground seeding potential (Figure 1).

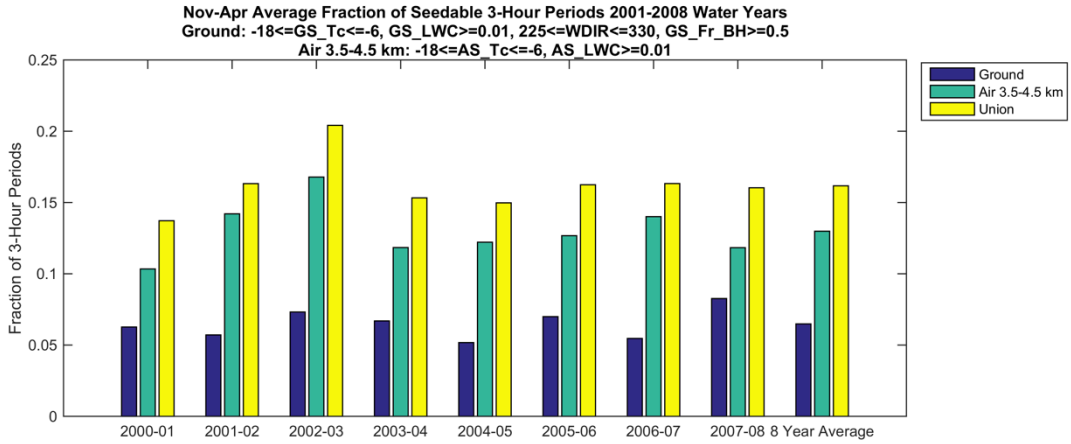


**Figure 1. Ground (0–1 km AGL; blue) versus airborne (3.5–4.5 km MSL; cyan) seeding opportunities by November–April season in the western region (fraction of hours in the season that meet the designated criteria, listed atop the figure), and the 8-year average. The frequency of occurrence of cases from the union of both ground and airborne seeding potential is shown in the yellow bar for each time period.**

Note that airborne seeding has the additional advantage of allowing seeding in October, May, and June, potentially doubling the amount of seedable precipitation with an aircraft program. However, from a logistical perspective, it is less likely that all airborne "seedable" hours can be seeded, especially with a single aircraft operation, given limited flight and on-station times. Even if the program is restricted to the November–April period, airborne seeding at the 3.5–4.5 km MSL level is likely to yield more seeding opportunities than ground-based operations, considering the stability factors that limit effective AgI transport.

Most of the time when cloud seeding conditions were present, precipitation occurred naturally over the Bighorn Mountains. Study results show that only 19% of the precipitation that fell in a given season was seedable based on the full ground-seeding criteria being met, while 39% of the precipitation that fell in a given November–April winter season was seedable by aircraft.

## Preliminary Project Design and Model Evaluation

In order to test a wide variety of program design options, and based upon results of the climatological analysis, several groups of ground-based generator sites were developed. Initially, just five groups of generators were tested, but based on an iterative process with the model evaluation of these design options, a sixth group was also created and tested with the model. The design focused on ground-based seeding and/or airborne seeding with an operational season of mid-November through mid-April (i.e., 15 November–15 April), utilizing AgI as the seeding agent.

Three test cases were simulated to evaluate the impact of the six groups of proposed ground generators and several potential aircraft tracks (Figure 2). The test cases were selected to represent various meteorological scenarios encountered in the Bighorn Mountains, but not every scenario may have been represented by this limited sample. If resources allow, more cases should be tested to obtain more robust results.

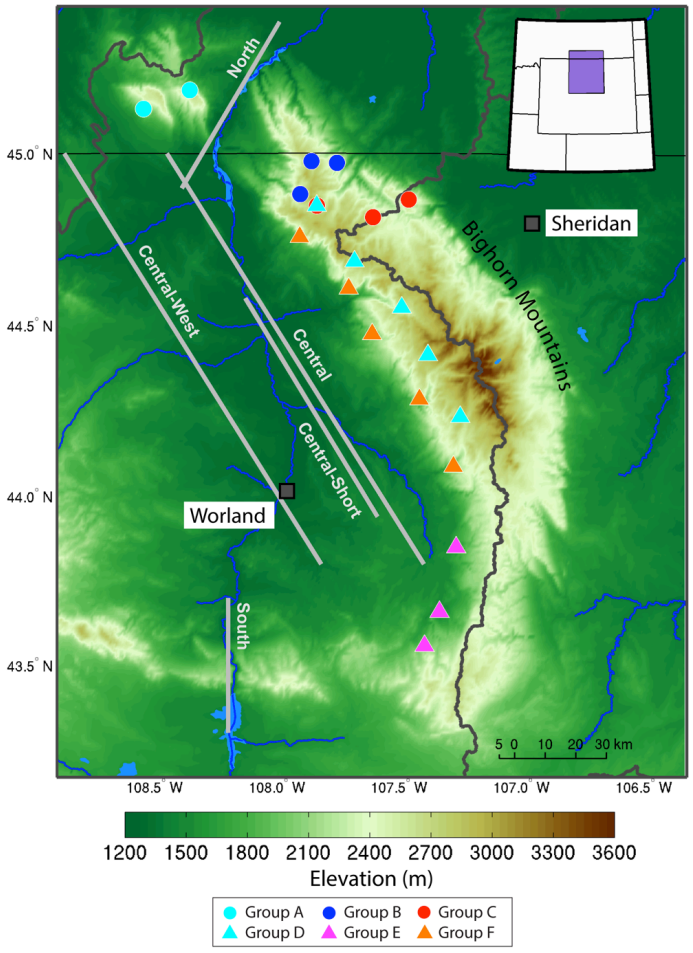


**Figure 2. Map of the proposed ground generator groups and potential airborne seeding flight tracks tested with the model.**

Based upon the model simulations of the three test cases, ground seeding had very limited spatial impact on the region with Groups A and B rarely impacting the target area.

Group C showed positive simulated seeding effects in some meteorological conditions, especially when the winds had a north-northeasterly component. Groups D and F yielded the best results for ground-based seeding, yet the impact area was rather small and confined to very narrow plumes (Figure 3). Group E ended up being a rather versatile group of generators, given they could impact the southern extent of the Bighorn Mountains under northwest to westerly winds, but could also impact the Cloud Peak area under southwesterly winds. Nonetheless, in the cases that were tested, Group E showed minimal overall simulated impacts (Figure 3).

Airborne seeding tended to yield the most widespread and greatest simulated seeding effects (Figure 3). However, shorter seeding flight tracks are recommended because the shorter central track experiment produced a greater simulated seeding effect more often than the longer track due to the simulated AgI plume being more concentrated using the shorter track length. The benefit of airborne seeding is that it can be performed wherever SLW is present. This can include situations where elevated SLW extends quite far upwind (to the west) of the mountains, as occurred in some of these cases. Airborne seeding is the only way to impact elevated SLW layers over the Bighorn River Basin because the air is often too stable in this valley to use ground generators to reach those higher altitudes. It should be noted that not all of the simulated seeding effects from seeding further upwind impact the higher elevations of the Bighorn Mountains; rather they often broadly impact the Bighorn Basin. Based on the modeled climatology, easterly upslope events include SLW, but occur infrequently. Therefore, due to the lower frequency of occurrence, siting ground generators on the eastern slope of the Bighorns is not advised, but it should be noted that airborne seeding is versatile enough that it can also be used to target easterly upslope events.

A field survey was conducted to assess the suitability of potential generator locations for seeding effectiveness, land access issues, and the impacts of land ownership. During the field survey, many of the originally proposed generator sites were moved short distances to more suitable locations. Six alternate sites were also added, because the original sites were not accessible, or the alternate sites were determined to be better suited for operational deployment. As a result of the field surveys and modeling analysis, a total of 21 generator sites—12 on United States Forest Services (USFS) lands, 5 on Bureau of Land Management (BLM) lands, 3 on private lands, and 1 on State lands—were considered to be viable options from a permitting and operational perspective.

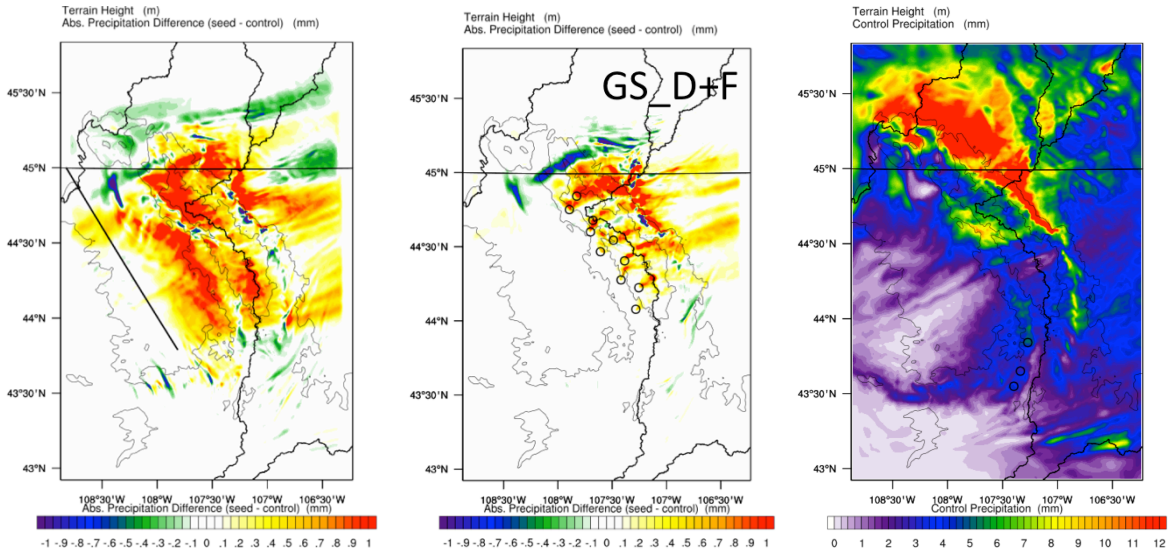


**Figure 3. Simulated seeding effects (changes in precipitation, mm) for the 20 November 2007 case from simulated airborne seeding along the Central-West track (left) and ground-based seeding with Groups D+F (middle). The total accumulated precipitation (mm) from the unseeded control simulation is shown on the right.**

## Operational Criteria and Other Considerations

Operational seeding criteria were developed for possible ground-based seeding operations as well as for potential seeding with an aircraft. Observations to determine when the operational criteria are met are available in real time via a variety of products available on the internet. However, given the dearth of observations in the region, deploying project-specific instrumentation (i.e., radiometer and soundings) or the use of numerical models can play vital roles in making seeding decisions. Other programs in the region, such as the operational cloud-seeding program in the Wind River Range, may provide leveraging opportunities to obtain data from such additional operational tools. Cloud-seeding suspension criteria were also developed based on the criteria developed for the Wind River Range operational program.

Common questions regarding the implementation of a cloud-seeding program are concerned with possible extra-area effects of cloud seeding on precipitation, and possible environmental impacts of the cloud-seeding agent (AgI). Recent studies on these topics were reviewed, including the most recent WWMPP study. These studies concluded that seeding effects outside of the intended target area would be negligible, and that no environmentally harmful effects would occur from the use of AgI as a cloud-seeding agent.

## Potential Benefits and Benefit/Cost Analysis

Estimates of streamflow changes due to seeding impacts were calculated using preliminary results from the WWMPP, which were based on three levels of estimated seasonal seeding effects of 5, 10, and 15% in seedable storms. The remaining parameters needed to calculate seeding impacts are the percentage of seasonal precipitation that occurs during seedable

conditions, the target area coverage of the seeding effects, and the ratio of increase in streamflow relative to an increase in snowpack. The seasonal seedable precipitation was determined from the climatological analysis for the Bighorn Mountains, while the target area coverage was assumed to vary between 30–80%, substantiated by the model simulations. Estimates of streamflow input into the Bighorn and Powder/Tongue River basins from the Bighorn Mountains were determined using the 8-year Weather Research and Forecasting (WRF) CONUS model simulations, since other estimates provided in local water plans were not specific to drainage solely from the Bighorn Mountains. These model estimates indicated average April–July streamflow from the Bighorn Mountains into the Bighorn Basin is approximately 515,000 AF and into the Powder/Tongue River Basin is roughly 465,000 AF. The streamflow estimates from the local water plans and the model simulation agreed relatively well. The ratio of increase in streamflow relative to an increase in snowpack was estimated to be 0.49 using the WRF CONUS model-simulated snowpack compared to simulated runoff. This ratio accounts for the evapotranspiration of some of the additional snowpack from cloud seeding.

Average estimates of streamflow increase (April–July runoff increase from seeding) based upon the parameters described above and combined across the two river basins produced estimates of streamflow increases ranging from ~1,400 AF to ~10,900 AF for ground-based seeding depending on the level of the estimated seeding effect and the assumed area of seeding coverage (Figure 4). Assuming a 50% area coverage of seeding effects, the range for ground-based seeding was between ~2,300 AF to ~6,800 AF (based upon the 5–15% assumption of seasonal seeding effect in seedable storms). These values were used in the benefit/cost analysis. For airborne seeding, which had a much higher fraction of seedable precipitation from the climatological analysis (i.e., 39% compared to only 19% for ground seeding), the estimates of streamflow increases ranged from ~2,800 AF to ~22,500 AF, depending on estimated seeding effect and area of coverage. However, limited aircraft on-station time was not accounted for in the fraction of seedable precipitation calculation, which for a single aircraft operation could conceivably limit the frequency of time that can be seeded in a given season. Nonetheless, assuming a 50% area coverage of seeding effects from airborne seeding, the range of estimated additional streamflow was between ~4,700 AF to ~14,000 AF. These values were used in the benefit/cost analysis.

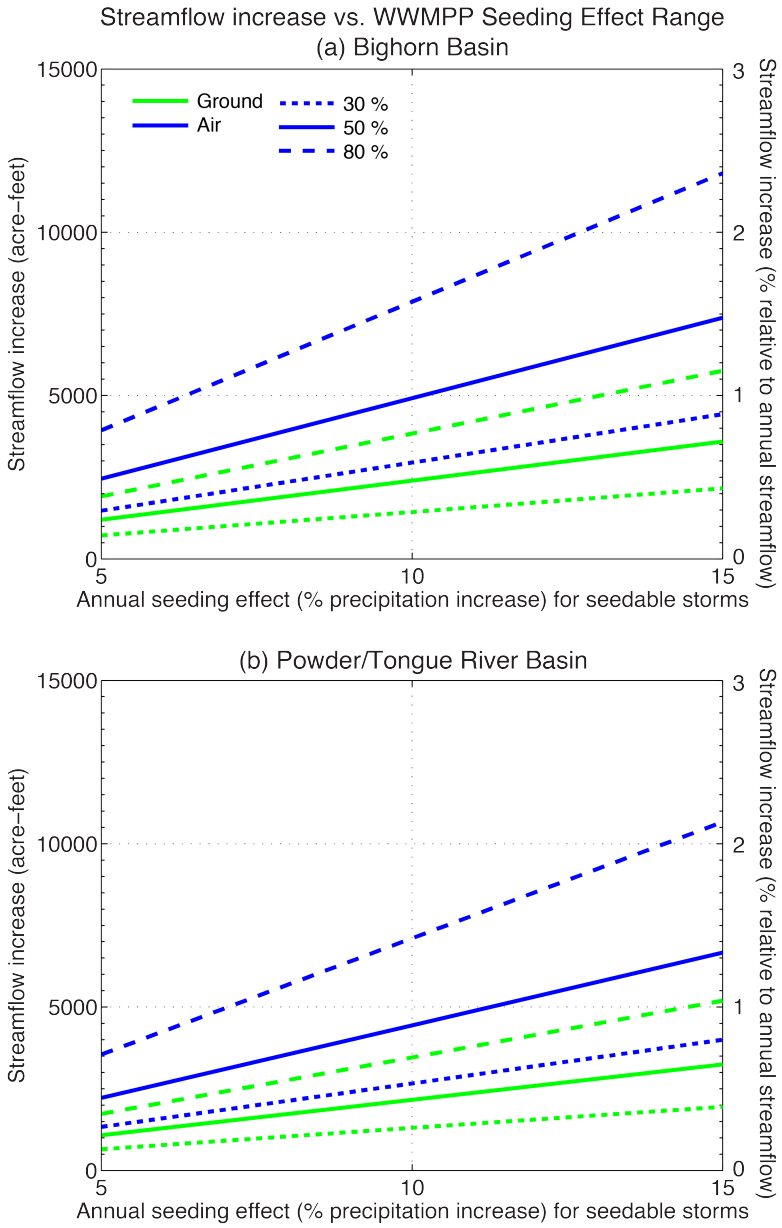


**Figure 4. Estimates of streamflow increases in acre-feet (left ordinate) and percent increase relative to annual streamflow (right ordinate) into (a) the Bighorn River Basin and (b) Powder/Tongue River Basin using the levels of seasonal seeding effects for seedable storms from the draft WWMPP report (5, 10 15%). The streamflow calculations include adjustments to relate the seeding effects to total target area precipitation, which requires an estimate of target area seeding coverage. The streamflow estimates for the various levels of area coverage (30-80%) are denoted by the different line styles. Different line colors represent the estimates based on a ground-based (green) or an airborne-based (blue) seeding program. The 50% area coverage (solid lines) is used for streamflow estimates assumed in the benefit/cost calculations.**

Cost estimates were prepared for two different cloud-seeding program options:

1) A program with 15 remote-controlled ground-based generators (estimated annual cost: $479,655), and
2) A single, stand-alone aircraft seeding program (estimated annual cost: $352,421).

A preliminary benefit/cost analysis was performed using the estimated range of enhanced average April–July runoff values. American Society of Civil Engineers (ASCE) Guidelines were considered to determine whether the program would be considered feasible. These Guidelines have two basic considerations: is the program technically feasible, and is the proposed program economically feasible? An affirmative answer to both questions is required in order for the program to be considered feasible. The evidence presented in this study is that the program is technically feasible.

For a proposed program to be economically feasible, the ASCE Guidelines recommend that a proposed program have an estimated benefit/cost ratio of 5/1. Several assumptions were made concerning the possible benefit/cost ratios for the proposed program (e.g., allocation of the water, value of the water, etc.). At the assumed costs of water ($30–$50 per AF), neither seeding program option yielded the 5/1 ratio with the assumed area impact of 50% (Figure 5), nor when assuming an 80% impact area. As a result, this proposed program would not be economically feasible based upon the ASCE Guidelines. Of the two seeding program options (ground or airborne), airborne resulted in a higher benefit/cost ratio than ground, given the lower cost of the airborne program and the higher amount of seedable precipitation for airborne seeding found in the climatology analysis. Sharing operational resources with another nearby cloud-seeding program might reduce costs and make a cloud-seeding program in this region more cost effective; however, it is beyond the scope of the present study to make this determination.

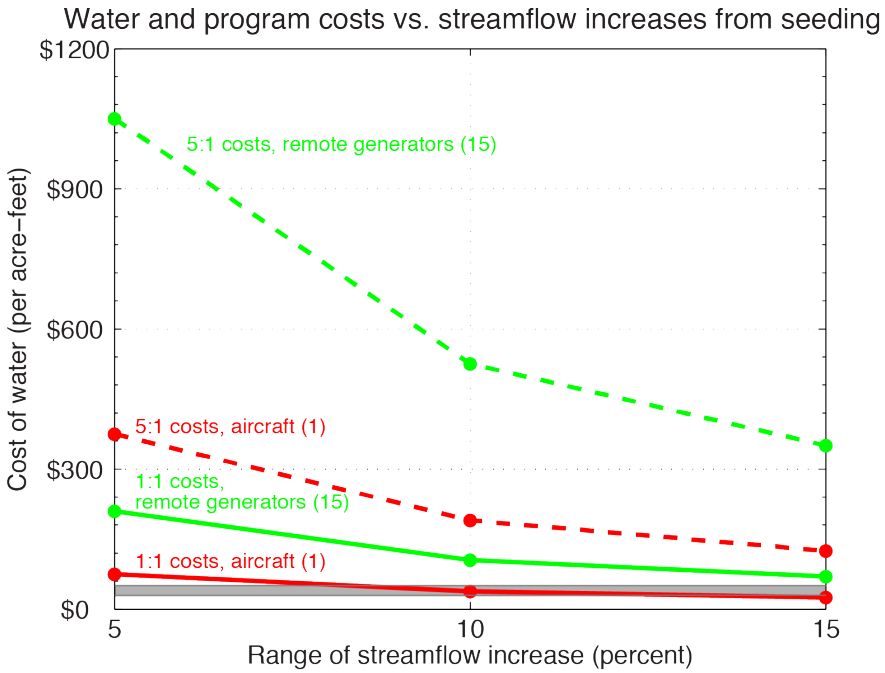


**Figure 5. Cost of water for usage categories and for two estimates of annual seeding program costs for the three levels of estimated streamflow increases resulting from WWMPP annual seeding effects for seedable storms. Gray shading indicates estimated water costs. The solid green and red lines indicate the cost for the 15 remote generator ground-seeding option versus the single aircraft airborne seeding option, respectively, expressed as program costs per acre-feet of streamflow increase (essentially a 1:1 ratio). The dashed green and red lines show the corresponding 5:1 ratios of water costs to program costs.**

## Conclusions and Recommendations

This study concludes that it is technically feasible to develop an AgI cloud-seeding program to target the Bighorn Mountains. This is supported by the climatological analysis and model evaluation, as well as radiometer measurements collected over the winter of 2015–2016. Ground-based cloud-seeding opportunities are less frequent due to the complex terrain that limits siting generators in locations that will effectively disperse the AgI plumes over the mountains. Opportunities for airborne seeding are more frequent and promising. Numerical simulations of airborne cloud seeding in the three tested cases indicated that airborne seeding is far more effective than ground-based seeding for enhancing precipitation both over the mountains and upwind of the mountains. However, it is important to note that three cases is not a large enough sample to draw robust conclusions, and therefore additional cases would be needed to thoroughly assess this recommendation.

The study also concludes that the program is not economically feasible based upon the ASCE guidelines. The cost effectiveness of a cloud-seeding program is dependent on several factors, including the benefit/cost ratio desired, actual water costs, and the level of seeding effect achieved. The benefit/cost analysis indicated that an airborne seeding program (~$25–75/AF) targeting the Bighorn Mountains was more cost effective than a ground-based program ($70–210/AF). The implementation of a collaborative weather modification program to share an aircraft, staff, and/or other operational resources (e.g., observations and forecast models) might yield the most cost-effective opportunity for a cloud-seeding program in this region; however, it is beyond the scope of the present study to make this determination.

The recommendations based on the results of this study are provided below. Given the complexity of the terrain and short duration of the study, only a few representative cases were evaluated in this study. To increase confidence in the results, it is recommended that additional studies be conducted with the atmospheric model coupled to a hydrological model. Specifically:

- Additional test cases (ideally an entire season of seeding cases) should be simulated to better represent the wide variety of storm types and/or the seasonal seeding impacts from seeding with a proposed operational design.
- A spatially-distributed hydrological model coupled to the WRF cloud-seeding simulation output should be run for multiple winters to better estimate hydrological benefits of cloud seeding. This modeling system would utilize the 3D spatial distribution and magnitude of the model-simulated seeding effects on snowpack to drive the hydrological model, which would calculate the water balance and routing of the streamflow driven by the snowmelt for every basin in the domain, obviating the need for fixed assumptions across the domain.

Recommendations specific to the design and implementation of an operational cloud-seeding program in the Bighorn Mountains include:

- Seeding should be conducted using AgI as the seeding agent.

- The seeding season should be November–April for ground-based seeding, but could be extended from October into May or June if airborne seeding is utilized.
- The climatology analysis and cost estimates indicate that airborne seeding has the potential to be more cost effective than ground-based seeding. Therefore, airborne seeding is recommended.
- If airborne seeding is implemented, shorter aircraft tracks should be used to achieve better coverage of AgI over the target area. In particular, the central track, using an altitude where the maximum LWC resides, was found to give the best result.
- Basic seeding criteria should be based on readily available (and quickly accessible) meteorological data. Given the lack of regular meteorological observations in the region, a program would benefit from deploying project-specific instrumentation (i.e, radiometer and soundings), but these would add additional costs to operate the program that have not been considered in the present benefit/cost analysis.
- In order to reduce costs, opportunities to share resources (especially an aircraft) with other nearby cloud-seeding programs should be explored. Specifically, a climatological analysis should be conducted to determine if the timing of seedable storm systems would allow for cost effective resource sharing (i.e., utilizing a single aircraft to target multiple mountain ranges).
- If the State of Wyoming were to operate multiple cloud-seeding programs across the State, it is recommended that a real-time forecast modeling system be implemented statewide to provide guidance on whether passing storm systems are suitable for seeding. A forecast modeling system would generate a cost savings by identifying when storms have high seeding potential, therefore maximizing cloud seeding impacts and avoiding seeding of cases with only limited potential. The model can also serve as a basis for seasonal program evaluation.

***Disclaimer***

*All rights to the underlying data collected and/or generated with funding from the Wyoming Water Development Office (WWDO) from which this report was created remain with the WWDO. This report does not constitute the opinions of the State of Wyoming, the Wyoming Water Development Commission, or the Wyoming Water Development Office.*

# 1. Introduction

A conceptual siting and design feasibility study was completed for the Wyoming Water Development Commission (WWDC) to assess the feasibility of conducting an operational weather modification program targeting the Bighorn Mountains in north central Wyoming. As part of the study, 16 tasks were identified and are briefly described below. The organization of this report follows this tasking, as requested by the WWDC.

## 1.1 Task Overview

### *Task 1: Scoping and Project Meetings*

In order to familiarize the WWDC, Technical Advisory Team (TAT), governmental agencies, and local stakeholders with the scope of the project, as well as obtain input from affected parties, a scoping meeting should be held early in the project.

### *Task 2: Review and Summarization of Previous Data*

This review will include all available background information regarding previous weather modification research and/or activities within the State of Wyoming and within the target area (as possible), and projects within close proximity having the potential to affect the Bighorn Mountains program operations or evaluation.

### *Task 3: Climatology of the Project Area*

The purpose of this analysis is to determine the characteristics of the storms producing precipitation over the Bighorn Moountains and determine the seeding potential of the project area.

### *Task 4: Development of Preliminary Project Design*

Based on the information gathered in Tasks 1–3, a preliminary weather modification project design for the Bighorn Mountains will be developed. The design shall include the methodology, materials, equipment, siting considerations, available meteorological observation systems, and other components necessary to operate and maintain a weather modification program in the target area.

### *Task 5: Model Evaluation of Preliminary Project Design*

The goal of this task is to use numerical models to evaluate the suggested locations of ground-based seeding generators and optimize seeding strategies for the proposed project design, including the possibility for airborne seeding.

### *Task 6: Field Surveys of Proposed Ground Generator Locations*

Field surveys will be conducted of the target area to inspect proposed ground-based generator locations as determined from Tasks 4–5.

### *Task 7: Access/Easements and Environmental Permitting/Reporting*

A review of all local area plans, county ordinances, and other regulations that may affect the proposed weather modification operations in the project area will be conducted. This will include identifying all easements and/or access agreements that will be necessary to

implement siting of the equipment as directed by the preliminary project design, as well as summarize all permitting and/or reporting requirements necessary to implement the proposed project design.

#### *Task 8: Establishment of Operational Criteria*

Preliminary operational seeding criteria will be developed for the project area, containing protocols and procedures necessary to operate the program within the established guidelines as set forth by the American Society of Civil Engineers (ASCE).

#### *Task 9: Environmental and Legal Considerations*

A summary of any potential environmental and legal considerations associated with implementation of the project design will be provided.

#### *Task 10: Evaluation Methodology*

Methodologies for evaluating the efficacy of the cloud-seeding program in the target area will be summarized, including both physical and statistical methods.

#### *Task 11: Hydrologic Assessment*

The goal of this task is to assess the potential streamflow benefits from cloud seeding utilizing the long-term high-resolution model simulation (Task 3) to conduct a water balance approach.

#### *Task 12: Cost Estimates*

Costs for establishing, operating, and maintaining the proposed weather modification program will be estimated and summarized.

#### *Task 13: Preliminary Cost/Benefit Analyses*

Based on the information from Tasks 1–12 of the project, cost/benefit estimates for conducting weather modification operations in the target area will be produced on a per acre-foot (AF) basis.

#### *Task 14: Reports and Executive Summaries*

Digital and paper copies of the final report and executive summary will be provided to the WWDC.

#### *Task 15: Report Presentations*

A meeting/public hearing will be held in the local project area to present the final results of the study.

#### *Task 16: Climatological Monitoring of the Study Area*

Pertinent climatological information and data will be collected and archived during the November 2015–April 2016 winter season for the study area. In addition, a radiometer will be deployed to measure the magnitude and frequency of liquid water in the region.

### 1.2 Personnel and Organizations

The Research Applications Laboratory (RAL) of the National Center for Atmospheric Research (NCAR) collaborated with Weather Modification International (WMI) and

Heritage Environmental Consultants (HEC) to conduct this study. Key personnel from each institution are listed in Table 1.1.

**Table 1.1. List of key personnel from each institution that was involved in conducting this study.**

| Organization | Key Personnel |
|---|---|
| NCAR | Sarah Tessendorf<br>Roy Rasmussen<br>Lulin Xue<br>Kyoko Ikeda<br>Courtney Weeks<br>Jamie Wolff<br>Michelle Harrold<br>Duncan Axisa<br>Scott Landolt<br>Al Jachcik<br>Dan Breed |
| WMI | Bruce Boe |
| HEC | Patrick Golden |

# 2. Task 1: Scoping Meeting/Project Meetings

The purpose of the scoping meeting is to familiarize the WWDC, TAT, governmental agencies, and local stakeholders with the scope of the project, as well as obtain input from affected parties.

## 2.1 Scoping Meetings in Sheridan and Worland, WY

Two public scoping meetings were held at the beginning of the project. The first scoping meeting was held on 22 September 2015 in Sheridan, Wyoming at the Sheridan County Fulmer Library. The second was held the next day on 23 September 2015 in Worland, WY at the Washakie Museum and Cultural Center.

The meetings were opened by Mr. Barry Lawrence, the Wyoming Water Development Office (WWDO) Project Manager, who facilitated introductions and provided a brief history and purpose for the study. Presentations at the meeting then included an overview of the scientific concept of cloud seeding (Mr. Bruce Boe, WMI), a summary of the previous studies in Wyoming (Dr. Roy Rasmussen, NCAR), an overview of the current study (Dr. Sarah Tessendorf, Mr. Bruce Boe, and Mr. Patrick Golden). The complete attendee list is included in Table 2.1.

**Table 2.1. List of attendees (other than presenters) at the scoping meeting in Sheridan.**

| Name | Agency | | Name | Agency |
|---|---|---|---|---|
| Jeni Cederle | WWDO | | Dan Coughlin | SAWSJPB |
| Brent Sosotka | BLM | | John Kane | Rancher |
| Kevin Chartier | IML Inc. | | Mike Dunn | The Sheridan Press |
| Bernie Burnong | Bighorn NF | | Bill White | Self |
| Carrie Rogaczewski | SCCD | | Susan Wells | UW Alumnus |

**Table 2.2. List of attendees (other than presenters) at the scoping meeting in Worland.**

| Name | Agency | | Name | Agency |
|---|---|---|---|---|
| Jeni Cederle | WWDO | | Caitlin Youngquist | UW Extension |
| Kristin Tilley | Shoshone Conservation Dist. (SCD) | | Keith Grant | SCD and Lovell Irrigation Dist. |
| Josh Fredrickson | WY State Engineers Office (SEO) | | Phil Bower | WY SEO |

## 2.2 27 January 2016, Cheyenne, WY

A TAT meeting was held on 27 January 2016 in Cheyenne, Wyoming at the WWDO. Ms. Jeni Cederle, the new WWDO Project Manager, facilitated the meeting. At the meeting, NCAR gave a presentation updating the TAT on the preliminary results and progress of the Bighorn Mountains Siting and Design Study, as well as the next steps to be completed in the study. NCAR representatives included Dr. Roy Rasmussen and Dr. Sarah Tessendorf. The

complete list of attendees is included in Table 2.3.

**Table 2.3. List of attendees at the January 2016 TAT meeting in Cheyenne.**

| Name | Agency | | Name | Agency |
|---|---|---|---|---|
| Lee Hacklemen | National Resources Conservation Service | | John Mejia | Desert Research Institute (DRI) |
| Ty Wattenberg | -- | | Frank McDonough | DRI |
| Steve Wolff | WY SEO | | Brian Lovett | WY Dept Environmental Quality (DEQ) |
| Jeff Frazier | WY Dept Transportation | | Jeff French | Univ. Wyoming (UW) |
| Sean Collier | Southern Nevada Water Authority | | Kate Dwire | USFS Rocky Mtn Research Station (RMRS) |
| Nathan Haynes | USFS Medicine Bow-Routt NF and Thunder Basin NF (MBRTB) | | Scot Rogers | USFS MBRTB |
| Terry Deshler | UW | | Mitchel Cottenoir | Tribal Water Engineer |
| Robert Musselman | USFS RMRS | | Binod Pokharel | UW |
| Sandy Henny | USFS | | Mohammed Mahmoud | Central Arizona Project |
| Lee Arrington | WY SEO | | Jeri Trebelcock | Popo Agie Conservation Dist. |
| Bruce Boe | WMI | | Pat Golden | HEC |
| Bart Geerts | UW | | Barry Lawrence | WWDO |
| Ray DeLuna | TREC Inc. | | Roy Rasmussen | NCAR |
| Sarah Tessendorf | NCAR | | Joe Busto | Colorado Water Conservation Board |
| Joan McGraw | Medicine Bow Conservation Dist. | | Jeni Cederle | WWDO |

# 3. Task 2: Review and Summarization of Previous Data

## 3.1 Background

The potential for modifying supercooled clouds with artificial *ice nuclei* (IN) was initially espoused in the literature by Findeisen (1938). After artificial ice nucleation by both dry ice and silver iodide (AgI) became known, many researchers became interested in modifying precipitation from supercooled clouds (e.g., Schaefer 1946; Vonnegut 1947; Kraus and Squires 1947; Langmuir 1948; Coons *et al*. 1948; and Bergeron 1949). Such modification is termed glaciogenic seeding, as it results in the formation of cloud ice.

These "early" scientists recognized that winter orographic clouds might be particularly well suited to seeding due to the frequency and persistence of supercooled water. Ludlum (1955) was among the first to present a conceptual model for seeding orographic clouds to enhance snowfall, a model that has remained unchanged in the essential details. However, the microphysical precipitation processes in winter clouds have proven to be far more complex than originally envisioned. This has led to many refinements and clarifications of the conceptual model details.

Precipitation in winter orographic storms generally develops when ice crystals form on natural IN (typically certain dust particles) and grow through *deposition* (water vapor forming ice directly, the process that builds the smallest snow crystals), *riming* (the collection of unfrozen cloud droplets by ice crystals), and/or *aggregation* (the entanglement of ice crystals with each other to form snowflakes). Measurements suggest that most orographic clouds do not contain much ice until temperatures cool to less than −12 °C (e.g., Geresdi et al. 2005). Natural IN are scarce at such relatively warm subfreezing temperatures (Hoose and Möhler 2012). During many storms, the precipitation process is inefficient due to the lack of natural IN active at warmer cloud temperatures.

Furthermore, the weak updrafts in orographic clouds (composed mostly of very small droplets of similar sizes), limit the activity of ice multiplication processes that create cloud ice without additional IN (e.g., Hallett and Mossop 1974). As a result, many shallow clouds, especially winter orographic clouds, may largely lack ice crystals and thereby have inefficient precipitation processes. The absence of ice crystals allows supercooled cloud droplets to persist for long periods in such orographic clouds instead of being depleted by vapor diffusion, riming, and/or aggregation. This fact is well documented by the measurement of sustained supercooled liquid water (SLW) in orographic clouds taken by aircraft and ground-based instruments, such as radiometers (e.g., Rauber et al. 1986; Huggins 1995). In contrast to natural IN, artificial IN, such as AgI, will nucleate ice crystals at temperatures as warm as −5 °C, enabling the creation of ice crystals in clouds warmer than −12 °C by "seeding" them with an AgI aerosol (DeMott et al. 1995).

One alternative to glaciogenic seeding with AgI is to seed with liquid propane (LP). Rather than producing ice via heterogeneous nucleation, liquid propane is released directly into the cloud to be seeded, where the rapid evaporation of the droplets results in extreme supercooling and homogeneous nucleation. At temperatures colder than −2 °C,

approximately $10^{12}$ ice crystals are produced per gram of propane (Hicks and Vali 1973). Seeding with LP is easy and efficient; however, there are disadvantages. First, the release must occur within a supercooled cloud. If LP is released in clear air, there are no droplets to freeze, and if the cloud is not supercooled, the ice formation will be very transient. Further, if the resulting ice that is formed should warm and melt or sublimate, it will not reform (Reynolds 1996). Therefore, to be effective, the ice produced by LP seeding must continue to grow to precipitation. If the ice thus formed melts or sublimates, there are no nuclei left behind to re-initiate ice development (as there would be when seeding with AgI), even if, or when the environment becomes saturated and supercooled again.

### *3.1.1 Conceptual Model*

The following chain of events is hypothesized for seeding the Bighorn Mountains.

In ground-based seeding, AgI is released from IN generators near and/or on the target mountain range, and carried upward by the wind. The plume of AgI rises and disperses within a relatively large volume of cloudy air. The AgI particles nucleate cloud ice at temperatures colder than −5 °C. However the nucleation efficiency increases by orders of magnitude (a factor of 100 to 1,000) at temperatures of −8° to −10 °C[1]. The ice crystals then rapidly grow in conditions of water saturation (within the cloud), where supercooled water droplets exist. The ice crystals first grow by vapor deposition and then by riming and/or aggregation, forming precipitation-sized ice particles that fall to the surface as snow. These crystals are enhanced in number, size, and/or density from what would have fallen naturally, but otherwise are indistinguishable from natural snowfall.

The chain of events for airborne seeding is essentially the same, except transport of the AgI into the cloud is ensured given it is released in cloud, or just above cloud. By this method, the AgI creates ice within 1 min (at −6° to −8 °C) of release via flare[2] (DeMott 1999), and rapidly grow as ice crystals in regions of SLW. The chain is otherwise identical to ground-based seeding, although the precipitation particles may originate at greater heights.

Airborne seeding eliminates some of the uncertainties inherent in ground-based releases of AgI because the seeding agent is delivered immediately and directly to the target clouds. Through the use of pyrotechnics, an aircraft can deliver more seeding agent to the cloud faster than ground-based generators can. A typical ground-based generator release rate is 25 grams per hour (per generator), while airborne release rates begin at ~37 grams per

[1] These numbers apply to the seeding solution used in the WWMPP, which functions rapidly through the condensation-freezing mechanism. More "traditional" formulas producing $AgI{\cdot}NH_4I$ nuclei function through the contact-freezing mechanism, and thus may require many minutes more to nucleate in clouds of lesser LWC.

[2] The activity of the silver iodide-based pyrotechnic quoted here is for the glaciogenic flare presently manufactured by Ice Crystal Engineering, LLC, of Kindred, North Dakota. The IN output and activity of pyrotechnics manufactured by others may vary considerably, and should be determined before any program is undertaken.

minute. Aircraft can also effectively treat clouds in some circumstances when ground-based seeding cannot.

However, operation of an aircraft is more expensive than ground-based generators, in large part because deployment costs are greater. Aircraft also have limited on-station (seeding) times as crew endurance and fuel consumption limit the length of operations while ground-based generators can be readily operated continuously for a day or more.

The model for LP seeding is essentially the same, but the targeting is different. While AgI nuclei can be released from any location where the flow will carry it into supercooled clouds, the LP can only be used within supercooled clouds, and must be sited exactly where the clouds develop. The advantage of LP is that it can be used to produce ice crystals if any SLW is present, and does not require clouds to be −6 °C or colder. The advantages and disadvantages of various seeding methods are listed in Table 3.1.

**Table 3.1. Advantages and disadvantages of various seeding types and modes.**

| *Type/ Mode* | *Siting/Positioning* | *Target Temperature Threshold* | | *Seeding Rate*[4] | *Advantages* | *Limitations* |
|---|---|---|---|---|---|---|
| | | °C | °F | | | |
| ***Manual, Ground-based AgI*** | Fixed, upwind of target. Distance from target and elevation depend upon typical flows during seeding conditions. | ~ -6 °C[1] | ~(+21°F) | $1.25*10^{11}$ nuclei per minute. | Lower cost, as communications electronics to actuate generator are not required. | Requires an on-site operator, so must be sited where an operator is available. Fixed location, so useful for a limited range of wind speeds. |
| ***Remote-Controlled Ground-based AgI*** | Fixed, upwind of target. Distance from target and elevation depend upon typical flows during seeding conditions. | ~ -6 °C[1] | ~(+21°F) | $1.25*10^{11}$ nuclei per minute. | Requires no on-site operator; can be sited anywhere the equipment can be moved. | Fixed location, so useful for a limited range of wind speeds. |
| ***Airborne AgI*** | Upwind of target clouds, at an appropriate altitude and distance from target. | ~ -4 to -6 °C[1,2] | ~+25 to +21°F | At -6 °C, $2.3*10^{14}$ nuclei per minute with pyro, $6*10^{11}$ nuclei per minute with seeding solution used by ground IN generators. | Upwind distance and altitude can be adjusted according to the cloud depth, temperature, and ambient wind speed. Deployment of surface-based equipment not required. | Minimum safe altitude must be maintained, so seeding at low altitudes close to barrier as needed in slow wind speeds is not possible. |
| ***Ground-based Liquid Propane*** | Fixed, elevation high enough to be routinely within supercooled cloud. | < 0 °C[3] | <32°F | $7*10^{12}$ ice crystals per minute from 0 to -2 °C, $\sim 7*10^{14}$ ice crystals per minute at temperatures colder than -2 °C.[3] | Propane is inexpensive.<br><br>Any supercooled cloud can be treated, regardless of temperature. | Only effective if within supercooled cloud. Most reliable when a real-time indicator of supercooled cloud is available, such as an icing rate meter. Utilizes homogeneous nucleation, so no nuclei are left behind to re-nucleate if the ice formed initially melts or sublimates. Fixed location, so useful for a limited range of wind speeds. Must be remote-controlled. |
| | [1]This temperature is based upon the nucleation efficiency of the seeding solution used in the WWMPP, which functions by the condensation-freezing mode. This solution contains an oxidizer, so the generator must be constructed with corrosion-resistant (e.g. stainless steel) components.<br>[2]Glaciogenic pyrotechnics manufactured by Ice Crystal Engineering produce $10^{11}$ IN per gram active at -4 °C, and $10^{13}$ IN active at -6 °C (1.5 orders of magnitude more than the seeding solution cited), which can further broaden the seeding opportunity window. See Figure 12.1.<br>[3]Per Hicks and Vali (1973).<br>[4]Seeding rates for AgI nuclei calculated from efficiencies measured by DeMott (1997, 1999). | | | | | |

## 3.2 History of Wintertime Orographic Cloud Seeding

The fundamental hypothesis underlying increasing precipitation through winter orographic cloud seeding is that natural precipitation efficiency can be improved by seeding. If conducted upstream of the mountain range, it will convert supercooled water to ice crystals. The newly created ice particles then grow by diffusion, riming, and/or aggregation, and precipitate as additional snow to the surface, increasing the natural snowfall.

Scientific evaluation of this hypothesis has been attempted over the last half a century using statistical comparison of surface precipitation in treated versus untreated events (randomized studies), observational studies to understand natural cloud structure and effects of seeding (physical studies), and numerical modeling of both natural and seeded clouds. Since 1948, numerous research programs have been completed in order to determine whether or not AgI seeding could produce additional precipitation in winter orographic clouds (see Huggins 2009 for a summary).

### *3.2.1 Randomized Studies - Historical*

Two randomized programs conducted in the Rocky Mountains are of immediate relevance to winter orographic cloud seeding in Wyoming. These are: the Climax experiments in the central Colorado mountains (Mielke et al. 1981; Grant 1986), and the Bridger Range Experiment (BRE) in southwestern Montana (Super and Heimbach 1983).

The Climax Experiments (Climax I, 1960–1965, and Climax II, 1965–1970) were exploratory and confirmatory randomized seeding experiments that used instruments and observations as covariates and for ancillary (*ex post facto*) studies. The Climax I and II research used experimental units of one-day (24-hour) duration, which were declared in accordance with design criteria established prior to the start of the respective experiments (Grant and Mielke 1967, Mielke et al. 1971). Both Climax I and the replication, Climax II, reported precipitation increases with high statistical confidence (Mielke et al. 1981). A reanalysis of the complete Climax dataset (I and II) showed that for warm 500-hPa temperatures, precipitation increases of 25% were realized. However, the validity of the experiments was questioned on the basis of the experimental execution and evaluation methodology (Rangno and Hobbs 1987, 1993). Much was learned from the Climax experiments, but ultimately the validity of these experiments left the conclusions in doubt.

The Bridger Range Experiment (BRE) was conducted in the Bridger Mountains of southwest Montana from 1969 to 1972 (Super 1974; Super and Heimbach 1983). To avoid trapping the seeding agent below stable atmospheric layers above, the BRE utilized ground-based IN generators that burned an AgI solution that were sited more than midway up the upwind (western) side of the barrier. The Bangtail Ridge was the expected target, and is a secondary barrier located from 5 to 20 km east of the main ridge of the range.

Randomized experiments were conducted during the winters of 1970–1971 and 1971–1972, and follow-on physical measurements were later made (Super and Heimbach 1988). This project produced strong statistical evidence of seeding effects, and also considerable documentation of the physical "chain-of-events" that began with seeding and led to the observed precipitation changes. A *post hoc* statistical analysis strongly suggests that increased target area snowfall resulted from seeding when Agl plume temperature was colder than approximately −9 °C. An estimate of ~15% more seasonal target area precipitation than predicted on non-seeded days resulted, while a target-control analysis of independent snow-course data strongly suggested seeding enhanced the seasonal snowpack more than 15%. Additional exploratory analysis of the BRE was later carried out by sub-partitioning the original 24-hour experimental units into 6-hour data blocks (Super 1986). That analysis was limited to those 6-hour periods having rawinsonde observations, Main Ridge temperatures ≤−9 °C and westerly flow. The results showed that AgI seeding was particularly effective in increasing precipitation in a small fraction of the 6-hour blocks, but had little or no effect most of the time. Seeding appeared to be especially effective when cloud-top temperatures were warmer than about −25 °C and the wind had a strong cross-barrier component. Super (1986) notes that, "…this analysis has not suggested any significant decreases in target precipitation due to seeding. This implies that the treatment used could be applied whenever potential storm conditions existed without concern of decreasing snowfall." These results have been accepted, but because of the limited scale, different geography and climate, the direct transferability to Wyoming was in doubt.

### 3.2.2 Randomized Studies - Recent

Randomized experiments with many similar design elements were recently carried out in two very distant areas, the Snowy Precipitation Enhancement Research Program (SPERP) in the Snowy Mountains of Australia (Manton et al. 2011, Manton et al. 2015), and the recently completed Wyoming Weather Modification Pilot Program (WWMPP) in southern Wyoming (Breed et al. 2014, WWDC Draft Executive Summary 2014).

The Australian experiment, SPERP (Phase I), provided recent evidence of an increase in precipitation due to AgI seeding of winter orographic clouds based on a 5-year statistical program (Manton and Warren 2011). Analysis of the confirmatory experiment showed a 7–9% increase in snow water equivalent (SWE), depending on whether the analysis used the primary control area or an extended "total" control area. However, these experimental results did not meet the accepted level of significance and therefore cannot be considered to be statistically different than no-seeding effect.

The operational procedures of, and measurements made during SPERP were designed to address and verify the issue of targeting – that is, ensuring that seeding material was affecting the seedable portion of the clouds. Therefore, exploratory analyses were performed with the targeting issue, and others, in mind. Use of the extensive sampling measurements for trace chemistry (silver-in-snow), tracers, integrated liquid water within the targeted clouds, and trajectory modeling, supported partitioning the precipitation data

by the total time generators were operating during a case. Seasonal precipitation increases of 14% were established (relative to seedable storms), at a 3% significance level (p-value of 0.03) after thresholding the cases according to generator hours, indicative of probable AgI coverage of the target area (e.g., more generator hours being equivalent to more AgI seeding material reaching the target area). Physical studies included silver-in-snow measurements that verified effective targeting of the AgI seeding agent.

The findings from the SPERP analysis prompted a second seeding experiment in the same area, but with expanded target and control areas and different seeding criteria. Although the study is not yet published, drafts of the project description and results have been circulated within the scientific community (Manton et al. 2015; Reynolds 2015). Although the changes in the target and control areas led to a range of seeding effects, the overall result is very similar to that found in the SPERP study: a 13% increase in precipitation (in the target area for seedable storms) at a 6% significance level (p-value of 0.06). The replication of the results in response to experimental changes from the SPERP analysis is very encouraging as far as substantiating the efficacy of winter orographic cloud seeding.

The results of the Wyoming project, WWMPP, were recently summarized in a draft executive summary (WWDC 2014) and included statistical, physical, and modeling analyses. The accumulation of evidence from these analyses suggests that "cloud seeding is a viable technology to augment existing water supplies, for the Medicine Bow and Sierra Madre Ranges." The primary statistical analysis implied a 3% increase in precipitation with a 28% probability that the result occurred by chance, which did not meet the acceptable level of significance. While this primary statistical analysis did not show a significant impact of seeding, statistical analysis stratified by generator hours, similar to the SPERP analyses, showed seasonal increases of 3–17% for seeded storm periods. Furthermore, high-resolution modeling studies that simulated three of the experimental seasons, or about half of the total number of seeding cases, showed positive seasonal seeding effects between 10–15% (relative to seedable storms).

Though no seeding effect was discerned in the primary randomized statistical experiment (RSE), ancillary studies using physical considerations (e.g., hours of generator operations, surface-based ice nucleus measurements, and numerical modeling) to stratify the WWMPP precipitation data and modeling studies over three full winter seasons yielded more positive evidence from the statistical, modeling, and physical analysis. This evidence suggested "a positive seeding effect on the order of 5 to 15%" relative to seedable storms in a given season. These increases apply to a single control site in the target area, so a seeding effect applicable to the whole target area needs to be calculated based on an estimate of effective seeding coverage of the target area. For example, if the areal coverage of effective seeding were 60%, then the seeding effect for the target would be 3–9%.

Important design and operational aspects of the WWMPP included confirming the presence of SLW over the target mountain ranges. This was accomplished using a dispersion model to guide initial generator placement, radiometers, soundings, and high-resolution real-time forecast models to inform operational decisions, and additional observations from ancillary instruments and "piggy-back" experiments, such as the AgI Seeding Cloud Impact

Investigation (ASCII, e.g. Pokharel et al. 2014). Based on the preliminary results of the WWMPP, the recommendation was made to consider implementing cloud-seeding technology in Wyoming by carefully addressing each of five components: 1) barrier identification; 2) program design; 3) operational criteria; 4) program evaluation; and 5) program management. These were further detailed in the executive summary.

The consensus of a post-SPERP, post-WWMPP panel discussion was that technological advances, particularly in remote sensing and numerical modeling, bode well for the advancement of cloud seeding operations (Tessendorf et al. 2015).

### *3.2.3 Physical Experiments*

Several randomized seeding experiments have included some physical studies aimed at verifying the seeding conceptual model. However, a number of other non-randomized research programs have also contributed to the refinement of the seeding conceptual model. Much of this work has been summarized by Golden (1995) and Super (1999), and more recently, Huggins (2009), who compiled a summary of past research studies related to winter orographic cloud seeding. The overall results of the various studies provided support for the National Research Council (NRC) (2003) conclusions that "strongly suggested positive seeding effects" in these types of storms.

Observational studies, in concert with the WWMPP and SPERP randomized seeding experiments, have evaluated or verified steps in the seeding conceptual model. The silver-in-snow sampling technique has advanced to the point of being a preferred method of evaluating the effectiveness of targeting (Warburton et al. 1995). Results have been presented in the analysis of SPERP (Manton et al 2011) and in the draft conclusions of the WWMPP (WWDC 2014). Additionally, AgI IN measurements using the NCAR acoustic IN counter (AINC) have demonstrated the variability of the seeding plume in targeting small areas, using both airborne and ground-based instruments (Heimbach et al. 2008; Boe et al. 2014).

Geerts et al. (2010) applied a high-resolution vertically-pointing millimeter-wavelength airborne Doppler radar to investigate wintertime seeding effects in orographic clouds for seven cases in conjunction with the WWMPP. Those results showed that the increase in near-surface reflectivity could be attributed to AgI seeding with statistical significance. However, the large natural variability of meteorological conditions and the small number of cases rendered the results cautionary. Consequently, the ASCII field program was carried out to better quantify the seeding signals by reducing the impact of natural variability of the orographic storms. Results showed that in some cases, increased reflectivity at low levels observed by the airborne Doppler radar was very likely to be induced by ground-released AgI particles (Pokharel et al. 2014a, b). The ASCII program also contributed surface radar, precipitation, and cloud physics observations, and airborne radar, lidar, and cloud physics measurements that have aided validation of numerical modeling studies of winter orographic cloud seeding.

These studies and evidence from randomized seeding experiments provide a detailed physical picture of AgI plume transport, ice nucleation, and snow development. More sophisticated measurements and improved numerical models developed over the last decade continue to refine and validate the seeding conceptual model.

### *3.2.4 Numerical Modeling*

Modeling of natural and seeded orographic clouds has been conducted in concert with physical studies. The Weather Research and Forecast (WRF) model (Skamarock et al. 2008) has been used in a number of winter snowpack studies and cloud-seeding evaluations that have verified the model's ability to reasonably simulate plume transport and snowfall over a variety of time and space scales. For example, the WRF model was used to simulate eight seasons of snowfall in the Rocky Mountains, covering all of Colorado and parts of adjacent states (Ikeda et al. 2010). The model runs at various resolutions were compared to Snow Telemetry (SNOTEL) data, and grid spacings of 6 km at a minimum were needed for reasonable agreement. Although 6-km resolution was adequate, the model run at 2-km grid resolution captured the local topographic forcing of regional snowfall even better.

Recently, Xue et al. (2013a, b) implemented an AgI cloud-seeding parameterization into the Thompson bulk microphysics scheme (Thompson et al. 2008) within the WRF model to systematically investigate how orographic seeding outcomes are influenced by atmospheric and cloud properties under idealized and realistic conditions. Almost all idealized and realistic case simulations showed that ground-based glaciogenic seeding enhances precipitation in stable stratified orographic clouds, but were ineffective in convective clouds deep enough to produce abundant ice nucleation near the top. By examining seeding effects under various meteorological and microphysical conditions, the model simulations presented in Xue et al. (2013a, b) demonstrated that the seeding effects increase with decreasing natural precipitation efficiency and vice versa.

For smaller domains, the WRF model can be configured at very high resolution, called a large eddy simulation (LES). The LES model was run on a case in the Medicine Bow Range of southern Wyoming at 100-m resolution and proved to be successful in simulating details of the airflow and plume dispersion for that case, validated by results of airborne mapping of the seeding plumes (Xue et al. 2014; Boe et al. 2014).

These recent modeling studies incorporating AgI seeding into the processes that lead to precipitation have shown promise in simulating seeding effects. Likewise, the emergence of this state-of-the-art cloud seeding microphysics scheme together with sufficient computing power to resolve large eddies now allows examination of the chain of events associated with glaciogenic seeding.

## 3.3 Meteorological Observations Relevant to the Bighorn Mountains

Public data sources include SNOTEL precipitation and snowpack measurements and United States Geological Survey (USGS) streamflow records. Meteorological data are also available

through the National Oceanic and Atmospheric Administration (NOAA). Some historical data are also listed in the Powder/Tongue River Basin Plan (HKM Engineering et al. 2002) and the Wind Bighorn Basin Plan (MWH Americas et al. 2010).

## 3.4 History of Cloud Seeding In and Near the Bighorn Mountains

Cloud-seeding operations are regulated and permitted by the Wyoming State Engineer's Office (WSEO). The earliest record of cloud-seeding activities near the Bighorn Mountains dates back to 1951, when a permit was issued to Water Resources Development Corporation under the direction of the Powder River Weather Research Corporation to engage in weather modification activities covering the counties of (those adjacent to the Bighorn Mountains are in bold italics) Campbell, Crook, ***Johnson***, Niobrara, ***Sheridan***, Weston and Converse north of the North Platte River (Figure 3.1). As stated in the permit, the seeding period was 1 May 1951 to 31 December 1951, and no more than 10 AgI generators were permitted to operate at one time. Seeding was primarily done in summer months with more than 1,000 hours of generator time during the months of June and August 1951.

Another permit, also in 1951, allowed operations in parts of Park, ***Big Horn***, ***Washakie,*** and Hot Springs Counties.

Additional permits were issued in 1951 to North American Weather Consultants for cloud seeding in Platte, Goshen, Laramie, Campbell, and ***Sheridan*** Counties.

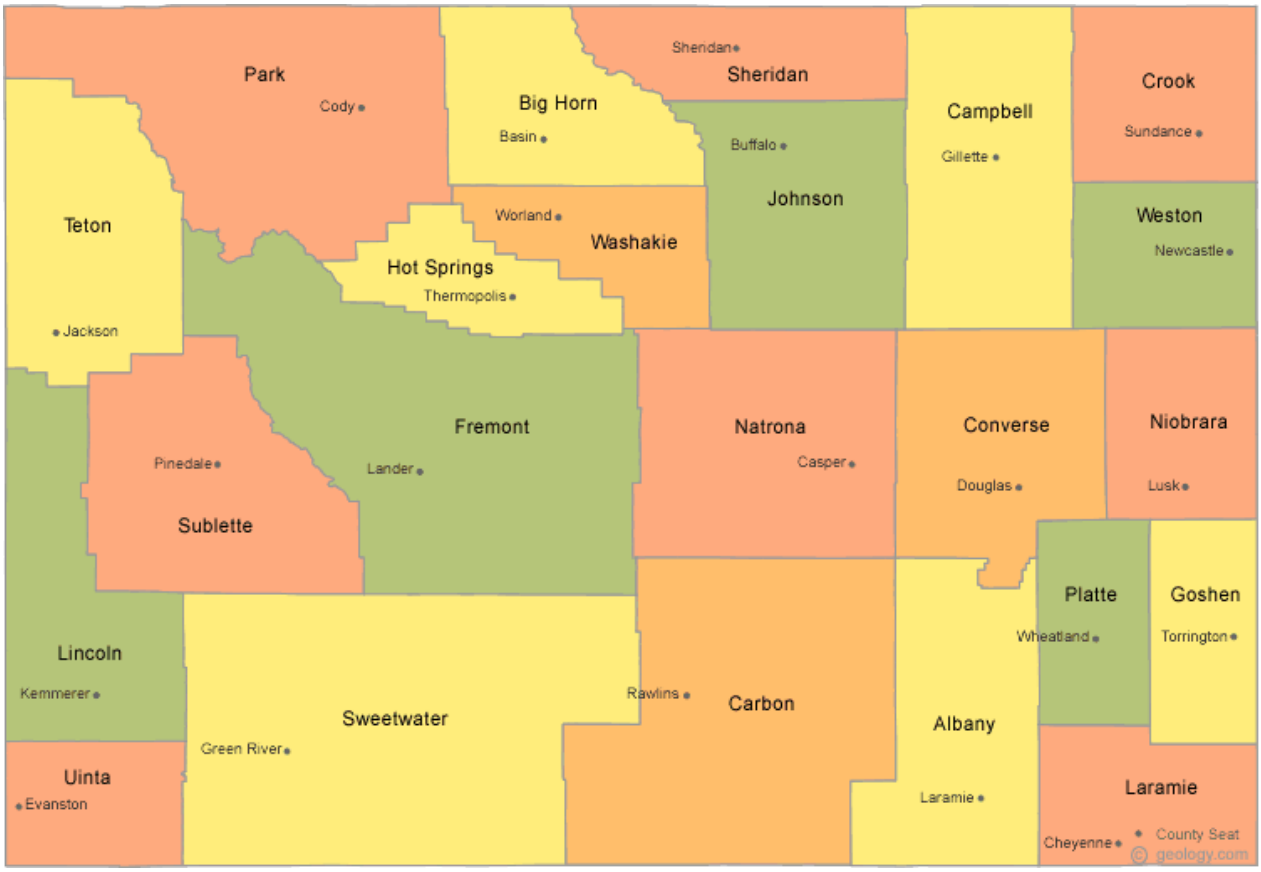


**Figure 3.1. Wyoming county borders.**

In 1952, North American Weather Consultants were permitted to operate under sponsorship and direction of Sheridan County Weather Association to conduct cloud seeding in ***Sheridan County*** for the period 23 April–15 October. Also in 1952, a permit was issued to Johnson County Weather Modification Inc. of the town of Buffalo, ***Johnson County*** to conduct cloud seeding in Johnson County for the period 1 April–31 December. Each permit required that the amount of AgI generators would not exceed 10 in number.

In 1953, a permit was issued to Water Resources Development Corporation to conduct cloud seeding in the following counties: Converse, Weston, Goshen, Niobrara, Platte, Laramie, and ***Sheridan***. The permitted seeding period ran from 1 May–31 December, and the permit required that the number of AgI generators were not to exceed 30. Though permits were issued, records do not show any operations in Sheridan County; however, only in those further south.

In 1954, another permit was issued to Water Resources Development Corporation to increase snowpack precipitation for benefit of the Wheatland Irrigation District in Platte County from 11 February –11 May , utilizing 10 AgI generators, but were required not to exceed the use of 40 generators. The counties listed in the permit were Campbell, Crook, Weston, Niobrara, Converse, Carbon, Albany, Platte, Goshen, Laramie, ***Sheridan,*** and ***Johnson***.

No other permits for cloud-seeding operations over or near the Bighorn Mountains were issued after 1954.

## 4. Task 3: Climatology of the Project Area

The purpose of this task is to determine the characteristics of storms producing precipitation over the Bighorn Mountains. and to determine the fraction of time that seedable conditions are present in winter storms impacting the project area, including the fraction of the winter precipitation that could be effectively seeded. The following questions were addressed.

- What are the prevailing winds, temperatures, cloud depths, stabilities, and liquid water content (LWC) during precipitation over the Bighorn Mountains?
- What fraction of the time are ground or airborne seeding conditions present?
- During which months do the most opportunities for ground or airborne seeding occur?
- What fraction of the precipitation occurs when ground or airborne seedable conditions are present?

In order to be defined as a "seedable condition," several criteria must be met. First, the temperature needs to be in an appropriate range for nucleation of AgI. Studies have shown that AgI nucleates at temperatures as warm as −5 °C, and the activation efficiency increases rapidly as temperatures cool toward −8 °C and colder (DeMott 1999). To ensure moderate to strong AgI activiation efficiency in this study, the seedable temperature range was defined to be between −6 °C and −18 °C.

In addition to an appropriate activation temperature for AgI, liquid water needs to be present for there to be potential for cloud seeding. SLW is a sign that natural precipitation processes are inefficient, and if additional ice crystals are nucleated (via AgI activation) they could grow at the expense of the SLW and fall out as additional snow. The criteria utilized in this study define seedable LWC as greater than 0.01 g/kg and within the appropriate temperature range to be considered SLW. Therefore, at a minimum, both appropriate temperature and LWC criteria need to be met to determine seeding potential.

Additional variables, such as atmospheric stability and winds, play a role in determining seeding potential, especially with regard to how effectively the AgI will be transported into the seedable cloud. Therefore, assessing the atmospheric stability and wind direction is important for determining locations to release AgI and the method of delivery (i.e., ground-based generators or aircraft).

Observations needed to evaluate these meteorological criteria include atmospheric soundings (to assess temperature, stability, and winds at heights where clouds form), radiometer data (to assess the presence of SLW in the atmosphere), and precipitation gauge data (to determine when and how much precipitation fell). With the exception of SNOTEL gauge measurements, these types of observations are quite rare, especially in the western U.S. mountains. Therefore, an alternative way to get this important information is to utilize high-resolution model reanalysis data. Because not all publicly available model reanalyses include LWC as an output variable (as explained in Ritzman et al. 2015), an 8-year high-resolution model simulation from NCAR (similar to Rasmussen et al. 2014) that

does include all of these necessary variables was utilized for the majority of this climatological analysis.

## 4.1 Data and Methodology

Precipitation climatology in the project area was investigated using SNOTEL observational data and a high-resolution WRF model simulation over an 8-year period between 1 October 2000 and 30 September 2008.

### *4.1.1 Observations*

Data from 14 SNOTEL sites were available in the Bighorn Mountains (Figure 4.1). SNOTEL observations provide a long-term record of precipitation from gauges that weigh precipitation and snow water content data via pressure-sensing snow pillows located at numerous sites throughout the Western U.S. These sites are owned and operated by the Department of Agriculture Natural Resource Conservation Service (NRCS), and are typically located at elevations between 2,400 and 3,600 m above mean sea level (MSL). Historical and real-time data are available from the NRCS web site (http://www.wcc.nrcs.usda.gov/snow/), and have been widely used for climatological studies. These studies also describe known measurement deficiencies (Serreze et al. 1999; Serreze et al. 2001; and Johnson and Marks 2004; for example) such as an undercatch of snowfall due to wind (Serreze et al. 2001; Yang et al. 1998; Rasmussen et al. 2012). The SNOTEL gauges are placed in a forest clearing where the wind speed is typically 2 m $s^{-1}$ or less, and an undercatch of 10–15% is expected. The SNOTEL dataset used in this study has been corrected for the undercatch following the procedure described in Serreze et al. (1999). The SNOTEL data resolution is 0.1 inch (2.5 mm), making it difficult to study precipitation characteristics or verify model data on a sub-daily basis. However, these data are suitable for use over monthly or longer periods.

Regular atmospheric sounding data were available twice daily at 0000 and 1200 UTC from the National Weather Service (NWS) office located in Riverton, WY. These data were analyzed to determine the frequency of 700-hPa wind direction when precipitation was observed at the Grave Springs SNOTEL site in the southern portion of the Bighorn Mountains. The wind rose produced from this analysis can be compared with the same from the model-based analysis of winds over the Riverton, WY site.

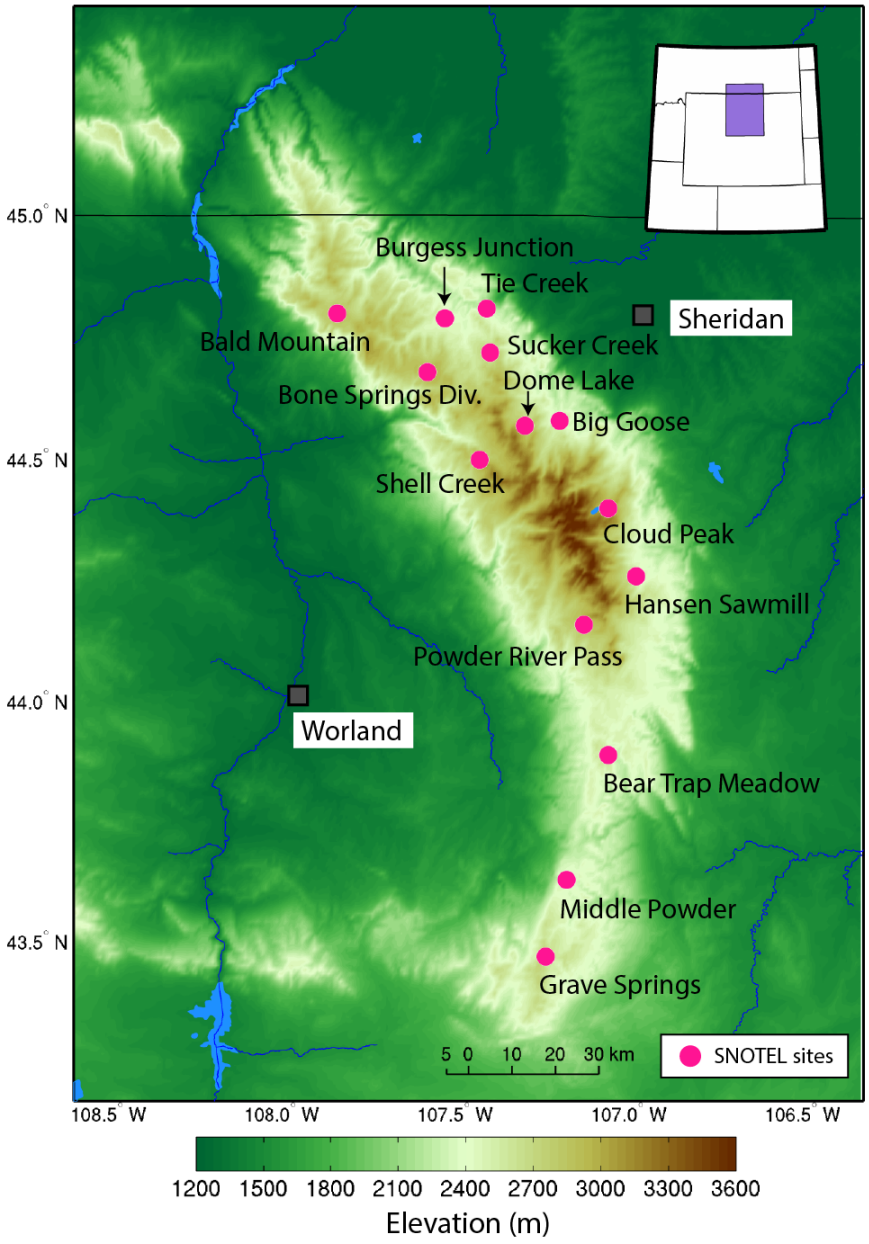


**Figure 4.1. SNOTEL site locations (magenta dots) in the Bighorn mountain range. Near-by towns are indicated by filled squares.**

### *4.1.2 Model*

Model data used to examine the climatology of the Bighorn Mountains came from a high-resolution (4 km) regional climate model (RCM) simulation performed over the Continental United States (CONUS) using the WRF model (Skamarock et al. 2005). The simulation was performed for a period from 1 October 2000 to 30 September 2013. However, the analysis presented herein focuses on the first eight water years in this simulation because the complete 13-year simulation was not yet complete at the time that this climatology analysis was performed. The WRF-CONUS model simulation (hereafter,

WRF-CONUS) was carried out as a follow-up study to a preceding high-resolution RCM study discussed in Rasmussen et al. (2014). The WRF-CONUS outputs are currently used in a number of climate studies. Figure 4.2 shows the WRF-CONUS model domain, and Table 4.1 lists the key model physical parameterizations used. The model was forced with 6-hourly European Reanalysis (ERA) Interim reanalysis data, and spectral nudging was used in the upper levels of the model atmosphere. See Liu et al. (2016) for a full description of the simulation setup, as well as simulated precipitation and temperature validation against observations over the model domain.

The model output is 3-hourly; therefore, any model results involving conditions for a single model output will be in terms of 3-hour periods. This does not imply that conditions were uniform within the 3-hour period, only that finer temporal analysis is not possible with this model output. Further, discussion concerning total fractions of modeled wintertime hours is also relative to the total number of 3-hour periods in a winter season.

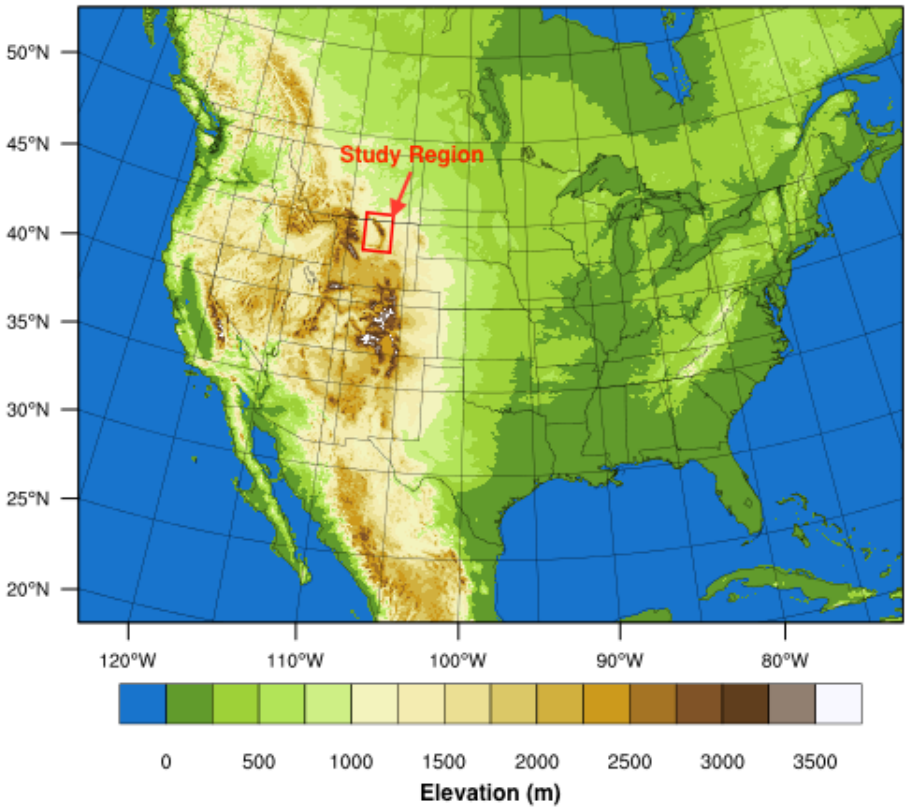


**Figure 4.2. WRF-CONUS model domain and elevation. Red box indicates the region of the Bighorn Mountains where the analysis focuses. For a close-up image of the study region see Figure 4.1.**

Table 4.1. WRF model physics options.

| WRF physics | Parameterization schemes | References |
|---|---|---|
| Land surface | Noah-MP (muti-physics) Land Surface Model | Niu et al. (2011) |
| Microphysics | Thompson aerosol-aware mixed phase scheme | Thompson and Eidhammer (2014) |
| Planetary boundary layer | Yonsei University PBL | Hong et al. (2006) |
| Longwave and shortwave radiation | RRTMG | Iacono et al. (2008) |

To establish a basis for using the model data for this study, the model data were compared to measurements from 14 SNOTEL sites in the Bighorn Mountains (Figure 4.1), which had a continuous record during the model simulation period (Section 4.2.2). The model data at the SNOTEL sites were obtained by taking the inverse-distance weighted average of the four data points closest to each SNOTEL site. In addition, the regular atmospheric sounding data from the Riverton NWS office were compared to the model (Section 4.2.3).

### *Seeding Potential Analysis Methods*

Three methods were used to determine the seeding potential of the project area: a single site analysis of 700-hPa conditions, a spatial mapping of seeding potential, and an area-based analysis.

The single site analysis was performed to examine conditions at 700 hPa for individually selected grid points surrounding the target area. Since the 700-hPa pressure level intersects the crest of the mountain range, using the 700-hPa data for an area-based analysis is not possible. Rather, nine representative sites were chosen to assess 700-hPa temperature and wind conditions on all sides of the Bighorn Mountains (Figure 4.3). The four sites most representative of the region used for this report: Sheridan, Wyoming to the northeast of the range; Kaycee, Wyoming to the southeast; Worland, Wyoming to the southwest of the range; and Twenty Mile Creek, Wyoming to the northwest (Figure 4.3). Riverton, Wyoming was also assessed in order to include a comparison of observational data from the NWS sounding site. The modeled 700-hPa temperature and wind conditions at those single grid points were also assessed during simulated precipitation conditions. For the Sheridan single site analysis, precipitation was determined using the model output at the grid point closest to the Sucker Creek SNOTEL site; for Kaycee, the grid point nearest the Bear Trap Meadow SNOTEL site was used; for Worland, the grid point nearest the Shell Creek SNOTEL site, and for the Twenty Mile Creek site, the grid point nearest the Bone Springs SNOTEL site was used (Figure 4.3).

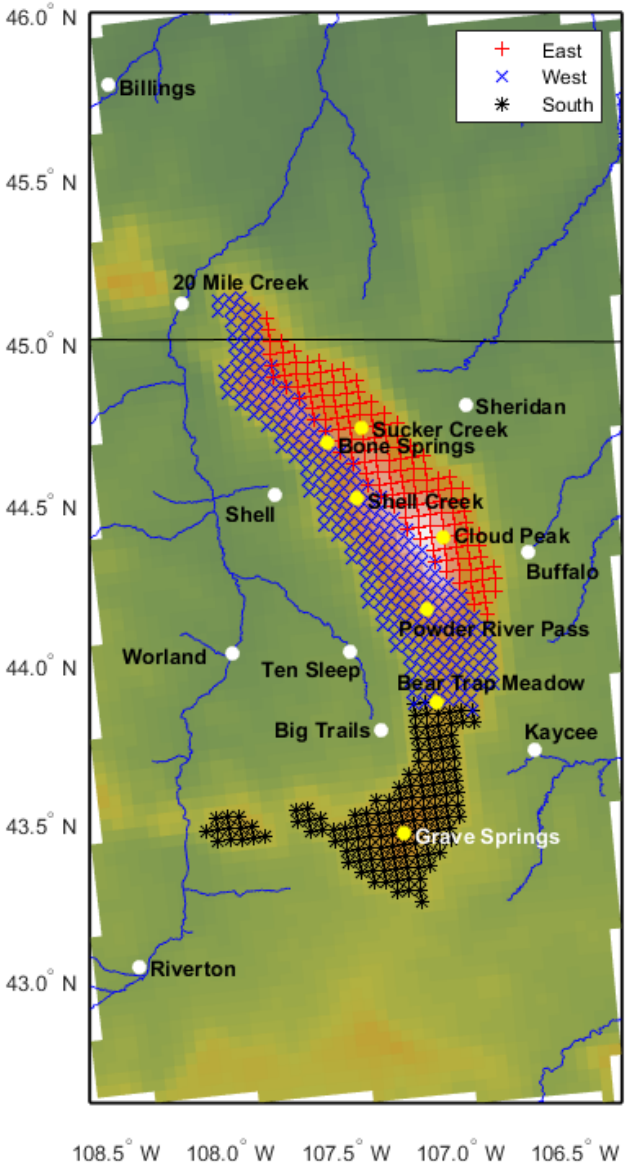


**Figure 4.3. Map of the model terrain height highlighting the grid points used in the seeding potential analysis along with other key sites where model output was analyzed. The west area is shown in blue, the east area in red, and the south area in black. Precipitation sites are marked by yellow circles. Sites used for analysis of 700-hPa conditions are marked by white circles.**

For the spatial mapping and area-based analyses, ground-based seeding potential was analyzed separately from airborne seeding potential using the vertical layer of the atmosphere under study. For ground-based seeding, the 0–1 km Above Ground Level (AGL) layer was investigated and each criterion assessed was averaged over that layer at every model grid point (4-km spacing) and output time (3-hourly). For airborne seeding potential, the 3.5–4.5 km MSL and the 4.5–5.5 km MSL layers were assessed by averaging each criterion over that vertical layer as was done for the ground-seeding layer.

Key criteria produced by the model output and utilized in this analysis were temperature, liquid water path (LWP; defined as column integrated liquid water per unit area), LWC mixing ratio, horizontal components of wind velocity (U and V) and derived stability parameters (e.g., square of Brunt-*Väisälä* frequency, Froude number, and Bulk Richardson number). Of these, the primary criterion used to indicate the presence of a cloud seeding opportunity was the presence of liquid water at temperatures appropriate for AgI activation. This leads to the following criteria for assessing whether cloud seeding is viable in a region:

- Temperature (−6 °C > T > −18 °C)
- LWP > 0.01 mm and/or
- LWC > 0.01 g $kg^{-1}$

The LWP criterion resembles information that would be available to an operational forecaster using a radiometer. In contrast, the LWC criterion identifies the vertical location of liquid water and thus can be used to discriminate ground from airborne seeding opportunities.

Meeting the above criteria indicates the potential for cloud seeding, whether ground-based or airborne. This potential can only be realized, however, if the seeding material reaches the regions where those criteria are satisfied. Because ground-based seeding requires the AgI plume to be carried over the barrier and into the suitable clouds, the inclusion of wind direction and atmospheric stability criteria are necessary. The requisite wind direction criteria varied by the region:

- For the west region, wind direction on the west side of the range between 225 and 330 degrees
- For the east region, wind direction on the east side of the range between 350 and 75 degrees
- For the south region, wind direction on the south side of the range between 270 and 350 degrees
- Froude number > 0.5

The wind direction criterion was based on the preliminary design of the ground-based seeding program after determining the dominant wind regimes affecting the target area. These additional criteria were not required for airborne seeding potential, given that an aircraft can introduce AgI directly into the atmosphere where seeding conditions occur, and the flight track can be oriented to account for wind direction.

Spatial maps were produced by utilizing the 3-hourly model output and mapping the frequency of 3-hour periods in a given time frame, such as monthly or seasonally, that the primary criteria were met at each grid point. This produced frequency of seedability maps at each grid point, for each month, and each season starting November 2000 and ending April 2008.

For the area-based analysis, western, eastern, and southern regions (Figure 4.3) were defined. In each region, areal-averaged values for each criterion (for both the ground and airborne seeding layers separately) were produced at every model output time (3-hourly). The same microphysical conditions assessed in the spatial mapping analysis (e.g., temperature and liquid water content in particular) were assessed over these regions by producing histograms of the areal-averaged values. Additionally, the frequency of time (in a given month or winter season) that the areal-averaged conditions met the thresholds defined above, was determined. In order to normalize the results by when precipitation occurred, a representative SNOTEL site for the given region was selected for each region. SNOTEL sites were selected that had a good comparison with the model (based upon the SNOTEL model evaluation, Section 4.2.2). The model grid point nearest that SNOTEL site was used to determine if precipitation occurred in that region or not.

Stability indices were also derived from the model output and analyzed to evaluate its impact on ground-based seeding potential. The primary index analyzed was the Froude number (Fr). The Froude number expresses the ability of upslope airflow to go over a mountain barrier. The flow will typically be blocked by the barrier when Fr < 0.5. The flow will freely move over the barrier (unblocked) when Fr > 1. Froude number is computed from

$$Fr = \frac{U/h}{N},$$

where $U$ is the average wind speed (m $s^{-1}$) perpendicular to the mountain barrier orientation over a depth of $h$ (in m), and $N$ is an average of the Brunt-Väisälä frequency between the same depth. In this case, $h$ is assumed to be 1000 m. $N$ ($s^{-1}$) is expressed as

$$N = \left( \frac{g}{T_v} \frac{\partial \theta_v}{\partial z} \right)^{1/2},$$

where $g$ is the gravitational acceleration (9.8 m $s^{-2}$), $T_v$ is the layer average virtual temperature (K), and $\partial \theta_v / \partial z$ is the vertical gradient of virtual potential temperature (K $m^{-1}$).

## 4.2 Characteristics of Wintertime Clouds and Precipitation

### *4.2.1 SNOTEL Precipitation Observations*

In this section, annual precipitation characteristics in the study area are presented using the SNOTEL precipitation data. Average monthly precipitation from 14 SNOTEL sites in each water year (panels a – h) and 8-year average (panel i) are shown in Figure 4.4. Table 4.2 lists annual precipitation and the fraction of annual precipitation that occurred in November–April. Of the years examined, the 2002–2003, 2004–2005, 2006–2007 and 2007–2008 water years were wetter years in terms of annual precipitation compared to the other four years. These years typically had strong precipitation in the spring months (March–May). In most years, the peak precipitation fell in the spring, with a secondary maximum in precipitation amounts observed in the autumn (October).

Of the four years with the highest *annual* precipitation, the November–April precipitation amounts were also high in three of those water years (i.e., 2002–2003, 2006–2007, and 2007–2008). In 2004–2005, however, the high annual precipitation was driven by strong precipitation in May, but the first part of the winter (November–February) period was quite dry. From November through April, the Bighorn Mountains tends to receive about half, if not just less than half, of its annual precipitation (Table 4.2).

In Wyoming, a single snowstorm can bring heavy snowfall and the month of maximum wintertime precipitation is heavily dependent on when such large snowstorms occur (e.g., March 2003). Furthermore, a large weather system in late spring can bring snowfall at high elevations and rainfall at lower elevations. For example, a single storm in May 2007 produced rain at lower elevations of the Bighorns, while snow fell across higher elevations where temperatures below freezing persisted (and where SNOTEL sites are located, see Figure 4.4). Similarly, the precipitation that occurred during the peak periods of May 2005 and 2008 was snowfall at high elevations. Typically, peak snowpack based on co-located snow pillow measurements at these sites occurs anytime between early April and late May, revealing that wintertime and early spring snowfall is an important source for water in this region.

Figure 4.5 shows the spatial distribution of the November–April precipitation at SNOTEL sites in each of the eight winter seasons. Overall, there is no evidence of a significant precipitation gradient existing between the sites on the western and eastern slopes of the mountains. Three sites located in the southern part of the range (Bear Trap Meadow, Middle Powder, and Grave Springs) tend to receive less precipitation than their northern counterparts. These three sites are also located at a lower elevation than the rest (Figure 4.1). Interestingly, the northern-most sites tend to have the most wintertime precipitation, which does not correlate with the areas of highest elevation.

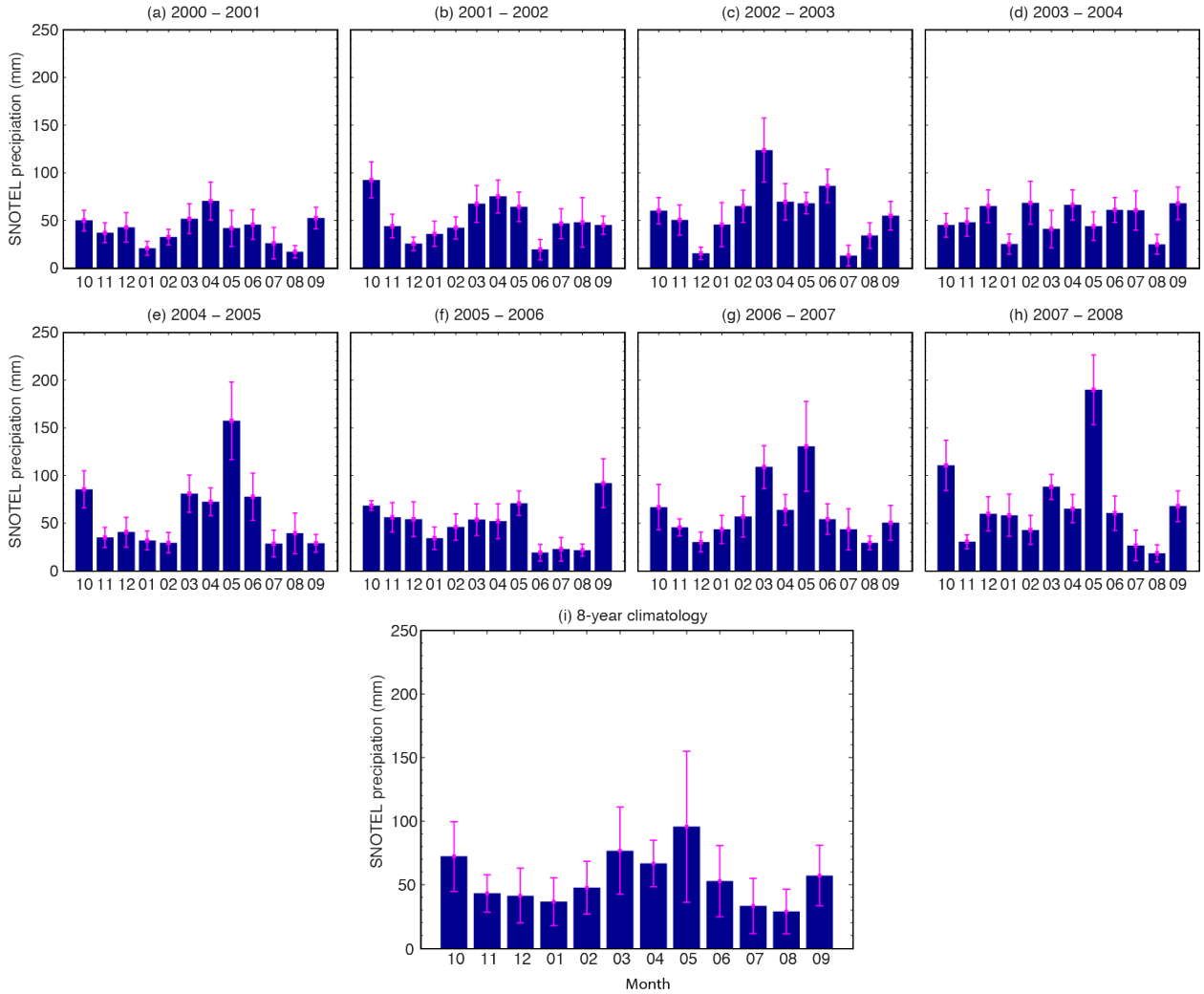


**Figure 4.4. (a) – (h) Monthly observed precipitation averaged from 14 SNOTEL sites in the study area in each water year. (i) The 8-year climatology of monthly SNOTEL-observed precipitation. Magenta vertical bars indicate +/– one standard deviation from the areal average, indicating spatial variability.**

**Table 4.2. Average annual precipitation from SNOTEL sites and the fraction of the annual precipitation that fell between 1 November and 30 April in each water year.**

| Water year | Annual precipitation (mm) | November – April precipitation (mm) | Fraction of November – April precipitation (%) |
|---|---|---|---|
| 2000 – 2001 | 485.7 | 252.6 | 52 |
| 2001 – 2002 | 603.0 | 289.4 | 48 |
| 2002 – 2003 | 683.7 | 369.2 | 54 |
| 2003 – 2004 | 614.8 | 313.5 | 51 |
| 2004 – 2005 | 704.6 | 288.9 | 41 |
| 2005 – 2006 | 587.4 | 293.7 | 50 |
| 2006 – 2007 | 721.2 | 346.2 | 48 |
| 2007 – 2008 | 815.9 | 342.7 | 42 |
| 8-year climatology | 651.4 | 312.7 | 48 |

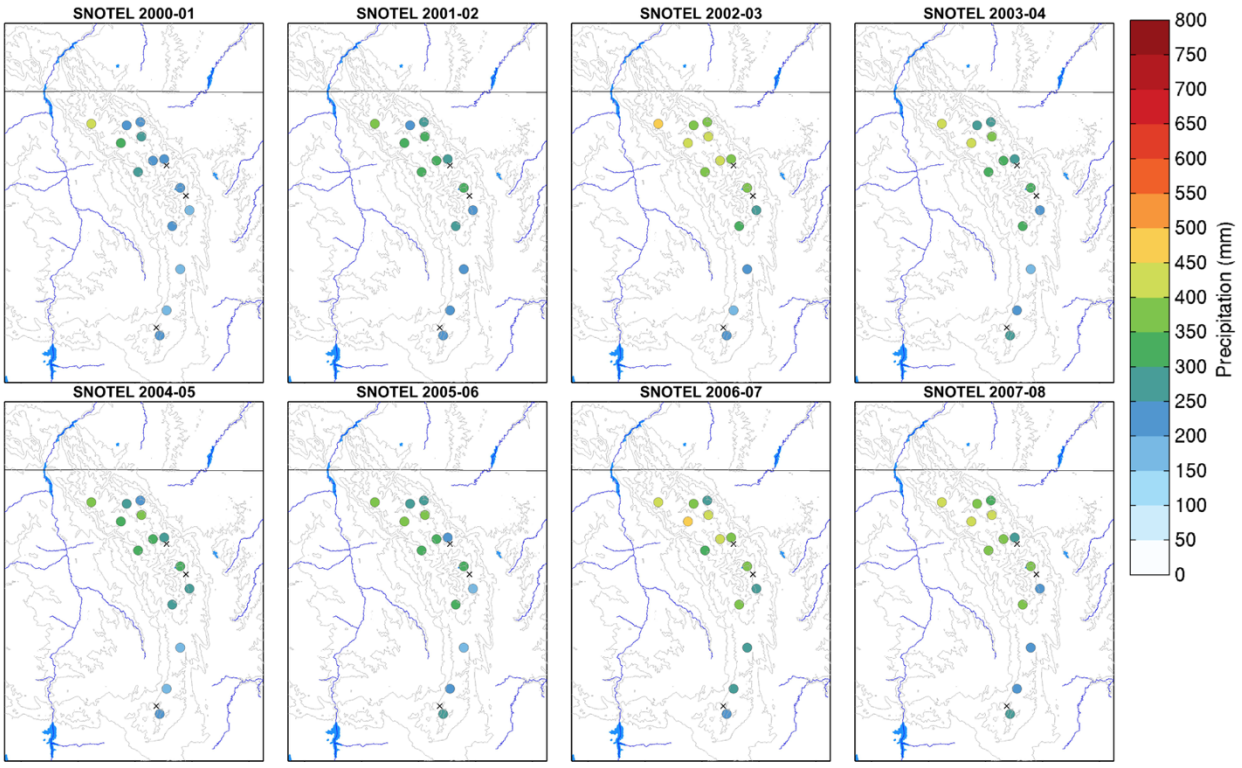


**Figure 4.5. The November – April precipitation at SNOTEL sites in each water year. Contours indicate elevation. The color scale is intended to match the range of model precipitation shown in Figure 4.9.**

To determine if any relation in the precipitation pattern exists between different parts of the Bighorn Mountains, the temporal correlation coefficient of daily SNOTEL precipitation was computed from 1 November–30 April over the 8-year period. Figure 4.6 shows the correlation coefficient between every pair of SNOTEL sites. Bright colors indicate high correlation in daily precipitation between a given pair of sites. The correlation coefficients for each season (November–April) are given in Figure 4.7. On these plots, site names for the sites in the western, eastern, and southern parts of the Bighorn Mountains are highlighted in black, blue, and red, respectively.

The 8-year seasonal correlation coefficient of daily precipitation (Figure 4.6) highlights that precipitation at the southern sites are not well correlated with precipitation at sites in the north or the western and eastern slopes. There is, however, a consistency between nearby sites that are on the same slope of the Bighorns. While this trend is evident on both slopes of the range, stronger correlations are found on the eastern slopes (e.g., Burgess Junction and Sucker Creek, Big Goose, and Tie Creek/Dome Lake). On the western slope, the highest correlation coefficient is seen between Bald Mountain and Bone Spring Divide—the two northern-most sites. Although the correlations are much lower than in the north, the southern sites are correlated among each other as well.

Similar correlations can be found between sites on different sides of the mountains. Shell Creek and Dome Lake are examples of such a case for all years except in 2007 – 2008. These two sites sit close to each other with the peak of the mountains in between. Bone Spring Divide's precipitation is fairly well correlated with precipitation at Burgess Junction, Tie Creek, and Sucker Creek—three sites on the eastern side across from Burgess Junction. The correlation coefficient between Powder River Pass and Cloud Peak/Hansen Sawmill (also close by on either side of the mountains.) is fairly high. The relationship between the "cross-mountain barrier" pairs of SNOTEL sites results from westerly weather systems. There is a year-to-year variability in correlation coefficient values (Figure 4.7), but the general pattern observed from the 8-year seasonal correlation coefficient can be seen in most individual years. The year-to-year variability is related to a number of factors such as dominant wind regimes and amount of snowfall associated with snow-producing events. In particular, strong and widespread snowstorms would result in a high correlation coefficient among all pairs, while drier November – April seasons yield low correlation coefficients (e.g., 2000–2001). In particular, the 2002–2003 and 2006–2007 seasons have very strong correlations for sites on the eastern slopes. These two years also happened to have a prominent peak in wintertime (November–April) precipitation in March, so these years could have been affected by a few strong and widespread easterly upslope storms.

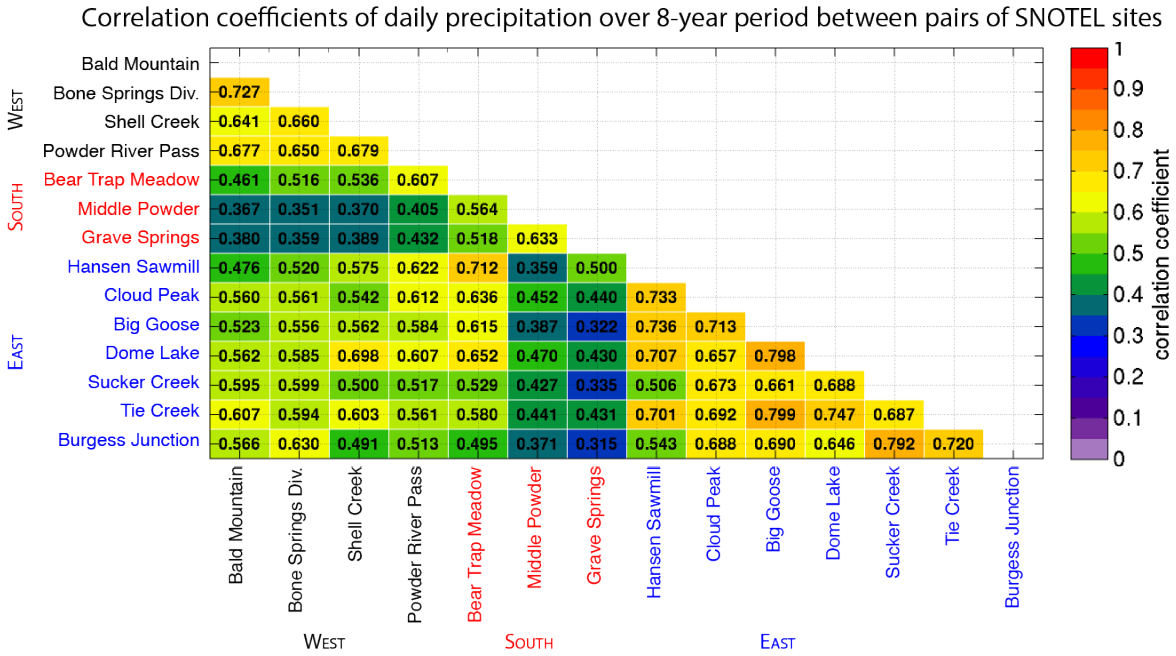


**Figure 4.6. Temporal correlation coefficients of daily precipitation over eight years at each pair of SNOTEL sites based on the November – April measurements from eight water years. Site names in black, red, and blue indicate sites in the western, southern, and eastern regions of the Bighorn Mountains.**

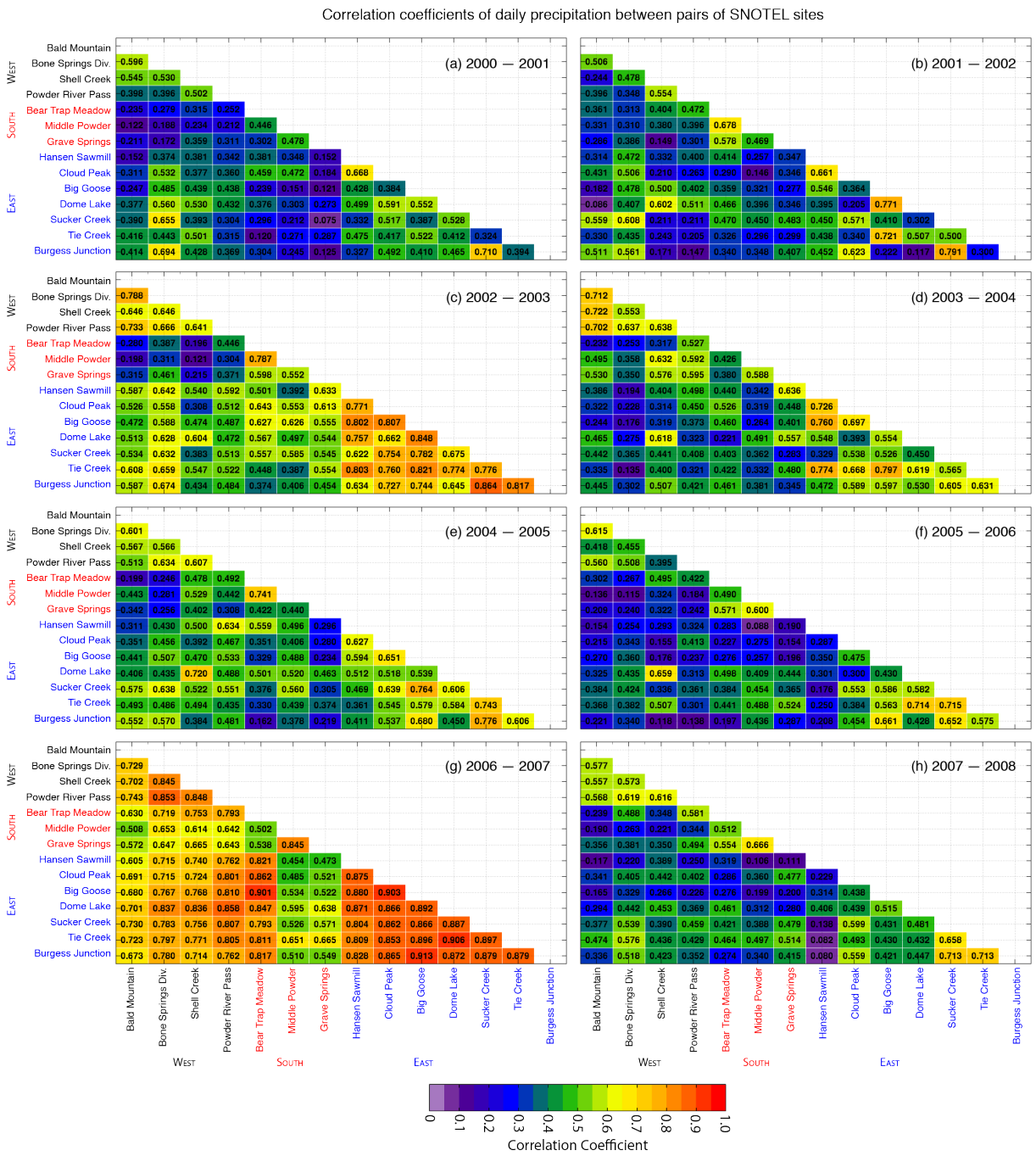


**Figure 4.7. Same as Figure 4.6 but for each water year.**

### *4.2.2 Comparison of model vs SNOTEL*

The WRF-CONUS model provides a more complete view of the precipitation distribution in the Bighorn Mountains. The 8-year average November–April map compares fairly well with the model, although the model overestimates at a few higher elevation sites. The model indicates two precipitation accumulation maximums: one at the Cloud Peak (highest elevation) area and one in the northern-most extent of the mountains (Figure 4.8). The maximum precipitation along the highest elevations of the Bighorn Mountains is expected and common in other mountainous regions. However, the simulated precipitation

maximum in the northern-most part of the mountains, at the Montana-Wyoming state border, is a feature unique to this mountain barrier. Unfortunately, there are no SNOTEL sites in this region to verify the model results, but the SNOTEL analysis did indicate that in most years the northern-most sites received the greatest amounts of precipitation, despite not being at the highest elevation of the mountain range.

Figure 4.9 shows the spatial distribution of the November–April precipitation from the WRF-CONUS simulation results for each winter season (recall Section 4.1.2). In general, the model simulated the observed precipitation pattern at SNOTEL sites well (compare with Figure 4.5). The spatial correlation of the seasonal total precipitation from the model at the corresponding SNOTEL location ranged from 0.70 to 0.85 over the eight individual November–April seasons (sample size of 5 months x 14 sites in each winter season). Averaged over the eight seasons, the spatial correlation coefficient was 0.83.

The months of November–February are much drier than the months of March–May and even October (Figure 4.10). The precipitation over the eastern Plains primarily comes from these latter months, while the precipitation remains confined to the mountain barrier in the November–February time period.

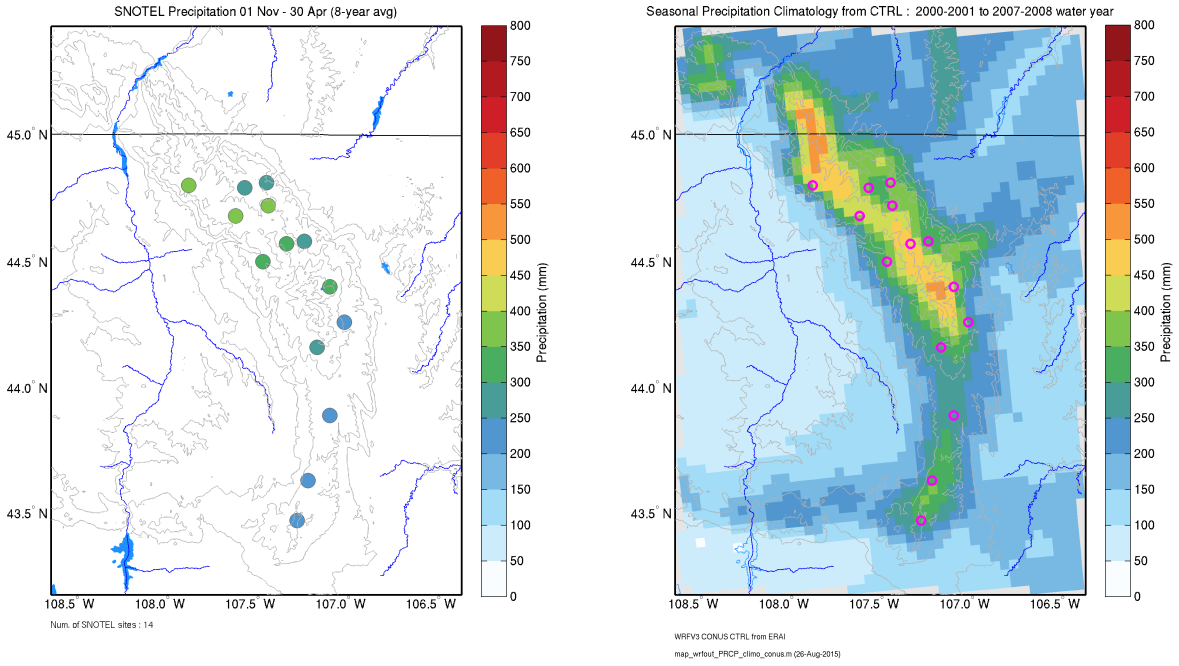


**Figure 4.8. Map of the 8-year average accumulated wintertime precipitation (mm) between November–April from SNOTEL (left) and the WRF-CONUS model (right).**

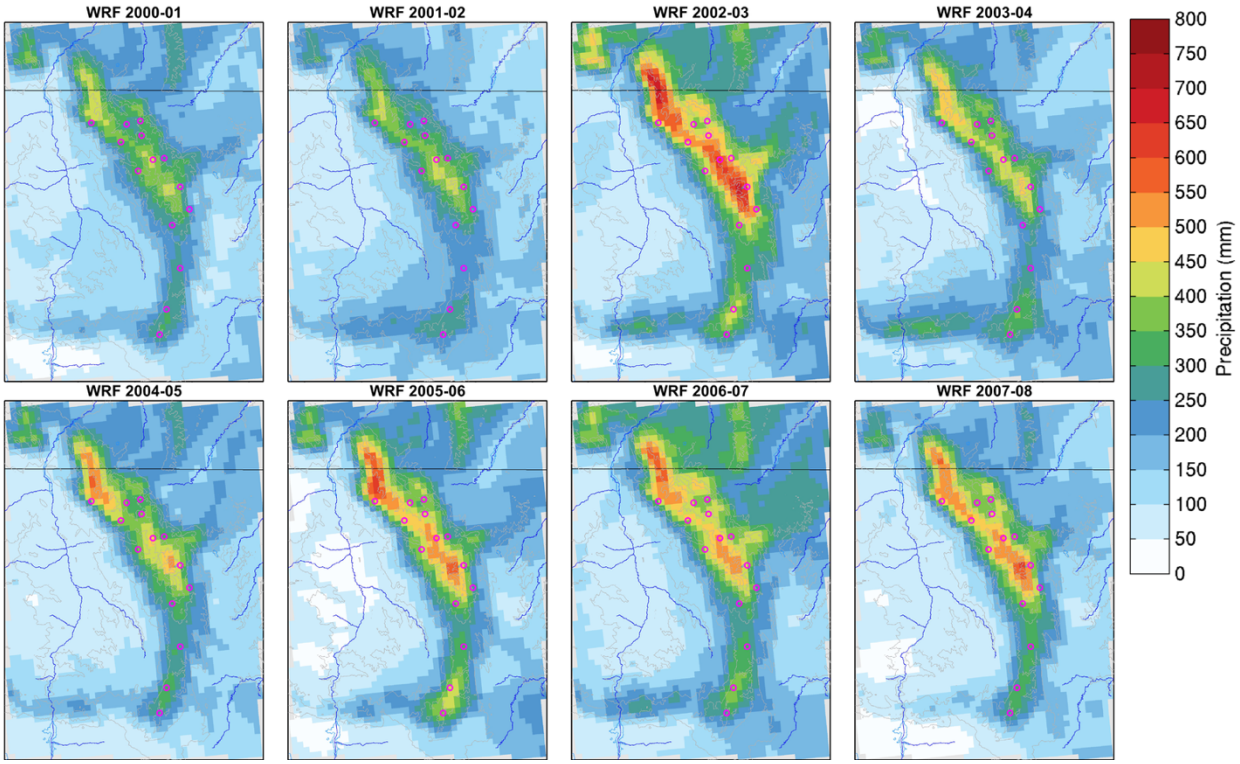


**Figure 4.9. The November – April precipitation in each water year from the WRF-CONUS model simulation. Magenta circles mark the SNOTEL site locations.**

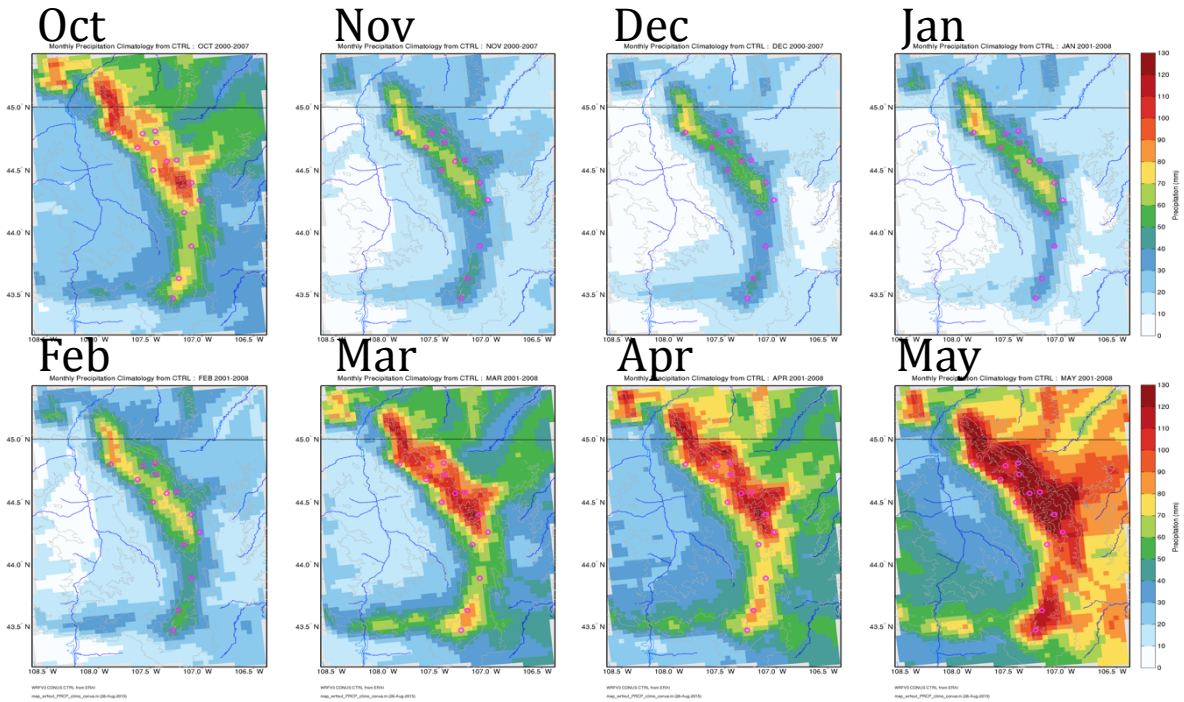


**Figure 4.10. Maps of 8-year average monthly precipitation accumulation (mm) from the WRF-CONUS model for the months of October to May.**

The ability for the model to reproduce observed precipitation at each site is demonstrated by Figure 4.11. The figure shows the 8-year climatology of precipitation accumulation from the model, and observations at each SNOTEL site. The agreement between the WRF-CONUS model and observations are nearly perfect for many sites during the potential seeding season (November–April, grey-shaded in Figure 4.11). However, sites such as Bald Mountain, Bear Trap Meadow, and Middle Powder indicate that the model overestimated precipitation. At these sites, the bias was not systematic in all simulation years.

The annual precipitation accumulation comparison from each simulation year, averaged over all SNOTEL sites, also shows that the model simulated winter (November–April) snowfall very well (Figure 4.12). Perhaps the only year that the model slightly overestimated the seasonal precipitation at SNOTEL sites is 2005–2006, in which the bias at Bald Mountain and Middle Powder was large (not shown; systematic bias was not from any single storm). As a result, the 8-year, 14-site average precipitation shows very good agreement between the model and observations (Figure 4.13).

While it occurred outside of the seeding season (November–April) and is therefore not related to the purpose of this study, the model's overestimation in annual total precipitation generally came from summertime precipitation.

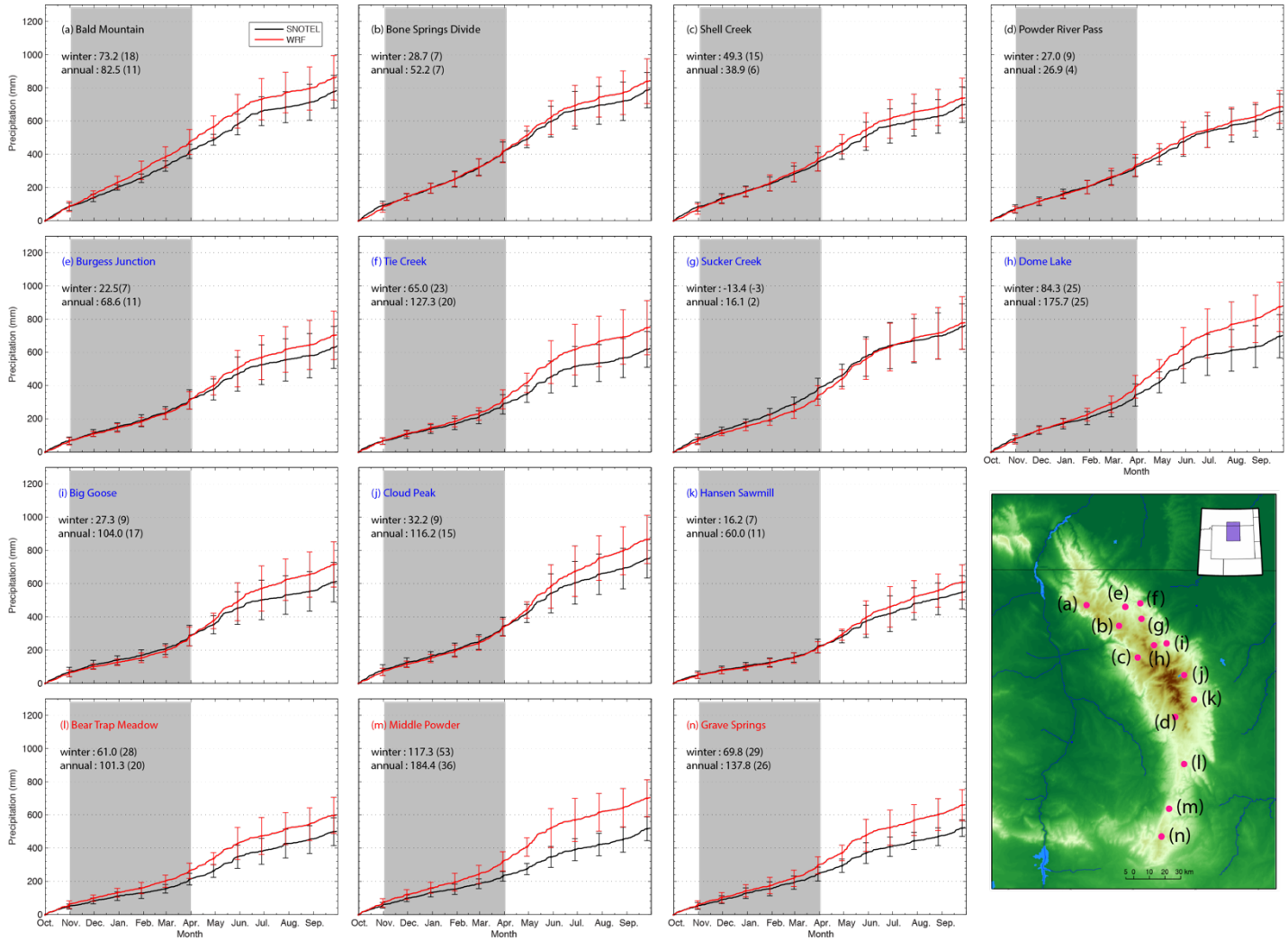


**Figure 4.11. 8-year average of annual precipitation accumulation at each SNOTEL site (SNOTEL in black, model in red). Vertical bars are one standard deviation about the 8-year mean. The difference (in mm) between the model and SNOTEL precipitation observations for November–April (winter) and the full year is indicated in the upper left corners. Values in parentheses indicate percent bias in the seasonal and annual biases with respect to the observations. Refer to the inlay map for the SNOTEL site locations.**

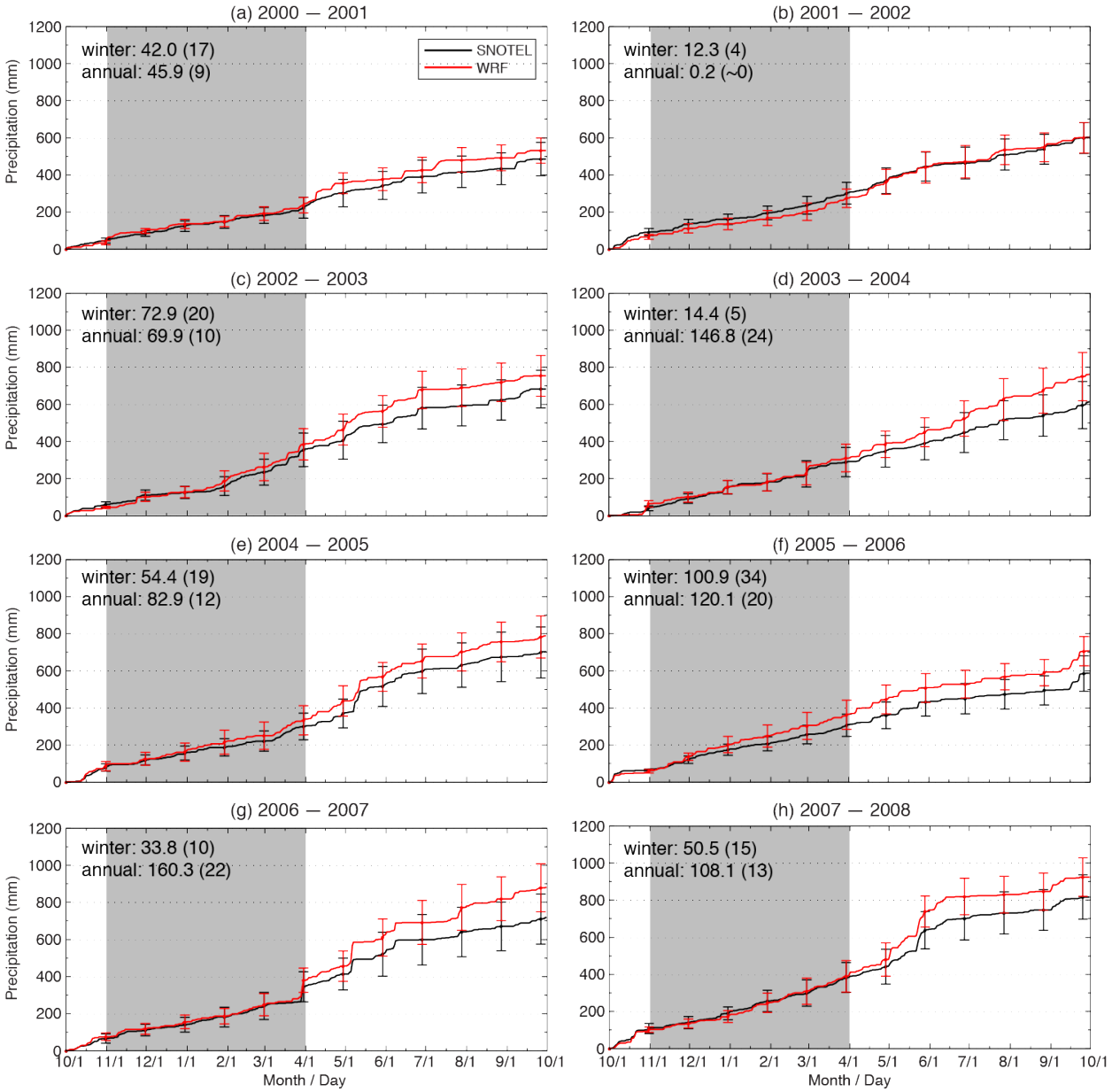


**Figure 4.12. Time history of observed and simulated precipitation accumulation averaged over SNOTEL sites in each water year. The difference (in mm) between the model and SNOTEL precipitation observations for November–April (winter) and the full year is indicated in the upper left corners. Values in parentheses are the percent bias from the observations. The biases are taken as model minus observation. Vertical bars present +/– one standard deviation from the areal mean, indicating spatial variability.**

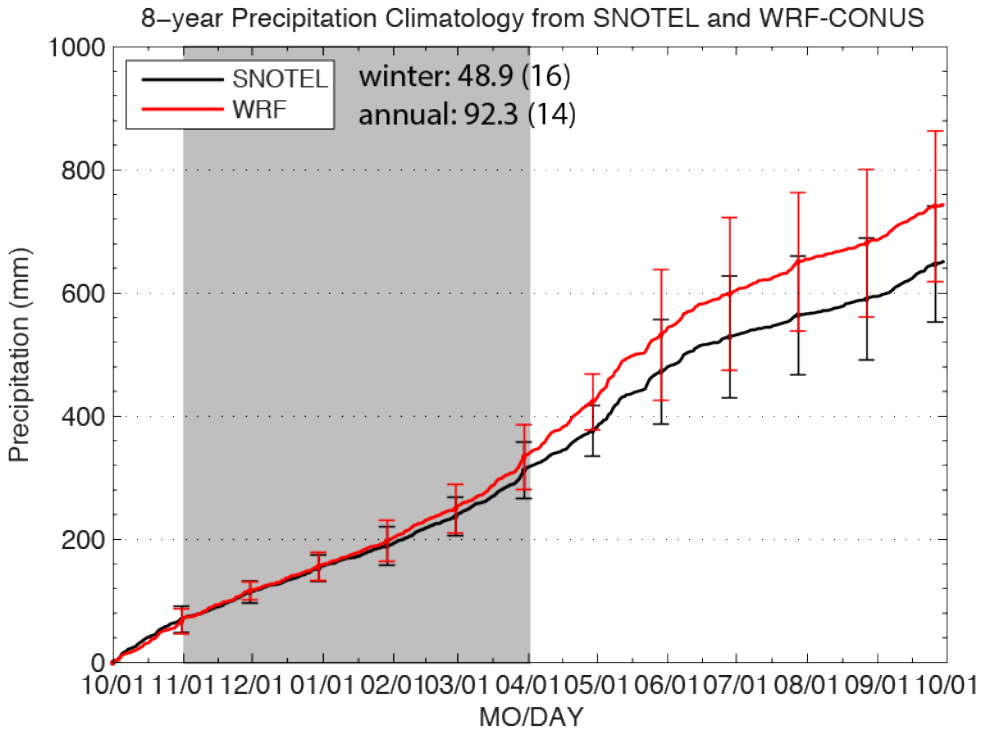


**Figure 4.13. The 8-year climatology of precipitation accumulation averaged over the SNOTEL sites in the study region. Vertical bars are one standard deviation from the 8-year mean, representing the year-to-year variability. The model bias in November – April (grey shaded) and annual precipitation (in mm) is indicated in the upper right corner. Values in parentheses are the percent bias from the observations. The biases are taken as model minus observation.**

### *4.2.3 Riverton Sounding Analysis*

A single site analysis was performed using eight years of observational data from NWS soundings at Riverton and observed daily precipitation data from the Grave Springs SNOTEL site within the time period of the model analysis (see below). This analysis shows that the observed predominant 700-hPa wind direction was northwesterly and westerly on days when precipitation occurred at Grave Springs (Figure 4.14a). Additionally, the observed 700-hPa temperature conditions at Riverton ranged from 10 °C to −24 °C for the winter season and 6 °C to −18 °C for precipitating events (Figure 4.15a). Around 60% of wintertime hours were warmer than −6 °C, dropping to roughly 45% for hours with precipitation.

The model-based Riverton wind rose is similar to that from the observations (Figure 4.14b), showing that northwesterly winds are dominant when precipitation occurs at the Grave Springs SNOTEL. The model-based wind rose shows slightly more of a north-northwesterly regime than the observations. The model results of temperature distribution at Riverton compare nearly identically with that observed by the NWS sounding at Riverton, but the distribution of temperature during precipitation events shifted to colder temperatures in the model, with only about 30% of model output hours (compared to ~50% of soundings) with precipitation having 700-hPa temperatures warmer than −6 °C (Figure 4.15b).

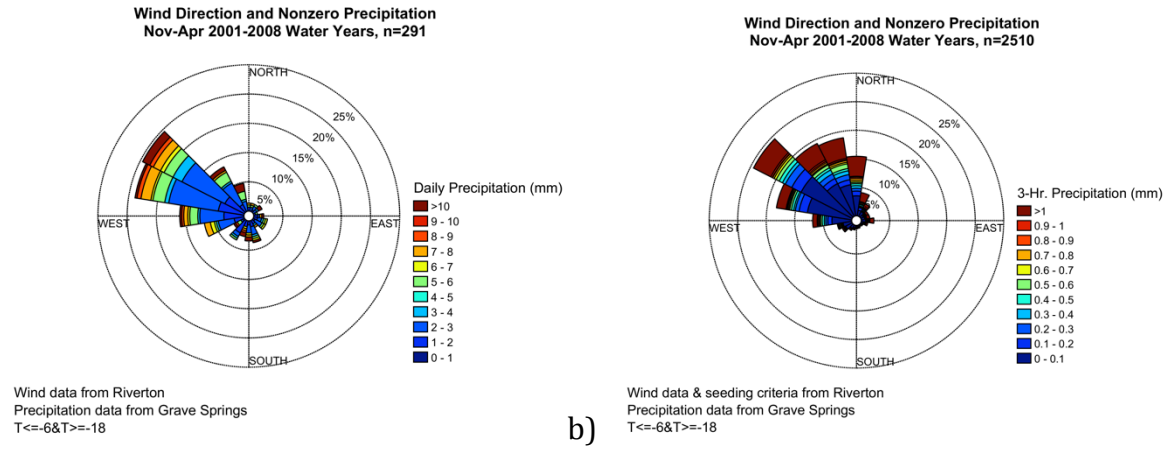


**Figure 4.14. Wind rose showing the frequency of (a) observed and (b) modeled 700-hPa wind direction over Riverton, Wyoming when precipitation occurred over the Bighorn Mountains, using daily observed data from the Grave Springs SNOTEL site in (a) and three-hourly modeled precipitation at Grave Springs in (b), over the 8-year period from November–April. The magnitude of daily observed or 3-hourly modeled precipitation for each wind direction is indicated by the color within each wind direction bin.**

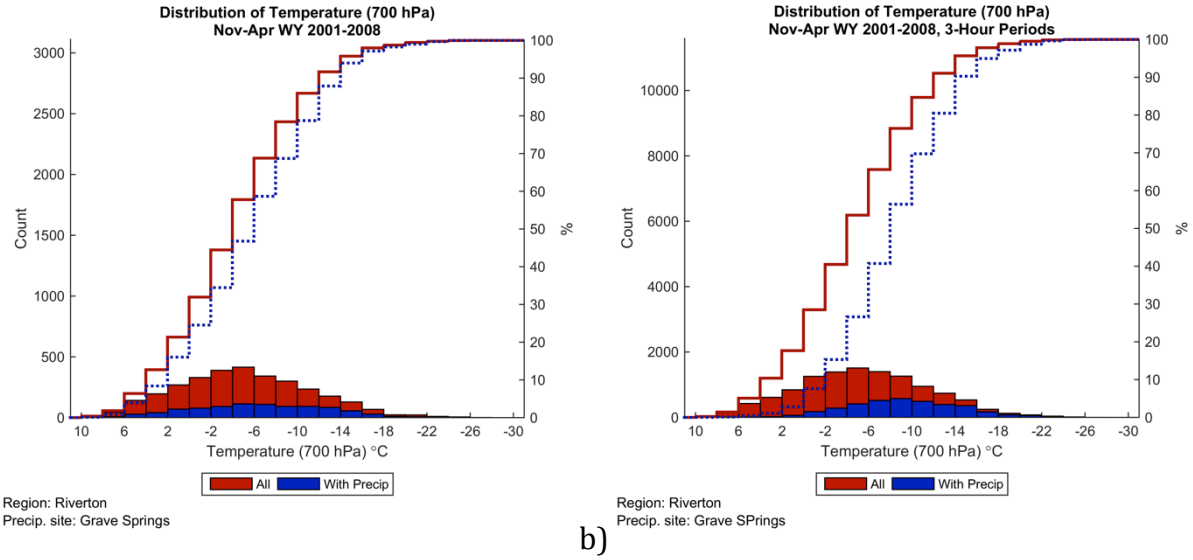


**Figure 4.15. Histogram counts (left ordinate) of the (a) observed and (b) modeled 700-hPa temperature at Riverton, Wyoming. In (a), it is shown for all soundings (red) from November–April during the 8-year period of study (water years 2001–2008) and for all soundings that had precipitation observed at the Grave Springs SNOTEL site (blue); in (b) counts of modeled 700-hPa temperature at Riverton, Wyoming for all three-hour model periods (red) and three-hour model periods with modeled precipitation at the Grave Springs SNOTEL site (blue). Cumulative distributions for all (red) and with precipitation (blue dotted) are also overlaid using the right ordinate (%).**

### *4.2.4 Model-based Analysis Results*

#### *Single Site Analysis*

Single-site analysis for Sheridan, Kaycee, Worland, and Twenty Mile Creek shows that the predominant 700-hPa wind direction when precipitation occurs and during seedable conditions (LWP > 0.01 mm, −6 °C < T < −18 °C) in the WRF-CONUS simulations is northwesterly (Figure 4.16–Figure 4.19). The Sheridan site shows a small number of highly precipitating events with northerly and north-northeasterly winds (Figure 4.16). While still predominantly northwesterly, roughly a quarter of the precipitating events at the Kaycee

site have winds with an easterly component (Figure 4.17). The Worland site indicates seedable precipitating events can also often have westerly and occasionally some southwesterly 700-hPa winds (Figure 4.18). The sites closest to the mountain range, especially on the west slope (i.e., Big Trails, Ten Sleep, and Shell), indicated very prominent northwesterly winds, with very little westerly component. The winds at these sites may have been influenced by blocking from the mountain barrier, causing westerly winds to turn south and flow more northwesterly along the barrier. This is why sites, such as Worland, that are located a bit farther from the barrier, were analyzed.

The 700-hPa winds during precipitation events have small variations from month to month at the northern sites (Sheridan and Twenty Mile Creek, as illustrated in Figure 4.22 and Figure 4.23), with the winds being largely northwesterly. Monthly analysis at the Kaycee and Sheridan sites shows increasing frequency of the northeasterly winds during precipitation events in the latter half of the winter season (Figure 4.20, Figure 4.21). Specific to Kaycee is a small amount of high precipitation events with southeasterly winds in January and April (Figure 4.21); since these events are relatively sporadic as opposed to following any kind of temporal trend, it does not support designing a fixed-asset seeding program (i.e., ground generators) to target them. Winds at Twenty Mile Creek have a small southwesterly component evident towards the end of the winter season (Figure 4.23). In Worland, the winds have more of a westerly component during seedable precipitation events, especially during the strongest precipitation events in January–February (Figure 4.22).

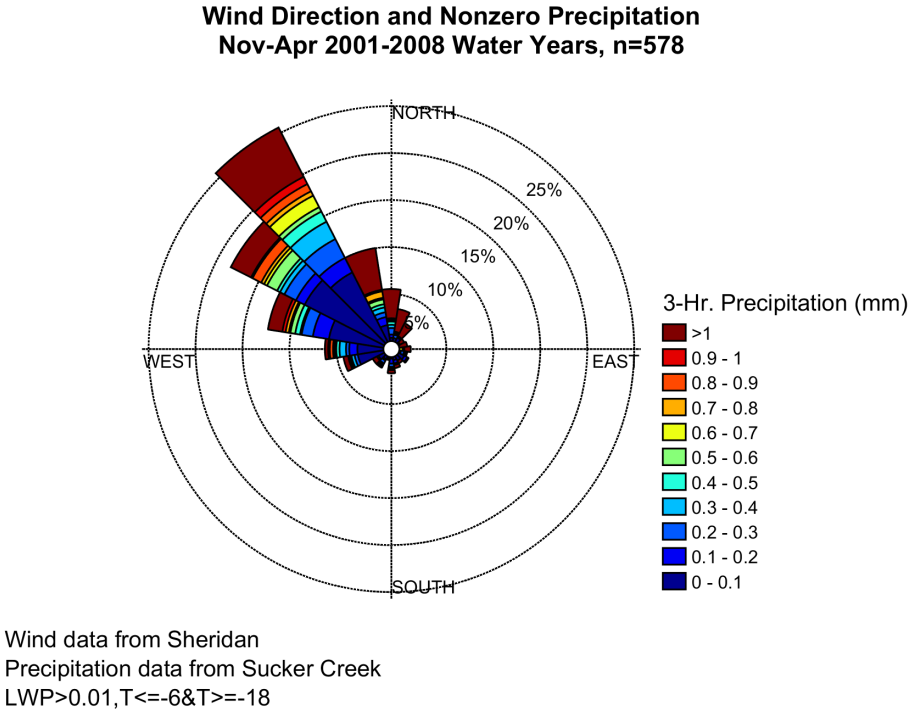


**Figure 4.16. Wind rose showing the frequency of modeled 700-hPa wind direction over Sheridan, Wyoming when precipitation occurred over the Bighorn Mountains (using the Sucker Creek SNOTEL site) over the 8-year period from November–April. The magnitude of precipitation per 3-hourly model output time for each wind direction is indicated by the color within each wind direction bin.**

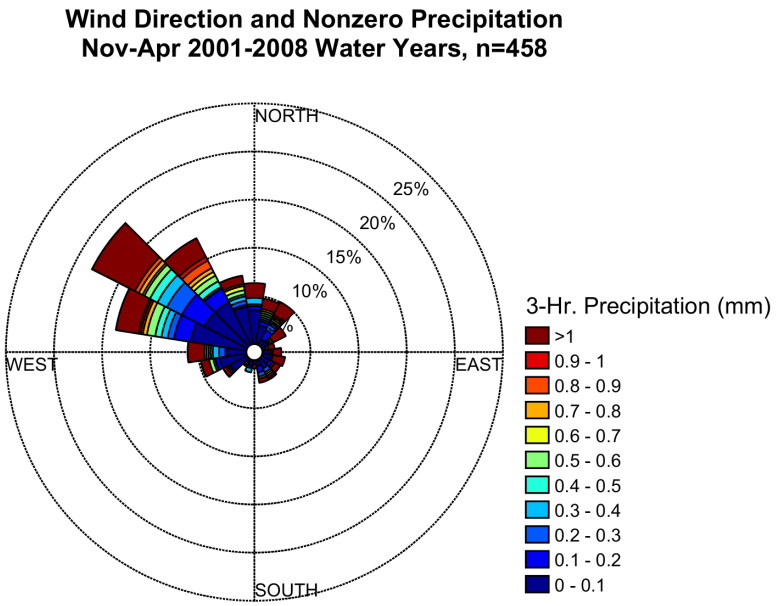


Wind data from Kaycee
Precipitation data from Bear Trap Meadow
LWP>0.01,T<=-6&T>=-18

**Figure 4.17. As in Figure 4.16, except for modeled 700-hPa winds over Kaycee when precipitation occurred at the Bear Trap Meadow SNOTEL site.**

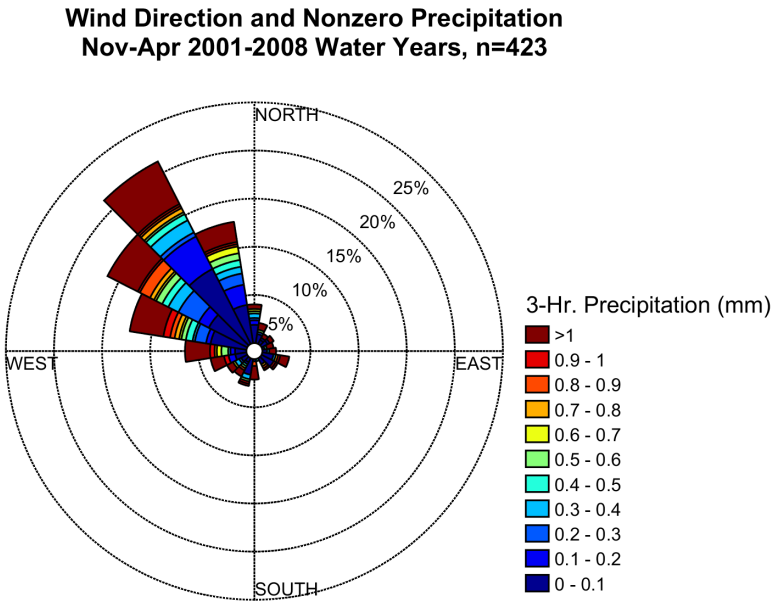


Wind data & seeding criteria from Worland
Precipitation data from Shell Creek
LWP>0.01,T700MB<=-6&T700MB>=-18

**Figure 4.18. As in Figure 4.16, except for modeled 700-hPa winds over Worland when precipitation occurred at the Shell Creek SNOTEL site.**

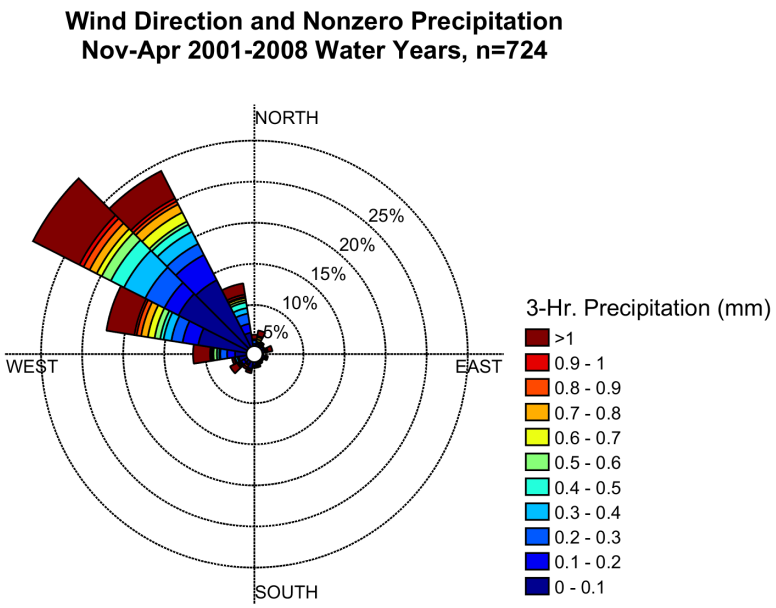


**Figure 4.19. As in Figure 4.16, except for modeled 700-hPa winds over Twenty Mile Creek when precipitation occurred at the Bone Springs SNOTEL site.**

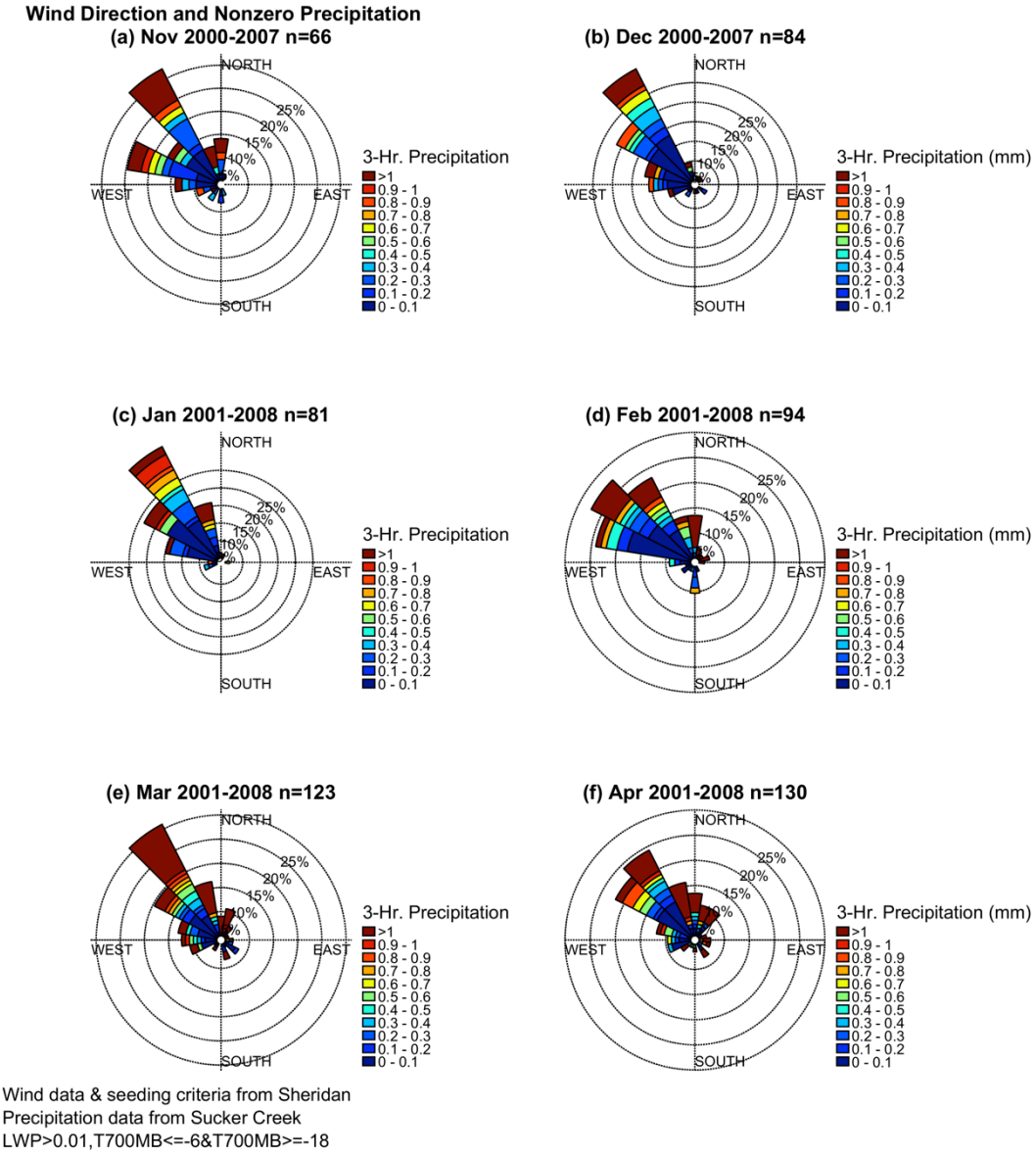


**Figure 4.20. Month-by-month model wind roses of 700-hPa wind direction over Sheridan during model hours with seedable conditions and precipitation at the Sucker Creek SNOTEL site from November–April.**

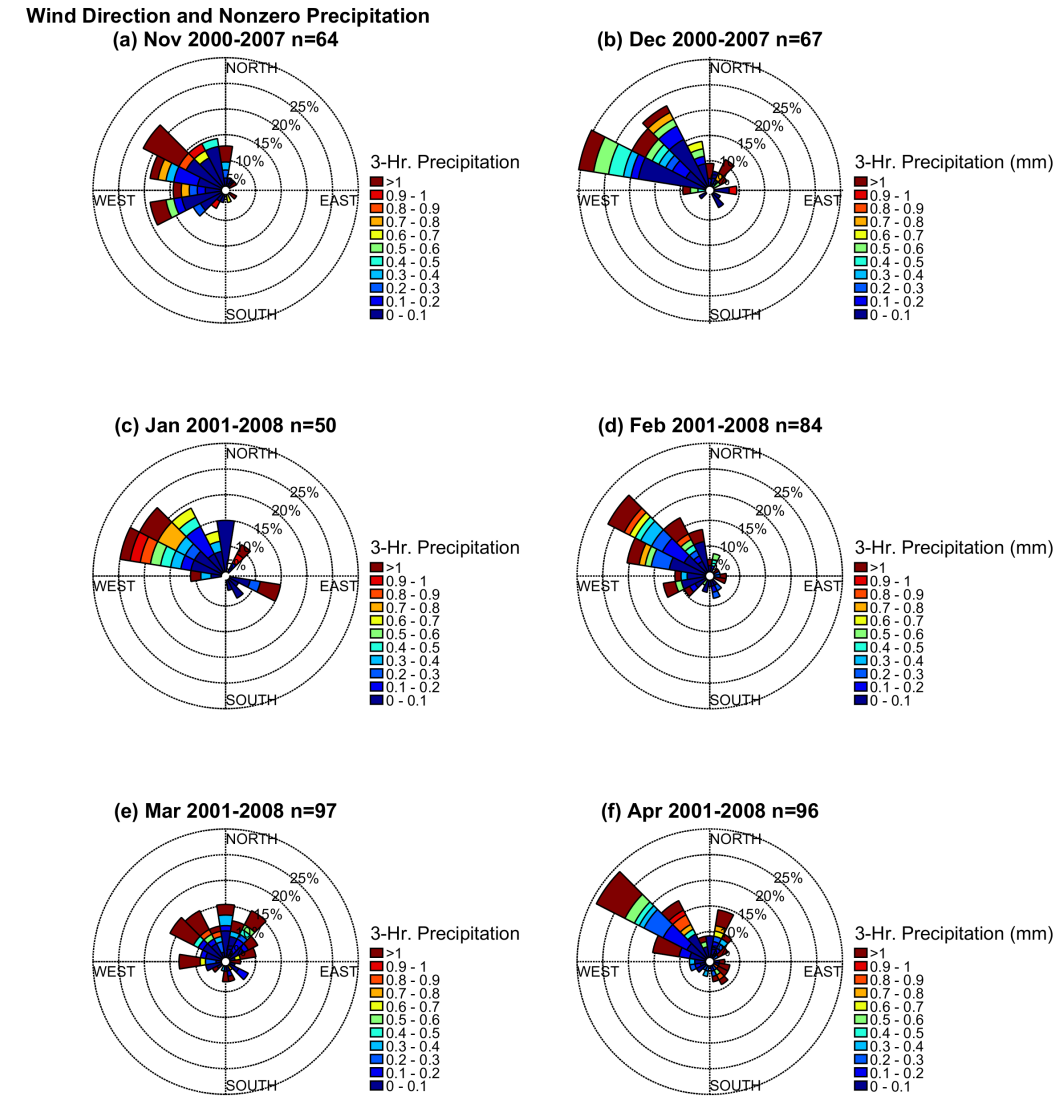


**Figure 4.21. As in Figure 4.20, but for model winds over Kaycee and precipitation at the Bear Trap Meadow SNOTEL site.**

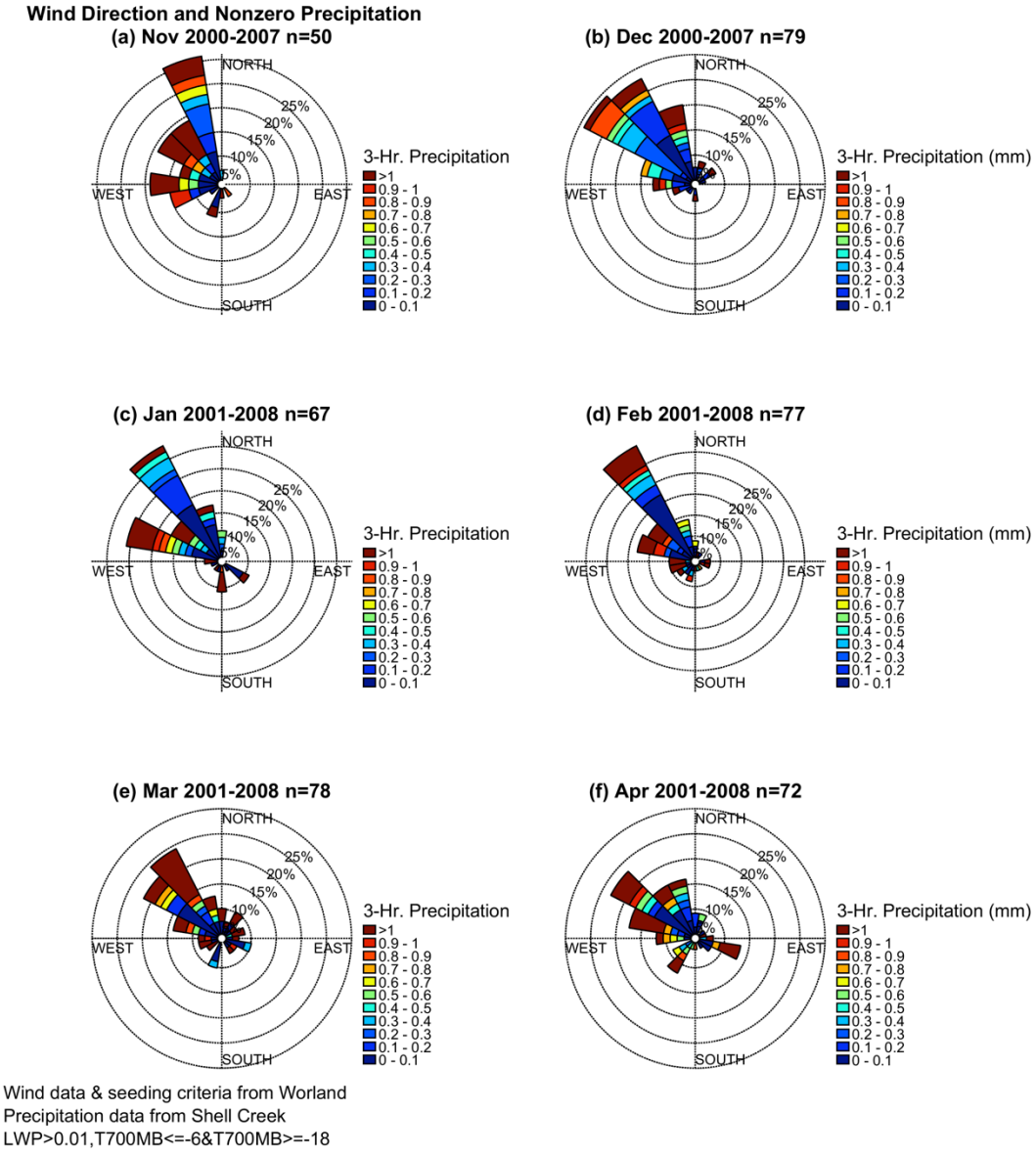


**Figure 4.22. As in Figure 4.20, but for model winds over Worland and precipitation at the Shell Creek SNOTEL site.**

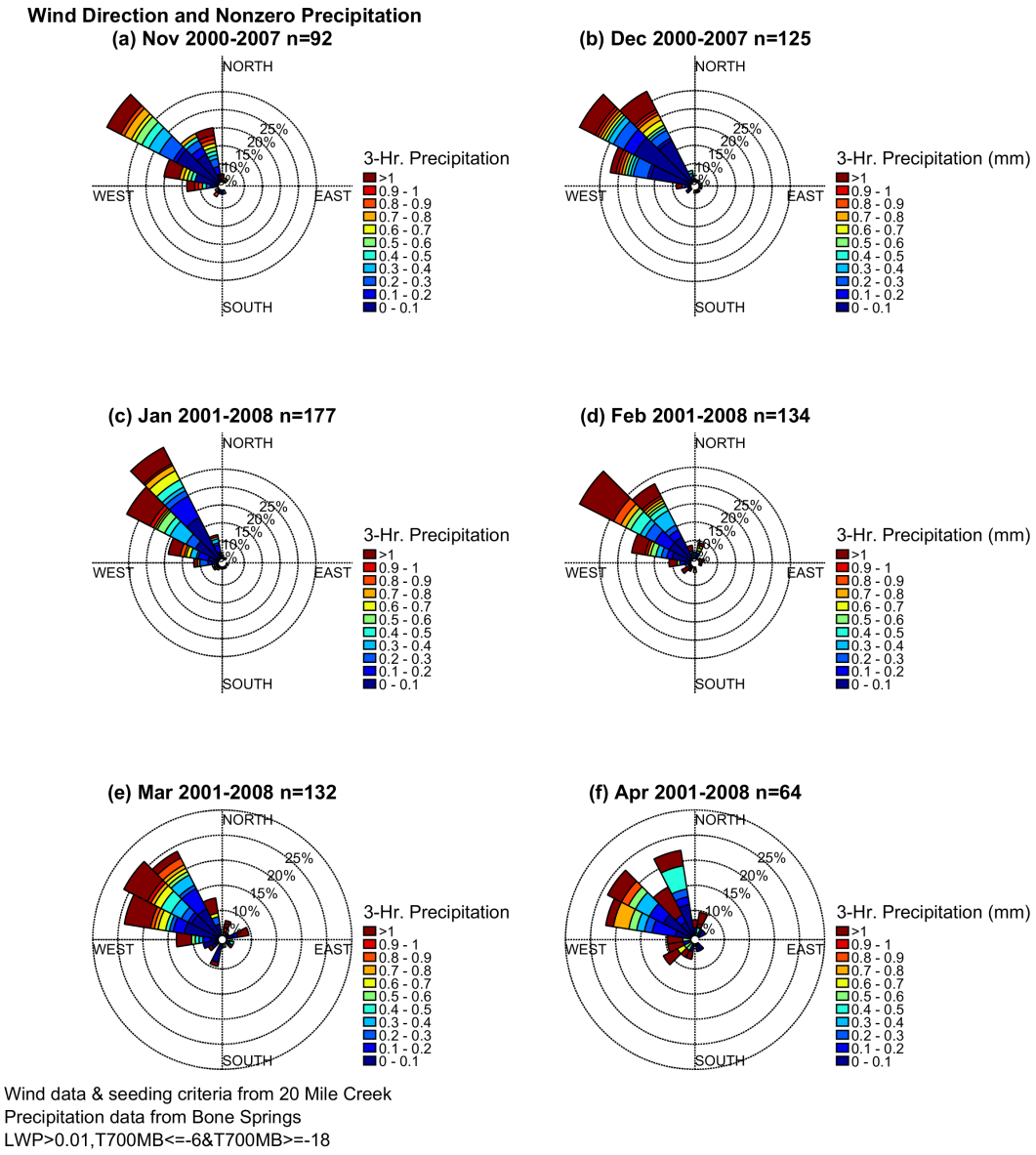


**Figure 4.23. As in Figure 4.20, but for model winds over Twenty Mile Creek and precipitation at the Bone Springs SNOTEL site.**

The modeled 700-hPa temperatures at all four sites are very similar. Over an average winter season, these temperatures were mostly concentrated from 6 °C to −22 °C; however, when precipitation occurred, the temperatures were more concentrated between 0 °C and −20 °C (Figure 4.24–Figure 4.27). At all four sites, roughly 45–50% of the wintertime hours over the 8-year period were warmer than −6 °C whereas approximately 20–25% of the hours with precipitation were warmer than −6 °C. The range of Riverton 700-hPa temperatures very closely resembles those at Sheridan, Kaycee, Worland, and Twenty Mile Creek (recall Figure 4.15b), and the ratio of wintertime hours with and without precipitation is very similar in the model results. However, the observed distributions of

700-hPa temperature at Riverton with precipitation shifted to warmer temperatures, resulting in roughly 30% of precipitating hours having temperatures warmer than −6 °C.

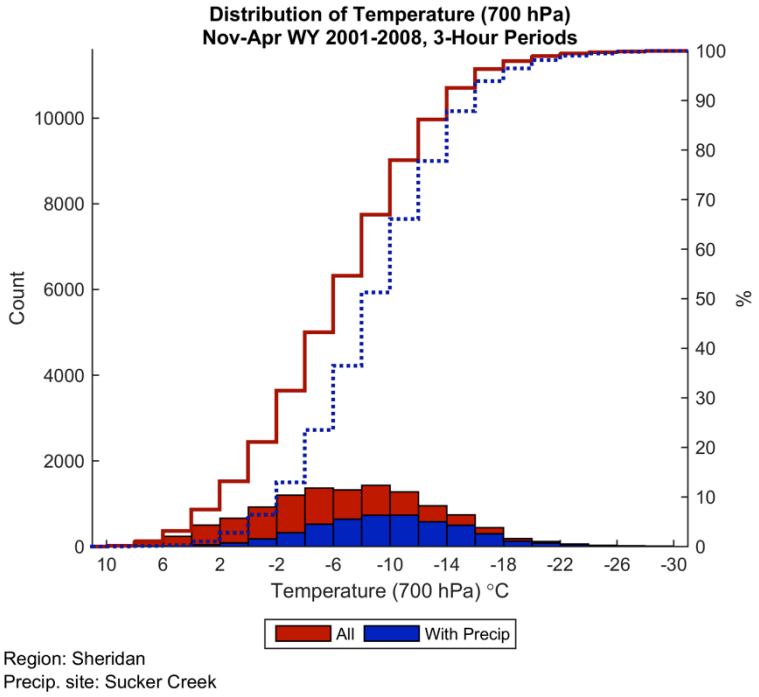


**Figure 4.24. Histogram counts (left ordinate) of the modeled 700-hPa temperature at Sheridan, Wyoming for all 3-hourly output from November–April from the 8-year (water years 2001–2008) model runs (red) and for all 3-hourly output that had precipitation at the Sucker Creek SNOTEL site (blue). Cumulative distributions for all (red) and with precipitation (blue dotted) are also overlaid using the right ordinate (%).**

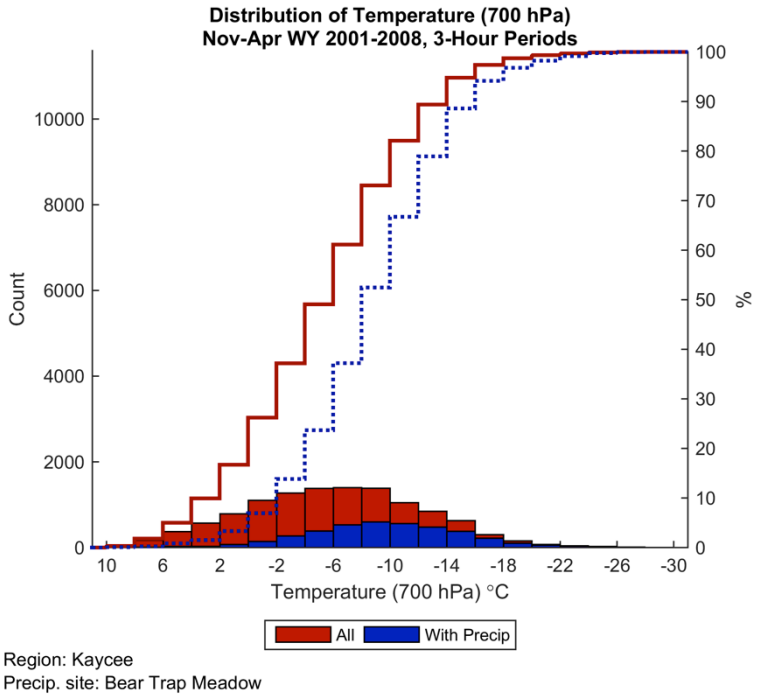


**Figure 4.25. As in Figure 4.24, but using modeled 700-hPa temperature at the Kaycee, Wyoming site and precipitation from the Bear Trap Meadow SNOTEL site.**

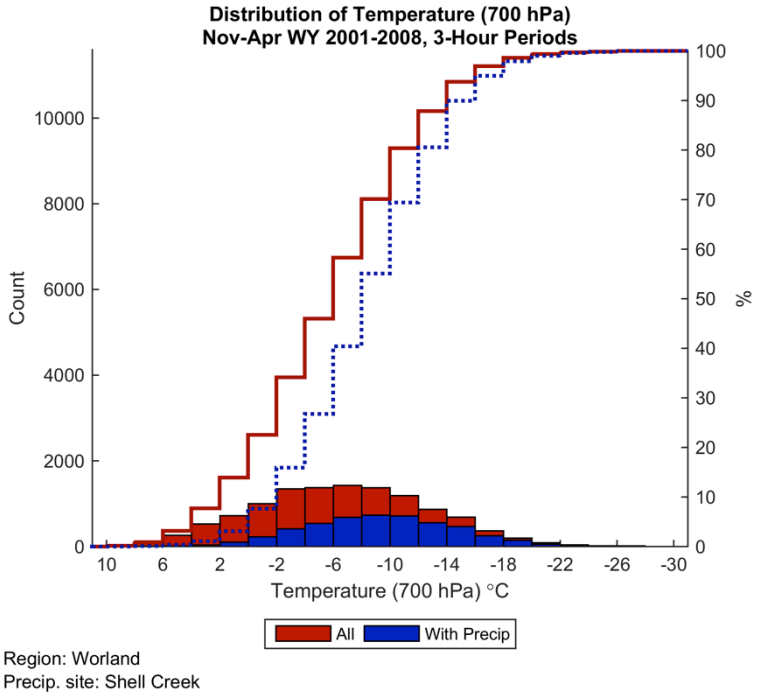


**Figure 4.26. As in Figure 4.24, but using modeled 700-hPa temperature at the Worland site and precipitation from the Shell Creek SNOTEL site.**

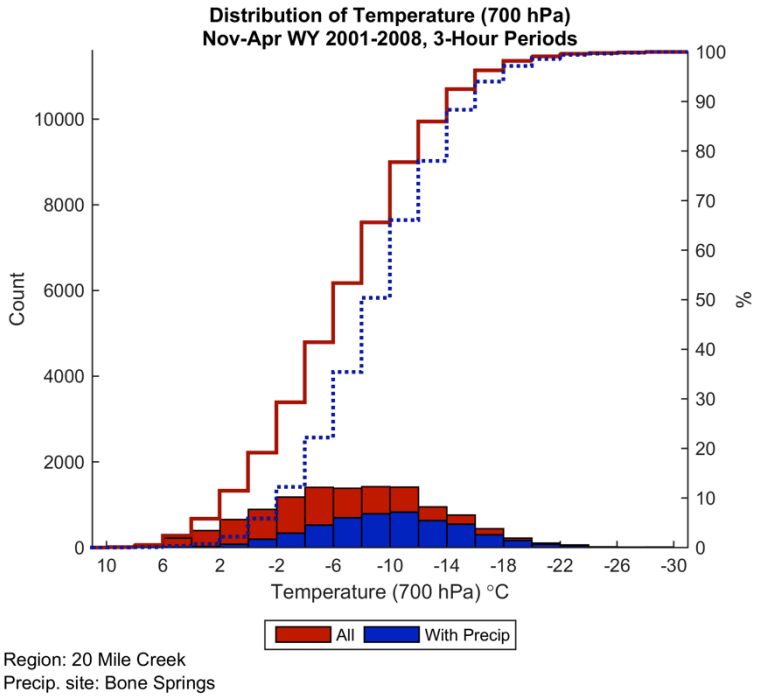


**Figure 4.27. As in Figure 4.24, but using modeled 700-hPa temperature at the Twenty Mile Creek site and precipitation from the Bone Springs SNOTEL site.**

### *Area-based Analysis*

Wintertime temperatures in the ground-seeding layer (0–1-km AGL) averaged over the western region ranged from 6 °C to −22 °C; however, when precipitation occurred, the span was more concentrated between 0 °C and −22 °C (Figure 4.28). The 0–1-km AGL temperatures averaged over the eastern region, shown in Figure 4.29, ranged from 8 °C to −22 °C for all hours, and 0 °C to −22 °C when precipitation occurred. The southern region 0–1-km AGL temperatures ranged from 10 °C to −18 °C, and 0 °C and −16 °C when precipitation occurred (Figure 4.30).

The distribution of LWC in the ground-seeding layer over the western region shows that just under 50% of all wintertime hours have no LWC, while less than 10% of the hours with precipitation have no LWC. In the eastern area, about 50% of all wintertime hours and roughly 15% of the hours with precipitation have no LWC. Nearly 70% of the wintertime hours and 20% of hours with precipitation in the southern region have no LWC, indicating less frequent LWC in the ground-seeding layer in the southern region. These results indicate that in all three regions, most precipitation occurs in situations with LWC and therefore, some seeding potential could exist 80–90% of the time precipitation occurs, as long as temperatures are also suitable (more detailed explanation below). Furthermore, the relatively high frequency of hours with non-zero LWC *without* precipitation — especially in the southern region — suggests a high frequency of conditions where precipitation could be initiated through seeding if the other conditions (e.g., temperature) are also suitable.

The differences in the distributions of LWC in the three areas are primarily in the ratio of zero LWC to nonzero LWC events. Conversely, the distributions of the nonzero values are very similar in the three regions, with the majority of values in the 0–0.05 mm range and very few occurrences of LWC greater than 0.1 mm.

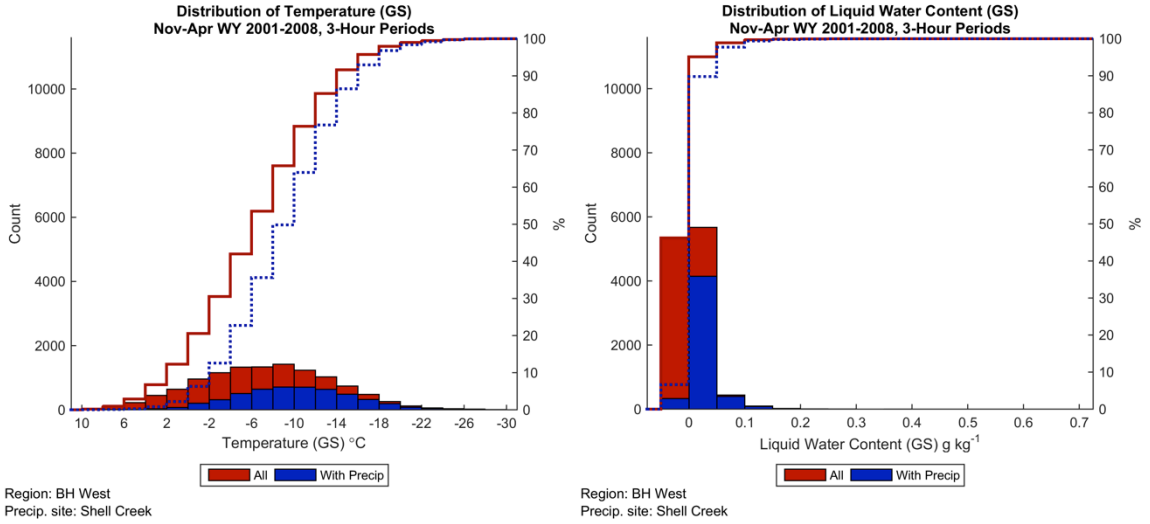


**Figure 4.28. Histogram counts (left ordinate) of the west region average 0–1 km AGL temperature (left) and 0–1 km AGL LWC (right) for ground seeding (GS) for all three-hourly output from Nov–Apr from the 8-year (Water Years 2001–2008) model runs (red) and for all three-hourly model output that had precipitation at the Shell Creek precipitation site (blue). Cumulative distributions for all (red) and output hours with precipitation (blue dotted) are also overlaid using the right ordinate (%). The bar to the left of the zero includes all values equal to zero.**

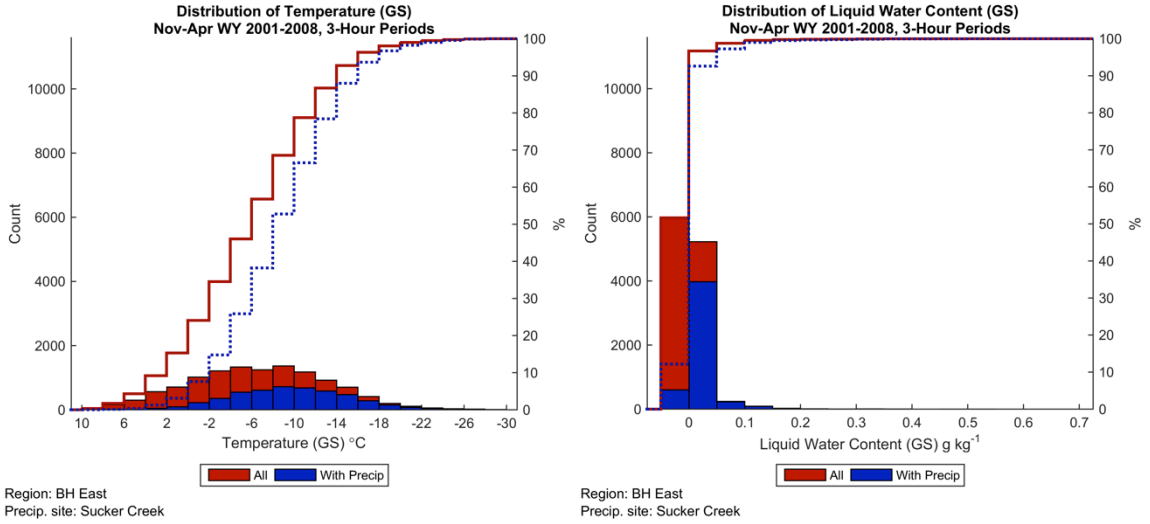


**Figure 4.29. As in Figure 4.28, but areal-averaged values from the eastern region and precipitation from the Sucker Creek site.**

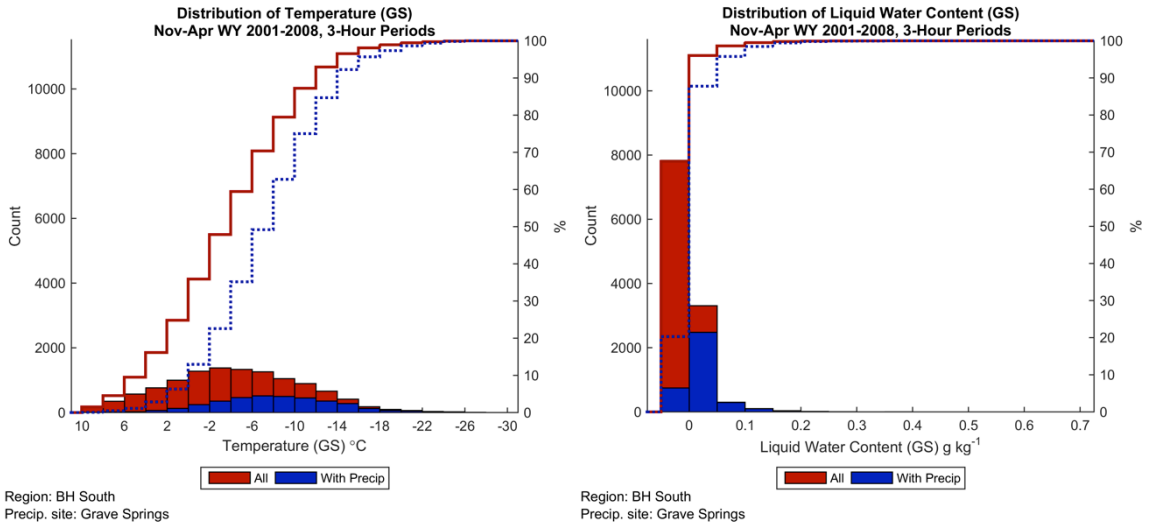


**Figure 4.30. As in Figure 4.28, but areal-averaged values from the southern region and precipitation from the Grave Springs site.**

The distribution of LWP is similar to that of LWC for the ground-seeding layer for all three regions (Figure 4.31). The most pronounced difference is that there are relatively fewer occurrences of zero LWC, both with and without precipitation, in the western and eastern regions in particular. This suggests more liquid water at higher levels. This has implications for the feasibility of airborne seeding, as will be described more below.

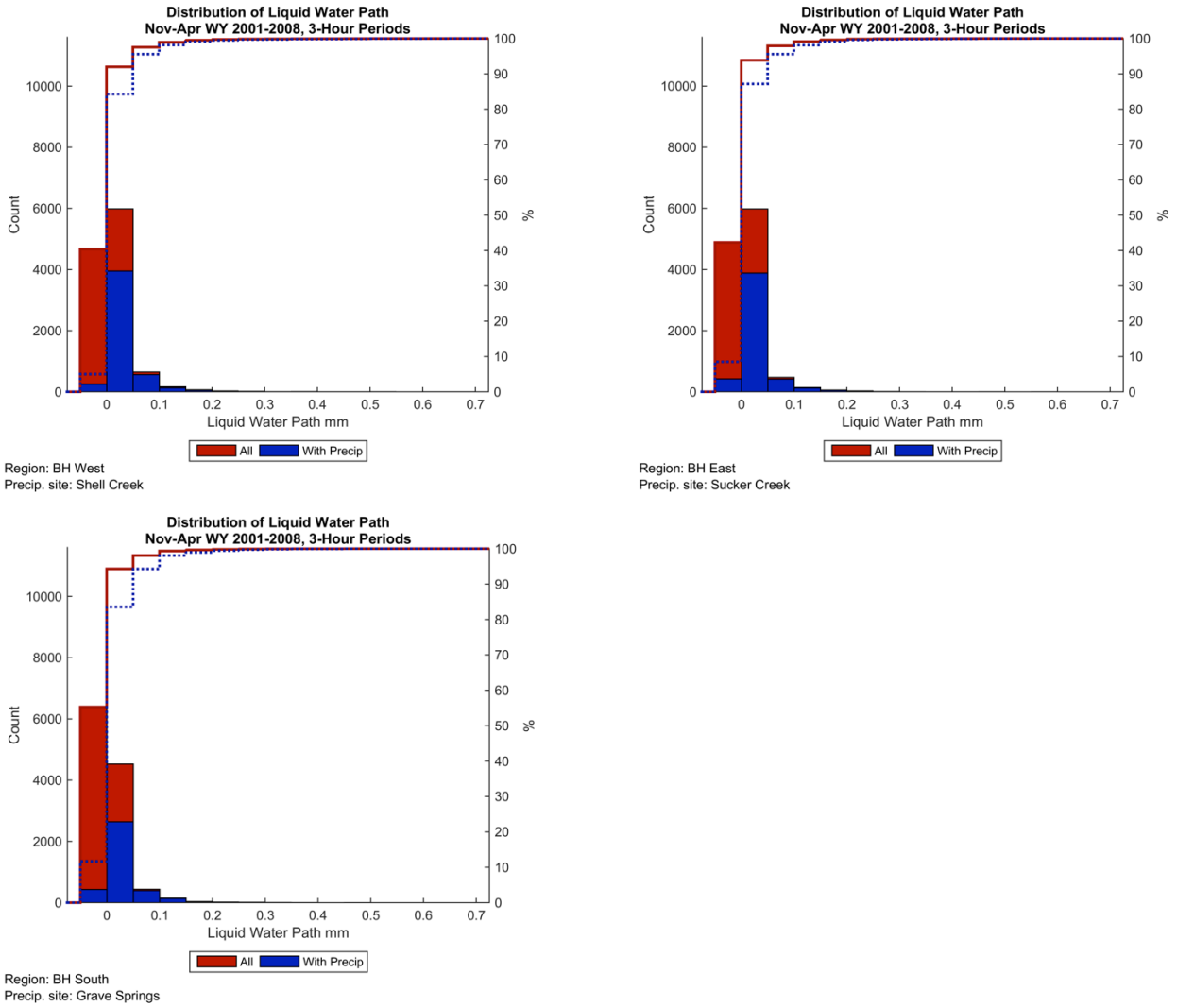


**Figure 4.31. As in Figure 4.28, except for average model LWP in the western (top left), eastern (top right), and southern (bottom) regions. The model precipitation was from the Shell Creek (west), Sucker Creek (east), and Grave Springs (south) sites.**

The Froude number distribution illustrates that for roughly 60% of wintertime hours in the western region, 55% in the eastern region, and 75% in the southern region, the conditions are conducive to flow being blocked by the mountain barrier (Fr<0.5, Figure 4.32). These percentages are reduced to 55% and 45% of the time when precipitation occurs in the western and eastern regions, respectively, but rises to 80% for the southern region. The high frequency of blocking situations was also evident in the wind direction analysis, as indicated above, resulting in sites close to the barrier having a stronger dominance of northwesterly winds than sites farther from the barrier.

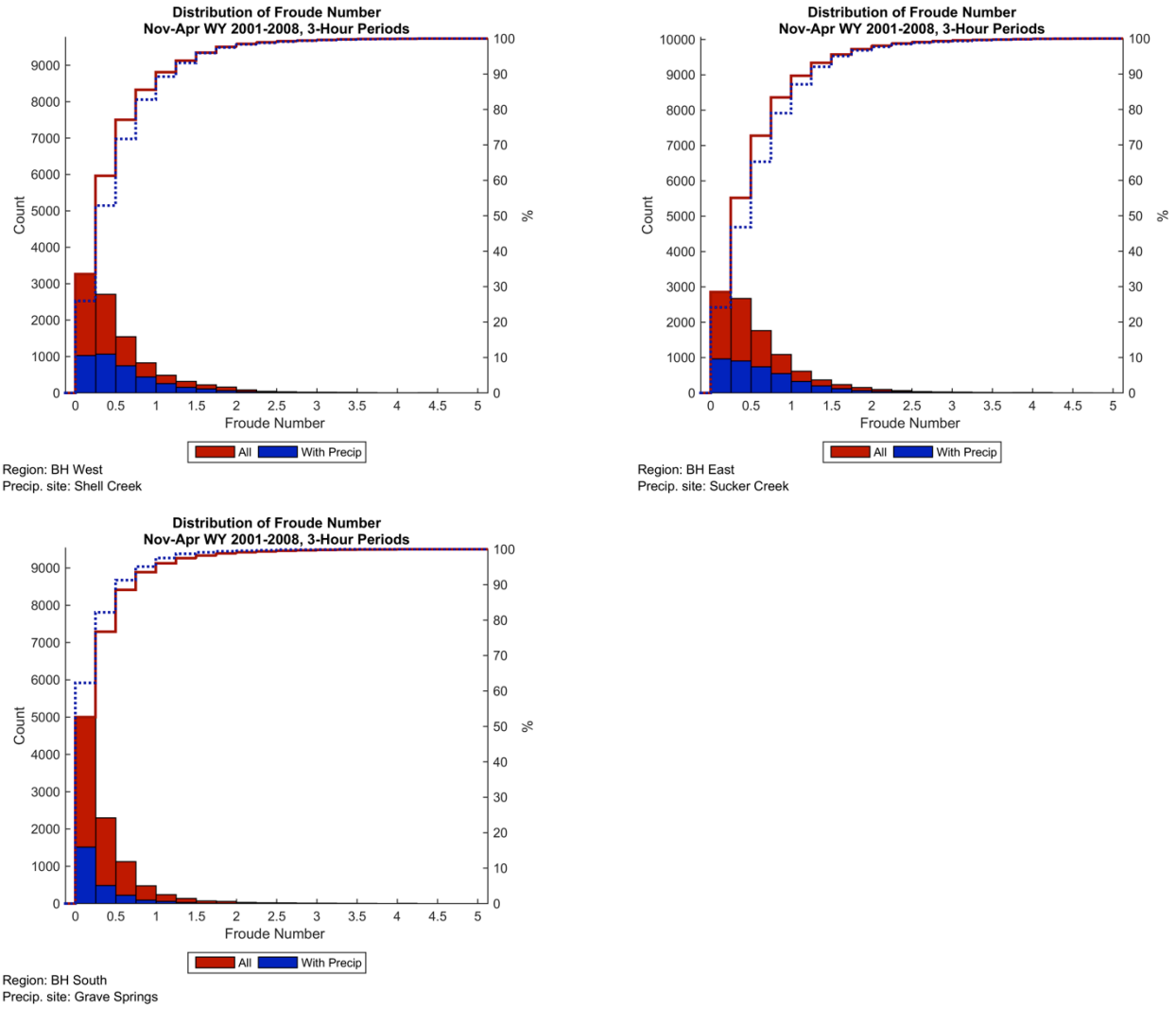


**Figure 4.32. As in Figure 4.28, except for average Froude number.**

Characteristics of clouds, such as base height, depth, and top temperature, relate to the cloud's natural precipitation efficiency. Clouds with colder cloud tops, and that are deeper, most likely have some natural ice formation processes leading to precipitation growth. Moreover, if cloud bases are too high, then ground-based AgI generators may have a hard time targeting the clouds. Cloud-base heights in the western region during winter are typically between 2,500 and 3,500 m MSL (~65% of all hours in winter have cloud-base heights in this range), and over 90% of the cloud-base heights during winter hours with precipitation are in this range (Figure 4.33). The distribution of cloud-base heights in the eastern region is nearly identical to that of the western region. Cloud depths in all three regions range as deep as 8,000 m, with 50% of occurrences having depths less than 2,000 m (Figure 4.34). The distributions in the eastern and western regions are nearly identical while the southern region has relatively fewer shallow clouds (Figure 4.34). The distributions of precipitating and non-precipitating clouds in all three regions are very similar to one another (within each individual region), except for a slightly smaller ratio of clouds with depths less than 500 m. All three regions show a high frequency of non-

precipitating clouds with cloud top temperatures colder than −20 °C, with only roughly 30% of clouds having top temperatures warmer than −20 °C (35–45% of precipitating clouds).

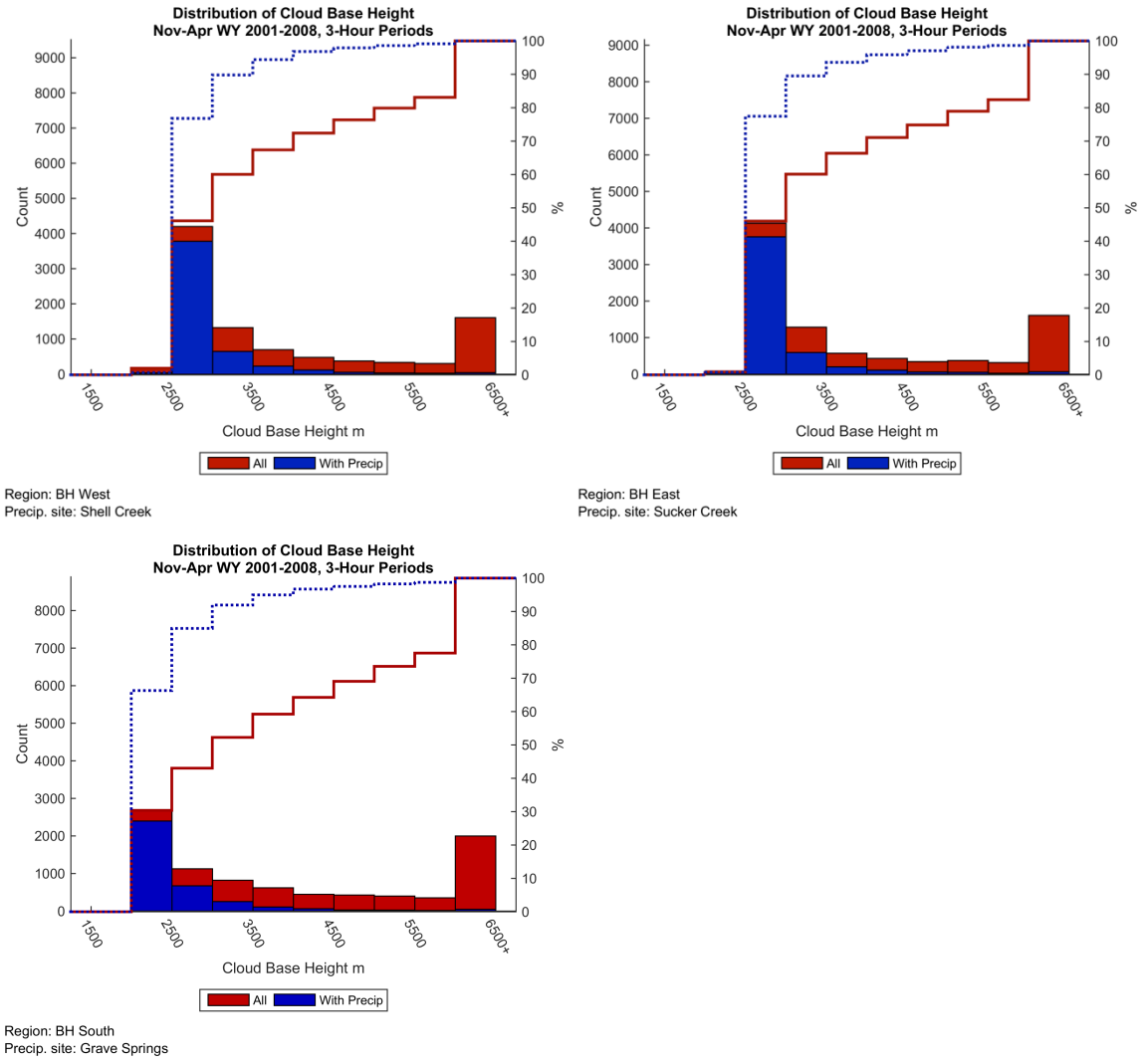


**Figure 4.33 As in Figure 4.28, except for average cloud base height in the western (left), eastern (right), and southern (bottom) regions. The model precipitation was from the Shell Creek (west), Sucker Creek (east), and Grave Springs (south) sites.**

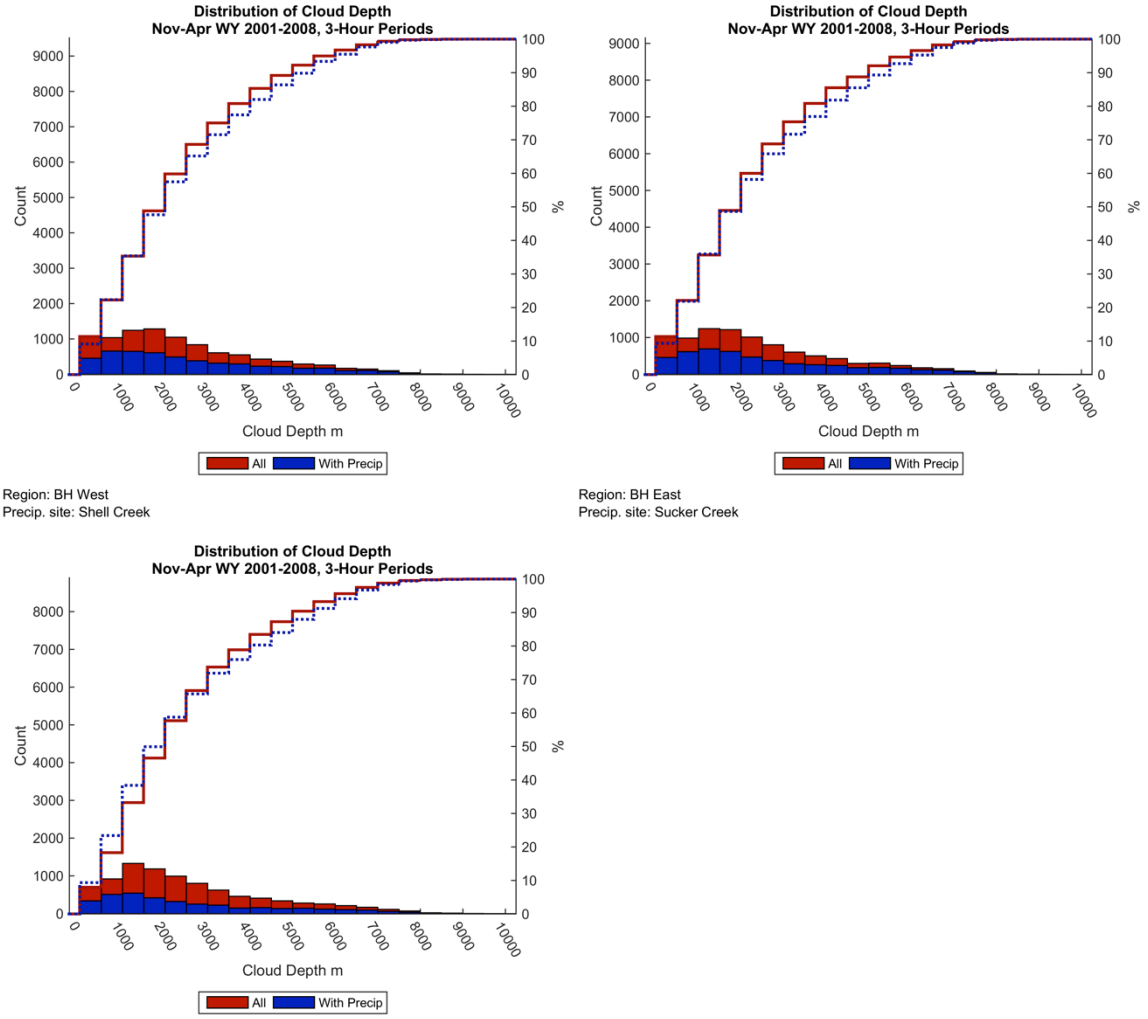


**Figure 4.34. As in Figure 4.28, except for average cloud depth in the western (left), eastern (right), and southern (bottom) regions. The model precipitation was from the Shell Creek (west), Sucker Creek (east), and Grave Springs (south) sites.**

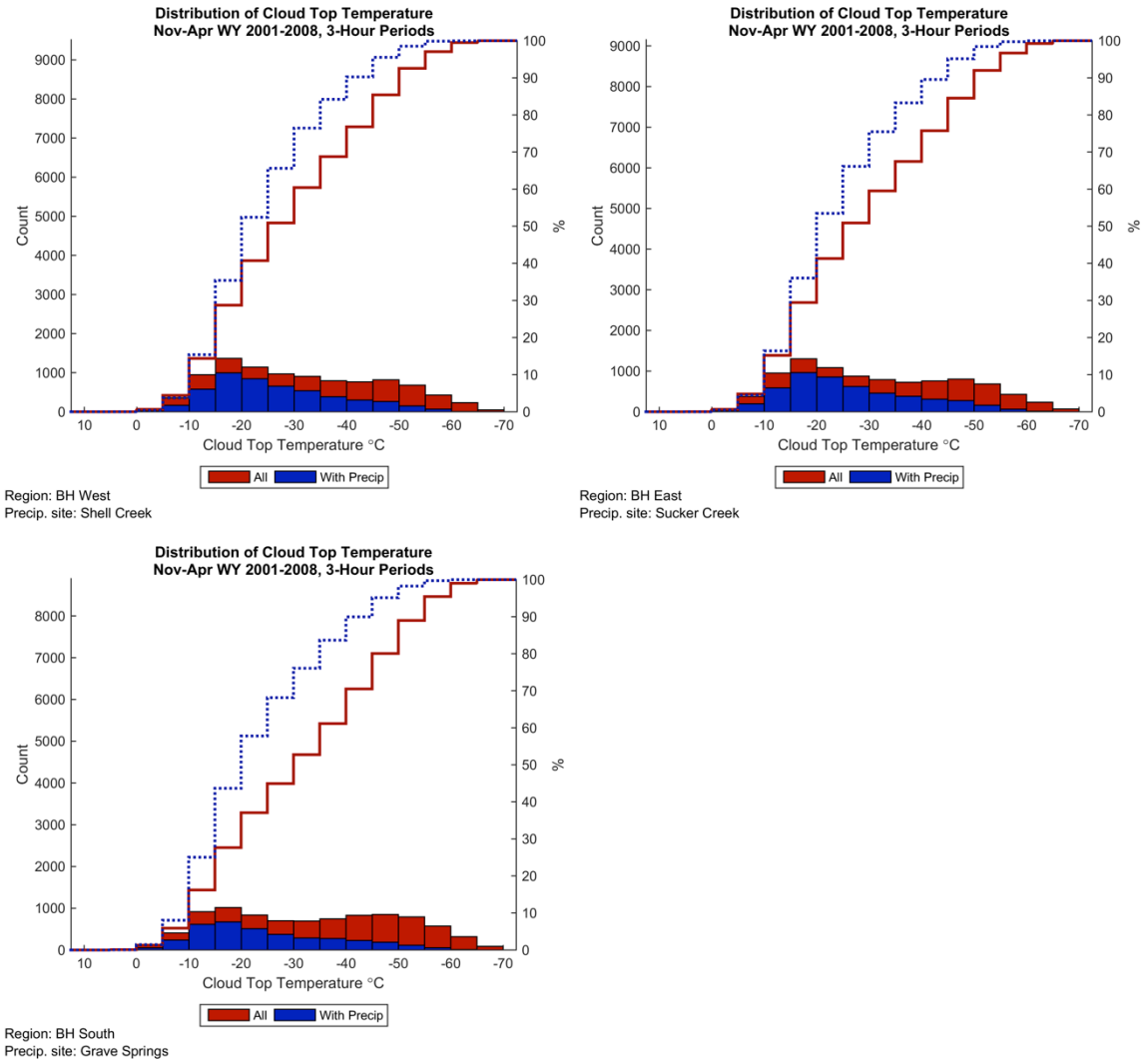


**Figure 4.35. As in Figure 4.28, except for average cloud top temperature in the western (left), eastern (right), and southern (bottom) regions. The model precipitation was from the Shell Creek (west), Sucker Creek (east), and Grave Springs (south) sites.**

The amount (and percent) of wintertime precipitation that falls when the area-averaged 700-hPa temperatures are cooler than −6 °C is shown by water year in Table 4.3–Table 4.5. The 8-year seasonal average over all three regions was very similar, with roughly three quarters of the precipitation falling when 700-hPa temperatures were cooler than −6 °C. In each of the three regions, there were year-to-year variations, ranging from 65–93%. Despite the large variations, the year-to-year results are very similar across the three regions, indicating that the year-to-year differences were greater than the areal differences. In all regions, water year 2008 had the most precipitation falling when temperatures were cooler than −6 °C. Precipitation totals in the eastern and western regions are very similar both year-to-year and in the 8-year average, and consistently higher than in the southern area. As a result, all three regions have a large fraction of precipitation that falls under temperature conditions suitable for AgI seeding.

**Table 4.3. Seasonal (November–April) model precipitation totals from Shell Creek and the amount of precipitation that fell when the western area average 700-hPa temperature was < −6 °C.**

| Season (Water Year) | Seasonal Precipitation (mm) | Seasonal Precipitation (mm) when 700-hPa T < −6 °C |
|---|---|---|
| 2001 | 344 | 263 (77%) |
| 2002 | 318 | 226 (71%) |
| 2003 | 415 | 290 (70%) |
| 2004 | 315 | 214 (68%) |
| 2005 | 362 | 235 (65%) |
| 2006 | 430 | 303 (70%) |
| 2007 | 414 | 264 (64%) |
| 2008 | 440 | 380 (86%) |
| 8-yr Average | 380 | 272 (72%) |
| Standard Deviation | 51 | 53 |

**Table 4.4. As in Table 4.3, but precipitation totals from Sucker Creek and 700-hPa temperatures averaged over the eastern area.**

| Season (Water Year) | Seasonal Precipitation (mm) | Seasonal Precipitation (mm) when 700-hPa T < −6 °C |
|---|---|---|
| 2001 | 310 | 252 (81%) |
| 2002 | 268 | 205 (76%) |
| 2003 | 465 | 309 (66%) |
| 2004 | 364 | 277 (76%) |
| 2005 | 343 | 246 (72%) |
| 2006 | 374 | 279 (75%) |
| 2007 | 400 | 300 (75%) |
| 2008 | 384 | 352 (92%) |
| 8-yr Average | 364 | 278 (76%) |
| Standard Deviation | 59 | 45 |

**Table 4.5. As in Table 4.3, but precipitation totals from Grave Springs and 700-hPa temperatures averaged over the southern area.**

| Season (Water Year) | Seasonal Precipitation (mm) | Seasonal Precipitation (mm) when 700-hPa T < −6 °C |
|---|---|---|
| 2001 | 287 | 237 (83%) |
| 2002 | 265 | 208 (78%) |
| 2003 | 322 | 228 (71%) |
| 2004 | 312 | 223 (71%) |
| 2005 | 277 | 188 (68%) |
| 2006 | 398 | 325 (82%) |
| 2007 | 302 | 223 (74%) |
| 2008 | 297 | 276 (93%) |
| 8-yr Average | 307 | 238 (78%) |
| Standard Deviation | 41 | 43 |

In the airborne-seeding layer (3.5–4.5 km MSL), the temperature range in wintertime is shifted slightly cooler than in the ground-seeding layer, as would be expected since air

temperature typically cools with increasing altitude. Additionally, the airborne layer temperature distributions are very similar for the eastern, western, and southern regions. In the airborne layer, it ranges from 0 °C to −30 °C, with the range slightly cooler between −6 °C and −26 °C when precipitation occurred (Figure 4.36–Figure 4.38). Specifically, ~10–15% of all wintertime hours were warmer than −6 °C; whereas, roughly 2% of the wintertime hours with precipitation were warmer than −6 °C. Roughly 20% of all wintertime hours and 30% of precipitating wintertime hours are colder than −18 °C, becoming too cold for AgI cloud seeding.

The range of LWC in the airborne-seeding layers is only slightly diminished compared to that in the ground-seeding layer (Figure 4.28–Figure 4.30, Figure 4.36–Figure 4.38). The primary difference in all three regions is a decrease in the frequency of non-zero LWC events with precipitation. Recall that the frequency of non-zero LWC without precipitation indicates potential seeding opportunities; the airborne layer shows a similar frequency of these opportunities.

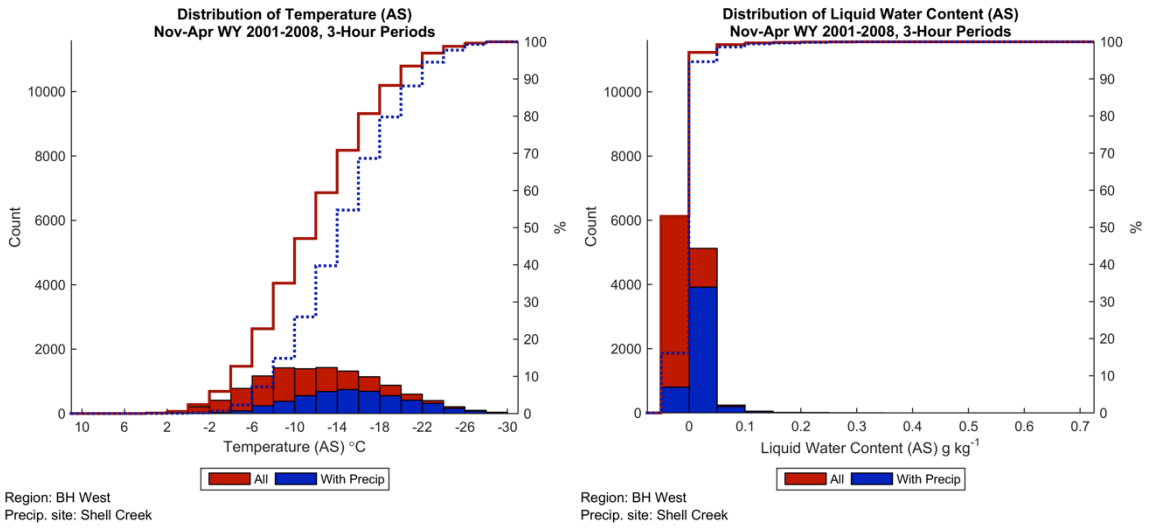


**Figure 4.36. As in Figure 4.28, except for in the 3.5–4.5 km MSL layer (for airborne seeding; AS).**

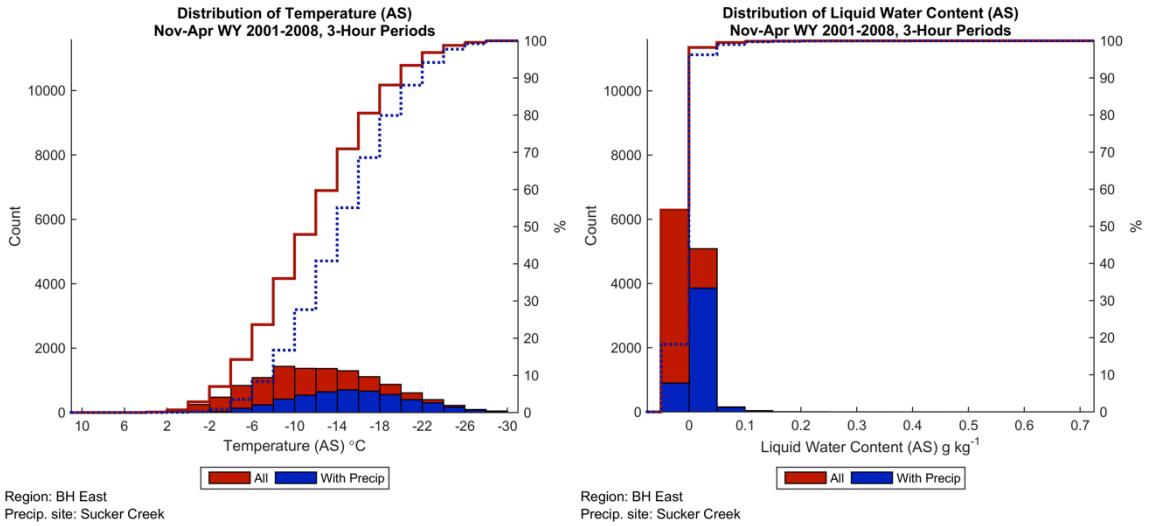


**Figure 4.37. As in Figure 4.29, except for in the 3.5–4.5 km MSL layer.**

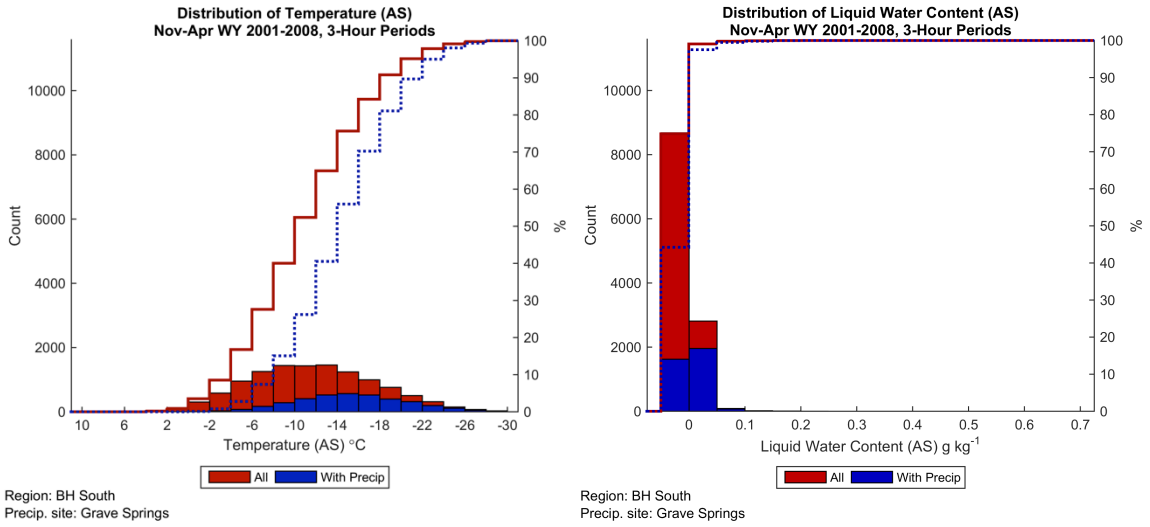


**Figure 4.38. As in Figure 4.30, except for in the 3.5–4.5 km MSL layer.**

A higher airborne layer was also examined for seeding opportunities (4.5–5.5 km MSL), but ~50% of all wintertime hours and 70–80% of precipitating wintertime hours had temperatures colder than −18 °C, and all three regions show very little LWC in this range (not shown). As a result, the higher airborne layer will not be the focus of the remaining discussion, but will be examined in later sections for seeding potential outside of the November–April months.

As mentioned above for both ground and airborne seeding, the occurrence of LWC when no precipitation occurred shows potential for cloud seeding if the temperature is suitable. Therefore, histograms of the layer average temperature during periods when there was LWC present for the ground-seeding layer and the 3.5–4.5-km MSL airborne seeding layer are provided (western region, Figure 4.39; results in the eastern and southern regions are practically identical and thus not shown). Interestingly, the cumulative temperature distributions when LWC was present both with and without precipitation are very similar.

This suggests that when LWC is present, there is no dependence on the layer temperature for precipitation to occur. Generally, 30% (5%) of the time that LWC was present for ground seeding (airborne seeding) the temperature was warmer than −6 °C. About 5% (15%) of ground seeding (airborne seeding) temperatures were colder than −18 °C, resulting in roughly 65% (80%) of wintertime events for which LWC was present having suitable temperatures for cloud seeding.

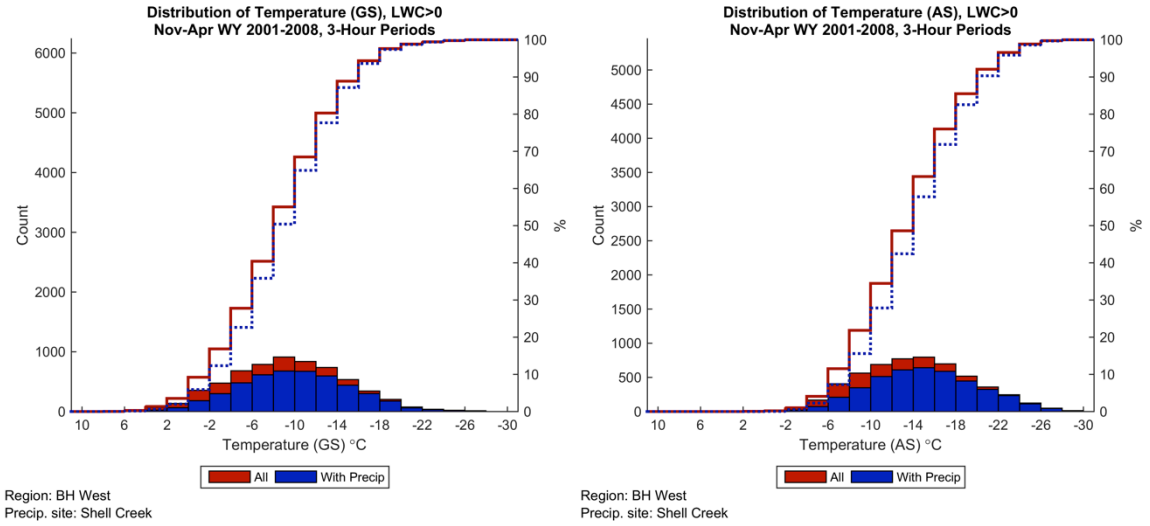


**Figure 4.39. Histogram counts (left ordinate) of the western region average 0–1 km AGL temperature when LWC was present (> 0) in the layer (left) and 3.5–4.5 km MSL temperature when LWC was present in the layer (right) for all hourly output between November and April from the 8-year (Water Years 2001–2008) model runs (red) and for all hourly output that had precipitation at the Shell Creek SNOTEL site (blue). Cumulative distributions are included as in Figure 4.28.**

## 4.3 Climatology of Cloud-Seeding Opportunities

When considering the two key criteria for cloud-seeding potential, appropriate temperature and the presence of liquid water, the frequency that these criteria are met can be established using either observations (if available) or model output. This provides a general sense of the frequency of cloud-seeding opportunities.

Due to the lack of observations available in the region, model output is used to calculate the fraction of hours in a given month or the entire winter season (November–April) in which those two criteria are both met. Additional criteria that may affect the potential for ground-based seeding are wind direction and atmospheric stability indices. These variables will be analyzed via the spatial mapping analysis and the area-based analysis below for both ground and airborne seeding potential.

### *4.3.1 Model-based Analysis Results*

#### *Ground Seeding Spatial Mapping Analysis*

Figure 4.40 shows the frequency (fraction of time analyzed for all eight seasons) that seeding criteria are met within the 0–1-km AGL ground-seeding layer. LWP frequencies have slightly higher magnitudes than LWC, especially over the adjacent plains, indicating

some of the LWC is above the ground-seeding layer. The LWP or LWC mixing ratio and their spatial distribution compared to Figure 4.40d (LWP and temperature criteria combined) indicate that the presence of liquid water is the most important factor controlling the frequency of seeding opportunities. The western slope shows a greater frequency in adequate LWP and LWC. Temperature criteria are satisfied at a high frequency and have very little impact on limiting seedability over the mountain barrier itself, but in the surrounding plains are met less frequently thereby limiting the potential for seeding from ground generators in those locations. The combination of temperature and LWP concurrently shows a maximum frequency of seeding opportunities of about 25% near Cloud Peak and only around 15% along the rest of the mountain barrier.

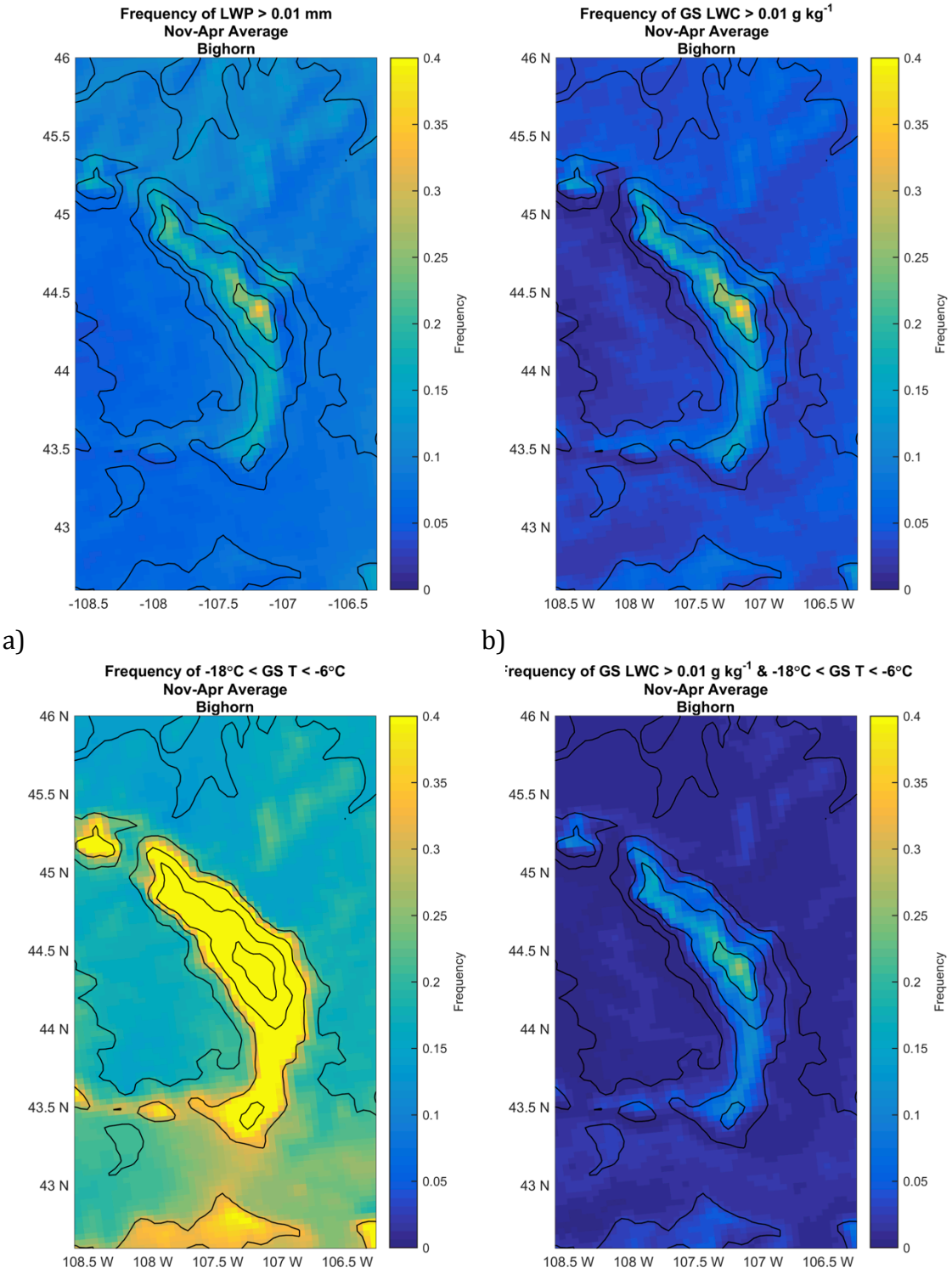


**Figure 4.40. Frequency (fraction of time) that seeding criteria are met within the 0–1 km AGL layer for all seasons (2000–2008): a) LWP, b) LWC, c) Temperature, d) LWC and Temperature concurrently. Note: the colorbar has a maximum value of 40% (same across all figures) and values greater than 40% are not shown. Thin black contours indicate the topography.**

### *Airborne Seeding Spatial Mapping Analysis*

Figure 4.41 shows the seedability frequency maps for a potential airborne seeding layer (3.5–4.5-km MSL) in the November–April winter months. The spatial patterns for all meteorological parameters are consistent with that shown for the ground-seeding layer, except temperature, which has greater than 40% frequency of being in the seedable range everywhere in the region for this layer. Differences can be observed in the magnitude of the frequencies (especially for LWC and temperature plus LWC), but the similarity in the contour pattern persists. This suggests that the LWC is strongly correlated with terrain features. The slight reductions in airborne seedability compared to the ground-seeding layer during November–April are driven by a lower frequency of LWC and colder temperatures that may get colder than seedable values, but the airborne layer still shows about a 10–20% frequency of seedable three-hour periods across the western and northeastern slopes.

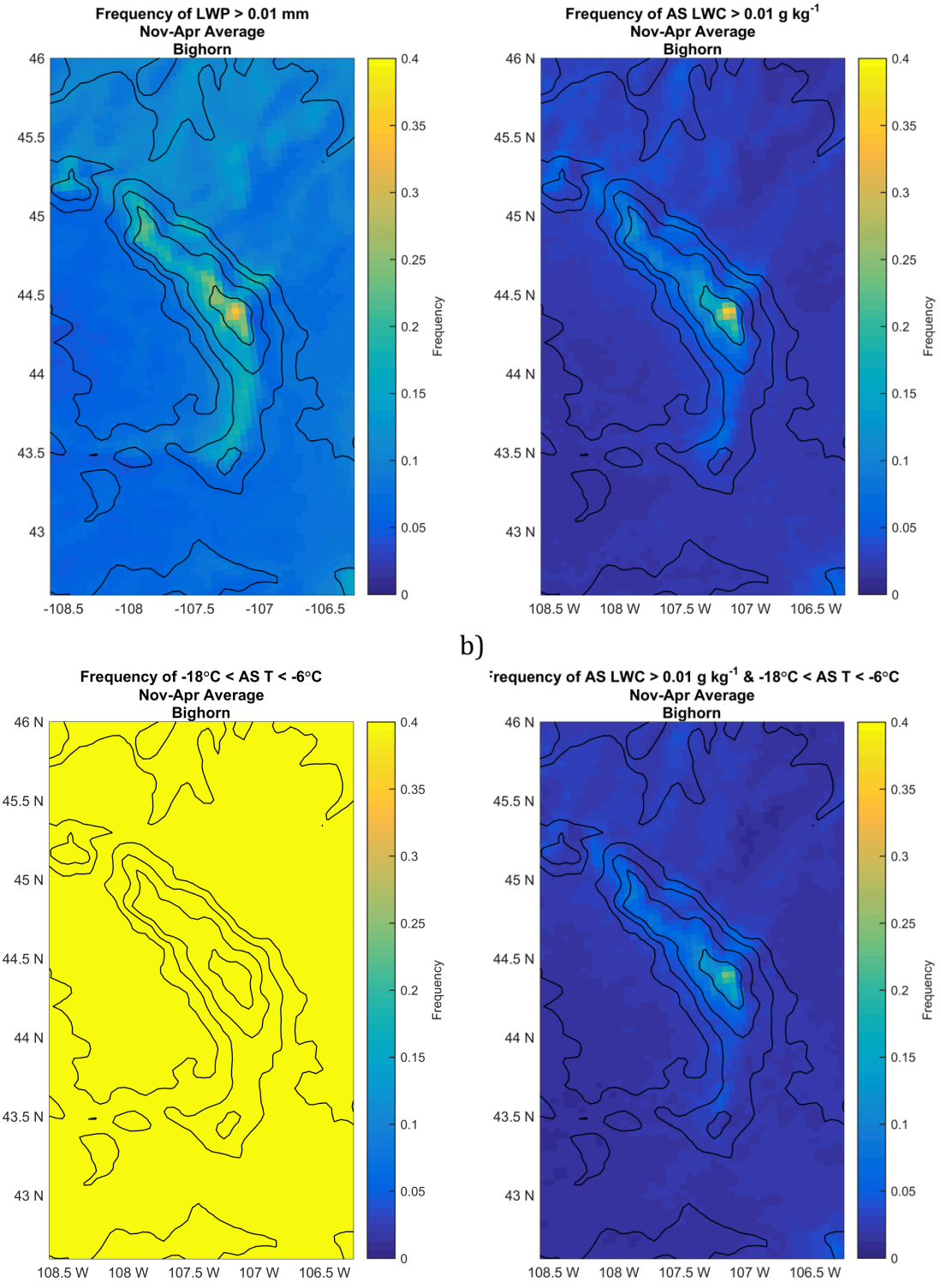


**Figure 4.41. As in Figure 4.40, but for the 3.5–4.5 km MSL airborne seeding layer.**

### *Ground Seeding Area-based Analysis*

#### Western Area

On a monthly basis, the seasonality of ground-based cloud-seeding opportunities (defined as meeting the temperature and LWC criteria) occurs primarily between November and April (where monthly fractions are > 0.1, Figure 4.42). When these results are normalized by the presence of precipitation over the target area (using modeled precipitation from the Shell Creek SNOTEL site), the fraction of hours is only slightly reduced. This indicates few non-precipitating opportunities for cloud seeding.

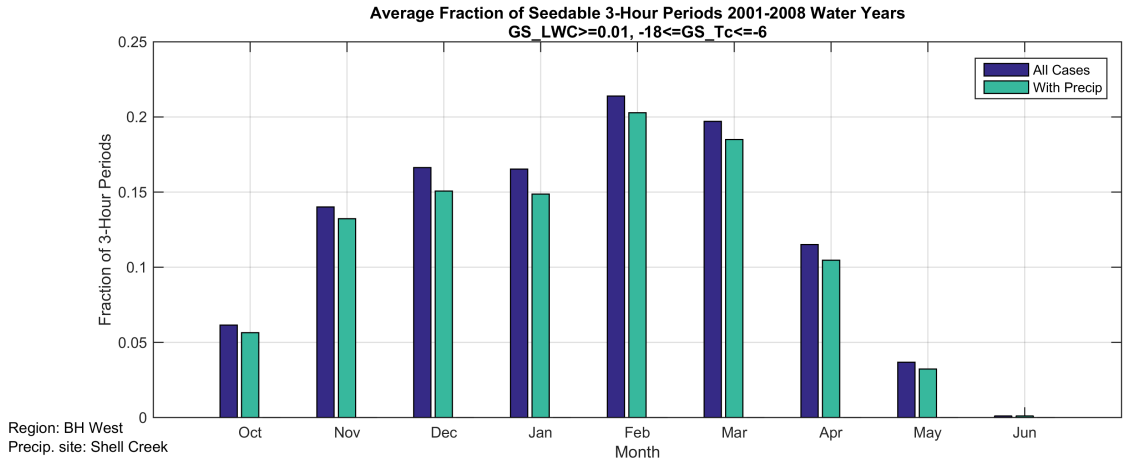


**Figure 4.42. Bar chart showing the average fraction of hours per month that met the temperature and LWC criteria averaged over the western area for ground-based seeding (0–1 km AGL; blue) and the same for hours that also had precipitation in the model near the Shell Creek SNOTEL site (cyan).**

When the monthly distribution of wintertime hours that met temperature and LWC criteria are broken down by season, the interannual variability in seeding opportunities for some months is apparent (Figure 4.43). December–February are fairly consistent year-to-year, but the remaining months show a greater degree of variability. However, with the exception of the first and last years of study, the season-wide fraction of seedable hours is fairly consistent, indicating that one weak month may generally be made up over the course of a season (Figure 4.44). Over the 8-year period of study, most seasons had between 15 and 20% of the wintertime hours meeting the temperature and LWC criteria. The 8-year average shows 17% of the wintertime hours as being seedable, based on meeting the primary criteria in the ground-seeding layer. Considering only cases when precipitation was simulated over the target area reduces these fractions only slightly, to an 8-year average of 15% of all wintertime hours being seedable with precipitation. Roughly 30% of all wintertime clouds over the 8-year period meet the ground seeding criteria (not shown).

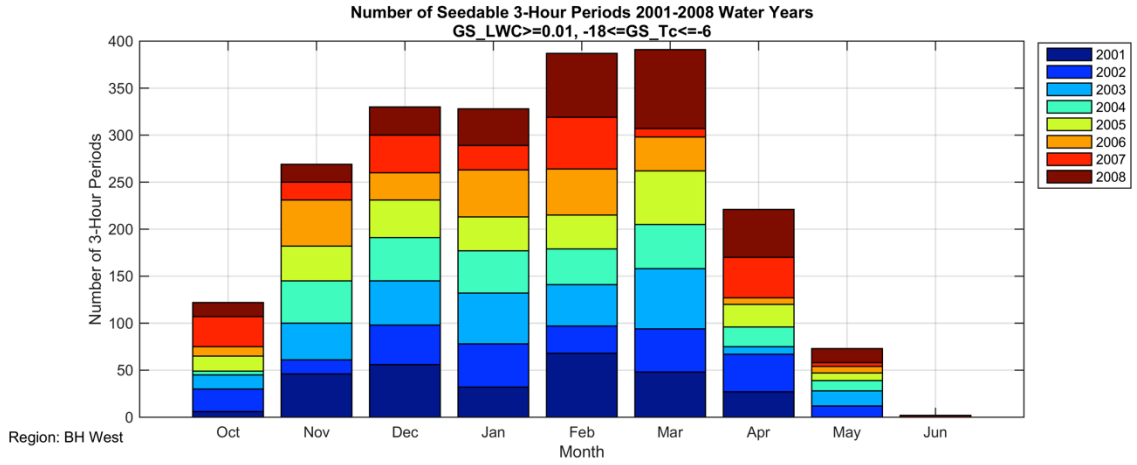


**Figure 4.43. Bar chart showing the number of hours in a given month that met the temperature and LWC criteria averaged over the western area for ground-based seeding (0–1 km AGL). Each color represents one of the 8 years simulated by the model.**

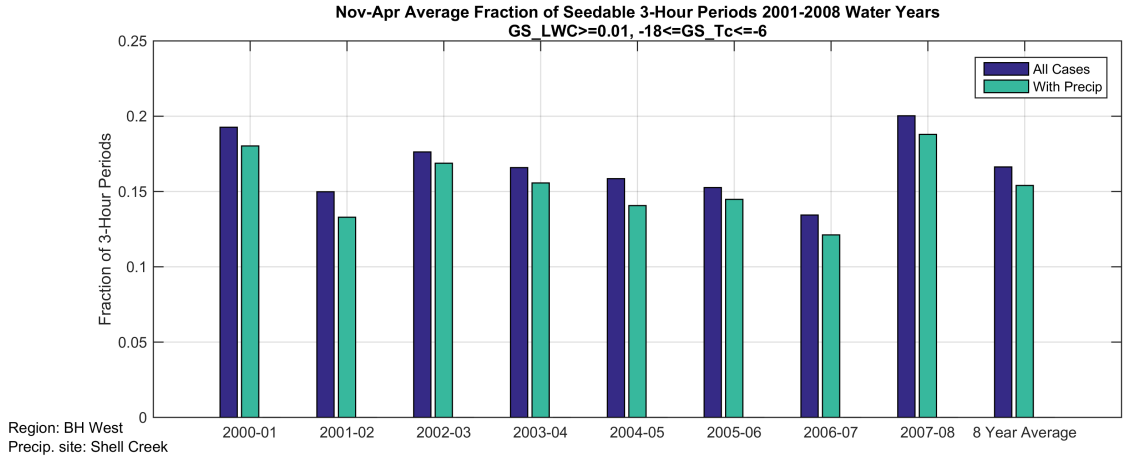


**Figure 4.44. Bar chart showing the average fraction of hours in a winter season (Nov–Apr) that met the temperature and LWC criteria averaged over the western area for ground-based seeding (0–1 km AGL; blue) and the same for hours that also had precipitation in the model near the Shell Creek SNOTEL site (cyan).**

Since ground-based seeding generators are typically at fixed locations, a wind direction criterion can be added to this analysis to identify the frequency at which seeding conditions occur when the wind directions are favorable for transport of the ground-based seeding material over the barrier (between 225 and 330 degrees for the western area). When imposing a 700-hPa wind direction criterion on the ground-based seeding potential, the frequencies were only reduced, from an 8-year average of 17% to 13% of all wintertime hours, and from 15% to 12% of wintertime hours that also had precipitation (Figure 4.45).

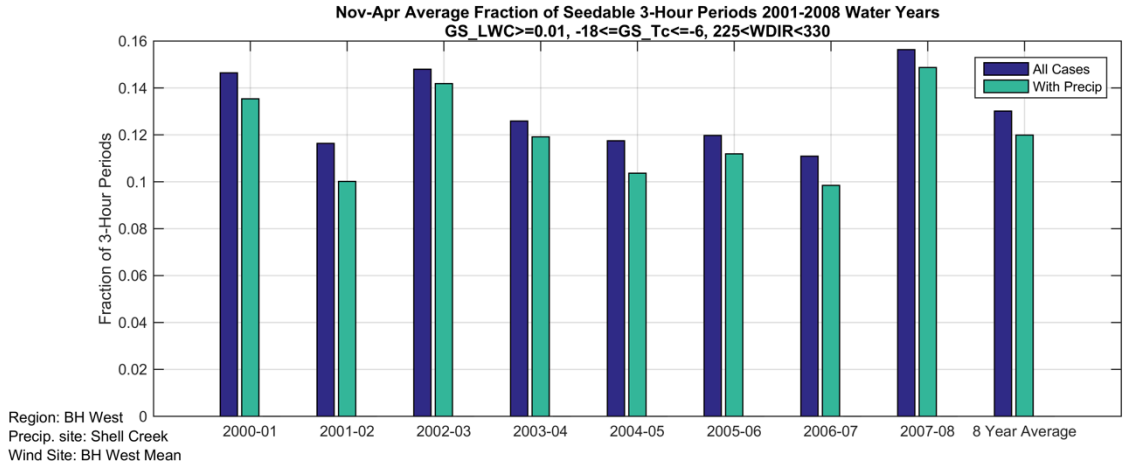


**Figure 4.45. As in Figure 4.44, except also including 700-hPa wind direction as an additional criterion for ground seeding potential.**

Moreover, since AgI released from ground-based generators needs to be able to disperse vertically up and over the mountain barrier, it is important to also assess the stability of the atmosphere. When including the additional criterion of Fr > 0.5 to the analysis of frequency of ground-seeding conditions (indicative that flow would be less likely to be blocked by the mountain barrier), the frequency of opportunities for ground-based seeding during all wintertime hours was reduced substantially (Figure 4.46) to roughly 6.5% of the season, based on the 8-year average.

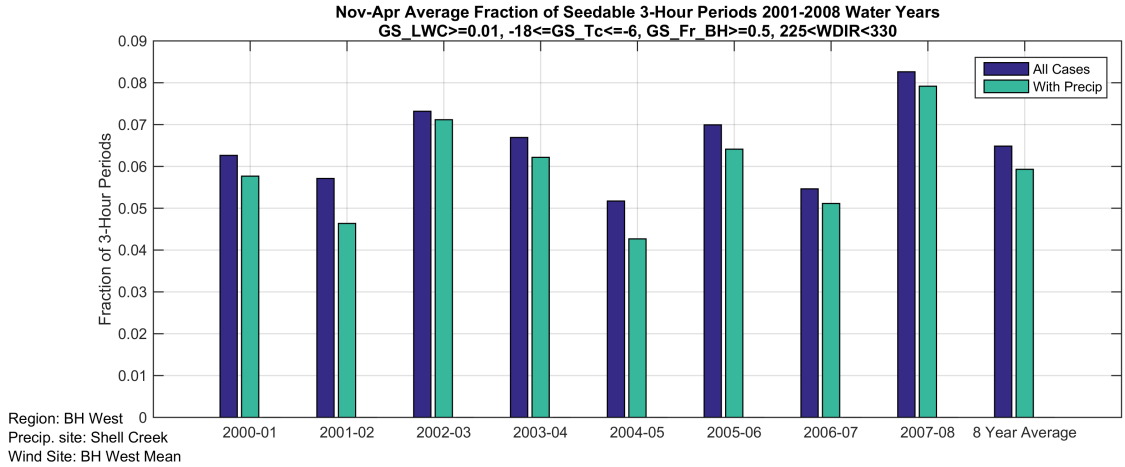


**Figure 4.46. As in Figure 4.44, except also including 700-hPa wind direction and Froude number > 0.5 as additional criteria for ground seeding potential.**

## Eastern Area

Ground-seeding opportunities in the eastern area increase steadily from October to March, but overall, occur at a lower rate than in the western area (maximizing at about 13% as opposed to consistently greater than 15% over several of the winter months in the western area; Figure 4.42 and Figure 4.47). The monthly mode occurs later in the winter season (March) for the eastern area, yielding the primary season for seeding (where monthly fractions are > 0.1) only between February and April.

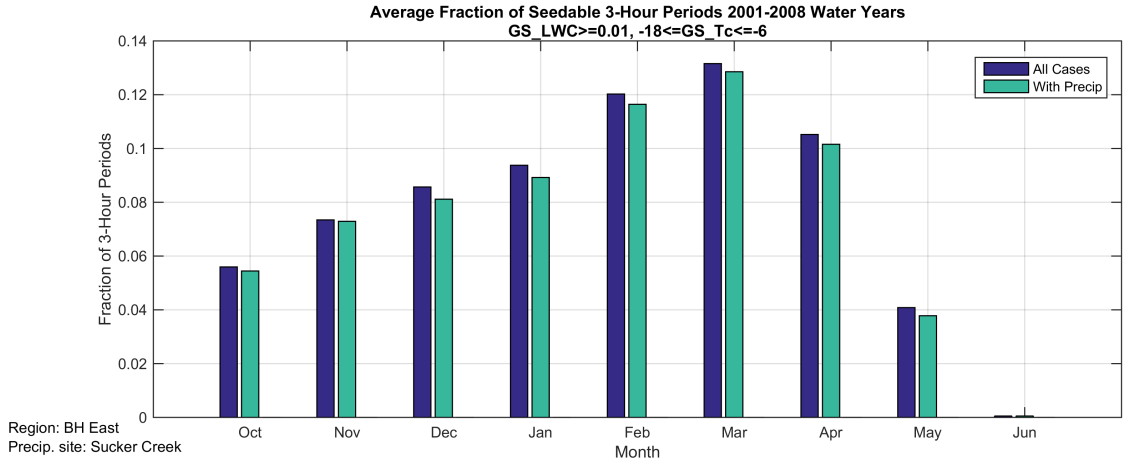


**Figure 4.47. As in Figure 4.42, but over the eastern area and using precipitation near the Sucker Creek SNOTEL site.**

Addition of a wind-direction criterion alone (350–75 degrees for the eastern slope) reduces the maximum fraction of seedable wintertime hours to less than 2% (for single years and the 8-year average; not shown); further addition of the Froude number threshold reduces the fraction of wintertime hours conducive to ground seeding to 0 in all months (not shown).

## Southern Area

The monthly distribution of seedable 3-hour periods in the southern area more closely resembles that of the western area, but reduced roughly in half (Figure 4.48). Recall that the November–March period in the western area ranged from about 15–20% of seedable 3-hour periods (Figure 4.42) whereas the southern area ranges from about 8–10%.

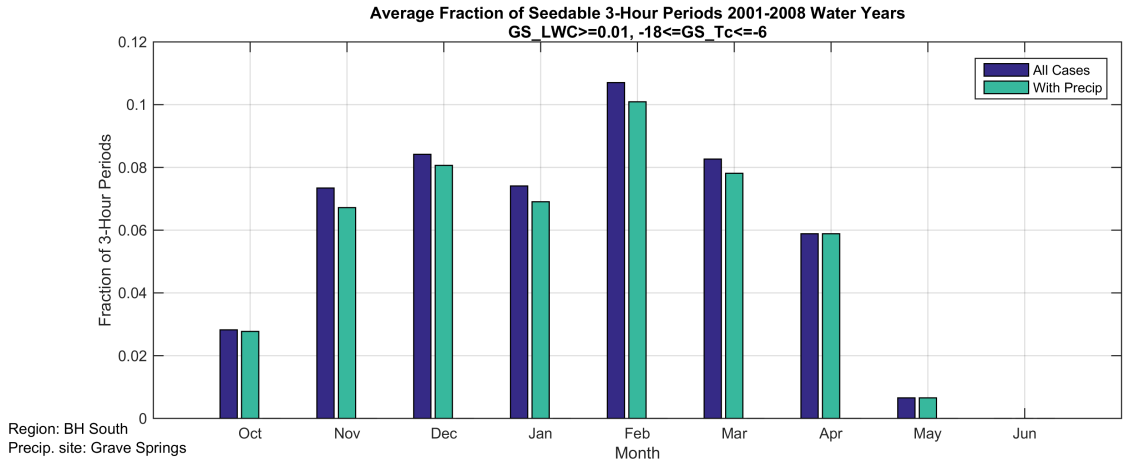


**Figure 4.48. As in Figure 4.42, but over the southern area and using precipitation near the Grave Springs SNOTEL site.**

Using a wind-direction criterion of 270–350 degrees for the southern region, the wintertime fraction of seedable hours is reduced only slightly, similar to the western area. However, similar to the eastern area, including the Froude number reduces the favorable fraction of wintertime hours to essentially zero (not shown).

### *Airborne Seeding Area-based Analysis*

Analysis of the airborne-seeding opportunities in the Bighorn Mountains is focused on two layers, 3.5–4.5 km MSL and 4.5–5.5 km MSL. The earlier histogram analysis focused only on the lower airborne layer as it was restricted to November–April, which is frequently too cold in the higher layer. However, as will be shown, the higher airborne layer has more frequent opportunities in late fall and early summer that may be worth considering.

#### Western Area

The monthly frequencies meeting the temperature and LWC criteria, shown in Figure 4.49, illustrate that the airborne opportunities are similar overall compared to ground, and they extend the seedable portion of the year beginning in early fall into early summer, as opposed to being primarily in the November–April months as in the ground-seeding layer. When these are normalized by precipitation occurring at the Shell Creek SNOTEL site, the frequencies are reduced at about the same rate as in the ground-seeding layer. These results vary little year-to-year (Figure 4.50), with the exception of the 2002–2003 being (slightly) anomalously high. This indicates that when airborne seeding conditions are met, there is a similar likelihood that it is precipitating at the surface. Since the precipitation may not always be snow, the same normalization by when snow was modeled at the Shell Creek SNOTEL site is included as well. The periods of precipitation that were snow were slightly lower than all precipitating periods in all months, indicating that even in the middle of winter, precipitation is not entirely falling as snow. A reviewer of this report expressed concern over the validity of the model simulating some occurrences of rain in any month of the winter, yet this finding is supported by a preliminary comparison of the daily precipitation gauge and snow pillow data at the Shell Creek SNOTEL site. Nonetheless, this comparison is not the most accurate way to check for the occurrence of rain versus snow, and therefore we recommend that further analysis be done to evaluate the modeled precipitation phase in the Bighorn Mountains to remedy this concern.

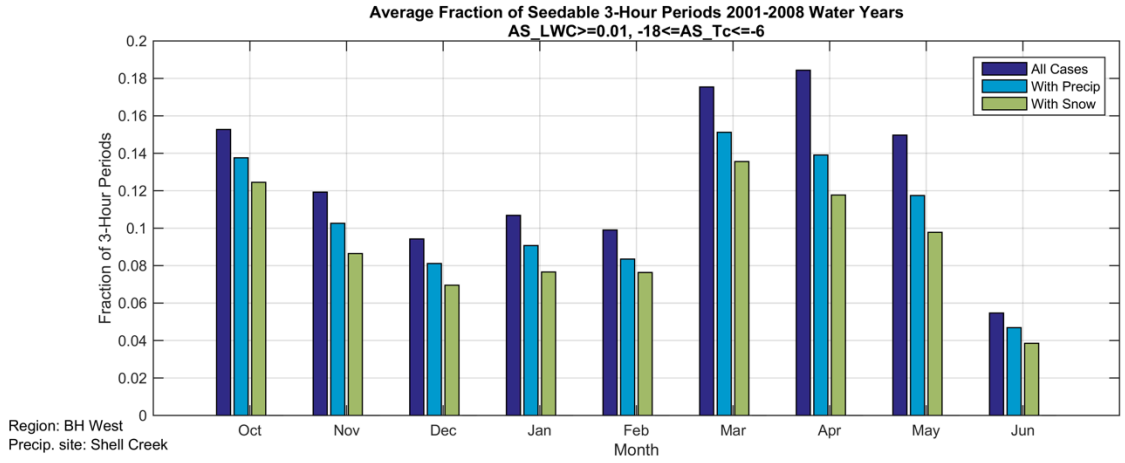


**Figure 4.49. Bar chart showing the average fraction of 3-hour periods in a month that met the temperature and LWC criteria averaged over the western area for airborne seeding (3.5–4.5 km MSL; blue) and the same for hours that also had any precipitation (cyan) and snow (green) in the model near the Shell Creek SNOTEL site.**




**Figure 4.50. Fraction of 3-hourly periods in the November–April period for each water year meeting the temperature and LWC criteria in the 3.5–4.5 km MSL layer over the western area (blue), and the same using the Shell Creek SNOTEL site for precipitation (cyan) and snow (green).**

As with the ground-seeding layer, there is month-to-month variability from year-to-year in the number of seedable hours (Figure 4.51). It is important to note that including May and October, and to a lesser degree June, provides a substantial increase in number of seedable hours for nearly every season in this period of study. The seasonal (November–April) and extended seasonal (October–June) total number of seedable 3-hour periods are shown in Figure 4.52 and Figure 4.53. Note the change from fraction of hours to number of periods; the fraction in the extended season naturally decreased due to a larger total number of 3-hour periods despite roughly 100 more 3-hour periods per year in the extended season.

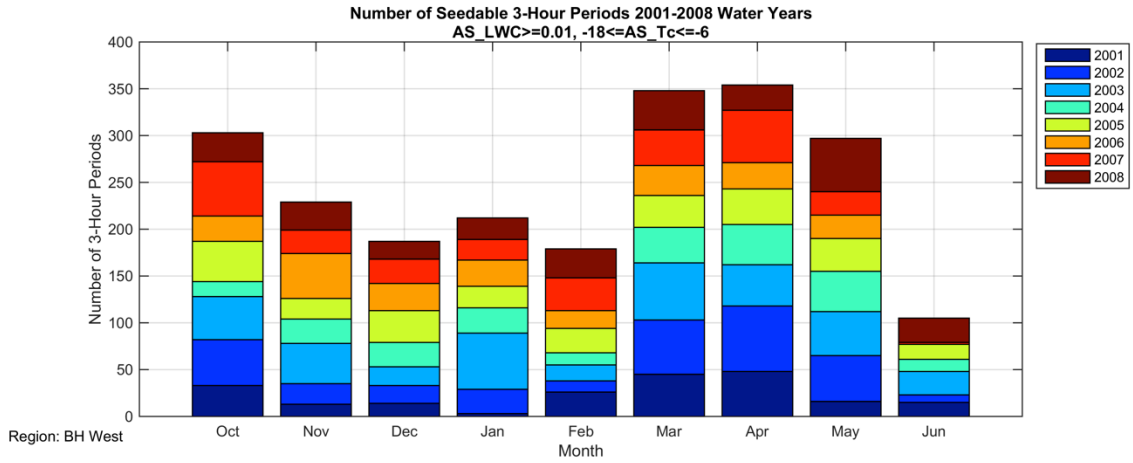


**Figure 4.51. As in Figure 4.43, except for airborne seeding (3.5–4.5 km MSL).**

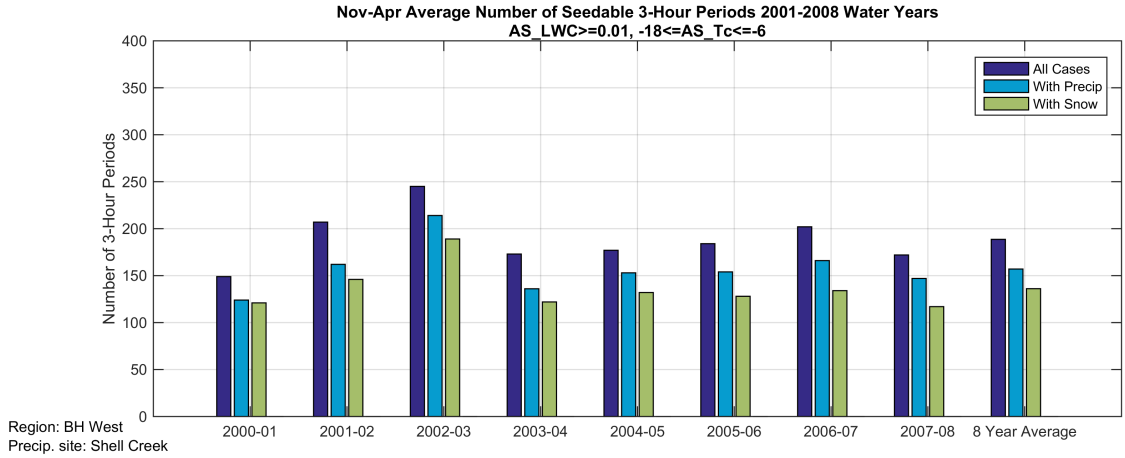


**Figure 4.52. As in Figure 4.50, except for number of 3-hourly periods rather than fraction.**

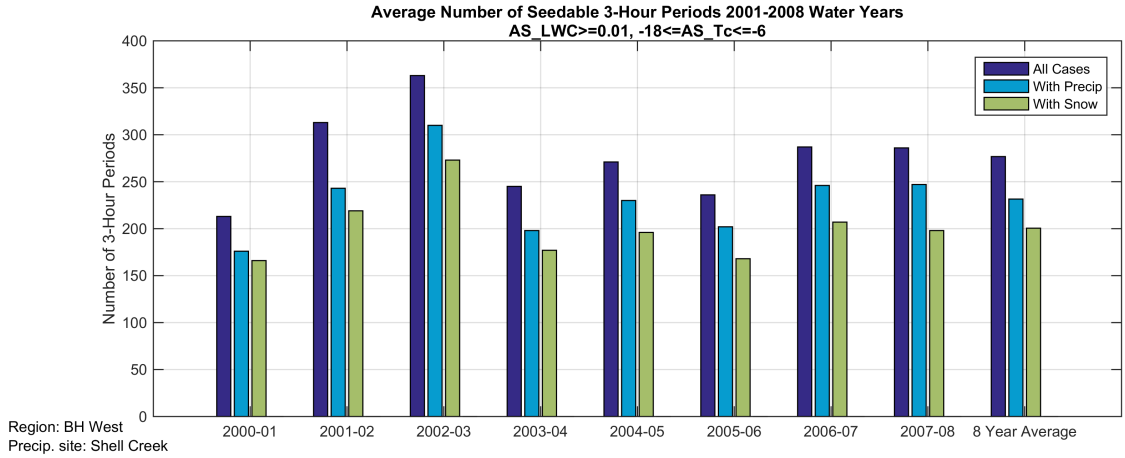


**Figure 4.53. As in Figure 4.50, except for number of 3-hourly periods in the extended October–June period.**

The higher airborne seeding layer (4.5–5.5 km MSL) shows infrequent opportunities in the winter months, largely due to temperatures being too cold (Figure 4.54). However, there are substantial opportunities in October and April–June, at nearly equal or greater frequencies than the lower airborne layer. However, when considering the frequency when snow is falling, the higher airborne layer frequencies are reduced well below 4% in those months, whereas they were 12%, 10%, and 4% in October, May, and June, respectively for the lower airborne layer when snow was falling.

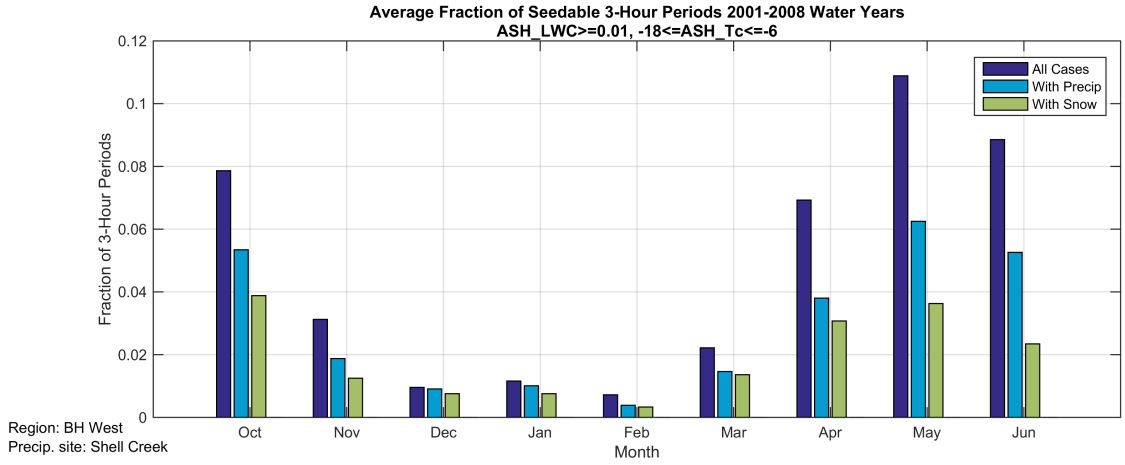


**Figure 4.54. As in Figure 4.49, except for the 4.5–5.5 km MSL layer.**

## Eastern Area

Airborne seeding opportunities in the eastern area show a similar monthly distribution as in the western area, with favorable conditions extending into the early summer and fall months (Figure 4.55). As with ground seeding, the eastern area presents seeding opportunities at a slightly lower rate compared to the western area.

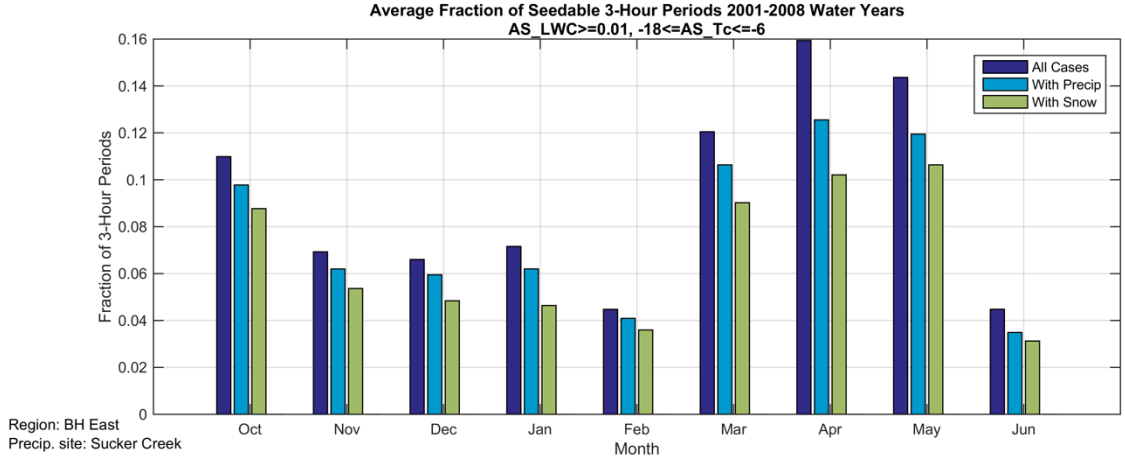


**Figure 4.55. As in Figure 4.49, except for the eastern region and the Sucker Creek SNOTEL site.**

Similar to the western area, the higher (4.5–5.5-km MSL) airborne layer in the eastern region has very few opportunities in November–March, but an even more pronounced increase in opportunities in early summer (Figure 4.56). Also similar to the western region, the frequencies for seeding in the warmer months are greatly reduced when considering if snow was falling.

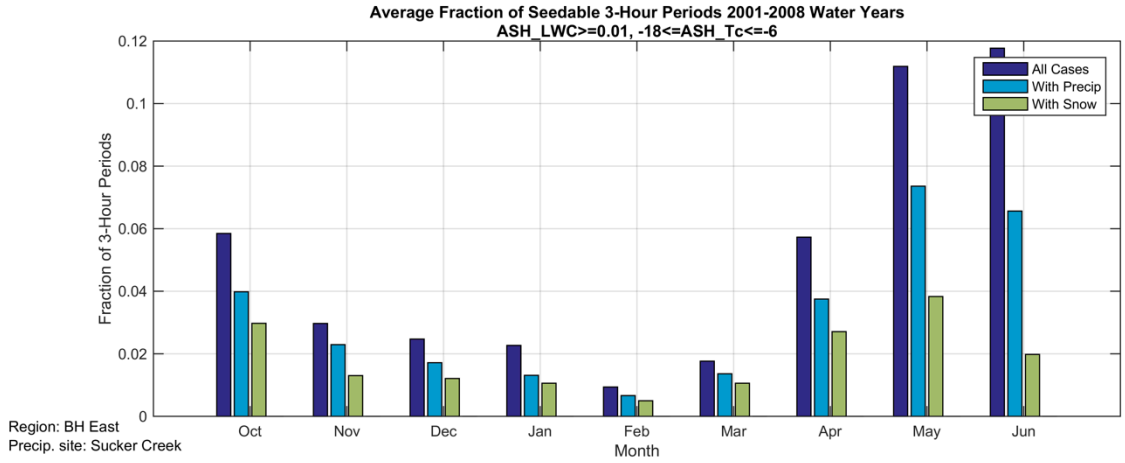


**Figure 4.56. As in Figure 4.49, except for the eastern region and Sucker Creek SNOTEL site, in the 4.5–5.5 km MSL layer.**

## Southern Area

The shape of the overall monthly distribution of 3.5–4.5-km MSL opportunities in the southern area is similar to that of the western and eastern areas, but at a lower rate than either one (Figure 4.57). Again, favorable conditions peak in April and extend into May, June, and October. Analysis of the 4.5–5.5-km MSL layer again reveals opportunities in early summer and late fall, but as with the lower airborne layer, at a lower frequency than in the eastern and western regions (Figure 4.58).

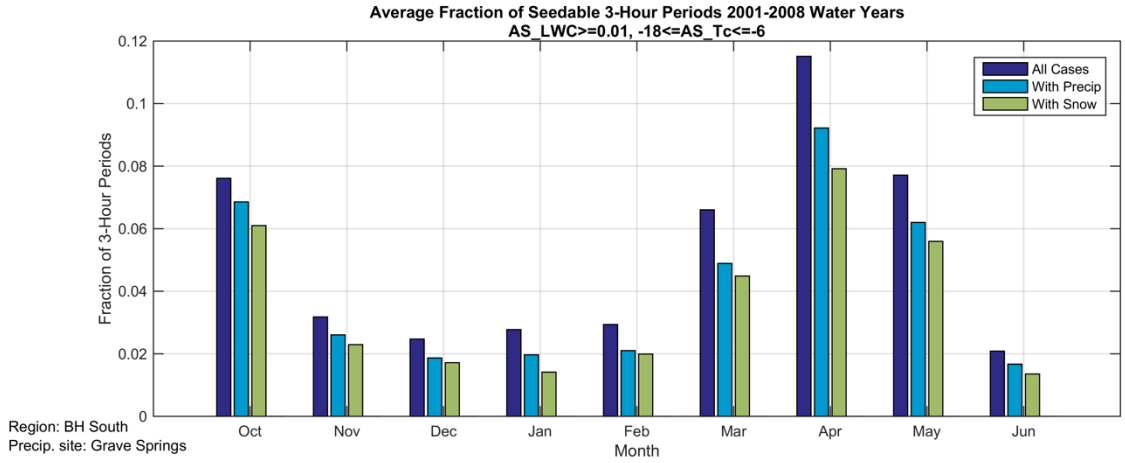


**Figure 4.57. As in Figure 4.49, except for the southern region and the Grave Springs SNOTEL site.**

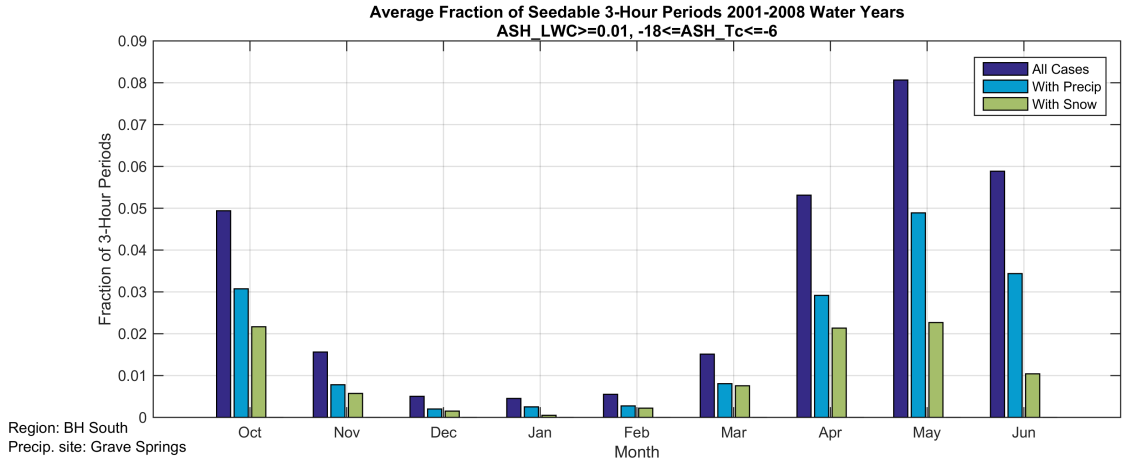


**Figure 4.58. As in Figure 4.49, except for the southern region and Grave Springs SNOTEL site, in the 4.5–5.5 km MSL layer.**

There is a slight increase overall (about 3%) in the average fraction of seedable hours when including the eastern region with the western region (Figure 4.59). This increases by about another 2% when including the southern area as well (Figure 4.60). Thus, while including the eastern and southern regions adds negligible opportunities in the ground-seeding layer due to wind direction and blocking, there is a small increase in the airborne layer.

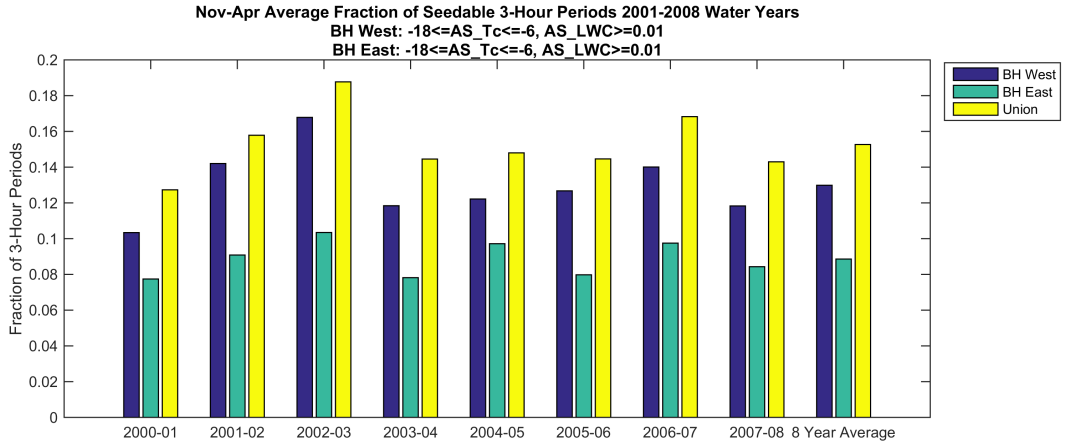


**Figure 4.59. Fraction of seedable three-hour periods meeting temperature and LWC criteria in the 3.5–4.5 km MSL airborne seeding layer for the western (blue) and eastern (cyan) areas, and the union of the two (yellow).**

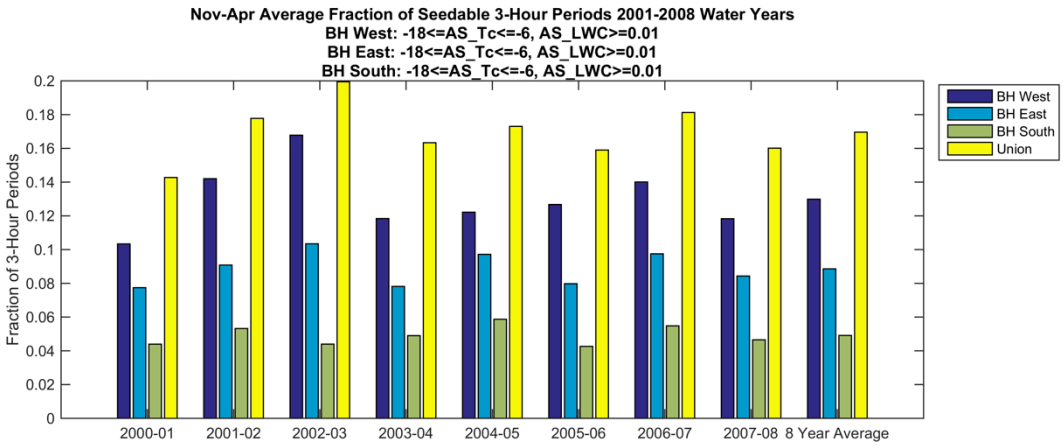


**Figure 4.60. As in Figure 4.59, except including the southern area as well (green).**

### *Ground versus Airborne Seeding Opportunities*

Using the area-based model analysis and when considering all of the additional criteria that impact ground-seeding opportunities, the airborne-seeding opportunities at the 3.5–4.5-km MSL layer are regularly greater in number than ground-seeding opportunities month-to-month (Figure 4.61). Comparison of ground and airborne layers is presented only for the western area, since the eastern and southern areas have zero or nearly zero opportunities in the ground-seeding layer when including Froude number and wind direction; the two airborne layers are compared against one another for all three regions. The winter months are best for ground-based seeding, while a focused period of October and April–June is more favorable for seeding in the airborne layer. The union of ground and airborne opportunities substantially increases the seasonal fraction of hours that are seedable. Based on the 8-year wintertime average it is just over 15% (Figure 4.62). This suggests that several seeding cases do not occur simultaneously in both layers.

As mentioned earlier, a higher airborne layer at 4.5–5.5-km MSL was also assessed, but has much less potential during the winter months for airborne seeding given low LWC and temperatures frequently colder than −18 °C. However, comparing the two airborne layers indicates substantial increases in airborne seeding opportunities outside of winter, particularly in October, May, and June (Figure 4.63). If the season were extended to be from October–June, there are roughly 60% more seedable 3-hourly output periods with a combined ground and air program (using both airborne layers) based on an 8-year average (Figure 4.64, Figure 4.65). However, recall that most of these seeding opportunities in these months for the higher airborne layer produced non-freezing precipitation (Figure 4.54).

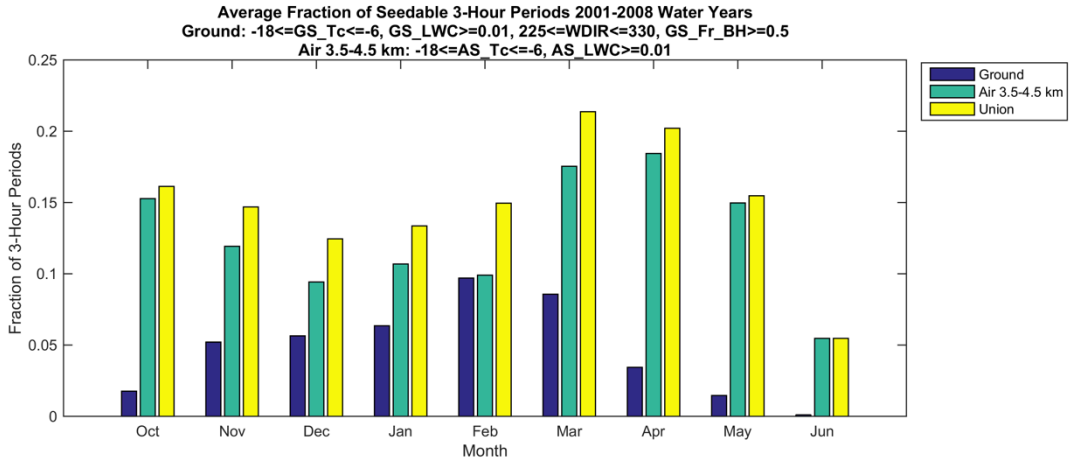


**Figure 4.61. Ground (0–1 km AGL; blue) versus airborne (3.5–4.5 km MSL; cyan) seeding opportunities by month in the western region (fraction of hours in the month that meet the designated criteria, listed atop the figure, on average over the 8-year period). The frequency of occurrence of cases from the union of both ground and airborne seeding potential is shown in the yellow bar for each time period.**

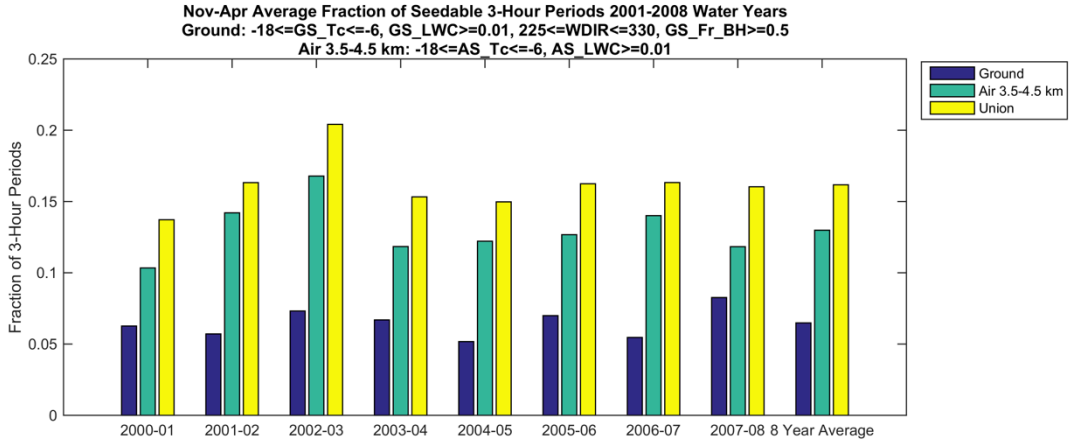


**Figure 4.62. Ground (0–1 km AGL; blue) versus airborne (3.5–4.5 km MSL; cyan) seeding opportunities by November–April season in the western region (fraction of hours in the season that meet the designated criteria, listed atop the figure), and the 8-year average. The frequency of occurrence of cases from the union of both ground and airborne seeding potential is shown in the yellow bar for each time period.**

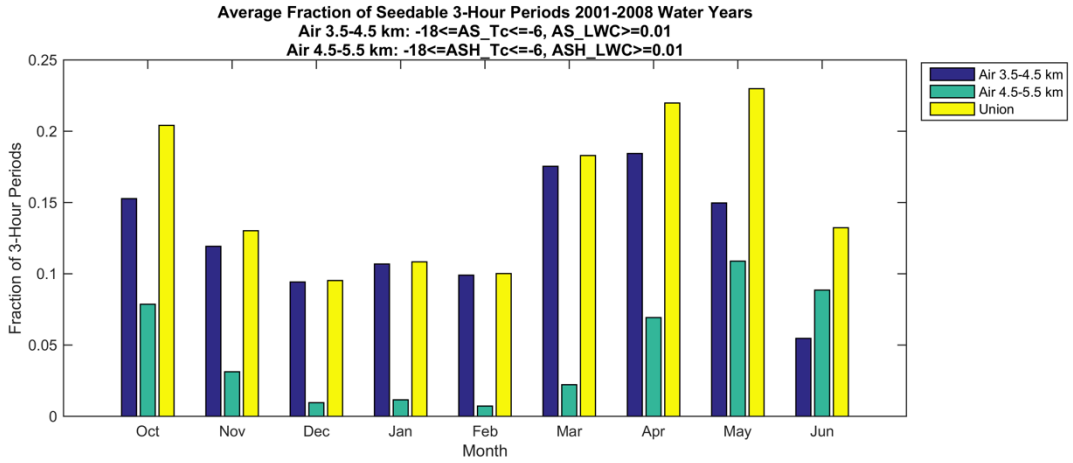


**Figure 4.63. Lower airborne (3.5–4.5 km MSL; blue) versus higher airborne (4.5–5.5 km MSL; cyan) seeding opportunities by month in the western region (fraction of hours in the month that meet the designated criteria, listed atop the figure, on average over the 8-year period). The frequency of occurrence of cases from the union of both ground and airborne seeding potential is shown in the yellow bar for each time period.**

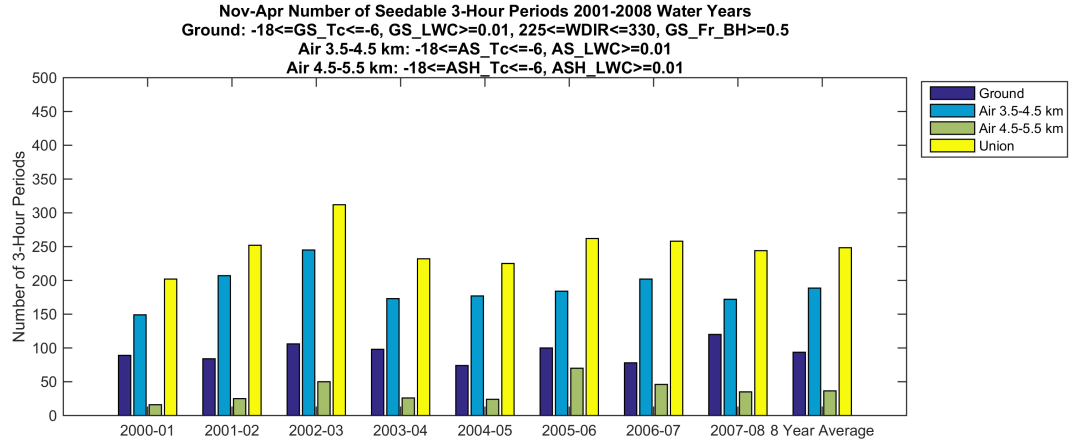


**Figure 4.64. Ground (0–1 km AGL; dark blue), lower airborne (3.5–4.5 km MSL; cyan), and upper airborne (4.5–5.5 km MSL; green) seeding opportunities in the western region by November–April season (total number of 3-hourly periods in the month that meet the designated criteria, listed atop the figure) and the 8-year average. The frequency of occurrence of cases from the union of both ground and airborne seeding potential is shown in the yellow bar for each time period.**

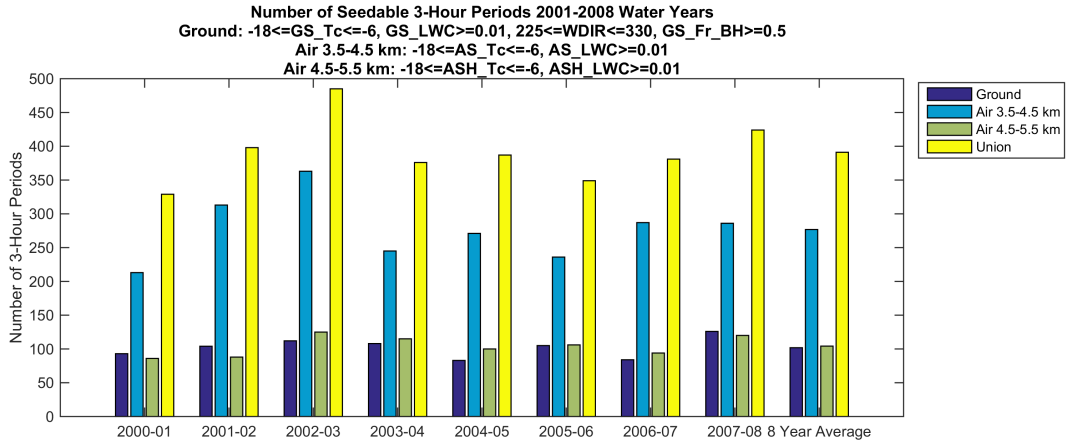


**Figure 4.65. As in Figure 4.64 but for the October–June period.**

Similar to the western region, including the upper airborne layer in the eastern and southern regions increases the number of seeding opportunities in October and April–June compared to the lower airborne layer alone (Figure 4.66–Figure 4.67). If it is feasible for the project to extend beyond the winter months, it may be worthwhile to include airborne seeding to provide additional seeding opportunities. This is of particular interest in the eastern and southern regions, since there are far fewer ground-seeding opportunities when considering wind direction and Froude number.

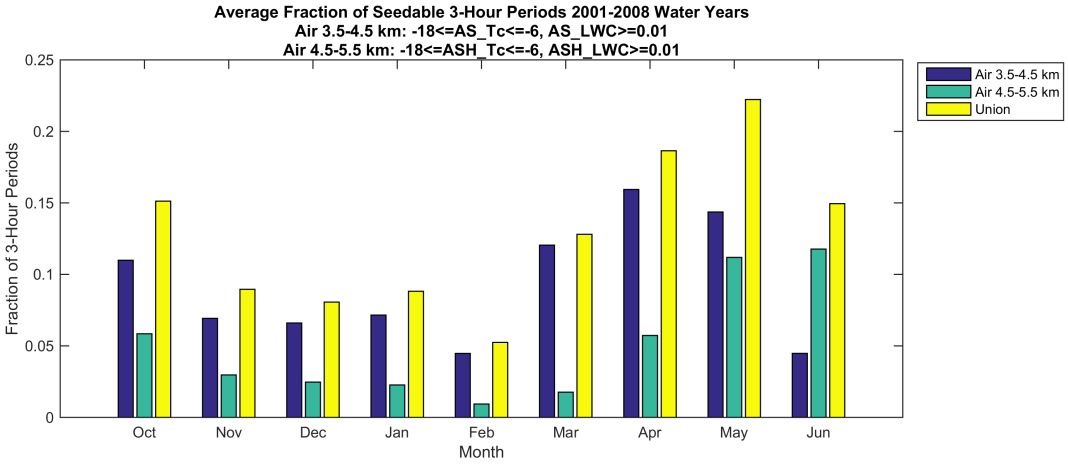


**Figure 4.66. As in Figure 4.63 but for the eastern region.**

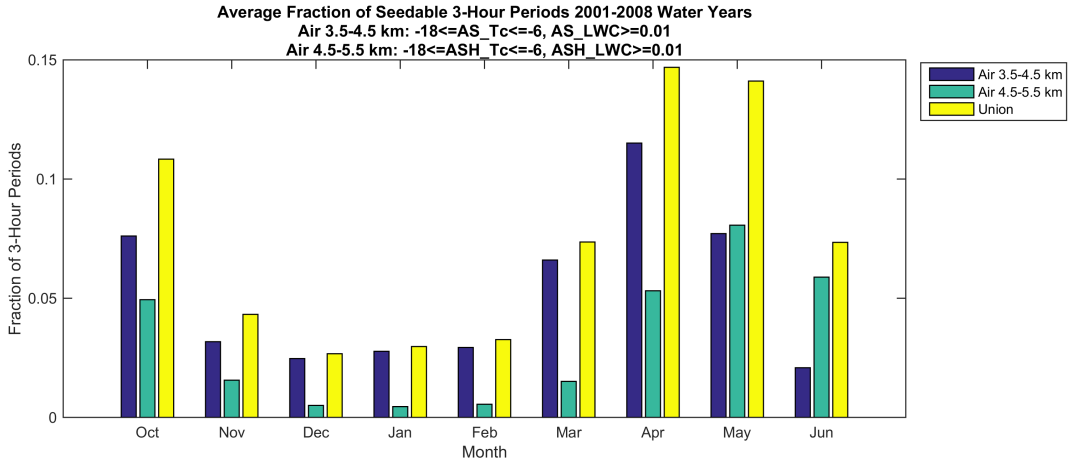


**Figure 4.67. As in Figure 4.63 but for the southern region.**

## 4.4 Seedable Precipitation Calculations

Model precipitation that fell during hours with seedable conditions was totaled throughout the wintertime months (November–April) and a wider period (October–June) to determine the total seasonal and extended-seasonal "seedable precipitation." This can then be compared to the total precipitation that fell to determine what fraction of the total precipitation could have been seeded. Note, however, that there may be seedable storms that did not produce precipitation (recall discussion above about instances when temperature and LWC are suitable, but no precipitation occurred as being potentially seedable). Without precipitation occurring during seedable periods, it is impossible to quantify the potential impact relative to natural precipitation for those situations.

As shown in Table 4.6 and Table 4.7, 41% (24%) of the seasonal (extended seasonal) precipitation for the western area fell when conditions met basic seeding criteria (temperature and LWC) in the ground-based layer (0–1 km AGL), 39% (33%) in the lower airborne seeding layer of 3.5–4.5 km MSL, and 8% (12%) in the upper airborne seeding layer of 4.5–5.5 km MSL. For ground-based seeding, additional criteria (wind direction and atmospheric stability) are needed to effectively transport AgI over the target area. When considering those additional criteria and assessing the ground-seeding layer in the western region, only 19% (11%) of seasonal (extended seasonal) precipitation was seedable. This reduction comes in part from the wind-direction criterion being applied, but also from the atmospheric stability (Fr) limiting the seeding opportunities. The additional ground-based criteria drop the eastern and southern regions to 0%. In the eastern region, this is primarily due to the wind direction being so predominantly west-northwesterly and the eastern region requires easterly winds for upslope conditions. In the southern region, however, the primary limitation is the criterion for atmospheric stability. Despite similar total precipitation, the precipitation that fell during seedable periods in the eastern area was lower for all types of seeding, both absolutely and relatively. Seedable precipitation amounts in the southern area were also lower than the western or eastern areas, both in total and percentage. In all three regions, including late fall and late spring/early summer has limited impact on the total seedable precipitation in the ground-seeding layer, but nearly (if not more than) doubles the seedable precipitation in mm in the airborne layers.

Table 4.6. Seasonal (November–April) 8-year average simulated total precipitation (mm) compared to the seasonal precipitation that fell during ground-seedable ("GS", 0–1 km AGL) time periods versus lower airborne-seedable ("AS", 3.5–4.5 km MSL) and upper airborne seedable ("ASH", 4.5–5.5 km MSL) times. The percent of the total seasonal precipitation that was seedable is provided in parentheses next to the absolute seedable precipitation. For the ground-seeding layer, the criteria builds starting with the basic temperature criteria, the the primary criteria (temperature and LWC), then the wind direction (WDIR) is included (T+LWC+WDIR) and finally the scenario with all additional criteria is included (T+LWC+ WDIR+Fr, "GS_all").

| | Precipitation (mm) | | | | | | | |
|---|---|---|---|---|---|---|---|---|
| **Region & Precip site** | **Season Total** | **GS: T** | **GS: T+LWC** | **GS: T+LWC+ WDIR** | **GS_all: T+LWC+ WDIR+Fr** | **AS: T+LWC** | **ASH: T+LWC** | **GS_all +AS** |
| West & Shell Creek | 380 | 258 (68%) | 155 (41%) | 124 (33%) | 73 (19%) | 146 (39%) | 30 (8%) | 178 (47%) |
| East & Sucker Creek | 364 | 261 (72%) | 120 (33%) | 31 (9%) | 0 (0%) | 94 (26%) | 23 (6%) | 94 (26%) |
| South & Grave Springs | 307 | 188 (61%) | 100 (33%) | 82 (27%) | 1 (0%) | 59 (19%) | 17 (6%) | 60 (20%) |

Table 4.7. Extended-seasonal (October–June) 8-year average simulated total precipitation (mm) compared to the extended-seasonal precipitation that fell during ground-seedable ("GS", 0–1 km AGL) time periods versus lower airborne-seedable ("AS", 3.5–4.5 km MSL) and upper airborne seedable ("ASH", 4.5–5.5 km MSL) times. The percent of the total precipitation that was seedable is provided in parentheses next to the absolute seedable precipitation. For the ground-seeding layer, the criteria builds starting with the basic temperature criteria, the the primary criteria (temperature and LWC), then the wind direction (WDIR) is included (T+LWC+WDIR) and finally the scenario with all additional criteria is included (T+LWC+ WDIR+Fr, "GS_all").

| | Precipitation (mm) | | | | | | | |
|---|---|---|---|---|---|---|---|---|
| **Region & Precip site** | **Extended Total** | **GS: T** | **GS: T+LWC** | **GS: T+LWC +WDIR** | **GS_all: T+LWC+ WDIR+Fr** | **AS: T+LWC** | **ASH: T+LWC** | **GS_all +AS** |
| West & Shell Creek | 719 | 285 (40%) | 173 (24%) | 136 (19%) | 80 (11%) | 236 (33%) | 85 (12%) | 270 (38%) |
| East & Sucker Creek | 748 | 308 (41%) | 150 (20%) | 41 (5%) | 0 (0%) | 182 (24%) | 80 (11%) | 182 (24%) |
| South & Grave Springs | 644 | 208 (32%) | 111 (17%) | 91 (14%) | 1 (0%) | 107 (17%) | 63 (10%) | 108 (17%) |

## 4.5 Summary

The typical wind regimes were westerly to northwesterly, with few easterly events on the eastern slopes of the Bighorn Mountains. The spatial mapping analysis revealed that LWC was most frequently located on the western and northeastern slope of the Bighorn Mountains, while the most frequent seeding opportunities occur on the western slope.

Based on 0–1-km AGL average temperature and LWC criteria, seeding criteria were met similar to, or more frequently than, in the airborne seeding layer during the November–April wintertime period. When the additional criteria for ground-based seeding (wind direction and atmospheric stability for transporting ground-released AgI into the targeted clouds) were considered, ground-seeding opportunities drop to nearly zero in the eastern

and southern regions, and were even substantially reduced in the western region. In fact, airborne-seeding opportunities (3.5–4.5 km MSL) in the western region are considerably more frequent than opportunities for ground seeding when considering the additional criteria required for ground-based seeding.

Including October, May, and June can potentially double seedable precipitation with an aircraft program. However, from a logistical perspective it is less likely that all airborne "seedable" hours can be seeded, especially with a single aircraft operation, given limited flight on station times. Even if the airborne program is restricted to the November–April period, airborne seeding at the 3.5–4.5-km MSL level is likely to yield more opportunities than ground seeding (considering factors that allow for AgI transport).

Most of the time when cloud-seeding conditions were present, precipitation occurred over the Bighorn Mountains. This indicates that there are few situations with low precipitation efficiency in which cloud seeding could have potential benefits. Only 19% of the precipitation that fell in a given season in the western region was seedable based on the full ground-seeding criteria being met, while 39% of the precipitation that fell in a given winter season was seedable by airborne seeding.

# 5. Task 4: Development of Preliminary Project Design

The overall goal of this task was to examine and develop the components of a cloud-seeding project design for the Bighorn Mountains area. The process followed the steps outlined in ASCE Standard#42-04 (ASCE 2004):

1. Definition of project scope
2. Targeting and delivery methods
3. Seeding agent selection
4. Meteorological data collection and instrumentation
5. Selection and siting of seeding equipment
6. Legal issues
7. Environmental concerns

Some of the steps in developing a project design are reported in separate sections of this report, such as meteorological data and instrumentation (Section 9) and legal issues and environmental concerns (Section 10). The remaining steps are described in more detail below.

The design process of selecting and siting of seeding equipment relies on the WRF model configured with a seeding parameterization to assess potential seeding effects resulting from different seeding scenarios and changes in the seeding delivery method (e.g., siting of ground-based seeding generators). The WRF modeling system was used as a tool to iteratively assess and improve the preliminary operational design by simulating selected case studies. Available meteorological observations in the region were used to evaluate the model performance for each case. This design process is described in this chapter, and the model evaluation of the design is described in Section 6. The design process was iterative based upon the results of the model evaluation, and therefore there are several additional aspects of the design described below that came about as a result of initial model simulations.

## 5.1 Project Scope and Targeting

The proposed target area is the Bighorn Mountains, with drainage into the Bighorn and Powder/Tongue River basins. The Bighorn Mountains are oriented from northwest to southeast in north central Wyoming. The highest peak is Cloud Peak at 4,013 m (13,167 ft) MSL located roughly in the central portion of the Mountains. There is a curved ridge of higher terrain that extends to the southwest from the south end of the Mountains. The total target area, defined as elevations above 8,000 ft MSL, is approximately 2,200 $km^2$ for the Bighorn Basin and 1,865 $km^2$ for the Powder/Tongue River basin. The climatology analysis (presented in Section 4), illustrated that the dominant wind direction is northwesterly to westerly, therefore the project designs primarily focused on targeting the western slope of the Mountains. A few additional project designs were tested to target the southern extension of the Mountains, as well as the northeast slope to capture results from other less frequent wind-flow patterns. The climatology analysis also defined that the best season for seeding in this region is between November and April for ground-based seeding, whereas airborne seeding could take place between October and May or June.

## 5.2 Delivery Methods and Seeding Agent Selection

The arguments outlined in Section 3 support AgI as the seeding agent to be used for glaciogenic seeding activities. Effective targeting of supercooled cloud regions depends on several factors related to the mode of seeding: adequate dispersion and concentration of the seeding material, costs, and logistical constraints (e.g., permissible flight altitudes, access to ground-based sites, permits and leases, reliable operation of the delivery mode). Two modes of ground-based AgI seeding (manually-operated generators and remotely-controlled generators) and the airborne release of AgI were reviewed with pros and cons identified for each approach. Figure 5.1–Figure 5.2 demonstrate the equipment used for the different seeding dispersion modes (i.e., ground and airborne).



**Figure 5.1. Example of a remotely-controlled AgI generator.**




**Figure 5.2. Example seeding aircraft .**

## 5.3 Selection of Test Cases

Section 6.2 describes the selection process for the test cases (seeded storms) used to assess the seeding impacts through numerical modeling of various generator and aircraft track locations. Three storms, two from the 2007–2008 season and one from the 2015–2016 season, were selected based on the climatology results and, for the 2015–2016 case, radiometer observations at Lovell, WY. The test cases represent different types of storm systems/wind regimes that resulted in different precipitation distribution patterns over the Bighorn Mountains. A comparison of the numerical model results for these test cases using several different seeding scenarios guided the design process. The various seeding scenarios, which varied the AgI dispersal modes and location of AgI release, were simulated in each of the cases when conditions from those scenarios were suitable for seeding. In each case, the wind, temperature, and liquid water conditions varied over time, typically related to a frontal passage, and therefore influenced times when suitable conditions for seeding occurred for each seeding scenario.

## 5.4 Initial Exploratory Ground-based Tests

The initial groups of generator location scenarios were designed to test the impacts of remote generators in varying locations along the Bighorn Mountains located on elevated terrain with a typical seeding rate of 25 g $h^{-1}$. As such, five groups (A-E, see Figure 5.3) of ground-based generators were designed to test seeding effectiveness in the northern-most regions of the Bighorn Mountains, down to the southern extension of the barrier.

Group A was designed based on the wind-direction results of the climatology analysis and previous research indicating that siting generators on upwind barriers (or elevanted terrain) can aid in transporting AgI plumes released from ground-based generators over downwind barriers (i.e., siting above any inversions). However, the logistics of siting generators in the State of Montana may have made these sites prohibitive, yet they were still tested in the model for thoroughness.

Group B was selected using a similar motivation as Group A; however, these sites are located in the state of Wyoming, just south of the Montana/Wyoming border.

Group C was designed to simulate seeding opportunities in the northern portion of the Bighorn Mountains under northwesterly, northerly, and northeasterly wind directions.

Group D was designed to cover the entire western slope under westerly wind directions.

Group E was designed to simulate seeding opportunities that occurred along the southern extension of the Mountains. The Group E design could be quite verstatile, in that a wide range of wind directions could be utilized for operations. Group E generators could be operated in westerly or northwesterly flow in order to target southern portions of the Mountains, as well as operated in southerly flow to transport AgI northward to the higher mountain peaks.

Results of the model simulations testing these design groups are presented in Section 6.

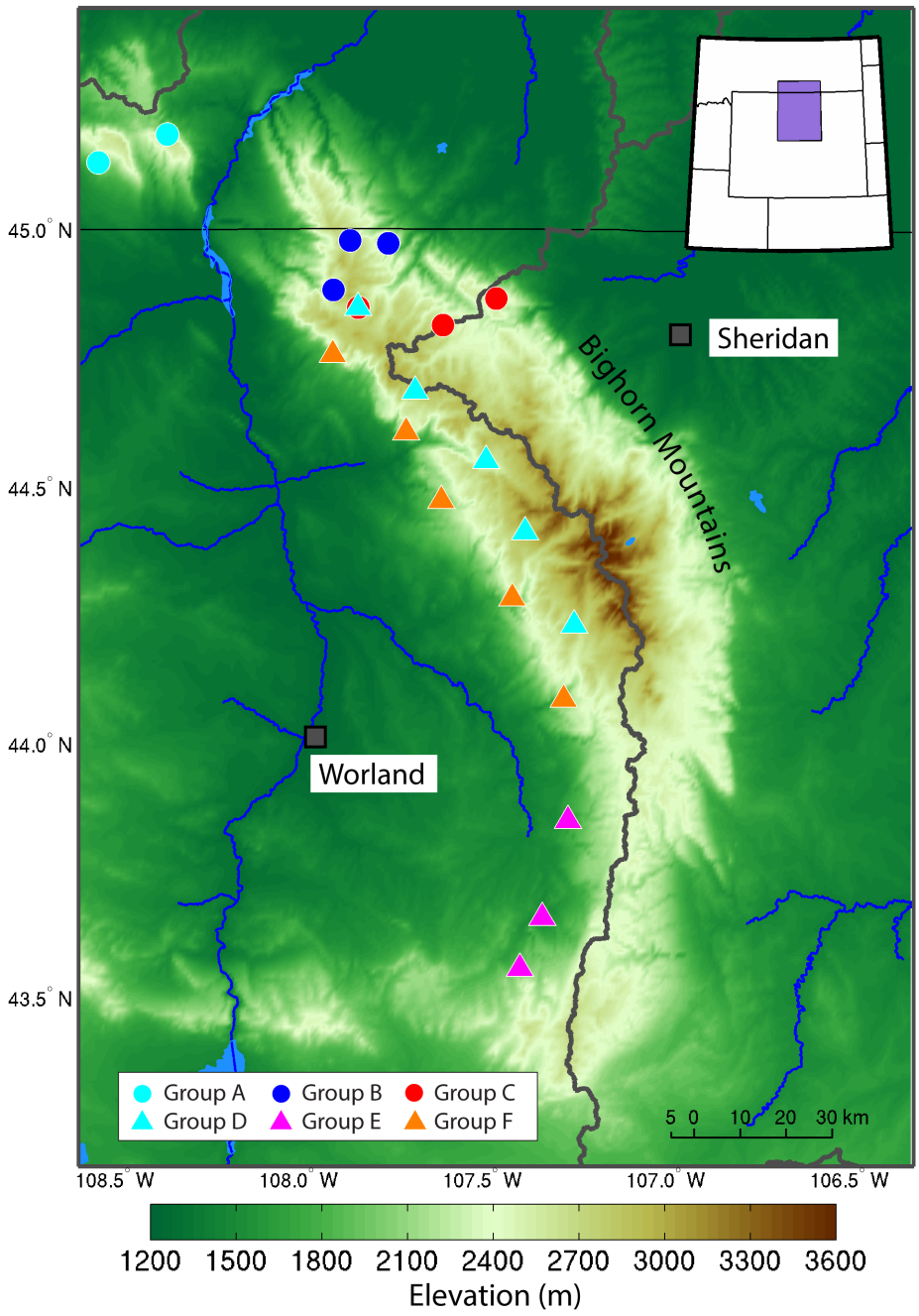


**Figure 5.3. Topography map of the Bighorn Mountains (m) illustrating the locations of all ground-based generator design groups.**

## 5.5 Airborne Tests

Three airborne track locations were evaluated in the seeding experiments with the three cases (Figure 5.4). Tests were performed to assess the impact of upwind distance or altitude of the aircraft track on simulated seeding effects in the target area.

A short northeast-southwest-oriented track (~60 km) in between Group A and Group B was designed as an airborne alterative (or complement) to these two ground-based generator groups to target the northern portion of the Range ( “North” track in Figure 5.4). A “Central” track, oriented northwest-southeast parallel to the Bighorn Mountains (~160 km long), was simulated to target the main portion of the Mountains. This track was tested farther upwind (“Central-West”) and at higher altitudes, as well as with a shorter track distance (~80 km; “Central-short” in Figure 5.4) to understand how these changes affected the simulated seeding response. A third track location was designed with a north-south orientation to target the southern extension of the Range (“South” in Figure 5.4). Details of the results from these test simulations are provided in Section 6.3.

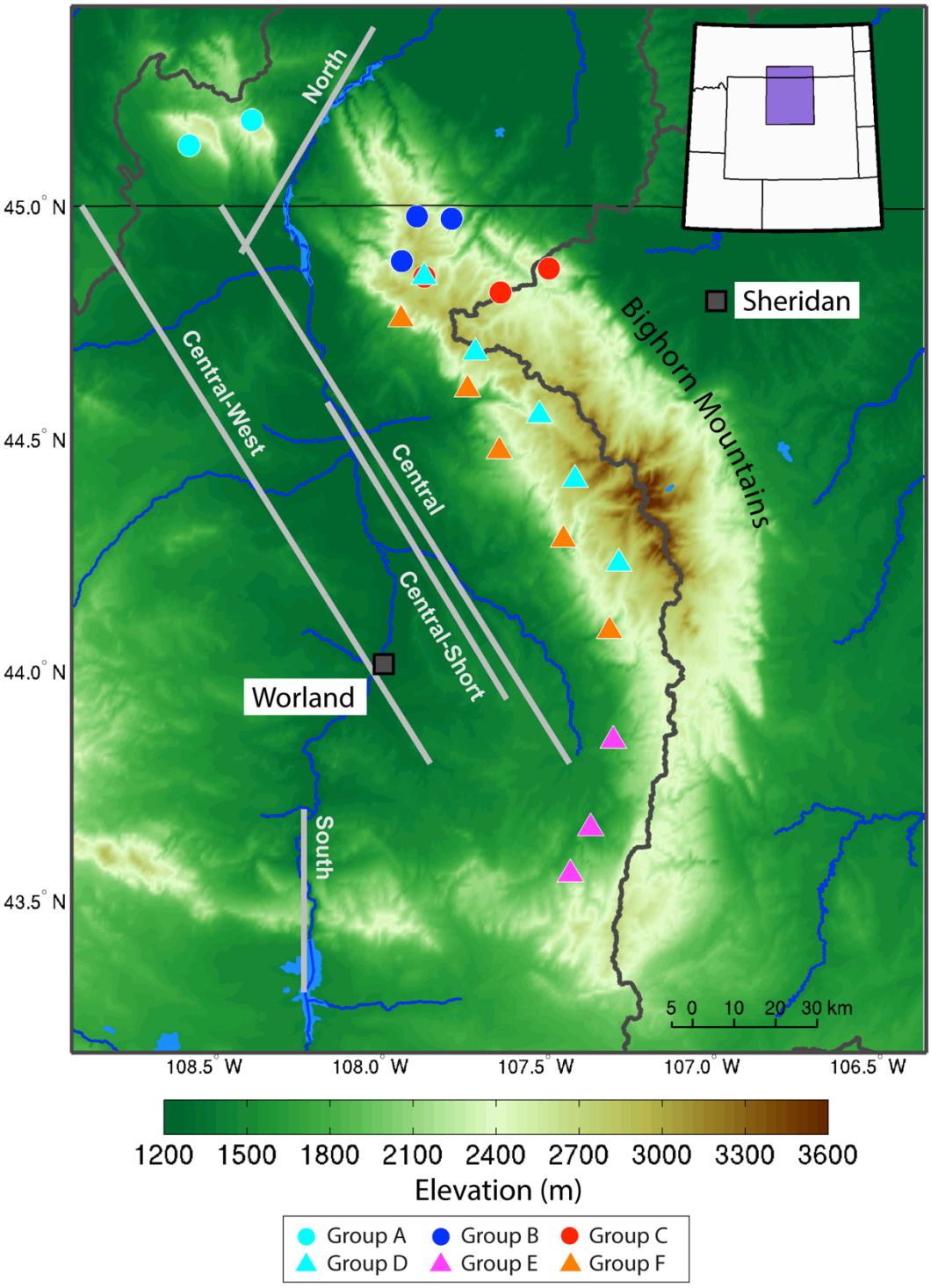


**Figure 5.4. Map of the proposed ground generator groups and potential airborne seeding flight tracks tested with the model.**

## 5.6 Additional Tests

The western slope of the Bighorn Mountains is very steep. Based on the results of the case study simulations, it became clear that AgI from the Group D generators was not fully

dispersing where there was SLW on the western slope given how high up the slope these sites were. As a result, Group F was created to site generators further west and at slightly lower elevations on the western slope (Figure 5.3). Group F generators were sited at the western-most edge of the higher terrain in order to prevent their plumes from being too easily blocked by the steep terrain (e.g., if they had been sited at the base of the steep slope).

## 5.7 Final Ground-based Generator Locations

After reviewing the results of the site visits to many of the generator locations (Section 7), and the iterative model evaluation (Section 6), Groups A and B were ruled out as ineffective generator site locations. Groups C-F were all determined to be effective in at least some, if not all, of the test cases simulated. While Group E did not result in substantial simulated seeding effects in the cases evaluated, the versatility of how the AgI dispersed from these sites makes them important to consider further in a final design process. If cost becomes an issue, both Groups C and E could be eliminated given they both had minimal simulated impacts and/or can only be used in limited situations based upon the climatology results.

Nevertheless, it is important to note that the conditions varied substantially with time and across the large area of the Bighorn Mountains, and therefore, one Group was not suitable for all situations. Based on the findings of the preliminary project design, and if resources allow, it is recommended that Groups C–F all be considered as potential ground-based seeding sites in a final project design (Figure 5.5).

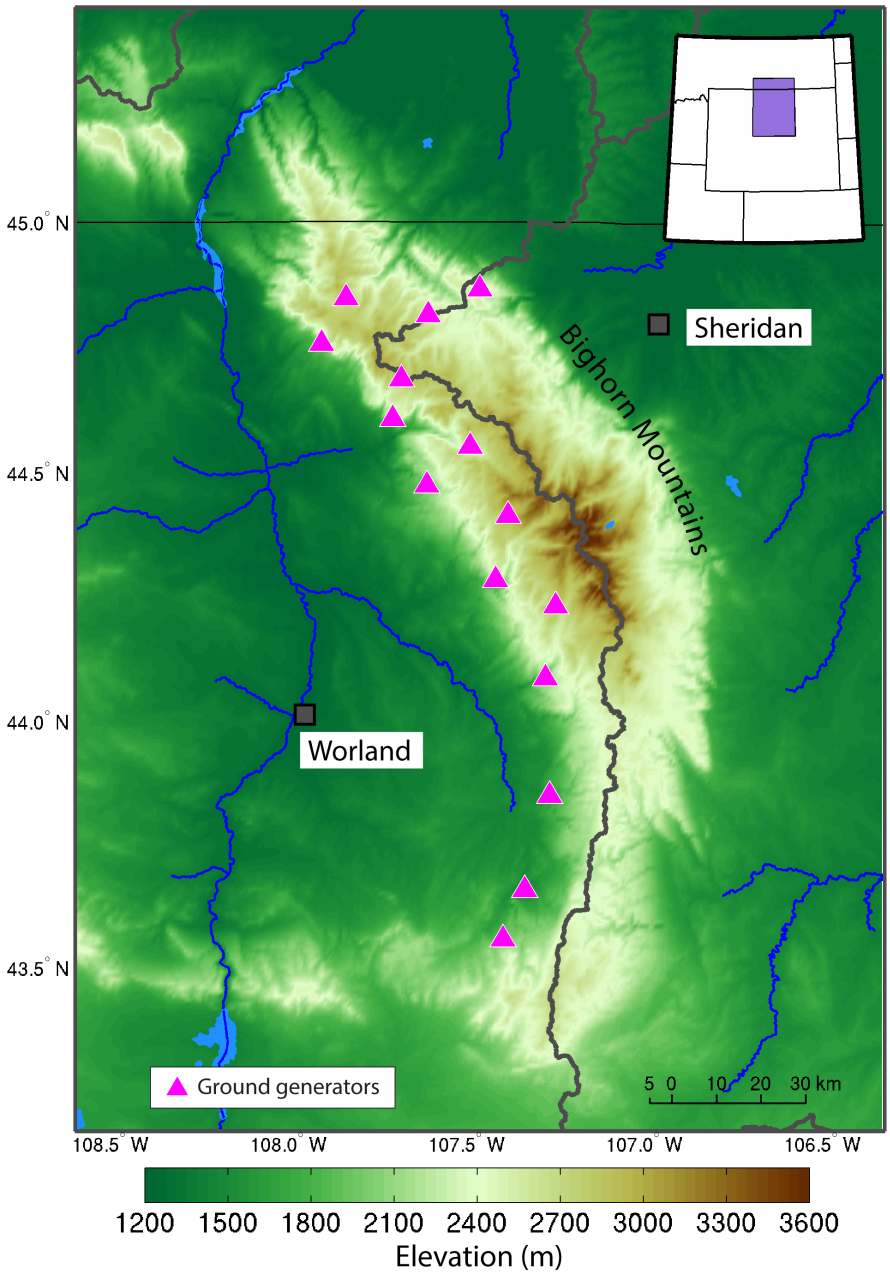


**Figure 5.5. Map of the Bighorn Mountains with the locations of potential ground-based generators. The thick gray line illustrates the divide between the Bighorn and Powder/Tongue River basins.**

## 5.8 Summary Remarks

A summary of the proposed Bighorn Mountains cloud-seeding preliminary design to enhance precipitation and streamflow into the Bighorn and Powder/Tongue River basins includes the following.

- A target area in the Bighorn Mountains encompassing the Bighorn and Powder/Tongue River basins above 8,000 ft MSL (2,438 m). This area is approximately 2,200 km$^2$ (850 square miles) for the Bighorn Basin and covers the western and northwestern slopes of the Bighorn Mountains, and is approximately

1,865 $km^2$ (720 square miles) for the Powder/Tongue River basin covering the eastern slopes of the Bighorn Mountains.

- An operational season of November through mid-April (e.g., 15 November–15 April) for ground-based seeding. This season could be extended longer to cover 1 October–31 May for airborne seeding.
- Silver iodide, or more specifically, a silver iodide-salt compound is recommended to be used as the seeding agent.
- A ground-based seeding operation that relies on the remotely-controlled generator network across the Bighorn Mountains, primarily on the western slope of the barrier; and/or an airborne seeding operation that can be positioned to target the regions of the barrier that are most suitable for seeding that cannot be targeted using ground-based techniques, including farther upwind/west of the mountains over the Bighorn River Basin
- The use of a prognostic numerical model with frequent updates to aid in identifying suitable seeding opportunities, possibly with an automated seeding criteria assessment.
- In addition to, or in place of, the numerical model, it is recommended that direct observations of seeding criteria parameters, such as liquid water and temperature and wind profiles are included in the project design.

Various aspects of the design are covered in other sections of this report, such as the recommended criteria for seeding, criteria for suspending operations, environmental concerns, and the advantages and disadvantages of the different seeding dispersion modes (manual, remote, and airborne).

# 6. Task 5: Model Evaluation of Preliminary Project Design

The purpose of this task was to use a numerical model to evaluate, through an iterative process, the suggested locations of ground-seeding generators and aircraft seeding flight tracks in order to optimize seeding strategies for the preliminary project design.

## 6.1 Model setup

The WRFV3.7.1 model was used to simulate three test cases. Two 1-way nested domains were set up for the simulations (Figure 6.1). The outer domain covers most of the western U.S. using a horizontal grid spacing of 2,700 m. The inner domain centered on the Bighorn Mountains has a horizontal grid spacing of 900 m (Figure 6.1). The vertical coordinate consisted of 81 terrain-following vertically-stretched levels. This includes an extra 20 levels in the lowest 4 km to better resolve AgI dispersion compared to the 61-level setup that was used in many previous studies (Xue et al. 2010, 2012, 2013a, 2013b, 2014).

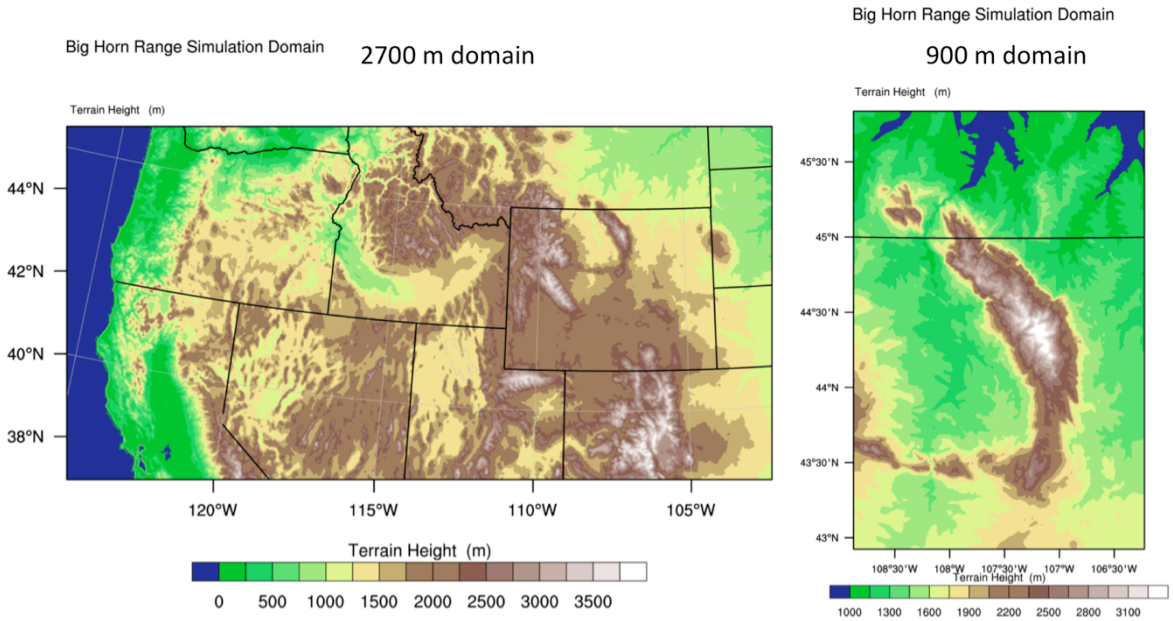


**Figure 6.1. Model domain for all cloud seeding project design evaluation simulations.**

The simulations of the outer domain were driven by analysis data from ERA-Interim. For each case, the outer domain was integrated for 48 hours with the first 12 hours as the spin-up period. Then the hourly outputs for the latter 36 hours were processed through the program ndown.exe to generate the initial and boundary conditions for the inner domain simulations. In this study, the new Thompson-Eidhammer microphysics scheme was applied. The climatological CCN and IN distributions were used to simulate the cloud activation and natural ice nucleation processes. To make such information available for the 900-m inner domain, the program ndown.exe was modified. The detailed configurations are listed in Table 6.1.

Table 6.1. Model configuration for cloud seeding project design evaluation simulations.

| Domain | 2700-m domain | 900-m domain |
|---|---|---|
| Horizontal grids | 720 x 360 | 240 x 360 |
| Vertical levels | 81 terrain-following Eta levels | |
| Time step | 12 s | 5 s |
| PBL scheme | Mellor–Yamada–Nakanishi–Niino (MYNN) 2.5 order | |
| Microphysics scheme | Thompson-Eidhammer with the new AgI seeding parameterization | |

### *6.1.1 Cloud-Seeding Parameterization in WRF*

The WRF numerical modeling system (Klemp et al. 2003; Skamarock 2004; Mikalakes et al. 2004; Barker et al. 2004; Chen and Dudhia 2000) is a community model developed through a collaborative effort led by NCAR. Modifications to the physics parameterization in the model code simulate the dispersion and activation of AgI seeding material within the cloud (i.e., AgI cloud-seeding parameterization, Xue et al. 2013a, b), and the subsequent microphysical responses leading to precipitation.

The wintertime AgI seeding parameterization (WASP) was embedded in the Thompson microphysics scheme (Thompson et al. 2004, 2008, Thompson and Eidhammer 2014). The Thompson scheme originated from a study that tested several different microphysics schemes in an attempt to determine which one best simulated mixed-phase clouds, including those with large amounts of SLW (Thompson et al. 2004). Several modifications to the Reisner et al. (1998) scheme resulted from this study, which produced the Thompson bulk microphysical scheme that handles the sensitive balance of cloud water, snow, and graupel suitably for this proposed study. The newest version of the Thompson scheme (Thompson and Eidhammer 2014) incorporates the explicit cloud droplet activation and ice nucleation as a function of the background CCN and IN concentration. Such an "aerosol-aware" version (known as the Thompson-Eidhammer scheme) simulates more realistic clouds. The WASP has been incorporated into the new Thompson-Eidhammer scheme and was modified to simulate more AgI removal processes that were absent in the original version.

Using WASP, AgI particles can be released in the computing domain as a function of location, time, and source strength. In other words, it can represent the release of AgI from ground-based generators and/or airborne platforms (Xue et al. 2013a, b). With a

prescribed source strength or release rate (g $h^{-1}$) and a known mean mass diameter (m), the number of AgI particles is retrieved. These AgI particles, acting as passive scalars, are advected and dispersed horizontally and vertically by model dynamics. The vertical diffusion, or mixing, of these particles is calculated by the planetary boundary layer (PBL) schemes. By default, the PBL schemes only mix water vapor, cloud water, and cloud ice vertically. To make vertical mixing of AgI particles more realistic, the PBL schemes were modified to mix all AgI-related scalars vertically. In the WRFV3.7.1, the vertical mixing of all scalars have been realized by all PBL schemes.

The AgI particles are assumed to be monodisperse in the AgI cloud-seeding parameterization. Modifications were made to the parameterization so that a lognormal distribution of AgI particles could be simulated.

AgI particles can be collected by drops and ice-phase particles through Brownian, phoretic, and turbulent diffusion. When the conditions are favorable, these AgI particles can nucleate ice crystals through deposition, condensation freezing, contact freezing, and immersion freezing. Both mixing ratios and number concentrations are predicted for dry AgI and AgI within each of the hydrometeor categories: cloud and rain drops, ice, snow, and graupel. The new version of WASP also simulates the AgI scavenging by precipitation particles (rain, snow, and graupel), AgI self-coagulation, mainly through the Brownian diffusion, and AgI dry deposition is now included as a function of surface roughness and PBL height. The detailed interactions between AgI and hydrometeors are illustrated in Figure 6.2.

The WRF model with this wintertime AgI seeding parameterization has been previously used to simulate the seeding effect over the target ranges for the WWMPP, Wyoming Range Phase II Feasibility study, and for program design and evaluation for Idaho Power Company (IPC). While efforts have been made to evaluate the model against available observations (e.g., soundings, radiometer, precipitation gauges), the required measurements to evaluate the physics of the cloud-seeding parameterization itself have not been available. Therefore, the parameterization has not been fully evaluated and all simulated seeding results should be considered approximate. Nonetheless, the model's ability to simulate the meteorological conditions needed for a seeding effect (i.e., temperature, winds, liquid water), which can be validated with sounding and radiometer data, can be evaluated. If these conditions are well represented by the model, it is a general indication that the resulting simulated seeding effects may be reasonable.

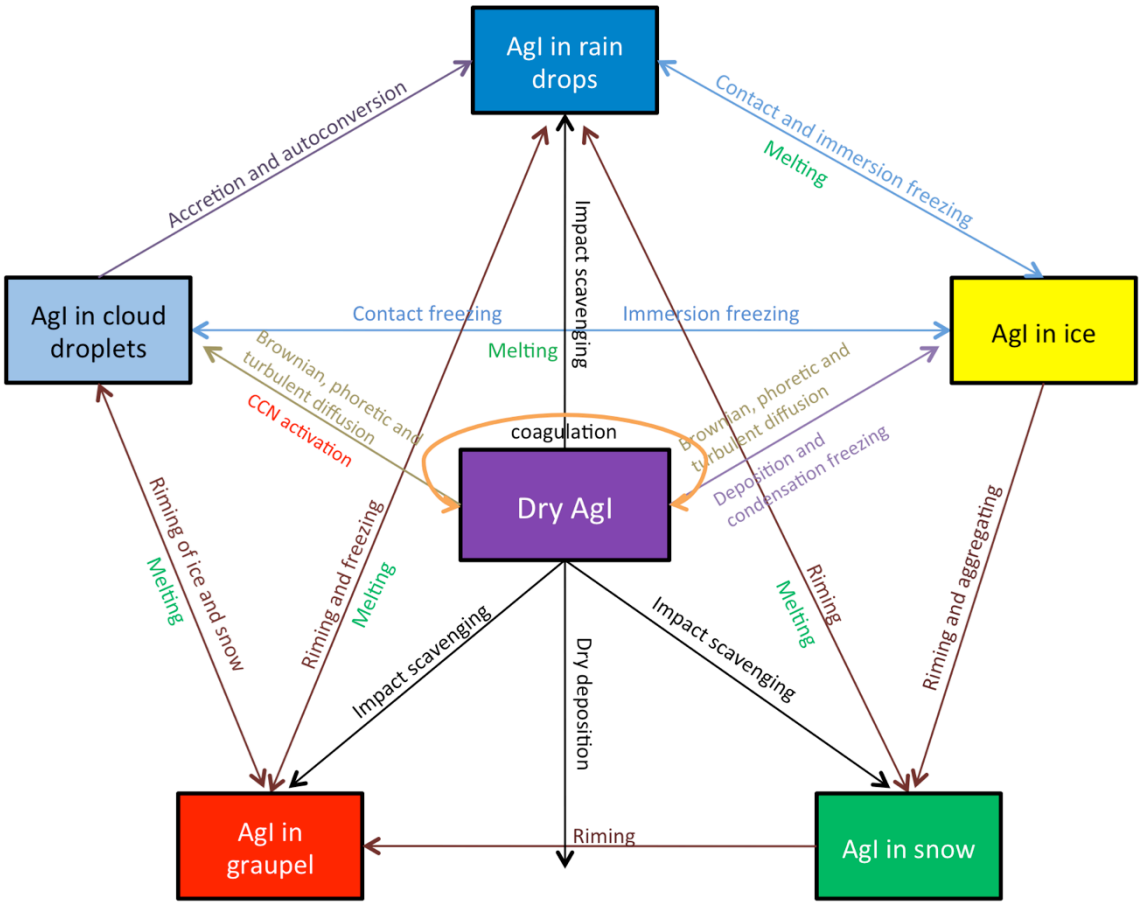


**Figure 6.2. Interactions between AgI and hydrometeors simulated in the cloud-seeding parameterization (updated from Xue et al. 2013a to include coagulation, impact scavenging, and dry deposition for AgI).**

## 6.2 Case Selection and Overviews

In order to assess a variety of different program design options, cases were selected to represent a variety of different meteorological scenarios suitable for seeding. Given the lack of data in the region, some cases were selected based on the WRF-CONUS model simulation. One case was also selected based on the data collected with instrumentation deployed in the target area during the 2015–2016 winter. Cases were chosen to represent different types of storm systems/wind regimes that resulted in different precipitation distribution patterns over the Bighorn Mountains (Table 6.2).

### *6.2.1 Case Selection using WRF-CONUS Model*

The most recent winter season analyzed with the WRF-CONUS model (2007–2008) was examined in detail for possible cases suitable for seeding that could be simulated to test the preliminary design for the project. The 3-hourly and 4-km WRF-CONUS model outputs over the Bighorns during the 2007–2008 winter were analyzed by the Wintertime AgI Seeding Case-calling Algorithm (WASCA) based on three sub-regions (Figure 6.3). WASCA is a tool

that assesses the conditions from a model simulation for their suitability for seeding over pre-selected areas. The conditions it assesses are temperature, LWP, LWC within the vertical layer of the atmosphere being targets (i.e., 0–1 km AGL for ground seeding, higher levels for airborne seeding), and winds. It also assesses the stability of the atmosphere for ground seeding scenarios. These results identified a multitude of possible cases, and from that list of cases a visual investigation of the LWP, 700-hPa winds, and 700-hPa temperatures was performed to select cases that might be suitable to test the various preliminary design scenarios (Section 5). From that analysis, two cases (13 November and 20 November 2007) were chosen to test the seeding efficacy of several ground-generator groups and various flight tracks.

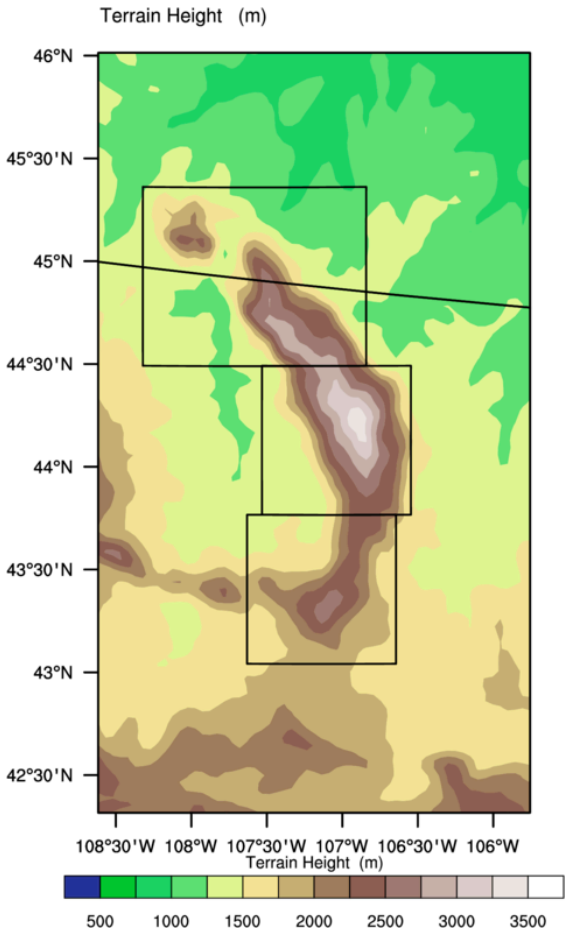


**Figure 6.3. The Bighorn sub-domain extracted from the WRF-CONUS model runs. The three black boxes indicate the three sub-regions used by WASCA to assess conditions suitable for seeding. The black line at 45°N is the Wyoming-Montana state border.**

### *6.2.2 Case Selection Using Observations from 2015–2016*

Analysis of observed radiometer LWP data at Lovell, WY (see Section 17.2.1 for more detail) indicated periods with liquid water that may be suitable for seeding. What made case selection from this past winter more challenging, however, was the lack of data or

high-resolution model output to indicate if the temperature and winds were also suitable for seeding. Nonetheless, reanalysis data were utilized to help aid in this determination, which led to the selection of a third case on 17 January 2016.

**Table 6.2. Summary of wind regime and precipitation for the selected cases.**

| Case Date | 700-hPa Wind Direction | Precipitation Distribution |
|---|---|---|
| 13 November 2007 | Shifts from westerly to northwesterly with cold frontal passage | Local northern end maximum, second maximum around Cloud Peak |
| 20 November 2017 | Shifts from westerly to variable around the barrier, including northeasterly on northeast slope with cold frontal passage | Widespread northeastern slope maximum |
| 17 January 2016 | West-northwesterly | Widespread maximum over high elevations of entire barrier |

## 6.3 Case Study Simulation Results

For each case, first a control simulation was run without seeding. Then, the WASCA was run on the half-hourly 900-m control outputs for the entire simulation periods to further identify times within the control simulation period to simulate seeding. The seeding conditions over three sub-regions (north, central, and south, or BHN, BHC, and BHS, respectively) were assessed (Figure 6.4). The cases identified by the WASCA and the associated plots will be present in each case's results sections below. While data are limited in this region, precipitation-gauge data are available and will be compared to the modeled precipitation for each case. However, the SNOTEL hourly accumulation data fluctuates, such that taking the difference between the end and beginning of the simulation period often results in negative accumulations (even when precipitation was actually occurring). Therefore, both the minimum and maximum precipitation accumulation were computed based on the hourly SNOTEL observations to give the possible range of observed precipitation during these simulated periods. The generator groups and aircraft tracks to be tested were plotted in Figure 5.4. Flight tracks for airborne seeding will be shown in each case separately.

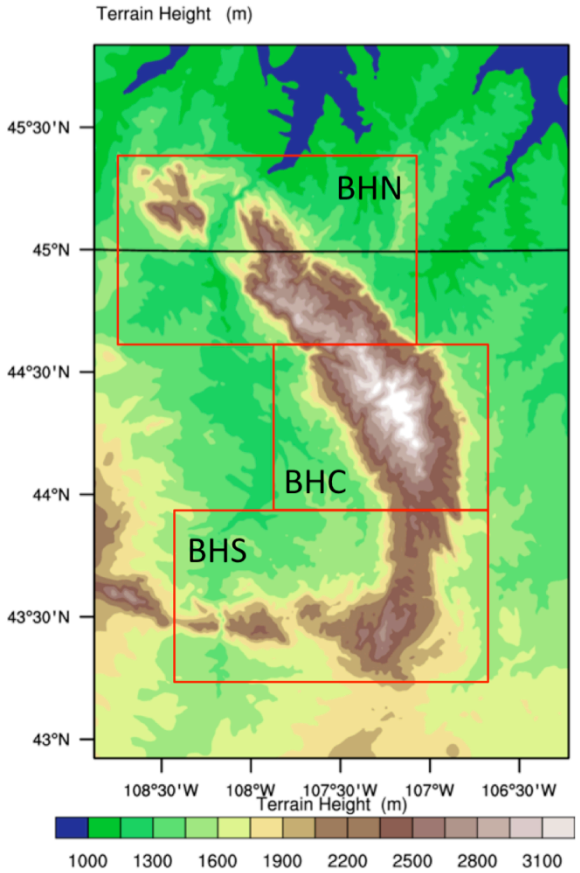


**Figure 6.4. Three sub-regions (areas with terrain greater than 2100 m within each red box) for WASCA.**

### *6.3.1 13 November 2007 case*

For this case, the outer domain was integrated for 48 hours from 0000 UTC 13 November 2007 to 0000 UTC 15 November 2007. The control simulation in the inner domain spanned from 1200 UTC 13 November 2007 to 0000 UTC 15 November 2007. The seeding cases identified by WASCA based on the 900-m control simulation results are listed in Table 6.3. The associated seeding criteria plots are shown in Figure 6.5 for this case.

**Table 6.3. WASCA output for the 13 November 2007 experiment.**

| |
|---|
| No ground seeding for BHN<br>For BHN, number of suitable airborne seeding period[s]: 1<br>Period 1 ranges from 2007-11-13_16:30:00 to 2007-11-14_04:00:00<br>Best case of period 1 seeds from 2007-11-13_22:00:00 to 2007-11-14_00:00:00 at track[s] BHNA1<br>For BHN, number of suitable higher airborne seeding period[s]: 1<br>Period 1 ranges from 2007-11-13_16:00:00 to 2007-11-14_05:00:00<br>Best case of period 1 seeds from 2007-11-13_23:30:00 to 2007-11-14_01:30:00 at track[s] BHNA1 |
| No ground seeding for BHC<br>For BHC, number of suitable airborne seeding period[s]: 1<br>Period 1 ranges from 2007-11-13_20:30:00 to 2007-11-14_06:00:00<br>Best case of period 1 seeds from 2007-11-14_02:30:00 to 2007-11-14_04:30:00 at track[s] BHCA1<br>For BHC, number of suitable higher airborne seeding period[s]: 1<br>Period 1 ranges from 2007-11-13_20:00:00 to 2007-11-14_07:30:00<br>Best case of period 1 seeds from 2007-11-14_01:30:00 to 2007-11-14_03:30:00 at track[s] BHCA1 |
| No ground seeding for BHS<br>For BHS, number of suitable airborne seeding period[s]: 1<br>Period 1 ranges from 2007-11-14_04:30:00 to 2007-11-14_13:00:00<br>Best case of period 1 seeds from 2007-11-14_09:00:00 to 2007-11-14_11:00:00 at track[s] BHSA1<br>For BHS, number of suitable higher airborne seeding period[s]: 1<br>Period 1 ranges from 2007-11-14_03:00:00 to 2007-11-14_13:00:00<br>Best case of period 1 seeds from 2007-11-14_09:00:00 to 2007-11-14_11:00:00 at track[s] BHSA1 |

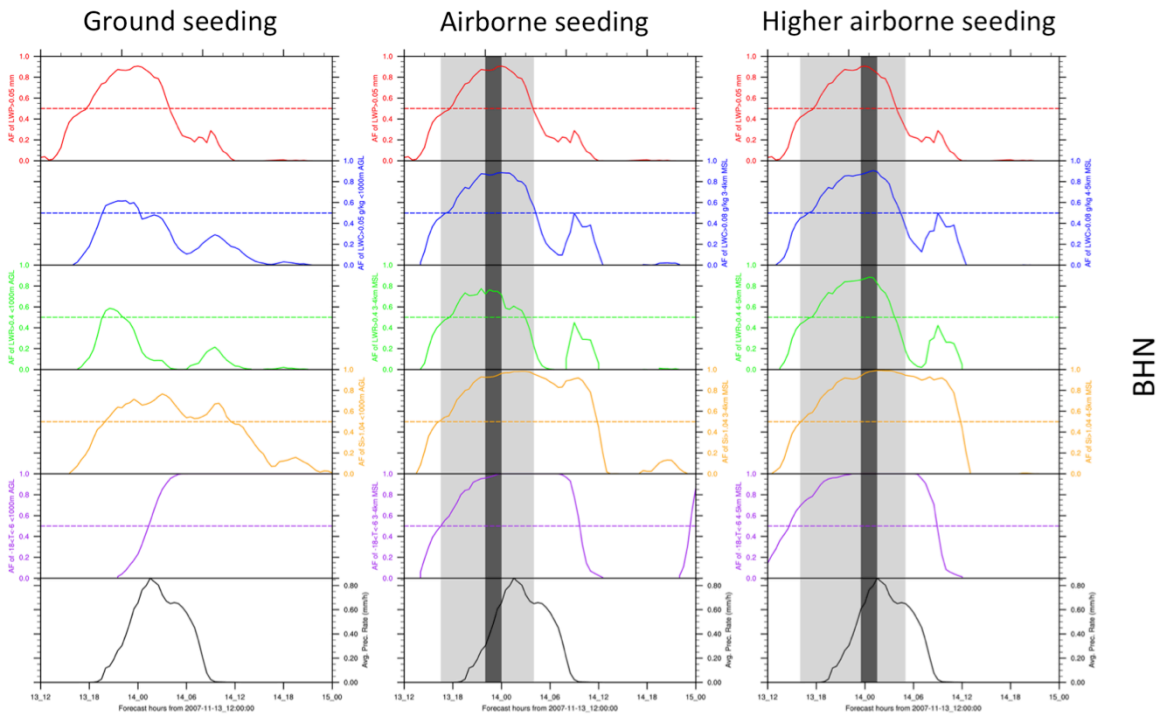
Ground seeding
Airborne seeding
Higher airborne seeding
BHN

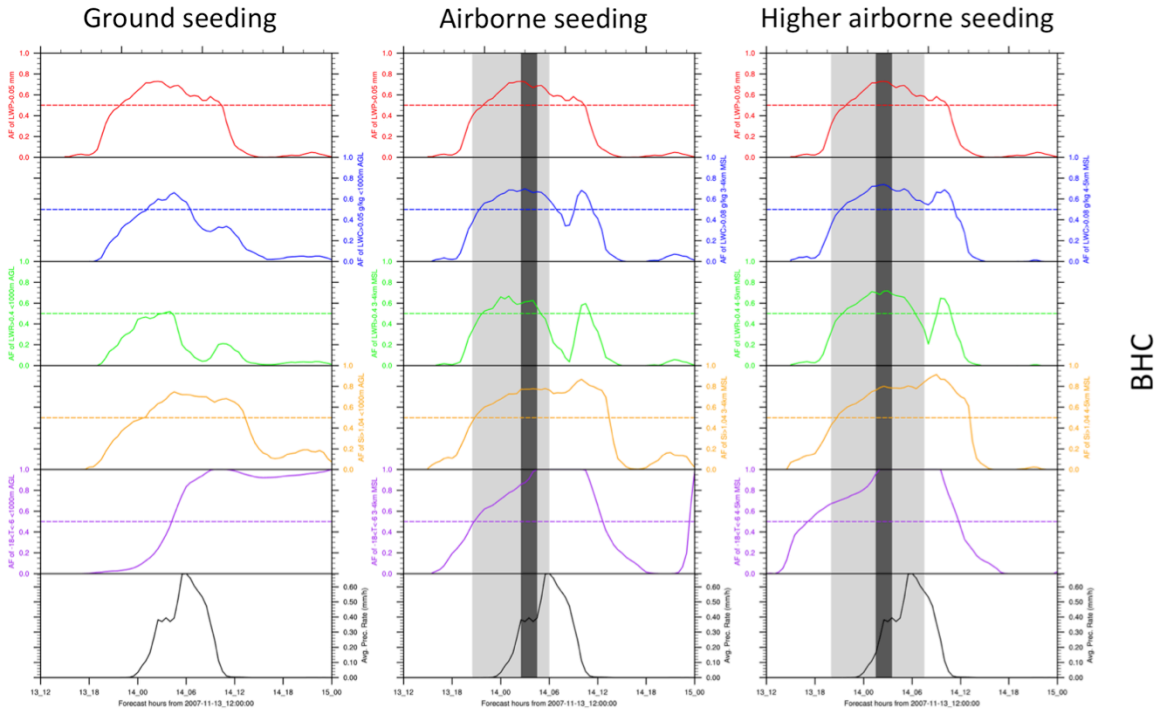
Ground seeding
Airborne seeding
Higher airborne seeding
BHC

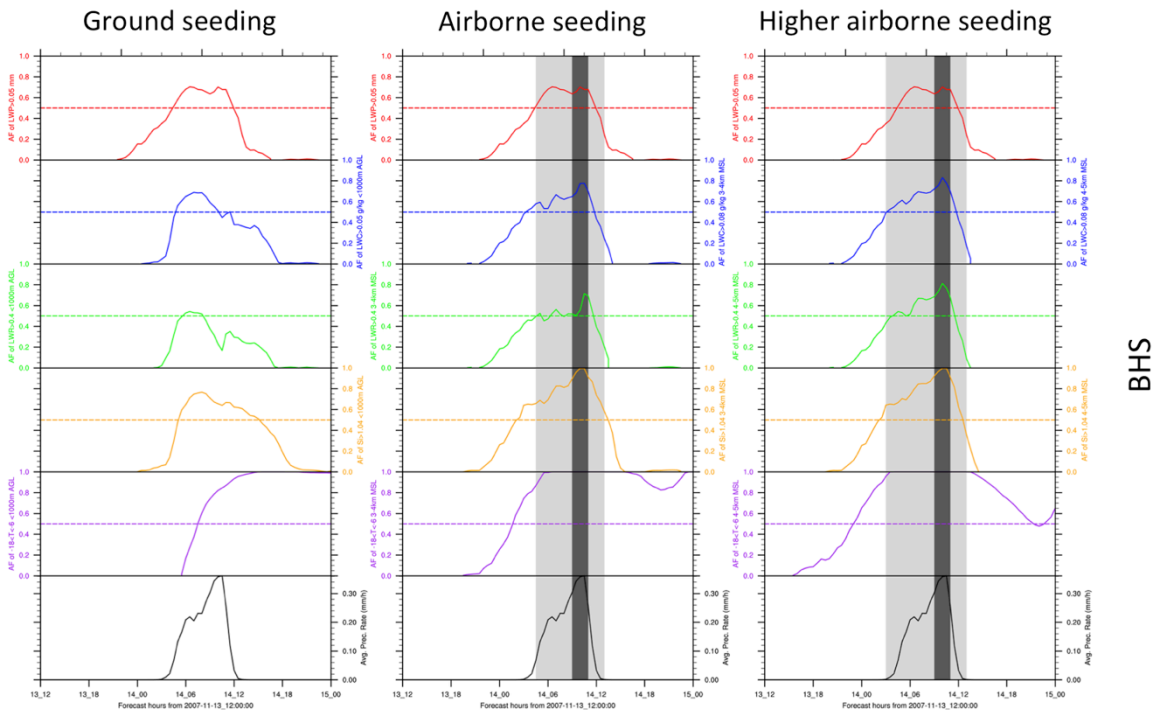


**Figure 6.5. Microphysical seeding criteria plots for ground seeding, airborne seeding (3750 m MSL) and higher level airborne seeding (4250 m MSL) for the BHN, BHC and BHS regions for the 13 November 2007 case. Each horizontal panel (and color) represents a different criterion assessed and the horizontal dashed line indicates the threshold that must be reached for the algorithm to consider that criterion met. Not all microphysical criteria assessed are required to be met for a case to be called, and even if all microphysical criteria are met there are additional criteria (especially for ground seeding, such as atmospheric stability and wind direction) that need to be met as well (not shown). Gray shading indicates time periods when seeding cases were identified. For airborne seeding, a 2-hr window is shaded in dark gray, representing the "best" period for seeding (given shorter time on station using a single aircraft).**

As illustrated above, WASCA did not identify any ground-seeding opportunities in any sub-region, mainly because once the temperature cooled to meet seeding criteria (purple line greater than dashed line in Figure 6.5), the LWC (blue and green lines in Figure 6.5) and/or winds were not suitable (Figure 6.5). However, WASCA identified that conditions were suitable for airborne seeding at both the regular and higher flight levels. The cases were identified sequentially from north to south indicating suitable seeding conditions moved from north to south during the simulation period. In fact, a cold front moved into the area from the north, and in the process, conditions for seeding shifted from north to south, as illustrated in the LWP plot (Figure 6.6) and the 700-hPa temperature and wind-field plot (Figure 6.7). The control precipitation for the entire 36 hours simulation is plotted in Figure 6.8.

During the simulation period on this case, roughly 2-10 mm of precipitation were observed at SNOTEL sites, with higher amounts generally at the northern sites (Figure 6.9). There are a few sites with greater (maximum) accumulations, and the primary exception is the Bone Springs site, which was a notable outlier in the observations for this case and the 20 January 2007 case (Figure 6.9-Figure 6.10). The measurement at the Bone Springs site on

this day and for the 20 November 2007 case is questionable, but the data were not excluded because the time series of precipitation showed that the timing of precipitation onset and cessation agreed with nearby SNOTEL sites. The model predicted precipitation accumulations generally in the observed range, with the highest accumulations also in the northern portion of the region (Figure 6.9).

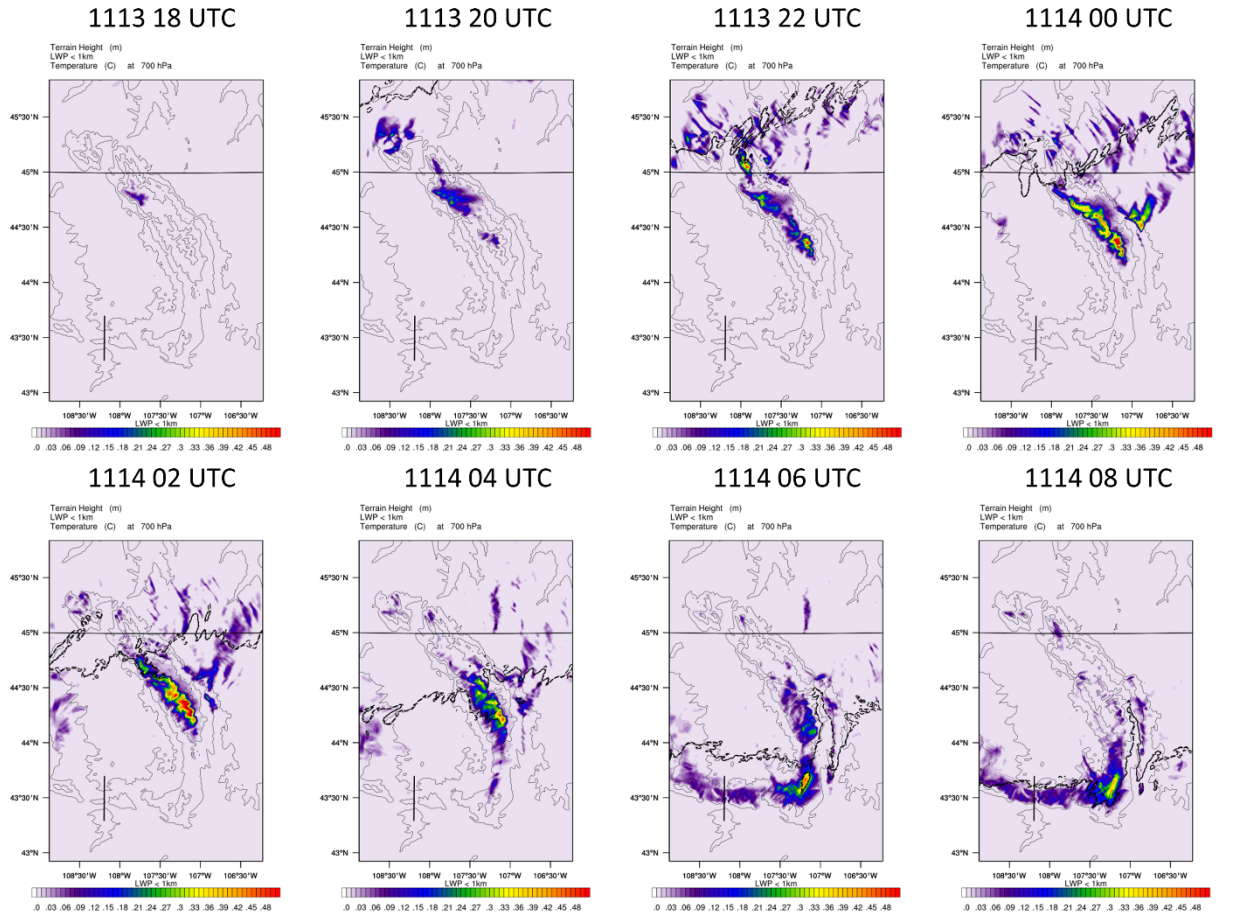


**Figure 6.6. Liquid water path below 1 km AGL (kg m$^{-2}$) from 18 UTC 13 November to 08 UTC 14 November every 2 hours. The scale ranges from 0 to 0.5 kg m$^{-2}$. The horizontal solid black line is the Montana-Wyoming state border, and the curved dark black line indicates temperature isotherm of –6 $^{o}$C at 700 hPa. The vertical short black line is the southern flight track.**

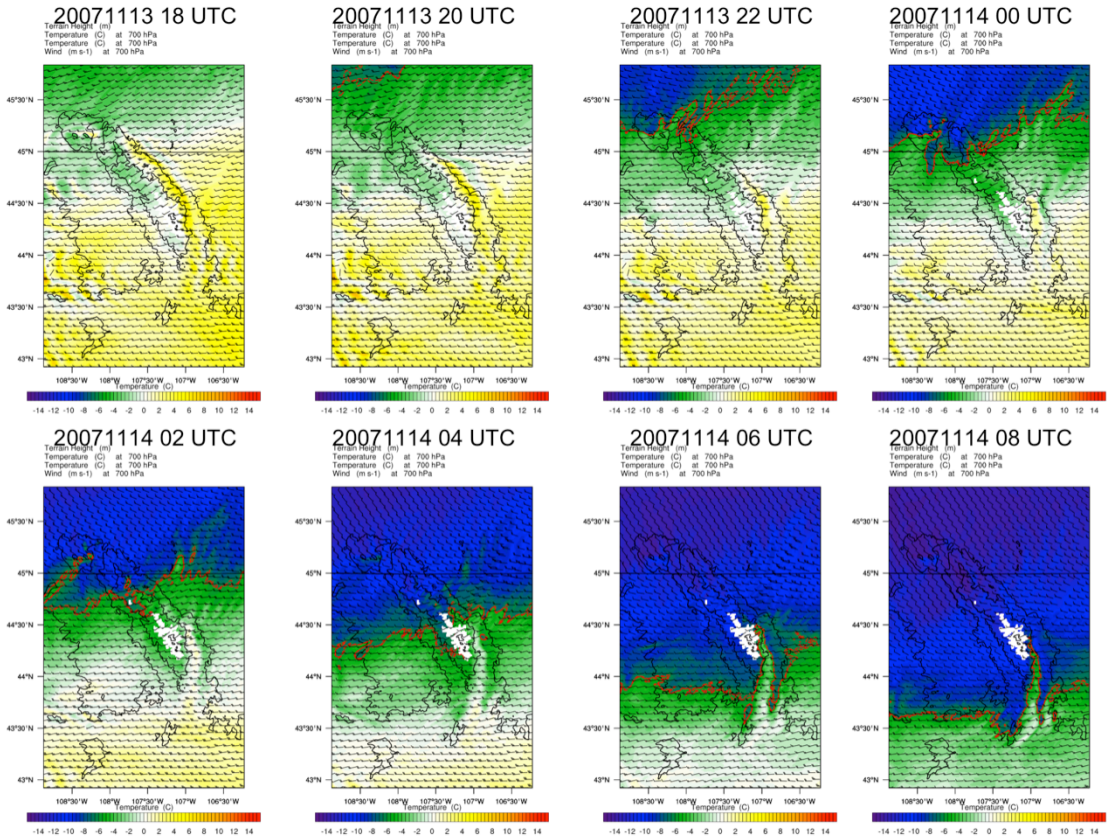


**Figure 6.7. The 700-hPa temperature (°C) and wind field for the same period as Figure 6.6. Temperature ranges from -14 to 14 °C. The red line indicates the temperature contour at -6 °C.**

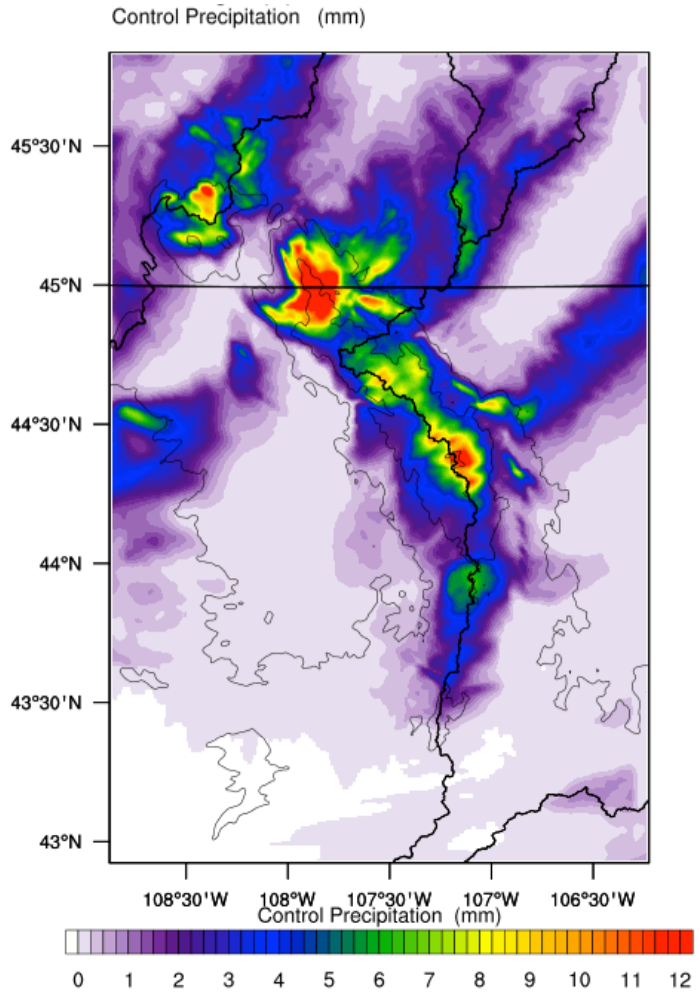


**Figure 6.8. Accumulated precipitation (mm) of the 13 November 2007 control simulation.**

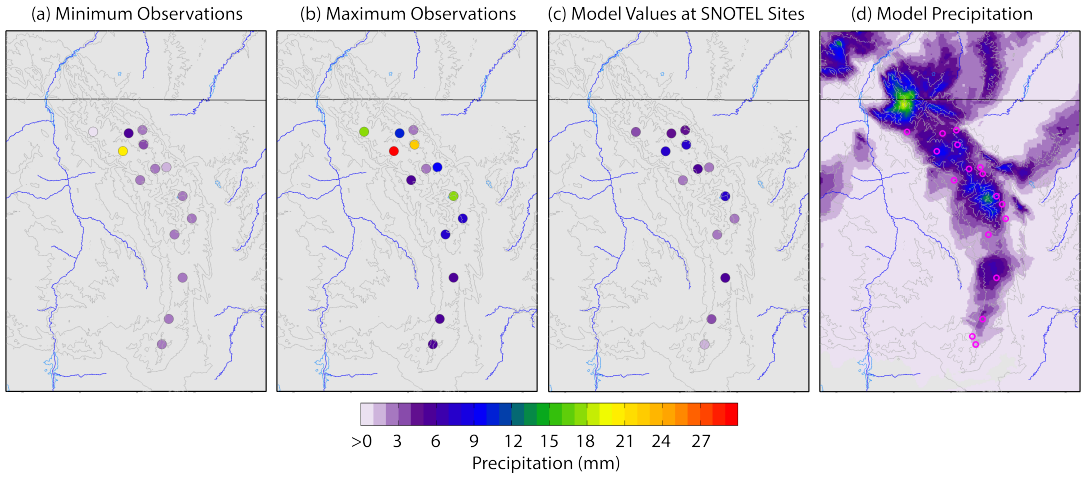


**Figure 6.9. Maps of observed precipitation accumulation (mm) over the simulation period for the 13 November 2007 case from SNOTEL sites, with minimum accumulation in (a) and maximum accumulation in (b), compared to model-simulated precipitation accumulation at the SNOTEL sites (c) and the complete simulation of precipitation across the domain (d).**

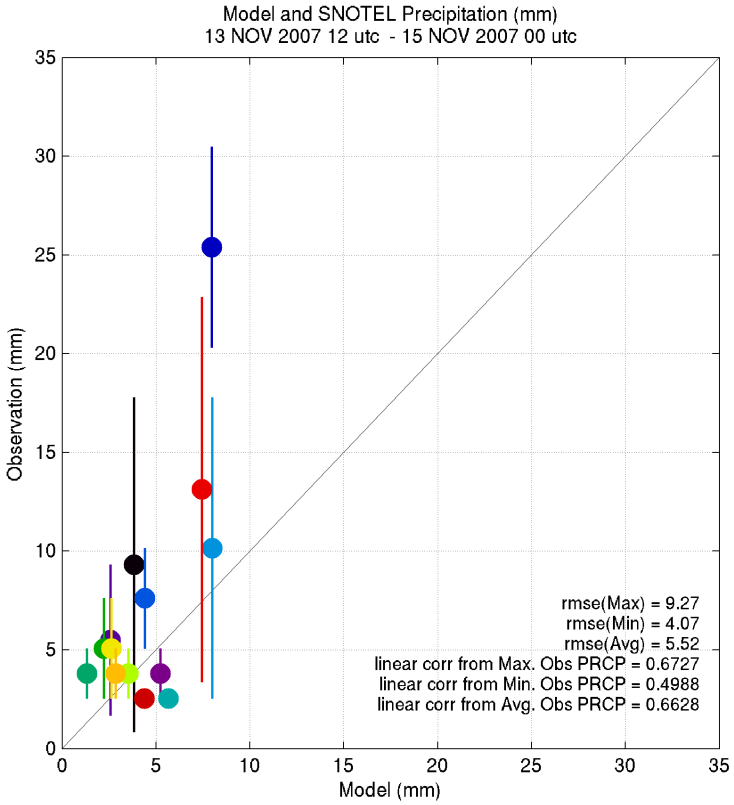


**Figure 6.10. Scatterplot comparing observed precipitation accumulation at SNOTEL sites versus the modeled precipitation accumulation at the same sites for 13 November 2007. Dots represent the average of the maximum and minimum possible precipitation accumulation at each SNOTEL site during the simulation period. Vertical bars represent the range of possible observation (i.e., minimum to maximum observation amount). Each point (color coded) represents single SNOTEL site.**

Though no ground-seeding cases were called by the WASCA, groups D and E of the ground generators were tested individually in separate simulations. The group D seeding was simulated from 0330 to 0600 UTC on 14 November and the group E seeding was simulated from 0700 to 1100 UTC on 14 November (Table 6.4). The simulated change in precipitation (seeding simulation minus control, hereafter the simulated seeding effect) in mm and percentage relative to the control precipitation (%) are plotted in Figure 6.11 for these two tests. The figure shows negligible seeding effects were simulated by these two groups of generators, especially Group D.

**Table 6.4. Seeding times of the ground seeding simulations for the 13 November 2007 case.**

| Experiment | GS_D | GS_E |
|---|---|---|
| T_start (UTC) | 1114 0330 | 1114 0700 |
| T_end (UTC) | 1114 0600 | 1114 1100 |

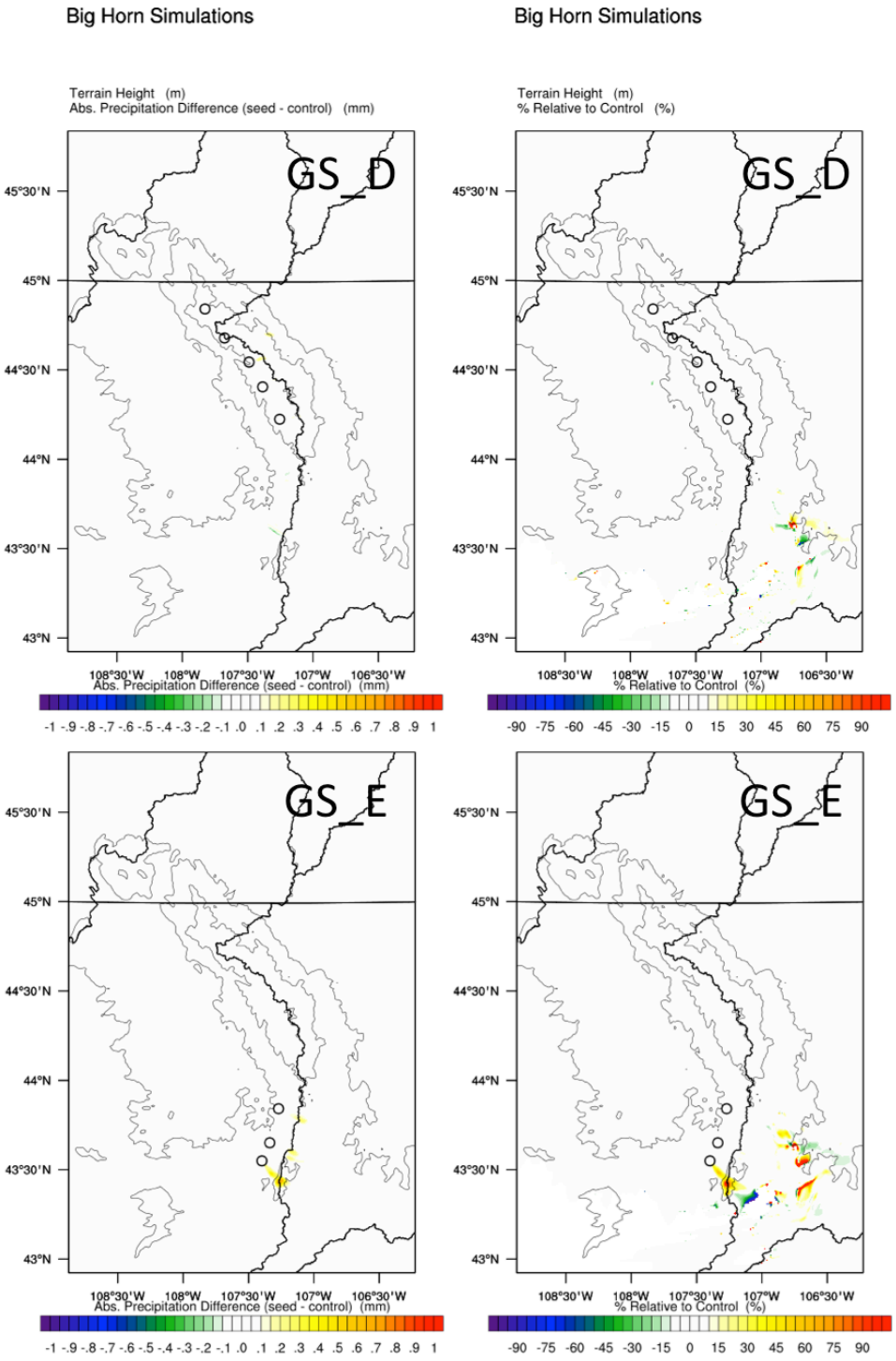


**Figure 6.11. The absolute simulated seeding effect (mm) on the left and relative simulated seeding effect (%) on the right for the group D simulation on the top and the group E simulation at the bottom.**

The simulated AgI plumes dispersed over the mountain without blocking, but they missed the SLW content in the upwind side and aloft (Figure 6.12). Also, the warm temperature close to the mountaintop limited the AgI nucleation ability.

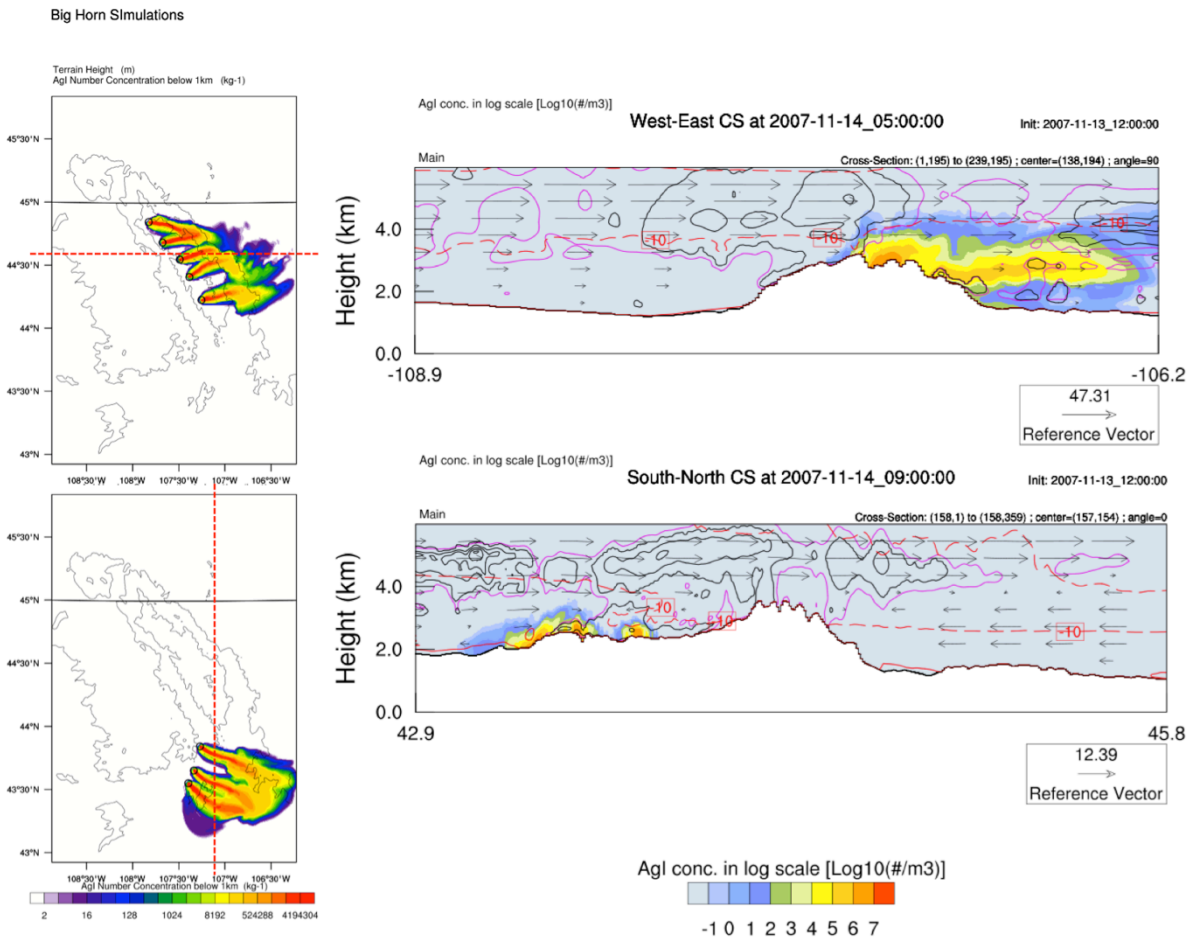


**Figure 6.12. Plan view maps of average simulated AgI concentration below 1 km AGL on the left and vertical cross sections of simulated AgI concentration (color shaded), liquid water mixing ratio (black contours in g/kg), temperature (red contours), ice supersaturation at 1.04 and wind vectors on the right. The cross-section locations are indicated by red dashed lines on the plan view maps. The time was 05 UTC 14 November 2007 for ground D simulation (top) and 09 UTC 14 November 2007 for group E (bottom).**

The ground-seeding simulations indicated that ground seeding may be ineffective in this case, which agrees with that lack of ground-seeding cases identified by WASCA once it was run on the 900-m control simulation. However, WASCA identified airborne seeding cases for all three sub-regions. Therefore, five different airborne seeding scenarios were tested for this case (see Figure 6.13 for flight track positions and seeding times). For the northern track (AS_N), only the regular altitude (3,750 m MSL) was tested. For the central long track, both regular and high altitudes (4,250 m MSL) were tested (AS_C and ASH_C, respectively). For the high track test, the seeding time was from 0130 to 0330 UTC. A shorter, central track was then simulated, only at the high altitude, and with regular and ¼ of the regular seeding rates (ASH_CS and ASH_CSQ, respectively). The seeding times of all airborne seeding cases are listed in Table 6.5.

Table 6.5. Seeding times for the airborne seeding simulations of the 13 November 2007 case.

| Experiment | AS_N | AS_C | ASH_C | ASH_CS | ASH_CSQ |
|---|---|---|---|---|---|
| T_start (UTC) | 1113 2200 | 1114 0230 | 1114 0130 | 1114 0130 | 1114 0130 |
| T_end (UTC) | 1114 0000 | 1114 0430 | 1114 0330 | 1114 0330 | 1114 0330 |

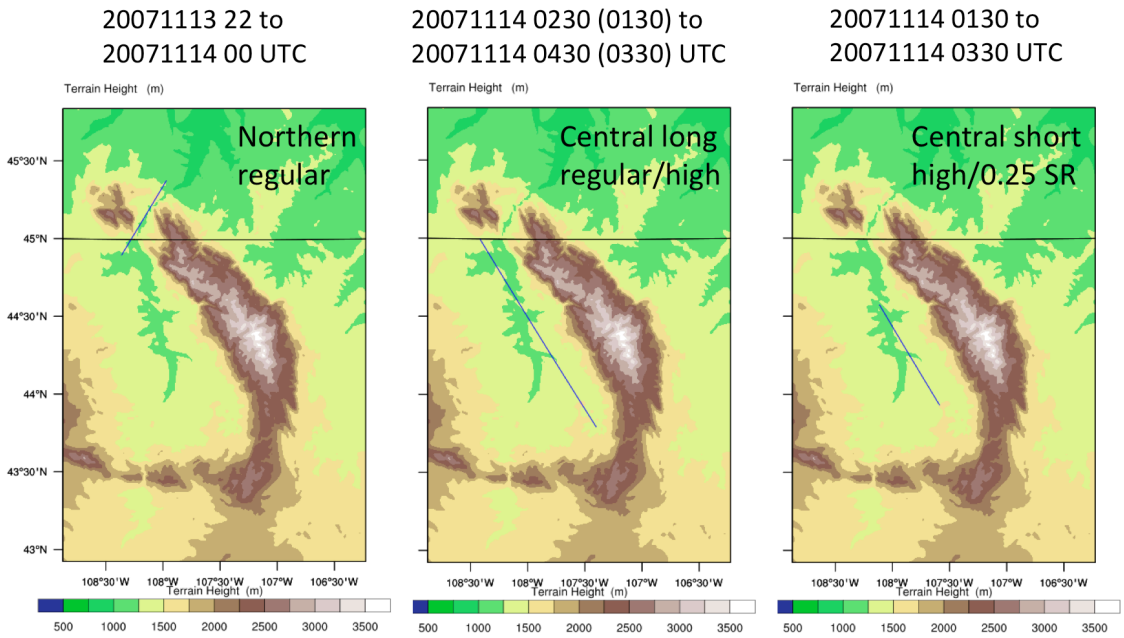


Figure 6.13. Three flight tracks, the corresponding altitude or seeding rates for the airborne seeding experiments in the 13 November 2007 case. The seeding times for each are also annotated atop each map.

The simulated seeding effect at the end of the simulation (mm), the average LWP difference (mm), and the relative LWP difference (%) of the AS_N case are plotted in Figure 6.14. The seeding from the northern track generated a focused area of LWP depletion in the immediate downwind region of the track due to the southwesterly wind at the seeding level (Figure 6.7 and Figure 6.15). The simulated seeding effect corresponds to the LWP depletion well.

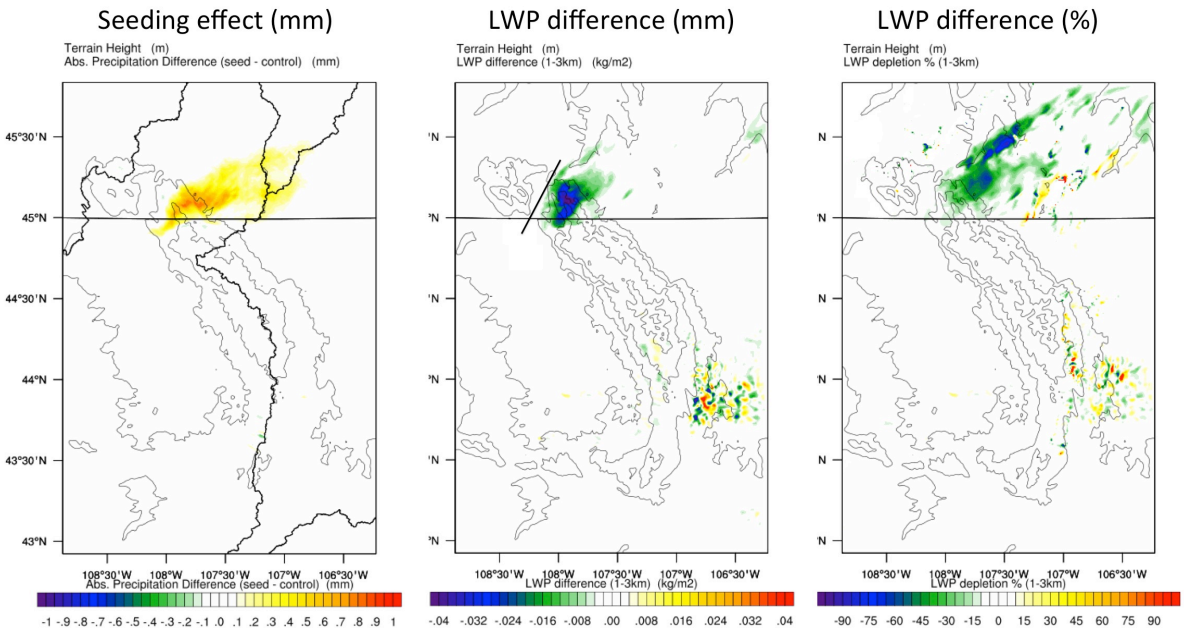


**Figure 6.14. The simulated seeding effect (mm) at the end of the simulation, average LWP difference (mm), and the relative LWP difference (%) for the AS_N case on 13 November 2007. The straight black horizontal line is the Wyoming-Montana state border. The thin black curves are the underlying terrain contours. The thick black curves in the left panel are the basin divides. The AS_N flight track is overlaid in the center panel.**

The simulated AgI plumes between 1 and 3 km MSL at 2300 UTC 13 November and 0100 UTC 14 November and the corresponding LWP are shown in Figure 6.15 and Figure 6.16. The AgI particles only covered the northern area with LWP at 2300 UTC 13 November, thereby explaining the spatial pattern of the simulated seeding effect shown in Figure 6.14. After the seeding stopped, most of the simulated AgI particles were transported to the lee side of the Bighorn Mountains where little liquid water was available.

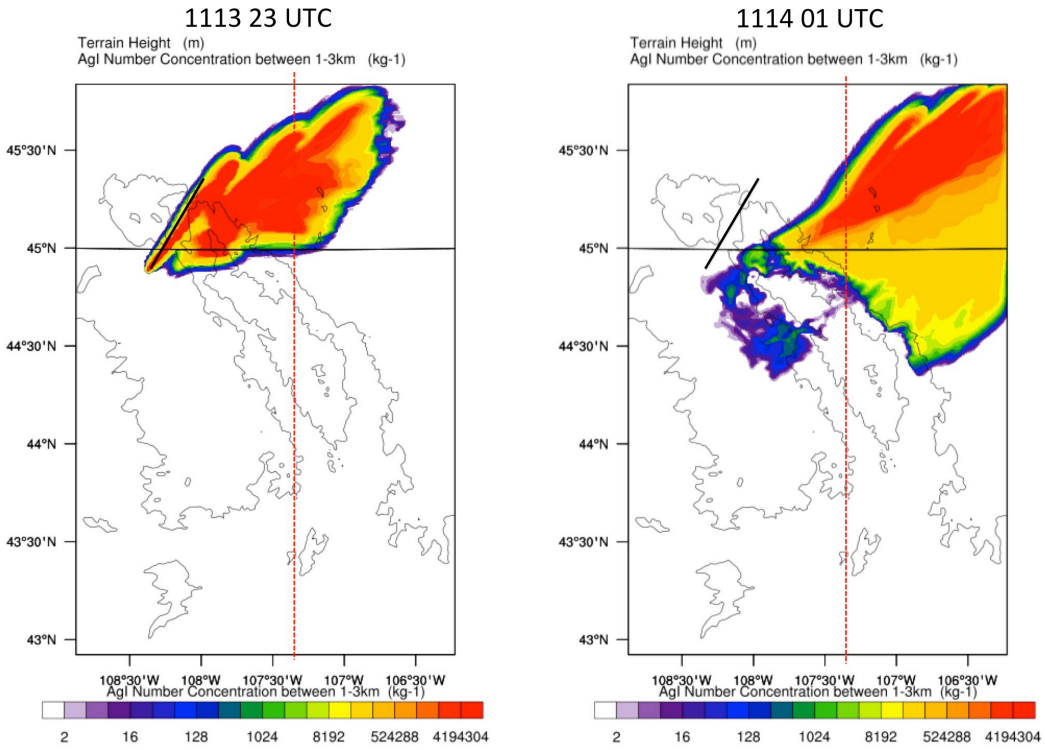


**Figure 6.15. The average simulated AgI number concentration between 1 and 3 km MSL at 1113 2300 UTC and 1114 0100 UTC. The red dashed lines indicate the cross section location as show in Figure 6.17. The AS_N flight track is overlaid as a thick black line.**

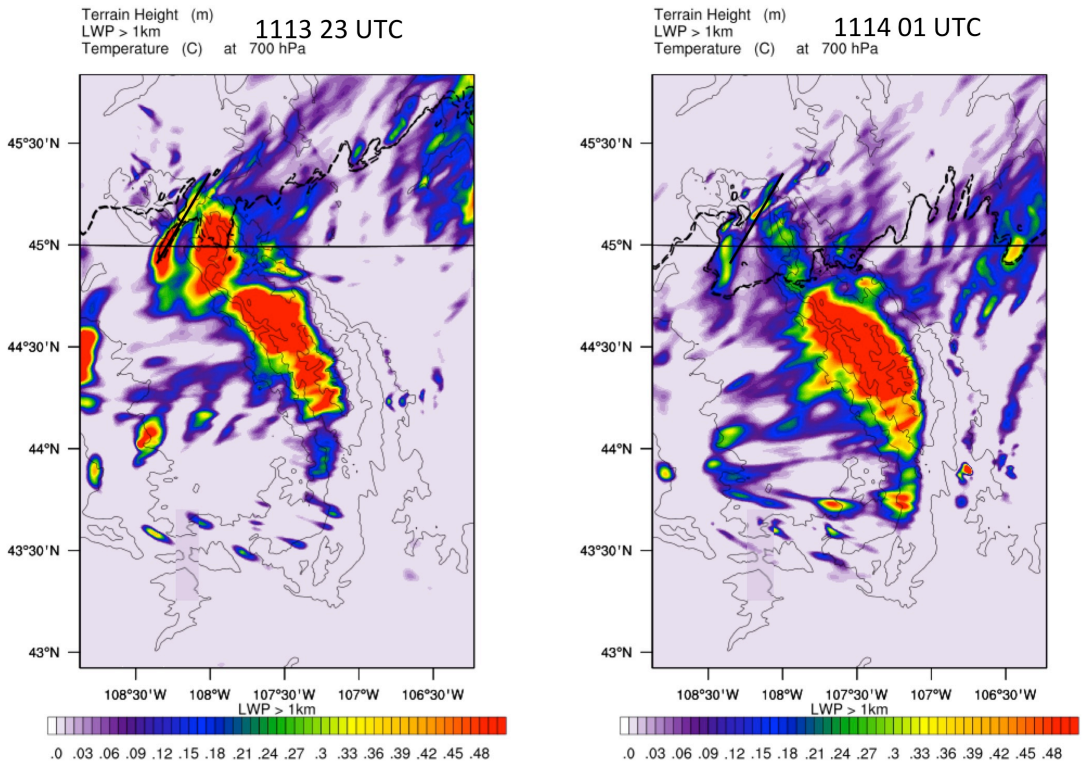


**Figure 6.16. The LWP between 1 and 3 km MSL at 1113 2300 UTC and 1114 0100 UTC. The black contour represents the isotherm of -6 °C at 700 hPa. The AS_N flight track is overlaid as a thick black line.**

The south-north cross sections at these two times show that the aircraft-released AgI particles depleted the supercooled liquid water at about −10 °C and formed precipitating ice particles (Figure 6.17). The plume did not reach the most abundant liquid water content above the top of the ridge.

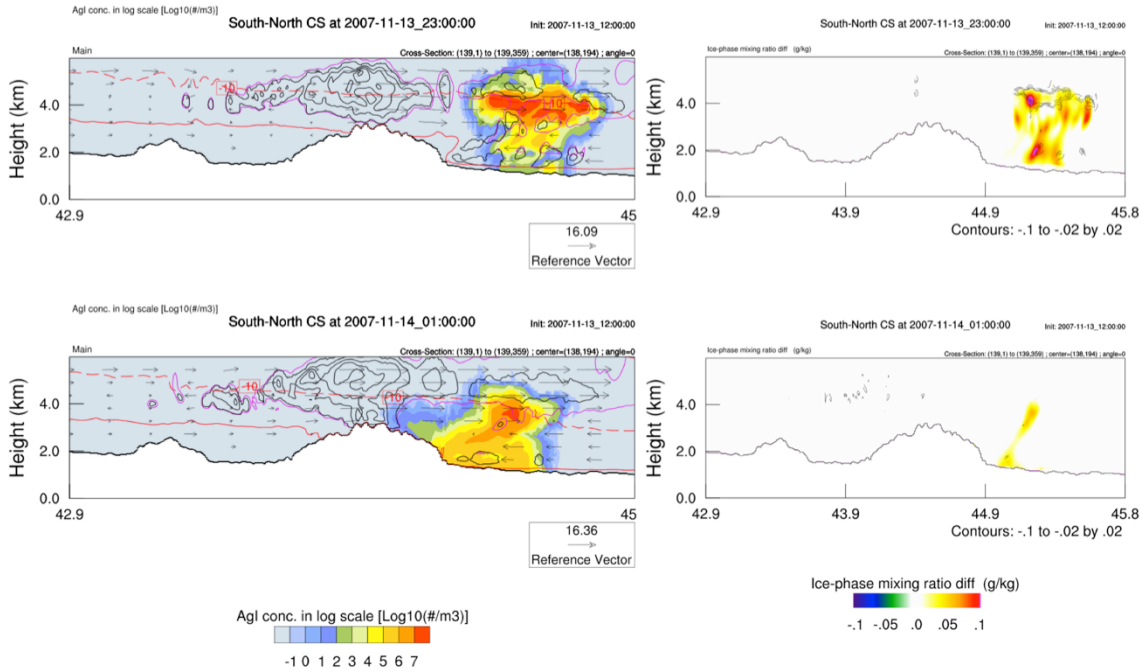


**Figure 6.17. South-north cross sections at 1113 2300 UTC and 1114 0100 UTC for the AS_N case. The left panels show the simulated AgI number concentration in logarithmic scale (color shaded), the cloud water mixing ratio in black starting at 0.01 g kg$^{-1}$ with an interval of 0.2 g kg$^{-1}$, the ice saturation ratio of 1.04 in purple, isotherm in every 10 °C and wind vectors. The right panels show the cloud water mixing ratio difference in black (g kg$^{-1}$) and ice-phase mixing ratio difference in color (g kg$^{-1}$).**

The same sets of plots are shown in Figure 6.18 through Figure 6.25 for the AS_C and ASH_C cases. The times of the simulated AgI plumes, LWP, and cross sections in these figures are 0330 and 0530 UTC 14 November for the AS_C case while they are 0230 and 0430 UTC 14 November for the ASH_C case, since the seeding starting time of ASH_C case is one hour earlier than AS_C case. It is found that the ASH_C case simulation depleted more liquid water and generated greater simulated seeding effects than the AS_C case (Figure 6.18 and Figure 6.22). This difference is partially due to the maximum LWC available at higher altitudes, which the ASH_C flight track targeted better (Figure 6.21 and Figure 6.25). These cross-section plots also show that the simulated AgI plumes cover most of the liquid water content (LWC) areas and extend over the peak. The SLW was almost completely depleted and converted into ice particles in the center of the AgI plume where the highest concentrations of AgI particles were simulated.

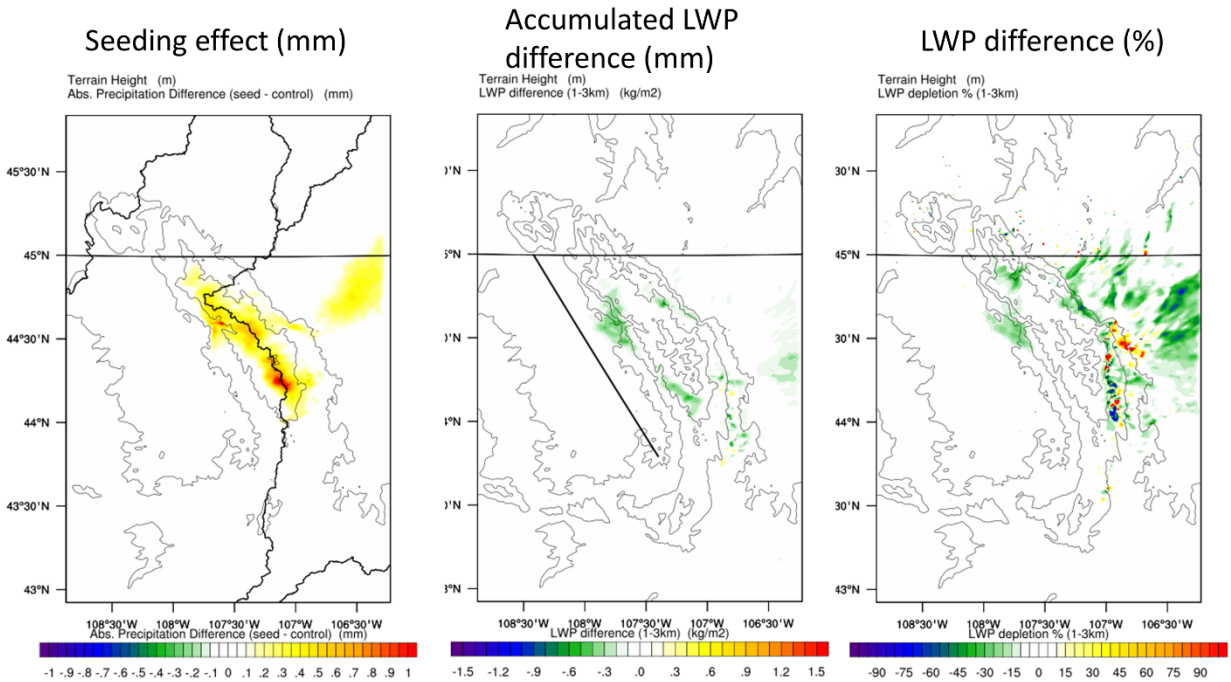


**Figure 6.18. The simulated seeding effect (mm) at the end of the simulation, average LWP difference (mm), and the relative LWP difference (%) for AS_C case. The straight black horizontal line is the Wyoming-Montana state border. The thin black curves are the underlying terrain contours. The thick black curves in the left panel are the basin divides. The AS_C flight track is overlaid in the center panel.**

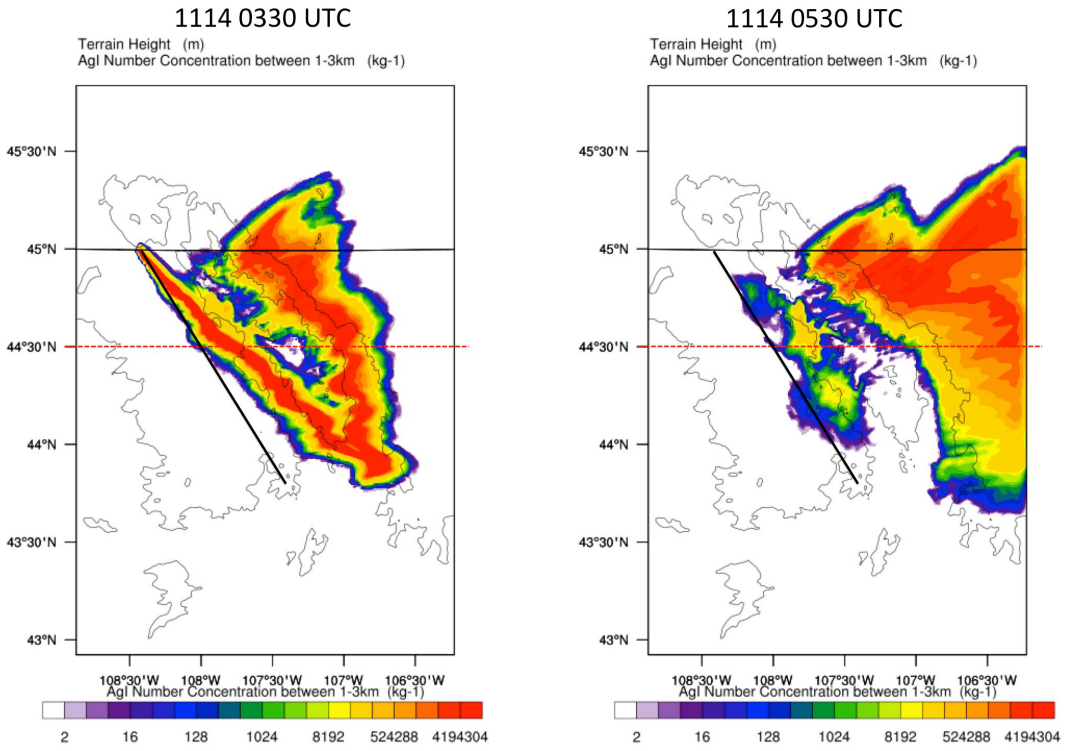


**Figure 6.19. The average simulated AgI number concentration between 1 and 3 km MSL at 1113 2300 UTC and 1114 0100 UTC for AS_C case. The red dashed lines indicate the cross section location. The AS_C flight track is overlaid as a thick black line.**

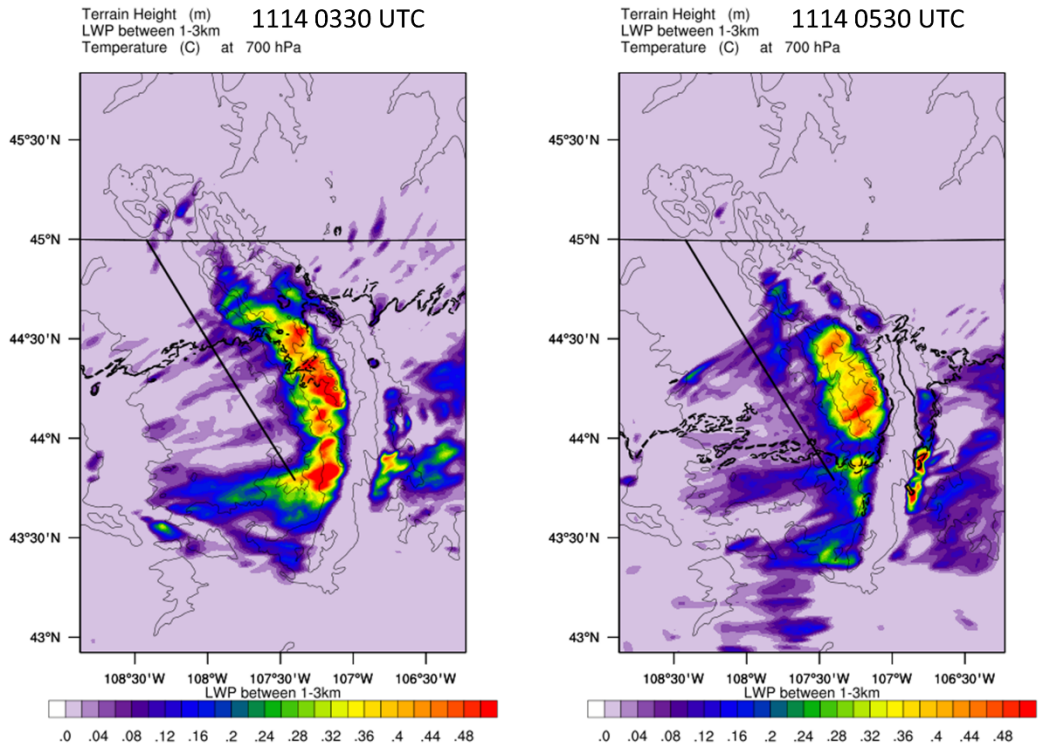


**Figure 6.20. The LWP between 1 and 3 km MSL at 1113 23 UTC and 1114 01 UTC for AS_C case. The black contour represents the isotherm of -6 °C at 700 hPa. The AS_C flight track is overlaid as a thick black line.**

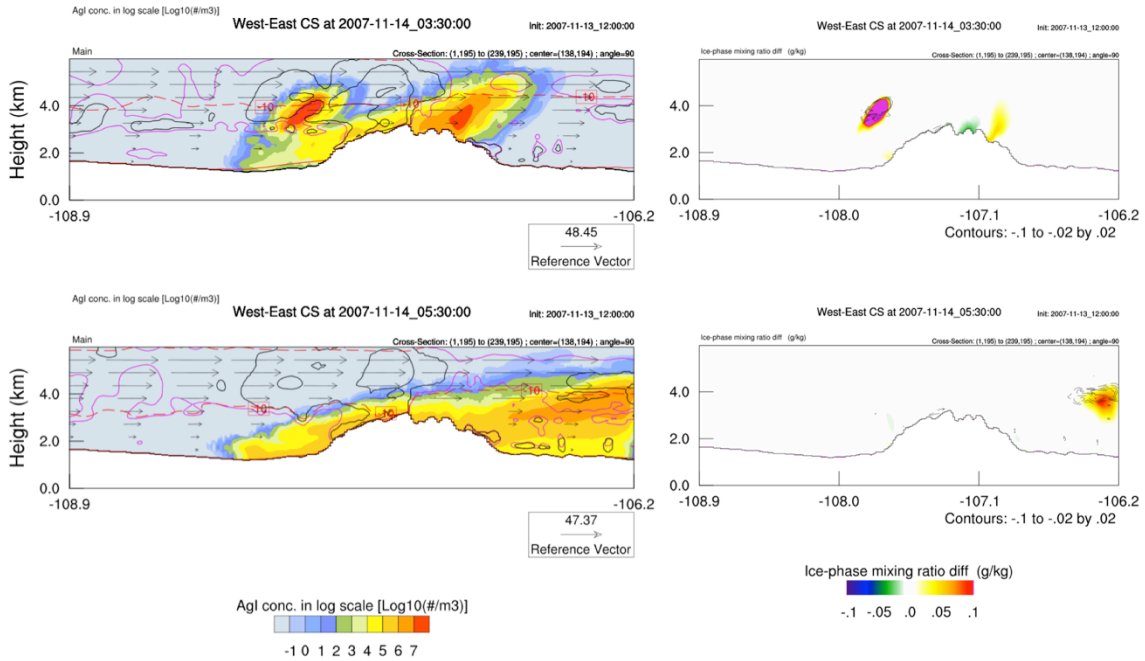


**Figure 6.21. West-east cross sections at 1114 0330 UTC and 1114 0530 UTC for the AS_C case. The left panels show the simulated AgI number concentration in logarithmic scale (color shaded), the cloud water mixing ratio in black starting at 0.01 g kg$^{-1}$ with an interval of 0.2 g kg$^{-1}$, the ice saturation ratio of 1.04 in purple, isotherm in every 10 °C and wind vectors. The right panels show the cloud water mixing ratio difference in black (g kg$^{-1}$) and ice-phase mixing ratio difference in color (g kg$^{-1}$).**

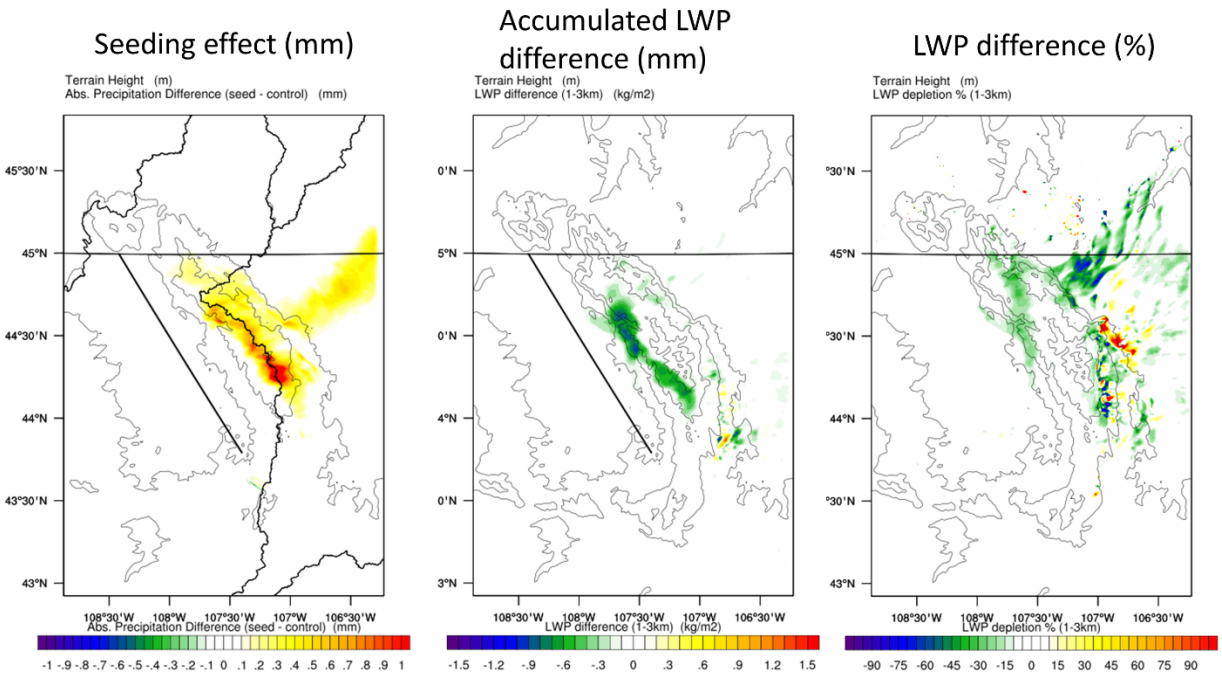


**Figure 6.22. The simulated seeding effect (mm) at the end of the simulation, average LWP difference (mm), and the relative LWP difference (%) for ASH_C case. The straight black horizontal line is the Wyoming-Montana state border. The thin black curves are the underlying terrain contours. The thick black curves in the left panel are the basin divides. The AS_C flight track is overlaid as a thick black line (left and center).**

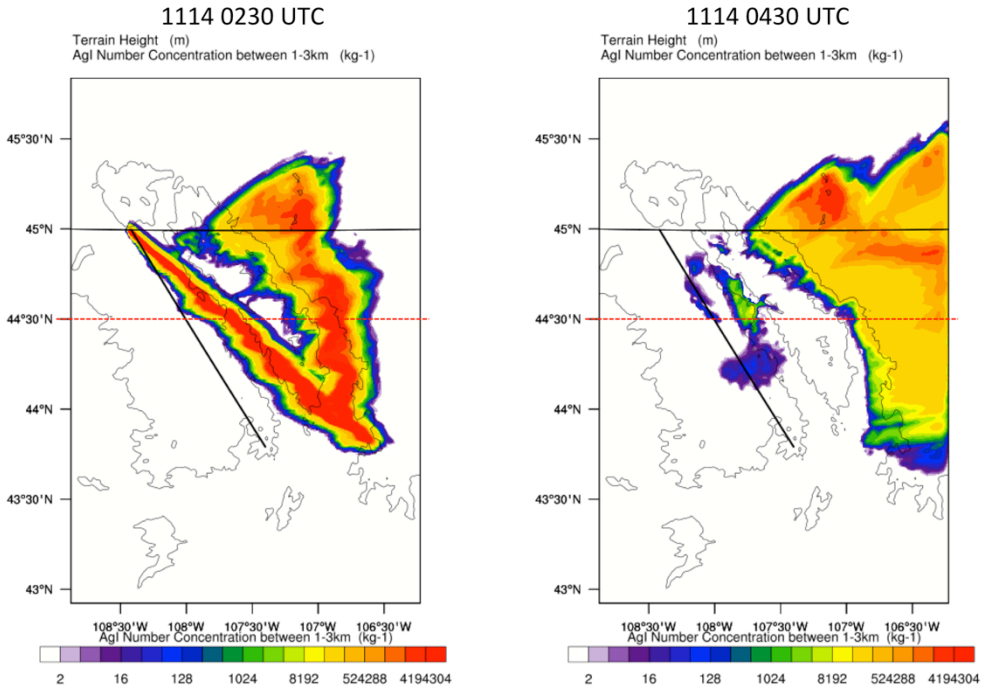


**Figure 6.23. The average simulated AgI number concentration between 1 and 3 km MSL at 1113 2300 UTC and 1114 0100 UTC for ASH_C case. The red dashed lines indicate the cross section location.**

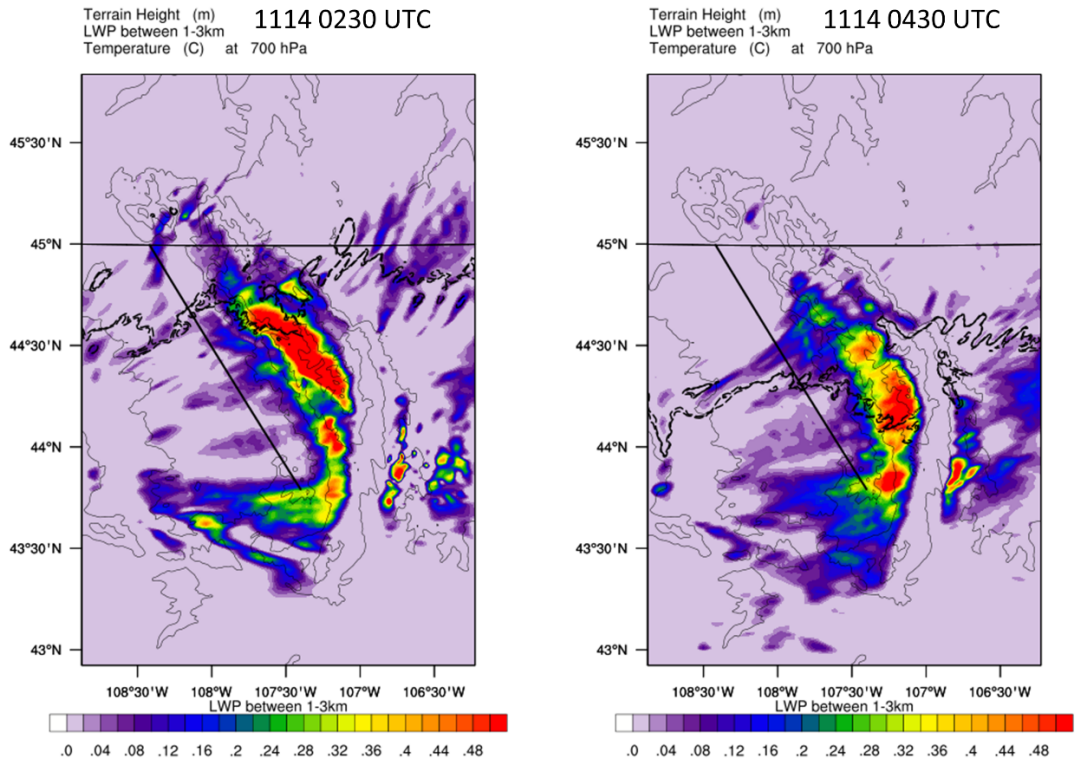


**Figure 6.24. Same as Figure 6.16, but for ASH_C case.**

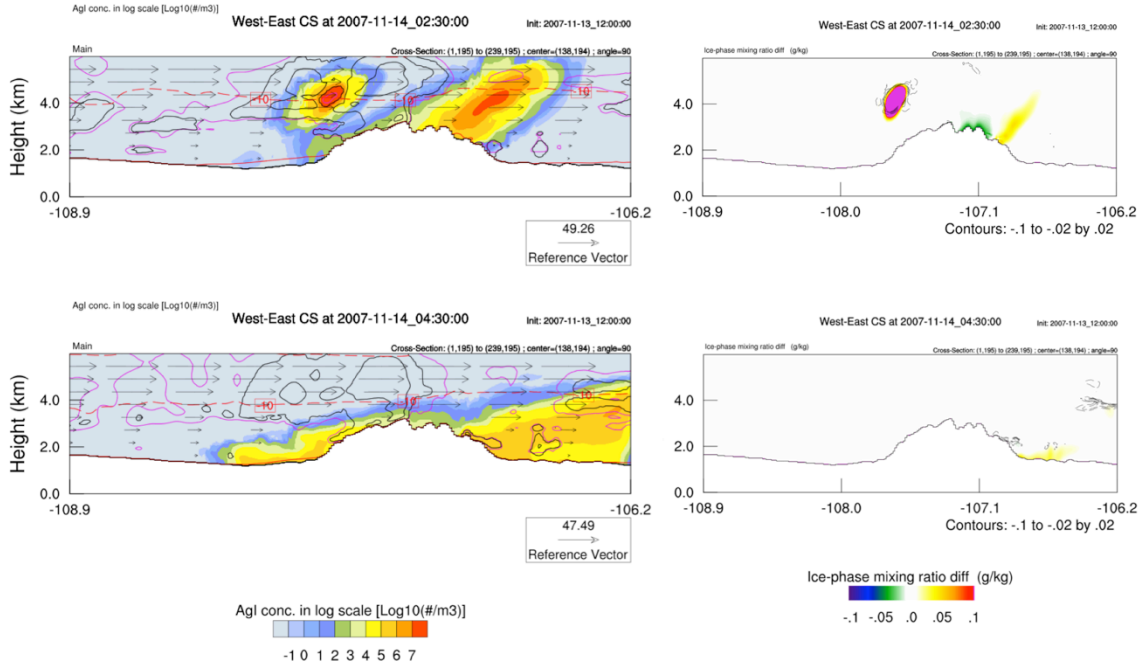


**Figure 6.25. West-east cross sections at 1114 0230 UTC and 1114 0430 UTC for the ASH_C case. The left panels show the simulated AgI number concentration in logarithmic scale (color shaded), the cloud water mixing ratio in black starting at 0.01 g kg$^{-1}$ with an interval of 0.2 g kg$^{-1}$, the ice saturation ratio of 1.04 in purple, isotherm in every 10 °C and wind vectors. The right panels show the cloud water mixing ratio difference in black (g kg$^{-1}$) and ice-phase mixing ratio difference in color (g kg$^{-1}$).**

Based on the limited spatial coverage of the high LWC over the peak and the better simulated seeding effect from the higher flight track, another airborne seeding experiment at the same altitude, but with a shorter track, was carried out (ASH_CS in Figure 6.13). At the same time, an extra experiment with the same setup as ASH_CS, but with one quarter of the seeding rate, was also conducted (ASH_CSQ) to test if the current seeding rate from the aircraft might cause over seeding. Both of these cases used the same seeding time as the ASH_C case.

The simulated seeding effects of the regular seeding rate simulation are greater than in the ASH_CSQ simulation, indicating that the regular seeding rate does not overseed the cloud. The AgI plumes at 0230 and 0430 UTC (Figure 6.27) show that the simulated AgI plumes from the ASH_CSQ covered a similar area as the ASH_CS case, but with a smaller area of high concentration of AgI particles. The shorter track makes the zigzag pattern tighter than the ASH_C so that a higher concentration of AgI was dispersed into the cloud. The cross sections (Figure 6.28) show that the aircraft-released AgI plumes covered the areas with LWC very well. The ASH_CSQ case simulated lower concentrations of AgI than ASH_CS, and as a result did not simulate as strong of a seeding effect on precipitation.

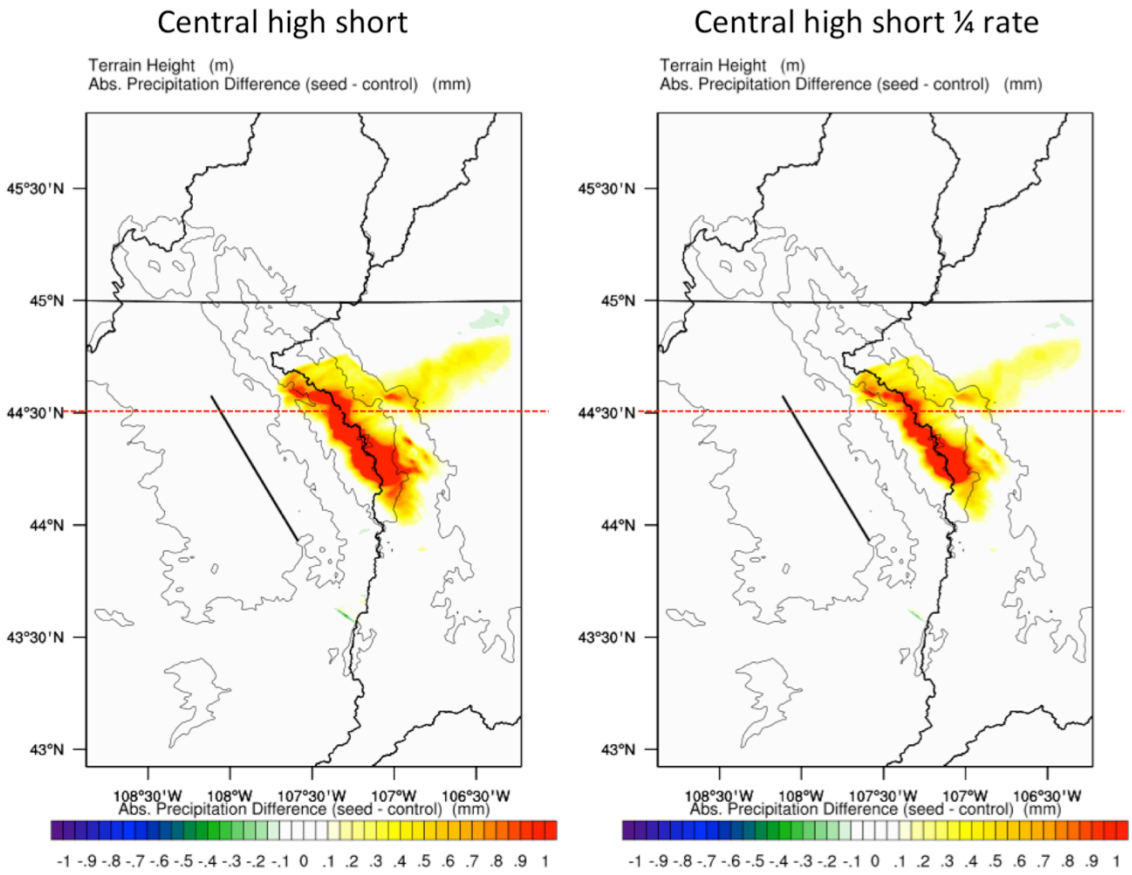


**Figure 6.26. The simulated seeding effect of ASH_CS (left) and ASH_CSQ (right) cases (mm). The location of the cross section shown in Figure 6.28 is indicated by the red dashed lines.**

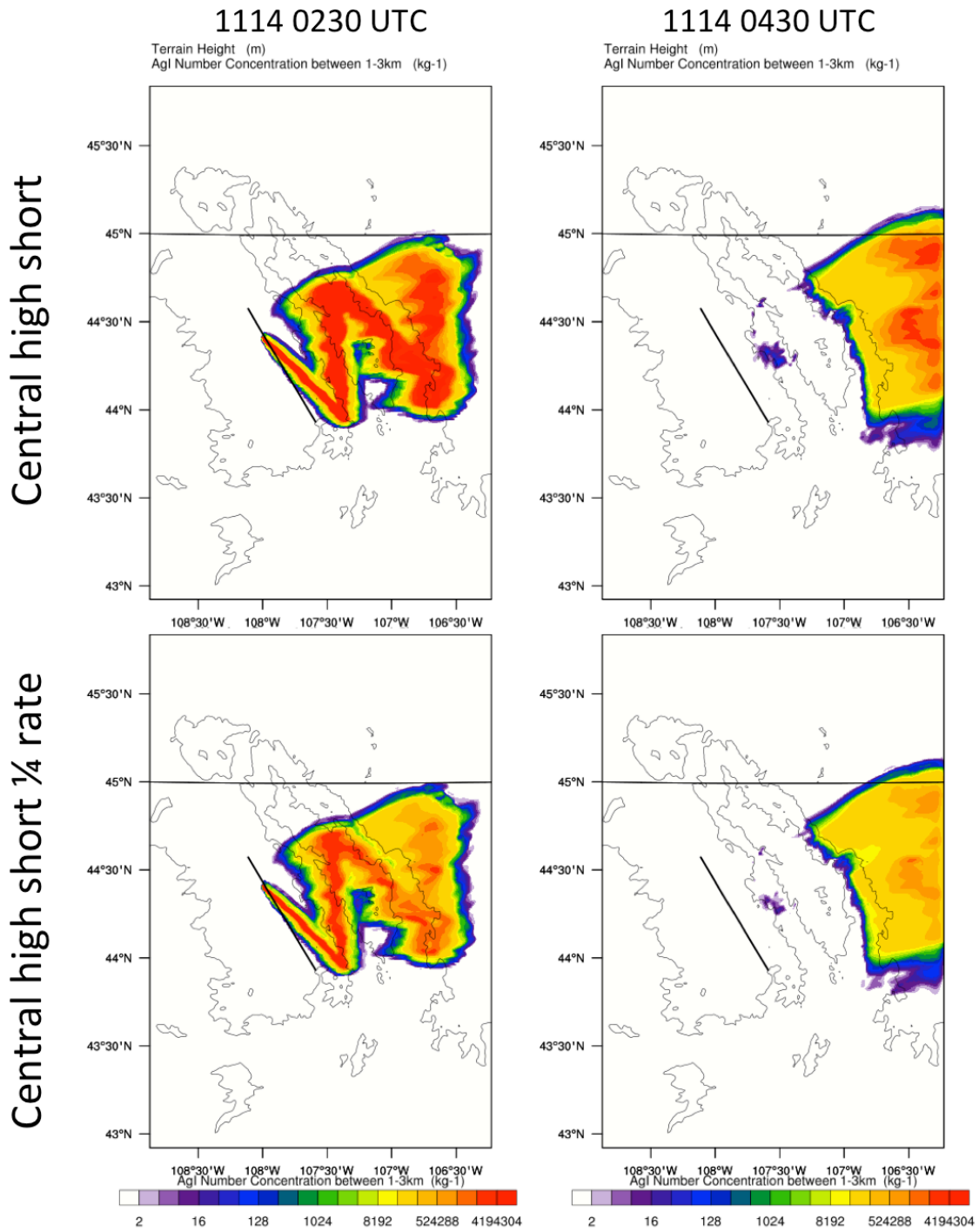


**Figure 6.27. The average simulated AgI number concentration between 1 and 3 km MSL at 1113 2300 UTC and 1114 0100 UTC for ASH_CS (top) and ASH_CSQ (bottom) cases. The red dashed lines indicate the cross section.**

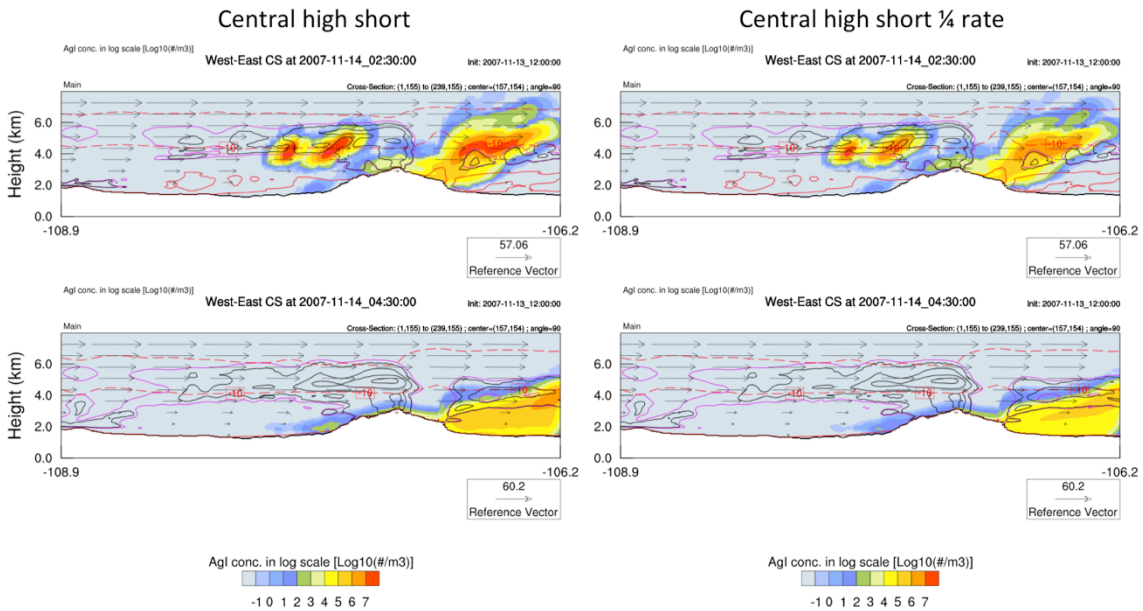


**Figure 6.28. West-east cross section at 0230 and 0430 UTC for ASH_CS (left) and ASH_CSQ (right).**

The watersheds within the simulation domain are plotted in Figure 6.29. The control precipitation and simulated seeding effect in the two primary watersheds are given in Table 6.6. Ground seeding generated negligible simulated seeding effects for this case, while the airborne seeding experiments generated moderate to large simulated seeding effects in the different watersheds. AS_N enhanced precipitation in the Bighorn Basin, but had little simulated seeding effect at the high-altitude regions of the Bighorn Mountains themselves. All of the central track experiments increased precipitation in both the Bighorn and Powder/Tongue River basins with notable enhancement over the high altitude (>8,000 ft) target regions. The higher altitude tracks tended to spill more simulated seeding effect over to the east slope feeding the Powder/Tongue River basin. The ASH_CS experiment, with the higher altitude and shorter track, generated the highest simulated seeding effect for both basins of all the experiments. Even using ¼ of the seeding material, ASH_CSQ produced more simulated seeding effect in the high elevations of the Bighorn Mountains than the longer track experiments, given the simulated AgI plume was more concentrated using the shorter track length. For all experiments with simulated seeding effects in the high-altitude target regions > 1%, the percent of the target areas impacted ranged from 44–88% (Table 6.7).

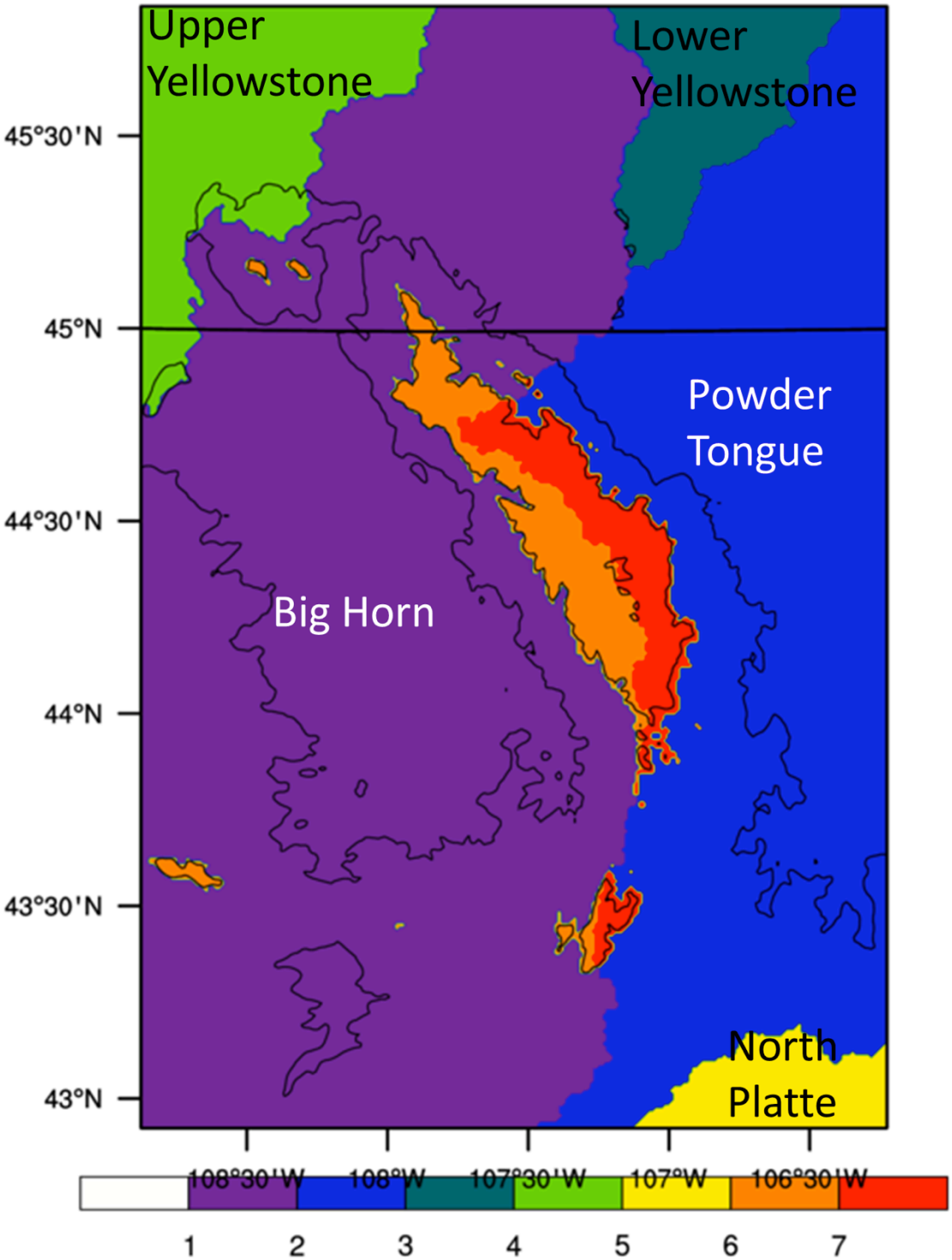


**Figure 6.29. Watersheds in the simulation domain (Bighorn =BH, Powder/Tongue =PT). The orange area is the Bighorn basin above 8000 ft (BH mtns) and the red area is the Powder/Tongue basin above 8000 ft (PT mtns).**

**Table 6.6. Control precipitation and simulated seeding effects for each seeding simulation (acre-feet on top and % effect on bottom for each experiment row) over the full model domain and in the two primary watersheds (entirely, BH and PT, and just above 8,000 ft in those watersheds, BH mtns and PT mtns) for each of the seeding experiments. The experiment with the best simulated seeding effects is shaded. Relative simulated seeding effects within the target regions (BH mtns and PT mtns) > 1% are listed in bold. Results shown for the 13 November 2007 case.**

| | Domain | BH | PT | BH mtns | PT mtns |
|---|---|---|---|---|---|
| CTRL (af) | 76343 | 49967 | 26376 | 8844 | 7737 |
| GS_D | 23 | 2 | 21 | 4 | 3 |
| | 0.03 | 0.00 | 0.08 | 0.04 | 0.03 |
| GS_E | 43 | 22 | 21 | 9 | 13 |
| | 0.06 | 0.04 | 0.08 | 0.10 | 0.17 |
| AS_N | 836 | 601 | 234 | 26 | -5 |
| | 1.09 | 1.20 | 0.89 | 0.29 | -0.07 |
| AS_C | 1304 | 421 | 884 | 373 | 354 |
| | 1.71 | 0.84 | 3.35 | **4.22** | **4.57** |
| ASH_C | 1772 | 436 | 1336 | 397 | 470 |
| | 2.32 | 0.87 | 5.07 | **4.49** | **6.07** |
| ASH_CS | 2190 | 665 | 1525 | 669 | 812 |
| | 2.87 | 1.33 | 5.78 | **7.56** | **10.49** |
| ASH_CSQ | 1631 | 479 | 1152 | 487 | 640 |
| | 2.14 | 0.96 | 4.37 | **5.50** | **8.27** |

**Table 6.7. Simulated seeding areas of impact for the 13 November 2007 case. The simulated positive seeding areal impacts are listed as area in km² (rows labeled A_SE) and the portion of the seeding impacted area relative to the total area in percentage (rows labeled P_SE). The CTRL precipitation impacted area is calculated based on grid points with accumulated precipitation greater than 0.01 mm (in km², "A", and in percent of total area, "P"). The total area (A_total) within each domain is listed in the first row (km²). For experiments and target areas (either BH mtns or PT mtns) with simulated seeding impacts > 1% (shown in Table 6.6), the P_SE values have been listed in bold.**

| | | Domain | BH | PT | BH mtns | PT mtns |
|---|---|---|---|---|---|---|
| Case | A_total | 69984 | 43367 | 26617 | 2206 | 1865 |
| CTRL | A | 57089 | 34115 | 22974 | 2160 | 1865 |
| | P | 81.57 | 78.66 | 86.31 | 97.91 | 100.00 |
| GS_D | A_SE | 1627 | 437 | 1191 | 109 | 162 |
| | P_SE | 2.33 | 1.01 | 4.47 | 4.96 | 8.69 |
| GS_E | A_SE | 597 | 223 | 374 | 60 | 94 |
| | P_SE | 0.85 | 0.51 | 1.41 | 2.72 | 5.04 |
| AS_N | A_SE | 8975 | 3934 | 5041 | 263 | 172 |
| | P_SE | 12.82 | 9.07 | 18.94 | 11.93 | 9.21 |
| AS_C | A_SE | 10770 | 3064 | 7706 | 1717 | 1649 |
| | P_SE | 15.39 | 7.07 | 28.95 | **77.83** | **88.44** |
| ASH_C | A_SE | 11990 | 3211 | 8779 | 1532 | 1511 |
| | P_SE | 17.13 | 7.40 | 32.98 | **69.42** | **81.02** |
| ASH_CS | A_SE | 8379 | 1733 | 6646 | 1089 | 1369 |
| | P_SE | 11.97 | 4.00 | 24.97 | **49.34** | **73.41** |
| ASH_CSQ | A_SE | 7482 | 1521 | 5961 | 989 | 1328 |
| | P_SE | 10.69 | 3.51 | 22.40 | **44.82** | **71.20** |

### *6.3.2 20 November 2007 case*

For this case, the outer domain was integrated for 48 hours from 1200 UTC 19 November 2007 to 1200 UTC 21 November 2007. The control simulation in the inner domain spanned from 0000 UTC 20 November 2007 to 1200 UTC 21 November 2007. The seeding cases identified by WASCA based on the 900-m control simulation output are listed in Table 6.8. The associated seeding criteria plots are shown in Figure 6.30 for this case.

**Table 6.8. WASCA output for the 20 November 2007 case.**

| |
|---|
| No ground seeding for BHN<br>For BHN, number of suitable airborne seeding period[s]: 1<br>Period 1 ranges from 2007-11-20_14:00:00 to 2007-11-21_05:30:00<br>Best case of period 1 seeds from 2007-11-20_23:30:00 to 2007-11-21_01:30:00 at track[s] BHNA1<br>For BHN, number of suitable higher airborne seeding period[s]: 1<br>Period 1 ranges from 2007-11-20_17:00:00 to 2007-11-21_01:30:00<br>Best case of period 1 seeds from 2007-11-20_20:00:00 to 2007-11-20_22:00:00 at track[s] BHNA1 |
| No ground seeding for BHC<br>For BHC, number of suitable airborne seeding period[s]: 1<br>Period 1 ranges from 2007-11-20_18:30:00 to 2007-11-21_08:30:00<br>Best case of period 1 seeds from 2007-11-20_23:00:00 to 2007-11-21_01:00:00 at track[s] BHCA1<br>For BHC, number of suitable higher airborne seeding period[s]: 1<br>Period 1 ranges from 2007-11-20_18:30:00 to 2007-11-21_04:30:00<br>Best case of period 1 seeds from 2007-11-20_21:30:00 to 2007-11-20_23:30:00 at track[s] BHCA1 |
| No ground seeding for BHS<br>For BHS, number of suitable airborne seeding period[s]: 1<br>Period 1 ranges from 2007-11-20_23:30:00 to 2007-11-21_12:00:00<br>Best case of period 1 seeds from 2007-11-21_07:30:00 to 2007-11-21_09:30:00 at track[s] BHSA1<br>For BHS, number of suitable higher airborne seeding period[s]: 1<br>Period 1 ranges from 2007-11-20_23:30:00 to 2007-11-21_09:30:00<br>Best case of period 1 seeds from 2007-11-21_03:30:00 to 2007-11-21_05:30:00 at track[s] BHSA1 |

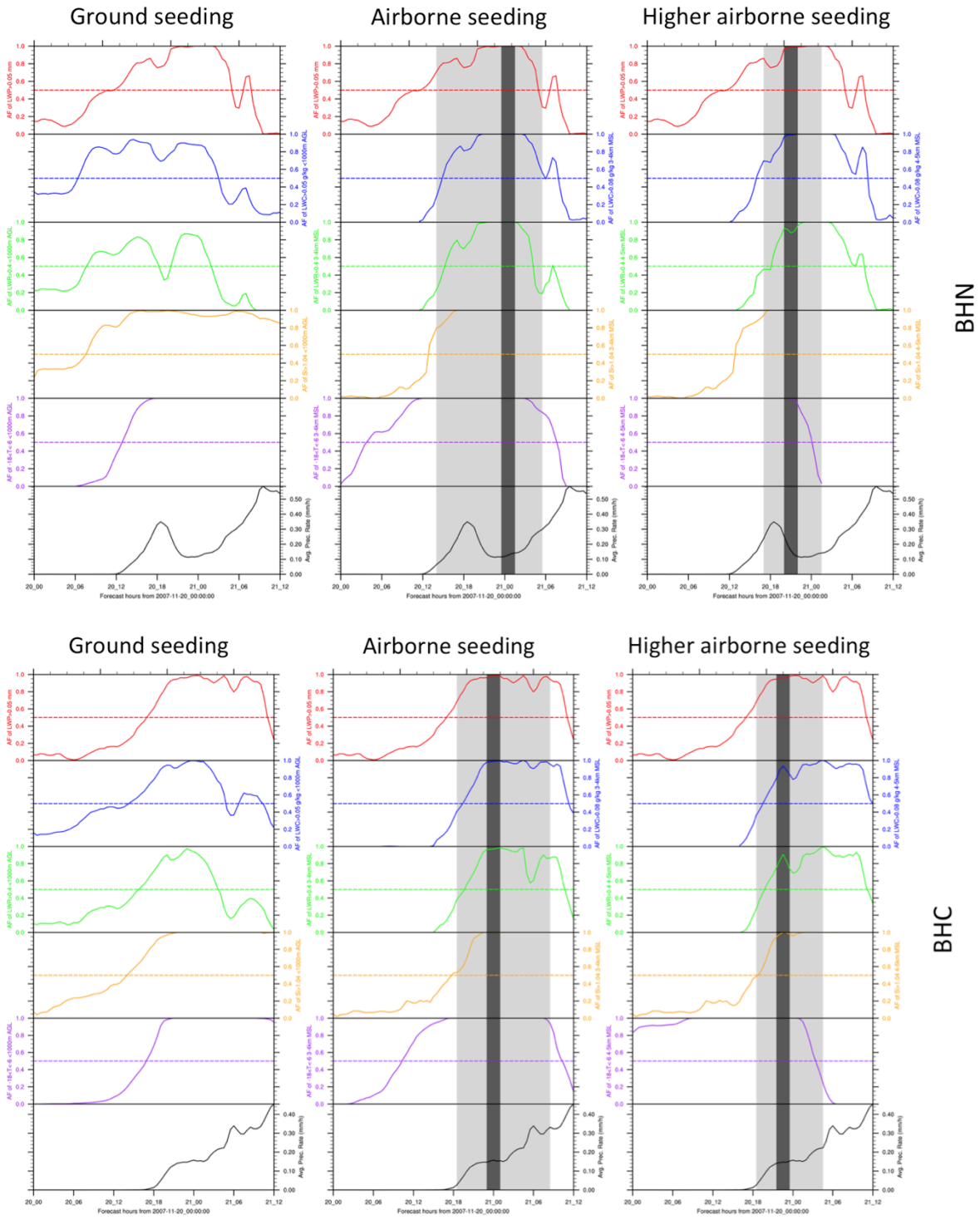
Ground seeding
Airborne seeding
Higher airborne seeding
BHN
Ground seeding
Airborne seeding
Higher airborne seeding
BHC

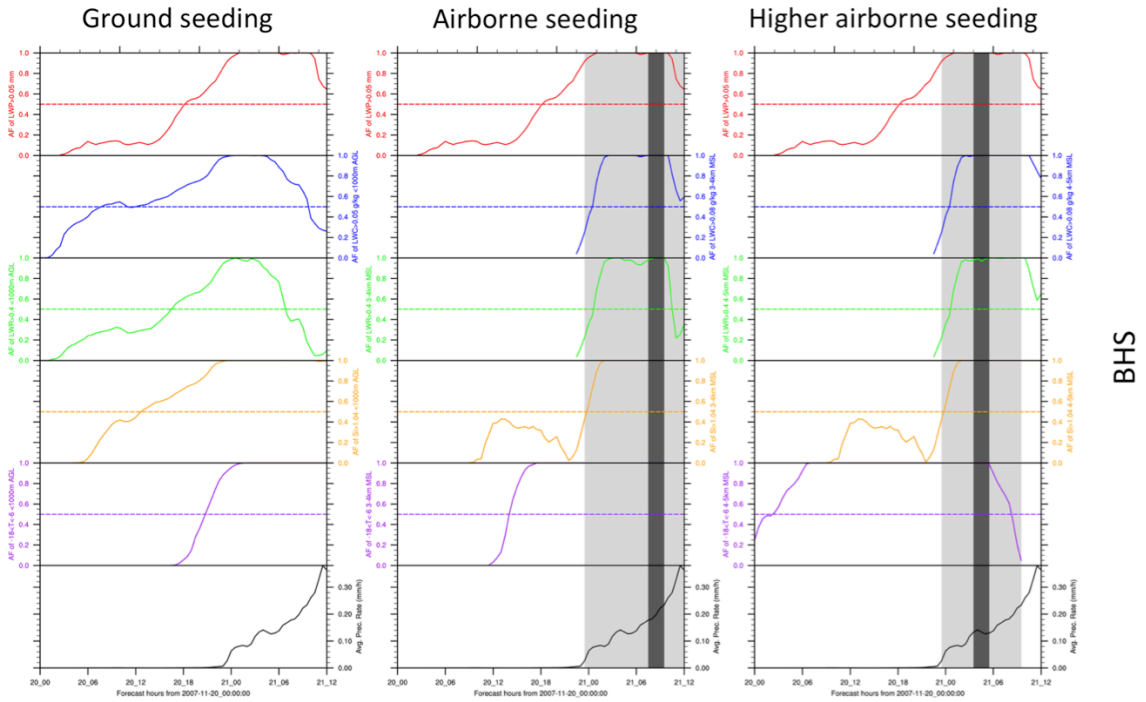


**Figure 6.30. Microphysical seeding criteria plots for ground seeding, airborne seeding (3750 m MSL) and higher level airborne seeding (4250 m MSL) for the BHN, BHC and BHS regions for the 20 November 2007 case. Each horizontal panel (and color) represents a different criterion assessed and the horizontal dashed line indicates the threshold that must be reached for the algorithm to consider that criterion met. Not all microphysical criteria assessed are required to be met for a case to be called, and even if all microphysical criteria are met there are additional criteria (especially for ground seeding, such as atmospheric stability and wind direction) that need to be met as well (not shown). Gray shading indicates time periods when seeding cases were identified. For airborne seeding, a 2-hr window is shaded in dark gray, representing the "best" period for seeding (given shorter time on station using a single aircraft).**

Similar to the 13 November 2007 case, no ground-seeding cases were called by WASCA, yet airborne seeding scenarios at both the regular and high altitudes were identified. The cold front moving from north to south is reflected by the sequential airborne cases from north to south identified by WASCA. Unlike the 13 November 2007 case, the microphysical conditions for ground seeding were met for the ground-seeding scenarios, but instead the dispersion (i.e., wind and stability) criteria in WASCA were not met in this case. Nonetheless, six ground-seeding experiments were conducted for this case, one for each of the five original ground generator groups, plus an additional simulation combining the new Group F with Group D (Section 5.6). The seeding times of these ground-seeding experiments are listed in Table 6.9. For GS_B, two seeding periods were simulated, one from 1400 to 1700 UTC and the other from 2000 to 0100 UTC. For the GS_D (and GS_D+F) case(s), five pairs of generators were turned on sequentially from north to south every hour from 1600 to 2000 UTC. All generators were powered off at 0300 UTC 21 November in these latter two cases. The sequential manner to powering on the generators was done to reflect the movement of seedable conditions from north to south as the cold front passed over the area.

Table 6.9. Seeding times of the ground seeding simulations for the 20 November 2007 case.

| Exp. | GS_A | GS_B | GS_C | GS_D | GS_E | GS_D + F |
|---|---|---|---|---|---|---|
| T_start (UTC) | 1120 12 | 1120 14<br>1120 20 | 1120 14 | (1) 1120 16<br>(2) 1120 17<br>(3) 1120 18<br>(4) 1120 19<br>(5) 1120 20 | 1121 00 | (1) 1120 16<br>(2) 1120 17<br>(3) 1120 18<br>(4) 1120 19<br>(5) 1120 20 |
| T_end (UTC) | 1120 14 | 1120 17<br>1121 01 | 1121 01 | 1121 03 | 1121 06 | 1121 03 |

The control-simulation precipitation accumulation and the LWP below 1 km AGL throughout the seeding period are plotted in Figure 6.31 and Figure 6.32. The control precipitation showed a broad maximum along the northeastern flank of the Bighorn Mountains. During the simulation period for this case, roughly 2-5 mm of precipitation were observed at SNOTEL sites in the southern portion of the region, with higher accumulations of 10-12 mm at the northern sites (Figure 6.33-Figure 6.34). As with the 13 November case, the primary exception is the Bone Springs site, which was an outlier again in this case. The model predicted precipitation accumulations of up to 10 mm, with the spatial pattern matching the observations very well (Figure 6.33).

The LWP below 1 km moved south generally with the movement of the cold front. The temperature and wind fields at 700 hPa (Figure 6.35) show that the cold front cooled the temperature from north to south and changed the wind direction in the northern and southern areas of the Bighorn Mountains. However, the wind direction in the central mountain region continued westerly through most of the seeding period.

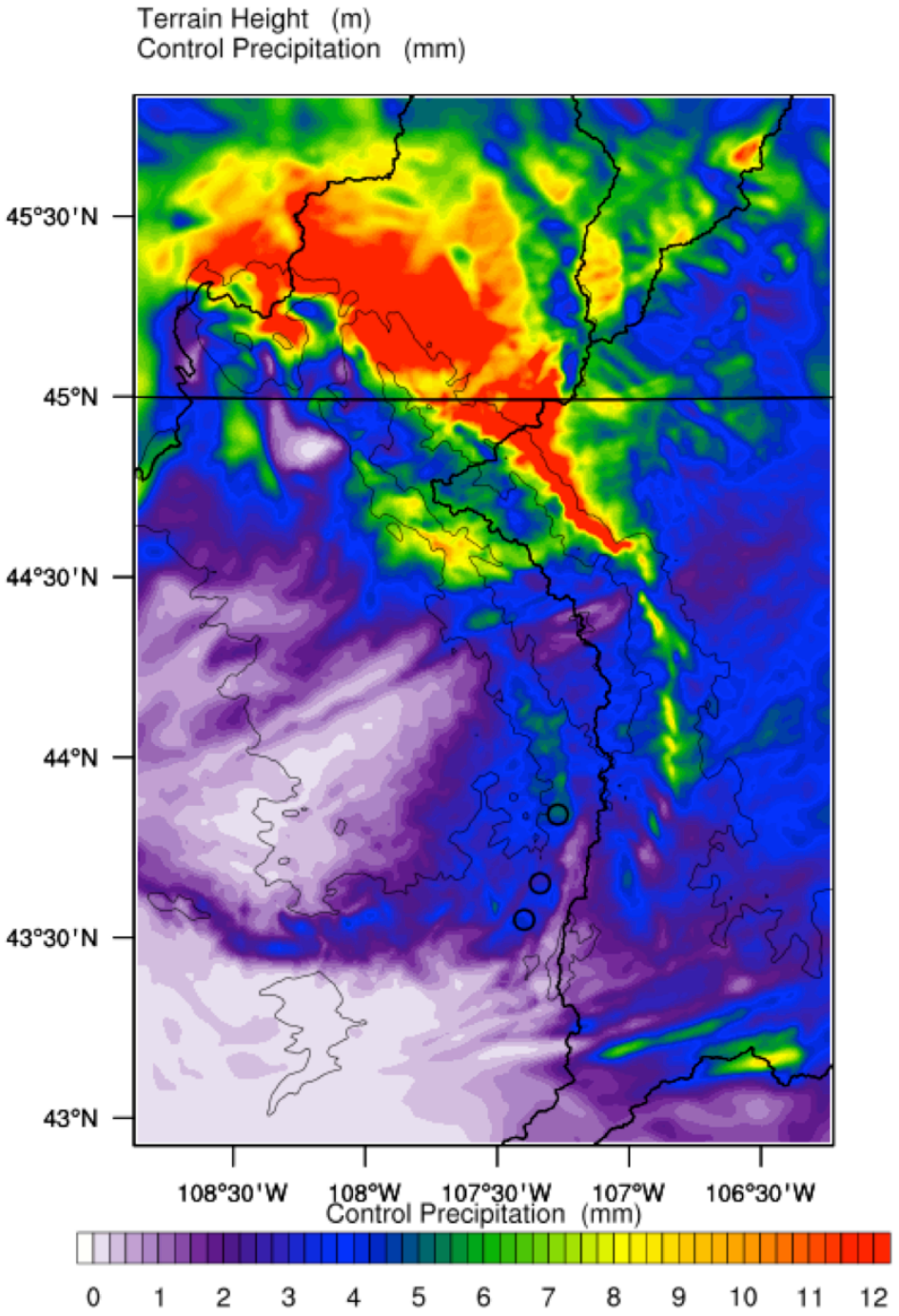


**Figure 6.31. Model simulation accumulated precipitation (mm), as Figure 6.8, but for the 20 November 2007 case.**

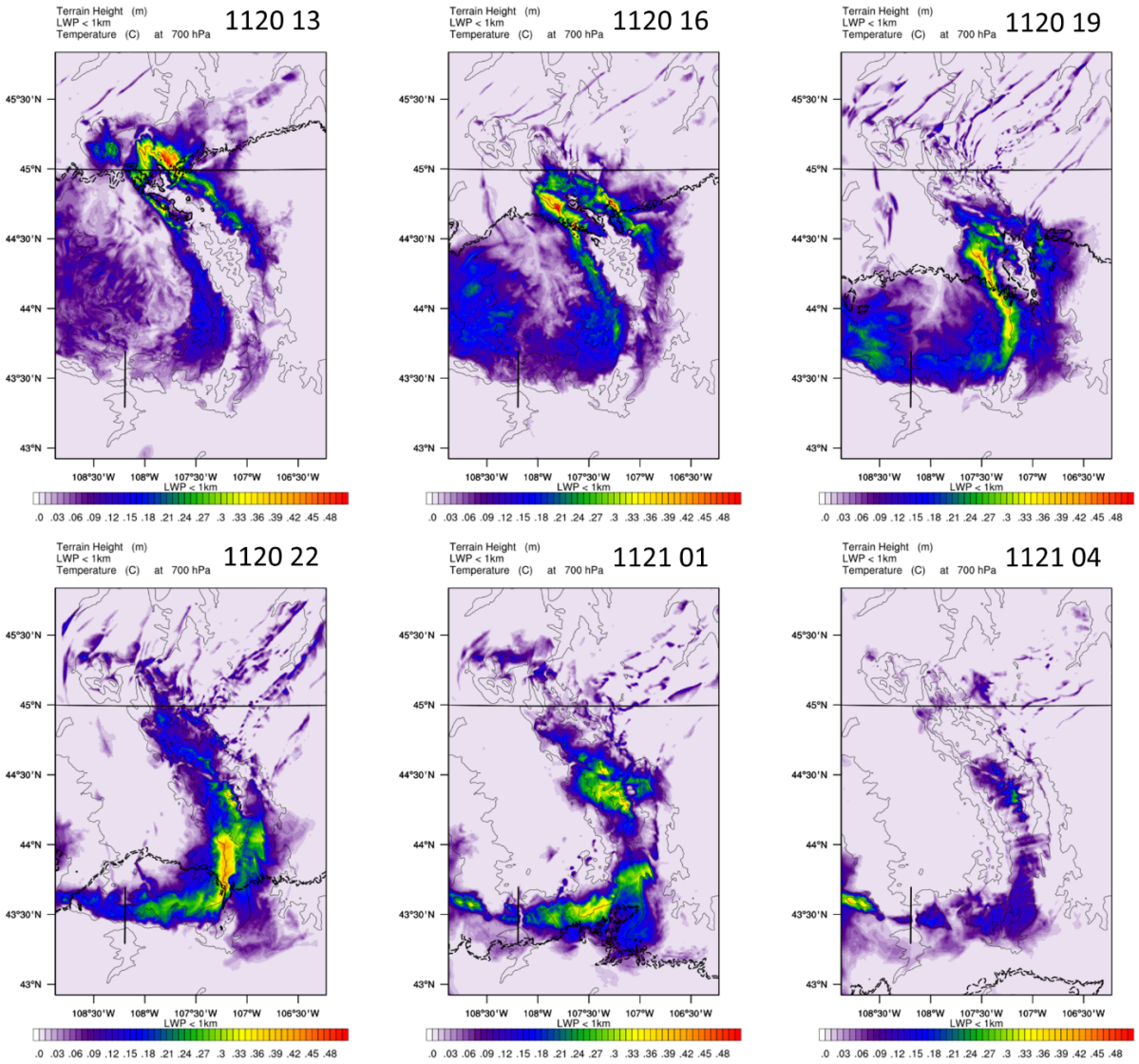


**Figure 6.32. Plan views of LWP below 1 km AGL (mm) from 1300 UTC 20 November to 0400 UTC 21 November every 3 hours. Black contour indicates the -6 °C isotherm at 700 hPa.**

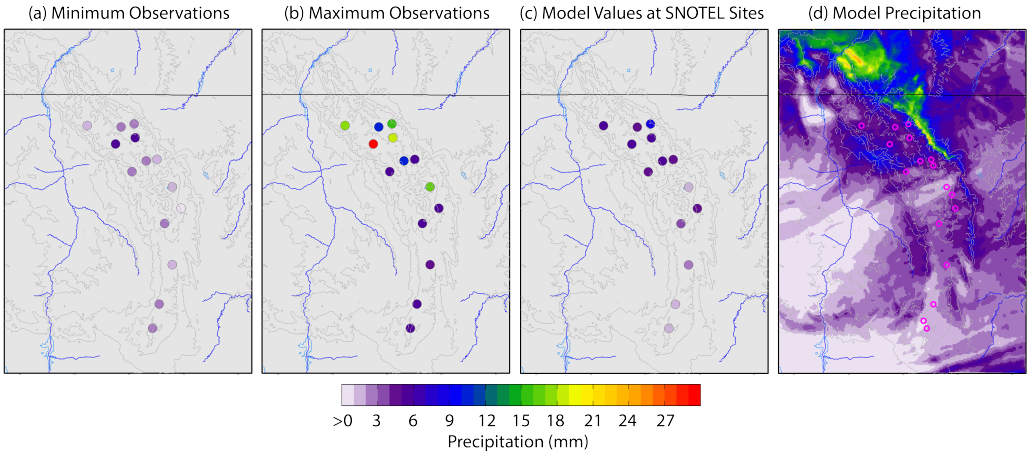


**Figure 6.33. Maps of observed precipitation accumulation (mm) over the simulation period for the 20 November 2007 case from SNOTEL sites, with minimum accumulation in (a) and maximum accumulation in (b), compared to model-simulated precipitation accumulation at the SNOTEL sites (c) and the complete simulation of precipitation across the domain (d).**

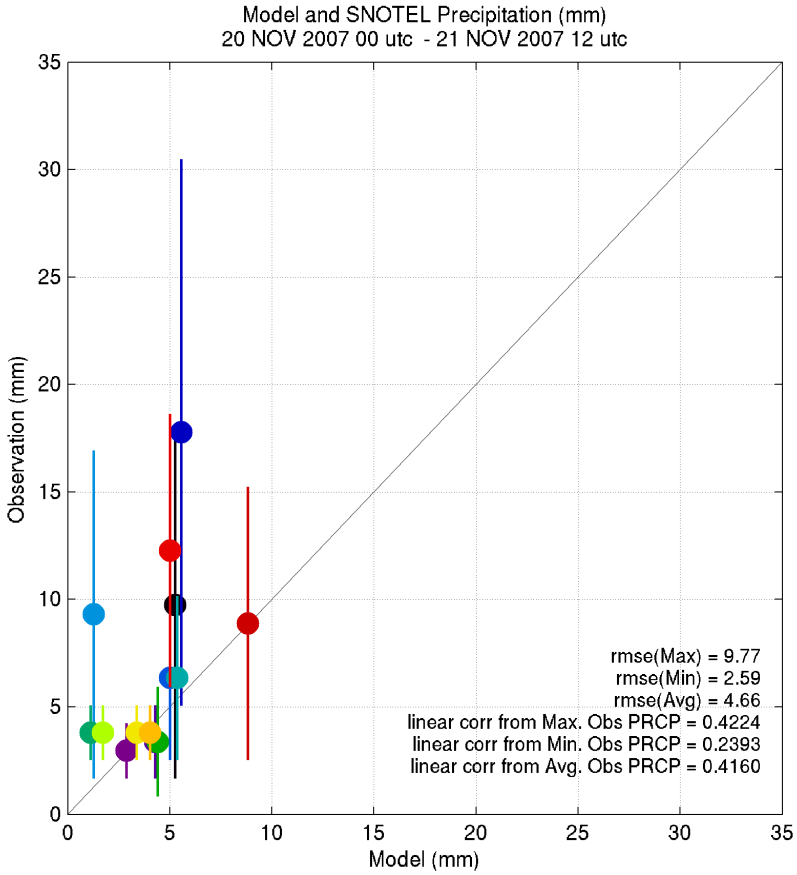


**Figure 6.34. Scatterplot comparing observed precipitation accumulation at SNOTEL sites versus the modeled precipitation accumulation at the same sites for 20 November 2007. Dots represent the average of the maximum and minimum possible precipitation accumulation at each SNOTEL site during the simulation period. Vertical bars represent the range of possible observation (i.e., minimum to maximum observation amount). Each point (color coded) represents single SNOTEL site.**

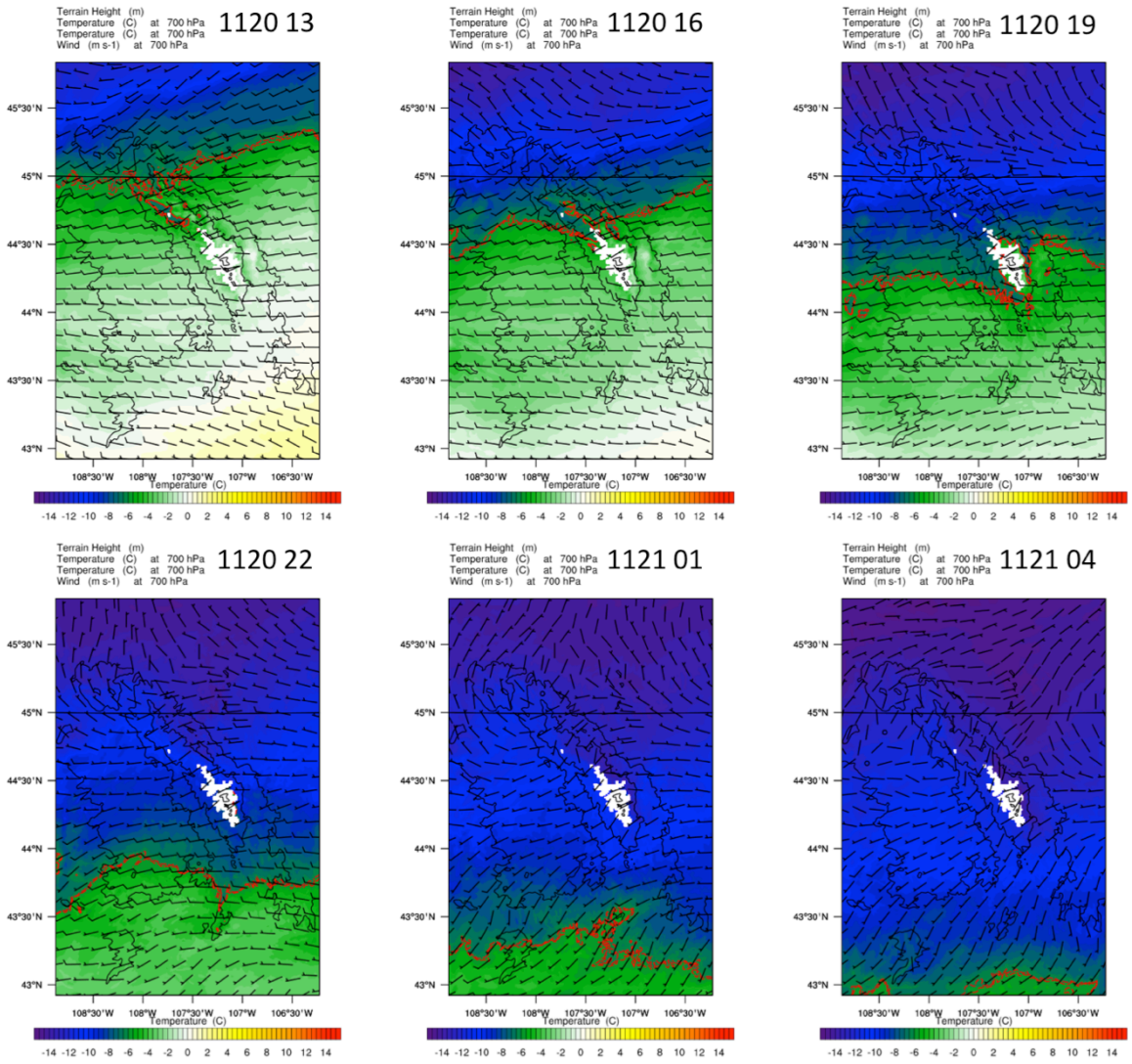


**Figure 6.35. 700-hPa temperature (color shaded) and wind barbs at the same times as Figure 6.32. Red line indicates the -6 °C isotherm.**

The average AgI concentration below 1 km AGL at the end of the corresponding seeding period is plotted in Figure 6.36 for each ground-seeding case. The simulated AgI plumes from the northern-most and the southern-most generators on the west slope were somewhat blocked by the range. Only the generators at high elevations or located in the central portion of the range had simulated AgI plumes passing over the mountain. The areal coverage of the highest concentrations of AgI is very limited in these cases.

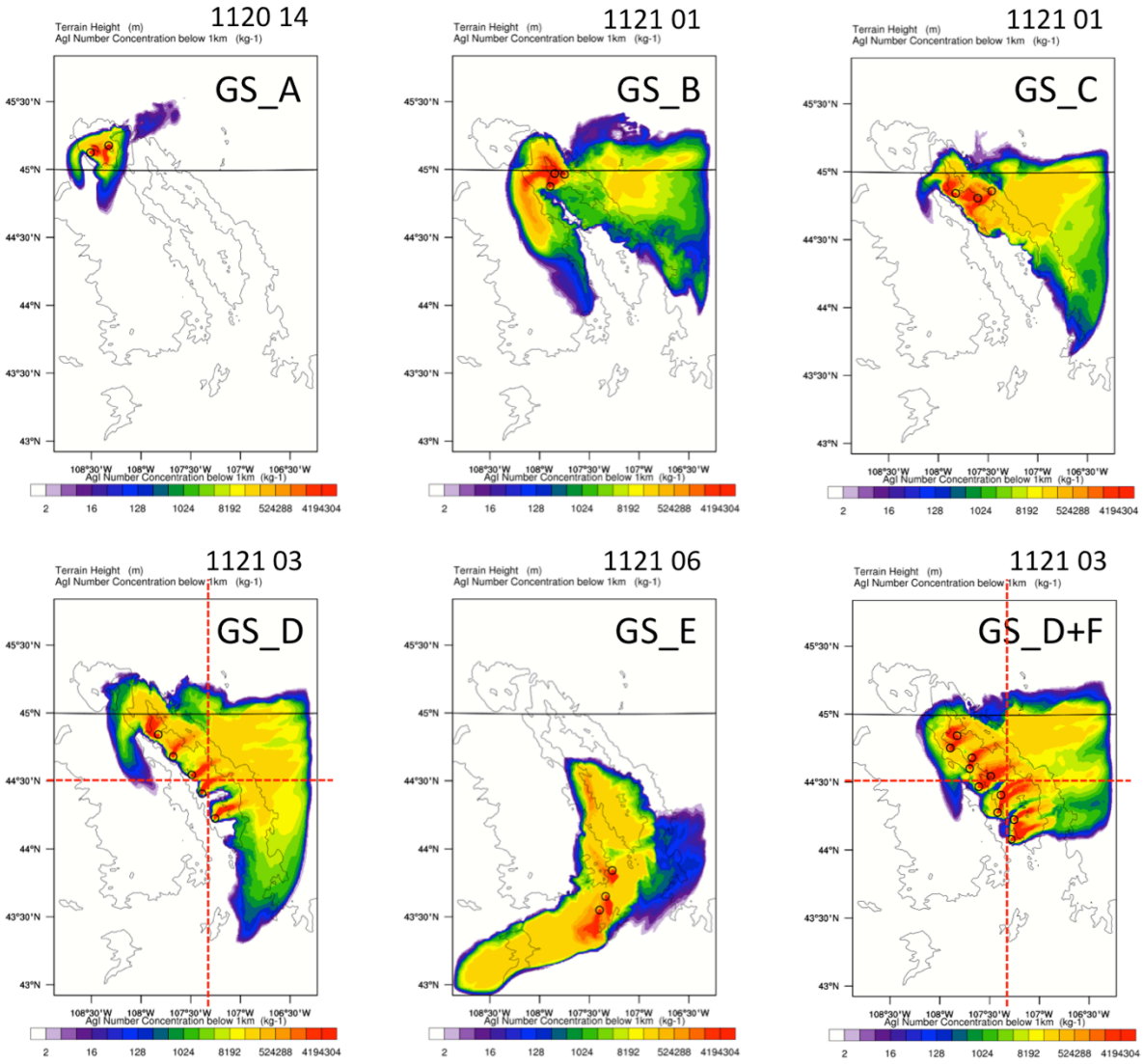


**Figure 6.36. Average simulated AgI concentration below 1 km AGL at the end of the seeding period of each ground seeding case. Red dashed lines indicate the cross section locations.**

The west-east and south-north cross sections are plotted in Figure 6.37 for the GS_D and GS_D+F experiments. The blocked portions of the simulated AgI plumes from the northern-most generators in these groups show up on the western side of the west-east cross sections at low levels. The SLW was most prevalent on the upwind (i.e., western) side of the range. The Group D generator locations were already high upslope at higher elevations, and therefore did not produce AgI plumes to tap this moisture. The addition of Group F, however, produced an AgI plume on the upwind/western slope, as it was designed to do, yet the AgI remained very shallow and close to the surface along this slope. Since most of the SLW was further aloft, this result still prevented most of the SLW from being depleted by the simulated seeding.

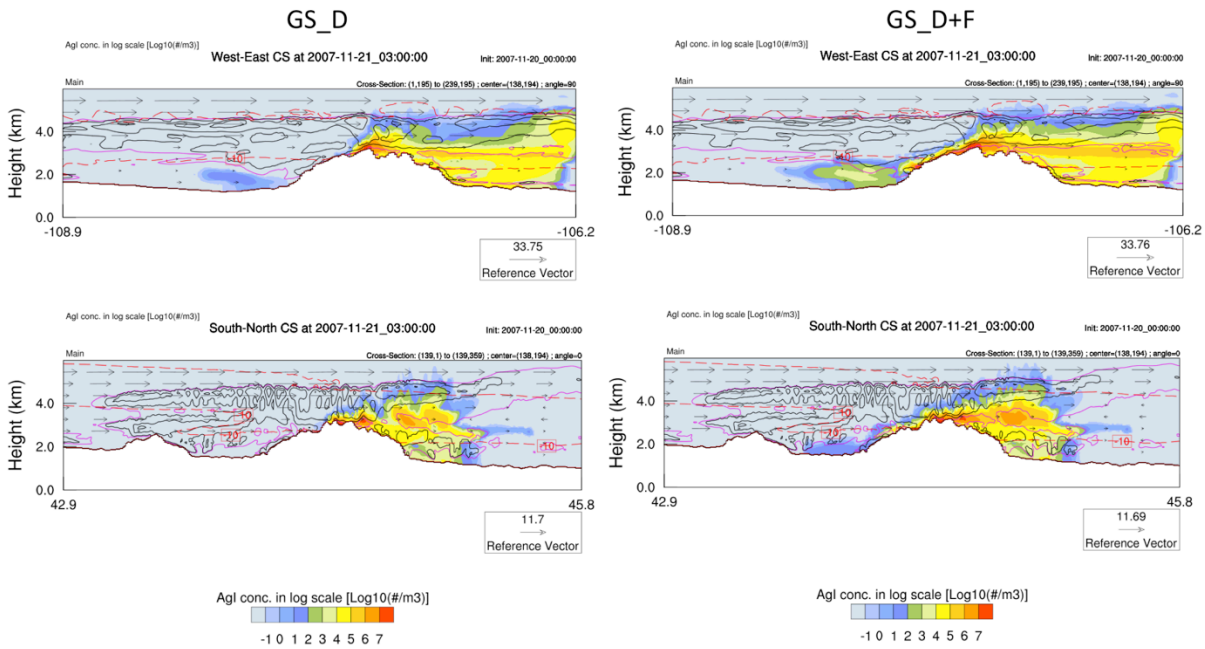


**Figure 6.37. West-east (top) and south-north (bottom) cross sections at 0300 UTC for the GS_D (left) and GS_D+F (right) experiments.**

The simulated seeding effect maps (Figure 6.38) show that all ground seeding experiments generated noticeable impacts except for the GS_A experiment. The GS_A experiment likely did not produce much of an effect due to having only two generators, and the plume from them was mostly blocked and remained localized (Figure 6.36). The other northern groups, GS_B and GS_C, produced focused seeding signals in the northeastern side of the Bighorn Mountains along the state border. Central groups GS_D and GS_D+F, showed narrower seeding impact areas in the downwind region of each generator pair. The southern group, GS_E, impacted the precipitation close to the generator sites, which, like for GS_A, was the result of blocking (Figure 6.36). The GS_D+F experiment generated greater simulated seeding effects than the GS_D experiment.

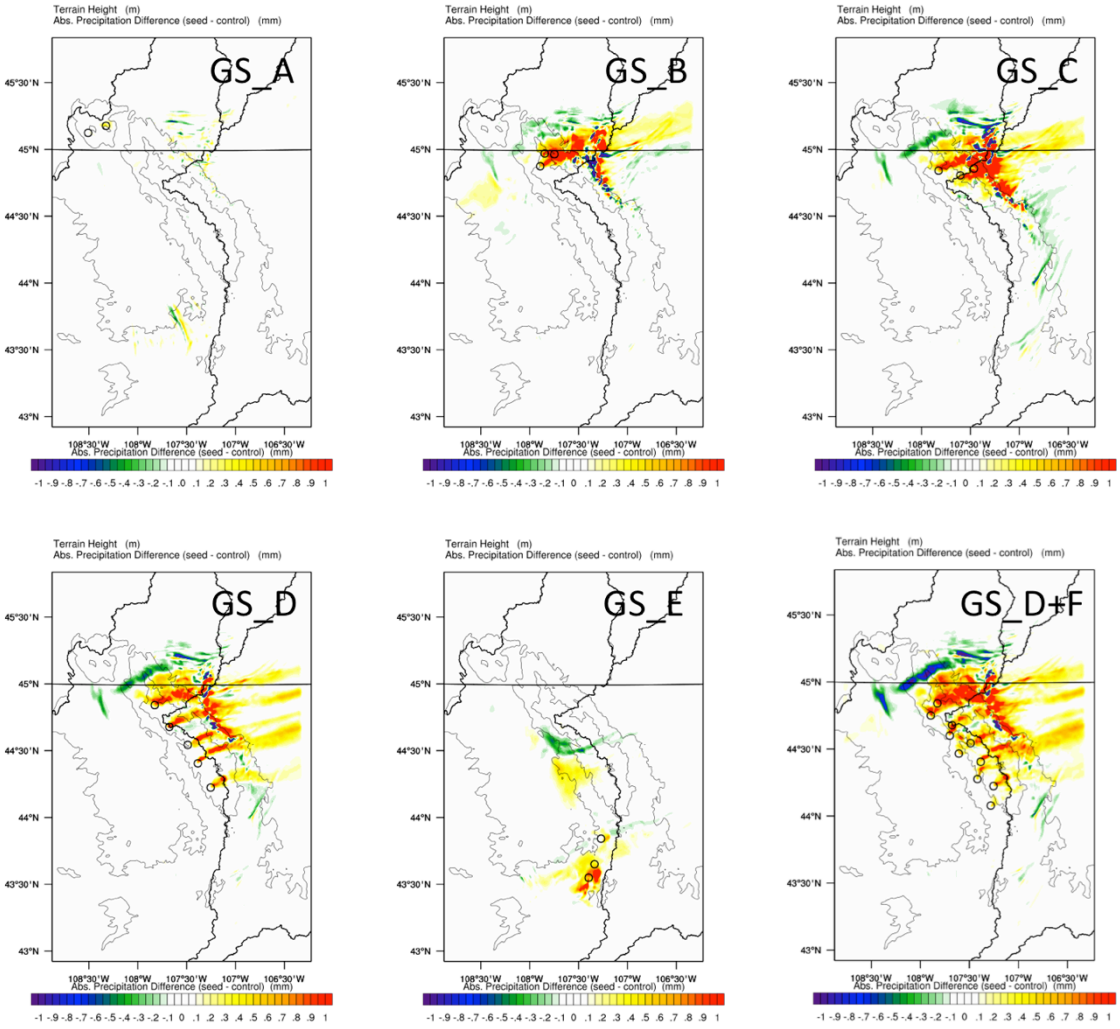


**Figure 6.38. The simulated seeding effect (mm) for all ground seeding experiments on 20 November 2007.**

Two airborne experiments were simulated for this case. One is the central track at the regular altitude but farther upwind than was tested in the 13 November case (AS_UC), and the other is a short north-south-oriented track at 4 km MSL in the southern region (AS4km_S). The location of these two tracks are plotted in Figure 6.39. The seeding periods of these two cases are given in Table 6.10.

**Table 6.10. Seeding times of the airborne seeding simulations.for the 20 November 2007 case.**

| **Experiment** | **AS_UC** | **AS4km_S** |
|---|---|---|
| T_start (UTC) | 1120 23 | 1121 0330 |
| T_end (UTC) | 1121 01 | 1121 0530 |

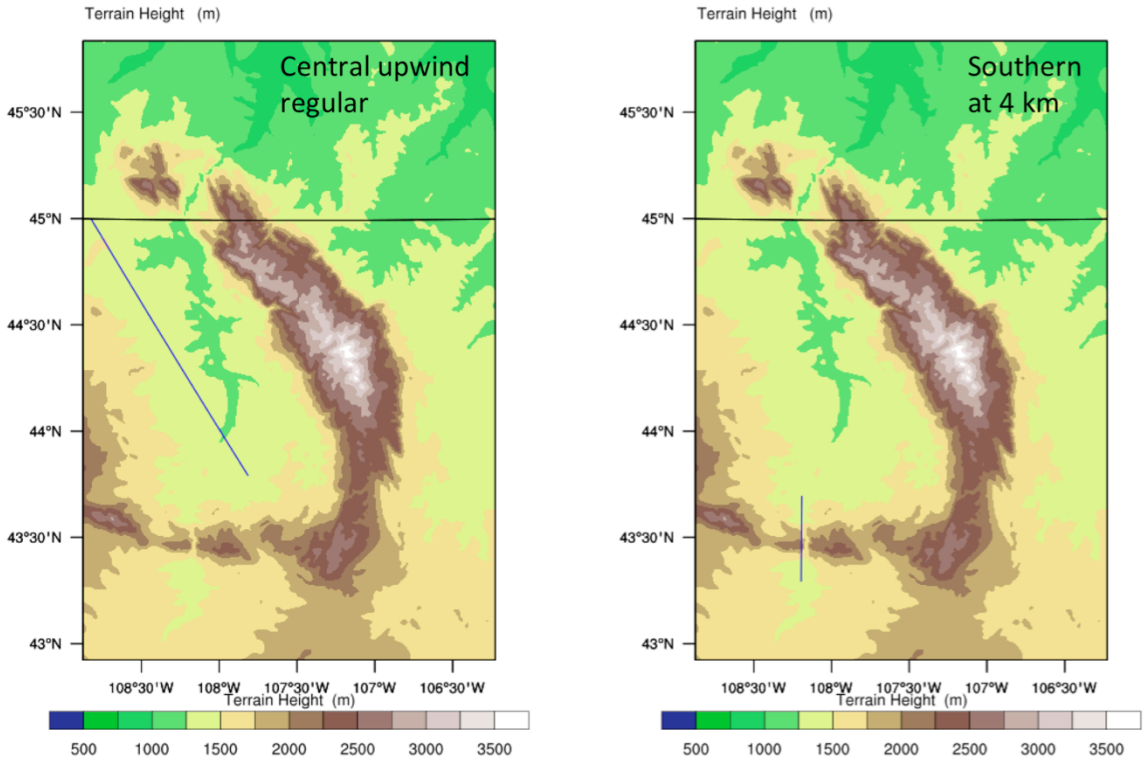


**Figure 6.39. The aircraft track location for the AS_UC (left) and AS4km_S (right) experiments.**

The simulated seeding effect and average absolute and relative LWP difference between 1 and 3 km (mm and %) are plotted in Figure 6.40 for the AS_UC experiment. The design of the upwind track was to cover more of the high-level SLW that was present in this case (Figure 6.37). The simulated seeding effect and LWP depletion indicate that the upwind design was successful in tapping much more of the available SLW that was simulated in this case, thereby yielding a broad area of positive simulated seeding effects on precipitation.

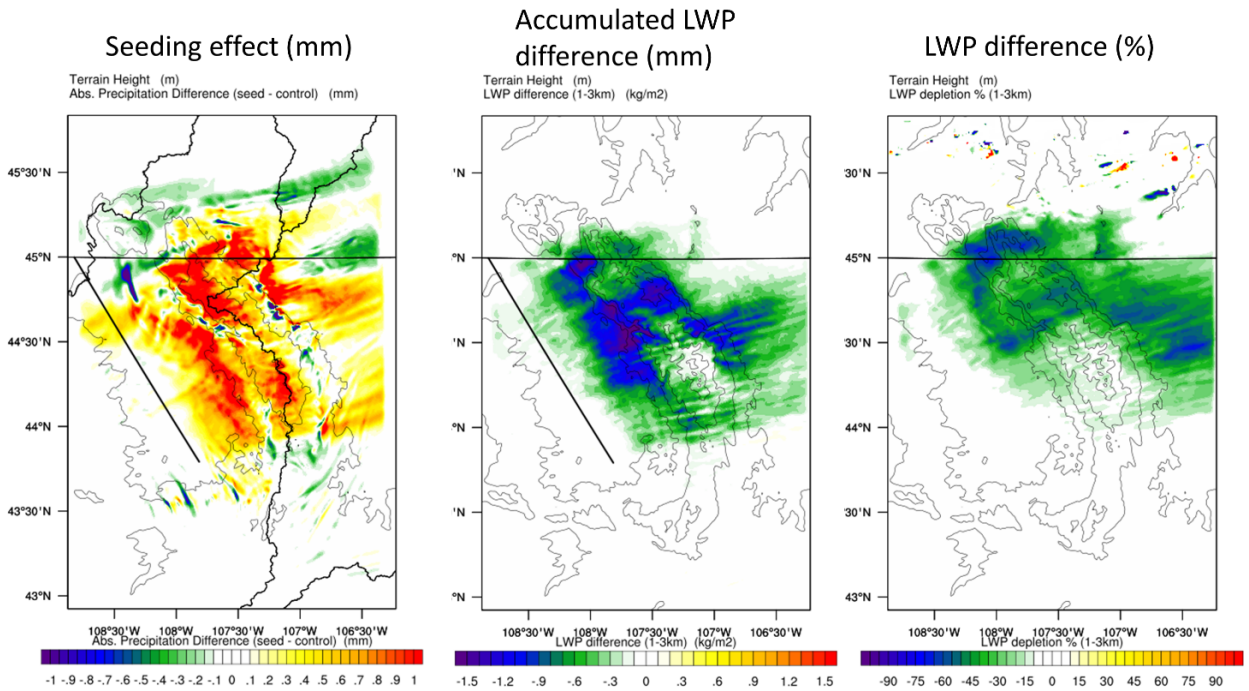


**Figure 6.40. The simulated seeding effect (mm) at the end of the simulation, average LWP difference (mm), and the relative LWP difference (%) for the AS_UC experiment in the 20 November 2007 case. The straight black horizontal line is the Wyoming-Montana state border. The thin black curves are the underlying terrain contours. The thick black curves in the left panel are the basin divides. The AS_C flight track is overlaid in the left and center panels.**

The simulated AgI plume and LWP between 1 and 3 km MSL at 00 and 02 UTC are shown in Figure 6.41 and Figure 6.42. The plume covered most of the Bighorn Mountains. The depletion of LWP between 1 and 3 km MSL by the simulated AgI plume is obvious over the mountain. The streaky feature of the LWP field is the result of interpolation of LWC at vertical levels close to 1 and 3 km MSL.

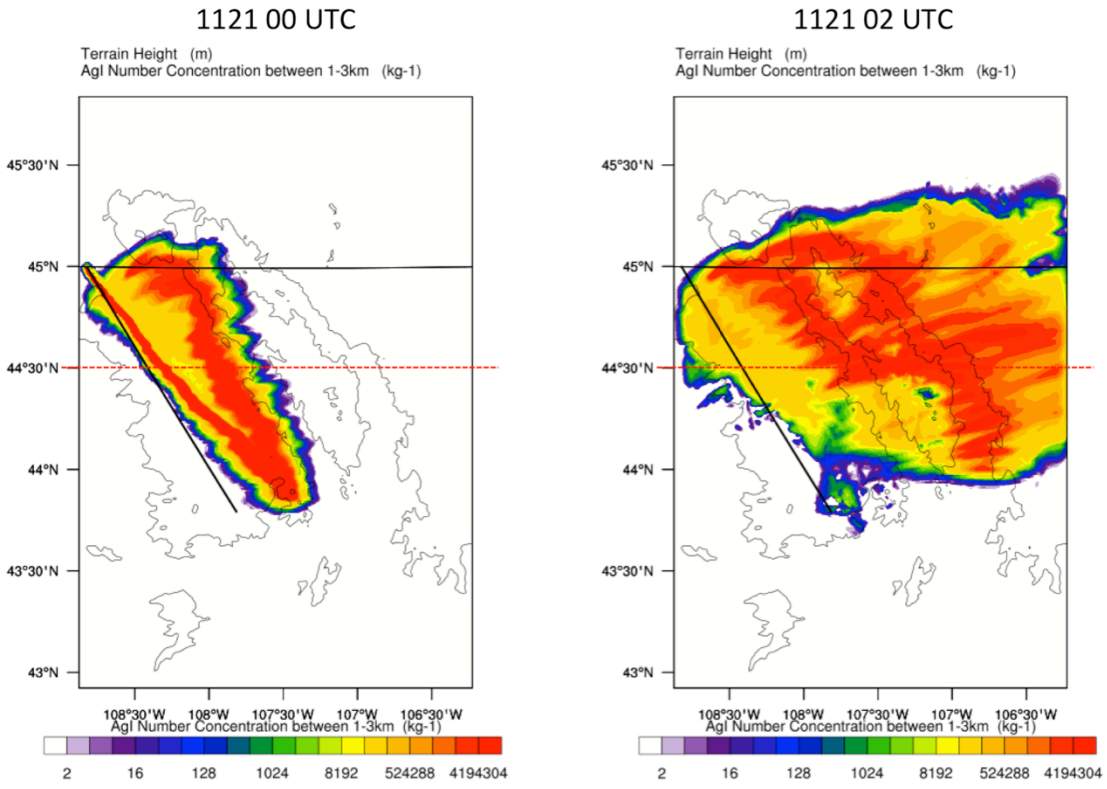


**Figure 6.41. Average simulated AgI concentration between 1 and 3 km MSL at 1121 00 and 02 UTC for the AS_UC experiment. The AS_C flight track is overlaid as thick black line.**

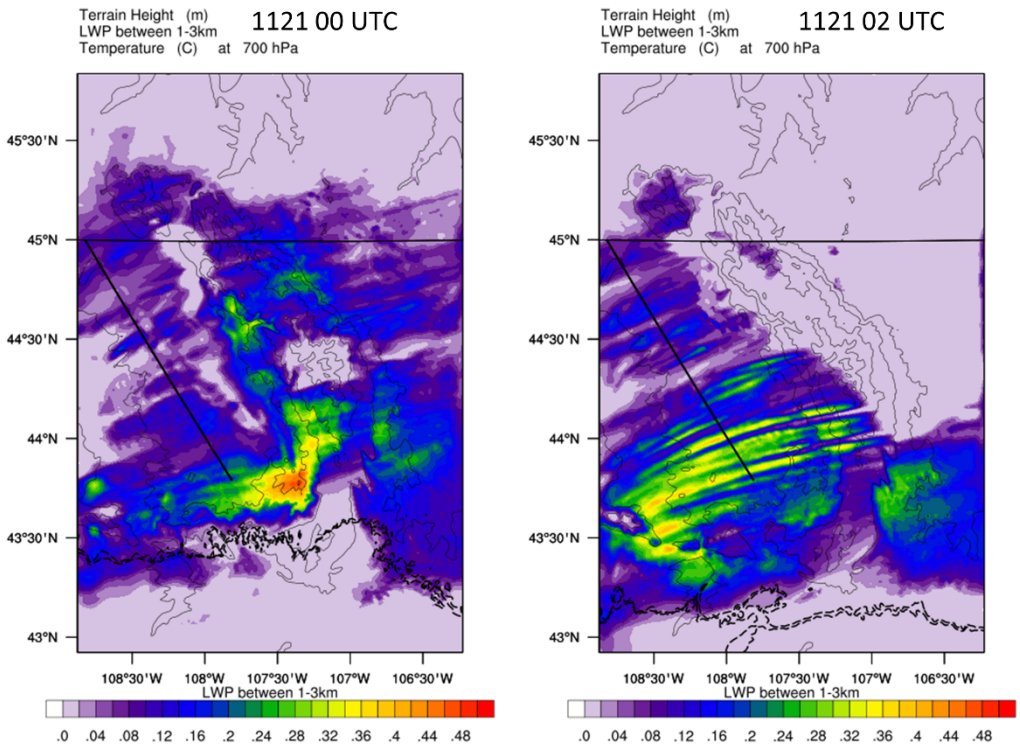


**Figure 6.42. The LWP between 1 and 3 km MSL at1121 00 and 02 UTC for the AS_UC experiment.**

The vertical cross sections (Figure 6.43) show that the aircraft-released AgI plume hovered in a temperature range between −17 and −11 °C. The high concentration of AgI particles converted all the SLW both upwind and downwind of the mountain into ice-phase particles (Figure 6.43). The optimum temperature range and abundant SLW aloft make this seeding case very efficient.

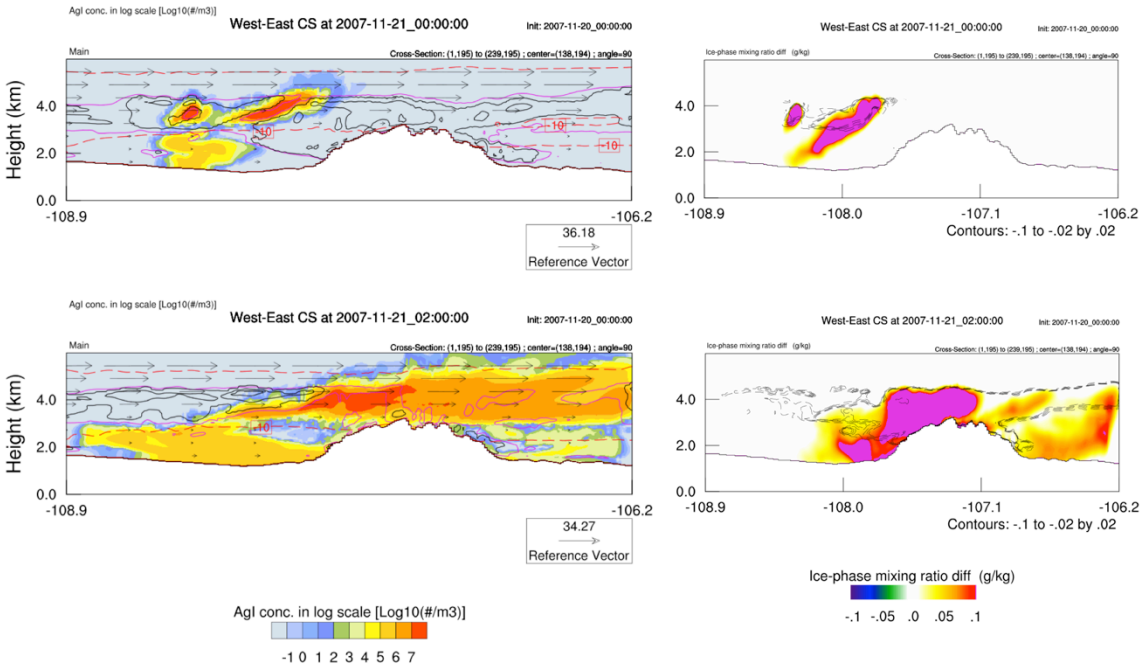


**Figure 6.43. West-east cross sections at 1121 0000 UTC and 1121 0200 UTC for the AS_UC case. The left panels show the simulated AgI number concentration in logarithmic scale (color shaded), the cloud water mixing ratio in black starting at 0.01 g kg$^{-1}$ with an interval of 0.2 g kg$^{-1}$, the ice saturation ratio of 1.04 in purple, isotherm in every 10 °C and wind vectors. The right panels show the cloud water mixing ratio difference in black (g kg$^{-1}$) and ice-phase mixing ratio difference in color (g kg$^{-1}$).**

The southern region was slightly warmer than the central and northern regions during the seeding period of AS4km_S (Figure 6.35). Therefore, a slightly higher track was used to capture the better temperature range. The simulated seeding effect and LWP depletion maps (Figure 6.44) showed that the simulated seeding impacted the upwind region substantially. Similar to the ASH_CS experiment in the 13 November 2007 case, the short track produced a more continuous AgI plume with high concentrations that completely converted the SLW into ice particles (Figure 6.45 and Figure 6.46). The simulate AgI plume in this case substantially depleted the SLW aloft upwind of the mountain barrier (Figure 6.47). Though the simulated precipitation was enhanced substantially in this experiment, the simulated seeding effects were mostly upwind of the mountain range, and therefore, the impacts to the highest elevations of the mountain range were minimal.

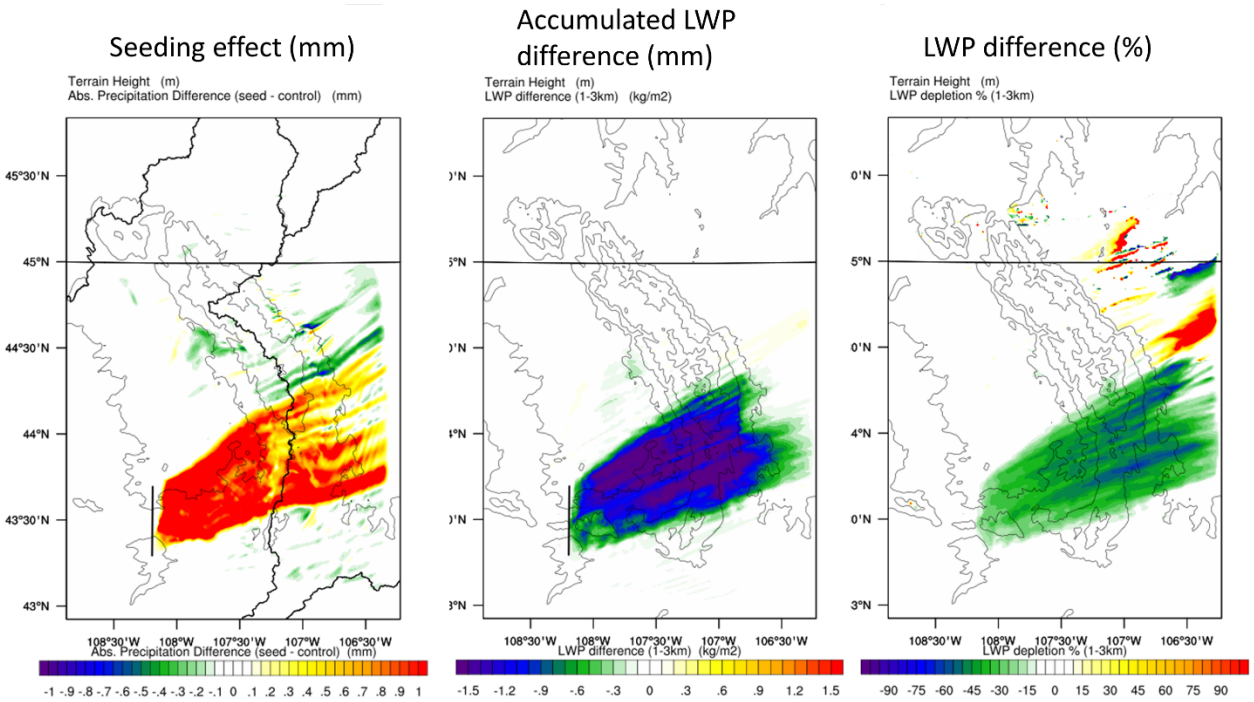


**Figure 6.44. The simulated seeding effect (mm) at the end of the simulation, average LWP difference (mm), and the relative LWP difference (%) for the AS4km_S experiment. The straight black horizontal line is the Wyoming-Montana state border. The thin black curves are the underlying terrain contours. The thick black curves in the left panel are the basin divides. The AS_S flight track is overlaid in the left and center panels.**

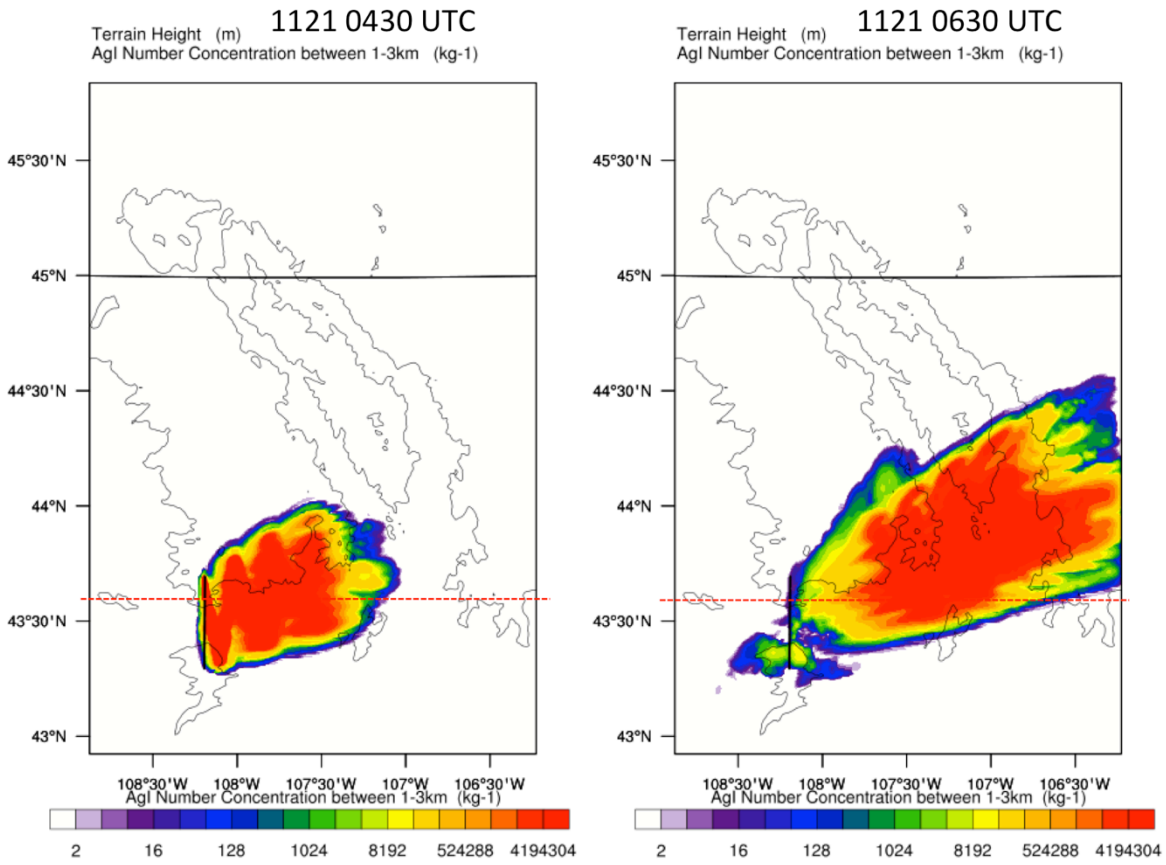


**Figure 6.45. Average simulated AgI concentration between 1 and 3 km MSL at 1121 00 and 02 UTC for the AS4km_S experiment.**

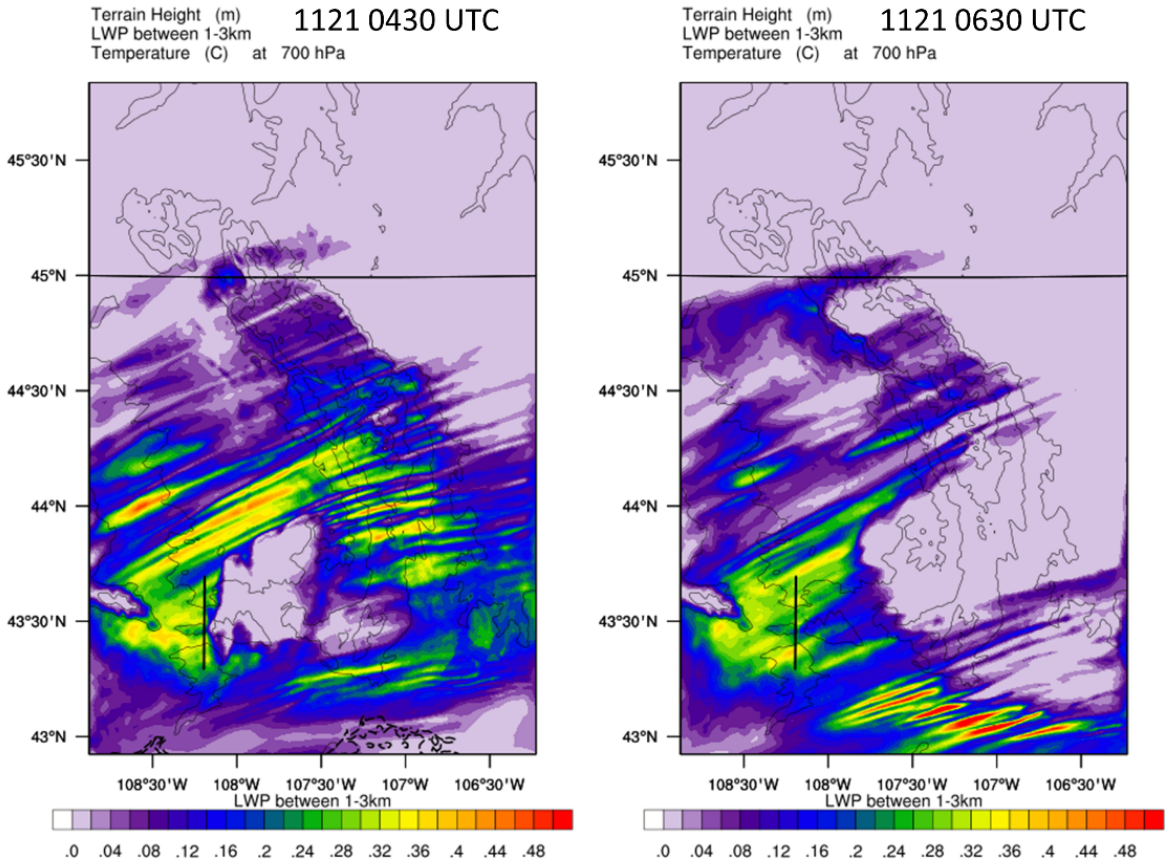


**Figure 6.46. The LWP between 1 and 3 km MSL at1121 00 and 02 UTC for the AS4km_S experiment.**

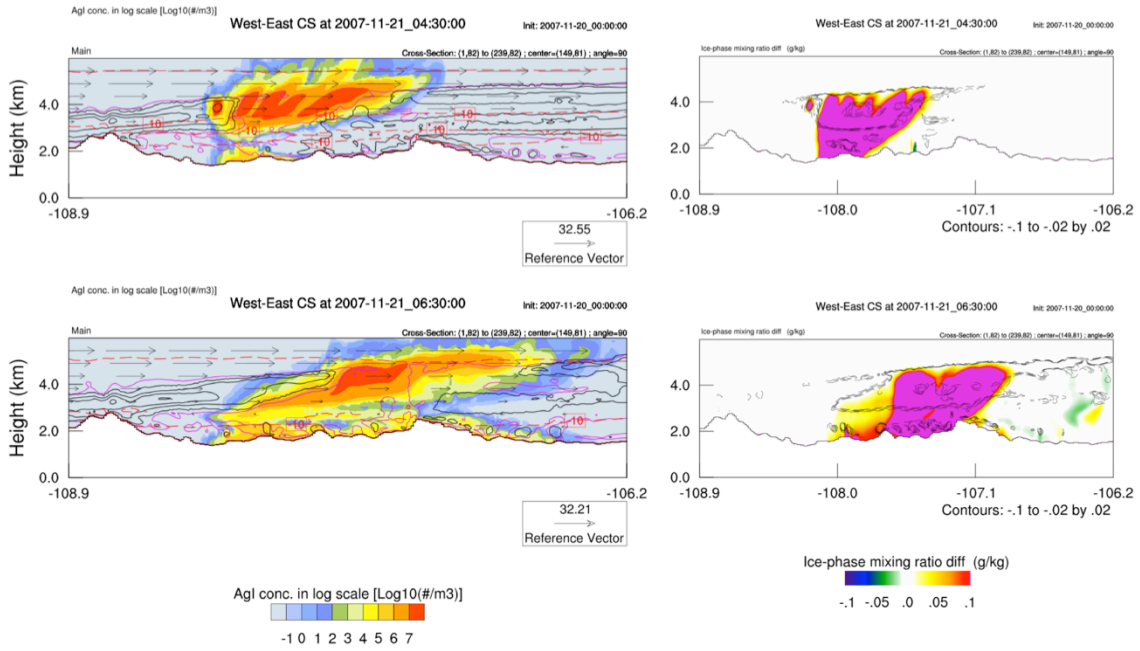


**Figure 6.47. West-east cross sections at 1121 0430 UTC and 1121 0630 UTC for the AS4km_S case. The left panels show the simulated AgI number concentration in logarithmic scale (color shaded), the cloud water mixing ratio in black starting at 0.01 g kg$^{-1}$ with an interval of 0.2 g kg$^{-1}$, the ice saturation ratio of 1.04 in purple, isotherm in every 10 °C and wind vectors. The right panels show the cloud water mixing ratio difference in black (g kg$^{-1}$) and ice-phase mixing ratio difference in color (g kg$^{-1}$).**

The control precipitation and simulated seeding effects in the two primary watersheds for all the seeding experiments are listed in Table 6.11 for the 20 November 2007 case. Ground-seeding experiments using northern and southern generator groups (GS_A, GS_B, GS_C and GS_E) produced negligible simulated seeding effects in the highest elevation regions (i.e., BH mtns and PT mtns). Central groups (GS_D and GS_D+F) generated reasonable simulated seeding effects, mostly focused at the higher elevations. In fact, the GS_D+F experiment simulated similar seeding effects as the airborne experiments in the 12 November 2007 case. The central flight track generated the highest simulated seeding effect of all the experiments, but like the southern airborne track experiment (AS4km_S), most of the enhanced precipitation fell upwind of the mountain range more than at the higher elevations. Since the track was further upwind, the simulated seeding effect was higher in the Bighorn than in the Powder/Tongue basin. The AS4km_S generated similar simulated seeding effects as the AS_UC case in the entire domain, but a negligible amount fell out at the higher elevation regions. The range of target areas impacted by positive simulated seeding effects ranged from 25–86% (Table 6.12).

**Table 6.11. Control precipitation and simulated seeding effects for each seeding simulation (acre-feet on top and % effect on bottom for each experiment row) over the full model domain and in the two primary watersheds (entirely, BH and PT, and just above 8,000 ft in those watersheds, BH mtns and PT mtns) for each of the seeding experiments. The experiment with the best simulated seeding effects is shaded. Relative simulated seeding effects within the target regions (BH mtns and PT mtns) > 1% are listed in bold. Results shown for the 20 November 2007 case.**

| | Domain | BH | PT | BH mtns | PT mtns |
|---|---|---|---|---|---|
| CTRL (af) | 221352 | 134136 | 87216 | 7330 | 5885 |
| GS_A | 231 | 185 | 46 | 16 | 1 |
| | 0.10 | 0.14 | 0.05 | 0.22 | 0.02 |
| GS_B | 919 | 686 | 233 | 100 | 9 |
| | 0.42 | 0.51 | 0.27 | **1.37** | 0.15 |
| GS_C | 1447 | 390 | 1057 | 95 | 85 |
| | 0.65 | 0.29 | 1.21 | **1.30** | **1.44** |
| GS_D | 1760 | 359 | 1401 | 172 | 248 |
| | 0.80 | 0.27 | 1.61 | **2.34** | **4.21** |
| GS_E | 600 | 554 | 46 | 40 | 5 |
| | 0.27 | 0.41 | 0.05 | 0.55 | 0.08 |
| GS_DF | 2783 | 804 | 1979 | 514 | 385 |
| | 1.26 | 0.60 | 2.27 | **7.01** | **6.53** |
| AS_C | 7436 | 4945 | 2491 | 1205 | 740 |
| | 3.36 | 3.69 | 2.86 | **16.44** | **12.58** |
| AS4km_S | 6430 | 4190 | 2239 | 68 | 224 |
| | 2.90 | 3.12 | 2.57 | 0.93 | **3.80** |

**Table 6.12. Simulated seeding areas of impact for the 20 November 2007 case. The simulated positive seeding areal impacts are listed as area in km² (rows labeled A_SE) and the portion of the seeding impacted area relative to the total area in percentage (rows labeled P_SE). The CTRL precipitation impacted area is calculated based on grid points with accumulated precipitation greater than 0.01 mm (in km², "A", and in percent of total area, "P"). The total area (A_total) within each domain is listed in the first row (km²). For experiments and target areas (either BH mtns or PT mtns) with simulated seeding impacts > 1% (shown in Table 6.11), the P_SE values have been listed in bold.**

| | | Domain | BH | PT | BH mtns | PT mtns |
|---|---|---|---|---|---|---|
| Case | A_total | 69984 | 43367 | 26617 | 2206 | 1865 |
| CTRL | A | 69015 | 42853 | 26162 | 2206 | 1865 |
| | P | 98.62 | 98.81 | 98.29 | 100.00 | 100.00 |
| GS_A | A_SE | 15836 | 9765 | 6072 | 832 | 372 |
| | P_SE | 22.63 | 22.52 | 22.81 | 37.70 | 19.94 |
| GS_B | A_SE | 15717 | 9756 | 5961 | 568 | 625 |
| | P_SE | 22.46 | 22.50 | 22.40 | **25.73** | 33.54 |
| GS_C | A_SE | 18398 | 9408 | 8990 | 770 | 909 |
| | P_SE | 26.29 | 21.69 | 33.78 | **34.88** | **48.74** |
| GS_D | A_SE | 16744 | 7160 | 9584 | 693 | 861 |
| | P_SE | 23.92 | 16.51 | 36.01 | **31.39** | **46.18** |
| GS_E | A_SE | 15504 | 9709 | 5795 | 1312 | 940 |
| | P_SE | 22.15 | 22.39 | 21.77 | 59.47 | 50.43 |
| GS_DF | A_SE | 21725 | 9804 | 11921 | 1699 | 1372 |
| | P_SE | 31.04 | 22.61 | 44.79 | **77.02** | **73.59** |
| AS_C | A_SE | 31172 | 18448 | 12724 | 1913 | 1618 |
| | P_SE | 44.54 | 42.54 | 47.81 | **86.71** | **86.75** |
| AS4km_S | A_SE | 18159 | 10165 | 7995 | 889 | 927 |
| | P_SE | 25.95 | 23.44 | 30.04 | 40.27 | **49.74** |

### *6.3.3 17 January 2016 case*

For this case, the outer domain was integrated for 48 hours from 1800 UTC 16 January 2016 to 1800 UTC 18 January 2016 UTC. The control simulation in the inner domain spanned from 0600 UTC 17 January 2016 to 1800 UTC 18 January 2016. The seeding cases identified by WASCA based on the 900-m control results are listed in Table 6.13. The associated seeding criteria plots are shown in Figure 6.48 for this case.

**Table 6.13. WASCA output for the 17 January 2016 case.**

| |
|---|
| No ground seeding for BHN<br>No airborne seeding for BHN<br>No higher airborne seeding for BHN |
| For BHC, number of ground seeding case[s]: 1<br>Case 1 seeds from 2016-01-17_18:30:00 to 2016-01-18_00:00:00<br>For BHC, number of suitable airborne seeding period[s]: 1<br>Period 1 ranges from 2016-01-17_18:00:00 to 2016-01-18_04:00:00<br>Best case of period 1 seeds from 2016-01-17_23:30:00 to 2016-01-18_01:30:00 at track[s] BHCA1<br>No higher airborne seeding for BHC |
| No ground seeding for BHS<br>For BHS, number of suitable airborne seeding period[s]: 2<br>Period 1 ranges from 2016-01-17_09:00:00 to 2016-01-17_13:30:00<br>Best case of period 1 seeds from 2016-01-17_10:30:00 to 2016-01-17_12:30:00 at track[s] BHSA1<br>Period 2 ranges from 2016-01-17_13:00:00 to 2016-01-17_18:30:00<br>Best case of period 2 seeds from 2016-01-17_14:30:00 to 2016-01-17_16:30:00 at track[s] BHSA1<br>No higher airborne seeding for BHS |

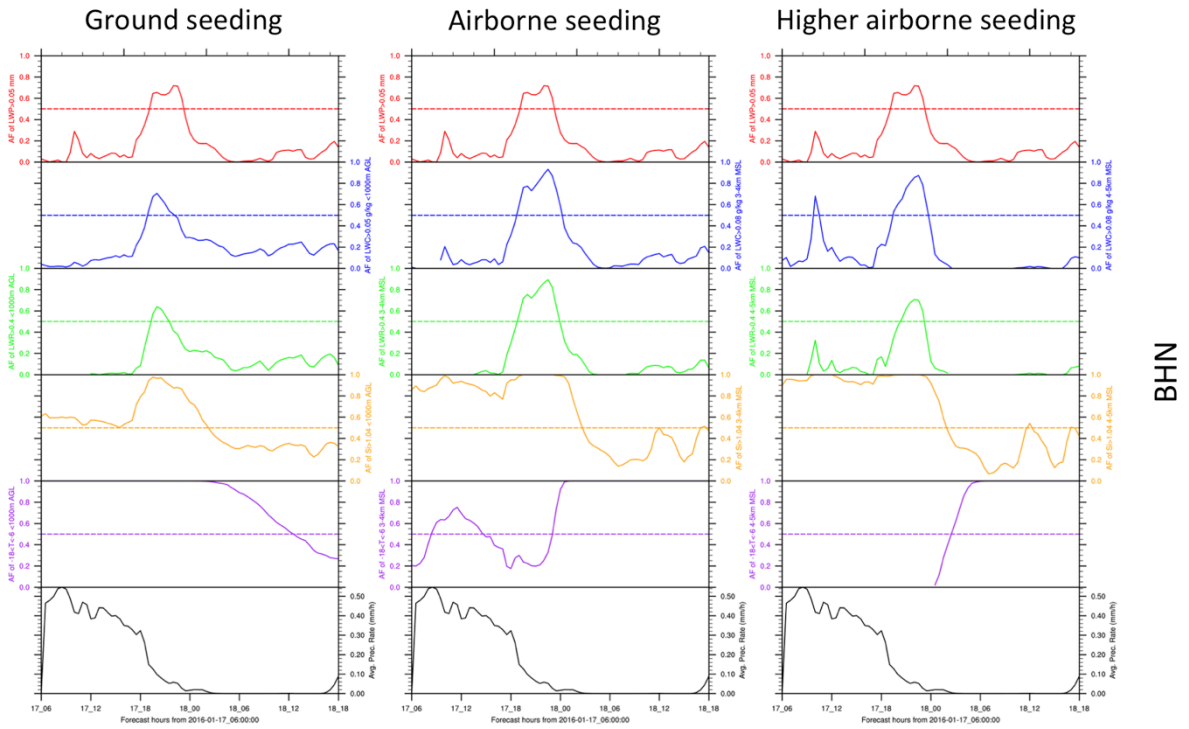
Ground seeding
Airborne seeding
Higher airborne seeding
BHN
Forecast hours from 2016-01-17_06:00:00
Avg. Prec. Rate (mm/h)

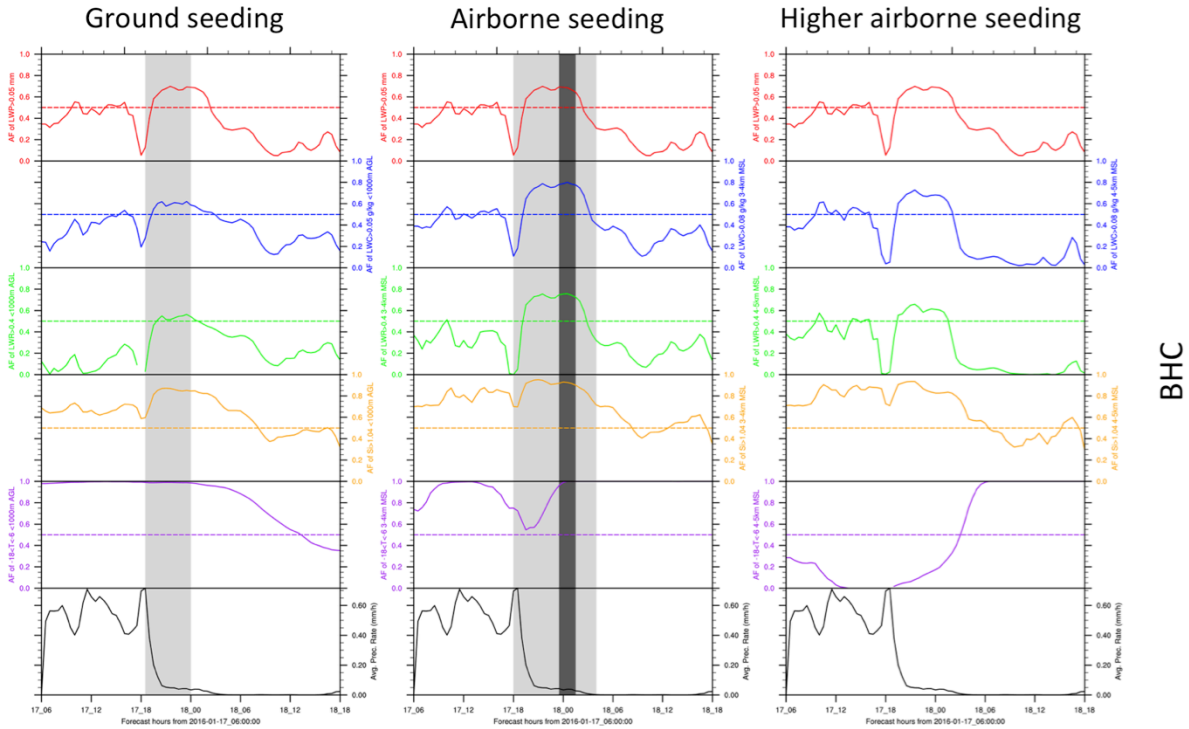
Ground seeding
Airborne seeding
Higher airborne seeding
BHC
Forecast hours from 2016-01-17_06:00:00
Avg. Prec. Rate (mm/h)

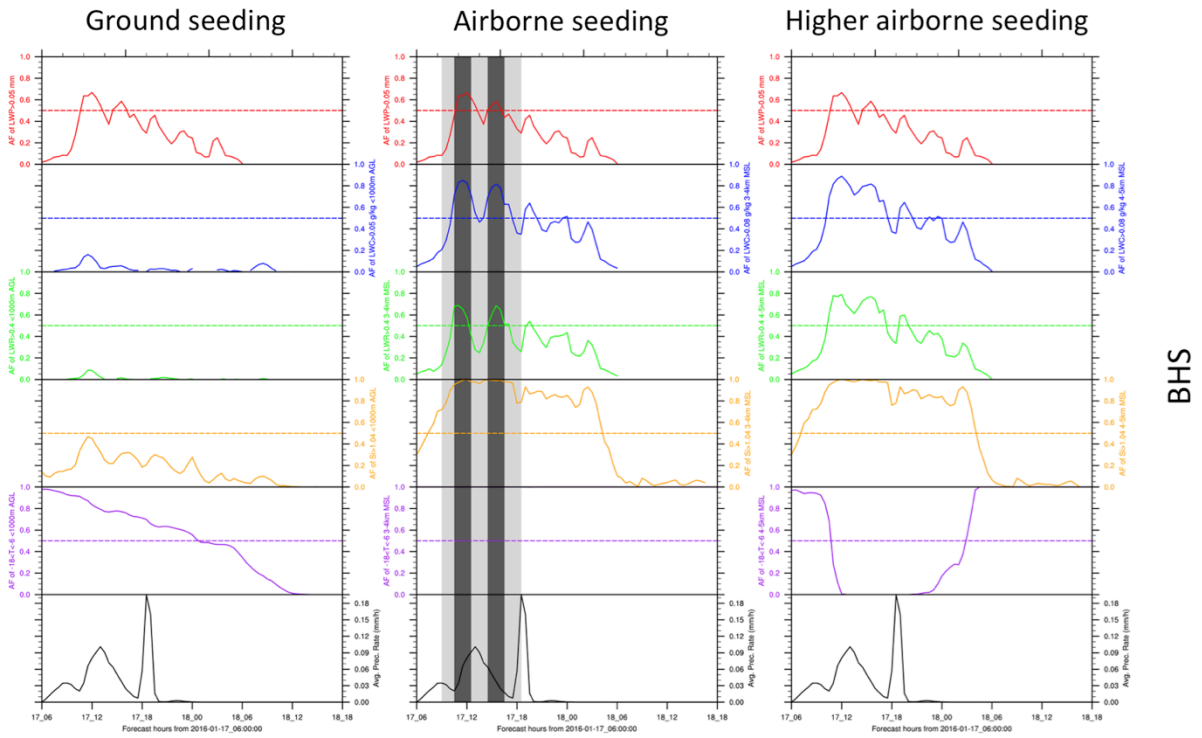


**Figure 6.48. Microphysical seeding criteria plots for ground seeding, airborne seeding (3750 m MSL) and higher level airborne seeding (4250 m MSL) for the BHN, BHC and BHS regions for the 17 January 2016 case. Each horizontal panel (and color) represents a different criterion assessed and the horizontal dashed line indicates the threshold that must be reached for the algorithm to consider that criterion met. Not all microphysical criteria assessed are required to be met for a case to be called, and even if all microphysical criteria are met there are additional criteria (especially for ground seeding, such as atmospheric stability and wind direction) that need to be met as well (not shown). Gray shading indicates time periods when seeding cases were identified. For airborne seeding, a 2-hr window is shaded in dark gray, representing the "best" period for seeding (given shorter time on station using a single aircraft).**

Radiometer data was available for this case, so the simulated LWP was evaluated at the Lovell radiometer site using the zenith observations (Figure 6.49). The modeled peaks in LWP are temporally mismatched with the observed peaks and peak values are generally lower than observed in the first half of the simulation period. In the latter half of the simulation, the model simulated no LWP over Lovell, while the radiometer still observed two additional periods with notable LWP.

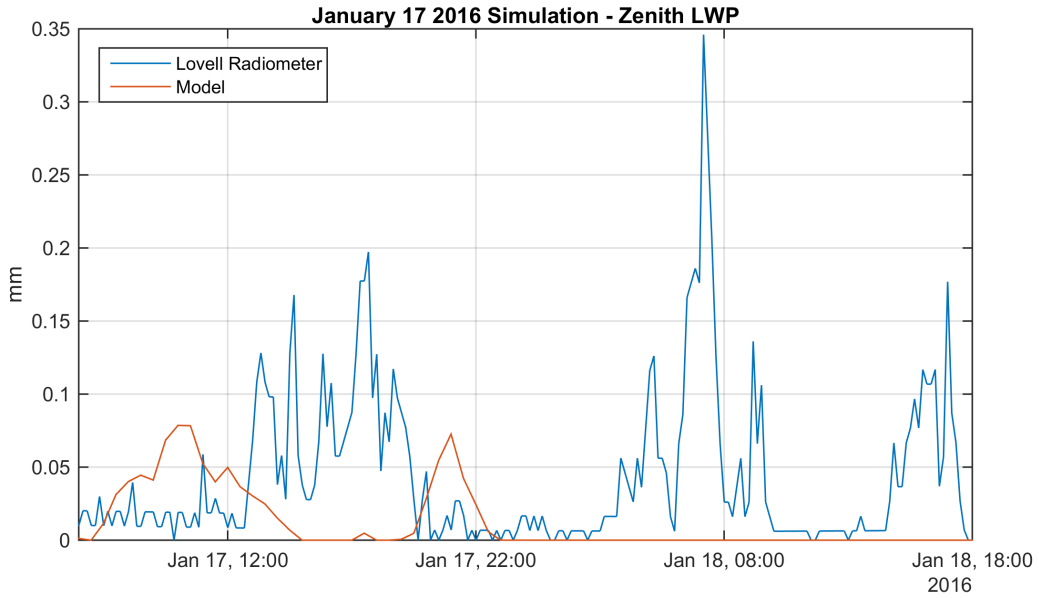


**Figure 6.49. Time series plot comparing the observed LWP from the Lovell radiometer (blue) against the modeled LWP at the same site (red).**

Unlike the 13 November and 20 November 2007 cases, a ground-seeding case was called by WASCA in the central region for this case. In the northern region, no seeding cases were identified. In the central and the southern regions, only the regular track airborne seeding cases were called. This indicates a colder temperature environment than the previous two cases. Five ground seeding experiments were performed for this case. The seeding times of these ground-seeding experiments are listed in Table 6.14.

**Table 6.14. Seeding times of the ground and airborne seeding simulations.for the 17 January 2016 case.**

| Experiment | GS_A | GS_B | GS_D | GS_F | GS_D+F | AS CS | AS_S |
|---|---|---|---|---|---|---|---|
| T_start (UTC) | 0117 1900 | 0117 1900 | 0117 1900 | 0117 1900 | 0117 1900 | 0117 2330 | 0117 1030 |
| T_end (UTC) | 0117 2100 | 0117 2300 | 0118 0600 | 0118 0600 | 0118 0600 | 0118 0130 | 0117 1230 |

Unlike the other two cases, this case did not have a frontal passage through the Bighorn mountain region. In addition, the precipitation distribution was different in that it has a maximum in the highest elevation terrain (Figure 6.50). Since a high-resolution snow gauge was operating in the Bighorn Mountains during this case, the data from it are also included in this comparison, along with the SNOTEL observations. During the simulation period on this case, roughly 2-8 mm of precipitation was observed at gauge sites (Figure 6.51). The observed precipitation accumulation is pretty uniform across the region on this case, as shown by the clustering of observed points in Figure 6.52, whereas the model simulated a broader range of precipitation accumulation at these sites. The Bone Springs site, which was a notable outlier in the previous two cases, seems to be performing better now. It is

possible there was a problem with the instrument at that site during the winter of 2007–2008 that was subsequently repaired. The model predicted the highest accumulations along the highest elevations of the mountains (Figure 6.51).

The low-level SLW occurred over the mountain peak and was quite persistent (Figure 6.53). The 700-hPa temperature was around −10 °C over the entire mountain and the environmental conditions were semi-steady through the seeding period (Figure 6.54). While the winds were from the northwest, they had more of a westerly component than northerly and as a result, the simulated AgI plumes from the northern generator groups (GS_A and GS_B) did not disperse over the main mountain barrier where the SLW existed (Figure 6.55). The simulated AgI plumes from the central groups (GS_D, GS_F and GS_D+F) dispersed over the main mountain barrier and therefore encountered more LWC than the northern groups (Figure 6.55). The simulated AgI plumes from the generators at lower elevations on the western slope (i.e., GS_F) were somewhat blocked by the mountain resulting in a broader area of AgI coverage than the case GS_D, especially upwind of the mountain barrier (Figure 6.55). The vertical cross sections show that GS_F impacted more SLW in the southern region (Figure 6.56). Since the SLW was very shallow and localized around the peak (Figure 6.53 and Figure 6.56), only the simulated AgI plumes with high concentrations close to the peak impacted the cloud and precipitation (Figure 6.57).

One airborne seeding simulation with two flight tracks was performed for this case. The seeding periods, based on the WASCA results, of the southern track (Figure 6.39) and the central short track (Figure 6.13) are listed in Table 6.14. Figure 6.58 shows the simulated seeding effect and LWP depletion of this airborne case. The central short track generated strong simulated seeding effects, while the southern track produced little simulated seeding effect on the ground. The AgI plumes between 1 and 3 km at the middle time segment for each seeding period are shown in Figure 6.59. The corresponding LWP maps are illustrated in Figure 6.60. The short tracks produced high concentrations of AgI and effectively depleted LWC along the wind. The west-east vertical cross sections (Figure 6.61) show that the southern seeding barely impacted the cloud, possibly because the LWC was higher than where the AgI plume was released and, as a result, generated minimal precipitation particles. Another test was simulated with a higher altitude southern track (4,250 m MSL, not shown), yet it also showed similar results. On the other hand, the central short track depleted almost all SLW over the peak and converted it into ice-phase precipitating particles.

The quantitative simulated seeding effects in all watersheds are listed in Table 6.15. As shown in Figure 6.57, northern ground generator groups generated null-simulated seeding effects throughout the domain. The GS_F experiment simulated a slightly greater seeding effect over the domain and similar simulated seeding effects at high elevations compared to GS_D. The simulated effect of the GS_D+F experiment is the greatest of all ground experiments, and is almost the summation of GS_D and GS_F cases due to little overlap in the seeding-impacted areas from these two cases. Similar to the previous two cases, the airborne seeding scenario was more effective than the ground-seeding scenarios. Simulated impact areas ranged from 37–64% for these ground-based seeding experiments, and as high as 55–73% for the airborne experiment. (Table 6.16).

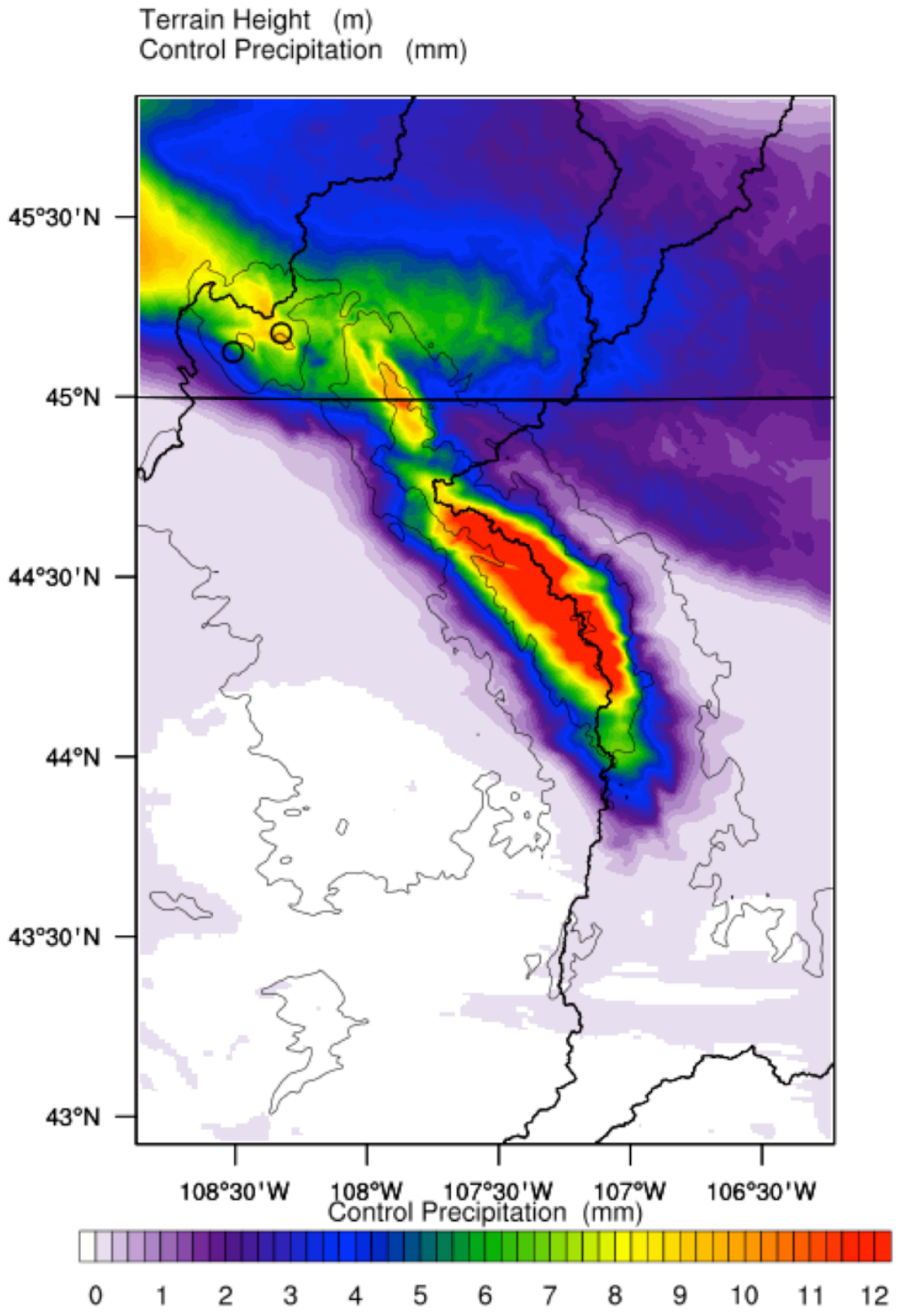


**Figure 6.50. Accumulated precipitation (mm) of the 17 January 2016 control simulation.**

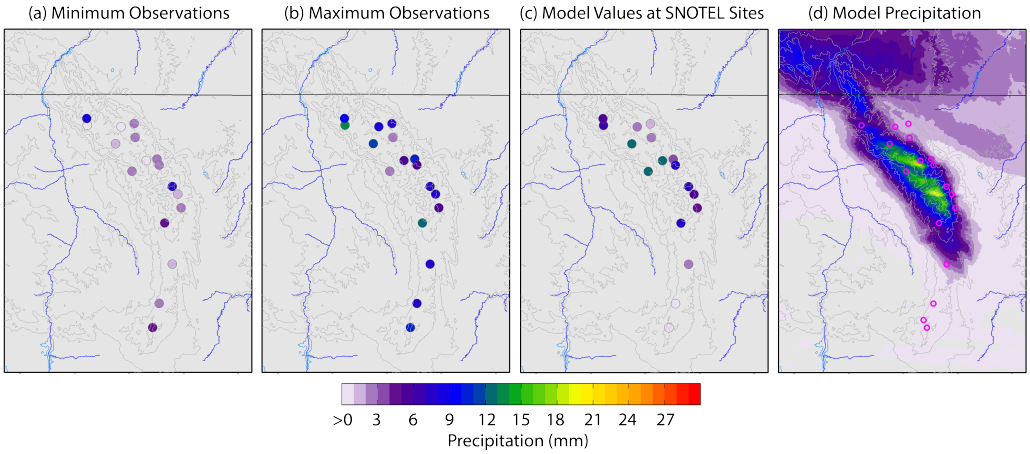


**Figure 6.51. Maps of observed precipitation accumulation (mm) over the simulation period for the 17 January 2016 case from SNOTEL sites, with minimum accumulation in (a) and maximum accumulation in (b), compared to model-simulated precipitation accumulation at the SNOTEL sites (c) and the complete simulation of precipitation across the domain (d).**

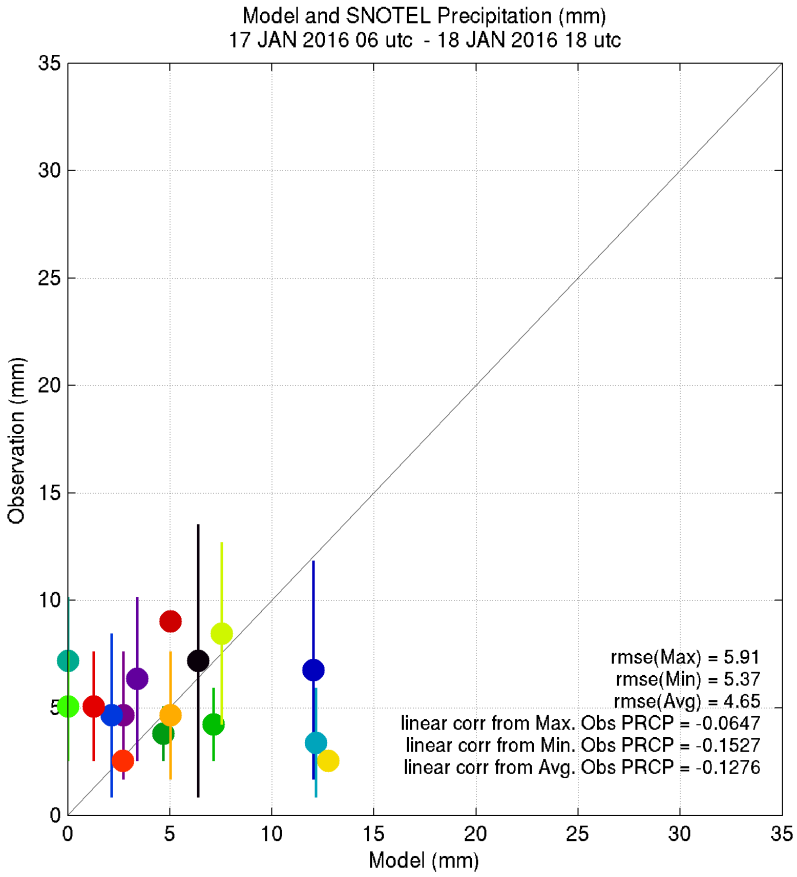


**Figure 6.52. Scatterplot comparing observed precipitation accumulation at SNOTEL sites versus the modeled precipitation accumulation at the same sites for 17 January 2016. Dots represent the average of the maximum and minimum possible precipitation accumulation at each SNOTEL site during the simulation period. Vertical bars represent the range of possible observation (i.e., minimum to maximum observation amount). Each point (color coded) represents single SNOTEL site.**

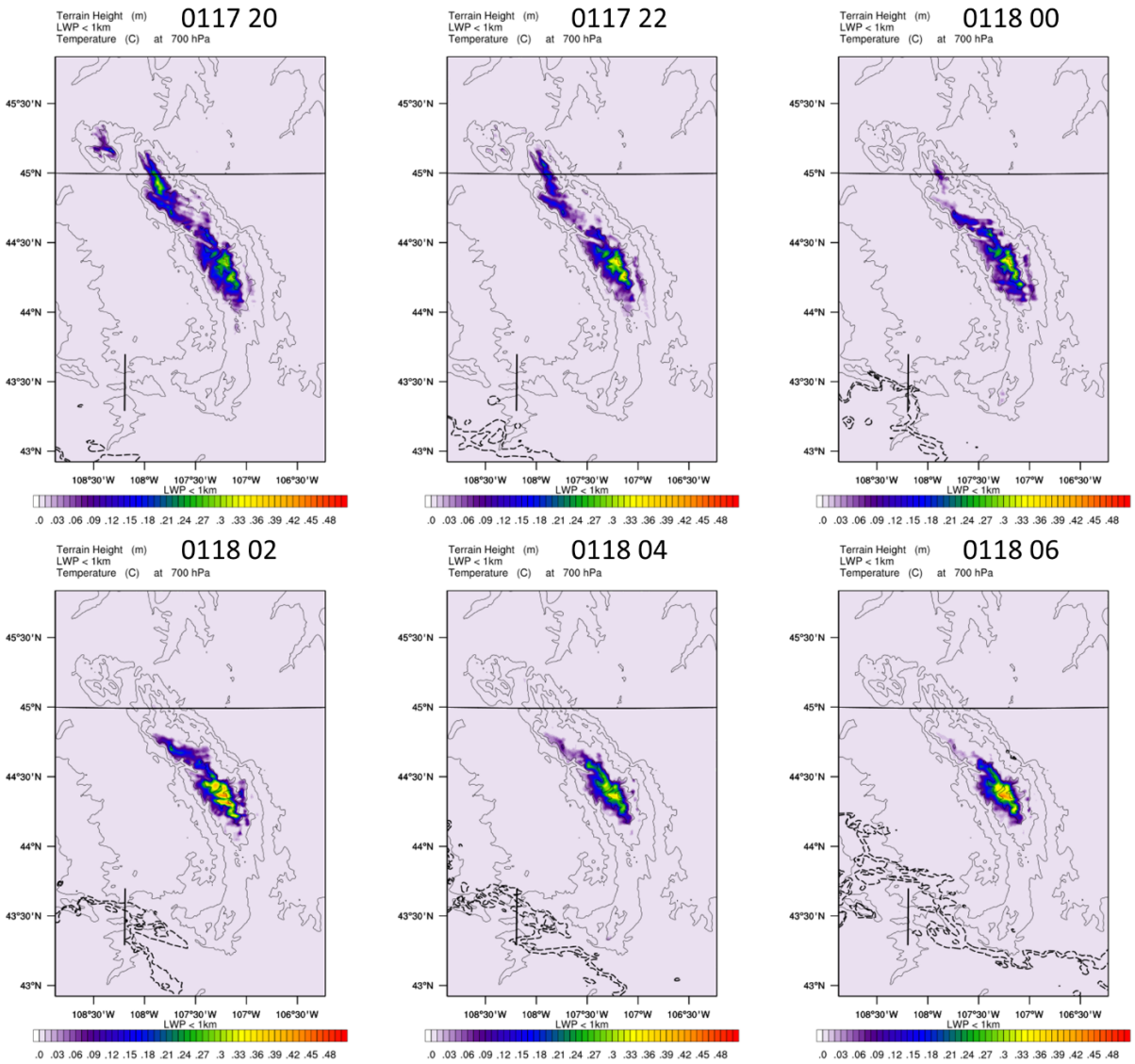


**Figure 6.53. Plan views of LWP below 1 km AGL (mm) from 2000 UTC 17 January 2016 to 0600 UTC 18 January 2016 every 2 hours. Black contour indicates the -6 °C isotherm at 700 hPa.**

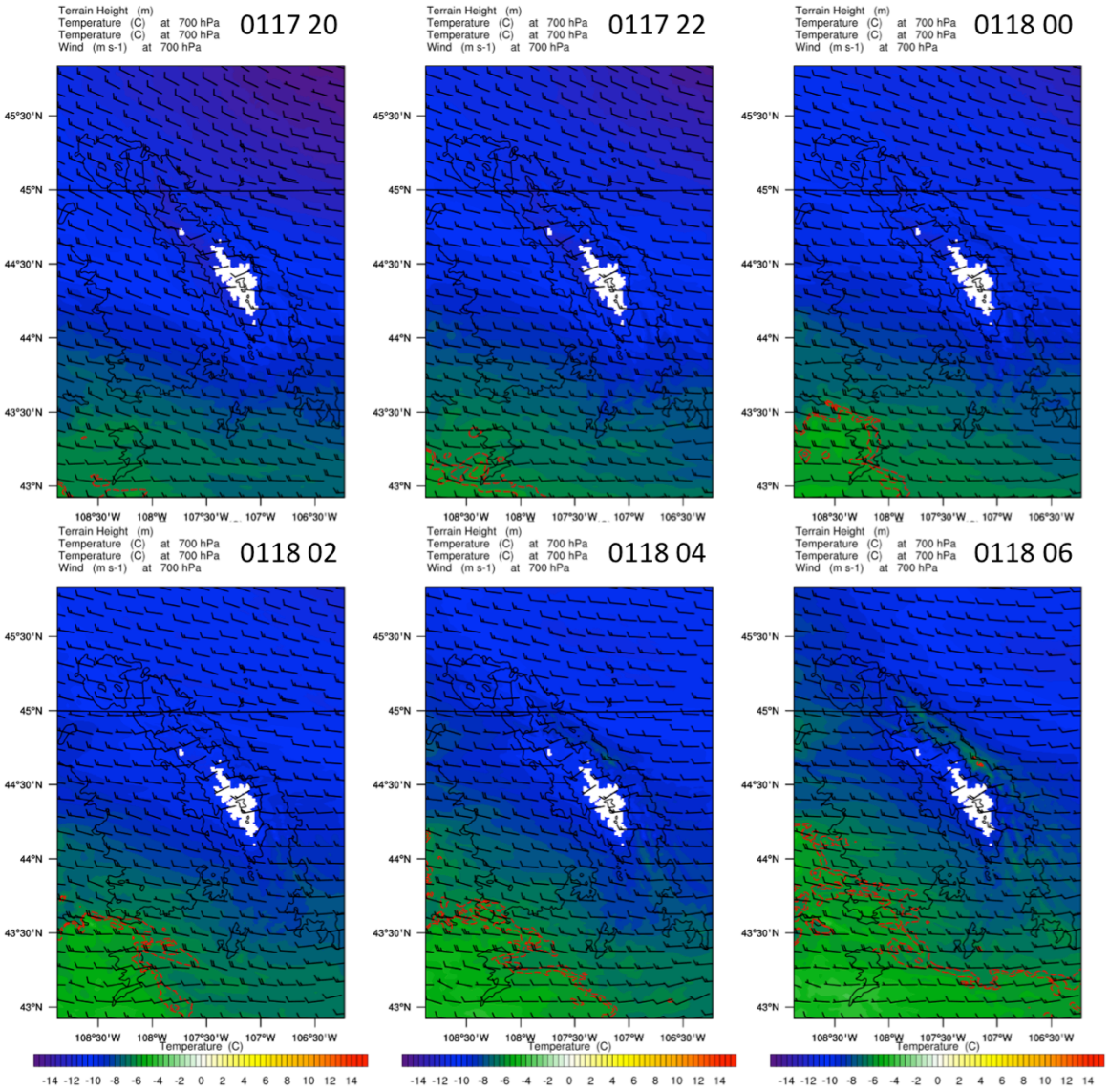


**Figure 6.54. 700-hPa temperature (color shaded) and wind barbs at the same times as Figure 6.53 for the 17 January 2016 case. Red line indicates the -6 °C isotherm.**

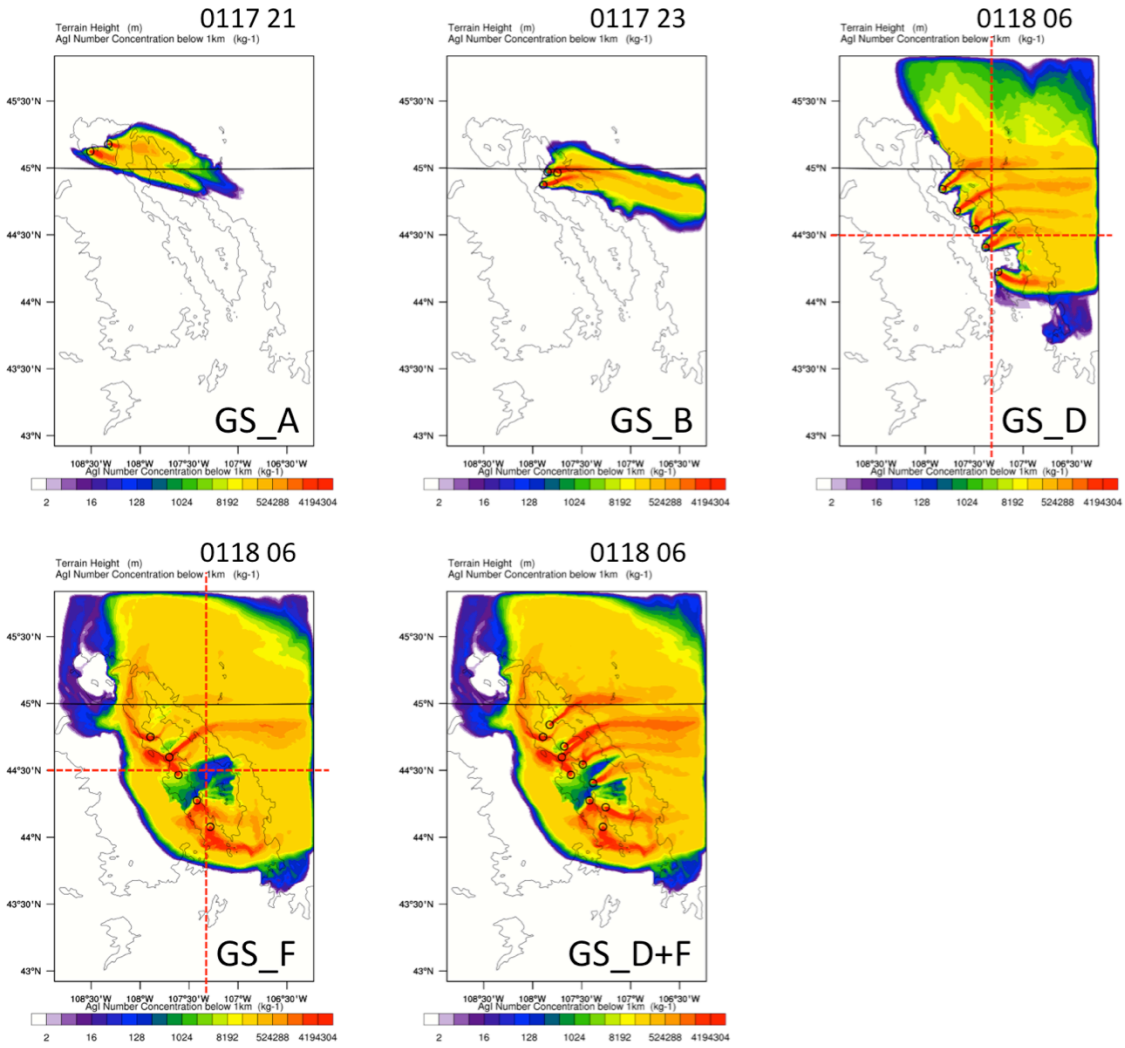


**Figure 6.55. Average simulated AgI concentration below 1 km AGL at the end of the seeding period of each ground seeding case on 17 January 2016. Red dashed lines indicate the cross section locations.**

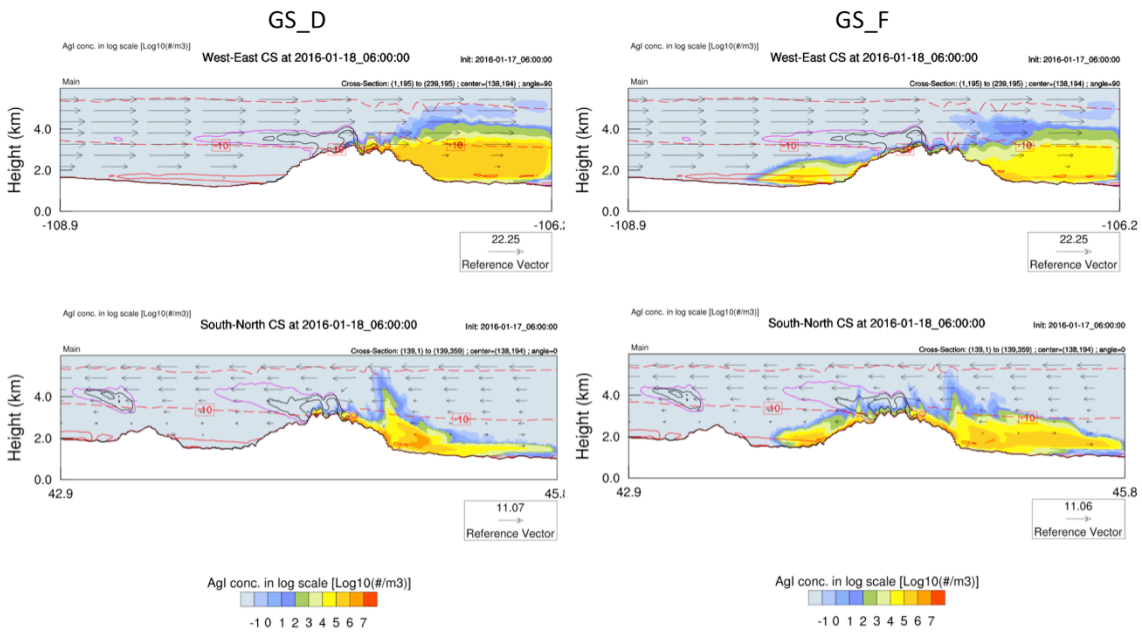


**Figure 6.56. West-east (top) and south-north (bottom) cross sections at 0600 UTC for the GS_D (left) and GS_F (right) experiments.for the 17 January 2016 case.**

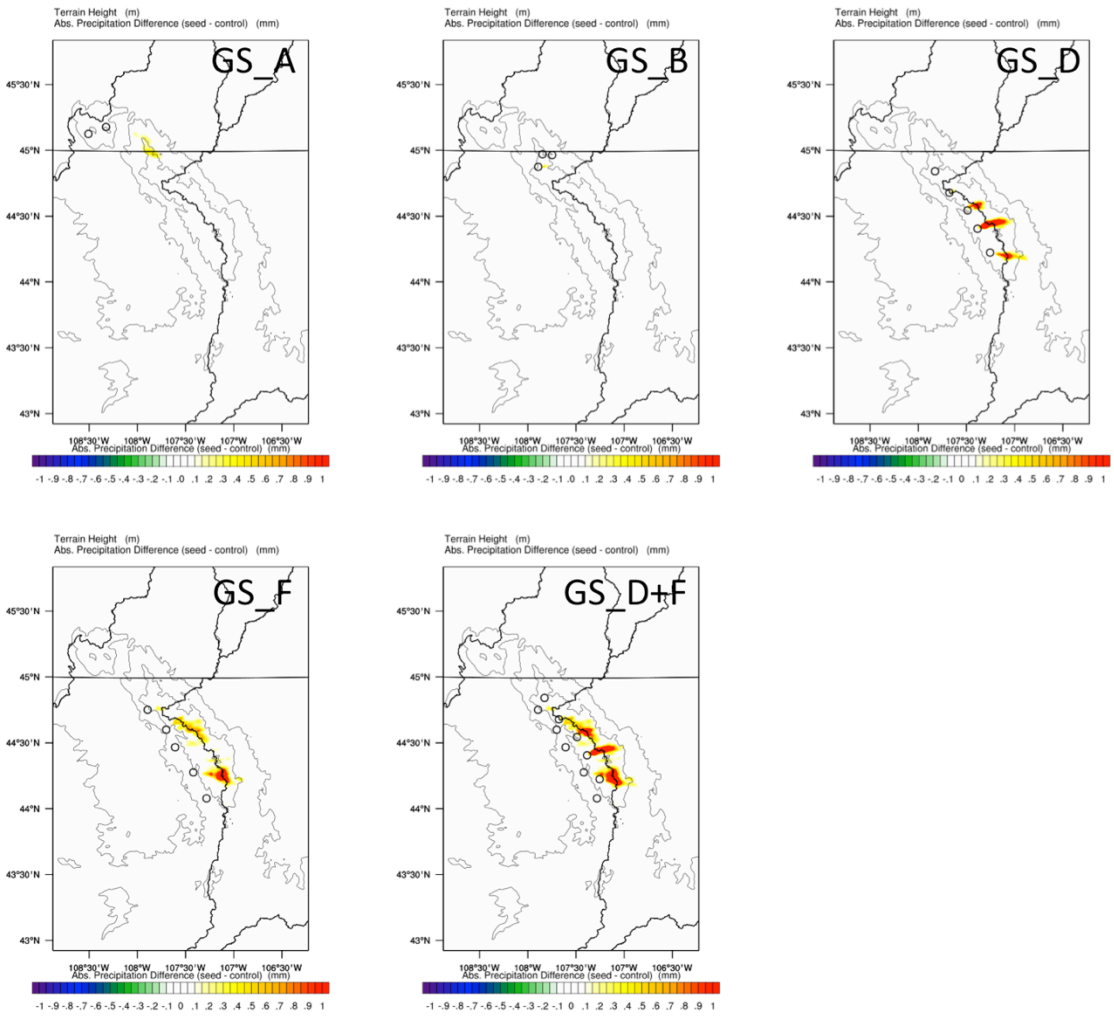


**Figure 6.57. The simulated seeding effect (mm) for all ground seeding experiments for the 17 January 2016 case.**

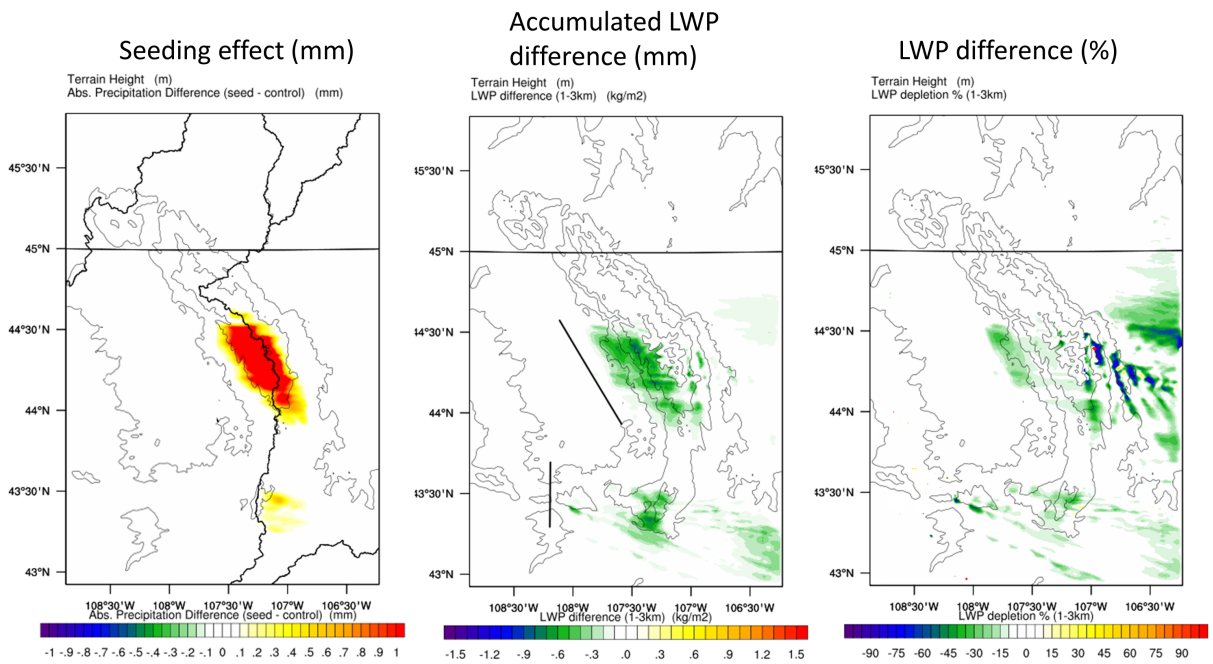


**Figure 6.58. The simulated seeding effect (mm) at the end of the simulation, average LWP difference (mm), and the relative LWP difference (%) for the AS experiment in the 17 January 2016 case. The straight black horizontal line is the Wyoming-Montana state border. The thin black curves are the underlying terrain contours. The thick black curves in the left panel are the basin divides. The AS_C and AS_S flight tracks are overlaid in the center panel.**

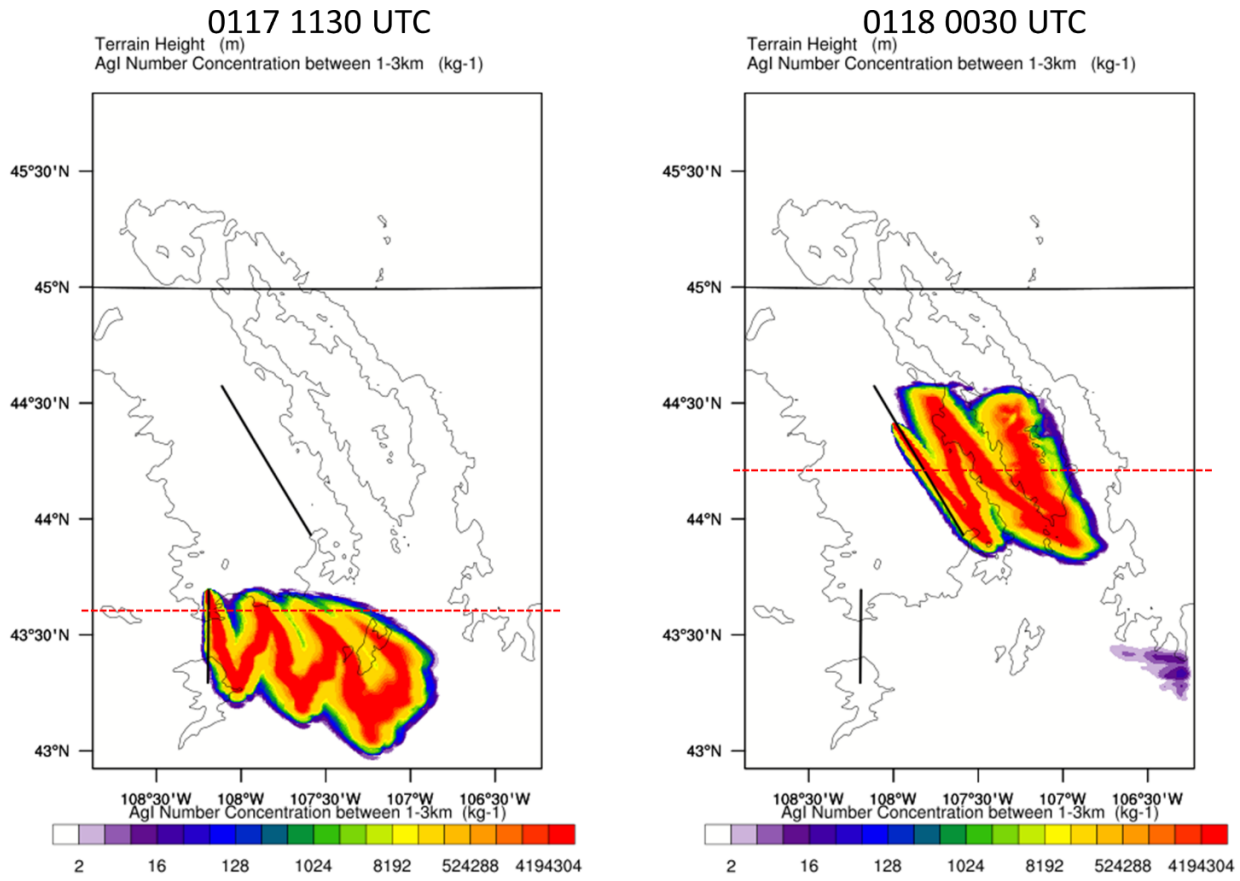


**Figure 6.59. Average AgI concentration between 1 and 3 km MSL at 17 January 1130 and 0118 0030 UTC for the AS experiment.**

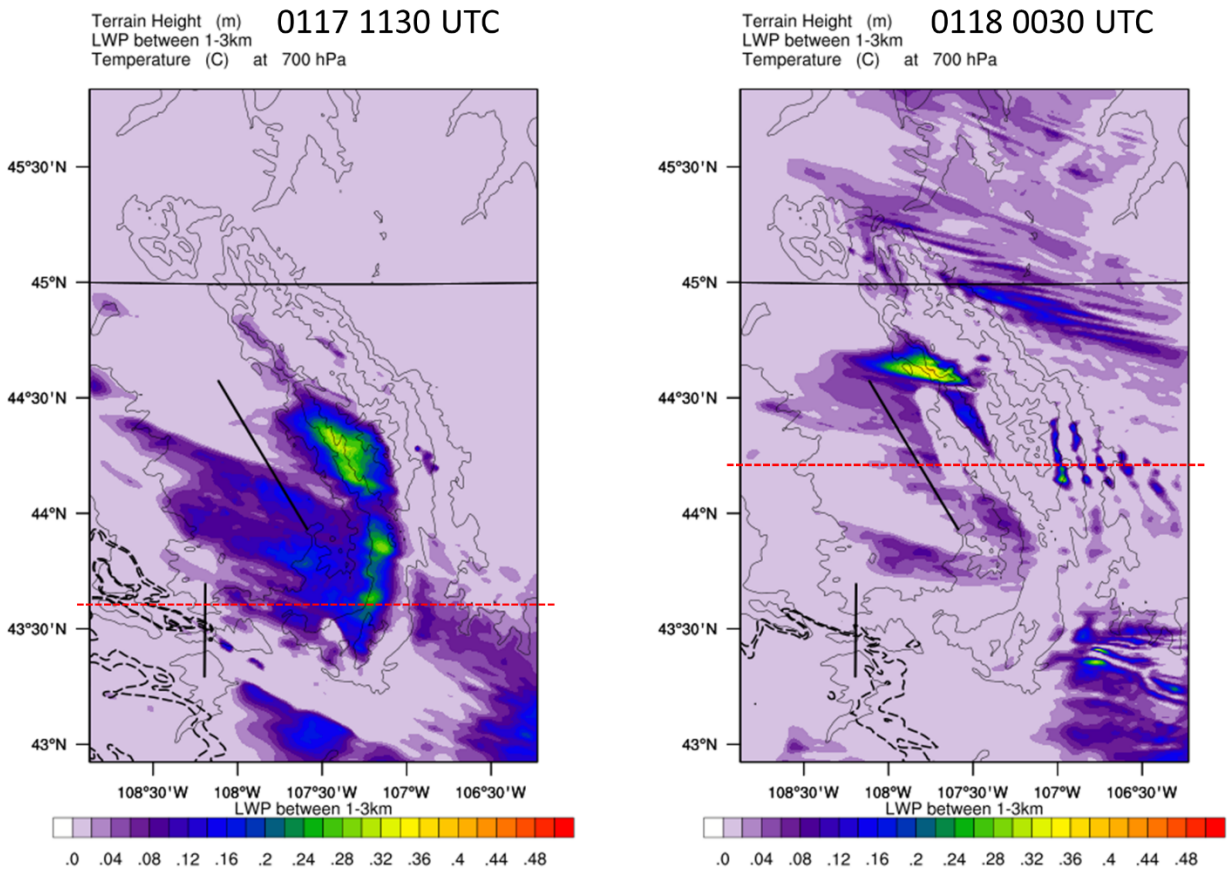


**Figure 6.60. The LWP between 1 and 3 km MSL at 17 January 1130 and 18 January 0030 UTC for the AS experiment.**

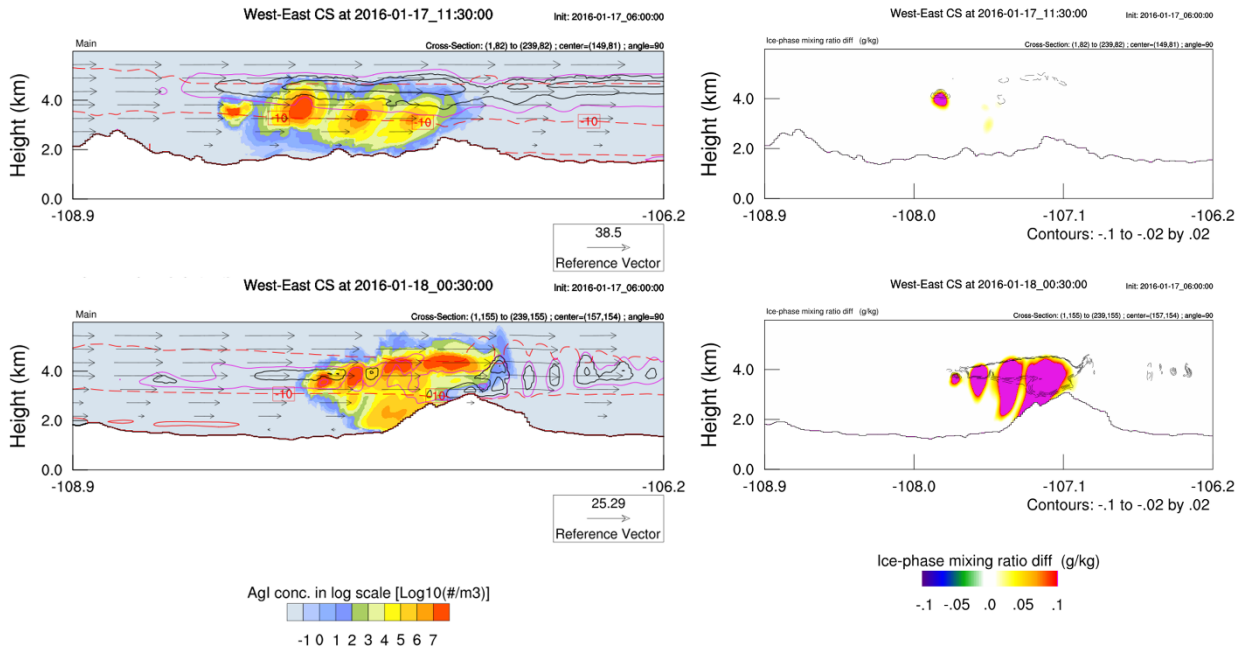


**Figure 6.61. West-east cross sections at 0117 1130 UTC and 0118 0030 UTC for the AS case. The left panels show the simulated AgI number concentration in logarithmic scale (color shaded), the cloud water mixing ratio in black starting at 0.01 g kg$^{-1}$ with an interval of 0.2 g kg$^{-1}$, the ice saturation ratio of 1.04 in purple, isotherm in every 10 °C and wind vectors. The right panels show the cloud water mixing ratio difference in black (g kg$^{-1}$) and ice-phase mixing ratio difference in color (g kg$^{-1}$).**

**Table 6.15. Control precipitation and simulated seeding effects for each seeding simulation (acre-feet on top and % effect on bottom for each experiment row) over the full model domain and in the two primary watersheds (entirely, BH and PT, and just above 8,000 ft in those watersheds, BH mtns and PT mtns) for each of the seeding experiments. The experiment with the best simulated seeding effects is shaded. Relative simulated seeding effects within the target regions (BH mtns and PT mtns) > 1% are listed in bold. Results shown for the 17 January 2016 case.**

| | Domain | BH | PT | BH mtns | PT mtns |
|---|---|---|---|---|---|
| CTRL (af) | 101038 | 68967 | 32072 | 14351 | 9973 |
| GS_A | 57 | 60 | -3 | 28 | 0 |
| | 0.06 | 0.09 | -0.01 | 0.19 | 0.00 |
| GS_B | 24 | 5 | 18 | 5 | 0 |
| | 0.02 | 0.01 | 0.06 | 0.03 | 0.00 |
| GS_D | 327 | 122 | 205 | 122 | 195 |
| | 0.32 | 0.18 | 0.64 | 0.85 | **1.95** |
| GS_F | 370 | 178 | 192 | 178 | 190 |
| | 0.37 | 0.26 | 0.60 | **1.24** | **1.90** |
| GS_DF | 651 | 290 | 360 | 291 | 351 |
| | 0.64 | 0.42 | 1.12 | **2.03** | **3.52** |
| AS_CS_S | 2089 | 1215 | 874 | 1100 | 638 |
| | 2.07 | 1.76 | 2.73 | **7.67** | **6.40** |

**Table 6.16. Simulated seeding areas of impact for the 17 January 2016 case. The simulated positive seeding areal impacts are listed as area in km² (rows labeled A_SE) and the portion of the seeding impacted area relative to the total area in percentage (rows labeled P_SE). The CTRL precipitation impacted area is calculated based on grid points with accumulated precipitation greater than 0.01 mm (in km², "A", and in percent of total area, "P"). The total area (A_total) within each domain is listed in the first row (km²). For experiments and target areas (either BH mtns or PT mtns) with simulated seeding impacts > 1% (shown in Table 6.15), the P_SE values have been listed in bold.**

| | | Domain | BH | PT | BH mtns | PT mtns |
|---|---|---|---|---|---|---|
| Case | A_total | 69984 | 43367 | 26617 | 2206 | 1865 |
| CTRL | A | 41229 | 22700 | 18529 | 2065 | 1677 |
| | P | 58.91 | 52.34 | 69.61 | 93.58 | 89.92 |
| GS_A | A_SE | 1044 | 956 | 88 | 165 | 13 |
| | P_SE | 1.49 | 2.20 | 0.33 | 7.49 | 0.70 |
| GS_B | A_SE | 1037 | 99 | 938 | 50 | 16 |
| | P_SE | 1.48 | 0.23 | 3.52 | 2.28 | 0.87 |
| GS_D | A_SE | 1278 | 317 | 961 | 299 | 692 |
| | P_SE | 1.83 | 0.73 | 3.61 | 13.55 | **37.10** |
| GS_F | A_SE | 2103 | 851 | 1251 | 832 | 1092 |
| | P_SE | 3.00 | 1.96 | 4.70 | **37.70** | **58.56** |
| GS_DF | A_SE | 2488 | 960 | 1528 | 924 | 1200 |
| | P_SE | 3.56 | 2.21 | 5.74 | **41.89** | **64.34** |
| AS_CS_S | A_SE | 5384 | 2063 | 3321 | 1223 | 1366 |
| | P_SE | 7.69 | 4.76 | 12.48 | **55.43** | **73.28** |

## 6.4 Summary of Model Evaluation

Three test cases were simulated to evaluate the impact of six groups of ground generators and several aircraft tracks. In general, ground seeding had very limited spatial impact on the region, resulting in simulated seeding impact areas of 30 – 50% of the target area (area > 8,000 ft). Moreover, Groups A and B rarely impacted the target area. Other meteorological scenarios not tested may have led to better simulated impacts from Groups A and B, but based on these three cases, these sites are not recommended to be included in the preliminary project design.

Group C showed positive simulated seeding effects when the winds had a north-northeasterly component. Groups D and F yielded the best results for ground-based seeding, yet the impact area was still rather small and confined to very narrow plume dispersion. This may be due to strong winds or very unidirectional winds that don't allow the plume to laterally disperse. Group E proved to be a versatile group of generators, since they could impact the southern extent of the Bighorn Mountains under northwest to westerly winds, but could also impact the central (i.e., Cloud Peak) area under southwesterly winds. Nonetheless, of the cases tested, Group E had quite minimal simulated impacts.

Airborne seeding tended to yield the most widespread effects, with simulated seeding impact areas often 50–80% of the target area (> 8,000 ft). Airborne seeding also tended to yield the greatest simulated seeding effects in these cases. However, shorter seeding flight tracks are recommended because they produce a more highly concentrated AgI plume. The benefit of airborne seeding is that it can be placed wherever the best SLW is located. This can include situations where elevated SLW extends quite far upwind (to the west) of the mountains, as occurred in some of these cases. In fact, airborne seeding is the only way to impact elevated SLW layers over the Bighorn River Basin because the air is too stable in this valley to use ground generators to reach those higher altitudes. Yet, it should be noted that not all of the simulated seeding effects from seeding further upwind impact the higher elevations of the Bighorn Mountains; rather they broadly impact the Bighorn Basin in general. Based on the modeled climatology, easterly upslope events include SLW, but occur infrequently. Therefore, due to the lower frequency of occurrence, siting ground generators on the eastern slope of the Bighorns is not advised, but it should be noted that airborne seeding is versatile enough that it can also be used to target easterly upslope events.

# 7. Task 6: Field Surveys: Proposed Ground Generator Locations

Field surveys were conducted within the project area to inspect proposed ground generator locations as determined from the modeling and design exercises presented in Sections 5 and 6. This section describes the selection of the potential sites, and the results of the actual field survey locations that were accessible during the study. Twenty potential generator locations were evaluated during the modeling design process (Section 7.1.1), 17 of these sites were visited during the field surveys (Section 7.1.2), at which time six alternate sites were also identified. As a result of the field surveys and modeling analysis, a total of 21 viable sites were considered for locating ground-based generators are presented in Figure 7.1. It should be noted that one potential generator location was used in two separate Groups (C and D).

## 7.1 Selection of Ground-based Generator Locations

As part of the preliminary program design process, ground-based generator locations were identified via topographic maps and on-line tools (e.g., Google Earth) to identify potential locations thought best suited for increasing snowpack in the target area. Generator spacing, ease of installation and maintenance, land ownership, access, elevation, and exposure were all considered.

Twenty potential remotely-operated generator sites on federal and private lands were evaluated in the design process:

1) US Forest Service (USFS) lands (14 sites);
2) Bureau of Land Management (BLM) lands (4 sites); and
3) private lands (2 sites).

The generator locations initially selected for consideration are shown in Figure 7.1.

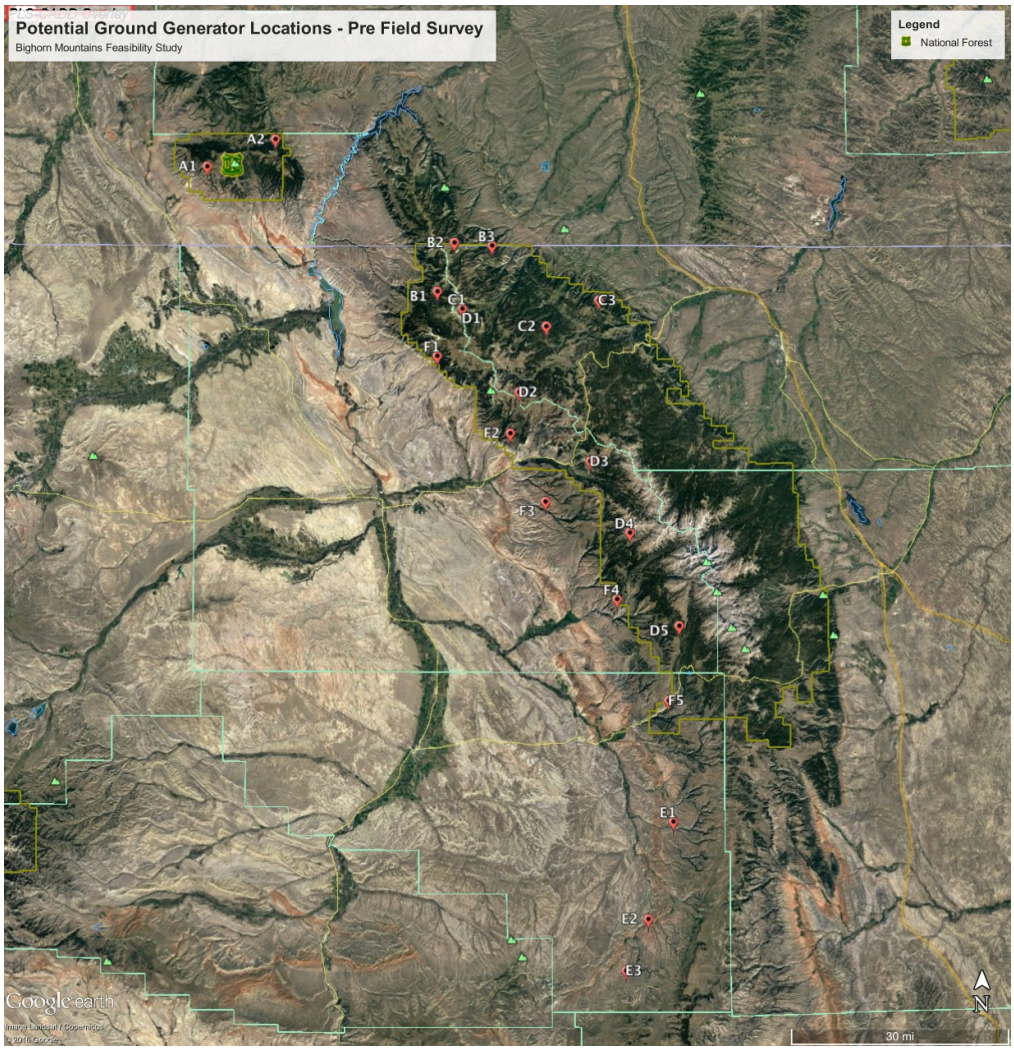


**Figure 7.1. Satellite-generated image of the project area with potential generator locations. These locations were selected prior to the field surveys.**

### *7.1.1 Remote Generator Locations – Pre-Field Survey*

HEC and WMI assessed the initial ground generator locations proposed in Section 5 for both access and ownership, prior to conducting actual site visits. The 20 generator locations selected for the study were organized into six generator "groupings." Group A (Generators A1 and A2) represents the northernmost group, and is located in Montana. Group B (B1, B2, and B3) is slightly south of Group A, and is located in Wyoming. Group C (C1, C2, and C3) is also located in the northern portion of the Bighorns, but further south of Group B. Group D (D1, D2, D3, D4, and D5) is aligned from north to south, west of, but closest to the Divide. Note that site C1 and D1 are at the same location, but were tested in different groups as part of the design process. Group E (E1, E2, and E3) represents the southernmost group, and is located on the west side of the Divide. Group F (F1, F2, F3, F4,

and F5) is aligned from north to south, to the west of Group D. Following are the site location details:

1. Group A
   A1: This site is located on the Custer National Forest off of Miller Road.
   A2: This site is located on the Custer National Forest near Pryor Mountain Road.
2. Group B
   B1: This site is located on the Bighorn National Forest off of National Forest Primary Route (FS) 14.
   B2: This site is located on the Bighorn National Forest near an unnamed two-track approximately 1.2 miles off of FS 11.
   B3: This site is located on the Bighorn National Forest off of FS 111.
3. Group C
   C1: This site is located on the Bighorn National Forest off of FS 11. It is the same location as generator D1.
   C2: This site is located on the Bighorn National Forest off of National Forest Primitive Route (FR) 179, which is accessed via FS 15.
   C3: This site is located on the Bighorn National Forest off of National Forest Secondary Route (FR) 168, which is accessed via FS 15.
4. Group D
   D1: This site is located on the Bighorn National Forest off of FS 11. It is the same location as generator C1.
   D2: This site is located on the Bighorn National Forest 0.15 miles off of FS 10.
   D3: This site is located on the Bighorn National Forest off of National Forest Primitive Route (FR) 277, which is accessed via FS 17.
   D4: This site is located on the Bighorn National Forest near National Forest Trail (FT) 025 which leads to nearby Cloud Peak Wilderness Area. The site would be accessed via FS 17.
   D5: This site is located on the Bighorn National Forest off of National Forest Primitive Route (FR) 411.
5. Group E
   E1: This site is located on private land off of BLM Road 1418 and is accessed via Spring Creek Road (Washakie County Road 58).
   E2: This site is located on BLM land off of Upper Norwood Road (Washakie County Road 82). There are private and state lands nearby.
   E3: This site is located on private land off of Cherry Creek Road (Washakie County Road 80). There does not appear to be existing road access.
6. Group F
   F1: This site is located on BLM land off of a primitive two-track road; it is accessed via BLM Road 1126. There is small private inholding nearby.
   F2: This site is located on the Bighorn National Forest off of National Forest Primitive Route (FR) 207.
   F3: This site is located on BLM land off of a very primitive two-track road (BLM 1114); it is accessed via Trapper Creek Road (Bighorn County Road 270).
   F4: This site is located on BLM land off of a very primitive two-track road accessed via National Forest Primitive Route (FR) 352.

F5: This site is located on the Bighorn National Forest off of an unnamed two-track that is accessed via National Forest Trail (FT) 412.

### *7.1.2 Generator Locations - Post-Field Survey*

A field survey of the generator locations was conducted from 13 June to 17 June 2016 to assess access restrictions (both for installation and maintenance during operations), exposure to winds that would loft the seeding plume into clouds upwind of and over the target, and permitting constraints.

The Group A (A1 and A2) sites were not visited in the field because modeling results indicated they were not effective sites for enhancing snowpack in the target area (Section 6). Even though Group B sites did not appear to be the most effective sites based on modeling results, sites B1 and B3 were visited in the field because they were easily accessible, however site B2 was not visited. All the remaining proposed generator Groups (C-F) were visited in the field, resulting in a total of 17 of the original 20 sites visited. During the field survey, many of the original sites were moved short distances to more suitable locations. Six alternate sites were added, in most cases because the original sites were not accessible or the alternate sites were determined to be better suited for operational deployment. Three of the alternate sites were also visited during the field survey, bringing the total number of actual generator site visits to 20.

Based on the modeling results, both Group A and Group B sites were eventually ruled out as proposed generator locations. The remaining Groups C through F combined with the six alternate sites resulted in a total of 21 viable site options for the preliminary project design (Figure 7.2). Of the final 21 site locations, 12 generators would be sited on USFS lands, five generators on BLM lands, three generators on private lands, and one generator on State lands (Figure 7.3). Proposed locations, land ownership, access ratings, and brief descriptions of the sites are included in Table 7.1. Appendix A provides photographs of the proposed sites.

**Table 7.1. Proposed Generator Locations Post-Field Survey**

| Initial ID | Ggen Name | Latitude | Longitude | T,R,S, ¼ ¼ | Elevation (feet) | Ownership | Access Rating | Notes |
|---|---|---|---|---|---|---|---|---|
| Group C | | | | | | | | |
| C1 | Cliffhanger | 44.849726 | -107.839043 | T56N R91W Sec 08 NWNW | 9377 | USFS | Class 1 | New location (moved about 500 feet upslope because original site is located underneath a cornice on very steep slope). May need to move another 50 to 100 feet upslope or to the west to avoid larger cornice in winter. Same location as D1. |
| C2 | Shuler Park | 44.815312 | -107.607264 | T56N R89W Sec 20 NESW | 8560 | USFS | Class 1 | Site is about 500 feet away from dispersed camping sites. Highly visible. |
| C3 | Freeze-out Point | 44.866921 | -107.456815 | T57N R88W Sec 35 SWSW | 8039 | USFS | Class 1 | New location (moved 0.25 miles up slope or east to get away from turnout area). Very exposed and highly visible. This area is likely subject to heavy snowmobile traffic. |
| Group D | | | | | | | | |
| D1 | Cliffhanger | 44.849726 | -107.839043 | T56N R91W Sec 08 NWNW | 9377 | USFS | Class 1 | Same site as C1. |
| D2 | Continental Divide | 44.687427 | -107.682576 | T54N R90W Sec 04 SENE | 9550 | USFS | Class 1 as sited; Class 1 closer to road | Original D2 is 0.15 miles off FS 10 without existing access. Site has good exposure and is hidden from road. Could move closer to road to reduce length of access but would be more visible FS 10. |
| D3 | Shell Creek | 44.552332 | -107.488000 | T53N R88W Sec 20 NESW | 8137 | USFS | Class 2 | New location is about 300 feet southwest to get farther from FR 277. Last 0.6 miles is rough going on primitive trail. Near Shell Ranger Station. |
| D4 | Moose Meadow | 44.414126 | -107.383099 | T51N R87W Sec 06 SWSW | 9257 | USFS | Class 2 | New location is about 130 feet to the west to make less visible from FS 17. |

| | | | | | | | | |
|---|---|---|---|---|---|---|---|---|
| D5 | Bald Ridge | 44.232718 | -107.249779 | T49N R86W Sec 07 SENE | 9235 | USFS | Class 1 | Site is easily accessible during summer. Winter maintenance would be a long snow mobile trip. |
| Group E | | | | | | | | |
| E1 | Holland Ranch | 43.849809 | -107.266626 | T45N R87W Sec 24 NWSW | 5690 | Private | Class 1 | Could Not Access - Posted. Site is 0.9 miles SE of the gate at private property on BLM Road 1418. Could move to BLM at property boundary if access is not granted (site E1A). |
| E1A | Holland Ranch Alternate | 43.854779 | -107.284120 | T45N R87W Sec 23 SWNW | 5406 | BLM | Class 1 | Site is easily accessible. |
| E2 | Cherry Creek | 43.659088 | -107.335531 | T43N R87W Sec 30 SESE | 5150 | BLM | Class 1 | Could not access. Site appears to be accessed from unnamed two-track on BLM which could not be located. Suggest moving to alternate site E2A. |
| E2A | Cherry Creek Alternate | 43.658650 | -107.330055 | T43N R87W Sec 29 SWSW | 5207 | State | Class 1 | Site is east of CR 82 on State land. Access is good but could be visible from the busy road. |
| E3 | Split Rock Creek | 43.558008 | -107.396438 | T42N R88W Sec 34 SWSE | 6635 | Private | Class 2 | Could not be accessed. Site is on top of the hill with no apparent existing access. Holland Ranch signs posted in area. Lewis Holland may be landowner. No alternate sites could be identified. |
| Group F | | | | | | | | |
| F1 | Pete's Hole | 44.758108 | -107.907504 | T55N R92W Sec 10 NWSE | 6735 | BLM | Class 1 | New location is 400 feet west to gain flatter ground. |
| F2 | Sunlight Mesa | 44.608217 | -107.705970 | T54N R90W Sec 32 SWSE | 7900 | USFS | Class 3 | New location is 100 feet east of original location. It was noted that wind was reduced significantly by large trees at the originally-proposed site. |
| F2A | Sunlight Mesa Alternate | 44.608451 | -107.696569 | T54N R90W Sec 33 SWSW | 8130 | USFS | Class 3 | New location is 0.48 miles east of F2. Site is more exposed and higher elevation. |

| | | | | | | | | |
|---|---|---|---|---|---|---|---|---|
| F3 | Bush Butte | 44.475178 | -107.610711 | T52N R90W Sec 13 NESW | 7041 | BLM | Class 5 | Site is located on BLM adjacent to private inholding - could be sited on either. |
| F3A | Bush Butte Alternate | 44.474230 | -107.610021 | T52N R90W Sec 13 SWSE | 7040 | Private | Class 5 | Alternate site is located 250 feet southeast on private inholding. Propane would have to be 100lbs. |
| F4 | Paint Rock Creek | 44.289827 | -107.413130 | T50N R88W Sec 23 NWSE | 7923 | BLM | Class 4 | New location is 0.4 miles northeast because road ended. |
| F5 | N/A | 44.086975 | -107.278367 | T48N R87W Sec 35 SWNE | 7395 | USFS | No access | Could Not Access - closed to motor vehicles 3.6 miles northeast of original site. F5A and F5B were identified as alternate sites. |
| F5A | High Park | 44.138019 | -107.197350 | T48N R86W Sec 9 SWSE | 9134 | USFS | Class 2 | Potential alternate. FR 429 good access but possible overland travel to access top of knob. 5.38 miles NE of F5. Good site, but scaffold would have to be carried piece-by-piece up a hill unless off-road driving is allowed. |
| F5B | Sarah's Folly | 44.076439 | -107.251697 | T47N R87W Sec 1 NENE | 7686 | USFS | Class 5 | Potential alternate. FR 436. Very rough access and slow. Propane would have to be delivered in 100-pound bottles. Several private inholdings very close by. A really good site, but difficult to access. May be easier over snow. |

[1] Township, Range, Section, quarter quarter

[2] Class 1 – access for installation/maintenance easy, propane truck accessible;
Class 2 – access for installation/maintenance relatively easy, may be short lengths of more difficult terrain or short distance with no existing access.
Class 3 – access for installation is more difficult; long distance and short sections rough roads; slow moving; winter access may be long distance
Class 4 - access for installation is more difficult; long distance and mostly rough roads; some tight turns; winter access may be long distance
Class 5 – extremely difficult; very rough and slow roads, more tight turns, steep slopes; winter access is a long snow mobile trip.

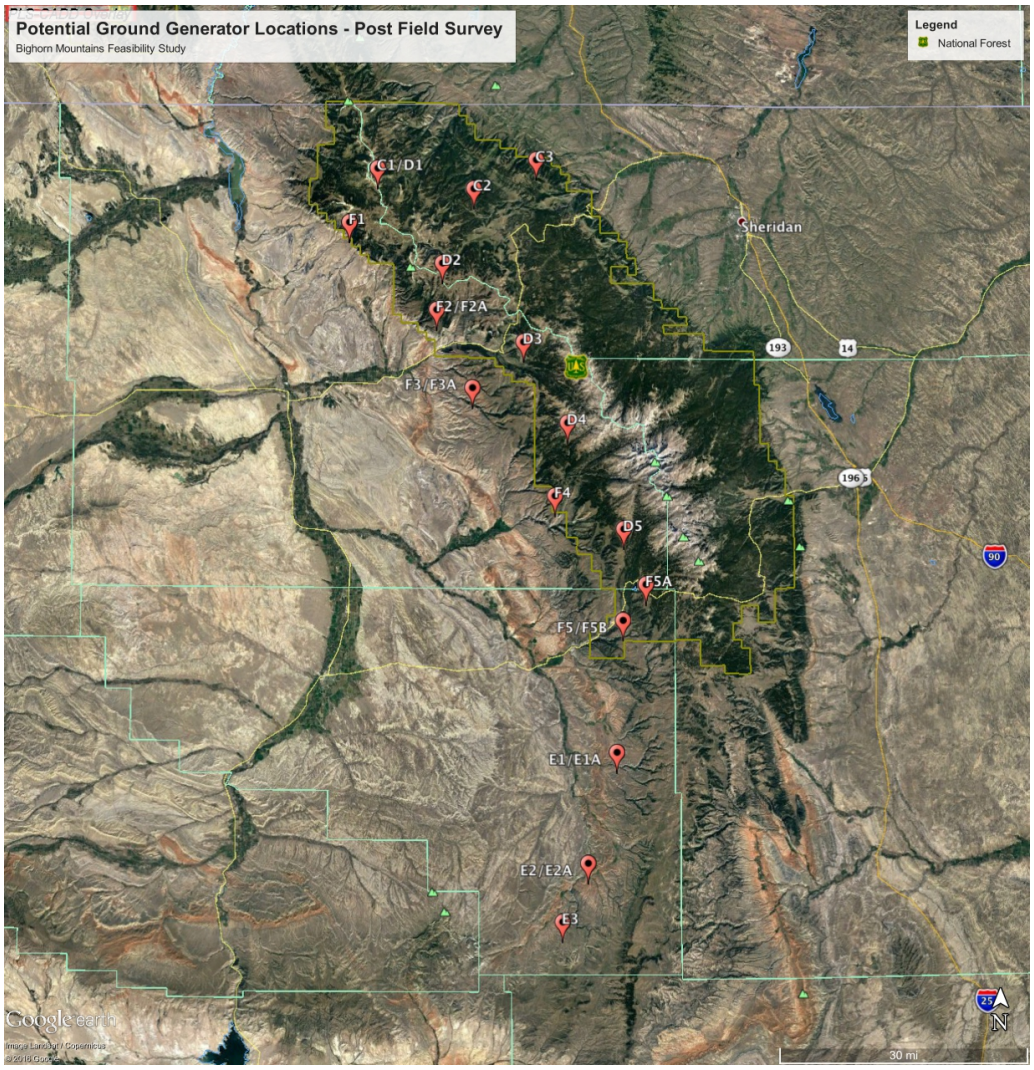


**Figure 7.2. Satellite-generated image of the project area with potential generator locations and alternate sites based on field surveys.**

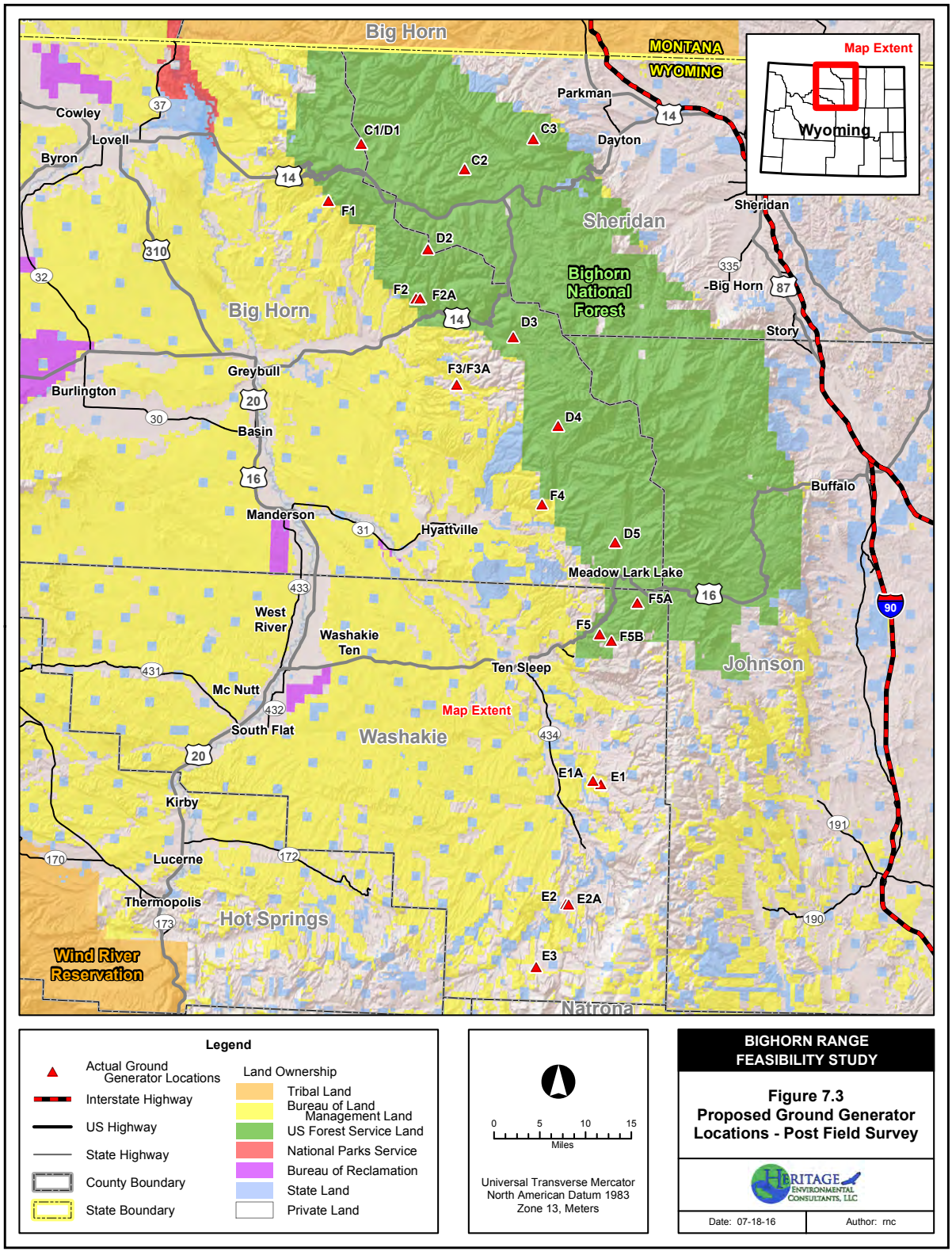


**Figure 7.3. Land ownership map indicating proposed generator sites.**

# 8. Task 7: Access/Easements & Environmental Permitting/Reporting

Effective targeting of clouds with seeding material is probably the most critical aspect affecting the outcome of cloud-seeding programs. For the Bighorn Mountains Feasibility Study, understanding the climatology of winds during seedable conditions (Section 4), aided by numerical modeling of trajectories, is necessary in determining the general placement of cloud seeding generators in order to reach the desired target area. Once the generator sites have been determined, logistical issues, such as site access and land ownership, become important. Accessibility of a potential generator site is necessary during both the summer (installation and pre-seaon preparatory work) and winter (operations and maintenance) months. One limiting factor for a site is sufficient access to deliver a large propane tank, and to be able to fill propane tanks during the summer. If this is not feasible, smaller tanks may be used, but this requires more deliveries to the site, sometimes during the winter months. The site must also be accessible during the winter months when access to remote sites requires a tracked vehicle or a snow machine.

Land ownership dictates the types of permissions needed for permit acquisition, site access, and use. Generators located on public lands often require additional permitting and periodic reporting. Section 7 described the selection process of choosing an array of potential ground-based generator sites. The majority of the locations that offered the best seeding opportunities are located primarily on federal lands administered by the USFS and BLM. Portions of State and private lands have been identified as possible generator locations, but are sparsely scattered throughout the area (Figure 7.3). Brief descriptions of the process for locating generators on private and public lands are presented in the following sections.

## 8.1 Private Lands

The first step in siting a generator on private land is to contact the Landowner and ask for permission to do so. If the Landowner is willing to allow a generator to be placed on their property, a lease agreement is made between the property owner and the operating entity, typically in the form of a Memorandum of Understanding (MOU). On some occasions, a fee is negotiated as part of the lease agreement, and can vary depending upon the willingness of the property owner and the desire of the operator to place a generator at that specific location. Private lands near the Bighorn Mountains tend to be located mainly in the valley bottoms that are located too far from the target area, and generally at too low an elevation to effectively deliver seeding agent to the clouds that are suitable for seeding.

Additionally, some counties require a permit for the placement of a cloud seeding generator on private lands. Proposed generators are located within three counties: Washakie County, Big Horn County, and Sheridan County. Washakie and Big Horn Counties do not require permits for ground generators. Sheridan County would consider this an accessory agricultural use, and would not require a permit.

## 8.2 Public Lands

The majority of the proposed generator locations are located on federally-owned lands because the area is dominated by BLM-administered and USFS-administered lands in and near the target area. The most effective generator locations will involve lands under public ownership, whether it be a federal or state entity.

If a location is under federal ownership, such as the USFS or the BLM, a Special Use Permit will be required for placement of the generator. As part of the permitting process, a National Environmental Policy Act (NEPA) review will be required. This process could result in a Categorical Exclusion (Cat Ex), an Environmental Assessment (EA), or an Environmental Impact Statement (EIS), as determined by the federal entity and the final project design. USFS lands include the Bighorn National Forest; BLM lands include those administered by the Casper, Worland, and Cody Field Offices.

Placement of a generator on state or local government lands requires the approval of that entity and a lease agreement. For placement on Wyoming State lands, a Temporary Use Permit is required from the Office of State Lands and Investments. This process involves a survey request prior to conducting any site visits, an application package that includes comments from the current lessee, and payment to the State. For example, each generator site in the Wind River Range costs $100 annually. These permits are valid for five years. Renewals would be required for longer-term operations.

## 8.3 Ownership Summary – Final Configuration of Generator Locations

A final configuration consisting of 21 potential generator locations for seeding operations, was determined by conducting field surveys as described in Section 7, and through an interative modeling exercise outlined in Sections 5 and 6. Of the final 21 site locations, 12 are located on USFS lands, five are located on BLM lands, three are located on private lands, and one is located on State lands.

## 8.4 Weather Modification Program Permitting

There have been no changes to the general permitting and reporting requirements for conducting cloud-seeding programs in the last ten years. There are essentially two entities that require some level of permitting and reporting: the State of Wyoming and the U.S. Department of Commerce, through NOAA.

### *8.4.1 State of Wyoming Permit Requirements*

Wyoming Statutes 9-1-905 to 9-1-907 contain legislative declarations concerning weather modification, the definition of weather modification, and weather modification permit requirements. These regulations are administered by the Wyoming State Engineer's Office (SEO). The permit process through the SEO requires an application outlining weather modification credentials, financial assurance, references, generator locations, target areas,

and proposed procedures. The SEO also requires that a monthly report is submitted during the operational season.

### 8.4.2 Wyoming Game and Fish Department

The Governor of Wyoming issued the Sage Grouse Executive Order in 2008, establishing Core Population Areas for sage grouse across the state to avoid federal listing of the species as threatened or endangered. Many types of development within these Core Population Areas are prohibited or limited. Core Population Areas were established based on habitat, not land ownership; therefore, they affect federal, state, and private lands. There are Core Population Areas located west, south, and east of the Bighorn Mountains.

The Wyoming Game and Fish Department (WGFD) requested to review the locations of all 26 ground-based generators associated with WWMPP, and it is anticipated that they would review the proposed generator locations for the Bighorn Mountains. If any are located in the Core Population Areas, an analysis on potential impacts to the species would need to be conducted and potential mitigation measures may be required.

### 8.4.3 National Oceanic and Atmospheric Administration Reporting

Public Law 92-205 requires that all non-federally sponsored attempts to modify the weather are reported to the Secretary of Commerce. The process involves the submittal of Initial, Interim, and Final reports covering weather modification activities for individual target areas. An initial report is required each year cloud seeding is planned, and at least 10 days prior to the start of the activity.

A final report must be submitted within 45 days after the completion of the weather modification activity. The information required in the interim activity and final reports include:

1) number of weather modification days each month;
2) number of modification days for purposes of increasing rain or snow, reduction of hail, fog or other;
3) hours of apparatus operation (airborne or ground); and
4) type and amount of cloud seeding agent used.

Public Law 92-205 is a reporting requirement, and establishes no regulatory authority, whereas the State of Wyoming permit requirements provide for non-compliance penalties.

# 9. Task 8: Establishment of Operational Criteria

Criteria for operational winter orographic cloud-seeding programs have been developed by the ASCE (ASCE 2004 and 2006), and by the Weather Modification Association (WMA 2014). Since this feasibility study examines the potential for effective glaciogenic seeding using AgI, the operational criteria summarized below will relate to a program using this seeding agent. Other agents for glaciogenic cloud seeding, such as liquid propane, were discussed in Section 3, yet AgI was determined to be the most suitable for the Bighorn Mountains.

## 9.1 Information Sources

Among the most critical data for establishing seeding thresholds are upper air temperatures and winds, and the existence of SLW relative to the project target area. The more accurate this information, the better the seeding decisions will be. Toward this objective, two instruments can play vital roles: soundings and a radiometer. In addition to these, or in the event these instruments are not available, high-resolution tailored forecast models can also provide valuable guidance for making seeding decisions.

### *9.1.1 Soundings*

On-demand project soundings would provide real-time temperature and wind profiles, and allow the use of Froude number (i.e., the stability index allowing prediction of whether environmental winds will flow up and over the mountains or around them, see Section 4.1.2). Project rawinsondes provide solid guidance for both wind flow and seeding temperatures. Though soundings are routinely made by the NWS Office in Riverton, WY, to the southwest of the target area, these are done at 0000 and 1200 UTC, and are too far removed to consistently reflect conditions in the Bighorn Mountains.

### *9.1.2 Radiometer*

A microwave radiometer sited with an unobstructed view of the Bighorn Mountains would provide real-time cloud LWC measurements over the range, critical for successful seeding. In the absence of real-time liquid cloud water data, its presence must be inferred by the presence of cloud mass over the range and/or prognostic numerical model output. One such option is the aircraft icing product from the NOAA Aviation Weather Center (AWC), available at https://www.aviationweather.gov/icing/fip.

### *9.1.3 Additional Information*

Additional real-time information useful for evaluating potential seeding conditions includes the following internet sources:

- NOAA and NWS data:
    - surface observations,
    - rawinsonde data,
    - prognostic numerical models, included gridded data,
    - satellite imagery: visible, infrared, and multi-spectral,

    - radar data from sites in Billings, MT, Riverton, WY, including reflectivity and upper-level winds;
- NRCS SNOTEL sites (can provide temperatures near the 700-hPa level), typically with a 1–2 hour latency;
- select real-time webcams near the range (during daylight, for cloud cover);
- University of Utah Mesowest mesonet data displays of surface winds and temperatures.

## 9.2 Ground-based Seeding with Ice Nuclei

When IN are generated, either by the combustion of seeding solution or pyrotechnic, the nuclei remain in the atmosphere until they (a) nucleate ice which grows into precipitation, or (b) they are scavenged by precipitation. With time, other processes may remove them more slowly. Once created, the IN plume can travel considerable distances downwind before becoming so dilute that it is no longer detectable. If ground-based IN generators are deployed, an array of remote-controlled IN generators would be used to seed clouds upwind of the targeted portions of the range, when flow regimes (winds) and temperature profiles are suitable. The proposed generator locations are shown in Figure 5.5. Manually operated generators would not be feasible because the proposed sites are all well removed from populated areas. Therefore, all proposed ground-based generators are recommended to be remotely controlled.

In any given seeding event, the generators activated would be determined by the prevailing wind speed and direction. The number of generators used will depend upon the extent of the seedable conditions over the target area. The AgI-based seeding agent would be released at a rate of approximately 25 grams per hour from each active generator.

Seeding would be guided by an on-site meteorologist, aided by weather observations, real-time microwave radiometer observations of cloud liquid water, atmospheric sounding data, and prognostic numerical models.

The recommended seeding criteria for ground-based IN seeding are:

1. The temperature at the 700-hPa pressure level (~10,000 ft MSL) should be less than or equal to −6 °C.
2. The wind direction is such that the proper transport of the IN will occur, from the selected ground-based generators to the target.
3. Liquid water is observed, predicted, or otherwise believed to exist over the range.
4. Atmospheric stability is conducive to allow seeding agent to disperse into the clouds and over the target area. Specifically, no temperature inversion is observed, predicted, or otherwise believed to exist that would trap the seeding agent in the boundary layer and Fr > 0.5. This can be determined from model or actual upper air sounding data.
5. No seeding suspension criteria are met.

The rationale for these criteria is taken largely from those employed by the WWMPP (Breed *et al*. 2014), but since some positive impacts (increases in snowfall) can be attained

at −6 °C, warmer than the WWMPP temperature criterion of −8 °C, the seeding window has been slightly expanded. These activation temperatures are for the IN from a seeding solution tested by DeMott (1997), known to function in the condensation-freezing mechanism. The AgI activation curve is shown in Figure 9.1, along with the analogous curve for the glaciogenic pyrotechnic manufactured by Ice Crystal Engineering (ICE). The pyrotechnic-generated IN are also known to function by the condensation-freezing mechanism (DeMott 1999).

Seeding with remote-controlled ground-based generators can begin whenever suitable conditions exist. Seeding can continue for as long as conditions remain favorable, at least as long as the requisite consumables are available at the generators in use. Since consumables are replenished between storm systems as needed throughout the season, this should not pose any limitations on the duration of any seeding events.

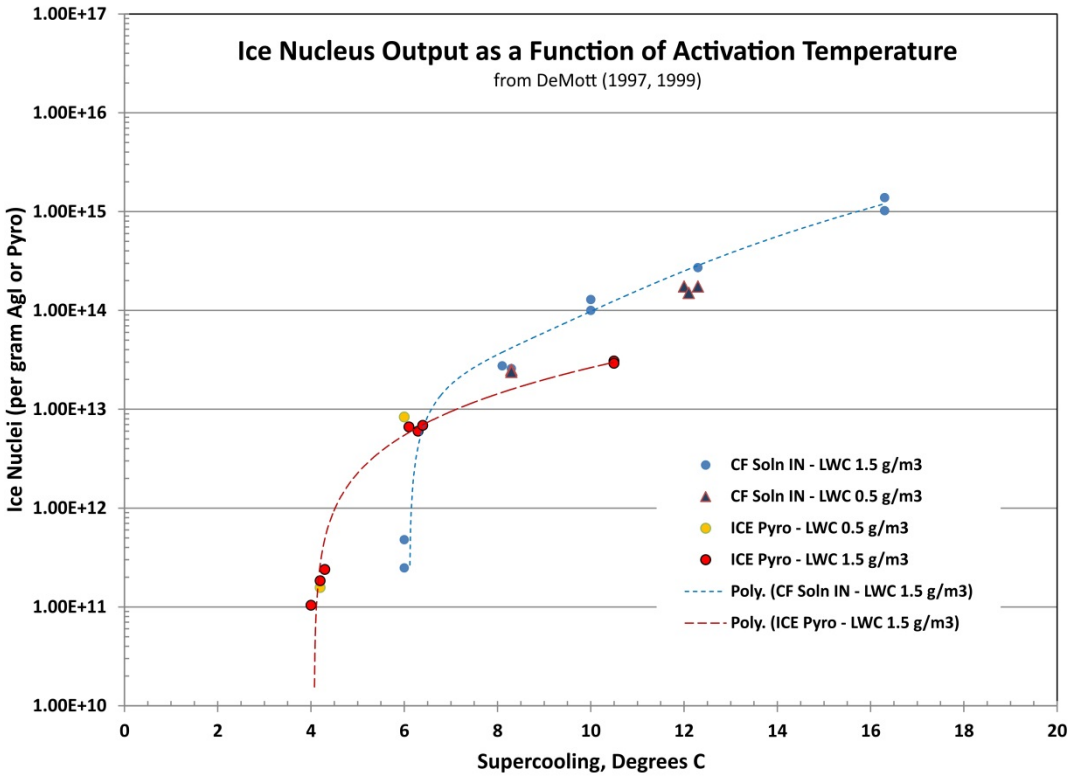


**Figure 9.1. Yield as a function of supercooling for a condensation-freezing nucleus produced by the seeding solution used in the WWMPP (blues), and another condensation-freezing nucleus produced by pyrotechnics manufactured by Ice Crystal Engineering (red, yellow). (Data from DeMott 1997, 1999.)**

## 9.3 Airborne Seeding with Ice Nuclei

Any aircraft deployed for wintertime glaciogenic seeding must be well-maintained and certified for flight in known icing conditions. Such a certification does not mean that flight operations can be conducted indefinitely in icing conditions, but rather that the aircraft has been proven to function safely in transient icing.

The recommended seeding criteria for airborne AgI seeding are:

1. The temperature at the flight altitude should be less than or equal to −6 °C. Given that the aircraft can fly higher[3] in order to target colder clouds, if necessary, the temperature criterion can often more easily be met for airborne seeding than for ground-based seeding.
2. The aircraft can be flown in a manner that allows the winds to transport the resulting ice crystals and precipitation to the target area.
3. The aircraft crew have observed aircraft icing, which verifies the presence of SLW.
4. No seeding suspension criteria are met.

The sequence for seeding via aircraft is as follows:

- fly to the desired seeding area, determined by the altitude, distance, and direction appropriate for the day;
- find the SLW to be targeted;
- climb slightly above the liquid water layer; and
- seed the SLW zone.

Since an aircraft will fly through portions of the orographic clouds not sampled by a radiometer, it is possible, even probable, that SLW may often be encountered by the aircraft when the radiometer sees none. Thus, the presence of SLW as indicated by a radiometer should not be the sole means of confirming its existence. Prognostic numerical model output may also be useful.

Seeding can thus continue as long as:

- the SLW persists, or
- the accumulation of ice on the aircraft makes descent to warmer atmospheric temperatures necessary, or
- all seeding materials on board are expended, or
- fuel is diminished, forcing a return to base.

## 9.4 Seeding Season

For the Wind River Range to the west, ground-based seeding research during the WWMPP ran from 15 November to 30 April of each season (after an early-project change). However, during the WWMPP seasons and also the two ensuing operational seasons, no ground-based seeding opportunities occurred later than 17 April. In the eight seasons of WWMPP and post-WWMPP operations, there were a total of eight ground seeding events during the first weeks of April, and only five more during the second weeks. Only once was there an opportunity to seed during the third week.

[3] There is an upper limit to the seeding altitude. The cloud must be deep enough and the precipitation process initiated early enough that resulting precipitation falls on the target. If the seeding altitude is too high and/or the wind is too strong, the resulting snow may not develop fast enough to precipitation on the barrier.

The scarcity of late-season ground seeding opportunities in the nearby Wind River Range suggests that it may not be cost-effective to prolong the seeding season in the Bighorn Mountains beyond 15 April. The Bighorn Mountains are similar in height and scale to the Wind River Range, and nearly adjacent as well, therefore using the applied Wind River Range cloud-seeding season to define an operational season for the Bighorn Mountains is reasonable.

## 9.5 Suspension Criteria

All seeding programs should have suspension criteria established prior to the commencement of field operations (ASCE Manual 81, as revised, 2014) to ensure personnel safety. Such criteria should identify thresholds at which cloud seeding will be stopped or suspended, and should also outline how any cessation of operations will be communicated to project personnel. Further, all cessations are expected to be documented for the public record.

Operational suspension criteria were established for the Wind River Range Weather Modification Program, conducted in the 2014–2015 and 2015–2016 winter seasons. These criteria were based on those implemented for the WWMPP, but modified to reflect differences between research (i.e., the WWMPP) and operations. The Wind River Range operational program criteria are likewise recommended for an operational program in the Bighorn Mountains. These criteria are expected to govern all decisions on the operations of the generators or seeding aircraft.

Snowfall histories are used to determine the Historic Range of Natural Variability (HRNV) for a given SNOTEL facility. These SWE are then combined and a "median" is established for a period of time, usually 10–20 years of recorded history. This "median" is then used to set the HRNV by the day or month of any recorded year.

Thresholds at which cloud seeding will be suspended for this operation are identified below. These criteria will be implemented to govern all decisions on the operation of the generators.

Thresholds and guidelines defining when cloud-seeding operations in the Bighorn Mountains are recommended to be suspended are listed below:

1. Seeding shall be suspended in any target area if and when range-wide SWE indicated by designated NRCS SNOTEL sites (see Figure 4.1) exceed a percentage of the long-term median defined by a linear upper limit of 85% of the thirty-year (1981–2010) median 1 April SWE for the site on November 15 (normal program start), and increasing to 140% of the median 1 April SWE as of 1 April. If seeding is to continue after 1 April, the upper limit will remain fixed at 140% of the 1 April median value, until season end[4].

[4]The operational excess snowpack seeding suspension criterion now uses medians rather than means, and the 1981-2010 period of record. The upper limit of 140% is used because this corresponds approximately to one standard deviation above the long-term medians, meaning that snowpack at this

2. Reservoir storage for flood control, based upon hydrologic estimates of total snowpack using all available data, is deemed insufficient.
3. There is potential for significant rain-on-snow events at elevations above 8,500 feet MSL. Occasionally, such events have the potential to produce short-term winter season flooding. The area of risk would not be targeted until after the risk had passed.
4. The NWS office responsible for the target area has forecast a severe winter weather event. The area forecast to be affected would not be targeted until the risk had passed.
5. There is an extreme avalanche risk in a specific portion of the target area. The area of risk would not be targeted until the risk had passed.
6. If a significant wildfire occurs within the watersheds of the target area, the Forest Service shall be consulted prior to the next cloud seeding season to determine if there is need for suspension(s) that account(s) for the newly burned areas.
7. Care will be taken to avoid targeting major highways to avoid impact on transportation corridors including U.S. Highway 14 and U.S. Highway 16, both of which transect the range[5].
8. Seeding will be suspended at any time, upon direction from the program sponsor.
9. In the event of a localized situation that affects only a portion of the target area, operational seeding activities will be restricted to non-affected portions of the target area[6].

In the event conditions change and suspension criteria no longer met, seeding operations may be resumed and documented appropriately.

---

level would still be well within the limits of natural variability. It is here noted that the *lowest* SWE suspension threshold currently employed in the western United States is 140%, including programs in Idaho, Utah, Nevada, and California.

[5] Modeling efforts conducted as part of this study suggest that in most circumstances the most additional water likely to be produced by seeding (per storm event) at any one location would be approximately 1 mm (liquid equivalent). This would translate to between 1 to 2 cm (0.4 to 0.8 inches) of additional snow depth. This is likely not enough to affect WYDOT plowing operations. However, to limit such impact, the north-south extent of seeding operations, especially airborne operations, can be readily restricted according to the environmental wind flow during each storm in attempt to avoid impacting these transportation corridors.

[6] An example of such a situation would be a wildfire burn scar that elevates erosion risks during spring runoff (Criterion 6). Conditions defined in Criterion 5 would also trigger this type of localized suspension. In such case(s), seeding activities that may impact the affected area would not be conducted.

# 10. Task 9: Environmental and Legal Considerations

As mentioned in Section 9, well-designed research and operational cloud-seeding programs incorporate seeding suspension criteria to stop or suspend seeding activities that could generate unsafe conditions due to increases in precipitation produced from the cloud seeding. These criteria tend to focus on specific concerns such as suspension of seeding when there is the potential for flash flooding.

There are other environmental concerns, such as downwind (extra-area) effects or potential impacts on water and soil quality, associated with the practice of cloud seeding. This section describes a few of the more common environmental concerns associated with cloud seeding.

## 10.1 Downwind (Extra-area) Effects

Perhaps the most frequently asked question regarding the possible establishment of a cloud-seeding program in an area that has not been involved in previous cloud-seeding programs is whether areas downwind of the intended target area will experience less precipitation during seeded periods. The analysis of precipitation in areas downwind of cloud-seeding programs suggest that the amount of downwind precipitation is not significantly changed.

As described in the WWMPP Draft Executive Summary (WWDC 2014), potential extra-area effects due to cloud seeding were evaluated for the Wind River, Sierra Madre, and Medicine Bow Mountains. Potential extra-area effects from seeding were evaluated using the WRF model coupled with the cloud-seeding parameterization (Xue *et al.* 2013a, b). Given the observational constraints of the WWMPP, no measurements were available to validate the model results beyond the intended seeding target areas, and therefore these results should be interpreted with the caveat that it was solely a numerical modeling exercise. Nonetheless, model validation studies to date show promise for the model's ability to capture the trends and distribution in precipitation, LWP, and thermodynamic structure; however, the validity of the model can vary by case and was not explicitly validated for this study.

During the WWMPP, WRF simulations were set up and conducted to investigate the simulated extra-area seeding effect from seeding the Wind River Range during the month of February 2013.

Figure 9.1 shows the natural precipitation from the non-seeded simulation as well as changes in precipitation due to the simulated seeding. The natural (CTRL) precipitation accumulated mostly on high altitude areas in the non-seeded simulation. The simulated seeding enhanced the precipitation in the Wind River Range, but also generated some positive and negative effects outside of that target area. The extra-area effects were small in area and magnitude and randomly distributed, except for two small areas just west of the Wind River Range, which had a large negative simulated seeding impact. Simulated

seeding enhanced precipitation in the target region by 3%, and an order of magnitude less in the extra-area region. It is also interesting to note that the very distant Sierra Madre/Medicine Bow ranges were also positively impacted by seeding during this seeding simulation. This is likely due to the predominant northwesterly flow transporting AgI southeastward during this simulation.

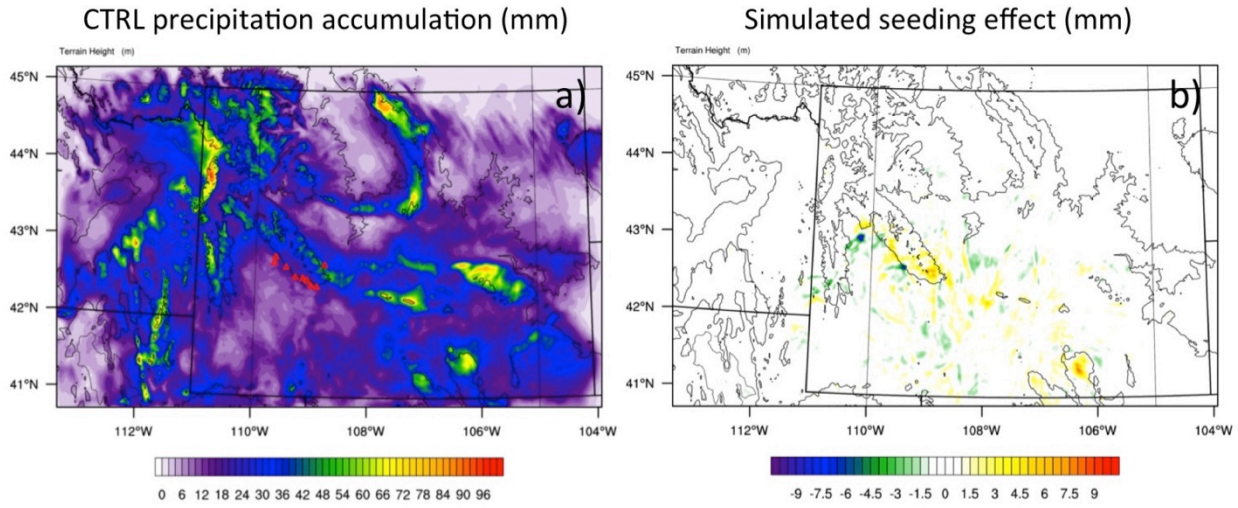


**Figure 9.1 The accumulated precipitation (mm) from CTRL (left), and the simulated seeding effect (difference in precipitation from the seeding simulation minus CTRL; mm) for the WR seeding cases (right).**

In addition to assessing the changes in precipitation, the model output was analyzed for changes in total precipitable water, which is a sum of all model-simulated atmospheric water vapor and hydrometeors (cloud droplets, rain, snow, ice, graupel) in the cloud. This was done to compare the impact of cloud seeding on the total mass of available water in the atmosphere. The maximum model-simulated change in total precipitable water was a reduction of 0.25% on 22 February. The simulated change in total precipitable water varied by seeding case, with some cases having much lower simulated percent changes. For instance, one seeding case had a simulated reduction in total precipitable water of only 0.07%.

The key preliminary result from the WWMPP study is that the net effect of all simulated seeding on precipitation in areas outside of the intended targets (i.e., extra-area effects) was quite small (less than 0.5%), which is consistent with conclusions from previous studies (Long 2001, DeFelice *et al.* 2014).

Long (2001) provides information from a variety of both winter and summer cloud-seeding programs in a review paper on the topic of extra-area effects. One winter research program that is perhaps most relevant to wintertime programs was conducted by Colorado State University scientists in the Climax, Colorado area. This mountainous area is located in the central Colorado Rockies. The randomized seeding program was conducted in two phases that came to be known as Climax I and Climax II. Quoting from Long (2001), "Grant et al. (1974) investigated downwind effects of the Climax I and II projects. In order to detect

downwind precipitation effects drifting from the Climax target area, various time lags of precipitation data from hourly stations in downwind locales were considered. Significant ratios of seeded to not-seeded precipitation were found downwind east and northeast of the Climax area. This suggests *increases* in precipitation on the order of 15–25% downwind of the intended target area. Long makes a summary statement in his paper as follows: "Downwind precipitation effects have been observed in geographic areas and time frames that are about the same magnitude as primary effects intended for the target area. There is little evidence of a decrease in precipitation outside the target area."

Solak et al. (2003) analyzed potential downwind effects from an operational winter program. This paper examined the precipitation that fell in areas of eastern and southeastern Utah and western Colorado located downwind of a long-term winter cloud-seeding program that has been conducted since 1974 in the central and southern Wasatch Mountains of Utah. The abstract from this paper states, "Estimations of effects on precipitation downwind of a long-standing operational snowpack augmentation project in Utah are made, using an adaptation of the historical target/control regression technique which has been used to estimate the seasonal effects over more than twenty seasons within the project's target area. Target area analyses of December–March high elevation precipitation data for this project indicate an overall seasonal increase of about 14%. Estimations of downwind effects are made for distance bands downwind as far as 150 miles. The downwind analyses indicate increases of similar magnitude to those for the target, expressed as percentages or ratio values, extending to about 100 miles downwind. Beyond 100 miles the ratio values decay, reaching about 1.0 (e.g., no effect) at about 125 miles. Expressed as average-depth precipitation amounts, the target area precipitation difference is about 1.4 inches of additional water, while the values within downwind distance bands range from 0.4 to 0.25 inches, reaching zero at about 125 miles."

A workshop, jointly sponsored by the WMA and the ASCE, was held at the annual meeting of the WMA in April 2012. The topic of this workshop was the potential for extra-area effects of cloud-seeding programs. Following this meeting, a paper was published on this topic (DeFelice et al. 2014). It states, "The results described in this paper make a strong case for enhanced precipitation, or a direct seeding effect, in extra-area regions from the conduct of seeding programs. They did not reveal regional impacts to the water balance, nor to the natural precipitation on a regional scale. This suggests that cloud seeding would not dry up the atmosphere or lead to summer drought, contrary to a popular belief. Cloud seeding typically benefits both 'Peter and Paul.'" Further, "The spatial extent of the positive 'extra area' seeding effect may extend to a couple hundred kilometers. Both microphysical (static) and dynamical (dynamic) effects of seeding appear to be contributors to these 'extra area' effects."

In summary, extra-area effects do not appear to show decreases in precipitation downstream of cloud-seeding activities, and often times show slight increases in downstream precipitation. Therefore, negative effects downstream of the Bighorn Mountains would not be expected as a result of cloud seeding in this area.

## 10.2 Environmental Impacts of Seeding Agents

Silver (Ag) in the form of AgI has been used as an ice nucleant in weather modification projects over the past 60 years. The ice nucleating properties of AgI were first reported by Vonnegut (1947). Vonnegut hypothesized that AgI acts as an effective ice nucleant because its crystal lattice structure resembles water ice. Vonnegut (1949) described a practical way to generate large numbers of AgI particles by combusting a solution of dissolved AgI in acetone. Using this method, one gram of AgI can produce $>10^{16}$ IN at temperatures of about −20 °C. Because of the extremely large number of IN produced by the method, very little AgI is required to significantly increase the local ice nucleus population. In ideal conditions, a large fraction of the AgI particles released during cloud-seeding operations create ice and are incorporated into the snowfall. Particles of AgI that do not act as IN may also be deposited on the ground by scavenging and dry deposition processes. Because the AgI particles are less than one micrometer, they will, if not captured in cloud particles, be transported in the atmosphere over large distances disappearing into the global atmospheric Ag background. Only a very small percentage of the AgI particle mass is expected to dissolve during snowmelt because it is a very insoluble salt. The impact of cloud seeding on natural levels of Ag in the environment (primarily aquatic ecosystems) has become an environmental concern because Ag in the form of its free ion ($Ag^+$) has been found to be toxic to fish and a subset of other aquatic organisms (Bianchini et al. 2002; Di Toro et al. 2001). It is important to note that *the toxic $Ag^+$ ion is not a product of AgI* and is not released into the environment by cloud seeding (Golden et al. 2011).

Several 1970s-era studies examined the environmental and health impacts of cloud seeding in the United States, including Harris (1981), Howell (1977), and Klein (1978). A more comprehensive list of worldwide laboratory and field studies is contained in the WMA's 2009 "Position Statement on the Environmental Impact of Using Silver Iodide as a Cloud Seeding Agent" (WMA 2009). The conclusion of the policy statement is, "The published scientific literature clearly shows ***no environmentally harmful effects*** arising from cloud seeding with silver iodide aerosols have been observed, nor would be expected to occur. Based on this work, the WMA finds that silver iodide is environmentally safe as it is currently being used in the conduct of cloud-seeding programs."

Cardno Entrix (2011) references four multi-year studies that have been conducted on cloud seeding from 1977 to 2006, including the geochemistry and toxicity of AgI. These studies are also unanimous in their conclusion that AgI used in cloud seeding is practically insoluble, does not tend to dissociate to its component ions of Ag and I, and is not bioavailable in the aquatic environment, but instead remains in soils and sediments.

Williams and Denholm (2009) provide an in-depth literature review of the toxicity of AgI on the environment, as well as the most recent monitoring results of the large-scale SPERP study, an eleven-year cloud-seeding research program designed to assess the technical, economic, and environmental feasibility of augmenting snowfall in the Snowy Mountain Region of New South Wales, Australia. The literature review summarizes findings from both field and laboratory toxicity studies, including studies on fish and amphibians. The authors concluded that there is no compelling evidence that the use of AgI for the SPERP would result in an adverse ecotoxicological impact on the study area environment.

Monitoring by the Desert Research Institute (DRI) of past cloud-seeding projects in and near the Walker Basin in Nevada has not been able to detect an increase in Ag above levels naturally present in soil and streams (i.e., baseline numbers are not elevated). DRI uses ultra-sensitive laboratory methods that can detect parts per trillion concentrations (Reclamation 2010).

Edwards and Simeral (2006) note the toxicity of $Ag^+$ in the aquatic environment is a function of its speciation, complexation, and interaction with competing cations. Thus, its toxicity is not necessarily related to the total aqueous metal concentration, but rather site-specific aquatic chemistry.

It is important to note that while laboratory studies have demonstrated the potential toxicity of $Ag^+$ to aquatic organisms, no actual reports of Ag toxicity in the environment were found, even for heavily polluted water bodies. Because of the lack of case studies, aquatic toxicity is still largely theoretical (Edwards and Simeral 2006).

Findings from the WWMPP state, "Trace chemistry analyses of water and soil samples were conducted for all three ranges following each operational season. These analyses demonstrated a negligible environmental impact of the seeding operations within the three mountain ranges, with silver concentrations in the water ranging in the parts per trillion and background concentrations in the soil being in the parts per billion range. These concentrations are far less than would be expected from other potential (background) sources of silver and measured concentrations in water sources were about three orders of magnitude less than values considered hazardous to environmental system or human health" (WWDC 2014).

All of these studies are consistent in concluding the contribution of AgI to the environment from cloud seeding is negligible (i.e., in quantities too small to be measured) compared to background levels and are well below threshold limits for human safety, aquatic organisms, and water quality standards.

Overall, the conclusions reached in the published scientific literature center around these points, and are applicable to the ecosystems contained within the area associated with the Bighorn Mountains:

- Background levels of Ag far exceed Ag contributed from cloud-seeding projects. Ag is found naturally and through industrial emissions. Ag is a trace element in many organisms. Numerous studies report no detected AgI in samples of cloud-seeded areas vs. control areas.
- In studies where Ag (all compounds and all sources) was detected, it was in the range of 0.1 to 0.01 micrograms per liter. The U.S. Public Health Service established a concentration limit of 50 micrograms per liter in public water supply. In a 1978 study, cloud seeding AgI was estimated to contribute 0.1 percent of overall silver emissions (Eisler 1996).
- The quantities of AgI used in cloud seeding are minute because very little material is needed to form the desired ice crystals. Furthermore, cloud seeding material is dispersed over very large areas. No detectable Ag above the natural background was

found in seeded target area water bodies, precipitation, and lake sediment samples, nor any evidence of Ag accumulation after more than 50 years of continuous seeding operations (Stone et al 1995; Stone 2006) after sampling water bodies in mountain areas of California subject to long-term cloud seeding.

- Silver toxicity depends on the concentration of active, free $Ag^+$ ions. AgI is considered water insoluble and not able to bioaccumulate to toxic levels. This insoluble property is what makes AgI maintain its structure and serve as an effective cloud-seeding agent. Some Ag compounds are toxic, especially to aquatic organisms in laboratory studies. However, in an environmental setting AgI is immobilized and is not bioavailable. Studies were conducted as part of an environmental monitoring effort to determine whether cloud seeding was impacting Sierra Nevada alpine lakes. No evidence was found that Ag from seeding operations was detectable above the background level. There was also no evidence of an impact on lake water chemistry, which is consistent with the insoluble nature and long times required to mobilize any AgI released over these watersheds. Comparisons of Ag with other naturally occurring trace metals measured in lake and sediment samples collected from the Mokelumne watershed in the Sierra Nevada indicate that the Ag was of natural origin (Stone 2006).
- Soil, sediment, and water-silver toxicity is very low even at high total Ag concentrations. Most Ag is bound into a compound such as AgI and is not available for absorption. Organic matter in the water column (colloids) and sediments bind $Ag^+$ ions, and Ag is strongly bonded to particulate matter. These factors result in low bioavailability, and therefore low toxicity. Because of this, very low amounts of Ag are absorbed from food; most is passed through the body of aquatic and terrestrial organisms.
- Although $Ag^+$ ions from soluble silver salts have been shown to be toxic to aquatic species, this is not the case with insoluble silver salts such as AgI, which is not bioavailable and thus of little environmental concern.

## 10.3 General Statements on Potential Environmental Impacts of Cloud Seeding

Numerous studies have been conducted in the western United States related to the potential environmental impacts of winter cloud seeding. Most of these studies were funded under the Bureau of Reclamation's "Project Skywater." Four programs of note concerned with wintertime programs were:

- Potential Ecological Impacts of Snowpack Augmentation in the Uinta Mountains, Utah. A 1981 report from Brigham Young University authored by Kimball Harper (Harper 1981) summarizing the results of a four-year study.
- Ecological Impacts of Snowpack Augmentation in the San Juan Mountains, Colorado. A 1976 report edited by Harold Steinhoff (Colorado State University) and Jack Ives (University of Colorado) summarizing the results of a five-year study (Steinhoff and Ives 1976).
- The Medicine Bow Ecology Project. A 1975 report on studies conducted in the Medicine Bow Mountains of southern Wyoming (Knight et al. 1975).

- The Sierra Ecology Study. A five-volume report summarizing work on possible impacts on the American River Drainage in California (Smith et al. 1980, Berg et al. 1980).

In general, the findings from these studies were that significant environmental effects due to the possible conduct of cloud-seeding programs in these areas were not expected to occur. A couple of examples that support this conclusion are as follows:

A statement made in the final report on the San Juan Mountains program (Steinhoff and Ives 1976): "The results of the San Juan Ecology Project suggest that there should be no immediate, large-scale impacts on the terrestrial ecosystems of these mountains following an addition of up to 30 percent of the normal snowpack, but with no addition to maximum snowpacks. Further, much of the work reported here suggests that compensating mechanisms within the study's ecosystems are such that any impacts would be buffered, at least for short periods of time, and of lesser magnitude than the changes in snow conditions required to produce them."

The Bureau of Reclamation published an "Environmental Assessment and Finding of No Significant Impact (Harris 1981) for the SCPP. Quoting from the introduction of this report:

"This document and the project environmental assessment serve as the basis for determination that no further action is necessary to comply with the National Environmental Policy Act of 1969 (Public Law 91-190) for the following reasons:

1) The Sierra Cooperative Pilot Project Environmental Assessment examines a research program designed to seed, on a randomized basis, some of the cloud types, which occur within winter storms in the Sierra Nevada of California and Nevada. The increase in annual precipitation expected from seeding all eligible storms during an average or less-than-average year would be 10 to 15 percent. The annual precipitation increase expected from randomized seeding of selected cloud types would be 5 to 7.5 percent. The report analyzes the potential effect of these increases upon weather elements, hydrologic and physiographic phenomena, plant and animal communities, the human environment, and land and water resource use in the project area. It also discusses possible impacts of the seeding agents, dry ice and silver iodide. The report concludes the research program will not result in significant or adverse effects upon the environment.
2) Consultation with Federal and State agencies has resulted in the determination that this project will not affect endangered or threatened species of plants or wildlife or their habitats in a significant or adverse manner.
3) Archeological and historic sites and sites of extraordinary aesthetic value will not be significantly or adversely affected by the project.
4) Project activities and resultant increases in precipitation will not affect the human environment, lifestyle, or existing land and water resource use in a significant or adverse manner. The project design includes suspension criteria to prevent operations during periods that would lead to public safety hazards."

A more recent environmental assessment was completed by the U.S. Bureau of Reclamation (USBR) for the Walker River Basin located in the east central Sierra Nevada Mountains of California and west central Nevada (Reclamation 2010). A Finding of No Significant Impact (FONSI) was issued for this project by the USBR (Reclamation 2010). The following is the summary statement from the FONSI: "Based on the analysis of the environmental impacts as described in the Environmental Assessment for the Walker River Basin Cloud Seeding Project, Reclamation has determined that the proposed federal action will not significantly affect the quality of the human environment, thus an environmental impact statement is not required. This Finding of No Significant Impact (FONSI) is supported by the Environmental Assessment for the Walker River Basin Cloud Seeding Project."

## 10.4 Legal Implications

There are legal implications associated with conducting cloud-seeding programs. For example, who should own the additional water produced from cloud-seeding activities? Most state regulations claim ownership of surface waters while they are within the state, and they can be distributed according to the existing water rights in the area. The State of Wyoming considers water developed by cloud seeding as part of the natural water supply and subject to all applicable laws.

Another legal consideration is whether cloud-seeding program sponsors have legal responsibilities for any perceived damages caused by the seeding activities. For example, if seeding is conducted and a flood occurs in or near the program's target area, would the sponsors be liable? Such situations are sometimes referred to as the possible "consequential effects" of cloud seeding. In order to prevent such situations, it is important to have adequate safeguards built into the design of seeding programs to suspend seeding operations in questionable circumstances (Section 9).

Weather modification operators also have the option to carry a special type of insurance commonly known as "consequential effects of cloud seeding liability insurance." This insurance protects the operator and sponsor from legal defense costs, and also provides reasonable assurance of protection to the public in the event that damages are caused as a result of cloud seeding.

Cloud-seeding programs are subject to permitting and reporting requirements. Both state and federal requirements would be associated with the proposed Bighorn Mountains cloud-seeding program. These requirements are summarized in Section 8.

# 11. Task 10: Evaluation Methodology

A critical issue for weather modification research and operational programs is the need for evaluation and validation of results. Objectivity, repeatability, and predictability are primary requirements in weather modification studies. Independent confirmation of a seeding effect with strong physical and statistical evidence is important. With more emphasis having been put on statistical studies and randomization in the past decade, there has been some improvement in the evaluation of cloud-seeding activities. The goal of this task is to develop and summarize statistical and physical methodologies for evaluating the efficacy of the proposed cloud-seeding program. The recent advances in the use of numerical models that simulate seeding are important, and can be considered complementary in contributing to both the statistical evidence and physical evidence of seeding.

The proposed cloud-seeding design for snowpack enhancement in the Bighorn Mountains is being developed as an operational cloud-seeding program, as opposed to a research-based program. Therefore, a randomized component for evaluation is not recommended, as it would reduce the number of times that seeding is actually conducted. As a result, the statistical methods discussed herein will focus on evaluating operational programs.

## 11.1 Statistical Evaluation

A statistical evaluation enables the detection, in an unbiased manner, of a change in a response variable (i.e., the seeding effect), as specified by the seeding conceptual model (Section 3.1.1). The objective is to show that the behavior of seeded clouds is clearly outside the range of natural occurrences. In a statistical experiment, the response variable is the variable being investigated for the seeding effect. While the variable could be any expected change along the steps of the conceptual model, such as AgI detection in the target area, increased concentrations of ice particles, or enhanced radar reflectivity, a measurement of the final result (seasonally accumulated precipitation, 1 April SWE, or a measure of streamflow) is usually of more interest. For example, in the WWMPP study, the response variable for the Medicine Bow and Sierra Madre targets was the 4-hour accumulation of liquid-equivalent precipitation in each target area as measured by high-resolution precipitation gauges. These changes, or seeding effects, have proven to be relatively small when compared to natural variability. Therefore, it is most common to compare target (seeded) measurements to control (unseeded) measurements — so-called target/control evaluation. This provides a method to detect and quantify seeding effects from an operational program with some measure of confidence. As such, it has been recognized or recommended as a preferred method in ASCE standards, and various weather modification permitting regulations.

### *11.1.1 Target/Control Method*

The most widely used approach to the evaluation of operational cloud-seeding programs is the comparison of events in the target area to events in one or more control areas (which are unaffected by the seeding). This approach assumes that the study area was adequately sampled. The 2006 Wyoming Range Feasibility Study (NAWC 2006) described this method

in great detail, and the review and results are still applicable to the Bighorn Mountains target area evaluation. The appeal of this method for operational programs is the use of measurements from the SNOTEL or streamflow gauge networks, which have been established for long periods of time. It is critical to identify appropriate controls that are highly correlated to the target area(s), and have been unaffected by precipitation augmentation activities for a long period of time. One simple technique is to calculate the precipitation as a percentage of normal (over a specific historical period). The target and control area can be compared in terms of percentage of normal, and a ratio of increase in precipitation can be calculated; however, the use of ratios carries a risk of error. Assuming that the target and control have similar precipitation patterns, the expected value of the target-control ratio is generally greater than one. However, its exact value depends on the distributions of rainfall events in the target and control area.

The validity of these ratios depends on two assumptions: 1) that no other differences are confounded with the operational/historical seed/no seed comparison; and 2) that variability of precipitation between one set of years and the next set behaves like the variability of two independent random samples of years. The first assumption, that no other differences are confounded with the operational/historical comparison, is referred to as a lack of "bias." Unknown biases arising from temporal or spatial trends that may have been present during the seeding period need to be resolved. For example, Silverman (2007) presents an analysis technique that accounts for biases due to natural differences in streamflow between the target and control and, by taking advantage of the high correlation between the target and control. The second assumption underlying the validity of the statistical methods regards the variability of precipitation from year to year. Knowledge about the effects of land use changes, climatic shifts, and large-scale dynamic cycles (e.g., El Nino) on precipitation in the West may be useful in further adjusting long-term records for these non-random variations. The practical issue is whether the statistical methods used in operational/historical evaluations of cloud seeding are valid when based on precipitation data that vary from year to year. Making the assumption of normality for precipitation is speculative. Different statistical approaches, such as historical regression and ratio statistics, can be used to compare target to control variables.

### *11.1.2 Evaluation by Historical Regression*

Relationships between target and control are commonly described statistically via regression calculations on historical data. The historical regression method of comparing target and control is considered more sophisticated than a ratio comparison. In addition to obtaining an estimate of the effects of seeding upon precipitation, the historical regression method provides an estimate of the probability that the departure from the predicted value for any seeded storm is entirely due to chance. Many examples of this technique have been described (e.g., Silverman 2007, 2010; Griffith et al. 2009, 2011; NAWC 2006).

The historical regression method consists of the following steps:

1. Select a variable that is affected by seeding (e.g., SWE, streamflow).

2. Records of the variable to be tested are acquired for a non-seeded historical period of more than 20 years duration (requires precipitation gauges with a long historical record).
3. Records are partitioned in the target and control area. The meteorology in the target and control area should be similar and the control area should be unaffected by the seeding. The correlation between precipitation in the target and control area should be greater than 0.9 and target and control area should not be downwind of other seeding projects. As more seeding programs are implemented in the Western U.S. mountains, this latter criterion will become more challenging to meet.
4. The target and control data from the unseeded period are then used to develop an equation (regression) that predicts the amount of target-area precipitation.
5. The regression equation is applied to the seeded period to estimate what target precipitation might have been without the seeding.

The target and control area is often the same fixed geographical area, and comparisons are made between measurements made during the seeding and those from a period without the seeding. Alternatively, the control area might be a geographically fixed area adjacent to (and meteorologically similar to) the target area. The historical regression method can also involve multiple control areas. One can also introduce controls based on observed meteorological variables other than precipitation. In this case, the objective is to find a multiple correlation coefficient higher than that for any single control area. The addition of new controls usually reaches a point of diminishing return due to intercorrelations amongst controls.

There is no guarantee that long-term climatological trends, or biases arising from temporal or spatial trends that may have been present during the seeding period, will not change a target-control relationship. In order to address this, it is recommended to follow the historical regression analysis method for the selection of control areas and to be aware of any changes in weather patterns that could distort the target-control relationship.

### *11.1.3 Evaluation by Ratio Statistics*

An alternative method for detecting and quantifying seeding effects, using target and controls, is based on the use of ratio statistics. Ratio statistics relate totals, or means, of precipitation at different times and in different areas (with seeding or without seeding), on a seeding target or a control area, or on two alternate targets. The totals accumulate all seeded or unseeded experimental units at all stations of a particular area. Since daily, or even weekly, precipitation tends to have highly skewed distributions, ratio methods may be considered as non-robust and prone to the effect of outliers. Replacing them by statistics that censor outliers increases robustness but does so at the risk of ignoring possible large effects of seeding. Biases occur when operational data are compared to historical records in an *a posteriori* evaluation of non-randomized seeding programs. Gabriel and Petrondas (1983) have shown that reliable conclusions cannot be drawn from comparisons of operational data with historical records, and have demonstrated the problems encountered in trying to do so. The calculated p-values are likely to be lower than the true level of significance and the calculated confidence limits are likely to be more precise than they

really are. Because of these problems, standard statistical methods are prone to indicate effects when there might not be any.

Although ratio statistics are explained in Gabriel (1999), a clear example is given in Silverman (2007) in the analysis of the Kings River operational seeding program (Henderson 2003). In this analysis, bias adjustments were made in accordance with Gabriel and Petrondas (1983) and robust results of seeding effects were presented. In general, the use of ratio statistics presents an analysis technique that addresses some of the caveats highlighted in other analysis methods. Using the regression ratio, which takes advantage of correlations over an entire measurement period (unseeded and seeded), and adjusting for biases decreases the variance and enables the detection of smaller effects due to seeding.

## 11.2 Numerical Model Evaluation

Computer models are now capable of predicting the transport of seeding plumes, their microphysical response in clouds, and the fallout of seeding-enhanced precipitation. Using the WRF model with a cloud-seeding parameterization (Xue et al. 2013a, b) to show spatial variability and quantifiable simulated seeding effects has been shown to aid in the design of cloud-seeding programs. The seeding parameterization in WRF can be applied to seeded and natural storms to statistically analyze seeding effects — like a virtual seeding experiment — as was done for the WWMPP (WWDC 2014). Although the model has yet to be thoroughly validated, this approach has the potential to transform how cloud-seeding programs are evaluated. Running seeded versus unseeded model simulations to determine a plausible seeding effect is less expensive than conducting a long-term, randomized, statistically significant seeding experiment. Moreover, the model provides a true "control" experiment to evaluate the effects of seeding. Therefore, an operational cloud-seeding program would not have to withhold seeding in some seedable storms, as would be the case if evaluating the program with a randomized experiment. For this approach to have merit, the ability of the model simulation to reproduce the actual observed storm characteristics in the control and seeded simulations needs to be validated with observations.

Additionally, various plume-modeling approaches have been successfully applied to winter orographic cloud-seeding conditions, based on spot observations for model verification. Plume models depend on input from observations or more often a 3D weather model to "drive" the plume model with winds, temperature, pressure, underlying topography, and land use. The advantage of using plume models is the ability to include many simulations with these relatively simple models (e.g., SCIPUFF – Sykes and Gabruk 1997; the Hybrid Single-Particle Lagrangian Integrated Trajectory [HYSPLIT], Stochastic Time-Inverted Lagrangian Transport [STILT], and Flexible Particle [FLEXPART] models). DRI's Lagrangian particle dispersion model (LAP) has been used to predict plume transport from AgI generators (NAWC 2006). Some of these simulations have been subject to independent verification through studies of the silver content of snow. Another method used to validate plume dispersion is using aircraft to map IN or tracer concentrations after they are released concurrently with the seeding (e.g., Boe et al 2014). Therefore, careful analysis of

observations to validate model output is required to gain confidence that such models faithfully portray seeding plumes.

## 11.3 Physical Evaluation

Physical evidence constitutes the measurement of key steps in the chain of events associated with the seeding conceptual model and can be used to establish the physical plausibility that seeding effects suggested by results of statistical evaluations could have been caused by the seeding intervention. The physical evidence enables the establishment of a cause-and-effect relationship between seeding and the changes in the response variables, as documented in the statistical evaluation. However, this relationship does not directly address whether seeding changes the total precipitation reaching the ground.

Physical evidence is usually accomplished 1) by means of case studies on the behavior of seeded and unseeded clouds, and 2) through the identification and measurement of response variables associated with the seeding conceptual model. Response variables are parameters that represent key steps in the chain of physical events as described by the seeding conceptual model. Such parameters must be measurable to the degree necessary to discern the anticipated changes due to seeding. A recent example of such an approach is the ASCII program, which utilized a suite of instruments to examine relevant parameters (Geerts et al. 2010; Pokharel et al. 2014a, b).

A number of instruments and analysis techniques to deploy for evaluating an operational program are listed below:

- Install additional precipitation measurement sites.
    - The accurately measuring SWE at unmanned high-elevation sites is difficult. The main issues are clogging at the top of the snow gauge and blow-by of snowflakes past the snow gauge. The best location for a snow gauge is in small clearings in forested areas to help reduce the impact of wind. Uncertainty in snow measurements could be greater in magnitude than a seeding effect. Siting multiple gauges at any given site (redundancy) is helpful to ascertain the uncertainty in the measurement itself.
    - SNOTEL sites provide the only type of standard precipitation measurements at high-elevation areas targeted by most winter cloud-seeding programs. They may not be well suited for use in estimations of seeding effect, given the low temporal (hourly) and measurement (0.1 inch) resolution of these gauges.
- Install additional streamflow gauges, especially at sites without a historical record. These sites could be the basis for statistical evaluation of streamflow changes. In addition, these gauges would augment streamflow information useful to the planning authorities.
- Add soundings and radiometer data. Not only are observations of current atmospheric conditions useful for making operational seeding decisions, but also for program evaluation and model validation.

- Install a meteorological tower site. While the location for the site would need to be assessed, meteorological observations in this data-sparse region would be useful for model validation.
- Deploy a millimeter-wave radar (e.g., the Wyoming Cloud Radar) during periods of opportunity. These radars measure the microstructure of the clouds, which provides insight into the precipitation formation processes. This type of radar was used during ASCII to document characteristics of seeded versus unseeded clouds.
- Deploy an X-band radar at a site that would allow remote operation. Radars serve as a great tool to map precipitation amounts and phases as it falls, however most mountainous regions are void of operational weather radar coverage. Deploying smaller, X-band radars in the mountains can help provide valuable data on where and how much precipitation is falling in the target area. This radar would not need to be continuously manned, but would require power and internet access.
- Collect snow samples for trace chemistry analysis to verify targeting. This technique is used in the assessment of the effectiveness of the targeting of seeding effect by determining whether silver is present in areas that use silver iodide as the seeding agent.
    - Snow samples collected prior to cloud seeding or from non-seeded storms are analyzed to establish the natural background silver content for comparison with snow samples taken from seeded storms.
    - Warburton et al (1996) demonstrates how trace chemical assessment techniques strengthen traditional target and control precipitation analyses.
    - Adding a control aerosol along with an active seeding aerosol (Warburton et al 1995) can give estimates of seeding effectiveness.
    - The combination of silver-in-snow along with model predictions of the transport of seeding plumes over sampling sites supports the presence of a positive seeding effect as determined through statistical evaluations.
- Measure IN concentrations, such as was done in the Medicine Bow Range during WWMPP. Without an easily accessible site in the target area, this may be best to measure downwind to investigate plume transport.
- Validate plume dispersion by either mapping tracer concentrations using aircraft in clouds after such tracer is released concurrently with the seeding or using trace gas releases at generator sites and gas samplers at the target area. Some work of this type was done using $SF_6$ as the tracer in Utah storm events (Holroyd et al. 1995, Heimbach et al. 1997).
- Instrument the seeding aircraft to be used simultaneously for cloud seeding and physical measurements. Such instrumentation would be used to measure the wind, amount of SLW, and the size of cloud hydrometeors less than 1 mm in diameter (e.g., LWC sensor, air data probe, back scatter cloud probe with polarization). The objective would be to keep the instrumentation at a minimum so that it could be utilized during operations without the need of an instrument operator and with minimal maintenance.
- Add icing meters to high-elevation remote generators to quantify the amount of SLW in clouds being seeded with ground generators.

- Consider new technologies for collecting atmospheric parameters relevant to the seeding conceptual model, such as other remote-sensing instruments or unmanned airborne vehicles as a platform for stability analysis (in valleys) or winds affecting plume transport and diffusion from lower elevation generators.

## 11.4 Evaluation Methodology Summary

Statistical analyses using the target/control method are commonly used to evaluate operational programs because of their history in developing the technique and the publically available data (i.e., SNOTEL, streamflow gauges) that are used. This method is capable of providing robust results and is cost effective; however, finding appropriate controls can be challenging. Numerical modeling using the recently developed seeding parameterization is evolving as another cost-effective tool for evaluating seeding effects. Validation efforts and continued development of the model are providing evidence of its applicability. Model studies can also be used in selecting suitable control sites. A number of physical measurements would also aid in the evaluation of the operational seeding program, such as adding streamflow gauges and local meteorological stations. Moreover, the addition of supplementary instrumentation (i.e., soundings, radiometers, numerical models) not only aids in program evaluation, but also in program decision making to identify suitable cases for seeding. Deploying specialized instruments (i.e., silver sampling, radar) would be useful for model validation and determining seeding effectiveness.

# 12. Task 11: Hydrologic Assessment

## 12.1 WRF model simulation of runoff

A first-order estimate of the potential change in streamflow (runoff) in the study area due to snowfall augmentation from cloud seeding was made using precipitation and runoff simulated by the high-resolution WRF-CONUS simulation (Section 4.1.2). Model output of runoff includes both surface and sub-surface runoff from the Noah-MP Land Surface Model (LSM). The WRF-CONUS simulation was not run with a hydrological model, which enables detailed hydrological routing of runoff to water bodies such as streams, rivers, and lakes. Therefore, the current dataset does not allow for an estimate of runoff amount that goes to particular rivers/streams; however, the model dataset does allow us to examine the spatial distribution of runoff and give insight to the relation between the distribution of precipitation and runoff.

Figure 12.1 shows precipitation, runoff[7], and evapotranspiration for the annual, November–April, and May–October periods using the averaged 2000–2008 WRF-CONUS simulation. On an annual basis, the results show more precipitation in the Powder/Tongue River basin, and the corresponding evapotranspiration is also higher compared to the Bighorn Basin. The largest amount of annual precipitation and runoff is found at high elevations (i.e. > 8,000 ft), revealing the importance of high elevation snowfall. However, a pattern unique to the Bighorn Mountains, as pointed out in Section 4.2.2, is a maximum in precipitation at the northern end of the mountain range, which is not the highest elevation area of the range. There is no second maximum in runoff in this northern region, presumably due to enhanced evapotranspiration in this lower elevation precipitation maximum. Annual runoff is the highest at the highest elevations along the divide (i.e., Cloud Peak), where evapotranspiration shows a local minimum due to lower temperatures at higher elevations. Across the whole domain, the runoff ratio (ratio of runoff to precipitation) is ~0.1–0.2, but there are regions, especially along the higher elevations of the Bighorn Mountains themselves, where it is ~0.4 or greater (Figure 12.2).

In November–April, only a small amount of runoff occurs at high elevations even though enough precipitation falls because high-elevation precipitation is snowfall during this period and is retained as snowpack. Furthermore, there is no snowmelt due to the cold wintertime temperatures, and the frozen soil prevents water from seeping into the sub-surface layer. Not surprisingly, the amount of evapotranspiration during the cold season is also small given cold temperatures and "*dormant*" vegetation activities. The November–April runoff at low elevations of the Powder/Tongue River basin comes from rainfall as well as slow snowmelt on warm days. The May–October runoff is greater than the cold-season runoff because of high-elevation snowmelt in early spring and rainfall. As

[7] Noah-MP LSM has an unconfined aquifer below the 2-m bottom of the Noah soil column to account for the exchange of water between the soil and the aquifer. Negative values in runoff means a flux of water from the aquifer into the soil column. All negative runoff values that appear in Figure 12.1 are small (~30 mm or less).

mentioned in Section 4.2.1, in some years, large precipitation events occurred in May. These precipitation events brought snow at high elevations and rain in the plains (Figure 12.3).

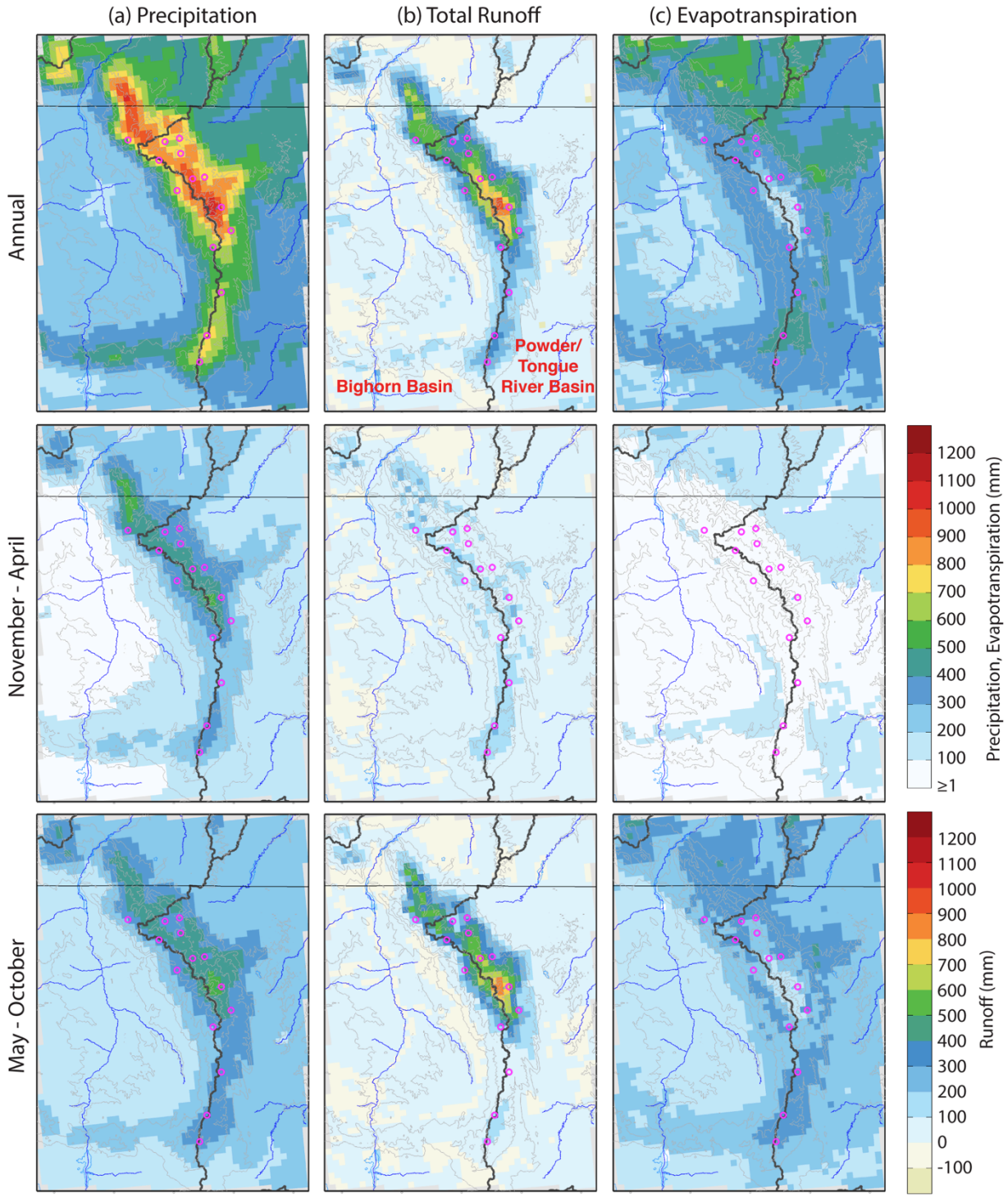


**Figure 12.1. WRF simulation of (a) precipitation, (b) total runoff (surface and sub-surface runoff), and (c) evapotranspiration averaged over 2000–2008. Top panels show annual precipitation, runoff, and evapotranspiration. Middle and bottom panels are for November – April, and May – October, respectively. Black**

solid lines indicate hydrological basins. West of the divide is the Bighorn basin and east of the divide is the Powder/Tongue River basin.

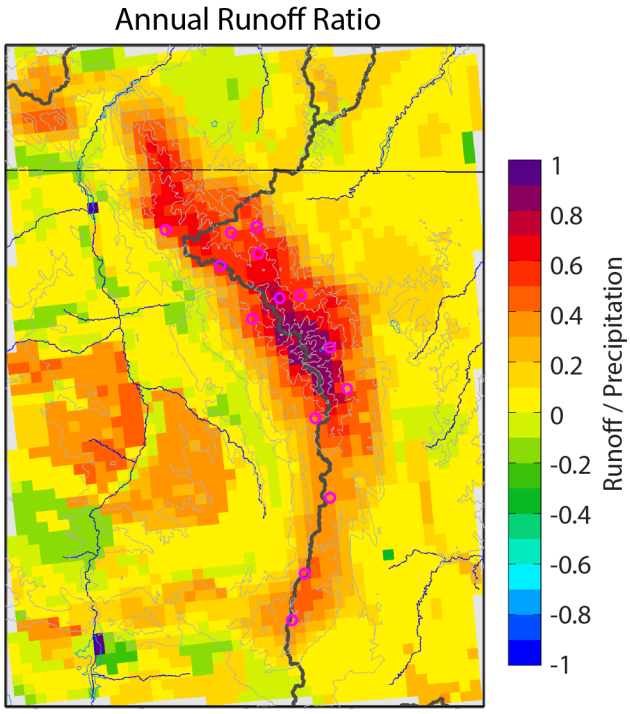


Figure 12.2. Ratio of annual total runoff to annual precipitation from the 8-year averaged model data.

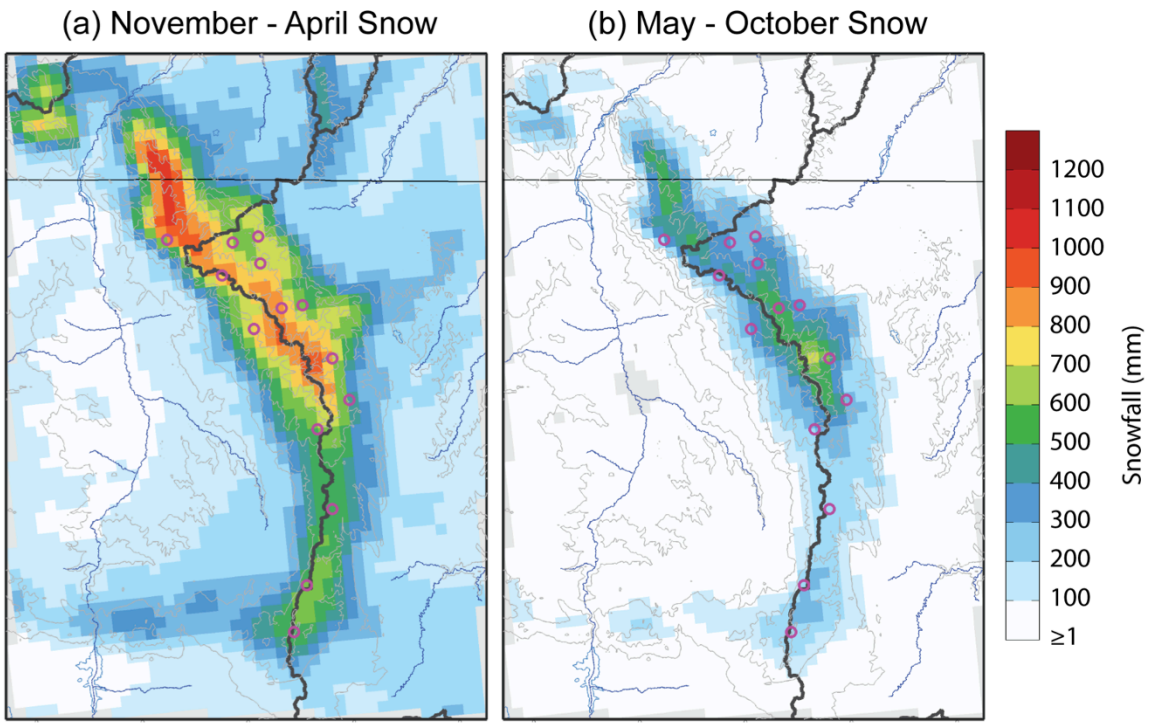


**Figure 12.3. 2000–2008 average snowfall in (a) November – April and (b) May – October.**

Figure 12.4 shows the annual cycle of monthly precipitation, snow, SWE, and runoff spatially averaged over the two key basins based on the 8-year averaged model data. The annual cycles are very similar in the Bighorn and Powder/Tongue River basins with peak snowfall occurring in April and a pronounced peak in total precipitation occurring in May, followed by peak runoff in May resulting from snowmelt as well as rainfall. There is a broad peak in the SWE curve between February and May, with the May peak associated with the high-elevation snowfall from the April–May events. Recall that these early spring high-elevation snow events present as rain at lower elevations (Section 4.2.2). The model results indicate that surface and subsurface runoff are small and similar in amount between November and March, but the April–June runoff mostly comes from subsurface runoff. The fact that the model provides runoff partitioned into surface and subsurface runoff components is an important added value of using model simulation results in assessing potential seeding-induced runoff increases. This is because observational streamflow data are only indicative of surface runoff, yet snowmelt also goes into subsurface runoff. As a result, observational assessments may be underestimating the potential change because they do not account for subsurface runoff changes.

Over the study area, the model-based annual precipitation is 457 mm, of which 17% goes to runoff (76 mm). Snowfall accounts for 43% of the annual precipitation. This means that ~43% of the 76 mm of runoff (i.e., 32 mm) derives from snowmelt and the other 44 mm from rainfall (Table 12.1).

The breakdown of these values for each of the two basins is similar to that determined for the entire study area (Table 12.1). Average total runoff in each basin was calculated for the areas > 8,000 ft (recall Figure 6.29) and is provided in Table 12.2.

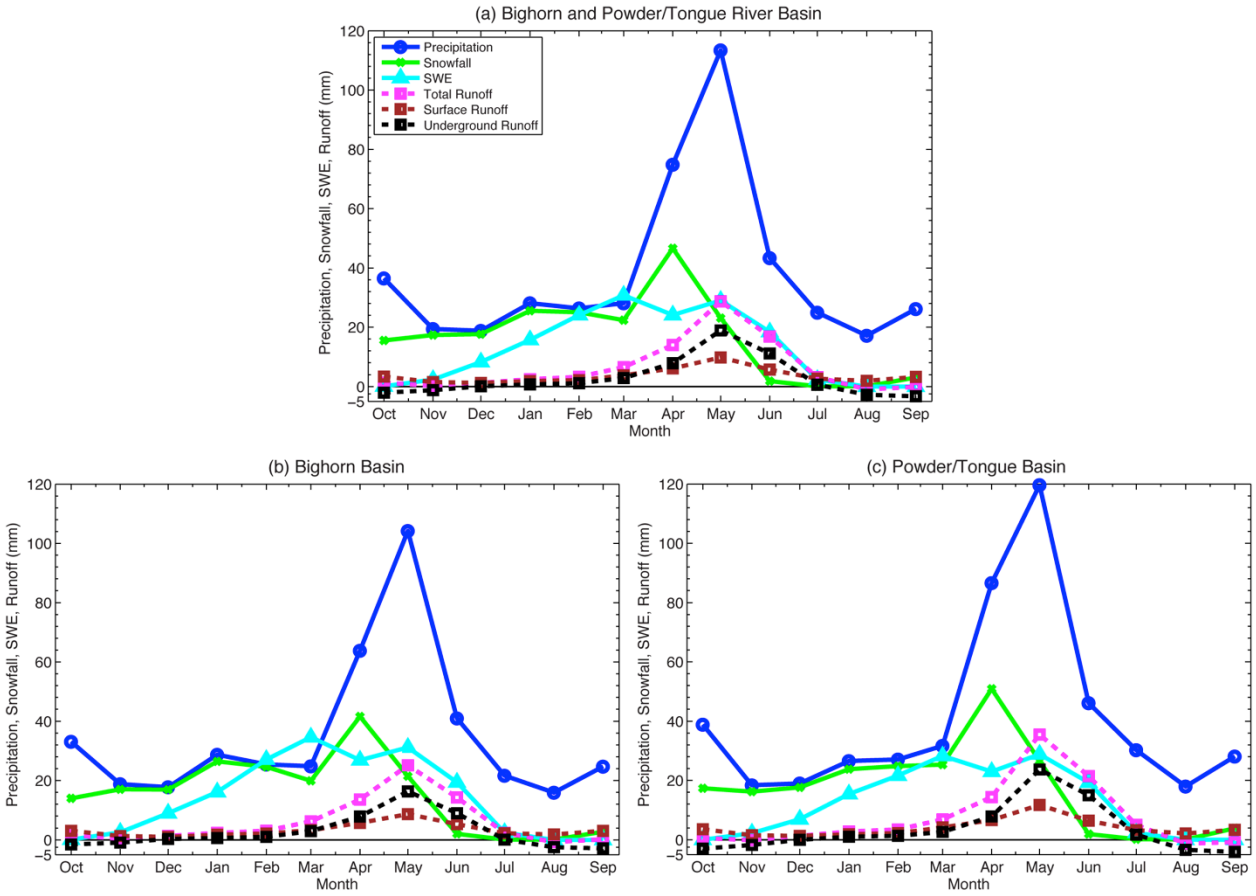


**Figure 12.4. Monthly precipitation, snow, SWE, and runoff (total, surface, and sub-surface) averaged over the (a) Bighorn and Powder/Tongue River basins, (b) Bighorn basin, and (c) Powder/Tongue River basin. The annual cycle is based on the 2000 – 2008 WRF simulation.**

**Table 12.1: 8-year average annual precipitation, runoff, runoff ratio, snowfall and rainfall averaged over the study area (Figure 12.1), Bighorn basin, and Powder/Tongue River basin. Values in parentheses for the snowfall and rainfall indicate the ratio of snowfall and rainfall to total precipitation. Note that the basin-averaged values are only for the area that appears in Figure 12.1, not including the entire basin.**

| | Annual Precipitation (mm) | Annual Runoff (mm) | Runoff / Precipitation | Annual Snowfall (mm) | Annual Rainfall (mm) |
|---|---|---|---|---|---|
| Study Area | 457 | 76 | 17 % | 198 (43%) | 259 (57%) |
| Bighorn Basin | 420 | 69 | 16 % | 188 (45%) | 232 (55%) |
| Powder/Tongue River Basin | 490 | 89 | 18 % | 209 (43%) | 281 (57%) |

**Table 12.2. 8-yr (2000–2008) average annual and April–July total runoff per river basin in acre feet for areas > 8000 ft in elevation calculated from the WRF-CONUS model simulations.**

| | Bighorn | Powder/Tongue |
|---|---|---|
| Avg annual total runoff (AF) | 600,231 | 591,360 |
| Avg Apr-Jul total runoff (AF) | 516,666 | 465,448 |

## 12.2 Observational Streamflow Data and Snowpack

In this section, the relationship between streamflow and snowpack is investigated by comparing the streamflow measurements from USGS (http://waterdata.usgs.gov/) to SNOTEL snowpack observations (i.e., SWE). The locations of the gauges analyzed are indicated in Figure 12.5. The streamflow gauges analyzed were selected if they had minimal regulation or diversions that could impact the relationships between the SNOTEL and streamflow gauge. For the eastern slope, which feeds the Powder/Tongue River basin, there were no streamflow gauges that had absolutely no regulation, but the Tongue River gauge was listed as having only a "small" diversion. Therefore, in order to calculate relationships for that basin, this site was selected. Nonetheless, the caveat that it was not a completely unregulated gauge site should be kept in mind. For the Bighorn Basin, the Shell Creek site was selected because there are no diversions upstream of the streamflow gauge.

For the Bighorn Basin, April–July streamflow from the 1980 to 2015 water years was used to compare to SWE on 1 April and 1 May from the streamflow gauge and SNOTEL sites at Shell Creek. For the eastern slope, two SNOTEL sites were paired with the Tongue River streamflow gauge site. For the Tie Creek-Tongue River observational site pair, measurements between the 1995 and 2015 water years were compared due to the shorter SNOTEL observational record. For the Burgess Junction-Tongue River pair, the 1983–2015 water year data were examined. Elevations of these sites are listed in Table 12.3.

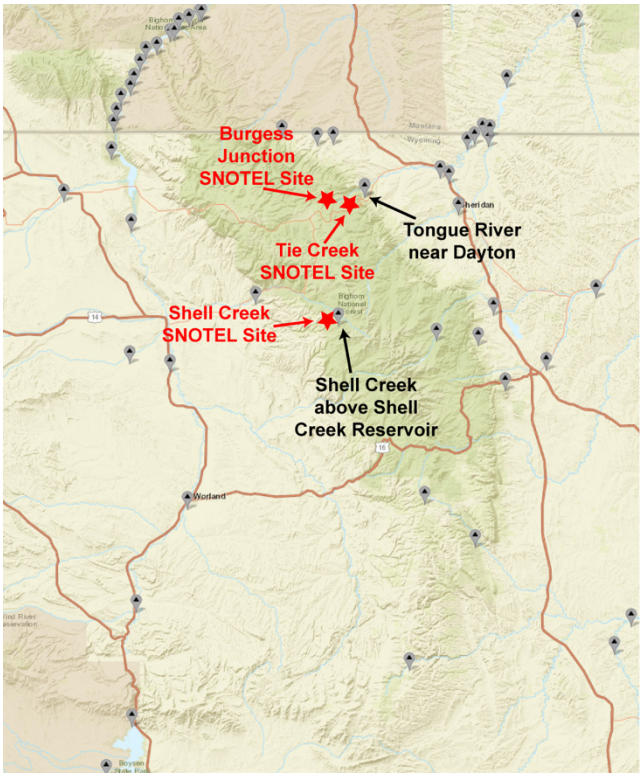


**Figure 12.5. USGS streamflow gauge sites. For this study, streamflow measurements from Tongue River gauge near Dayton and Shell Creek gauge above Shell Creek Reservoir were used. Correspondence of streamflow to snowpack were examined with SWE data from near-by SNOTEL sites (stars).**

**Table 12.3. List of site name, measurements, and site elevation used.**

| Site Name | Measurements | Site Elevation (ft) | Period of Record Used |
|---|---|---|---|
| Shell Creek above Shell Creek Reservoir | Streamflow | 9050 | 1980–2015 |
| Tongue River near Dayton | Streamflow | 4060 | 1995–2015 or 1983–2015 |
| Shell Creek SNOTEL | SWE | 9580 | 1980–2015 |
| Tie Creek SNOTEL | SWE | 6870 | 1995–2015 |
| Burgess Junction SNOTEL | SWE | 7880 | 1983–2015 |

The climatological annual cycle of streamflow from the Shell Creek gauge above Shell Creek Reservoir and SWE at the Shell Creek SNOTEL site are shown in Figure 12.6. The climatological annual cycle of streamflow was calculated for three different periods (since 1971, 1980, and 1995) to examine if there is any significant difference depending on the climatological period. These results showed similar ranges for the data as well as the median values, indicating no notable dependence on the period selected.

The streamflow variability from one year to another increases at the beginning of spring (i.e., start of the melting season) and maximizes in June with peak streamflow typically in

June. The SWE peaks generally in May and quickly decreases in June once the melting season begins. This is consistent with the peak streamflow timing.

Figure 12.7 is a scatter plot showing the relationship between April–July streamflow at Shell Creek gauge above Shell Creek to 1 May SWE at Shell Creek SNOTEL site. The streamflow from this slope of the range flows into the Bighorn Basin. Traditionally, 1 April SWE is compared to streamflow; however, the 1 May SWE is used as the parameter in this study because the peak SWE is in May and has shown a better relationship to the April–July streamflow. The two datasets show good agreement, having a linear correlation coefficient of 0.65. The least-squared fit through the data points have a coefficient of determination of 0.42.

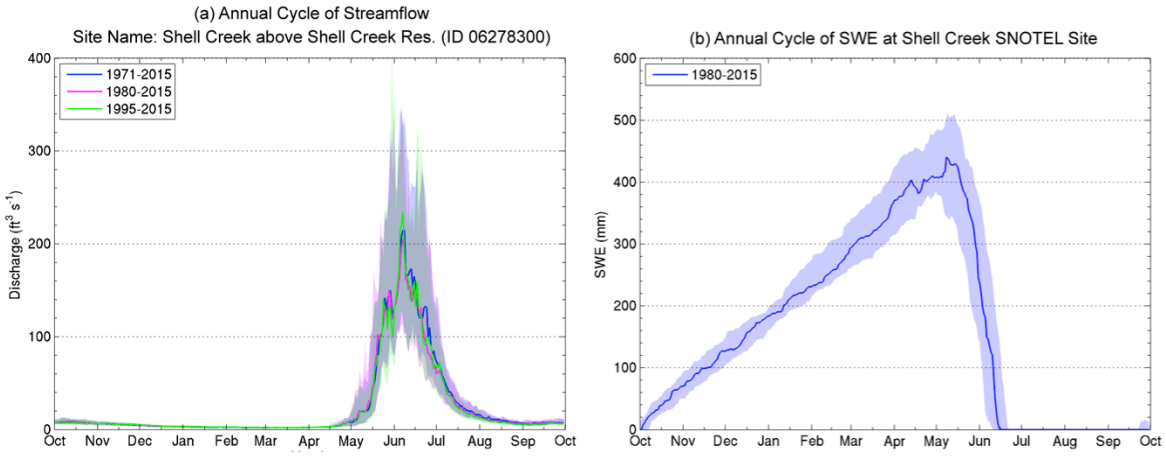


**Figure 12.6. (a) Annual cycle of daily mean discharge ($ft^3\ s^{-1}$) measured at the Shell Creek gauge above Shell Creek Reservoir over three different climatological periods: 1971–2015, 1980–2015, and 1995–2015. Lines are the median values of the data. Shaded region indicate 25th to 75th percentile of the data for each climatological period. (b) Annual cycle of SWE at Shell Creek SNOTEL site for the 1980–2015 period. Median (line) and the 25–75th percentile range (shaded) of the data are shown.**

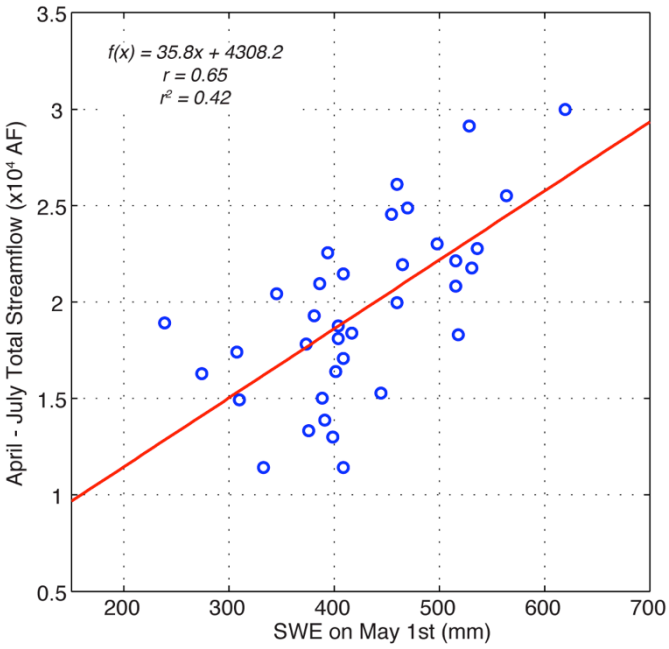


**Figure 12.7. Scatter plot of total streamflow (AF) from April through July compared to SWE (mm) on 1 May for Shell at Shell Creek SNOTEL site. Red line shows the least-squared fit. $r^2$ is the coefficient of determination and r is the linear correlation coefficient.**

The climatological annual cycle of streamflow and SWE for the Tongue River streamflow gauge near Dayton and SNOTEL sites at Tie Creek and Burgess Junction are shown in Figure 12.8 and scatter plots of streamflow versus SWE from these sites are in Figure 12.9. The streamflow from this slope flow into the Powder/Tongue River basin. These results indicate that streamflow peaks in June, as it did at the Shell Creek streamflow gauge site. Nonetheless, there is more streamflow at this site than the Shell Creek site, such that the peak flow is double the amount it was at Shell Creek. This is consistent with the spatial distribution of precipitation and runoff shown by the WRF-CONUS simulation being greater on the northeastern slopes (Figure 12.1).

There are some differences in the median curves around the peak flow season for the three climatological periods analyzed for the Tongue River streamflow gauge, indicating more variability and therefore dependence of the results on the period studied. SWE curves show that the peak SWE occurs a little earlier than at the Shell Creek site, likely because of the different elevation between the sites. Additionally, there is less SWE at the Tie Creek site compared to Burgess Junction, again attributed to the elevation difference between the sites.

The streamflow peak in June includes rainfall from May–June (recall earlier discussion about large precipitation events in May and high-elevation snowmelt). There is fairly good correlation between the Tongue River stream gauge and the Burgess Junction SWE measurements (Figure 12.9a) having a linear correlation coefficient of 0.75. However, there

is not a strong relationship between the Tongue River streamflow gauge and Tie Creek SWE measurements.

Table 12.4 gives a summary of the relationship between the streamflow and 1 May SWE. Climatological average April–July streamflow is 19,536, 86,054, and 85,069 AF at Shell Creek above Shell Creek Res. streamflow gauge site, Tongue River streamflow site during the 1995–2015 and 1983–2015 periods, respectively. The seasonal streamflow accounts for 88% of the total annual streamflow at Shell Creek and 73% at Tongue River streamflow sites.

The percentage increase in streamflow for a given percentage increase in SWE varies between dry and wet conditions. Based on the best-fit line for the streamflow and 1 May SWE, a 25% reduction of SWE during a "dry" season would result in 19% reduction in April–July streamflow at the Shell Creek site. A 50% increase of SWE during a "wet" season yields 39% more April–July streamflow at this site. At the Tongue River streamflow gauge site, a 25% decrease of SWE would decrease streamflow by 29% and a 50% SWE increase leads to 59% more streamflow if Burgess Junction SNOTEL SWE data were used. The impact of SWE change to streamflow is less, based on the SWE values at Tie Creek SNOTEL site (and also recall this site pair had fairly low correlation).

Using these single-point measurements, the ratio of snowpack increase to streamflow increase is quite variable (boldface row in Table 12.4). This is consistent with the results of Super and McPartland (1993) who found ratios varied between 0.6 and 2.1 with a median value of 1.05 for several geographical locations in Colorado, Utah, and Wyoming. However, such single-point measurements between well correlated streamflow and snow-gauge sites may underrepresent the evapotranspiration loss that occurs over an entire basin. Therefore, this ratio was also calculated using the WRF-CONUS model simulation April–July runoff relative to simulated 1 May SWE over the target area (> 8,000 ft MSL). This suggested the ratio is 0.49, which agrees with results from detailed hydrological models that have shown ratios much lower than 1.0 (e.g., Acharya et al. 2011). Based on all these factors, a ratio of 0.49, relating the increase in April–July streamflow to the increase in 1 May SWE, is used to calculate seeding effects on streamflow.

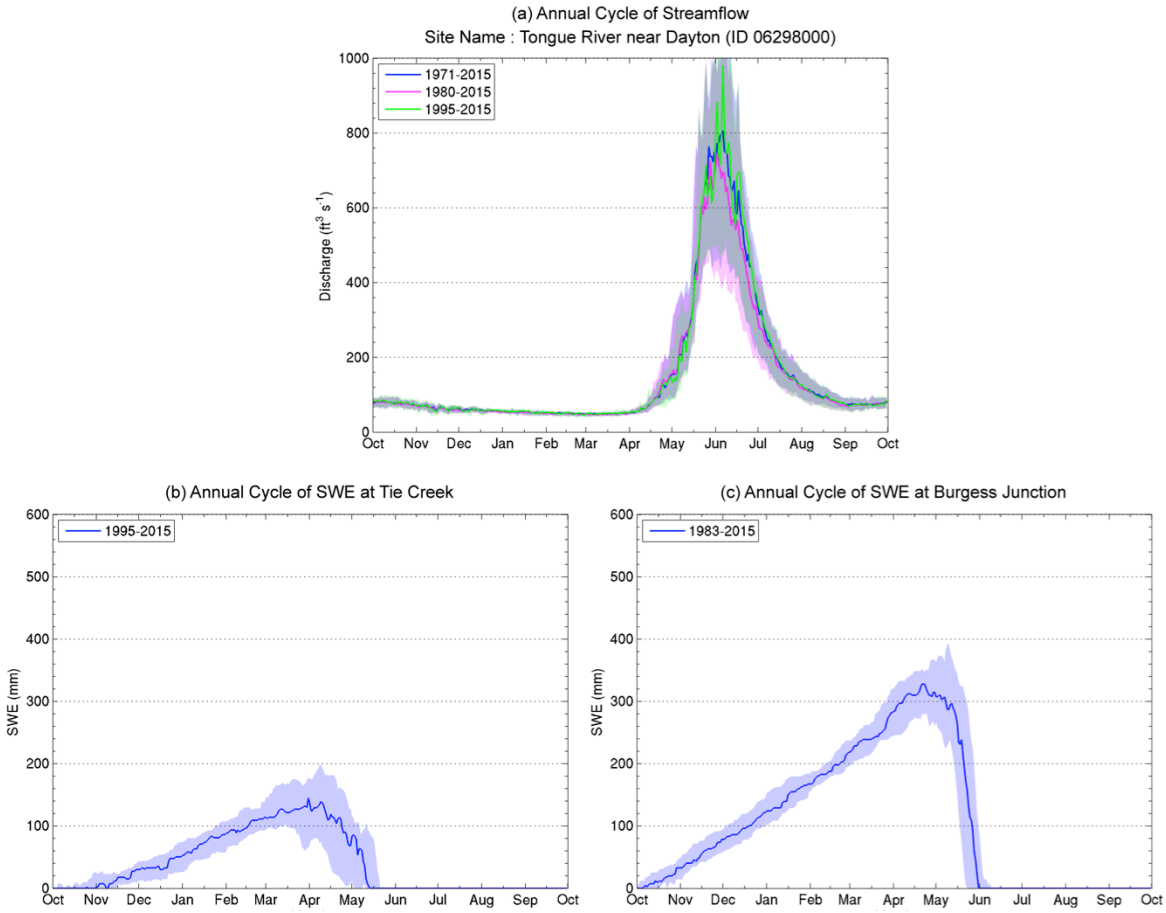


**Figure 12.8. Same as Figure 12.6 but for (a) the streamflow measurements at Tongue River near Dayton and SNOTEL SWE measurements at (b) Tie Creek and (c) Burgess Junction.**

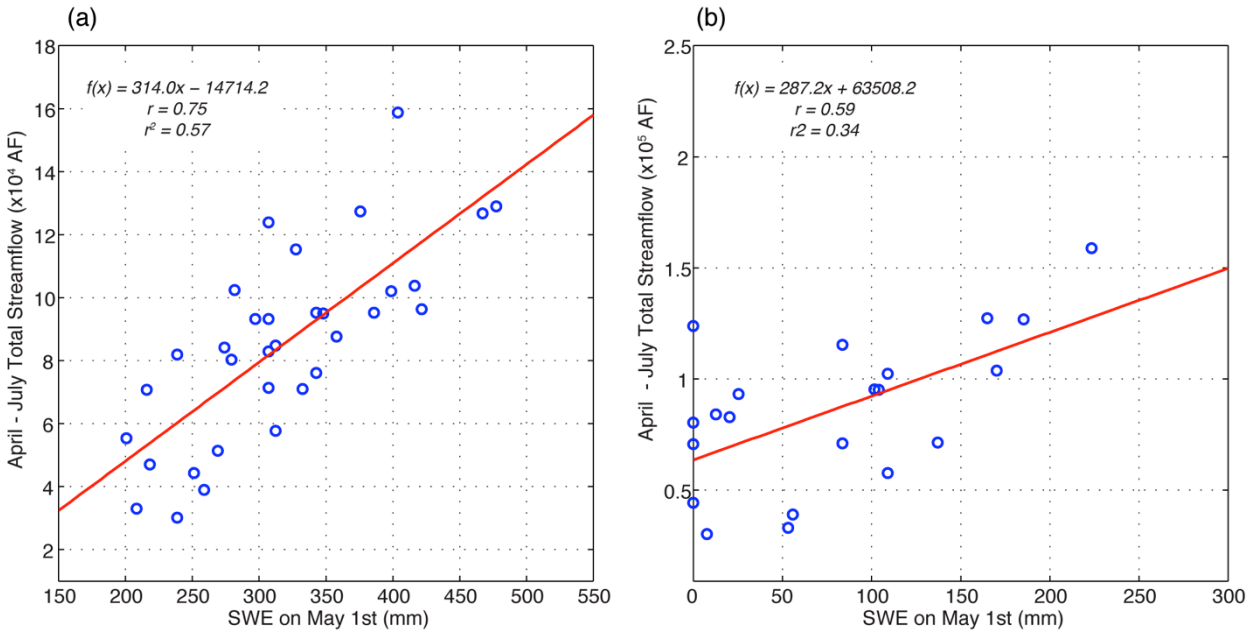


**Figure 12.9. Same as Figure 12.7 but for the (a) Tongue River streamflow gauge and Burgess Junction SNOTEL SWE, and (b) Tongue River streamflow gauge and Tie Creek SNOTEL SWE.**

**Table 12.4. Summary of relation between the April – July streamflow and the 1 May Snowpack from each pairs of streamflow gauge and SNOTEL site. Total annual runoff, average seasonal runoff and mean 1 May Snowpack are data values averaged over the regression period. Dry and wet season streamflow are determined from the best-fit equation shown in Figure 12.9. Ratio of % change in streamflow to % change in snowpack (in bold) are based on the "Dry" and "Wet" season streamflow estimates.**

| Streamflow gauges | Shell Creek | Tongue River | Tongue River |
|---|---|---|---|
| Snow sites used in the regression equation | Shell Creek SNOTEL | Tie Creek SNOTEL | Burgess Junction SNOTEL |
| Regression period | 1980–2015 | 1999–2015 | 1983–2015 |
| Correlation (R value) | 0.65 | 0.75 | 0.59 |
| Ratio of % change in streamflow to % change in snowpack: | **0.78** | **0.26** | **1.17** |
| Total Runoff (AF) | 22,274 | 118,352 | 117,026 |
| Average Seasonal Runoff (AF) | 19,536 | 86,054 | 85,069 |
| Dry Season Streamflow (75% of mean snowpack) (AF) | 15,729 | 80,418 | 60,123 |
| Wet Season Streamflow (150% of mean snowpack) (AF) | 27,150 | 97,327 | 134,960 |
| Mean SNOTEL Snowpack on 1 May (mm) | 425.8 | 78.5 | 317.8 |

## 12.3 Other parameters for Estimating Seeding Effects

### *12.3.1 Seasonal Percentage of Seedable Snowpack*

Results from seeding project evaluations have sometimes been interpreted incorrectly because of differences in the methods of estimating seeding effects. Some report seasonal seeding impacts, which are appropriate if the measurement is a seasonal or integrated value such as with streamflow gauge data and 1 May SWE measurements. Experimental seeding projects usually measure precipitation in some form on a case-by-case basis, such as with the Bridger Range Experiment, SPERP, and the WWMPP. When using results from these types of seeding evaluations to estimate seeding impacts on seasonal snowpack, it is necessary to also assess how often the experimental seeding events occur in a season or how much precipitation falls during "seedable" conditions. A climatological evaluation of a project design needs to include a parameter that translates seeding events or seedable conditions into a seasonal estimate.

Section 4.4 provides this parameter for the Bighorn Mountains. For ground-based seeding using the western region, seedable conditions occurred during periods accounting for 19% of the total winter (November–April) precipitation on average for the 8-yr climatology. For comparison, airborne seeding conditions over the same region occurred during periods

affecting 39% of the total precipitation. In the more restrictive seeding criteria of the WWMPP, about 30% of the total precipitation occurred during seedable conditions (Ritzman et al. 2015). If a combined airborne and ground-based seeding program were utilized, 47% of precipitation would be seedable. For the calculations used in estimating the streamflow changes due to seeding, each of these values for a ground-based, airborne-based, and combination program was determined from the climatological analysis.

### *12.3.2 Areal Coverage*

If the technique for estimating seasonal snowpack changes from seeding is based upon measuring the impact at a single point (as was the case for the WWMPP analysis), then a factor for areal coverage of the seeding impacts is required. This is because the response variable (i.e., the measure of the seeding effect) in the WWMPP was determined at basically one measurement point or small area. The areal coverage is then necessary to extrapolate that result to the larger target area. However, if the response variable, and hence the seeding effect, is derived from an areal measurement (i.e., over a target area), such as in the SPERP measurements and analysis or from three-dimensional model simulations, then there is no need to perform the extrapolation. The technique used in this study for estimating streamflow changes is based upon the preliminary WWMPP analysis, given it is an estimate of seeding impacts on a seasonal basis, which is needed for streamflow estimation. The model evaluation performed as part of Task 5 only simulated a few cases, given the resources available to this study, and therefore cannot be utilized directly to estimate streamflow benefits. Since these estimates are based upon the preliminary WWMPP analysis, an areal coverage parameter is needed.

Areal coverage of the Bighorn Mountains target area was approximated from the case-study results of simulated seeding (Section 6). The areal coverage of seeding effects varies across the cases, representing the different seeding conditions. The preliminary WWMPP technique used a range of 30–80% (WWDC 2014). An examination of the case studies in Section 6 show that a reasonable value for coverage of the Bighorn Mountains, in each basin above 8,000 ft, is about 50%, with a range of about 30–80%. In any given case, there may be more impact in one basin compared to another, but for the sake of these calculations, the same impact area is assumed in each basin.

## 12.4 Estimates of Streamflow Changes due to Seeding

The technique used in the draft WWMPP report (WWDC 2014) for calculating streamflow changes is essentially repeated here using the preliminary WWMPP seeding results (5–15% per season relative to seedable storms), but using other parameters specific to the Bighorn Mountains. Although there is a range of possible values, the percentage of precipitation accumulation that occurred when ground-based, airborne, or a combined program seeding criteria existed is assumed to be a fixed 19%, 39%, and 47%, respectively, of seasonal precipitation — the average value from the climatology results (Table 4.6). Similarly, the conversion of precipitation increase to streamflow increase (percentage) is assumed to be fixed at a ratio of 0.49. Parameters that are more variable include the total April–July streamflow into the Bighorn and Powder/Tongue River basins from the Bighorn Mountains (~515,000 AF – Bighorn Basin, ~465,000 AF – Powder/Tongue River basin, see

Table 12.2) and the areal coverage of seeding in the target area (30–80%). The combination of these variables on potential increases in streamflow are illustrated in Figure 12.10. Note that there is a difference in the maximum temperature threshold used in this study (−6 °C) compared to that used in the WWMPP (−8 °C). Since the AgI activation has been shown to be less efficient at warmer temperatures, the seeding effects (i.e., 5–15% per season relative to seedable storms) preliminarily reported by the WWMPP (WWDC 2014) may be greater than what could be realized for cases identified using this warmer temperature threshold. Nonetheless, the warmer temperature threshold allows for many additional cases to be considered seedable (Section 4.4), and if each of those cases also contribute to the seasonal seeding effect, the possible reduced magnitude of seeding effects due to reduced AgI activation efficiency could potentially offset the fact that more cases would be seeded and thereby could accrue similar seasonal results. Nonetheless, this caveat in the analysis should be kept in mind when interpreting the results.

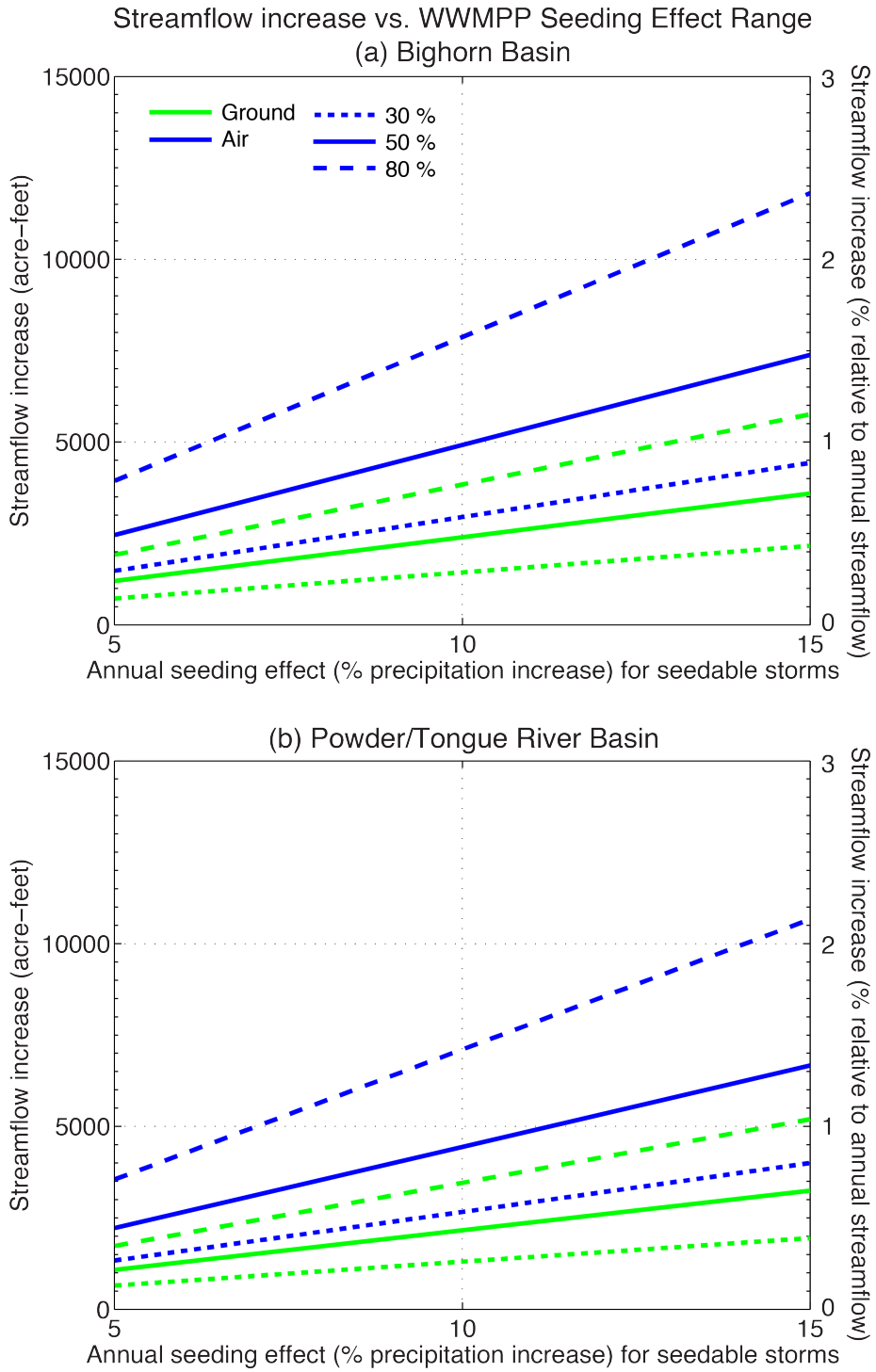


**Figure 12.10. Estimates of streamflow increases in acre-feet (left ordinate) and percent increase relative to annual streamflow (right ordinate) into the (a) Bighorn River Basin and (b) Powder/Tongue River Basin using the levels of seasonal seeding effects for seedable storms from the draft WWMPP report. The streamflow calculations include adjustments to relate the seeding effects to total target area precipitation, which requires an estimate of target area seeding coverage. The streamflow estimates for the various levels of area coverage (30–80%) are denoted by the different linestyles. Different line colors represent the estimates based on a ground-based (green) or airborne-based (blue) seeding program. The 50% area coverage (solid lines) are used for streamflow estimates assumed in the benefit/cost calculations.**

**Table 12.5. Streamflow increase estimates using various seeding impact parameters for a ground-based seeding program (5, 10, 15% seeding effect and 30–80% seeding impact area). *Estimated April–July streamflow increase per basin is provided for the 50% impact area scenario.**

| Method | Seeding Effect Scenario | | |
|---|---|---|---|
| Seeding effect (increase) | 5% | 10% | 15% |
| Seasonal seeding impact (19% seeding precip/total precip) | 0.47% | 0.93% | 1.40% |
| 30% target area coverage | 0.14% | 0.28% | 0.42% |
| *50% target area coverage | 0.23% | 0.47% | 0.70% |
| 80% target area coverage | 0.37% | 0.74% | 1.12% |
| Apr-Jul Streamflow Increase (AF) Bighorn @ 515,000 AF total | 1199 | 2397 | 3596 |
| Apr-Jul Streamflow Increase (AF) Powder/Tongue @465,000 AF total | 1082 | 2165 | 3247 |

**Table 12.6. Same as Table 12.5, except for an airborne seeding program.**

| Method | Seeding Effect Scenario | | |
|---|---|---|---|
| Seeding effect (increase) | 5% | 10% | 15% |
| Seasonal seeding impact (39% seeding precip/total precip) | 0.96% | 1.91% | 2.87% |
| 30% target area coverage | 0.29% | 0.57% | 0.86% |
| *50% target area coverage | 0.48% | 0.96% | 1.43% |
| 80% target area coverage | 0.76% | 1.53% | 2.29% |
| Apr-Jul Streamflow Increase (AF) Bighorn @ 515,000 AF total | 2460 | 4921 | 7381 |
| Apr-Jul Streamflow Increase (AF) Powder/Tongue @465,000 AF total | 2222 | 4443 | 6665 |

**Table 12.7. Same as Table 12.5, except for a combined ground and airborne seeding program.**

| Method | Seeding Effect Scenario | | |
|---|---|---|---|
| Seeding effect (increase) | 5% | 10% | 15% |
| Seasonal seeding impact (47% seeding precip/total precip) | 1.15% | 2.30% | 3.45% |
| 30% target area coverage | 0.35% | 0.69% | 1.04% |
| *50% target area coverage | 0.58% | 1.15% | 1.73% |
| 80% target area coverage | 0.92% | 1.84% | 2.76% |
| Apr-Jul Streamflow Increase (AF) Bighorn @ 515,000 AF total | 2965 | 5930 | 8895 |
| Apr-Jul Streamflow Increase (AF) Powder/Tongue @465,000 AF total | 2677 | 5354 | 8032 |

# 13. Task 12: Cost Estimates

The costs for an operational winter orographic cloud-seeding program designed to increase snowpack in the Bighorn Mountains of Wyoming would depend upon the following considerations:

- the portions of the range targeted;
- the number of ground-based IN generators deployed (Sections 6 and 7);
- annual program duration (when seeding starts and stops each season);
- service contract duration (the number of operational seasons);
- whether to use ground-based or airborne seeding;
- whether or not the project is conducted via contract with a commercial operator, in-house (by the sponsor(s), or a blend of the two; and
- sharing operational resources with other cloud seeding programs.

The details and scope of each of these is discussed in the following sections.

## 13.1 Project Scope

The most direct approach to estimating project cost is to consider the entire mountain range for the predominant flow regimes (wind conditions) identified in Section 4, in which the project scope will match that defined in Sections 5 and 6. However, it is feasible to reduce the scope of the project and still develop an effective cloud-seeding program that would target a smaller portion of the range, which would likely be less expensive. For the sake of these cost projections, the full mountain range will be considered, with generator groups C, D, E, and F deployed for a total of fifteen generators.

## 13.2 Deployment of Ground-based Ice Nucleus Generators

The deployment cost for fifteen ground-based IN generators will depend upon the following:

A. Whether the generators are leased or purchased, and whether the generators will be manually operated, remotely controlled, or a mix of the two. Given the locations of the generators proposed herein, manual operation is not considered a viable option, so this cost estimate assumes all fifteen will be remote-controlled units. For these cost estimates, the IN generators are assumed to be leased, rather than purchased.

B. The amount of seeding agent and other consumables (nitrogen, propane) used by each IN generator, which will vary depending upon the number and duration of the seeding opportunities. For these cost estimates, a frequency and duration of operations similar to that observed in the nearby Wind River Range is assumed, approximately 85 hours of seeding, per generator, per season.

C. The scope of the service and maintenance requirements for the IN generators. Based on previous cloud-seeding operations in the Wind River Range, it is evident that a team of two technicians can keep a large number of IN generators operating through an entire season. Therefore, this cost estimate assumes that one team will service all the generators.

   A final cost consideration is a requirement that special-use permits must be obtained for any equipment placed on Federally owned lands. Since a majority of

the fifteen ground-based generator sites identified are on Federal lands, these permits must be acquired. This process is described in Section 8. For a project being considered in proximity to designated wilderness areas, it can be expected that a NEPA impact assessment (i.e., EA or EIS) would be required, thus resulting in additional project costs. Depending on the type of environmental assessment to be completed, a front-end, one-time expense ranging from about $200,000 (for an EA) to approximately $750,000 (for an EIS) should be considered as part of the overall cost for a ground-based program. However, because the NEPA assessment is a one-time expense, it is not included in the cost estimates presented later in this section.

## 13.3 Length of Program Season

The duration of a winter seeding season is largely determined by the climatology (Section 4). Typically the beginning of the season is determined when cloud temperatures become cold enough to allow glaciogenic seeding to produce snow, as defined by a temperature criterion of −6 °C (Section 9). Likewise, the end of the season is determined by the typical date when the orographic clouds are no longer routinely cold enough.

In Section 9, it is noted that seeding opportunities in the Wind River Range typically end by early or mid-April. Given that the Wind River Range and Bighorn Mountains are similar in elevation (and therefore cloud temperatures), it is reasonable to believe that seeding seasons will be similar. This being the case, cost for a season duration of five months is presented.

## 13.4 Airborne Seeding

Recent investigations have found that winter orographic seeding via aircraft can often be effective when ground-based seeding is not (Xue et al. 2016, Geresdi et al. 2016). Thus, airborne seeding can effectively increase the window of opportunity.

A few winter programs in the western U.S. utilize airborne seeding only (e.g., the Northern California Power Association and the Sacramento Municipal Utilities District). The implementation of an aircraft-only program removes concerns regarding the deployment of or access to ground-based seeding equipment, and any of the logistics and costs associated with siting.

However, aircraft operations are expensive. Not only must the aircraft be leased and configured for seeding, but the flight crew must be trained for the work. To determine if the inclusion of airborne seeding is an economically viable option, the storm climatology of the region is used to identify the frequency of situations when the lower atmosphere is marked by stability or temperature inversions sufficient to inhibit effective targeting with ground-based generators. In addition, there may be situations when SLW is present in locations otherwise suitable for seeding, but exists at altitudes higher than can be reliably targeted with ground-based facilties.

For the cost estimates presented in Table 13.1, a single, piston-engine aircraft certified for flight in known icing conditions is considered. Such an aircraft would be operated by a crew

of two for 125 flight hours. Seeding agent (pyrotechnics) required for the 125 flight hours is estimated. Fuel and hangar costs are also included.

**Table 13.1. Estimated Operational Costs of Possible Five-Month Programs for the Bighorn Mountains.**

| | | *Remote-Controlled Generators (15)* | *Airborne Seeding One Aircraft*[4] |
|---|---|---|---|
| ***Deployment***[1] | ***Personnel*** | *$20,580* | *$4,641* |
| | ***Direct Costs*** | *$3,865* | *$3,844* |
| ***Operations***[2] | ***Personnel*** | *$235,400* | *$180,400* |
| | ***Direct Costs*** | *$114,025* | *$101,200* |
| ***Expendables and Other Reimbursable Costs***[3] | | *$106,185* | *$62,336* |
| ***Estimated Totals*** | | ***$479,655*** | ***$352,421*** |

[1] *Initial deployment costs for ground-based operations amortized over five seasons*
[2] *Assumes an average of 85 hours per generator for the ground-based seeding program*
[3] *Seeding agents, propane, aircraft fuel, etc., as applicable*
[4] *Assumes an average of 80 flares of each type, each month, 25 flight hours per month*

For a purely operational program using only remotely controlled ground-based IN generators, the estimated annual costs for a typical season are approximated at $480,000. For an airborne program using a single twin-engine seeding aircraft, costs would run just over $350,000. Both cost estimates are based on current costs for labor, fuel, seeding agents, and other expendables. The seasonal window of opportunity has been shown to be longer for an airborne program (Section 4.3.1), such that an airborne program could be conducted for six months. Adding an additional month of aircraft seeding would increase the cost of the program by approximately $69,000.

## 13.5 Possible Cost Savings

Costs presented here reflect all aspects of an operational program, and do not consider any of the various avenues through which savings might be realized. There are several means by which a program could potentially cut costs, and those options are explored in the sections that follow.

### *13.5.1 Sharing Operational Resources*

If there are other cloud-seeding programs operating in the vicinity, collaboration and cooperation with those projects could result in significant savings. For example, if the general weather patterns and storm events have similar timing, then the same meteorological support established for one program might service both. Since the majority of weather datasets used to predict, initiate, and terminate seeding events are readily available through the Internet, utilizing meteorological support teams to forecast for more than one project and/or target area is reasonable.

Similarly, current operational programs have shown that a single team of field technicians can support up to two dozen or more IN generators, providing they are not too widely spaced geographically. Thus, depending upon the number of generators operated by adjacent projects, it may make considerable sense to share technicians between programs for IN generator service and maintenance calls.

Sharing an aircraft between adjacent programs could also be a feasible source of cost savings; however, only if the storm systems move through the broader region in a way that yields seeding opportunities in a sequential order between the various target areas. In contrast, if seeding opportunities among the adjacent target areas always occur simultaneously, then multiple aircraft would be needed to be able to target them all at the same time.

### *13.5.2 The Number of Operational Seasons*

A cost savings can also be realized as the number of operational project seasons increase. Multi-season projects can be conducted more affordably than single-season projects for two reasons. First, a company contracted to conduct or assist with the program will know the engagement is longer than just a season, and can manage its resources accordingly. Resources include both physical resources, such as the IN generators, vehicles, and shops, as well as the seasonal project personnel. In general, the longer the project (contract), the greater are the savings. Secondly, expenses are spared when consumables not used during one season can be carried over to the next. Typically, this includes seeding agent, propane, nitrogen, and helium (if rawinsondes are part of the project). Another advantage to the multi-season project is that as project personnel expertise (e.g., local weather forecasting, knowledge of terrain, project logistics, etc.) increases from season to season, the efficiency and effectiveness of the program can be expected to increase. In the end, the longer a project (contract) is executed, the greater the potential savings.

### *13.5.3 Project Implementation Mode*

There are two methods of program implementation. One is to hire an experienced firm to provide the equipment, personnel, and consumables to conduct the cloud-seeding project. The other is for the project sponsors to purchase and/or construct the requisite equipment and consumables, and train their own personnel to conduct operations. A third option would be a blend of the two; to contract out certain project aspects while implementing other project activities "in house." A comparison of the pros and cons of the first two approaches is provided in Table 13.2.

The cost estimates presented in Table 13.2 (columns 1 and 2) are based upon turnkey operations. Columns 3 and 4 are included because significant cost savings can result if the sponsor's infrastructure and staffing allow for the implementation of certain project activities; however, the calculation of such circumstance-specific savings are beyond the scope of this feasibility study.

**Table 13.2. Contracted vs. Self-Run Projects, or Project Components.**

| | Element | Leasing / Hiring | | Purchasing / Self-Service | |
|---|---|---|---|---|---|
| | | 1<br>***Pros*** | 2<br>***Cons*** | 3<br>***Pros*** | 4<br>***Cons*** |
| A | ***Ice Nucleus Generators*** | Consultant in charge of equipment procurement, and/or construction. Consultant provides all technical services (i.e., siting, installation, maintenance, replacement, repair and dismantle services). No additional project sponsor staff is required (staff resource savings). | Lease fees may exceed actual generator purchase costs in long-term. Indirect expenses for technician services (i.e. salary, time, travel, company overhead fees, etc.) are incurred by the funding sponsor. | Purchase expenses will be recouped if equipment is utilized long-term (5 – 7 years, A2). Project sponsor is able to provide all technical services (A1). Indirect expenses (A2) for project sponsor staff are already accounted for. | A long-term cloud-seeding project is required to attain "ower/operator" cost savings. Additional expenses will occur if outside expertise is required to perform any technical services (A1). |
| B | ***Aircraft*** | Consultant responsible for aircraft and associated equipment procurement expenses. Consultant provides all required aircraft services and manpower. Lease fees include actual flight hours, and "stand-by" time. No purchase or installation of seeding equipment fees. No additional "in-house" project sponsor staff is required (staff resource savings). | The deployment costs include the salaries and living expenses for aircraft mechanics, technicans, meteorologists, and pilots), are paid by the funding sponsor | Project sponsor staff is able to provide all required aircraft services. Salaries for specialized professional services (B2), and indirect expenses (B2), are already accounted for. Aircraft can be used for ancillary purposes (i.e., transport) when not employed for cloud seeding. | Project sponsor responsible for aircraft & associated equipment procurement expenses. All aircraft expenses (e.g., "stand-by" fees) are absorbed by the project sponsor, however, if the sponsor regularly stores, operates & maintains aircraft, this may not greatly impact known expenditures. |
| C | ***IN generator Technicians*** | No training required. Technician fees are incurred only while "on project" at a pre-determined rate. No additional "in-house" project sponsor staff is required (staff resource savings). | Indirect expenses for technician services (A2) are incurred by the funding sponsor. | Project sponsor staff is able to provide all technical services (A1). Indirect expenses for project sponsor staff are already accounted for (A2). | Additional expenses will occur if outside expertise is required to perform any technical services (A1). Project sponsor staff workloads may increase. |

| | | | | | |
|---|---|---|---|---|---|
| D | ***Forecasting and Seeding Operations*** | Consultant meteorologist is able to perform required services, and posseses local weather expertise. Meteorologist expenses are incurred only while "on project" at a pre-determined rate. No additional "in-house" project sponsor staff is required (staff resource savings). Indirect expenses for meteorological services can be reduced if forecasting support is provided "off site" via the Internet. "On-site" expenses (lodging, per diem) are not incurred. | Indirect expenses for meteorological services are incurred by the funding sponsor (A2). A lack of local weather expertise may result in additional operational expenses. | Project sponsor meteorologist is able to perform required services and posseses local weather expertise. Indirect expenses for meteorological staff are already accounted for (A2). | Additional expenses will occur if outside expertise is required to perform any meteorological services. A lack of local weather expertise may result in additional operational expenses. Project sponor staff workloads may increase. |
| E | ***Radiometer*** | Consultant absorbs all equipment purchase expenses. Consultant provides all technical services (A1). No additional "in-house" project sponsor staff is required (staff resource savings). | Lease fees may exceed actual radiometer purchase cost in long-term. Indirect expenses for technician services (A2) are incurred by the funding sponsor. | Purchase expenses will be recouped if equipment is utilized long-term (~5 years). Project sponsor is able to provide all technical services (A1). Indirect expenses (A2) for project sponsor staff are already accounted for. | Project sponsor responsible for purchase of equipment. A long-term cloud-seeding project is required to attain "ower/operator" cost savings. Additional expenses will occur if outside expertise is required to perform any technical services (A1). |
| F | ***Rawinsondes*** | Consultant absorbs all equipment purchase expenses. Consultant provides all technical services (A1). No additional project sponsor staff is required (staff resource savings). | Lease fees may exceed actual sounding equipment purchase costs (i.e., calibration box and receiver) in long-term. Indirect expenses for technician services (A2) are incurred by the funding sponsor. | Purchase expenses will be recouped if equipment is utilized long-term (~5 years). Project sponsor is able to provide all technical services (A1). Indirect expenses (A2) for project sponsor staff are already accounted for | Project sponsor responsible for purchase of equipment. A long-term cloud-seeding project is required to attain "ower/operator" cost savings. Additional expenses will occur if outside expertise is required to perform any technical services (A1). |

## 13.6 Water Quantity, Use, and Value

### *13.6.1 Wind/Bighorn Basin*

The Bighorn Mountains provide a large fraction of the water in the Wind and Bighorn Basins to the west. The most recent document regarding these basins is the Wind/Bighorn Basin Plan Update (MWH Americas *et al*. 2010). This report provides the most current numbers available on water use for these basins.

Table 13.3 provides the water use, by category, for the Wind/Bighorn Basin. Agricultural use, primarily irrigation, accounts for most of it, both for diversion and consumptive use. The second greatest use (loss) is evaporation from the reservoirs.

**Table 13.3. Summary of Current (2010) Water Use by Category[4]**

| | ***Diversion (acre-feet)[1]*** | | ***Consumptive Use*** | |
|---|---|---|---|---|
| ***Water Use*** | ***Acre-feet*** | ***% of Total*** | ***Acre-feet*** | ***% of Total*** |
| ***Agricultural (Irrigation)*** | 3,136,728 | 92% | 1,079,971 | 85% |
| ***Stock Water[2]*** | 6,370 | 0.20% | 6,370 | 0.50% |
| ***Municipal/Domestic[3]*** | 21,324 | 1% | 8,743 | 1% |
| ***Industrial/Mining*** | 91,906 | 3% | 19,163 | 2% |
| ***Reservior Evaporation*** | 156,157 | 5% | 156,157 | 12% |
| ***Total*** | *3,412,485* | *100%* | *1,270,404* | *100%* |

*[1]includes both surface water and ground water use.*
*[2]Consumptive use not calculated for stock water use.*
*[3]A range of municipal/domestic water use was determined. Calculations performed using an average of the range.*
*[4]Table from the Wind-Bighorn Basin Water Plan Update (MWH Americas et al. 2010)*

Table 13.4 provides the annual streamflow by sub-basin for the Wind/Bighorn Basin. Note that the flow at Bighorn River at Kane is not entirely from the Bighorn Mountains, but also comes from other upwind areas to the west and south[8] (Figure 13.1).

[8] It should also be noted that the Bighorn River flows from south to north.

**Table 13.4. Summary of Natural Annual Streamflows by Sub-basin, Wind/Bighorn.**

| *Sub-Basin* | *USGS Gauge No.* | *Site Name* | *Period of Record* | *Average Annual Flow (AF)* |
|---|---|---|---|---|
| ***Nowood*** | | No current gauges | | |
| ***Bighorn Lake*** | 06278300 | Shell Creek Above Shell Creek Reservoir, Wyo. | Oct 1956 - Present | 22,906 |
| | 06278500 | Shell Creek Near Shell, Wy | Oct 1940 - Present | 85,940 |
| | 06279500 | Bighorn River At Kane, Wy | Oct 1928 - Present | 1,431,787 |

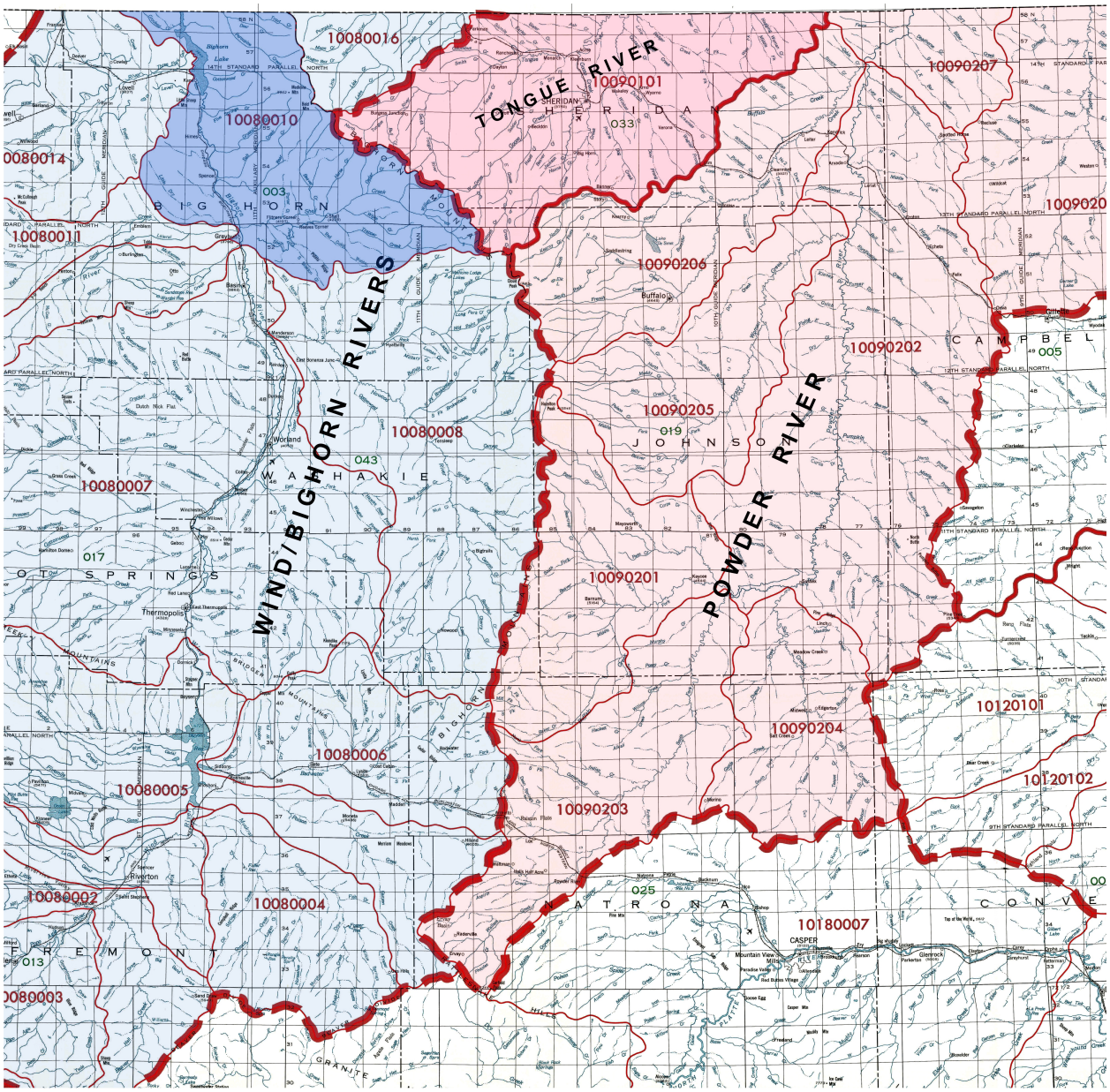


**Figure 13.1. Map of the river basins, and their respective sub-basins, surrounding the Bighorn Mountains. The Powder/Tongue Basin is in shades of pink, while the Wind/Bighorn Basin is in shades of blue. The darker blue shaded sub-basin is the Bighorn Lake drainage (that includes Shell Creek), while the darker pink shaded sub-basin is the Tongue River drainage. Streamflow gauges in each of these sub-basins were utilized in the hydrological assessment.**

### *13.6.2 Powder/Tongue River Basin*

The Bighorn Mountains provide a substantial fraction of the water in the Tongue and Powder River basins to the east as well (Figure 13.1). The most recent document regarding these basins is the Powder/Tongue River Basin Plan Final Report (HKM Engineering Inc. *et al.* 2002). This report provides the most current numbers available on water use for the Tongue and Powder River drainages (Table 13.5 and Table 13.6). The report provided streamflow at key gauges, with the driest 20 percent of years are considered dry years, the

wettest 20 percent of years are considered wet years, and the middle 60 percent of years are considered average years (Table 13.6).

**Table 13.5. Summary of Current (2002) Water Use By Category[1]**

| *Acre-feet per Year* | | |
|---|---|---|
| ***Water Use*** | ***Surface Water (AF)*** | ***Ground Water (AF)*** |
| ***Agricultural (Irrigation)*** | 184,000 | 200 |
| ***Municipal*** | 2700 | 500 |
| ***Domestic*** | 0 | 4,400 |
| ***Industrial/Mining*** | 0 | 68,000 |
| ***Reservoir Evaporation*** | 11,300 | -- |
| ***Total*** | *198,000* | *73,100* |

[1]After the Powder/Tongue River Basin Water Plan Final Report (HKM Engineering *et al*. 2002)

**Table 13.6. Summary of Natural Annual Streamflows by Sub-basin, Powder/Tongue.**

| ***Basin*** | ***USGS Gauge No.*** | ***Site Name*** | ***Gauged Annual Flow (acre-feet)[1]*** | | |
|---|---|---|---|---|---|
| | | | ***Dry*** | ***Average*** | ***Wet*** |
| ***Little Bighorn*** | 6288600 | Little Bighorn River below Dayton Gulch near Burgess Junction, WY | 9,348 | 14,937 | 19,851 |
| | 6288700 | Dry Fork Little Bighorn River below Lick Creek near Burgess Junction, WY | 25,935 | 35,720 | 46,785 |
| | 6288960 | Little Bighorn River near Parkman, WY | 61,087 | 88,877 | 122,841 |
| | 6288975 | Elkhorn Creek above Fuller Ranch Ditch near Parkman, WY | 1,621 | 2,213 | 3,196 |
| | 6288990 | West Fork Little Bighorn River near Parkman, WY | 13,505 | 19,677 | 28,152 |
| | 6289000 | Little Bighorn River at State Line near Wyola, MT | 80,523 | 112,704 | 152,367 |
| | 6289100 | Red Canyon Creek near Parkman, WY | 689 | 1,304 | 2,263 |
| | 6289800 | East Pass Creek near Parkman, WY | 7,524 | 9,211 | 10,995 |
| | 6291200 | Lodge Grass Creek at State Line near Wyola, MT | 10,349 | 14,620 | 19,456 |
| | | ***Subtotals, Little Bighorn Basin*** | ***210,581*** | ***284,326*** | ***405,906*** |
| | | | | | |
| ***Tongue*** | 6297000 | South Fork Tongue River near Dayton, WY | 38,639 | 53,216 | 77,970 |
| | 6297480 | Tongue River at Tongue Canyon Campground near Dayton, WY | 100,258 | 128,419 | 168,195 |
| | 6298000 | Tongue River near Dayton, WY | 103,051 | 131,306 | 168,904 |
| | 6298480 | Little Tongue River at Steamboat Point near Dayton, WY | 5,073 | 6,819 | 10,367 |
| | 6298490 | Little Tongue River above South Fork Little Tongue River near Dayton, WY | 3,639 | 5,427 | 8,538 |
| | 6298500 | Little Tongue River near Dayton, WY | 7,811 | 10,372 | 15,626 |
| | 6299480 | Wolf Creek below Alden Creek near Wolf, WY | 15,122 | 19,909 | 29,311 |
| | 6299490 | Wolf Creek above Red Canyon Creek near Wolf, WY | 15,089 | 19,565 | 28,664 |
| | 6299500 | Wolf Creek at Wolf, WY | 15,331 | 19,746 | 28,171 |
| | 6300500 | East Fork Big Goose Creek near Big Horn, WY | 18,042 | 22,980 | 32,133 |
| | 6301480 | Coney Creek above Twin Lakes near Big Horn, WY | 2,746 | 3,548 | 4,987 |

| | | | | | |
|---|---|---|---|---|---|
| | | ***Subtotals, Tongue River Basin*** | ***324,801*** | ***421,307*** | ***572,866*** |
| | | | | | |
| ***Powder*** | 6309200 | Middle Fork Powder River near Barnum, WY | 12,754 | 20,805 | 32,117 |
| | 6309260 | Buffalo Creek above North Fork Buffalo Creek near Arminto, WY | 1,294 | 2,429 | 4,070 |
| | 6309270 | North Fork Buffalo Creek near Arminto, WY | 2,284 | 3,639 | 5,518 |
| | 6309280 | Buffalo Creek below North Fork Buffalo Creek near Arminto, WY | 1,067 | 2,700 | 5,612 |
| | 6309450 | Beaver Creek below Bayer Creek near Barnum, WY | 3,060 | 5,106 | 7,634 |
| | 6309460 | Beaver Creek above White Panther Ditch near Barnum, WY | 7,882 | 10,154 | 13,553 |
| | 6311000 | North Fork Powder River near Hazelton, WY | 7,867 | 11,173 | 16,167 |
| | 6313950 | North Fork Crazy Woman Creek below Pole Creek near Buffalo, WY | 13,847 | 17,873 | 24,544 |
| | 6314000 | North Fork Crazy Woman Creek near Buffalo, WY | 13,744 | 17,577 | 24,767 |
| | 6314500 | North Fork Crazy Woman Creek below Spring Draw near Buffalo, WY | 15,483 | 22,032 | 32,766 |
| | 6315480 | Poison Creek Below Tetley Spring near Mayoworth, WY | 3,766 | 4,508 | 5,530 |
| | 6315490 | Poison Creek near Mayoworth, WY | 4,195 | 4,954 | 5,997 |
| | 6315500 | Middle Fork Crazy Woman Creek near Greub, WY | 15,009 | 19,565 | 25,906 |
| | 6317300 | Sourdough Creek near Buffalo ,WY | 1,545 | 2,504 | 3,462 |
| | 6317340 | Little Sourdough Creek near Buffalo, WY | 314 | 668 | 1,242 |
| | 6319470 | South Rock Creek at Forest Boundary near Buffalo, WY | 11,594 | 16,268 | 23,106 |
| | 6319480 | South Rock Creek abovev Red Canyon near Buffalo, WY | 11,288 | 15,949 | 22,788 |
| | 6321500 | North Piney Creek near Story, WY | 21,400 | 30,217 | 40,490 |
| | | ***Sutotals, Powder River Basin*** | ***148,393*** | ***208,121*** | ***295,269*** |

[1]Dry years are the lowest 20%, average years the middle 60%, and wet years the top 20%. Data from HKM Engineering et al. (2002).

### *13.6.3 The Value of Water near the Bighorn Mountains*

The value of water in the region varies considerably. According to the Bureau of Reclamation (Myler 2016), water from Boysen Reservoir is sold for irrigation, when available, on a one-year temporary basis, for $3.10/AF, with a minimum purchase of $400. Water for municipal and industrial uses is more representative of costs elsewhere in Wyoming, at $40/AF, again with a minimum purchase of $400. The latter is quite consistent with the range of $30–$50/AF found elsewhere in Wyoming. Boysen Reservior is a federally owned facility, whereas there are other non-federally owned facilities providing water at a much higher cost to the consumer. For example, a contract for water from Park Reservoir, near Sheridan, WY, presently sells at $4,200/AF. In this example, the high cost is not an annual fee, but rather a fee for use in perpetuity. While these numbers cannot be reasonably used to calculate cost-benefits, they do help to understand the variability in the cost of water. Nonetheless, for the purposes of this study, typical water costs ranging from $30 - $50/AF will be assumed.

# 14. Task 13: Preliminary Cost/Benefit Analyses

The ASCE Guidelines for Cloud Seeding to Augment Precipitation (2006) provides a discussion of feasibility studies that are recommended to be conducted prior to the initiation of an operational cloud-seeding program. The Guidelines suggest that two major questions need to be answered: 1) Is the program technically feasible, and 2) Is the program economically feasible? Both of these questions need to be answered in the affirmative for the program to be considered feasible. Evaluating the economic feasibility of a program can best be done by considering the potential benefit compared to the estimated cost of providing this benefit (i.e., the common benefit/cost ratio). For example, if the estimated additional streamflow produced through cloud seeding costs $5/AF and the value of this water to the primary users (there can be secondary and tertiary beneficiaries) is $20/AF, then a 4/1 ratio is the result; stated more pragmatically, a potential for $4 in return for each dollar spent. The ASCE Guidelines recommend that a target benefit-to-cost ratio should be ~ 5/1. The following will examine some preliminary benefit/cost estimates.

Section 12 of this report contains three estimates of the potential average increases in April–July runoff from the proposed Bighorn Mountains target area into the Bighorn and Powder/Tongue River basins separately. Considering the costs for the program are the same for (and shared by) each basin, basin-combined estimates of streamflow increases going forward are provided. Therefore, a combined estimate of streamflow increase (using a 50% impact area) for a ground-based seeding program range from ~2,300 AF to ~6,800 AF. For airborne seeding, the estimates in potential streamflow increase (using a 50% impact area) range from ~4,700 AF to ~14,000 AF. Note that the airborne seeding impact area is often between 50–80%, and therefore using an impact area of 80%, the basin-combined potential estimated streamflow increase from airborne seeding was between ~7,500–22,500 AF.

## 14.1 Value of Augmented April-July Streamflow

Assuming a value of water between $30–$50/AF, various benefit/cost ratios can be established for the ground versus airborne program scenarios. Table 14.1 and Table 14.2 illustrate the various program costs required to meet different benefit/cost ratios assuming water costs $50/AF. If water costs are higher, then the program can cost more and still meet recommended benefit/cost ratios. To achieve the 5/1 ratio recommended by the ASCE Guidelines, a ground-based seeding program would need to cost less than $68,000 and achieve a streamflow increase of 6,800 AF. For an airborne seeding program (assuming a 50% impact area) to achieve the 5/1 recommended ratio, it must cost less than $140,000 and provide a streamflow increase of 14,000 AF. Given the operational cost estimates provided in Section 13, none of these programs meet the 5/1 ratio. However, an airborne seeding program assuming an 80% impact area can produce an increase in streamflow (up to 22,500 AF) that meets the 5/1 ratio, if the program costs approximately $225,000 (Table 14.3).

Table 14.1. Cost of a Ground-based Program to Generate Different Benefit/Cost Ratios, assuming a water cost of $50 and impact area of 50%.

| Benefit/Cost Ratio | Cost of Program With 2,300 AF Increase | Cost of Program With 4,600 AF Increase | Cost of Program With 6,800 AF Increase |
|---|---|---|---|
| 2/1 | $57,500 | $115,000 | $170,000 |
| 3/1 | $38,333 | $76,667 | $113,333 |
| 4/1 | $28,750 | $57,500 | $85,000 |
| 5/1 | $23,000 | $46,000 | $68,000 |

Table 14.2. Cost of an Airborne Program to Generate Different Benefit/Cost Ratios (assuming $50 water cost and 50% impact area).

| Benefit/Cost Ratio | Cost of Program With 4,700 AF Increase | Cost of Program With 9,400 AF Increase | Cost of Program With 14,000 AF Increase |
|---|---|---|---|
| 2/1 | $117,500 | $235,000 | $350,000 |
| 3/1 | $78,333 | $156,667 | $233,333 |
| 4/1 | $58,750 | $117,500 | $175,000 |
| 5/1 | $47,000 | $94,000 | $140,000 |

Table 14.3. Cost of an Airborne Program to Generate Different Benefit/Cost Ratios (assuming $50 water cost and 80% impact area).

| Benefit/Cost Ratio | Cost of Program With 7,500 AF Increase | Cost of Program With 15,000 AF Increase | Cost of Program With 22,500 AF Increase |
|---|---|---|---|
| 2/1 | $187,500 | $375,000 | $562,500 |
| 3/1 | $125,000 | $250,000 | $375,000 |
| 4/1 | $93,750 | $187,500 | $281,250 |
| 5/1 | $75,000 | $150,000 | $225,000 |

## 14.2 Cost per Acre-Foot Estimates

The total cost summary from Table 13.1 for the remote generator and aircraft seeding options is reproduced in Table 14.4, along with the estimated program costs per acre-foot. The estimated costs per acre-foot are also illustrated in Figure 14.1. Based on the estimated operational program cost of $479,655 (Table 13.1) and assuming a cost of water at $50/AF, a ground-based seeding program would not be cost effective. This is in large part due to the low percent of seedable precipitation identified in the climatological analysis. An operational airborne program, costing approximately $352,421 (Table 13.1), would meet the 1/1 benefit/cost ratio assuming the annual seeding effect in seedable storms is greater than 10%. As illustrated in Figure 14.1 when the 5/1 line falls into or below the gray shaded area, attaining the 5/1 benefit/cost ratio cannot occur for either program with current water costs ranging from $30–$50/AF. Nonetheless, because the airborne seeding simulations often had impact areas greater than 50%, cost estimates based upon the 80% impact area for airborne seeding are not unrealistic. These results suggest that airborne

seeding would be cost effective at the 3/1 ratio (for water costs of $50 or less) if seeding effects are 15% (seasonally relative to seedable storms; Table 14.3 and Table 14.4). To make such a seeding program more cost effective, sharing operational resources with adjacent cloud-seeding programs would be advised.

**Table 14.4. Annual Costs Breakdown of Seeding Options for the Proposed Bighorn Mountains Winter Cloud-Seeding Program and Estimated Cost/AF of augmented streamflow (using 50% impact area assumption for ground, and both the 50 and 80% assumption for airborne).**

| Item | Remote Generators (15) | Seeding Aircraft (one)—50% area | Seeding Aircraft (one)—80% area |
|---|---|---|---|
| Est. Total Costs (Table 13.1) | $479,655 | $352,421 | $352,421 |
| Est. Cost/AF for 5% Seeding Effect | $210 | $75 | $47 |
| Est. Cost/AF for 10% Seeding Effect | $105 | $38 | $24 |
| Est. Cost/AF for 15% Seeding Effect | $70 | $25 | $16 |

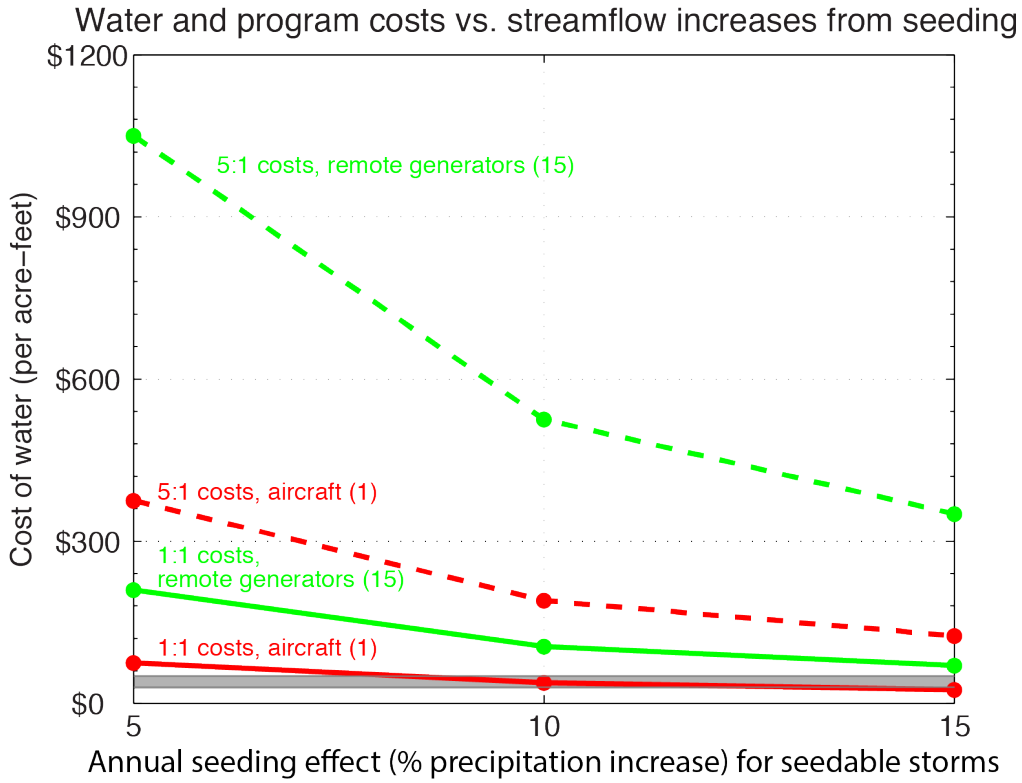


**Figure 14.1. Cost of water for usage categories and for two estimates of annual seeding program costs (using 50% impact area) for the three levels of estimated streamflow increases resulting from WWMPP annual seeding effects for seedable storms (5, 10. 15%; Section 12). Gray shading indicates estimated water costs ($30–$50/AF). The solid green and red lines indicate the cost for the 15 remote generator ground-seeding option versus the single aircraft airborne seeding option, respectively, expressed as program costs per acre-feet of streamflow increase (essentially a 1:1 ratio). The dashed green and red lines show the corresponding 5:1 ratios of water costs to program costs.**

## 14.3 Cost/Benefit Summary Remarks

There are a number of assumptions factored into calculating cost/benefit estimates. Perhaps the most significant assumption is that the seeding program options summarized in Table 14.4 produce the estimated increases in streamflow contained in Section 12. The streamflow estimates from Section 12 are based upon the range of preliminary WWMPP seasonal seeding effects for seedable storms, due to limited resources that prevented simulating seeding effects on a *seasonal* basis explicitly for the Bighorn Mountains seeding program designs that were tested. Moreover, the preliminary WWMPP results are based upon the program design of the WWMPP (i.e., up to eight generators per mountain barrier utilized in a given period). It is quite possible that the seeding effects would have scaled up (or down) with more (or less) generators used. In fact, the preliminary WWMPP results suggest that the number of generator hours impacted the seeding effect results. However, this is not adequately quantified to be able to apply it to this study. Therefore, this study assumes that the range of seeding effects from the draft WWMPP report encompasses the reasonable range of seasonal seeding effects that may be realized by the various program design options summarized in Table 14.4.

Additional assumptions include:

- Consistently being able to obtain the estimated seeding effects provided in Section 12.
- The ratio of the increase in April–July runoff to the increase in winter snowpack is 0.49.
- The value of the augmented streamflow would be $50/AF.
- The cost estimates in Table 14.4 do not provide for any additions to the programs. For example, collecting rawinsonde and radiometer data, the provision of near real-time sophisticated modeling support for identification of "seedable" situations or targeting the AgI nuclei and forecasting potential seeding effects on precipitation, or any evaluation exercises. Any additions of this type or encountering unexpected costs during the performance of the seeding program would lower the calculated benefit/cost ratio information.

Another point to consider is that the calculated values in Table 14.1 and Table 14.2 are for average conditions. Would the benefit/cost ratios rise in above normal years and fall in below normal years? A companion question to this one is whether the seeding increases would remain the same in above and below normal years or if these increases vary. Also, the estimated benefits are primary benefits to identifiable water users in the immediate area. There may be secondary and even tertiary benefits from augmenting precipitation in the Bighorn Mountains. Examples include benefits derived from augmented streamflow that flows out of the Wind/Bighorn River or Powder/Tongue River basins in Wyoming; value to agriculture, industrial and municipal uses; and enhanced hydroelectric generation (a non-consumptive use). Positive impacts may occur in the forests of the intended target areas as well as the enhancement of recreational activities like fishing and boating.

### *14.3.1 Uncertainties in the Analysis*

Given limited resources and/or data availability, the methods utilized in this study have several caveats and inherent uncertainties. Utilizing different methodologies could possibly reduce some of these uncertainties; however, this would primarily depend on the resources available. The following list will itemize the various sources of uncertainty and, when possible, highlight options to reduce the uncertainties.

1) The WRF cloud-seeding parameterization has not been thoroughly verified
    - Specialized data are needed to verify the model parameterization, such as *in situ* cloud physics measurements to measure the effect of AgI on the cloud and samples of Ag in the snow to measure where AgI is reaching the ground in snow.
    - Another option for verifying the cloud-seeding parameterization would be to see if it can successfully simulate the results of the WWMPP randomized experiment. This effort is being conducted as part of the Medicine Bow/Sierra Madre Final Design and Permitting study.
2) Assumed area of seeding impact (30-80% of the target area in this study)
    - Running 3D WRF simulations with the cloud-seeding parameterization can simulate the 3D location and magnitude of the seeding effect, as shown in the case study simulations. If this model were run for a full winter season or, better yet, multiple seasons (to provide a result more representative over time), then the 3D spatial pattern and magnitude of the simulated seeding effect on an annual basis could be estimated, obviating the need for an assumed seeding impact area. The cloud-seeding parameterization uncertainties would still exist without thorough verification as discussed in (1).
3) Assumed range of annual seeding effects on seedable storms from the preliminary WWMPP results (5–15%)
    - By running 3D WRF simulations with the cloud-seeding parameterization for every seeding opportunity over a full winter season or multiple seasons (to provide a result more representative over time), the 3D spatial pattern and magnitude of the simulated seeding effect on an annual basis could be estimated, obviating the need for an assumed range of seeding impacts. The cloud-seeding parameterization uncertainties would still exist without thorough verification as discussed in (1).
4) Assumed fraction of seedable precipitation from climatology analysis, used to calculate the annual snowpack increase using the WWMPP annual seeding effect estimates. This uncertainty has multiple aspects: (i) Is the climatology of "seedable precipitation" representative to calculate annual seeding impacts, especially given that there can be situations when no precipitation fell, but could have been seeded? (ii) The limitation of on station time when seeding with a single aircraft is not addressed in the climatology.
    - By running 3D WRF simulations with the cloud-seeding parameterization for every seeding opportunity over a full winter season or, better yet, multiple seasons (to provide a result more representative over time), where an

automated and objective case-calling algorithm could be used to identify when seedable opportunities occur and then simulate seeding in those cases. This would determine the exact amount of "seedable" opportunities and then explicitly simulate seeding in those identified opportunities, including those that may not have natural precipitation falling otherwise, thereby addressing (4i). Moreover, the case-calling algorithm can account for the limited on station time of an aircraft by only allowing aircraft seeding in limited time intervals, thereby reducing that uncertainty of (4ii) as well. The cloud-seeding parameterization uncertainties would still exist without thorough verification as discussed in (1). Since this would be done to replace an assumption from the climatology analysis, this would definitely need to be run for multiple seasons to avoid one season not being representative of a multi-year average as provided by the current 8-year climatology.

5) Assumed fixed ratio of the increase in streamflow for an increase in snowpack used in hydrological benefits analysis
    - Running a spatially distributed hydrological model coupled to WRF cloud-seeding simulation output would allow the 3D spatial distribution and magnitude of the simulated seeding effects to feed directly into the snowpack used to drive the hydrological model. This would allow the hydrological model to calculate the water balance and routing of the streamflow driven by the snowmelt for every basin in the domain, obviating the need for fixed assumptions across the domain. However, hydrological models also have inherent uncertainties. Access to good streamflow, soil, and land-surface data can help calibrate hydrological models, yet it is still a model and therefore, other uncertainties may still exist, as addressed in (6).
6) General uncertainties in the model simulations
    - Data assimilation techniques can improve model simulations by nudging them toward observations and/or ensemble modeling approaches can characterize and quantify uncertainty in model simulations.

In order to have a more robust understanding of the potential benefits of an operational seeding program targeting the Bighorn Mountains, it would be advised to try to reduce some of these uncertainties, as outlined above.

## 15. Task 14: Reports and Executive Summaries

This task requires preparing digital and paper copies of a final report and executive summary to be provided to the WWDC at the completion of this study. This report serves as the deliverable for this task. An executive summary has also been written that summarizes the purpose, primary results, and recommendations from this study in a short document.

# 16. Task 15: Report Presentations

Presentations on the study were given at several meetings during the project period, including the scoping meeting and two TAT meetings as described in Section 2 (for work under Task 1).

At the conclusion of the study, two public hearings were held pursuant to Wyoming Statute 41-2-114(b)(iii) on 15 and 17 August 2016 in Sheridan and Worland, WY, respectively. The hearings were conducted in order to present the final results of the study, and accept public comment. Ms. Jeni Cederle presided over the meeting, during which NCAR, WMI, and HEC representatives (Drs. Sarah Tessendorf and Roy Rasmussen, Mr. Bruce Boe, and Mr. Patrick Golden) presented results of each study task. During the course of the presentation, the consultants provided clarification and answered technical questions posed by the audience regarding the study results. No substantive public comment (verbal or written) was received for the public record. A list of attendees is included in Table 16.1 and Table 16.2, and the Meeting Notice Card, publication affidavits, agendas, and sign in sheets are included in Appendix B.

Wyoming Statute 41-2-115(a) also requires that the WWDO identify whether or not any person, association or corporation engaged in private enterprise is capable of, and willing to construct, operate and maintain the proposed cloud seeding activities in lieu of the Office doing so. This statutory requirement was addressed at each public hearing, and no interested or capable parties were identified.

In addition to these hearings, a short presentation was given at the TAT meeting on 16 August 2016 in Sheridan, WY.

**Table 16.1. List of attendees (other than presenters) at the results meeting in Sheridan.**

| Name | Agency | | Name | Agency |
|---|---|---|---|---|
| Jeff French | Univ. Wyoming | | Bill Bass | Bighorn National Forest |
| Sheridan Little | WWDC | | T. Carrie Little | WGF Commission |
| Carrie Rogaczewski | Sheridan County Cons. Dist. | | Steve Maier | Sheridan County |
| Jack Landon | | | Jo Fubes | |

**Table 16.2. List of attendees (other than presenters) at the results meeting in Worland.**

| Name | Agency | | Name | Agency |
|---|---|---|---|---|
| David McKamey | Highland Hanover Irrigation Dist. | | Jack Clucas | Basin, WY |
| Kristen Tilley | Shoshone Cons. Dist. | | John Elliott | BLM Worland |
| Phil Blamer | Wyoming SEO | | John Schenerman | Honover Irrigation Dist. |
| Barry Lawrence | WWDO | | | |

# 17. Task 16: Climatological Monitoring of the Study Area

Data that could be used to monitor the climatology of the study area have been collected and archived for the November 2015–April 2016 season. Given the general lack of data for the region, additional instrumentation was also deployed to the Bighorn Mountains for the 2015–2016 season, including a radiometer and high-resolution snow gauges. For the datasets that are publicly available on the internet, URLs to access those data have been provided. For any dataset that is not readily and/or publicly available on the internet (i.e., radiometers and snow gauges), the data files have been provided on a CD-ROM.

## 17.1 Available Datasets on the Internet

The following list provides URLs for the readily available observations and model data sets used in this study.

- SNOTEL precipitation and snowpack measurements
  - Real-time and historical precipitation and snowpack measurements are available at http://www.wcc.nrcs.usda.gov/snow/.
  - Temporal resolution of hourly and daily.
- USGS streamflow records
  - Real-time stream gauge measurements are available at http://waterdata.usgs.gov/wy/nwis/current/?type=flow&group_key=huc_cd
  - Historical data can be retrieved from a how-to page via http://waterdata.usgs.gov/nwis
- Model forcing data, such as that utilized by the WRF RT-FDDA model
  - Forcing data used for the real-time RT-FDDA runs can be found via https://madis.ncep.noaa.gov/user_resources.shtml

## 17.2 Additional Instrument Deployments

### *17.2.1 Radiometer*

A radiometer was deployed to the town of Lovell, Wyoming to collect measurements on the frequency and amount of LWP observed over the Bighorn Mountains during the winter of 2015–2016.

#### *Siting and Operation*

Utilizing contacts made during the project Scoping Meetings, a representative of the Shoshone Conservation District recommended property from local landowners for the radiometer. Two landowners were contacted and both were amenable to locating the radiometer on their property. The site that was selected had fewer trees that could block the view of the Bighorn Mountains (Table 17.1). Neither property had internet access (few in the area do), so a cell phone modem was required to transmit the data. The cellular service, Verizon, had a strong signal and 4G service at the radiometer site.

Table 17.1. Location information about the radiometer site.

| | |
|---|---|
| **Address** | 1080 Road 15, Lovell, WY. About 1/8 mile north of Highway 14A. |
| **Latitude, Longitude, Altitude** | 44.8441°, -108.3116°, 3816 ft MSL. |

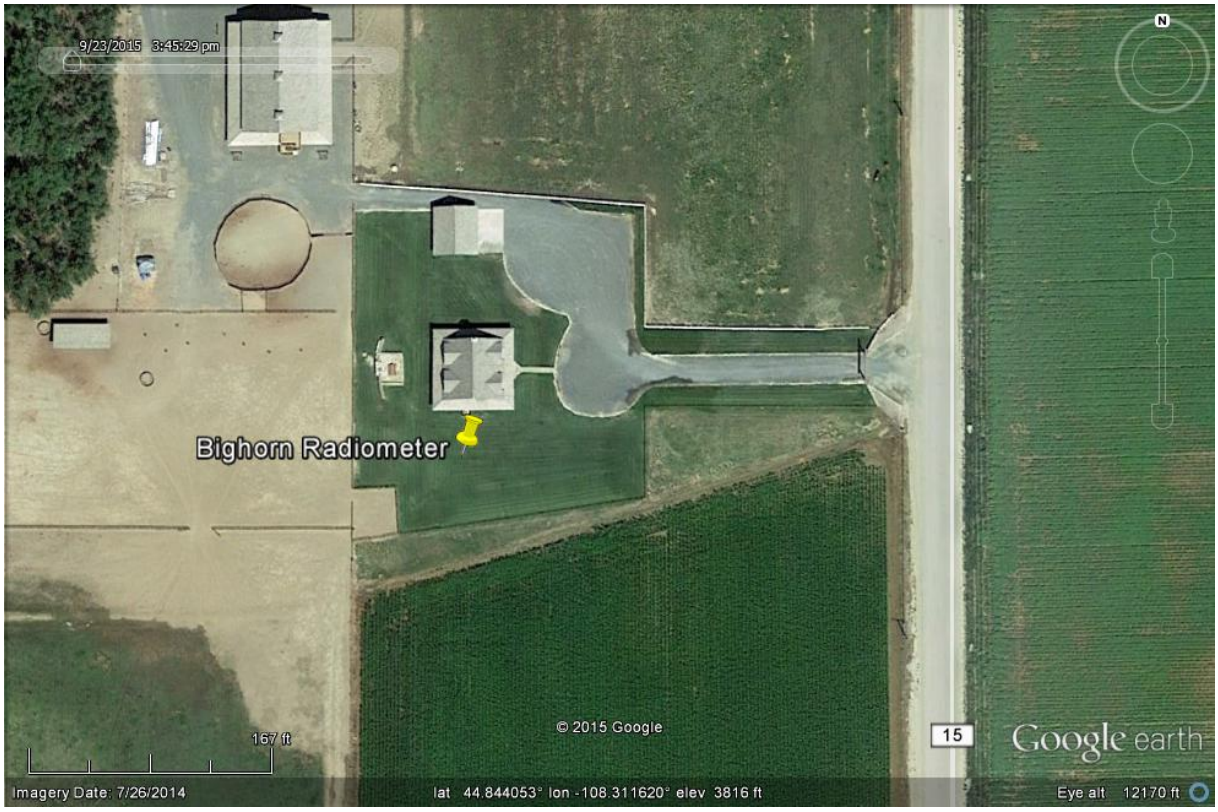


Figure 17.1. Google Earth map of the Lovell radiometer.

The radiometer was installed on 12 November 2015 (started at about 19:00 UTC) on the south side of a building on the property with a pointing angle (azimuth) about 074° at Sheep Mountain. This resulted in a distance to precipitation gauge sites of about 38 km (Figure 17.2). Figure 17.3 shows the installation and view of the radiometer. Five elevation angles plus a zenith angle scan were programmed into the radiometer (8.1°, 12.15°, 15.3°, 30.15°, 45.0°). These angles were scanned approximately every minute. Every 10 minutes, a black body calibration and a tipping curve were performed, which included the zenith scan (90°) with a water vapor profile, as well as the liquid water path. Data files cover one entire day from 0000 UTC to 2355 UTC. The radiometer operated until 9 April 2016, at which time the laptop (that was stored in a heated cooler throughout the winter) overheated and was unable to reboot. The radiometer was uninstalled on 23 May 2016.




**Figure 17.2. Google Earth map of the pointing angle from the Lovell radiometer over Sheep Mountain.**



*View of radiometer to Bighorn Mountains.*



*Zoomed view of radiometer*



*Interior of heated radiometer laptop shelter*

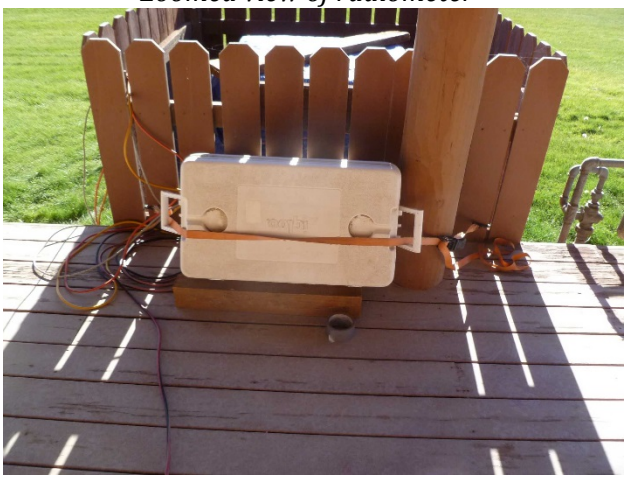

*Laptop shelter – closed up*

**Figure 17.3. Photos of the radiometer installation.**

### *Data and Analysis*

Data from the Lovell radiometer were analyzed for the November 2015–April 2016 period as part of the current study. Liquid water periods (hereafter, LW periods) were identified consisting of a minimum of one hour in which the median observed liquid water path exceeded 0.1 mm. Consecutive LW periods with less than an hour of separation were combined into a single period. While the model threshold for liquid water path for identifying seedable conditions was 0.01 mm, the observations require a higher threshold in order to account for high frequency noise during periods with no liquid water.

For the period spanning 13 November 2015 through 9 April 2016, 62 LW periods were identified, with an average duration of 2.79 hours. The average maximum value within the LW periods was 0.78 mm (range 0.12–4.81 mm), and the average mean value 0.24 mm (range 0.07–1.01 mm). The number and duration of LW periods by month are listed in Table 17.2, showing fairly consistent numbers in January–February and peaking in March. However, given that the months of November and April have incomplete data and there are several outages in the remaining months (one ~1-day outage in December, two ~1-day outages and one ~2-day outage in January, one ~2-day outage in February, one ~1-day

outage in March, and one ~1-day outage in April), the total number of LW periods is slightly misleading. Thus, the number of identified hours per month is normalized by the hours of data included in each month (second row, Table 17.2). The normalized values indicate that the percentage of hours in a given month meeting the liquid water path threshold increases throughout the season. The average duration is fairly consistent throughout the season, ranging from a low of 2.2 hours in December to a high of 3.2 hours in March. The slight increase in average duration also contributes to the increase in monthly percentage of hours meeting the liquid water path threshold.

It should be noted that not all of these LW periods are suitable for seeding. Additional measurements, from local soundings in particular, would be needed to determine if the winds and temperatures during these LW periods are suitable for seeding. However, these measurements do indicate that liquid water is present in the Bighorn Mountains and there are several instances in the winter where there could be the potential for cloud seeding.

**Table 17.2. Monthly break down of number and duration of LW periods.**

| | **Nov** | **Dec** | **Jan** | **Feb** | **Mar** | **Apr** |
|---|---|---|---|---|---|---|
| **# LW periods** | 4 | 13 | 11 | 12 | 17 | 5 |
| **% hours** | 2.48 | 3.92 | 4.57 | 5.48 | 7.56 | 9.07 |
| **Avg. duration(h)** | 2.71 | 2.18 | 2.63 | 2.90 | 3.20 | 3.09 |

Figure 17.4 shows the distribution of LW period durations. While the range of values extends out to 12 hours, the majority of LW periods are less than 2.5 hours long. Thus, the monthly average durations (nearly all greater than 2.5 hours) are skewed by a few long events.

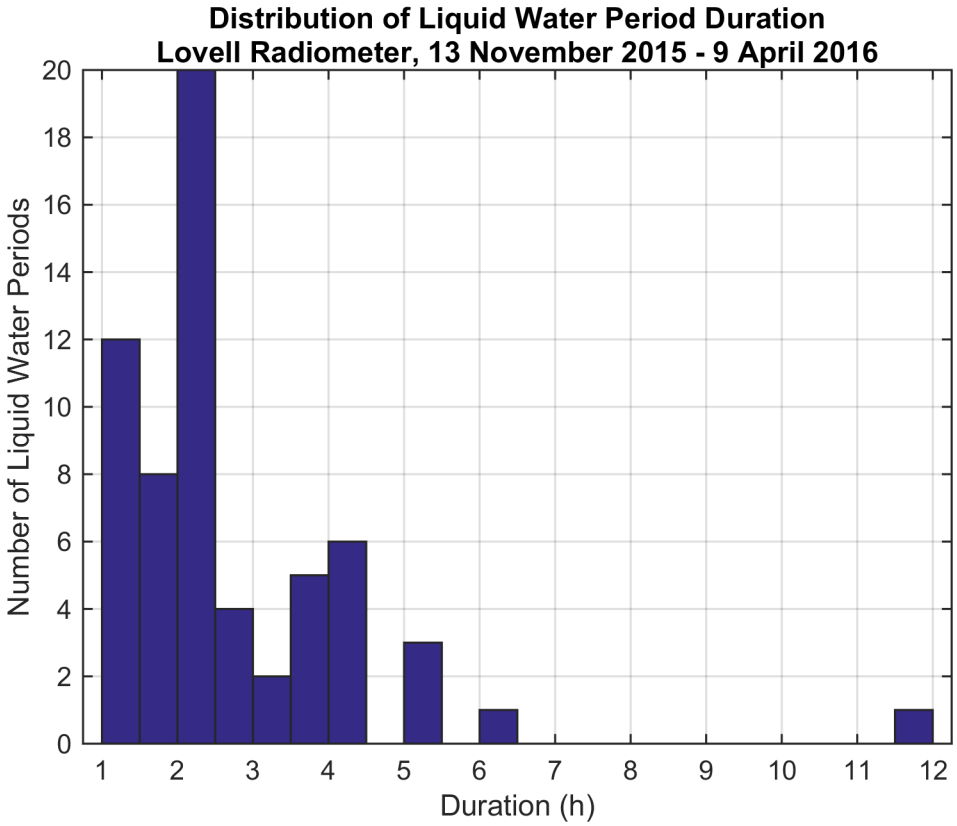


**Figure 17.4. Histogram of LW period duration (hours).**

Figure 17.5–Figure 17.10 show monthly time series of observed liquid water path with the identified LW periods highlighted in gray.

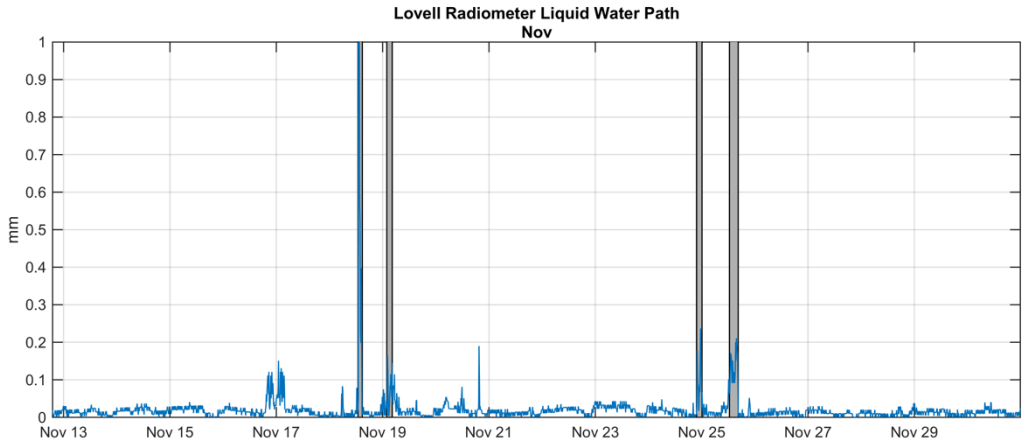


**Figure 17.5. Liquid water path (blue) and identified LW periods (gray) from the Lovell radiometer for the month of November, 2015.**

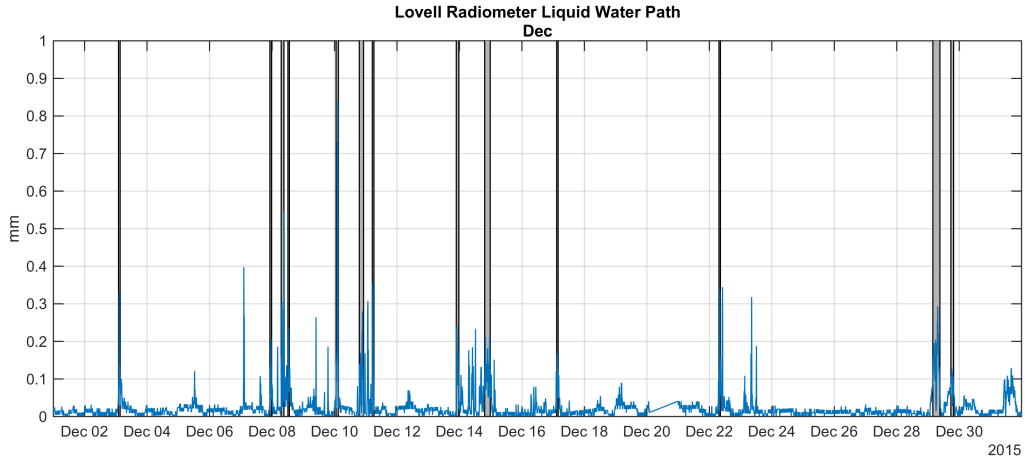


**Figure 17.6. As in Figure 17.5, but for December 2015.**

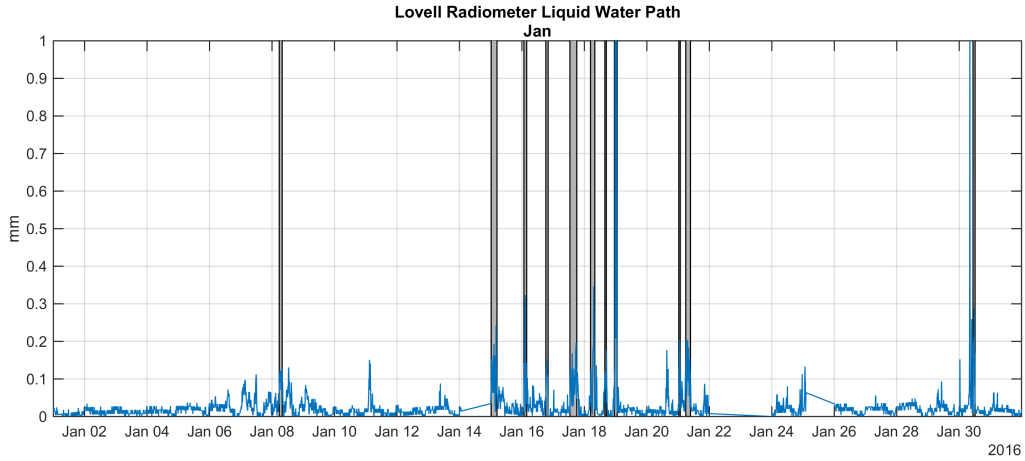


**Figure 17.7. As in Figure 17.5, but for January 2016.**

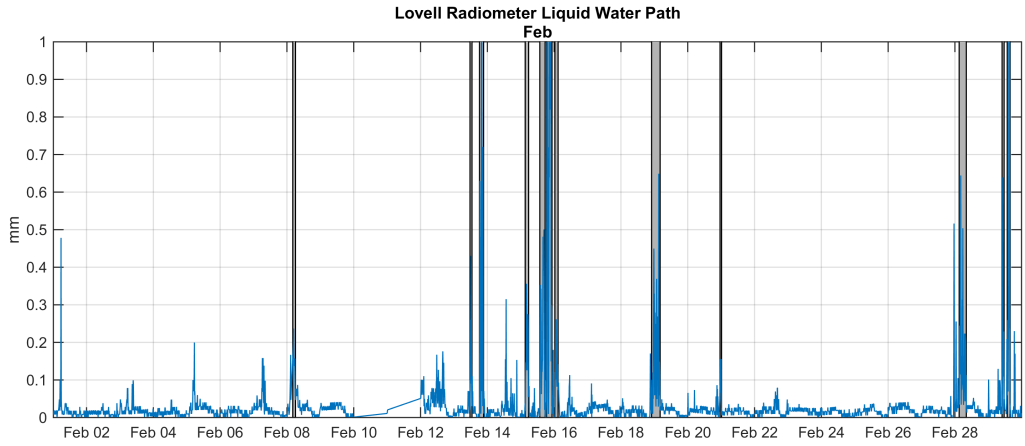


**Figure 17.8. As in Figure 17.5, but for February 2016.**

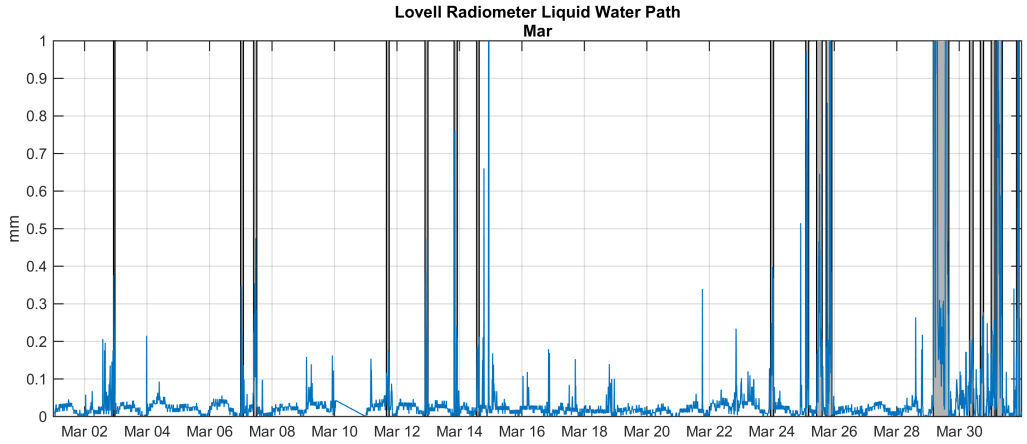


**Figure 17.9. As in Figure 17.5, but for March 2016.**

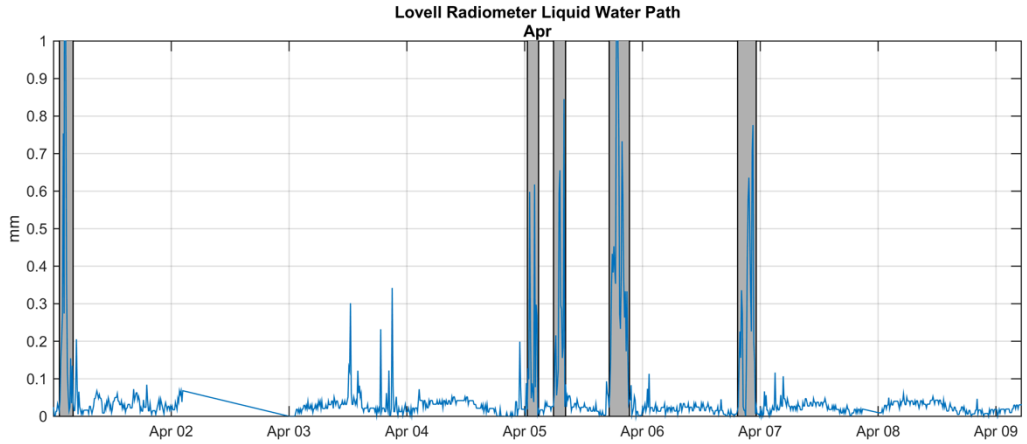


**Figure 17.10. As in Figure 17.5, but for April 2016.**

### *17.2.2 Snow Gauges*

A secondary maximum in precipitation in the northern-most region of the target area was identified by the WRF_CONUS simulation, and because the region is void of any gauge data to verify the model, high-resolution snow gauges were deployed to measure snowfall in this area for the winter of 2015–2016. The closest SNOTEL site to this area is the Bald Mountain SNOTEL (Figure 17.11, see also Figure 4.1).




Figure 17.11. Photo of the Bald Mountain SNOTEL gauge.

### *Siting and Operation*

The discovery of a secondary maximum in model-simulated precipitation occurred after the project had begun, during the course of conducting the climatology analysis. Therefore, the plan (and approval) to deploy snow gauges was rather last minute. Nonetheless, several potential sites were identified (see Figure 17.2), and a permit application was submitted to the USFS on 9 October 2015. The permit, which covers a 5-year period, was approved by 9 November 2015, but only four of the five proposed sites were approved (A, B, D, E as shown in Figure 17.12–Figure 17.13).

Table 17.3. Loaction information for the deployed snow gauge sites.

| Site Name | Latitude | Longitude | Instruments |
|---|---|---|---|
| Rd 14 | 44°50'37.5"N | 107°50'43.9"W | GEONOR, ETI |

The gauge site was deployed on 20 December 2015. At the time of deployment, all sites were evaluated to determine the best one for the installation. During the site surveys of the four potential sites, it was discovered that the sites at Locations D and E were inaccessible during the winter due to the dangerous buildup of snow along the ridge.

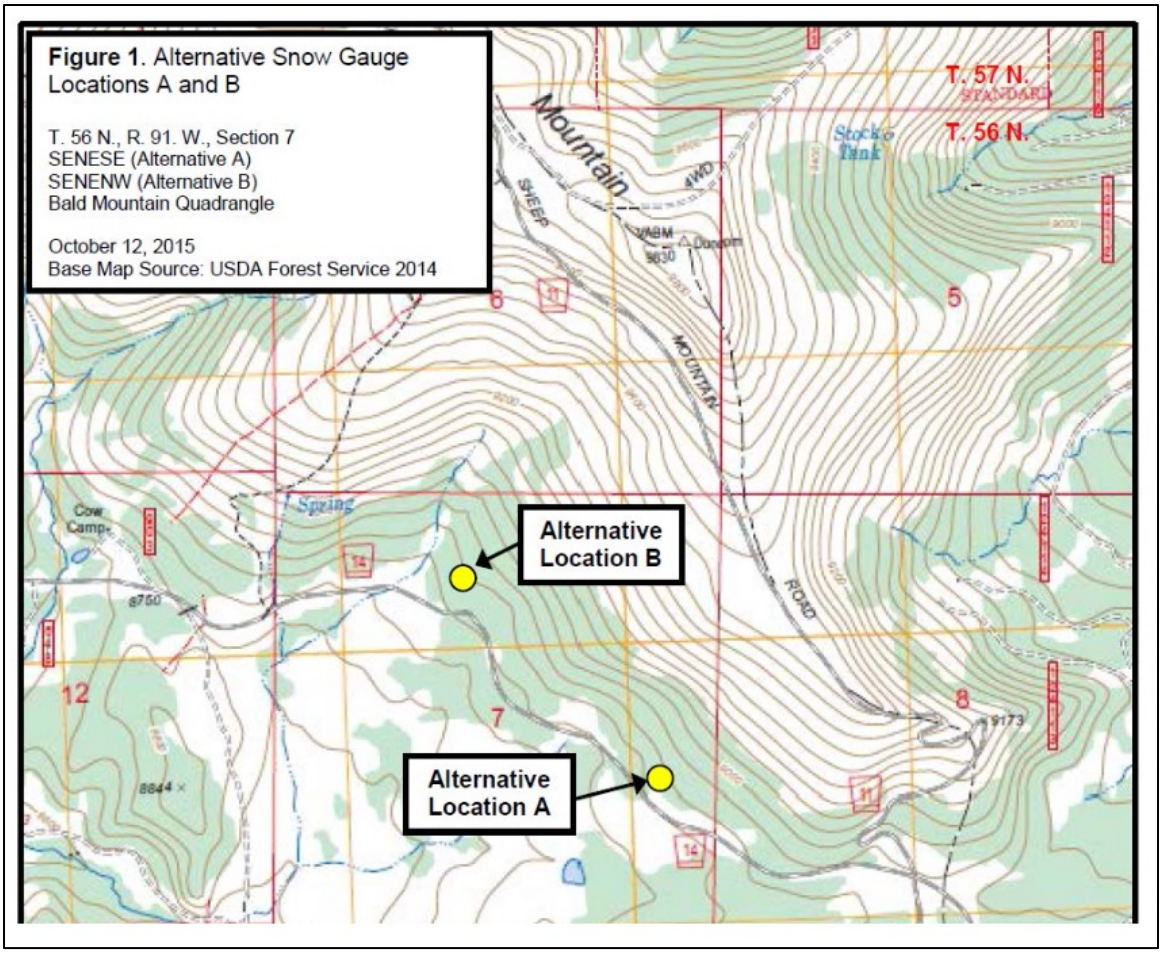


**Figure 17.12. Southern permitted potential site locations.**

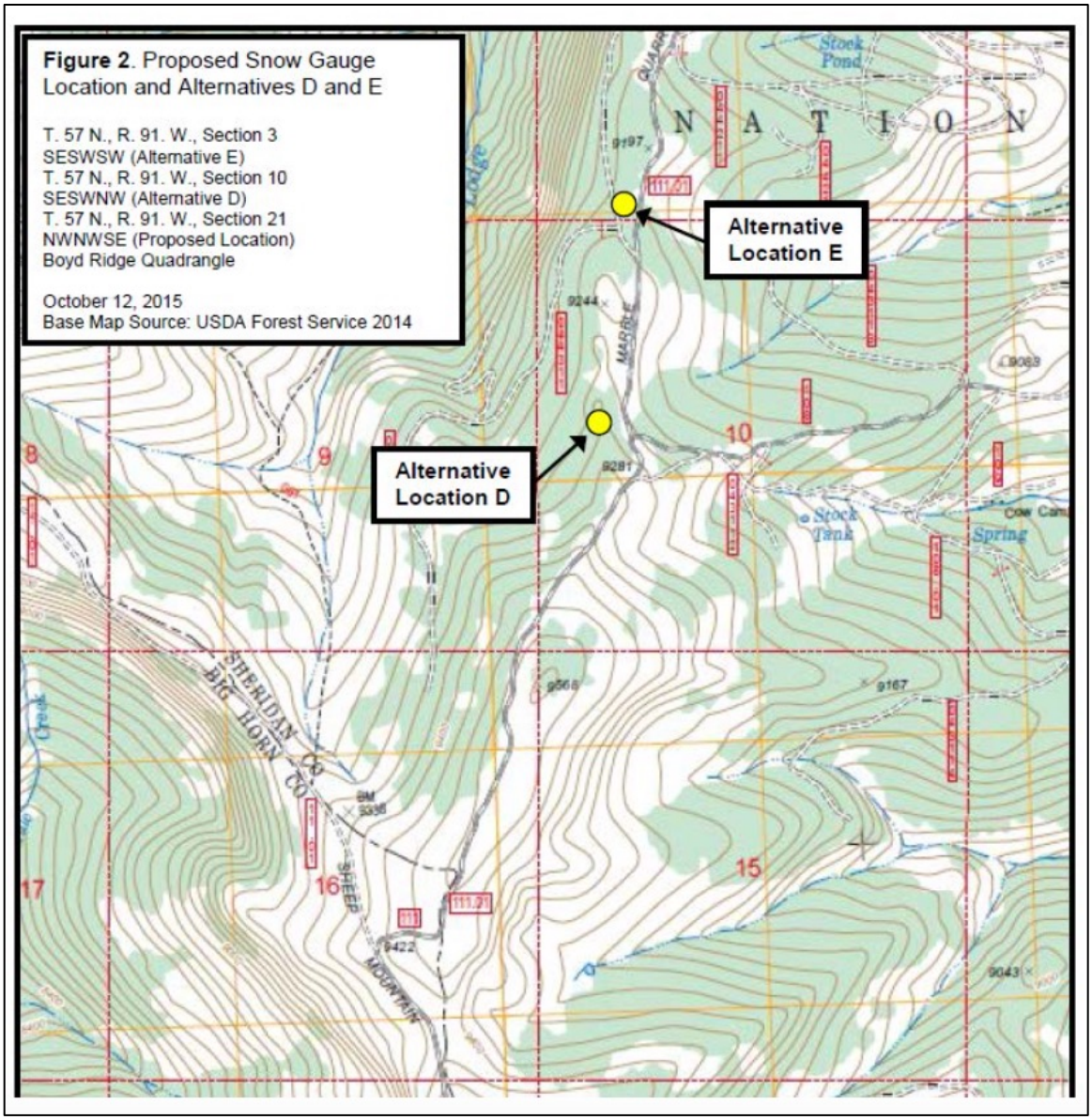


**Figure 17.13. Northern potential site locations.**

Locations A and B were both inspected for suitability to install the gauges. Location B appeared to have a significant amount of downed trees in the clearing, which would have made the gauge installation difficult. Also, the trees were too dense to get the UTV into the site to unload all the equipment. Location A (renamed site "Rd 14") was thus chosen as the location for the sensors for this winter season.

Two gauges were installed at the Rd 14 site; one ETI gauge and one GEONOR gauge. Wind, temperature and relative humidity sensors were also installed with the gauges. There is some sloping terrain in this area, with the east side of the site having a higher elevation (~10 feet) than the west side. The gauges were installed on the east side since the west side appeared to be collecting more snow due to blow-off from snow that collected in the trees.

Even though the gauges are at a higher elevation, the site is still relatively protected from the ambient wind flow. Figure 17.14–Figure 17.16 show the instrumentation setup looking towards each of the cardinal directions.

Weak cell signal was observed down the road from this site, but no signal was found at the site, even when a signal booster was used. The Rd 14 site was set up to run in standalone operation with manual data collection occurring as often as a technician could get to the site.

The High Country Lodge, which operates year round, maintains two snowcats and can transport people around the area for a small fee. The Lodge has internet access and an agreement was made with the Lodge to put an additional gauge there and use their network to transmit the data in real time (from their site) to monitor how much snow is falling in the region. This aided the determination of how often a site visit for maintenance was needed. This agreement could be renewed if the gauges remain in place beyond this winter. The agreement included one of their staff members visiting the Rd 14 site every few weeks to manually download the data and transmit it to NCAR using internet access at the lodge.



**Figure 17.14. North-facing view (left) and South-facing view (right) of the Rd 14 gauge installation.**



Figure 17.15. East-facing view of the Rd 14 gauge installation.



Figure 17.16. West-facing view of the Rd 14 gauge installation.

### *Data and Analysis*

The data from the Rd 14 site were analyzed to compare with the Bald Mountain SNOTEL in order to determine how well the SNOTEL site performed relative to nearby high-resolution gauges, as well as to determine if the deployed gauges could detect a trend in higher precipitation amounts north of the SNOTEL site. The analysis shows that the Bald Mountain SNOTEL site performed quite well compared to the Rd 14 gauge, only missing a few events (Figure 17.17–Figure 17.18). Furthermore, the Rd 14 site did not appear to accumulate excessive amounts of additional snowfall compared to the Bald Mountain SNOTEL, with the exception of the few missed events. It is possible that these missed events produced a more focused region of precipitation in the northern region, or that some other issue (e.g., wind undercatch, capping of the gauge) impacted the SNOTEL gauge from performing well. Nonetheless, we conclude that the Rd 14 site was not far enough north to verify the modeled maximum in precipitation and it is recommended to move the gauges farther north for an upcoming winter (likely to sites D or E).

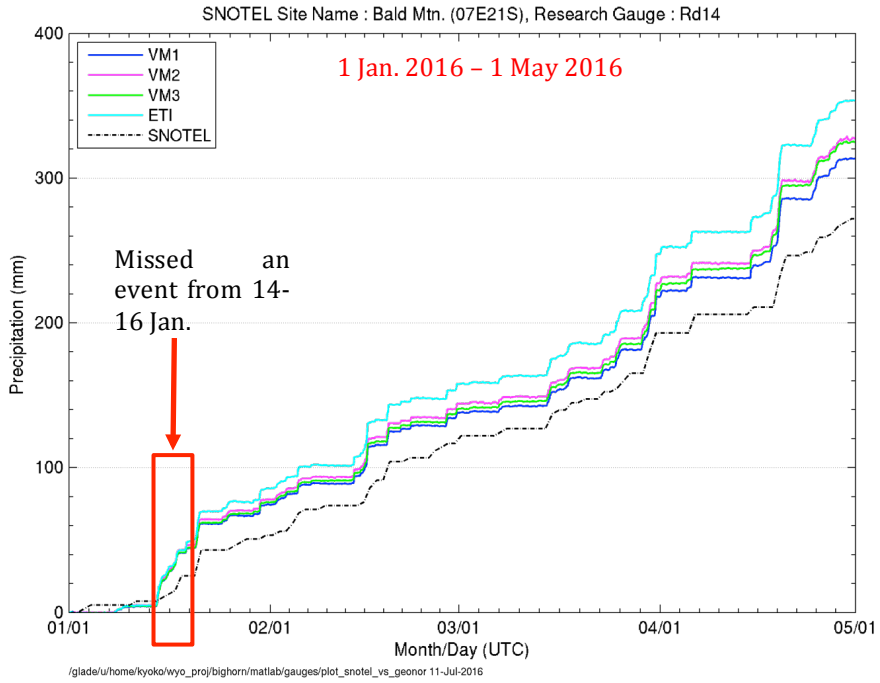


**Figure 17.17. Time series plot of accumulated precipitation (mm) measured by the Rd 14 Geonor (three wires each labeled VM1, VM2, VM3) and ETI gauge compared to the Bald Mountain SNOTEL for the period 1 January–1 May 2016.**

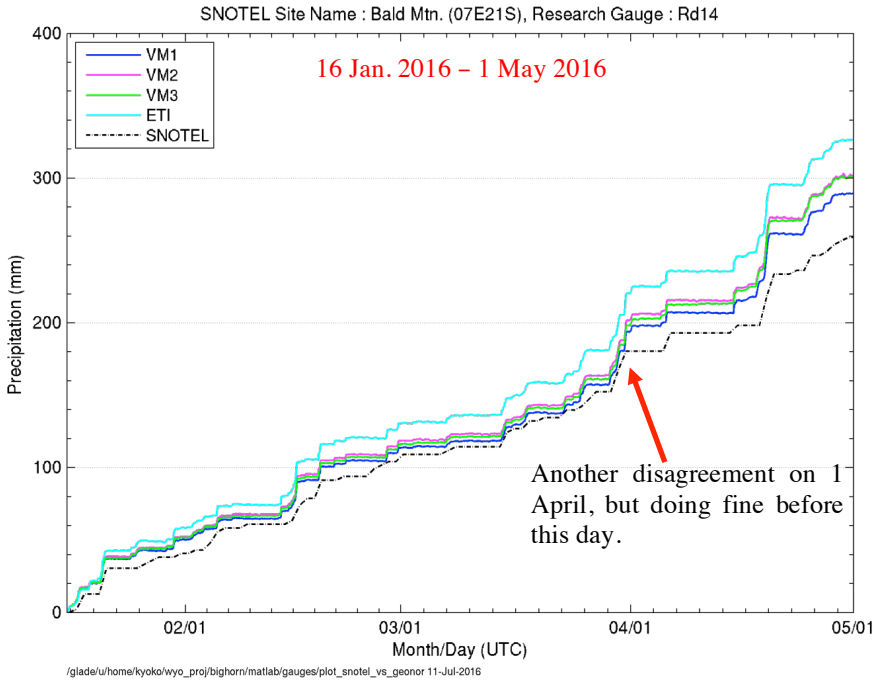


**Figure 17.18. Same as Figure 17.17, except this figure starts on 16 January 2016 in order to show that after the 15 January event, the Bald Mountain SNOTEL site compares fairly well with the Rd 14 gauges.**

# 18. Summary and Recommendations

A conceptual design and siting study was completed to assess the feasibility of conducting an operational weather modification program that would target the Bighorn Mountains in northern Wyoming. This study was led by NCAR with collaboration from WMI and HEC. Sixteen tasks were identified by the WWDC for the study, including: scoping and project meetings; reviewing previous studies and data; climatological analysis of the project area; development of a preliminary project design; model evaluation of the project design; field surveys of potential ground generator locations; assessing the access/easements and permitting/reporting for potential generator sites; operational criteria development; a review of environmental and legal implications; potential benefits analysis; cost estimates; development of a cost/benefit analysis of the potential program; preparation of the report itself; giving presentations on the final results; and climatological monitoring of the study area.

## 18.1 Summary

Two public scoping meetings were held at the beginning of the project in locations on opposite sides of the Bighorn Mountains. The meetings provided the public with an overview of the scientific concept of cloud seeding, a summary of the previous weather modification studies in Wyoming, and an overview of the current study.

A review of previous data found that there were previous cloud-seeding activities in the Bighorn Mountains, spanning the period of 1951–1954. Since that time, no additional permits for cloud seeding operations in the Bighorns were issued. These previous programs utilized ground-based AgI generators, and most operations targeted clouds in the summer months.

In more recent years, numerous research investigations have improved the understanding of how to use AgI seeding to enhance snowfall in winter orographic clouds. These include the recently concluded Wyoming Range Phase II Feasibility Study and the WWMPP. The results of these studies were reviewed in the preparation of this report, to ensure it remains consistent with the most recent recommendations for cloud-seeding program design. Noteworthy results from the draft WWMPP report included that the randomized seeding experiment found seasonal precipitation increases of 5–15% in seedable storms. It also demonstrated the capability of numerical models to realistically simulate snowfall distributions, as well as simulate seeding effects via a seeding parameterization. These results were utilized by the present study.

The review of previous data suggested that liquid propane seeding would be an inefficient option for the Bighorn Mountains because the liquid propane must be released in the supercooled cloud to be effective. Mannual, ground-based AgI generators were also determined to be challenging to deploy and operate in the target area, given the limited options for accessible and effective generator placement. In order for manual generators to be activated and deactivated during the winter months, locations would need to be sited at

lower elevations in the Bighorn River Basin, such that the AgI plume would frequently be trapped and unable to disperse over the mountains.

The climatology analysis indicated that the typical wind regimes in the Bighorn Mountains are westerly to northwesterly, with few easterly (upslope) events on the eastern slopes. The spatial mapping analysis revealed that LWC most frequently develops on the western and northeastern slopes of the Bighorn Mountains, while the most frequent seeding opportunities occur on the western slopes.

Based on 0–1-km AGL average temperature and LWC criteria, ground seeding opportunities were equal to, or more frequent than, airborne seeding opportunities during the November–April wintertime period. When the additional ground-based seeding criteria were considered (i.e., wind direction and stability for transporting ground-released AgI into the targeted clouds), ground-based seeding opportunities dropped to nearly zero in the eastern and southern regions, and were substantially reduced in the western region. In fact, when considering the additional criteria for ground-based seeding, airborne seeding potential in the western region is greater than ground seeding.

The inclusion of October, May, and June would potentially double seedable precipitation with an aircraft program. However, from a logistical perspective it is less likely that all airborne "seedable" hours can be seeded, especially with a single aircraft operation, given limited flight on station times. Even if the airborne program is restricted to the November–April period, seeding at the 3.5–4.5-km MSL level is likely to yield more opportunities than ground seeding (considering the factors that limit effective AgI transport).

Most of the time when cloud seeding conditions were present, precipitation occurred over the Bighorn Mountains. This indicates that there are few situations in which precipitation efficiency is low and cloud seeding could have potential benefits. Only 19% of the precipitation that fell in a given winter season (November – April) was seedable based on all of the ground-seeding criteria being met, while 39% of the precipitation that fell in a given November–April winter season was seedable by aircraft.

### *Project Design, Model Evaluation, and Field Surveys*

In order to test a wide variety of program design options, and based upon results of the climatological analysis, several groups of ground-based generator sites were developed. Initially just five groups of generators were tested, but based on an iterative process with the model evaluation of these design options, a sixth group was also created and tested with the model. The design focused on ground-based seeding and/or airborne seeding with an operational season of mid-November through mid-April (i.e., 15 November–15 April), utilizing AgI, or more specifically, a silver iodide-salt compound as the seeding agent.

Three test cases were simulated to evaluate the impact of seeding and six groups of ground generators and several aircraft tracks were tested. The cases were selected to represent various meteorological scenarios encountered in the Bighorn Mountains, but not every scenario may have been represented by this limited sample. In particular, this sample did

not yield the best cases for ground-based seeding. If resources allow, more cases should be tested to develop more robust results.

Based upon the model simulations of the three test cases, in general, ground seeding had very limited spatial impact on the region, and Groups A and B rarely impacted the target area. Other meteorological scenarios not tested may have led to better simulated impacts from Groups A and B, but based on these three cases, these sites are not recommended for implementation.

Group C showed positive simulated seeding effects in some meteorological conditions, especially when the winds were north-northeasterly. Groups D and F yielded the best results for ground-based seeding, yet the impact area was rather small and confined to very narrow plumes. Group E ended up being a rather versatile group of generators, given they could impact the southern extent of the Bighorn Mountains under northwest to westerly winds, but could also impact the Cloud Peak area under southwesterly winds. Nonetheless, in the cases that were tested, Group E had minimal overall simulated impacts.

Airborne seeding tended to yield the most widespread and biggest simulated seeding effects in these cases. However, shorter seeding flight tracks are recommended because the shorter central track experiment produced a greater simulated seeding effect more often than the longer track because the simulated AgI plume was more concentrated when using the shorter track length. The benefit of airborne seeding is that it can be located wherever the most SLW is present. This can include situations where elevated SLW extends quite far upwind (to the west) of the mountains, as occurred in some of these cases. In fact, airborne seeding is the only way to impact elevated SLW layers over the Bighorn River Basin, given the air is too stable in this valley to use ground generators to reach those higher altitudes. Yet, it should be noted that not all of the simulated seeding effects from seeding further upwind impact the higher elevations of the Bighorn Mountains; rather, they broadly impact the Bighorn Basin in general. Based on the modeled climatology, easterly upslope events include SLW, but occur infrequently. Therefore, due to the lower frequency of occurrence, siting ground generators on the eastern slope of the Bighorns is not advised, but it should be noted that airborne seeding is versatile enough that it can also be used to target easterly upslope events.

A field survey was conducted to assess the suitability of potential generator locations for seeding effectiveness, land access issues, and the impacts of land ownership (Sections 7 and 8). During the field survey, many of the originally proposed generator sites were moved short distances to more suitable locations. Six alternate sites were added, usually because the original sites were not accessible, or the alternate sites were determined to be better suited for operational deployment. In total, 21 potential ground-based generator sites were considered as viable options from a permitting and operational perspective. Of the final 21 site locations, 12 generators were sited on USFS lands, five generators on BLM lands, three generators on private lands, and one generator on State lands.

### *Operational Criteria and Other Program Considerations*

Operational seeding criteria were developed for possible ground-based seeding operations as well as for potential seeding with an aircraft. Observations used to determine when the operational criteria are met are available in real time via a variety of products available on the internet. However, given the dearth of observations in the region, deploying project-specific instrumentation (i.e., radiometer and soundings) or numerical models tailored to the region can play vital roles in making seeding decisions. Other programs in the region, such as the Wind River Range operational cloud-seeding program, may provide leveraging opportunities to obtain data from such additional operational tools. Suspension criteria were also developed based on the criteria developed for the Wind River Range operational program.

Common questions regarding the implementation of a cloud-seeding program are concerned with possible extra-area effects of cloud seeding on precipitation and possible environmental impacts of the cloud-seeding agent (AgI). Recent and relevant studies on these topics were reviewed, including the most recent WWMPP study. These studies concluded that seeding effects outside of the intended target area would be negligible, and that no environmentally harmful effects would occur from the use of AgI as a cloud-seeding agent.

### *Potential Benefits, Cost Estimates, and Benefit/Cost Analysis Summary*

Estimates of streamflow changes due to seeding impacts were calculated using preliminary results from the WWMPP, which were based on three levels of estimated seasonal seeding effects on seedable storms of 5, 10, and 15%. The remaining parameters needed to calculate seeding impacts are the percentage of seasonal precipitation that occurs during seedable conditions, the target area coverage of the seeding effects, and the ratio of increase in streamflow relative to an increase in snowpack. The seasonal seedable precipitation was determined from the climatological analysis for the Bighorn Mountains, while the target area coverage was assumed to vary between 30–80%, which was substantiated by the model simulations. Estimates of streamflow input into the Bighorn and Powder/Tongue River basins from the Bighorn Mountains were determined using the 8-year WRF-CONUS model simulations, since other estimates provided in local water plans were not specific to drainage solely from the Bighorn Mountains. However, the streamflow estimates from the local water plans and the model simulation agreed relatively well. The ratio of increase in streamflow relative to an increase in snowpack was estimated to be 0.49 using the WRF-CONUS model-simulated snowpack compared to simulated runoff. This ratio accounts for the evapotranspiration of some of the additional snowpack from cloud seeding.

Average estimates of streamflow increase (April–July runoff increase from seeding) based on the parameters described above and combined across the two river basins produced estimates of streamflow increases ranging from ~1,400 AF to ~10,900 AF for ground-based seeding, depending on the level of the estimated seeding effect and the assumed area of seeding coverage. Assuming a 50% area coverage of seeding effects, the range was between ~2,300 AF to ~6,800 AF, which was used in the benefit/cost analysis. For

airborne seeding, which had a much higher fraction of seedable precipitation from the climatological analysis, the estimates of streamflow increases ranged from ~2,800 AF to ~22,500 AF, depending on estimated seeding effect and area of coverage percentage. Assuming a 50% area coverage of seeding effects for airborne seeding, the range was between ~4,700 AF to ~14,000 AF, which was used in the benefit/cost analysis.

Cost estimates were prepared for two different seeding program options:

1) a program with 15 remote-controlled ground-based generators (estimated annual cost: $479,655), and
2) a single stand-alone seeding aircraft program (estimated annual cost: $352,421).

A preliminary benefit/cost analysis was performed using the estimated range of enhanced average April–July runoff values. ASCE Guidelines were considered to determine the feasibility of the program. These Guidelines have two basic considerations: is the program technically feasible and is the proposed program economically feasible? An affirmative answer to both questions is required in order for the program to be considered feasible. *The evidence presented in this study is that the program is technically feasible.*

For a proposed program to be economically feasible, the ASCE Guidelines recommend that a proposed program have an estimated benefit/cost ratio of 5/1. Several assumptions were made concerning the possible benefit/cost ratios for the proposed program (e.g., allocation of the water, value of the water, etc.). Given the assumed costs of water ($30–$50/AF), neither seeding program option yielded the 5/1 ratio with the assumed area impact of 50%, nor when assuming an 80% impact area. As a result, this program would not be economically feasible based upon the ASCE guidelines. Of the two seeding program, airborne resulted in a higher benefit/cost ratio than ground, given the lower cost of the airborne program and the higher amount of seedable precipitation for airborne seeding found in the climatology analysis. Sharing operational resources (i.e., aircraft, staff, weather data, etc.) between adjacent cloud-seeding programs may be the most cost effective way to target the Bighorn Mountains. Consolidating operational resources between projects would likely reduce project costs, and therefore, increase the cost effectiveness for the project, but it is beyond the scope of the present study to make this determination.

It should be noted that the cost effectiveness calculations were based upon estimated streamflow impacts in the highest ("target area") elevations of the Bighorn Mountains (>8000 ft), for seeding programs run between November and April, and also using an impact area of 50%. For airborne seeding, however, impacts were often simulated well upwind of the Bighorn Mountains, which would effectively enhance Bighorn Basin streamflow that much more, but additional cases would need to be simulated to determine exactly how much. Moreover, airborne seeding target-area impacts often were much greater than 50% (up to around 80%), and airborne seeding could be effective from October–early June, thereby providing even more opportunities to further enhance streamflow. Therefore, an airborne cloud-seeding program is expected to be more cost effective than these preliminary estimates imply, but would also depend on how much a limited aircraft on station time would reduce the annual seedable precipitation determined by the climatology.

## 18.2 Conclusions and Recommendations

The conclusion of this study is that there are opportunities for cloud seeding with AgI in the Bighorn Mountains area making a cloud-seeding program targeting this region technically feasible. This is supported by the climatological analysis and model evaluation, as well as the recent radiometer measurements collected over the winter of 2015–2016. The cloud-seeding opportunities are less frequent for ground-based seeding, however, due to the complex terrain that limits siting generators in locations that can release AgI plumes that will effectively disperse over the Mountains (as opposed to being blocked by the terrain). Rather, the opportunities for airborne seeding are more frequent and promising, given that numerical simulations of airborne cloud seeding in the three tested cases indicated that airborne seeding is far more effective than ground-based seeding at enhancing precipitation both over and upwind of the Bighorn Mountains.

The study also concludes that the program is not economically feasible based upon the ASCE guidelines. The cost effectiveness of such a cloud-seeding program is dependent on several factors, including the benefit/cost ratio desired, actual water costs, and the level of seeding effect achieved. This benefit/cost analysis indicated that an airborne seeding program was more cost effective than a ground-based program. Nonetheless, the implementation of a collaborative weather modification program to share an aircraft, staff, and/or other resources (e.g., observations, forecast models) with another seeding program would likely yield the most cost effective opportunity to enhance precipitation in this region; however, it is beyond the scope of the present study to make this determination.

### *18.2.1 Recommendations*

The recommendations based on the results of this study are provided below. Given the complexity of the terrain and short duration of the study, only a few representative cases were evaluated in this study. To increase confidence in the results, it is recommended that additional studies be conducted with the atmospheric model coupled to a hydrological model. Specifically:

- Additional test cases (ideally an entire season of seeding cases) should be simulated to better represent the wide variety of storm types and/or the seasonal seeding impacts from seeding with a proposed operational design.
- A spatially distributed hydrological model coupled to cloud-seeding model output should be run for multiple winters to better estimate hydrological benefits of cloud seeding. This modeling system would utilize the 3D spatial distribution and magnitude of the model-simulated seeding effects on snowpack to drive the hydrological model, which would calculate the water balance and routing of the streamflow driven by the snowmelt for every basin in the domain, obviating the need for fixed assumptions across the domain.

Recommendations specific to the design and implementation of an operational cloud-seeding program in the Bighorn Mountains include:

- Seeding should be conducted using AgI as the seeding agent.

- The seeding season should be November–April for ground-based seeding, but could be extended from October into May or June if airborne seeding is utilized.
- The climatology analysis and cost estimates indicate that airborne seeding has the potential to be more cost effective than ground-based seeding. Therefore, airborne seeding is recommended.
- If airborne seeding is implemented, shorter aircraft tracks should be used to achieve better coverage of AgI over the target area. In particular, the central track, using an altitude where the maximum LWC resides, was found to give the best result.
- Basic seeding criteria should be based on readily available (and quickly accessible) meteorological data. Given the lack of regular meteorological observations in the region, a program would benefit from deploying project-specific instrumentation (i.e, radiometer and soundings), but these would add additional costs to operate the program that have not been considered in the present benefit/cost analysis.
- In order to reduce costs, opportunities to share resources (especially an aircraft) with other nearby cloud-seeding programs should be explored. Specifically, a climatological analysis should be conducted to determine if the timing of seedable storm systems would allow for cost effective resource sharing (i.e., utilizing a single aircraft to target multiple mountain ranges).
- If the State of Wyoming were to operate multiple cloud-seeding programs across the State, it is recommended that a real-time forecast modeling system be implemented statewide to provide guidance on whether passing storm systems are suitable for seeding. A forecast modeling system will generate a cost savings by identifying when storms have high seeding potential, therefore maximizing cloud-seeding impacts. The model can also serve as a basis for seasonal program evaluation.

## 19. References


Acharya, A., T. Piechota, H. Steven, and G. Tootle, 2011: Modeled streamflow response under cloud seeding in the North Platte River watershed. *J. Hydrology*, **409**, 305–314.

ASCE, 2004: Standard Practice for the Design and Operation of Precipitation Enhancement Projects. ASCE/EWRI 42-04, Reston, Virginia, 58p.

ASCE, 2006: Guidelines for Cloud Seeding to Augment Precipitation. ASCE Manuals and Reports on Engineering Practice No. 81. ASCE, Reston, VA. 181 p.

Barker, D.M., W. Huang, Y.-R.Guo, A.J. Bourgeois and Q.N.Xiao, 2004: A three-dimensional variational data assimilation system for MM5: Implementation and initial results. *Mon. Wea. Rev.,* **132**, 897–914.

Barlage, M., and Coauthors, 2010: Noah land surface model modifications to improve snowpack prediction in the Colorado Rocky Mountains. *J. Geophys. Res.,* **115**, D22101, doi:10.1029/ 2009JD013470.

Berg, N. H., and Smith, J. L., 1980: "An Overview of Societal and Environmental Responses to Weather Modification." *The Sierra Ecology Project*, **5**, Office of Atmospheric Resources Management, Bureau of Reclamation, U.S. Department of the Interior (USDI), Denver, CO.

Bergeron, T., 1949: The problem of artificial control of rainfall on the globe. I. General effects of ice-nuclei in clouds. *Tellus*, **1**, 32–43.

Boe, B.A., J.A. Heimbach, Jr., T.W. Krauss, L. Xue, X. Chu, and J.T. McPartland, 2014: The dispersion of silver iodide particles from ground-based generators over complex terrain, Part 1: Observations with Acoustic Ice Nucleus Counters. *J. Appl. Meteor. Climatol*., **53**, 1325–1341.

Breed, D., R. Rasmussen, C. Weeks, B. Boe, and T. Deshler, 2014: Evaluating winter orographic cloud seeding: Design of the Wyoming Weather Modification Pilot Project (WWMPP*), J. Appl. Meteor. Climatol*., **53**, 282–299.

Brier, G.W., 1974: Chapter 5. Design and Evaluation of Weather Modification Experiments, in *Weather and Climate Modification*, Wilmot Hess, Ed., John Wiley and Sons, New York, 842 pp.

Chen, F., and J. Dudhia, 2001: Coupling an advanced land surface hydrology model with the Penn State–NCAR MM5 modeling system. Part I: Model implementation and sensitivity. *Mon. Wea. Rev*., **129**, 569–585, doi:10.1175/1520-0493(2001)129,0569: CAALSH.2.0.CO;2.

Chen, S. and J. Dudhia, 2000: Annual Report: WRF Physics. *NCAR/MMM Internal Report* available at http://www.mmm.ucar.edu/wrf/users/docs.

Collins, W. D., and Coauthors, 2006: The Community Climate System Model version 3 (CCSM3). *J. Climate*, **19**, 2122–2143, doi:10.1175/JCLI3761.1.

Coons, R.D., R.C. Gentry, and R. Gunn, 1948: First partial report on the artificial production of precipitation: Stratiform clouds, Ohio. *Bull. Amer. Met. Soc.,* **29**, 266–269.

DeFelice, T.P., J. Golden, D. Griffith, W. Woodley, D. Rosenfeld, D. Breed, M. Solak and B. Boe, 2014: Extra area effects of cloud seeding - An updated assessment. *Atmos. Res*., **135-136**, p. 193–203.

DeMott, P.J., 1995: Quantitative descriptions of ice formation mechanisms of silver iodide-type aerosols. *Atmos. Res.*, **38**, 63-99.

DeMott, P.J., 1997: Report to North Dakota Atmospheric Resource Board and Weather Modification Incorporated on tests of the ice nucleating ability of aerosols produced by the Lohse airborne generator. Report from Dept. Atmos. Sci., Colorado State Univ., Fort Collins, CO, 15 pp.

DeMott, P.J., 1999: Report to Ice Crystal Engineering on Tests of Ice Nucleating Ability of Aerosols Produced by New Formulation Pyrotechnics - July 1999. Cloud Simulation and Aerosol Laboratory, Department of Atmospheric Science, Colorado State University, Fort Collins, CO, USA 80523, 19 pp.

Dennis, A.R., 1980: *Weather Modification by Cloud Seeding*. Academic Press, New York, 267 pp.

Eilers, Paul H.C. and Hans F.M. Boelens, 2005: Baseline correction with asymmetric least squares smoothing. *Leiden University Medical Centre Report*.

Gabriel, K.R., 1999: Ratio statistics for randomized experiments in precipitation stimulation. *J. Appl. Meteor.*, **38**, 290-301.

Gabriel, K.R. and D. Petrondas, 1983: On using historical comparisons in evaluating cloud seeding operations. *J. Climate Appl. Meteor.*, **22**, 626-631.

Geerts, B., Q. Miao, Y. Yang, R. Rasmussen, and D. Breed, 2010: An airborne profiling radar study of the impact of glaciogenic cloud seeding on snowfall from winter orographic clouds. *J. Atmos. Sci*., **67**, 3286–3302.

Geresdi, I., L. Xue, R. Rasmussen, 2016: Evaluation of Orographic Cloud Seeding Using Bin Microphysics Scheme. Part I: Two-dimensional approach. *J. Appl. Meteor. Climatol*., in review.

Gochis, D.J., W. Yu, and D.N. Yates, 2013: *The WRF-Hydro model technical description and user's guide, version 1.0.* NCAR Technical Document. 120 pages. Available online at: http://www.ral.ucar.edu/projects/wrf_hydro/

Golden, J.H., 1995: The NOAA Atmospheric Modification Program – A 1995 update. *J. Wea. Modif.*, **27**, 110-112.

Griffith, D.A., M.E. Solak, D.P. Yorty, A.W. Huggins, and D. Koracin, 2006: A Level II Weather Modification Feasibility Study for the Salt River and Wyoming Ranges, Wyoming. Nroth American Weather Consultants (NAWC) Report to the Wyoming Water Development Commission, 261 pp. [also referenced as NAWC, 2006]

Griffith, D.A., M.E. Solak and D.P. Yorty, 2009: 30+ winter seasons of operational cloud seeding in Utah. *J. Wea. Modif.,* **41**, 23–37.

Griffith, D.A., D.P. Yorty and M.E. Solak, 2011: A winter operational cloud seeding program: Upper Gunnison River Basin, Colorado. *J. Wea. Modif.,* **43**, 29–43.

Harper, K.T., 1981: Potential Ecological Impacts of Snowpack Augmentation in the Uinta Mountains, Utah. Brigham Young University Report to the Utah Division of Water Resources, 291 pp.

Harris, E. R., 1981: "Sierra Cooperative Pilot Project - Environmental Assessment and Finding of No Significant Impact". U.S. Bureau of Reclamation Report, 196 pp.

Heimbach, J.A., A.B. Super, B.A. Boe, G. Langer, and J.T. McPartland, 2008: Comparison of two acoustic ice nucleus counters. *J. Wea. Modif.*, 4**0**, 54–63.

Henderson, T.J., 2003: The Kings River weather resources management program. *J. Wea. Modif.,* **35**,. 45–51.

HKM Engineering Inc., Lord Consulting, and Watts and Associates, 2002: *Powder/Tongue River Basin Plan Final Report*, a report to the Wyoming Water Development Commission, 203 pp.

Hong, S.-Y., Y. Noh, and J. Dudhia, 2006: A new vertical diffusion package with an explicit treatment of entrainment processes. *Mon. Wea. Rev.*, **134**, 2318–2341, doi:10.1175/MWR3199.1.

Huggins, A.W. 2007: Another wintertime cloud seeding case study with strong evidence of seeding effects. *J. Wea. Modif.*, **39**, 9–36.

Huggins, A.W. 2009: Summary of studies that document the effectiveness of cloud seeding for snowfall augmentation. *J. Wea. Modif.,* **41**, 119–126.

Iacono, M. J., J. S. Delamere, E. J. Mlawer, M. W. Shephard, S. A. Clough, and W. D. Collins, 2008: Radiative forcing by long-lived greenhouse gases: Calculations with the AER radiative transfer models, *J. Geophys. Res.,* **113,** D13103, doi:10.1029/2008JD009944.

Ikeda, K., and Coauthors, 2010: Simulation of seasonal snowfall over Colorado. *Atmos. Res.*, **97**,462-477.

Janjic Z. I., 1994: The step-mountain Eta coordinate model: Further developments of the convection, viscous layer, and turbulence closure schemes. *Mon. Wea. Rev.*, **122**, 927–945, doi:10.1175/1520-0493(1994)122,0927:TSMECM.2.0.CO;2.

Janssen, D.W., G.T. Meltsen, and L.O. Grant, 1974: Extended area effects from Climax, Colorado Seeding Experiment. *Preprints of Fourth Conference on Weather Modification*, Ft. Lauderdale, FL. AMS, Boston, 516–522.

Johnson, J. B., and D. Marks, 2004: The detection and correction of snow water equivalent pressure sensor errors. *Hydrological Processes*, **18**, 3513–3525.

Klein, D.A., 1978: *Environmental Impacts of Artificial Ice Nucleating Agents*. Dowden, Hutchinson & Ross, Inc., Stroudsburg, Pennsylvania.

Klemp, J.B., W.C. Skamarock, and O. Fuhrer. 2003: Numerical consistency of metric terms in terrain-following coordinates. *Mon. Wea. Rev.,* **131**, 1229–1239.

Knight, D. H., and Coauthors, 1975: "The Medicine Bow Ecology Project." *Final Report to Bureau of Reclamation*, University of Wyoming, Laramie, WY.

Kraus, E.B., and P. Squires, 1947: Experiments on the simulation of clouds to produce rain. *Nature,* **159**, 489–491.

Langmuir, I., 1948: The growth of particles in smokes and clouds and the production of snow from supercooled clouds. *Proc. Am. Philos. Soc.,* **92**, 167.

Liu, Y., and Coauthors, 2008: The operational mesogamma-scale analysis and forecast system of the U.S. Army Test and Evaluation Command. Part I: Overview of the modeling system, the forecast products, and how the products are used. *J. Appl. Meteor. Climatol.*, **47**, 1077–1092.

Liu. C., and co-authors, 2016: xxx, *Journal Name., in preparation.*

Long, A. B., 2001: Review of downwind extra-area effects of precipitation enhancement. *J. Wea. Modif.,* **33**, 24–45.

Manton, M.J., and L. Warren, 2011: A confirmatory snowfall enhancement project in the Snowy Mountains of Australia. Part II: Primary and associated analyses. *J. Appl. Meteor*. *Climatol*, **50**, 1448–1458.

Manton, M.J., L. Warren, S. L. Kenyon, A.D. Peace, S.P. Bilish, and K. Kemsley, 2011: A confirmatory snowfall enhancement project in the Snowy Mountains of Australia. Part I: Project design and response variables. *J. Appl. Meteor. Climatol.*, **50**, 1432–1447.

Manton, M.J., J. Denholm, K. Kemsley, S. L. Kenyon, A. Peace, J. Speirs, and L. Warren (2015): Analysis of a snowfall enhancement project in the Snowy Mountains of Australia. *Submitted to the J. Appl. Meteor. Climatol.*

Mielke, P.W. Jr., G.W. Brier, L.O. Grant, G.J. Mulvey, and P.N. Rosenweig, 1981: A statistical reanalysis of the replicated Climax I and II wintertime orographic cloud seeding experiments. *J. Appl. Meteor*., **20**, 643–659.

Mikalakes, J., J. Dudhia, D. Gill, T. Henderson, J. Klemp, W. Skamarock, and W. Wang, 2004: The Weather Research and Forecast Model: Software Architecture and Performance. *Proceeding of the Eleventh ECMWF Workshop on the Use of High Performance Computing in Meteorology. 25 - 29 October 2004, Reading, U.K.*

MWH Americas, Inc., Short Elliott Hendrickson, Inc., and Harvey Economics, 2010: *Wind-Bighorn Basin Plan Update*, a report to the Wyoming Water Development

Myler, L., 2016: U.S. Bureau of Reclamation, personal communication regarding the sale of water from Boysen Reservoir, Bighorn River, WY.

NAWC, 2006: [see Griffith et al. 2006]

NCAR, 2008: Wyoming Weather Modification 5-Year Pilot Program: Design of the Randomized Seeding Experiment with 2008 Additions, 80 pp. Available from the Wyoming Water Development Commission, Cheyenne, WY.

National Research Council (NRC), 2003: *Critical Issues in Weather Modification Research*. National Academy Press, 123 pp

Niu, G.-Y., and co-authors, 2011: The community Noah land surface model with multiparameterization options (Noah-MP): 1. Model description and evaluation with local-scale measurements. *J. Geophys. Res.*, **116**, D12109, doi: 10.1029/2010JD015139.

Pokharel, B., B. Geerts, and X. Jing, 2014a: The impact of ground-based glaciogenic seeding on orographic clouds and precipitation: a multi-sensor case study. *J. Appl. Meteor. Climatol*., **53**, 890-909.

Pokharel, B., B. Geerts, X. Jing, K. Friedrich, J. Aikens, D. Breed, R. Rasmussen, and A. Huggins, 2014b: The impact of ground-based glaciogenic seeding on clouds and precipitation over mountains: A multi-sensor case study of shallow precipitating cumuli. *Atmos. Res.*, **147-148**, 162-182.

Rasmussen, R., and Coauthors, 2011: High-resolution coupled climate runoff simulations of seasonal snowfall over Colorado: A process study of current and warmer climate. *J. Climate*, **24**, 3015–3048.

Rasmussen. R, and Coauthors, 2012: How well are we measuring snow? The NOAA/FAA/NCAR Winter Precipitation Test Bed: *Bull. Amer. Meteorol. Soc.*, **93**, 811–829.

Rasmussen. R., and Coauthors, 2014: Climate change impacts on the water balance of the Colorado Headwaters: High-resolution regional climate model simulations. *J. Hydro. Meteor.,* **15,** 1091–1116*.*

Reisner, J. R.M. Rasmussen, and R.T. Bruintjes, 1998: Explicit forecasting of supercooled liquid water in winter storms using the MM5 mesoscale model. Quart*. J. Roy. Meteor. Soc.*, **124**, 1071–1107.

Reynolds, D.W., 2015: Literature Review and Scientific Synthesis on the Efficacy of Winter Orographic Cloud Seeding. Draft Report to the U.S. Bureau of Reclamation, CIRES, Boulder, CO, 148 pp.

Ritzman, Jaclyn, 2013: What Fraction of Winter Precipitation over the Sierra Madres and Medicine Bows was Treated during the Wyoming Weather Modification Pilot Project?, MS Thesis, Univ. of Wyoming, 96 pp.

Ritzman, J., T. Deshler, K. Ikeda, and R. Rasmussen, 2015: Estimating the fraction of winter orographic precipitation that is produced under conditions meeting the seeding criteria from the Wyoming weather modification pilot project. *J. Appl. Meteor. Climatol.*, **54**, 1202–1215.

Ryan, T., 2005: Weather Modification for Precipitation Augmentation and its Potential Usefulness to the Colorado River Basin States. Metropolitan Water District of Southern California Report, 34 pp.

Schaefer, V.J., 1946: The production of ice crystals in a cloud of supercooled water droplets. *Science*, **104**, 457–459.

Serreze, M. C., M. P. Clark, R. L. Armstrong, D. A. McGinnis, and R. S. Pulwarty, 1999: Characteristics of the western United Stated snowpack from snowpack telemetry (SNOTEL) data. *Water Resour. Res.*, **35**, 2145–2160.

Serreze, M. C., M. P. Clark, and A. Frei, 2001: Characteristics of large snowfall events in the montane western United States as examined using snowpack telemetry (SNOTEL) data. *Water Resour. Res.,* **37**, 675–688.

Silverman, B.A., 2007: On the use of ratio statistics for the evaluation of operational cloud seeding programs. *J. Wea. Modif*., **39**, 50–60.

Silverman, B.A., 2009: An independent statistical evaluation of the Vail operational cloud seeding program. *J. Wea. Modif*., **41**, 7–14.

Silverman, B.A., 2010: An evaluation of eleven operational cloud seeding programs in the watersheds of the Sierra Nevada Mountains. *Atmos. Res*., **145**, 526–539.

Skamarock, W.C., 2004: Evaluating Mesoscale NWP Models Using Kinetic Energy Spectra. *Mon. Wea. Rev.,* **132**, 3019–3032.

Skamarock, W. C., J. B. Klemp, J. Dudhia, D. O. Gill, D. M. Barker, W. Wang, and J. G. Powers, 2005: A description of the Advanced Research WRF version 2. NCAR Tech. Note NCAR/TN-4681STR, 88 pp. [Available online at www.mmm.ucar.edu/wrf/users/docs/arw_v2.pdf.]

Skamarock, W. C., J.B. Klemp, J. Dudhia, D.O. Gill, D.M Barker, 2008: A description of the Advanced Research WRF version 3. NCAR Tech. Note NCAR/TN-475+STR

Solak, M.E., D.P. Yorty and D.A. Griffith, 2003: Estimations of downwind cloud seeding effects in Utah. *J. Wea. Mod*., **35**, 52–58.

Smith, J. L., Erman, D. C., Hart, D. D., Kelly, D. W., Klein, D. A., Koch, D. L., Linn, J. D., Moyle, P. M., Ryan,J. H., and Woodard, R. P., 1980. "An Evaluation of Possible Effects of Weather Modification On Lake and Stream Biota in the American River Basin, California." *The Sierra Ecology Project*, **2**, (5), Office of Atmospheric Water Resources Management, Bureau of Reclamation, USDI, Denver, CO.

Stauffer, N.E., and K. Williams, 2000: Utah cloud seeding program, increased runoff/cost analysis. Technical Report. Utah Department of Natural Resources, Division of Water Resources.

Steinhoff and Ives, 1976: Ecological Impacts of Snowpack Augmentation in the San Juan Mountains of Colorado, Final Report of the San Juan Ecology Project to the Bureau of Reclamation from Colorado State University, Contract No. 14-06-D-7052, 489 pp.

Super, A.B., 1974: Silver iodide plume characteristics over the Bridger Mountain Range, Montana. *J. Appl. Meteor*., **13**, 62–70.

Super, A.B., 1999: Summary of the NOAA/Utah Atmospheric Modification Program: 1990-1998. *J. Wea. Modif*., **31**, 51-75.

Super, A.B., and J.A. Heimbach, Jr., 1983: Evaluation of the Bridger Range winter cloud seeding experiment using control gauges. *J. Appl. Meteor*., **22**, 1989–2011.

Super, A.B., and J.A. Heimbach, Jr., 1988: Microphysical effects of wintertime cloud seeding with silver iodide over the Rocky Mountains, Part II: Observations over the Bridger Range, Montana. *J. Appl. Meteor*., **27**, 1152–1165.

Super, A.B., and A.W. Huggins, 1992: Investigations of the targeting of ground-released silver iodide nuclei in Utah – Part I: Ground observations of silver in snow and ice nuclei. *J. Wea. Mod*., **24**, 19-34

Super, A.B., and J.T. McPartland, 1993: Preliminary estimates of increased runoff from additional high elevation snowfall in the Upper Colorado River Basin. *J. Wea. Modif*., **25**, 74–81.

Super, A.B., and J. A. Heimbach, Jr., 2005: Feasibility of snowpack enhancement from Colorado winter mountain storms: Emphasis on supercooled liquid water and seeding with silver iodide and propane. Final Report to Technical Services Center, Bureau of Reclamation, Denver, CO, 13 November 2005, 73 pp.

Super, A.B., B.A. Boe, J.A. Heimbach, J.T. McPartland, and G. Langer, 2010: Comparison of silver iodide outputs from two different generators and solutions measured by acoustic ice nucleus counters. *J. Wea. Modif.*, **42**, 49–60.

Sykes, R. I., and R. S. Gabruk, 1997: A second-order closure model for the effect of averaging time on turbulent plume dispersion. *J. Appl. Meteor*., **36**, 1038-1045.

Tessendorf, S.A., B. Boe, B. Geerts, M.J. Manton, S. Parkinson, and R. Rasmussen, 2015: The future of winter orographic cloud seeding: a view from scientists and stakeholders. *Bull. Amer. Meteor. Soc*., **96**, 2195-2198.

Thompson, G., R. M. Rasmussen, and K. Manning, 2004: Explicit forecasts of winter precipitation using an improved bulk microphysics scheme. Part I: Description and sensitivity analysis. *Mon. Wea. Rev.*, **132,** 519–542.

Thompson, G., P. R. Field, R. M. Rasmussen, and W. D. Hall, 2008: Explicit forecasts of winter precipitation using an improved bulk microphysics scheme. Part II: implementation of a new snow parameterization. *Mon. Wea. Rev.*, **136,** 5095–5115.

Thompson, G. and T. Eidhammer, 2014: A study of aerosol impacts on clouds and precipitation development in a large winter cyclone. *J. Atmos. Sci.,* **71,** 3636–3658.

USBR, 2010: Finding of No Significant Impact, Walker River Basin Cloud Seeding Project. FONSI No: LO-10-05, 7 p.

Vonnegut, B., 1947: The nucleation of ice formation by silver iodide. *J. Appl. Phys.*, **18**, 593–595.

Warburton, J.A., R.H. Stone, and B.L. Marler, 1995: How the transport and dispersion of AgI aerosols may affect detectability of seeding effects by statistical methods. *J. Appl. Meteor*., **34**, 1929-1941.

Williams, B.D., and J.A. Denholm, 2009: Assessment of the Environmental Toxicity of Silver Iodide-With Reference to a Cloud Seeding Trial in the Snowy Mountains of Australia. *J. Wea. Modif.*, **41,** 75–96

WMA, 2009: Weather Modification Association (WMA) Position Statement on the Environmental Impact of Using Silver Iodide as a Cloud Seeding Agent. WMA, Salt Lake City, 5 pp.

WMA, 2014: Code of Ethics. Weather Modification Association document adopted April 2014 by WMA membership, Reno, Nevada.

WWC Engineering, AECOM, and ERO Resources Corp., 2010: *Green River Basin Plan.* Report to the Wyoming Water Development Commission, Basin Planning Program. 189 pp.

WWDC, 2014: The Wyoming Weather Modification Pilot Program – Level II Study, Draft Executive Summary, NCAR, 15 pp. (available at http://wwdc.state.wy.us/)

Xue, L., A. Teller, R. M. Rasmussen, I. Geresdi, and Z. Pan, 2010: Effects of aerosol solubility and regeneration on warm-phase orographic clouds and precipitation simulated by a detailed bin microphysical scheme. *J. Atmos. Sci.,* **67**, 3336 – 3354.

Xue, L., A. Teller, R. M. Rasmussen, I. Geresdi, Z. Pan, and X. Liu, 2012: Effects of aerosol solubility and regeneration on mixed-phase orographic clouds and precipitation. *J. Atmos. Sci.,* **69**, 1994 – 2010.

Xue, L., and Coauthors, 2013a: AgI cloud seeding effects as seen in WRF simulations. Part I: Model description and idealized 2D sensitivity tests. *J. Appl., Meteor. Climatol*., **52**, 1433–1457.

Xue, L., S. Tessendorf, E. Nelson, R. Rasmussen, D. Breed, S. Parkinson, P. Holbrook, and D. Blestrud, 2013b: AgI cloud seeding effects as seen in WRF simulations. Part II: 3D real case simulations and sensitivity tests. *J. Appl. Meteor. Climatol.*, **52**, 1458–1476.

Xue, L., X. Chu, R. Rasmussen, D. Breed, B. Boe, and B. Geerts, 2014: The dispersion of silver iodide particles from ground-based generators over complex terrain, Part 2: WRF Large-Eddy simulations vs. Observations. *J. Appl. Meteor. Climatol*., **53**, 1342–1361.

Xue, L., R. Edwards, A. Huggins, R. Rasmussen, S. A. Tessendorf, P. Holbrook, D. Blestrud, M. Kunkel, B. Glenn and S. Parkinson, 2016: WRF Large-Eddy simulations of chemical tracer deposition and seeding effect over complex terrain from ground- and aircraft-based AgI generators. *J. Appl. Meteor. Climatol.,* to be resubmitted.

Yang, D., B.E. Goodison, J.R. Metcalfe, V.S. Golubev, R. Bates, T. Pangburn, and C.L. Hanson, 1998: Accuracy of NWS 8" standard nonrecording precipitation gauge: results and application of WMO intercomparison. *J. Atmos. Oceanic Technol.*, **15**, 54–68.

Yorty, D.P, T.W. Weston, M.E. Solak, and D.A. Griffith, 2012: Low-level stability during icing periods in Utah: Implications for winter ground-based cloud seeding. *J. Wea. Modif.,* **44,** 48–68.

## 20. List of Acronyms

AF – Acre-feet
AgI – Silver iodide
AGL – Above Ground Level
AINC – Acoustic Ice Nucleus Counter, aka the NCAR ice nucleus counter
ASCE – American Society of Civil Engineers
ASCII – AgI Seeding Cloud Impact Investigation, a National Science Foundation-funded study of cloud seeding in Wyoming that utilized the seeding facilities from the WWMPP
ASOS – Automated Surface Observing System
BLM - U.S. Bureau of Land Management
BRE – Bridger Range Experiment (southwestern Montana)
CALTRANS—California Department of Transportation
CCMRB - Central Colorado Mountains River Basin
CRADP – Colorado River Augmentation Demonstration Program
CSU – Colorado State University
EA – Environmental Assessment
EIS – Environmental Impact Study
EPA – Environmental Protection Agency
FONSI – Finding of No Significant Impact
Fr – Froude Number, an index of how flow interacts with a mountain barrier
GFS – Global Forecast System
HEC – Heritage Environmental Consultants
HRRR – High Resolution Rapid Refresh
HYSPLIT – HYbrid Single-Particle Lagrangian Integrated Trajectory (http://www.arl.noaa.gov/documents/Summaries/Dispersion_HYSPLIT.pdf)
IN – Ice Nucleus
IPC – Idaho Power Company
LES – Large Eddy Simulation
LW – Liquid water
LWC – Liquid water content
LWP – liquid water path (a vertical integration of LWC)
MSL – Mean Sea Level
MYJ – Mellor Yamada Janjic PBL scheme
NAM – North American Mesoscale Model
NAWC – North American Weather Consultants
NCAR – National Center for Atmospheric Research
NEPA – National Environmental Policy Act
NEXRAD – Next-Generation Weather Radars used by the NWS
NOAA – National Oceanic and Atmospheric Administration
NRCS – Natural Resource Conservation Service
NWS – National Weather Service
PBL – Planetary Boundary Layer
RAL – Research Applications Laboratory, a part of NCAR
RAOB - Rawinsonde Observation
RAMS – Regional Atmospheric Modeling System

RT-FDDA – WRF real-time four-dimensional data assimilation modeling system
RUC – Rapid Update Cycle
SCIPUFF – Second-order Closure Integrated Puff
SCPP – Sierra Cooperative Pilot Project
SEO – State Engineer's Office
SLW – supercooled liquid water
SNOTEL – Snow Telemetry, a snow gauge network operated by the NRCS
SPERP – Snowy Precipitation Enhancement Research Program (Snowy Mountains of Australia)
SWE – Snow water equivalent
TAT – Technical Advisory Team, created as part of the WWMPP
USBR – Unites States Bureau of Reclamation
USFS – United States Forest Service
USGS – United States Geological Survey
WASCA – Winter AgI Seeding Case-calling Algorithm
WMA – Weather Modification Association
WMI – Weather Modification International
WRDS – Water Resources Data System, http://www.wrds.uwyo.edu
WRF – Weather Research and Forecast model
WWDC – Wyoming Water Development Commission, the State body directing the WWDO
WWDO – Wyoming Water Development Office
WWMPP – Wyoming Weather Modification Pilot Program

## 21. Appendix A

**Photos from the field surveys of potential generator sites**

Sites A1 and A2 were not visited, as both were determined to be ineffective.

Site B1 – Little Tepee Creek. Clockwise, from upper left: north, east, south, and west.




Site B2 was not visited due to time constraints.

Site B3 – Dry Ridge. Clockwise, from upper left: north, east, south, and west.



Site C1 and D1 – Cliffhanger. Clockwise, from upper left: north, east, south, and west.



Site C2 – Shuler Park. Clockwise, from upper left: north, east, south, and west.



Site C3 – Freeze-out Point. Clockwise, from upper left: north, east, south, and west.

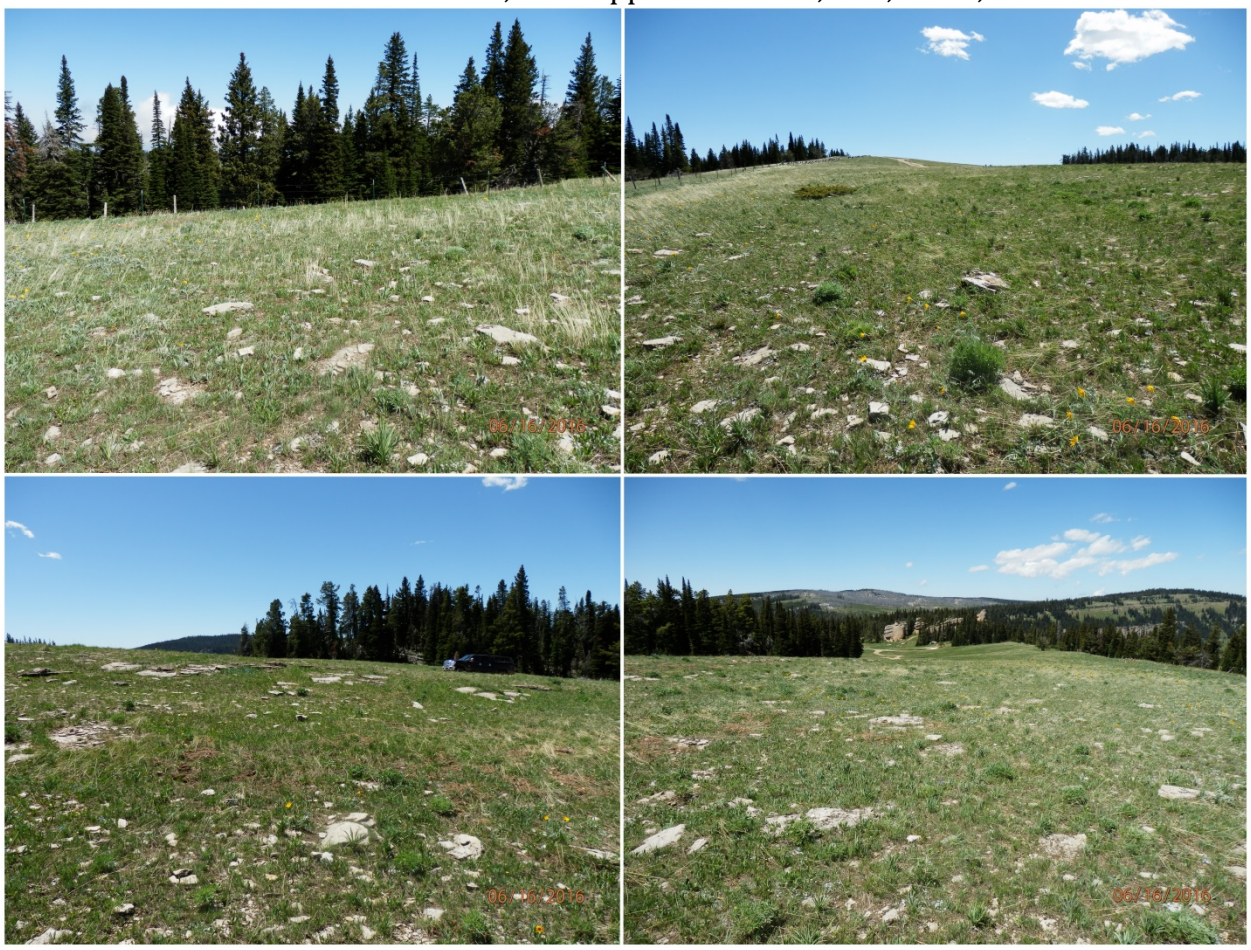

Site D1 – Same as Cliffhanger, previous.

Site D2 – Continental Divide. Clockwise, from upper left: north, east, south, and west.



Site D3 – Shell Creek. Clockwise, from upper left: north, east, south, and west.



Site D4 – Moose Meadow. Clockwise, from upper left: north, east, south, and west.



Site D5 – Bald Ridge. Clockwise, from upper left: north, east, south, and west.



Site E1 – Holland Ranch. Did not visit, gated, private land.

Site E1A. Holland Ranch Alternate, located about 0.9 mi W of E1. Clockwise, from upper left: north, east, south, and west.



Site E2 – Cherry Creek. Clockwise, from upper left: north, east, south, and west.




E2A – Cherry Creek Alternate. Site added via desktop analysis after field work was completed.

Site E3 – Split Rock Creek. Clockwise, from upper left: north, east, south, and west.



Site F1 – Pete's Hole. Clockwise, from upper left: north, east, south, and west.



Site F2 – Sunlight Mesa. Clockwise, from upper left: north, east, south, and west.



Site F2A – Sunlight Mesa Alternate. Clockwise, from upper left: north, east, south, and west.



Site F3 – Bush Butte. Clockwise, from upper left: north, east, south, and west.




F3A – Bush Butte Alternate. No photos were taken because site is 250 feet from F3 and looks the same.

Site F4 – Paint Rock Creek.  Clockwise, from upper left: north, east, south, and west.




Site F5 – No photos because was not accessible.

Site F5A – High Park. Possible alternative to F5, which was not accessible. Clockwise, from upper left: north, east, south, and west.



Site F5B – Sarah's Folly. Clockwise, from upper left: north, east, south, and west.



# 22. Appendix B

**Public Hearing Documents**

You are invited to attend the Big Horn Range
Weather Modification Feasibility Study
Draft Results Public Hearings

**Mon., August 15, 2016 @ 5:30pm**
Sheridan County Fulmer Library, 335 W. Alger St.
Sheridan, WY

**Wed., August 17, 2016 @ 2:00pm**
Bureau of Land Management Office, 101 S. 23rd St.
Worland, WY

**Learn about the results of the cloud seeding feasibility study in the Big Horn Range from representatives of the:**

- **National Center for Atmospheric Research**
- **Heritage Environmental Consultants, LLC**
- **Weather Modification, Inc.**

For more information contact the Wyoming Water Development Office at:
(307) 777-7626 http://wwdc.state.wy.us/

# MEMORANDUM OF PUBLICATION

**The Sheridan Press**
**144 E. Grinnell Avenue**
**Sheridan, WY 82801**
**Phone: (307) 672-2431**
**Fax: (307) 672-7950**
**www.sheridanpress.com**

Katie Talbott
Wyoming Water Development Office
6920 Yellowtail Road
Cheyenne, WY 82002
(307)777-7626

***Class Liner Ad #00074189***
***Summary:***

Ad Description: Public Hearing and draft
Size: 2.00 x 3.12

| | |
|---|---|
| Publication Cost | $173.55 |
| Adjustments | $0.00 |
| Net Cost | $173.55 |
| Prepaid Amount | $0.00 |
| Amount Due | $173.55 |

***Order Detail:***

| Publication | Run Date | Cost |
|---|---|---|
| Insertion | 7/2916 | $57.85 |
| Insertion | 8/5/16 | $57.85 |
| Insertion | 8/12/16 | $57.85 |

Public Hearing and draft report presentation on the:
Big Horn Range Weather Modification Feasibility Study
When: Monday, August 15, 2016, 5:30 pm
Where: Sheridan County Fulmer Library, Inner Circle Room, 335 W. Alger St., Sheridan, WY 82801
AND
When: Wednesday, August 17, 2016, 2:00 pm
Where: BLM building, 101 S. 23rd St., Worland, WY 82401

The Wyoming Water Development Commission will hold a public hearing to receive comments on the Big Horn Range Weather Modification Feasibility Study. The Commission will also be seeking information as to whether the proposed project functions and services can be served by any person, association or corporation engaged in private enterprise.
Representatives of the Water Development Commission will be present to explain the project and to record comments.
For further information contact:
Wyoming Water Development Office
6920 Yellowtail Road
Cheyenne, Wyoming 82002
307/777-7626
Publish dates: July 29, August 5, 12, 2016.

RECEIVED
AUG 0 1 2016

**Bighorn Range Weather Modification**
**Level II Feasibility Study**
**Draft Final Results Public Hearing**

Monday August 15th, 2016, 5:30-7:30 p.m.
Sheridan County Library
Sheridan, Wyoming

WELCOME – Jeni Cederle, Project Manager, Wyoming Water Development Office (WWDO), Cheyenne, WY
- A. Welcome and introduction
- B. Pass around sign-in sheet
- C. Brief history and purpose for this study / today's agenda

OVERVIEW OF CURRENT LEVEL II STUDY – Sarah Tessendorf, National Center for Atmospheric Research (NCAR)
- A. Introduction of project team
- B. Summary of tasks
- C. Climatology study
- D. Climatological monitoring instrument deployments
- E. Overview of design options

MODEL EVALUATION OF PRELIMINARY DESIGNS – Roy Rasmussen, NCAR
- A. Model evaluation of design options
- B. Design iterations based on model results
- C. Recommended design

PROGRAM CONSIDERATIONS – Bruce Boe, Weather Modification Inc. (WMI), and Patrick Golden, Heritage Environmental Consultants
- A. Review of previous data
- B. Operational criteria
- C. Field surveys of potential generator sites
- D. Environmental and legal implications

COST BENEFIT ANALYSIS – Roy Rasmussen, NCAR, and Bruce Boe, WMI
- A. Potential benefits analysis
- B. Cost estimates
- C. Benefit/cost analysis

SUMMARY AND RECOMMENDATIONS – Sarah Tessendorf, NCAR

DISCUSSION / WRAP UP

## WYOMING WATER DEVELOPMENT COMMISSION (WWDC) PUBLIC HEARING
### BIG HORN WEATHER MODIFICATION FEASIBILITY STUDY PUBLIC HEARING

ust 15, 2016 *Meeting Location: Sheridan County Fulmer Library, Sheridan, WY*

| Name | Representing / Location | Email |
|---|---|---|
| Cederle | WWDO | jeni.cederle1@wyo.gov |
| k Golden | Heritage Env Consultants | pgolden@heritage-ec.com |
| h Tessendorf | NCAR | Saraht@ucar.edu |
| f French | UW | JFrench@uwyo.edu |
| Bass | Bighorn Nat'l Forest | bbass@fs.fed.us |
| dan Little | WWDC | |
| rrie Little | WGF Commission | carrie.little@wyo.gov |
| Rogaczewski | SCCD | carrie.rogaczewski@sccdwy.org |
| ue Maier | Sheridan County | smaier@sheridancounty.com |
| k Landon | Self | jlandon@fiberpipe.net |
| e Boe | WMI | bboe@weathermod.com |
| Forbes | Dayton WY | |
| | | |
| | | |
| | | |

*Wyoming Water Development Office*
6920 YELLOWTAIL ROAD TELEPHONE: (307) 777-7626 CHEYENNE, WY 82002

## *** Proof of Publication ***

Casper Star-Tribune
P.O. Box 80, Casper, WY 82602-0080, ph 307-266-0500

AFFIDAVIT OF PUBLICATION

STATE OF WYOMING )
COUNTY OF NATRONA )

I, the undersigned, being a person in the employ of the Casper Star-Tribune, a newspaper published in CASPER, NATRONA COUNTY, WYOMING, and, knowing the facts herein set forth do so solemnly swear that a copy of the notice as per clipping attached was printed and published

Daily Weekly

In the regular and entire issue of said newspaper, and not in any supplement thereof, for 3 Consecutive Days Weeks

commencing with issue dated July 29, 2016
ending with issue dated August 12, 2016

Wyoming Water Development
6920 Yellowtail Rd.
Cheyenne, WY 82002

ORDER NUMBER 5743

Signed

Subscribed in my presence and sworn to before me this
16th day of August, 2016

Rebecca S. Harris

NOTARY PUBLIC
REBECCA S. HARRIS
STATE OF WYOMING
COUNTY OF NATRONA
My Commission Expires June 13, 2020

**Public Hearing and draft report presentation on the: Big Horn Range Weather Modification Feasibility Study**

When: Monday, August 15, 2016, 5:30 pm

Where: Sheridan County Fulmer Library, Inner Circle Room, 335 W. Alger St., Sheridan, WY 82801
AND

When: Wednesday, August 17, 2016, 2:00 pm

Where: BLM building, 101 S. 23rd St., Worland, WY 82401

The Wyoming Water Development Commission will hold a public hearing to receive comments on the Big Horn Range Weather Modification Feasibility Study. The Commission will also be seeking information as to whether the proposed project functions and services can be served by any person, association or corporation engaged in private enterprise. Representatives of the Water Development Commission will be present to explain the project and to record comments.
For further information contact:
Wyoming Water Development Office
6920 Yellowtail Road
Cheyenne, Wyoming 82002
307/777-7626
Published: July 29, August 5 & 12, 2016
Legal No: 5743

PUBLISHED ON: 07/29/2016, 08/05/2016, 08/12/2016

| | |
|---|---|
| TOTAL AD COST: | 228.76 |
| FILED ON: | 8/12/2016 |

**WYOMING WATER DEVELOPMENT COMMISSION (WWDC) PUBLIC HEARING**
**BIG HORN WEATHER MODIFICATION FEASIBILITY STUDY PUBLIC HEARING**

ıust 17, 2016 *Meeting Location: BLM Building, Worland, WY*

| Name | Representing / Location | Email |
|---|---|---|
| Tessendorf | NCAR, Boulder, CO | saraht@ucar.edu |
| Boe | WMI, Fargo, ND | bboe@weathermod.com |
| Cederle | WWDO | jeni.cederle1@wyo.gov |
| D McKamey | Highland Hanover J.D | — |
| Clucas | Basin WY | ClucasJM@Tctwest.net |
| Tilley | Shoshone Conservation District | shoshonecd@tctwest.net |
| Elliott | BLM - Worland Wy | j75ellio@blm.gov |
| Beamer | Wyo State Engineers Office | philip.beamer@wyo.gov |
| Schenerman | Hanover Irrigation District | |
| Lawrence | Wyo Water Development | Barry.lawrence@wyo.gov |
| Golden | Heritage EC | pgolden@heritage-ec.com |
| Rasmussen | NCAR | rasmus@ucar.edu |
| | | |
| | | |
| | | |

**Bighorn Range Weather Modification**
**Level II Feasibility Study**
**Draft Final Results Public Hearing**

Wednesday, August 17th, 2016 - 2:00 to 4:00 p.m.
Worland BLM Field Office
Worland, Wyoming

WELCOME – Jeni Cederle, Project Manager, Wyoming Water Development Office (WWDO), Cheyenne, WY
- A. Welcome and introduction
- B. Pass around sign-in sheet
- C. Brief history and purpose for this study / today's agenda

OVERVIEW OF CURRENT LEVEL II STUDY – Sarah Tessendorf, National Center for Atmospheric Research (NCAR)
- A. Introduction of project team
- B. Summary of tasks
- C. Climatology study
- D. Climatological monitoring instrument deployments
- E. Overview of design options

MODEL EVALUATION OF PRELIMINARY DESIGNS – Roy Rasmussen, NCAR
- A. Model evaluation of design options
- B. Design iterations based on model results
- C. Recommended design

PROGRAM CONSIDERATIONS – Bruce Boe, Weather Modification Inc. (WMI), and Patrick Golden, Heritage Environmental Consultants
- A. Review of previous data
- B. Operational criteria
- C. Field surveys of potential generator sites
- D. Environmental and legal implications

COST BENEFIT ANALYSIS – Roy Rasmussen, NCAR, and Bruce Boe, WMI
- A. Potential benefits analysis
- B. Cost estimates
- C. Benefit/cost analysis

SUMMARY AND RECOMMENDATIONS – Sarah Tessendorf, NCAR

DISCUSSION / WRAP UP